

AFWAL - TR - 80 - 2063



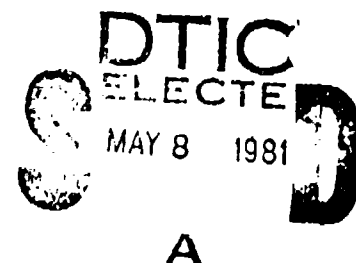
RELIABILITY ADVANCEMENT FOR ELECTRONIC ENGINE CONTROLLERS

Volume I: Final Report

HAMILTON STANDARD
DIVISION OF UNITED TECHNOLOGIES CORPORATION
WINDSOR LOCKS, CONNECTICUT 06096

JUNE 1980

TECHNICAL REPORT AFWAL - TR - 80 - 2063
FINAL REPORT FOR PERIOD AUGUST 1977 TO APRIL 1980



APPROVED FOR PUBLIC RELEASE: DISTRIBUTION UNLIMITED

AERO PROPULSION LABORATORY
AIR FORCE WRIGHT AERONAUTICAL LABORATORIES
AIR FORCE SYSTEMS COMMAND
WRIGHT - PATTERSON AIR FORCE BASE, OHIO 45433

AD A098623

DTIC FILE COPY

815 04101

**Best
Available
Copy**


NOTICE

When Government drawings, specifications, or other data are used for any purpose other than in connection with a definitely related Government procurement operation, the United States Government thereby incurs no responsibility nor any obligation whatsoever; and the fact that the government may have formulated, furnished, or in any way supplied the said drawings, specifications, or other data, is not to be regarded by implication or otherwise as in any manner licensing the holder or any other person or corporation, or conveying any rights or permission to manufacture use, or sell any patented invention that may in any way be related thereto.

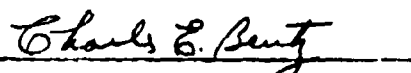
This report has been reviewed by the Office of Public Affairs (ASD/PA) and is releasable to the National Technical Information Service (NTIS). At NTIS, it will be available to the general public, including foreign nations.

This technical report has been reviewed and is approved for publication.


CHARLES E. RYAN, JR.
PROJECT ENGINEER


DAVID H. QUICK, LT COL, USAF
CHIEF, COMPONENTS BRANCH
TURBINE ENGINE DIVISION
AERO PROPULSION LABORATORY

FOR THE COMMANDER


CHARLES E. BENTZ
ACTING DEPUTY DIRECTOR
TURBINE ENGINE DIVISION
AERO PROPULSION LABORATORY

"If your address has changed, if you wish to be removed from our mailing list, or if the addressee is no longer employed by your organization please notify AFWAL/POTC, W-PAFB, OH 45433 to help us maintain a current mailing list".

Copies of this report should not be returned unless return is required by security considerations, contractual obligations, or notice on a specific document.

SECURITY CLASSIFICATION OF THIS PAGE (When Data Entered)

REPORT DOCUMENTATION PAGE		READ INSTRUCTIONS BEFORE COMPLETING FORM	
1. REPORT NUMBER	2. GOVT ACCESSION NO.	3. RECIPIENT'S CATALOG NUMBER	
AFWAL TR-80-2063 Vol 1	AD-A098623		
4. TITLE (and Subtitle)		5. TYPE OF REPORT & PERIOD COVERED	
RELIABILITY ADVANCEMENT FOR ELECTRONIC ENGINE CONTROLLERS. Volume I		Final Report August 1977 - April 1980	
6. AUTHOR(s)		7. PERFORMING ORG. REPORT NUMBER	
C. Rabinowitz K. Walworth J. Vernon R. Otterberg P. Cote K. Boucher M. McGlone (P&WA)		HSE-7667	
8. CONTRACT OR GRANT NUMBER(s)			
F33615-77-C-2055			
9. PERFORMING ORGANIZATION NAME AND ADDRESS		10. PROGRAM ELEMENT, PROJECT, TASK AREA & WORK UNIT NUMBERS	
Hamilton Standard Division United Technologies Corporation Windsor Locks, Connecticut 06096		Project 3066 / Task 306603 Work Unit 3066 03 75	
11. CONTROLLING OFFICE NAME AND ADDRESS		12. REPORT DATE	
Aero Propulsion Laboratory AF Wright Aeronautical Laboratories, AFSC Wright-Patterson Air Force Base, Ohio 45433		June 1980	
14. MONITORING AGENCY NAME & ADDRESS (if different from Controlling Office)		13. NUMBER OF PAGES	
Same		516	
		15. SECURITY CLASS. (of this report)	
		Unclassified	
		15a. DECLASSIFICATION, DOWNGRADING SCHEDULE	
16. DISTRIBUTION STATEMENT (of this Report)			
Approved for public release; distribution unlimited.			
17. DISTRIBUTION STATEMENT (of the abstract entered in Block 20, if different from Report)			
18. SUPPLEMENTARY NOTES			
19. KEY WORDS (Continue on reverse side if necessary and identify by block number)			
<ul style="list-style-type: none"> ● Electronic Engine Controller ● Reliability ● Redundancy Management ● Accelerated Stress Test 			
20. ABSTRACT (Continue on reverse side if necessary and identify by block number)			
<p>This study presents a comprehensive approach to the development of full-authority electronic engine controls which are capable of meeting the high reliability levels required of aircraft turbine engine controls.</p> <p>The primary groundrules and assumptions are defined, including the Variable Cycle Engine, its control requirements, and service environment. A preliminary design is developed, beginning with a system description and reliability evaluation of a baseline system, including implementation of redundancy, back-up</p>			

DD FORM 1 JAN 73, 1473

EDITION OF 1 NOV 68 IS OBSOLETE

SECURITY CLASSIFICATION OF THIS PAGE (When Data Entered)

20. ABSTRACT

control provisions, and self-test.

Through detailed system analyses and electrical and mechanical trade studies, a final preliminary design is derived. (Other topics covered include component baselines for reliability and cost studies, a discussion of reliability technology information exchanges with consulting organizations, a detailed description of reliability improvement measures including various levels of device screening and testing, and a Cost of Ownership Study.)

Through the effective use of measures such as fault tolerant coverage and selective duplex/triplex redundancy, the final RAEEC system developed can approach high flight safety levels and the goal for maintenance MBTF of 25,000 hours.

FOREWORD

This study was initiated to establish a comprehensive approach to the development of a high reliability, full-authority electronic engine control. The program was conducted by Hamilton Standard Division of United Technologies Corporation under the sponsorship of the Aero Propulsion Laboratory, Turbine Engine Division, Wright-Patterson Air Force Base, Ohio (Air Force Contract No. F33615-77-C-2055, Project No. 3066, Task No. 306603, Work Unit No. 3066 03 75. Sincere thanks are due the Project Officer, Charles E. Ryan, Jr., AFWAL/POTC for his direction, guidance, and encouragement during the course of this program. Mr. Ryan established a team of advanced technology advisors to add their considerable experience to appropriate parts of this effort. Hamilton Standard Division also expresses its sincere appreciation to these organizations and individuals listed below for their invaluable contributions:

Bell Telephone Laboratories

Conrad H. Fierdt Jr.
D. Stewart Peck
Irwin Schmidt

Delco Electronics Division, General Motors Corporation

Kenneth W. Doversberger
R. M. Siefken
W. Brown

Rome Air Development Center

Joseph B. Brauer
Clyde Lane

AFWAL Avionics Laboratory

Captain Roger E. Little
Captain Lawrence C. Hollatz

U.S. Army Electronics Command

U.S. Army Material Systems Analysis Activity

Dr. L. H. Crow

A

CONTENTS

<u>SECTION</u>		<u>PAGE</u>
I	INTRODUCTION	1
1.1	Background of Program	1
1.2	Purpose and Goals	1
1.3	Method of Investigation	1
II	DEFINITION OF VARIABLE CYCLE ENGINE (VCE)	10
2.1	Engine Cycle Definition	10
2.2	Duct and Core Stream Augmentation	12
2.3	Engine Ratings	13
2.4	Operational Limits	14
2.4.1	Basic Control Modes	15
2.4.2	Augmentation Control Mode	17
III	CONTROLLER PRELIMINARY DESIGN	19
3.1	Introduction	19
3.2	System Description	19
3.2.1	RAEEC Baseline System	19
3.2.2	Backup Control Provisions, Self Test and Diagnostic System	28
3.2.3	Self Test	31
3.2.4	RAEEC Final System	35
3.3	System Reliability Evaluation	48
3.3.1	Concepts	48
3.3.2	Baseline System	50
3.3.3	Reliability Groundrules	53
3.3.4	RAEEC Final System	54
3.3.5	System Coverage	61
3.3.6	Final System Flight Safety Probability	72
3.4	Electrical Design	77
3.4.1	Introduction	77
3.4.2	Analog-to-Digital Converter	77
3.4.3	Resolver-to-Digital Converter	77
3.4.4	Resolver Excitation	80
3.4.5	Torque Motor D/A's and Drivers	82
3.4.6	Solenoid Drivers	83
3.4.7	Pressure Sensors and Circuitry	83
3.4.8	Low Level DC Interface	89
3.4.9	Resolver Multiplexer	89
3.4.10	Discrete Signal Conditioner Circuit	89

TABLE OF CONTENTS (Continued)

<u>SECTION</u>		<u>PAGE</u>
3.4.11	Frequency to Digital Speed Interfaces	89
3.4.12	Turbo Pump Speed Interface	94
3.4.13	Fault Detection Logic	94
3.4.14	Power Supply System	94
3.4.15	CPU Design	100
3.4.16	Low Voltage Circuit Derating	121
3.5	Mechanical Design	126
3.5.1	General	126
3.5.2	Configuration and Installation	127
3.5.3	Physical Description	129
3.5.4	Maintainability	139
3.5.5	Environmental Design	140
IV	CONTROLLER ENVIRONMENT	158
4.1	Variable Cycle Engine Simulation	158
4.1.1	Aircraft and Engine Selection	158
4.1.2	Mission Profile Selection	158
4.1.3	Flight Envelope Definition	160
4.1.4	Simulation Methodology	160
4.2	Thermal Environment	165
4.2.1	Thermal Environment Definition	165
4.2.2	Cooling Methods	165
4.2.3	Moisture	173
4.2.4	Fuel and Oil Resistance	175
4.3	Vibration, Acoustic, and Impact Environment	178
4.3.1	Vibration Environment Definition	178
4.3.2	Acoustic Environment Definition	183
4.3.3	Impact Environment Definition	183
4.4.	Electrical Environment Definition	185
4.4.1	Summary	185
4.4.2	General	185
4.4.3	Lightning Environment	188
4.4.4	Electromagnetic Interference (EMI) Environment	198
4.5	Conclusions	199
V	COMPONENT BASELINES FOR RELIABILITY AND COST OF OWNERSHIP STUDIES	201
5.1	Baseline System Description, Functional	201
5.2	Baseline System Description, Mechanical	203
5.3	Part Quality Levels	205

TABLE OF CONTENTS (Continued)

<u>SECTION</u>		<u>PAGE</u>
VI	RELIABILITY TECHNOLOGY TRANSFER	206
VII	RELIABILITY IMPROVEMENT MEASURES	207
7.1	General	207
7.2	Thermal Environment	207
7.3	Redundancy	208
7.4	Vibration Environment	208
7.5	Interconnection Technology	209
7.6	Component Technology	209
7.7	Advanced Component Derating	210
7.8	Component Screens	211
7.9	Module Assembly Test and Screens	211
7.10	End Item Assembly Level Screening and Tests	212
7.11	Summary	212
VIII	TESTS TO ENHANCE RELIABILITY GROWTH	215
8.1	Introduction	215
8.2	Piece Part Screening	217
8.2.1	Integrated Circuits	217
8.2.2	Discrete Semiconductors	222
8.2.3	Tantalum Capacitors	224
8.2.4	Multilayer Epoxy or Polyimide Printed Circuit Boards	229
8.3	Subassembly Level (Module) Screening	231
8.3.1	Preproduction	233
8.3.2	Production	236
8.4	Final Assembly Level Screening	236
8.5	Reliability Development Testing	247
8.6	Reliability Growth Modeling	252
8.6.1	Generalized Statistical Analysis	252
8.6.2	Early Reliability Growth Evaluation	267
IX	ACCELERATED STRESS TESTING	270
9.1	Introduction	270
9.2	Test Program	271
9.2.1	Facility Evaluation	271
9.2.2	Initial Inspections and Tests	273
9.2.3	Bias Circuit Evaluation	273
9.2.4	High Temperature Accelerated Life Tests	274
9.3	Conclusion and Results	277

TABLE OF CONTENTS (Continued)

<u>SECTION</u>		<u>PAGE</u>
X	COST OF OWNERSHIP STUDY FOR RELIABILITY ADVANCE- MENT OF ENGINE ELECTRONIC CONTROLLERS	280
10.1	Introduction	280
10.2	Objective	280
10.3	Summary	280
10.4	Approach	281
10.4.1	Ground Rules	281
10.4.2	System Configurations	282
10.4.3	Major Cost Elements	284
10.5	Results	299
10.6	Conclusion	301
XI	DEVELOPMENT GUIDE	302
XII	CONCLUSIONS	303
XIII	RECOMMENDATIONS	305
APPENDIX A	ELECTRICAL DESIGN: BASELINE and TRADE STUDIES	307
APPENDIX B	MECHANICAL DESIGN TRADE STUDIES	435
APPENDIX C	TECHNOLOGY TRANSFER VISIT TO ROME AIR DEVELOPMENT CENTER	449
APPENDIX D	VIBRATION AND TEMPERATURE TRADEOFF STUDY	457
APPENDIX E	PARAMETRIC AND FUNCTIONAL DEVICE TESTING	469
APPENDIX F	CONSTRUCTION EVALUATION FOR ACCELERATED LIFE TESTS	475
APPENDIX G	COST BENEFITS OF SELF-TRIM CONTROL MODES	479
	REFERENCES	485

ILLUSTRATIONS

<u>FIGURE</u>		<u>PAGE</u>
SECTION I		
1	PROGRAM FLOW CHART RAECC	2
2	RAECC CONTROLLER EVOLUTION	3
3	ELECTRONICS SUPERVISORY CONTROL	6
4	ADVANCED TACTICAL FIGHTER MISSION PROFILE (BATTLEFIELD INTERDICTION MISSION)	7
5	ADVANCED TACTICAL FIGHTER MISSION PROFILE (DEEP STRIKE MISSION)	8
SECTION II		
6	VARIABLE CYCLE ENGINE	11
7	SIMPLIFIED BLOCK DIAGRAM CONTROL MODE	16
8	VARIABLE CYCLE ENGINE TOL MODE-DUCT STREAM AUGMENTOR CONTROL BLOCK DIAGRAM	18
SECTION III		
9	RAECC BASELINE SYSTEM SIMPLIFIED BLOCK DIAGRAM	20
10	FAILURE MODE SYNTHESIZATION CURVES	29
11	RAECC FINAL SYSTEM SIMPLIFIED BLOCK DIAGRAM	37
12	PRESSURE SENSOR TRANSDUCER WITH DUAL ELECTRONICS	47
13	BASLINE SYSTEM RELIABILITY BLOCK DIAGRAM	51
14	RELIABILITY BLOCK DIAGRAM - FINAL SYSTEM	62
15	FLIGHT SAFETY RELIABILITY BLOCK DIAGRAM	73
16	SAFETY MODEL RELIABILITY GRAPH	74
17	MULTI - RAMP A/D CONVERTER	78
18	RESOLVER TO DIGITAL CONVERTER	79
19	RESOLVER EXCITATION	81
20	TORQUE MOTOR DRIVER	84
21	SOLENOID DRIVER	85
22	SECTION VIEW OF PRESSURE SENSOR	86
23	SENSOR CIRCUIT BLOCK DIAGRAM	88
24	LOW LEVEL INTERFACE	90
25	RESOLVER MULTIPLEXER	91
26	DISCRETE SIGNAL CONDITIONER	92
27	SPEED INTERFACE	93
28	TURBINE PUMP SPEED INTERFACE	95
29	FAULT DISCRETES	96
30	POWER SUPPLY BLOCK DIAGRAM	97
31	A/C INTERFACE, POWER SUPPLY SYSTEM	98
32	RAECC DISTRIBUTIVE PROCESSING	101
33	THREE-CHIP HS 16/24 MACHINE	104

LIST OF ILLUSTRATIONS (Continued)

<u>FIGURE</u>		<u>PAGE</u>
34	RAECC CPU BLOCK DIAGRAM (FOR A PARALLEL MULTIPLE INSTRUCTION MULTIPLE DATA MACHINE ARCHITECTURE)	106
35	1024 WORD RAM	109
36	I/O ADDRESSING	112
37	DUAL PORT RAM "IMMEDIATE TRANSFER"	116
38	FULL CAPABILITY BACKUP USING AN ADDITIONAL, IDENTICAL CPU	118
39	CONDITIONAL CAPABILITY BACKUP USING THE FAILED CPU AT REDUCED PERFORMANCE CAPABILITY	120
40	TEST UART	122
41	RAECC PACKAGE OUTLINE	128
42	RAECC PACKAGE CONFIGURATION	130
43	ELECTRONIC MODULE	131
44	OVERBOARD DRAIN SCHEMATIC	136
45	RAECC CONTROL CROSS-SECTION	137
46	PRESSURE SENSOR MANIFOLD	138
47	FUEL FLOW DIAGRAM	144
48	CONDUCTIVE HEAT TRANSFER PATHS	147
49	PREDICTED VIBRATION ENVIRONMENT FOR VARIABLE CYCLE ENGINE; HIGHEST PEAKS IN FREQUENCY SPECTRUM AT OUTER ENGINE CASE JUST UPSTREAM OF DUCT FLAMEHOLDER	150
50	PREDICTED VARIABLE CYCLE ENGINE INSTANTANEOUS VIBRATION SPECTRUM AT THE ELECTRONIC CONTROL LOCATION	151
51	INSTANTANEOUS VIBRATION CURVE	152
52	COMPONENT MOUNTING	152
53	COMBINED MAX JFC90 INTERNAL COMPONENT RESPONSE TO ENGINE TESTS	153
54	FREQUENCY TUNED SYSTEM	155
55	ATTENUATION CHARACTERISTICS	157
SECTION IV		
56	ADVANCED TACTICAL FIGHTER MISSION PROFILE (BATTLEFIELD INTERDICTION MISSION)	159
57	ADVANCED TACTICAL FIGHTER MISSION PROFILE (DEEP STRIKE MISSION)	159
58	FLIGHT ENVELOPE AND FLIGHT POINTS FOR VARIABLE CYCLE ENGINE	161
59	ELECTRONIC CONTROL MOUNTING CONFIGURATION	166
60	COOLING FUEL ACCESS POINTS	171
61	MOISTURE DECREASE WITH ALTITUDE	174
62	PREDICTED VIBRATION ENVIRONMENT FOR VARIABLE CYCLE ENGINE	179

LIST OF ILLUSTRATIONS (Continued)

<u>FIGURE</u>		<u>PAGE</u>
63	EFFECT ON VIBRATION ENVIRONMENT OF MOVING CONTROL LOCATION AXIALLY	180
64	PREDICTED VARIABLE CYCLE ENGINE INSTANTANEOUS VIBRATION SPECTRUM AT THE ELECTRONIC CONTROL LOCATION	181
65	SCHEMATIC REPRESENTATION OF CONTROL MOUNTING WITH RESPECT TO VIBRATION	182
66	PREDICTED VARIABLE CYCLE ENGINE ACOUSTIC ENVIRONMENT	182
67	CARGO ENVIRONMENTS FOR HIGHWAY TRANSPORT	184
68	MAXIMUM SHOCKS RECORDED DURING AIRLINE TEST SHIPMENT	186
69	CARGO ENVIRONMENTS FOR AIR TRANSPORT	187
70	LIGHTNING STROKE MECHANISMS	190
71	NATURAL LIGHTNING STRIKE	191
72	LIGHTNING STROKE MODEL	196
73	ASSUMED EMI FIELD OUTSIDE AND INSIDE ENGINE NACELLE	200
SECTION V		
74	QUASI-REDUNDANT DUAL CHANNEL BASELINE SYSTEM	202
SECTION VII		
75	RELIABILITY ROADMAP	214
SECTION VIII		
76	ESTABLISHMENT OF ACCELERATED BURN-IN CONDITIONS (DESIGN & DEVELOPMENT PHASE, FOR INTEGRATED CIRCUITS)	219
77	100% SCREENING OF INTEGRATED CIRCUITS DURING PRODUCTION PHASE	220
78	100% ACCELERATED SCREENING FLOW FOR DISCRETE SEMICONDUCTORS	223
79	STEP STRESS, TEST OF SOLID TANTALUM CAPACITORS (PREPRODUCTION PHASE)	226
80	STEP STRESS TEST OF NON-SOLID TANTALUM CAPACITORS (PREPRODUCTION PHASE)	227
81	100% ACCELERATED SCREENING OF TANTALUM CAPACITORS (PRODUCTION PHASE)	228
82	100% SCREENING OF MULTILAYER POLYIMIDE LAMINATE PRINTED CIRCUIT BOARDS PREPRODUCTION AND PRODUCTION	230

LIST OF ILLUSTRATIONS (Continued)

<u>FIGURE</u>		<u>PAGE</u>
83	PRINTED CIRCUIT BOARD PLATED THRU HOLES	232
84	100% SCREENING OF POLYIMIDE P.C. BOARD MODEL DURING PREPRODUCTION PHASE	234
85	TEMPERATURE EXTREMES AT DWELL TIME	235
86	100% PREPRODUCTION SCREENING OF MODULES INCORPORATING LCC AND CERAMIC SUBSTRATES	237
87	100% SCREENING OF MODULES INCORPORATING POLYIMIDE P.C. BOARDS DURING PRODUCTION PHASE	238
88	100% SCREENING OF PRODUCTION MODULES INCORPOR- ATING LCC AND CERAMIC SUBSTATES	239
89	PRODUCTION ACCEPTANCE TEST OF END ITEM EQUIPMENT	241
90	GENERALIZED TEMPERATURE CYCLING FAILURE RATE CURVES AS A FUNCTION OF EQUIPMENT COMPLEXITY	242
91	DETERMINATION OF NUMBER OF TEMPERATURE CYCLES AS A FUNCTION OF EQUIPMENT COMPLEXITY	243
92	TEMPERATURE RATE OF CHANGE OF EQUIPMENT IN ITS USE ENVIRONMENT BY SEVERITY RANK	245
93	CERT OBJECTIVES	248
94	CERT TEST CONDITIONS	250
95	RELIABILITY GROWTH CYCLE	251
96	GENERALIZED STATISTICAL ANALYSIS FLOW CHART	253
97	CUMULATIVE FAILURES	255
98	AVERAGE FAILURE RATE	255
SECTION IX		
99	TEST PROGRAM FLOW	272
100	MC14163B BIAS CIRCUIT	275
SECTION X		
101	LIFE CYCLE COST ELEMENTS	283
102	USAF LOGISTICS SUPPORT COST MODEL	285
103	EQUATION 1 - PIPELINE SPARES	286
104	EQUATION 2 - ON-EQUIPMENT MAINTENANCE	287
105	EQUATION 3 - OFF-EQUIPMENT MAINTENANCE	288
106	EQUATION 6 - PERSONNEL TRAINING	289
107	EQUATION 7 - TECHNICAL DATA	290
108	ELECTRONIC ENGINE CONTROLLER COST COMPARISON	300

LIST OF TABLES

<u>TABLE</u>		<u>PAGE</u>
SECTION I		
1	ASSUMPTIONS	4
2	IMPERATIVES/ADMONITIONS	5
SECTION III		
3	RAECC BASELINE SYSTEM DEFINITION	21
4	RAECC FINAL SYSTEM DEFINITION	38
5	FAILURE EFFECTS-BASELINE SYSTEM	52
6	FIRST FAILURE FLAG ACTION MODIFIED BASELINE SYSTEM	55
7	FAILURE EFFECTS - FINAL SYSTEM	57
8	FIRST FAILURE FLAG ACTION FINAL SYSTEM	58
9	FINAL RAECC SYSTEM COVERAGE	68
10	BUILT-IN-TEST SUMMARY	71
11	POWER SUPPLY REQUIREMENTS	99
12	COMPUTER ARCHITECTURE "BOTTON-LINE"	102
13	SINGLE INSTRUCTION SINGLE DATA CPU	105
14	RAECC RAM DESIGN	110
15	RAECC ROM DESIGN	111
16	RAECC I/O ADDRESSING	113
17	RAECC DUAL-PORT DESIGN TRADEOFFS	117
18	RAECC TEST UART	123
19	CMOS STRESS DERATING IMPROVEMENT	124
20	TYPICAL ENGINE NACELLE THERMAL ENVIRONMENT - BATTLEFIELD INTERDICTION MISSION	142
21	TYPICAL ENGINE NACELLE THERMAL ENVIRONMENT - DEEP STRIKE MISSION	143
22	POWER DISSIPATION	146
SECTION IV		
23	PREDICTED ENGINE OPERATING CONDITIONS AT EXTREME FLIGHT CONDITIONS	162
24	TYPICAL ENGINE OPERATING CONDITIONS - BATTLEFIELD INTERDICTION MISSION	163
25	TYPICAL ENGINE OPERATING CONDITIONS - DEEP STRIKE MISSION	164
26	PREDICTED ENGINE NACELLE THERMAL ENVIRONMENT AT EXTREME FLIGHT CONDITIONS	167
27	TYPICAL ENGINE NACELLE THERMAL ENVIRONMENT - BATILEFIELD INTERDICTION MISSION	168
28	TYPICAL ENGINE NACELLE THERMAL ENVIRONMENT - DEEP STRIKE MISSION	169

LIST OF TABLES (Continued)

<u>TABLE</u>		<u>PAGE</u>
29	LOW PROBABILITY MODELS OF PRECIPITATION RATES AND LIQUID WATER ALOFT (SISSENWINE, AFCRL-72- 0369, 1972)	176
30	SUMMARY OF LIQUID WATER CONTENT AT ALTITUDE (SISSENWINE, AFCRL-72-0369, 1972)	177
SECTION VIII		
31	CONFIDENCE INTERVALS FOR MTBF FROM TIME TERMINATED TEST	261
32	CRITICAL VALUES FOR CRAMER-VON MISES GOODNESS OF FIT TEST	263
33	CONFIDENCE INTERVALS FOR MTBF FROM FAILURE TERMINATED TEST	265
SECTION IX		
34	BIAS CIRCUIT EVALUATION SUMMARY	276
35	PARAMETRIC TEST SUMMARY	278
SECTION X		
36	DEFINITION OF TERMS IN LSC MODEL EQUATIONS	291
37	WEAPON SYSTEM INPUT PARAMETERS	294

GLOSSARY

ACCELERATED STRESS TESTING - Testing in which the applied stress level is chosen to exceed that stated in the reference conditions in order to shorten the time required to observe the stress response of the item or magnify the response in a given time.

AVAILABILITY - A measure of the degree to which an item is in the operable and committable state at the start of the mission.

COVERAGE - The conditional probability that given the existence of a failure in an operational system, the system is able to recover and continue operation with no permanent loss of function.

CROSS CHANNEL MONITORING - The process by which the signals or outputs of the channels are compared and any disagreement, outside of a tolerance range, is classified a fault.

CROSS-STRAPPING - The physical hardwiring of an element in one channel to elements in other channels.

FAULT TOLERANCE - The ability of the system to experience a finite number of failures and continue operation, in either a fully operational or degraded mode.

FLIGHT SAFETY RELIABILITY - The probability, per flight, of not losing the aircraft due to failures in the engine control.

IN-LINE CHANNEL MONITORING - The process by which the signals or outputs of a single channel are checked (for faults) by the processor of the channel. Also referred to as BIT.

MAINTENANCE RELIABILITY - The probability that the device will not require a maintenance action in the manner and under the conditions of intended use.

MISSION RELIABILITY - The probability that the device will successfully complete its defined mission.

OPERATIONAL READINESS - See AVAILABILITY.

REDUNCANCY MANAGEMENT - The process of improving the coverage of failures with the purpose of making the system fault tolerant.

SYNTHESIS - The substitution of data calculated from the physical relationships of the system using other parameters for a failed element.

ABBREVIATIONS, ACRONYMS, AND SYMBOLS

A4 - High Pressure Turbine Inlet Area
A41 - Low Pressure Turbine Inlet Area
A/D - Analog-to-Digital Converter
AFAPL - Air Force Aero Propulsion Laboratory
AFCRL - Air Force Cambridge Research Laboratories
AGE - Auxiliary Ground Equipment
AGREE - Advisory Group on Reliability of Electronic Equipment
AIC - Air Inlet Control
AJD - Duct Stream Exhaust Nozzle Area
AJE - Core Stream Exhaust Nozzle Area
AMSAA - Army Material Systems Analysis Activity
AQL - Acceptable Quality Level
ASSY - Assembly
AUG - Augmentation
BIT - Built-In-Test
CMVT - Constant Match Varying Temperature
COS - Cost of Ownership Study
CPU - Central Processor Unit
CSVA - Compressor Stator Vane Angle
D/A - Digital-to-Analog Converter

Delta (Δ):

ΔP_3 - Compressor Discharge Differential Pressure

ΔP_{13} - Fan Discharge Differential Pressure

DIP - Dual In-Line Package

DMA - Direct Memory Access

DPRAM - Dual Port Random Access Memory

DPCTRAM - Dual Port Cross Talk Random Access Memory

EAROM - Electrically Alterable Read Only Memory

ECM - Electronic Counter Measures

ECU - Electronic Control Unit

EEC - Electronic Engine Control

E_f - Fan Excitation Order

E_H - High Rotor Excitation Order

EMC - Electromagnetic Compatibility

EMI - Electromagnetic Interference

EMP - Electromagnetic Pulse

EOC - End of Conversion

EPR - Engine Pressure Ratio

FADEC - Full Authority Digital Electronic Control

FET - Field Effect Transistor

FIFO - First In First Out

FIGV - Fan Inlet Guide Vane Angle

GOMAC - Government Microcircuits Application Conference

HCC - Hermetic Chip Carrier
HTOT - High Temperature Overstress Testing
HTRB - High Temperature Reverse Bias
I/O - Input/Output
JAN (JN) - Joint Army Navy
 JANS - Highest Procurement Level
 JANTX - Extra Testing
 JANTXV - Extra Testing and Internal Visual
KOPS - Thousand Operations Per Second
LCC - Leadless Chip Carrier
LOD - Light Off Detector
LRU - Line Replaceable Unit
LSB - Least Significant Bit
LSC - Logistic Support Cost
LSI - Large Scale Integration
MIMD - Multiple Instruction Multiple Data
MOS - Metal Oxide Semiconductor
MSB - Most Significant Bit
MSFC - Marshal Space Flight Center
MSI - Medium Scale Integration
MTBF - Mean Time Between Failures
MTBUR - Mean Time Before Unscheduled Removal
MUX - Multiplexer

N₁ (NL) - Low Rotor Speed
N₂ (NH) - High Rotor Speed
NHA - Next Higher Assembly
NOCS - Non-Operational Control System
P2 - Fan Inlet Total Pressure
P3 - Compressor Discharge Total Pressure
P5 - Low Pressure Turbine Discharge Total Pressure
P5/P2 - Engine Pressure Ratio
P12 - Fan Inlet Total Pressure
P13 - Fan Discharge Total Pressure
P_{am} - Ambient Pressure
P_b - Burner Pressure
PAT - Production Acceptance Test
PIND - Particle Impact Noise Detection
PLA - Power Lever Angle
PLADH - Duct Augmentor Power Lever Angle
POR - Power On Reset
PROM - Programmable Read Only Memory
PSR - Power Supply Reset
PS3 - Compressor Discharge Static Pressure
PS13 - Fan Discharge Static Pressure
PT2 - Total Fan Inlet Pressure
PT3 - Total Compressor Discharge Pressure
PT5 - Total Low Pressure Turbine Discharge Pressure
PT13 - Total Fan Discharge Pressure

Ptd - Fan Duct Total Pressure
PWM - Pulse Width Modulation
QPL - Qualified Products List (Mil)
RAM - Random Access Memory
R/D - Resolver-to-Digital Converter
RF - Rocket Fire Signal
RI - Receiving Inspection
RM - Redundancy Management
ROM - Read Only Memory
SDFTP - Self Diagnosing Fault Tolerant Microprocessor
SEM - Scanning Electron Microscope
SIMD - Single Instruction Multiple Data
SISD - Single Instruction Single Data
SOS - Silicon On Sapphire
SOV - Solenoid Operated Valve
SPM - Scratch Pad Memory
SSI - Small Scale Integration
T₃ - Compressor Discharge Total Temperature
T₂₂ - Compressor Inlet Total Temperature
T_{am} - Ambient Temperature
TBT - Turbine Blade Temperature
Thr. Bal. - Thrust Balance
TPS - Turbine Pump Speed

TT_2 - Fan Inlet Total Temperature
 T_{td} - Fan Duct Total Temperature
TTL or T^2L - Transistor to Transistor Logic
UART - Universal Asynchronous Receiver/Transmitter
VCE - Variable Cycle Engine
VLSI - Very Large Scale Integration
V/STOL - Vertical/Short Take-Off and Landing
 WA_{13} - Duct Air Flow
 W_{ad} - Fan Duct Airflow Rate
 W_f - Fuel Flow
 W_{fd1} - Duct Augmentor Fuel Flow, Zone 1
 W_{fd2} - Duct Augmentor Fuel Flow, Zone 2
 W_{fd3} - Duct Augmentor Fuel Flow, Zone 3
WFDH - Fuel Flow, Duct Heater
 W_{fep} - Gas Generator Primary Zone Fuel Flow
 W_{fes} - Gas Generator Secondary Zone Fuel Flow
WOW - Weight On Wheels Signal
 W_{td} - Duct Heater Fuel Flowrate
 W_{te} - Core Fuel Flowrate
XNH - High Rotor Speed
XNL - Low Rotor Speed
 θ_{t2} - Ratio of fan inlet air temperature to standard ambient temperature at sea level

SUMMARY

The employment of electronics technology in the full-authority control of aircraft turbine engines offers many advantages over the traditional hydromechanical technology; increased accuracy, improved control modes, better maintenance, and, because of no-trim-required capabilities, substantially reduced life cycle cost. In terms of the key element of reliability, however, considerable study and investigation of means to improve the reliability potential of electronic engine controllers has been deemed necessary to the end that, at maturity no reliability penalty need attend their use on military engines. The Reliability Advancement For Electronic Engine Controls (RAEEC) Final Report presents a comprehensive approach for the evolution of a controller design capable of providing a maintenance mean time between failures (MTBF) of nearly 25,000 hours after 500,000 engine flight hours. This compares favorably with the high reliability levels of mature hydromechanical systems.

The engine cycle definition for the RAEEC control study was the variable-cycle engine (VCE), derived from the Navy's "Full-Authority Digital Electronic Control" (FADEC) program (Contract No. N00019-76-C-0422). The operating requirements and service environment for this type of engine, during a given mission profile, provide the basis for the control system development in the RAEEC program.

The baseline system is a two channel (primary and secondary) configuration with each channel having its own set of input sensors and signals, a central processing unit (CPU), and a set of output function controls. The basic mode of operation for the controller is to establish function control by using the primary channel. If there is a detectable fault in the primary channel, control of the output functions is transferred to the secondary channel. In the two channel baseline system, most of the output functions and all input sensors and signals are redundant, with the exception of the six pressure sensors and two temperature sensors. Memory-to-memory communication between the channels is provided by a Universal Asynchronous Receiver/Transmitter (UART) data link.

The development of electronic control systems with high mean time between failures and high mission safety encompasses two conflicting goals. Mission safety is provided by several levels of redundancy, whereas maximum MTBF is achieved through simplicity. To reconcile these two opposing goals, a fault-tolerant design approach is necessary to extend trouble-free service life, to increase availability, and to minimize the probability of safety-critical failures. The RAEEC design goal is to keep the system operational in spite of single and multiple hardware failures.

In the course of the RAEEC study, the baseline system was altered to evaluate the benefit of successive application of Redundancy Management techniques such as selective triple redundancy, majority voting, fault coverage, Built-in-test (BIT), parameter synthesis, and reliability mathematical modeling methods.

Through the application of Redundancy Management in the design of highly reliable fault tolerant electronic fuel controls, an optimal mix of MTBF, safety, and hardware complexity can be achieved; specifically through selected triple

redundancy at the functional modular level with a high degree of cross-strap-ping. The configuration is such that the control can operate satisfactorily at a full performance level with several dissimilar failures in two channels. In many cases, the redundancy in the system also allows postponement of immediate maintenance actions without compromising effective fuel control performance.

Circuit design trades were conducted on fourteen circuit designs and partitions to define the optimal final system. The trades considered the application of any technology in production as of 1979, in terms of a design's salient features and drawbacks, circuit board area, and power dissipation. The final circuit choices included a distributive processing array CPU configuration.

The mechanical package design for the RAEEC control incorporates modular construction for standardization and simplification of assembly, troubleshooting, and repair. Design features are developed to accommodate the predicted thermal, vibratory, acoustic, impact, and humidity elements of the controller's operational environment.

Particular emphasis was placed on tests to enhance reliability growth. These involve screening of piece parts, sub-assembly, and final assembly, as well as Combined Environmental Reliability Testing (CERT) tests for hard "real world" data from actual equipment use before entry into service. High temperature accelerated stress testing of semiconductor devices was evaluated to determine the viability of such testing. The testing done demonstrated that the semiconductor devices subjected to test were very reliable. Clearly, such testing can be very useful for semiconductor device screening purposes and for the characterization of device life distribution.

In an effort to derive maximum benefit from the experience of other organizations in terms of their own reliability enhancement efforts in the electronics field, a number of technology transfer visits and many telephone discussions have been conducted as described herein.

Reliability improvement measures were targeted for the following areas:

1. Thermal Environment
2. Redundancy
3. Vibration Environment
4. Interconnect Technology
5. Component Technology
6. Advanced Component Derating
7. Component Screens
8. Assembly Tests and Screens

When all improvement measures were implemented, an MTBF improvement factor of 25 was obtained.

Cost of ownership studies and self-trim investigations support the expectation of substantial life cycle cost savings based upon assumed guidelines for an electronic engine control. Cost study results also show that increased reliability can reduce the cost of maintenance to low levels. There is a reliability level beyond which further improvements are not cost effective from a maintenance standpoint and must be justified by requirements for mission reliability and flight safety.

No single reliability improvement measure will result in a high degree of reliability enhancement for an electronic engine control (EEC), but a family of improvement measures, involving design, procurement, and manufacturing disciplines can result in a full-authority EEC with a maintenance reliability many times greater than the overhaul period of the engine it controls. Detailed conclusions and recommendations are presented separately at the end of the RAEEC Final Report.

SECTION I INTRODUCTION

1.1 Background of Program

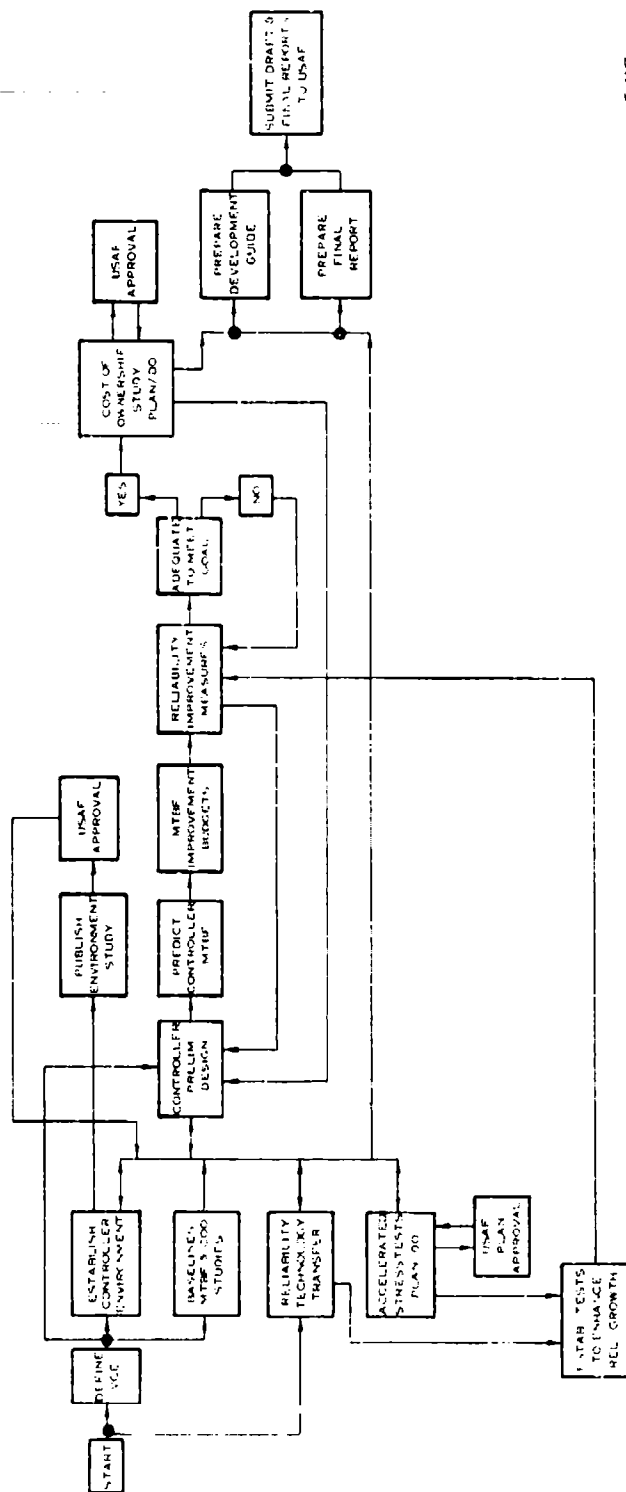
The historical trend in military high performance aircraft engines and engine controls has been toward higher levels of complexity, increased accuracy of control, and more stringent operational control requirements. The application of full-authority digital electronic control technology to meet this challenge is expected to provide economic benefits because of the ability to operate with greater precision, utilize improved control modes, and employ better maintenance procedures than the hydromechanical counterpart. However, engine-mounted digital electronic controls employ technology which is still in a developing and emerging state. Consequently, there is considerable concern about the ability of electronics technology to provide those levels of reliability which the users of aircraft turbine engines have come to expect. The intent of this study, therefore, is to investigate means of improving the reliability potential of electronic engine controls to the end that, at maturity, no reliability penalty need attend their use on military high performance engines in next generation aircraft.

1.2 Purpose and Goals

The overall objective of this program is to develop a comprehensive approach to the development of electronic engine controllers which can lead to the achievement of very high levels of reliability. The specific goal for this program is the evolution of a controller preliminary design capable of providing a maintenance reliability MTBF of 25,000 hours. Forty percent of this goal is to be reached at the 50,000 engine-flight-hour point and ninety-five percent of this goal is to be reached at the 500,000 engine-flight-hour point. This goal is comparable to the MTBF associated with the logic section of the hydromechanical "main fuel control" of J79 engines in the U.S. F-4 fighter aircraft fleet.

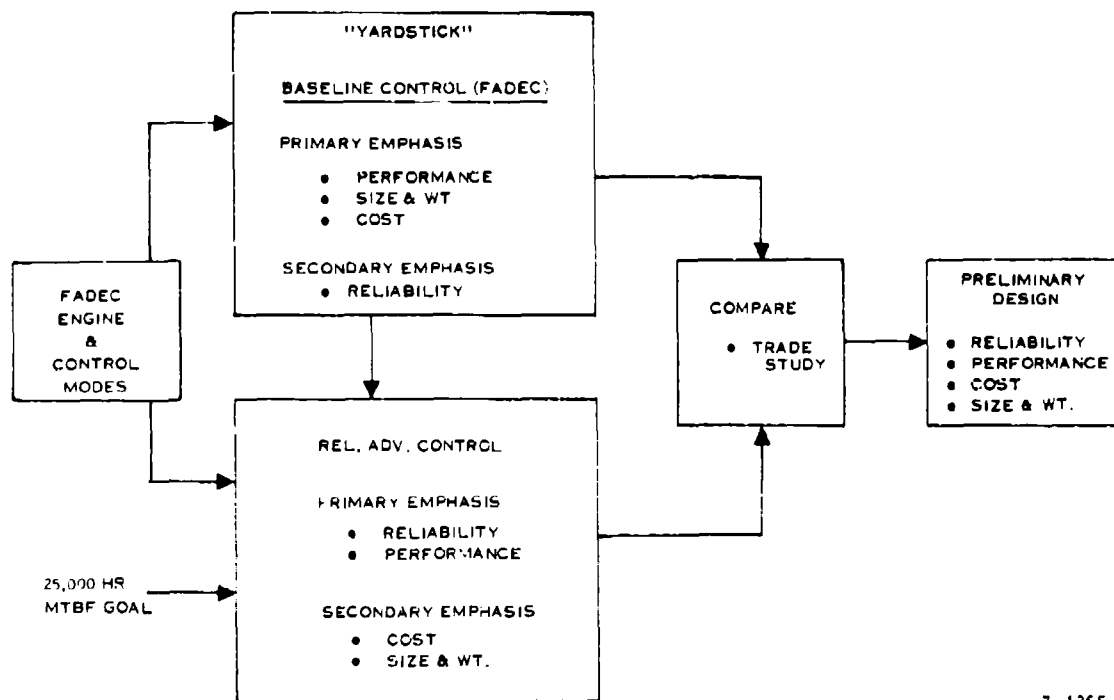
1.3 Method of Investigation

The method of investigation for this program is illustrated in the program flow chart of Figure 1. The heart of this program is the "reliability improvement measures" which are iterated many times during the program using the format shown in Figure 2. Selection of the variable cycle engine used in the Navy-sponsored FADEC program and the control modes developed for that VCE engine have allowed the focus of attention in the subject program to be on the improvement of reliability of the engine controller. A number of assumptions (Table 1) have been utilized in the program with the review and concurrence of AFAPL. In addition, a number of imperatives/admonitions have been provided by AFAPL (Table 2). In responding to the imperative/admonition regarding the importance of field reliability, field reliability experience has been utilized as appropriate from the only large-engine engine-mounted electronic control with significant field history, namely the F15/F16 engine controller shown in Figure 2. Component and assembly data based on USAF field



E-3657

FIGURE 1 PROGRAM FLOW CHART RAEEC



7-1365

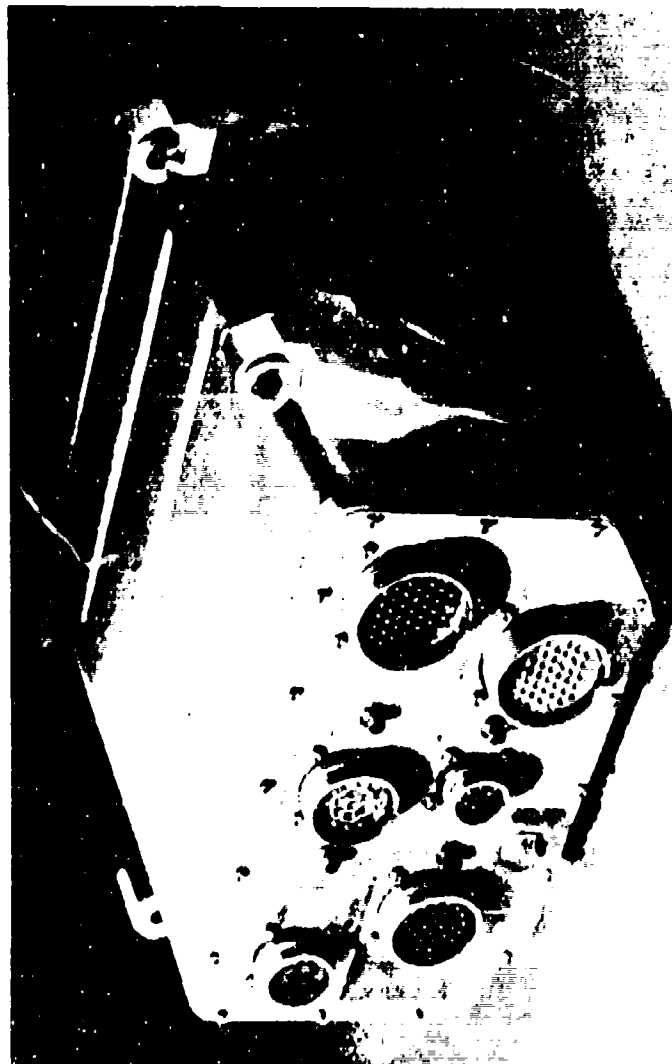
FIGURE 2 RAECC CONTROLLER EVOLUTION

TABLE 1 ASSUMPTIONS

- Definition of aircraft
 - Advanced tactical fighter
 - Two VCE engines
 - Located AFT fuselage
- Mission definition
 - Battlefield interdiction (See Figure 4)
 - Deep strike (See Figure 5)
 - Ten missions/day equally divided
- Shock and vibration sources other than engine
 - Gatling gun
 - Hard landings
- Maintenance philosophy and objectives
 - Forward front line base
 - Self contained health monitoring
 - No ground equipment
 - Pull entire control and replace
 - No trim or adjust
- Level II maintenance depot
 - AGE computer test set
 - Diagnostics and fault isolation
 - Module and parts inventory
 - Trim and adjust

TABLE 2 IMPERATIVES/ADMONITIONS

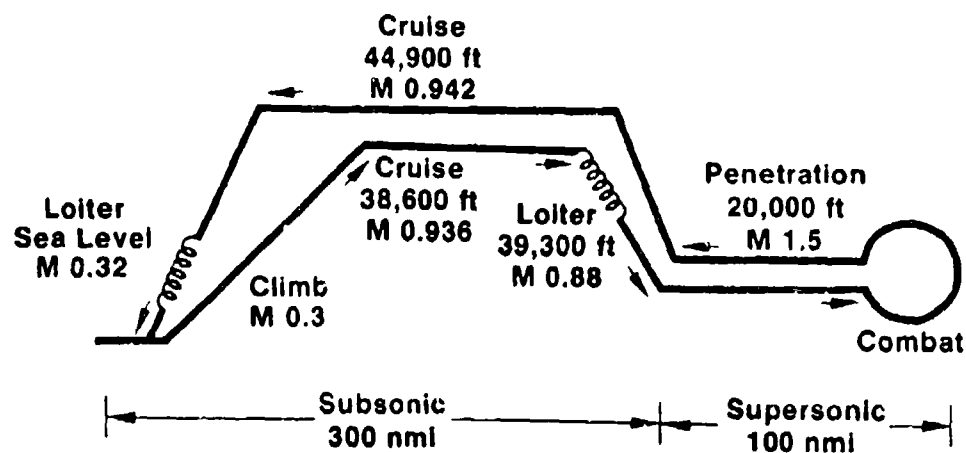
- Not bound by Mil specs. and conventional practices.
- Derive max., benefit from accelerated test technology at component and subassembly/assembly level enhanced by interface with industry advisors.
- Establish life cycle cost basis for future judgement regarding "How much reliability should Air Force seek to afford".
- Cognizant of current workshops/seminars.
- Use pragmatic approach to retain techniques which work, discard rest.
- Emphasize field MTBF as the most important reliability measure. Try to understand it, measure it, and correlate with it.
- For high reliability use high quality parts in conservative ways.
- Publish



- ☐ ENGINE MOUNTED
- ☐ FUEL COOLED
- ☐ TTL TECHNOLOGY
- ☐ PARALLEL DIGITAL
COMPUTER
- ☐ 24 LBS.

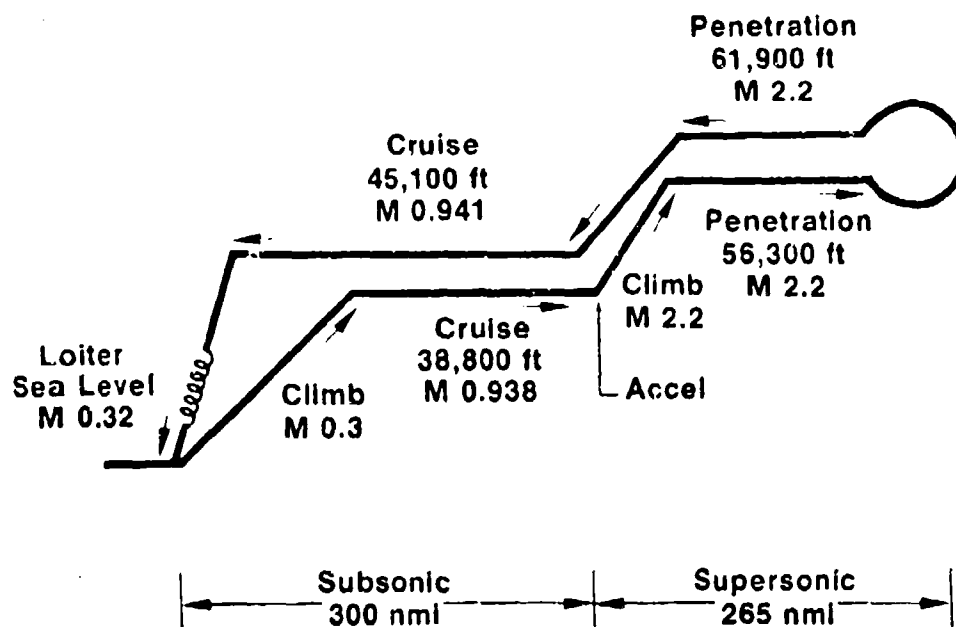
E-9188

FIGURE 3 SUPERVISORY ELECTRONIC CONTROL



E-4807

FIGURE 4 ADVANCED TACTICAL FIGHTER MISSION PROFILE
(BATTLEFIELD INTERDICTION MISSION)



E-4808

FIGURE 5 ADVANCED TACTICAL FIGHTER MISSION PROFILE
(DEEP STRIKE MISSION)

reliability history have been utilized in the definition of the "baseline" controller.

The work conducted by Hamilton Standard and its supporting contractors during the course of this study follows the flow chart of Figure 1 and is summarized in this report.

SECTION II DEFINITION OF VARIABLE CYCLE ENGINE (VCE)

2.1 Engine Cycle Definition

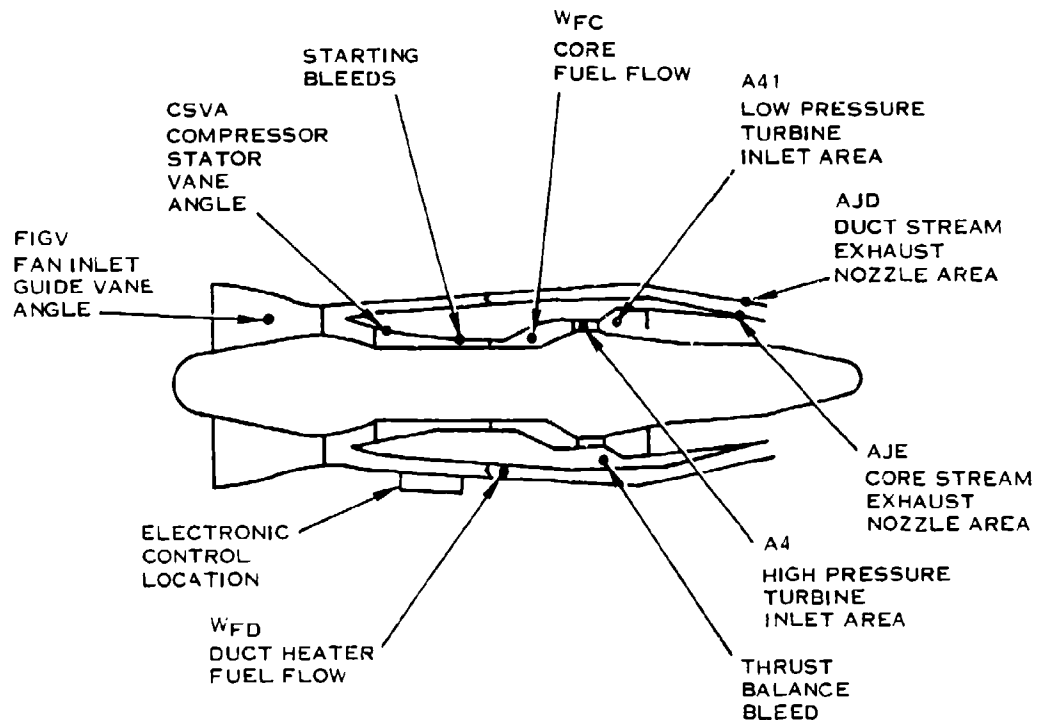
The Engine Cycle Definition, given below, was obtained from the FADEC VCE concept which serves as the baseline for the RAEEC Program. Variable cycle engines, such as the configuration shown in Figure 6, incorporate variable fan stator vanes, variable compressor stator vanes, variable high- and low-pressure turbine vane areas, and variable primary and fan duct exhaust nozzle areas in a two stream exhaust configuration. This degree of variable geometry provides the propulsion system designer with improved flexibility for controlling engine operating pressures, thrust-turbine temperature-airflow relationships, engine by-pass ratio, and transient response. Probably the single most important source of performance benefit for this engine configuration over a fixed-area turbine configuration is the capability to operate at constant inlet airflow over not only the augmented power range, but also over a significant portion of the nonaugmented high power range.

Maintaining constant airflow over a range of power settings is accomplished through a mode of operation referred to as constant match varying temperature (CMVT) operation. This mode of operation requires a constant match of rotor speeds, pressure ratios, and corrected airflow of the fan and compressor as turbine stator inlet temperature is varied. This is accomplished by changing fuel flow to set the power level, while modulating the turbine and exhaust nozzle areas to maintain constant values of high and low turbine work and constant gas flow through the compressor and fan duct. Power can be reduced in this manner from the intermediate level (highest nonaugmented power level), while maintaining a constant match of the fan and compressor until the low turbine exit flow parameter reaches its maximum allowable value, determined from consideration of pressure loss and flow separation of the exit guide vane. This power level is referred to as the breakpoint of CMVT. Below breakpoint power, constant airflow cannot be maintained, but fan and compressor operating lines and engine bypass ratio can be controlled.

Operation in the CMVT mode requires a two-stream, or nonmixed flow, exhaust nozzle configuration to avoid static pressure balancing of the two exhaust streams which would cause the fan to operate off the desired match point, and hence at lower efficiency.

The control flexibility provided by the variable geometry results in performance benefits which include the following:

- a. From a cycle point of view, the variable-area turbine engine operating with the CMVT mode has a higher compression ratio for a given turbine temperature, and therefore, a cycle advantage which yields lower fuel consumption at all powers below intermediate.



E-5655

FIGURE 6 VARIABLE CYCLE ENGINE

- b. The capability to reduce thrust at constant airflow leads to a reduction in inlet and exhaust nozzle drag at part power conditions, and therefore improvements in installed thrust specific fuel consumption.
- c. For operation at high supersonic conditions, accurate control of engine airflow resulting from the variable geometry plus the capability for constant airflow operation and better inlet/engine matching can result in a smaller inlet size, thus reducing weight and drag while maintaining aircraft thrust requirements and propulsion system stability.
- d. The variable areas can accommodate adjustments for cycle variation due to altitude, bleed air or horsepower extraction.
- e. In the area of aircraft-control integration, the variable-area turbine engine offers considerable advantages over a fixed turbine engine in its ability to accommodate changes in inlet distortion level resulting from evasive maneuvers, weapons firing or special modes of operation such as V/STOL. Thus, turbine and nozzle areas can be modulated to shift fan and compressor match points thereby providing stability accommodation.
- f. For transient operation, turbine and nozzle area modulation provides accurate control of fan and compressor operating lines resulting in improved stability during engine transients. During CMVT operation there is no requirement to change rotor speeds to change thrust which results in thrust response capabilities that are not possible with a fixed turbine engine.

2.2 Duct and Core Stream Augmentation

The duct stream augmentor typically is operational between intermediate and maximum power, and it is not operative during part-power engine operation. The range of operation is constrained from the minimum value of fuel-air ratio required to maintain stable combustion, up to one of three possible maximum limits. This is either a maximum mechanical limit on exhaust nozzle area, a maximum exhaust nozzle temperature for structural considerations, or a maximum fuel-air ratio to avoid stoichiometric conditions. In addition, a maximum limit on the duct augmentor inlet Mach number is imposed at minimum light-off fuel-air ratio to assure consistent light-off capability.

It is the purpose of the duct augmentor and nozzle control mode to not only maintain these operational limits, but also to provide smooth augmentor lights, fast continuous modulation, minimum disturbance to total engine airflow, minimum reduction in engine stability margin, good steady-state control accuracy, and safe gas generator operation in the event of blowout. Thrust response of

the duct augmentor must meet the time specifications of MIL-E-5007C. It is also desirable to obtain all of these objectives with a control mode of minimum complexity.

2.3 Engine Ratings

Four unique rating points can be identified for the variable cycle engine configuration shown in Figure 6. These are intermediate, breakpoint, idle, and maximum. Intermediate power is defined as the maximum power available without augmentation and without exceeding any engine operational limits. The intermediate rating schedules were established considering desired compressor and fan match points, maximum high-pressure turbine stator inlet temperature limit, and an inlet corrected airflow schedule typical for a fighter/bomber type aircraft application.

As noted previously, power can be reduced from intermediate while holding a constant match of the fan and compressor down to breakpoint power, which is the point at which the low-pressure turbine exit flow parameter reaches its maximum allowable value.

The idle rating point was varied as a function of aircraft Mach number for this study engine. At zero Mach number the idle point is set to be 6 percent of intermediate power. Idle was set at 10 percent of intermediate power for Mach numbers ranging between 0.3 and 1.0. For Mach numbers greater than 1.5, idle power was set equal to breakpoint power in order to prevent a decrease of airflow and subsequent inlet matching problems when decreasing power from intermediate to idle. Interpolation between the power settings of Mach numbers of 0.0 and 0.3, and Mach numbers of 1.0 and 1.5 provides the idle ratings for these ranges of Mach numbers.

The idle and intermediate rating points define two power settings which must be accurately scheduled by the engine control system as a function of the pilot power lever angle (PLA). However, this is not sufficient information to determine the complete shape of the control schedules. To provide ease of operation of the engine, it was found to be desirable to provide the breakpoint power setting at the same value of PLA for all flight conditions. Thus, the pilot is provided with a PLA setting above which he knows constant airflow can be maintained, and above which he can expect the engine response to be different. Finally, a requirement for an essentially linear relationship of thrust-versus-PLA between idle and breakpoint, and between breakpoint and intermediate was imposed.

The above constraints are sufficient for defining control schedules for a fixed-area turbine engine. For a variable-area turbine engine, however, these constraints can be met with a wide variety of turbine area settings between idle and breakpoint, and between breakpoint and intermediate power. Between break-

point and intermediate power, the requirement for constant match of the fan and compressor establishes the constraints on turbine area settings. Below breakpoint power, the establishment of the desired fan and compressor operating lines and the relationship between corrected rotor speeds provide the necessary constraints. These relationships might vary depending on the aircraft mission, and for this study the operating lines were established to minimize the variation of the turbine area settings between breakpoint and idle power.

With the addition of augmentation, the maximum rating point is obtained at either the maximum exhaust gas temperature, maximum exhaust nozzle area or maximum fuel-air ratio. A requirement for linearity of the thrust-versus-PLA relationships is imposed between minimum augmentation and maximum power.

2.4 Operational Limits

The operational limits of a variable cycle engine can be delineated into three categories: aerodynamic, thermodynamic, and mechanical or structural. Typical aerodynamic limits are choking of a nozzle, airflow separation along a compressor or turbine airfoil, maximum airflow, minimum augmentor inlet Mach number required for light-off, and compressor surge. The range of CMVT operation is limited by aerodynamic limits of the low turbine exit guide vane. For the low power end of the CMVT range, the low-pressure turbine exit flow parameter is limited to a maximum value determined from consideration of pressure loss and flow separation of the exit guide vane. For the high power end, a minimum limit of low-pressure turbine exit flow parameter can be correlated with blade stress limits and loss in turbine performance, resulting from efficiency and flow separation effects.

Thermodynamic limits include minimum burner fuel-air ratio required to maintain burning and maximum fuel-air ratio to avoid exceeding stoichiometric operation.

Mechanical and structural limitations include maximum rotor speeds, maximum burner case pressure, creep limits, maximum value of and rates of change of high-pressure turbine stator inlet temperature, maximum augmentor temperatures, and the entire set of control variable rate and amplitude limits.

All operational limits identified in these categories must be considered in the design of the control system. Some will affect control schedule requirements, others will affect control logic, and some will require individual control loops to guarantee avoidance of the limit. The impact of these limits on the control for this engine configuration will become more apparent in the discussion of the control schedules derived to meet the above requirements.

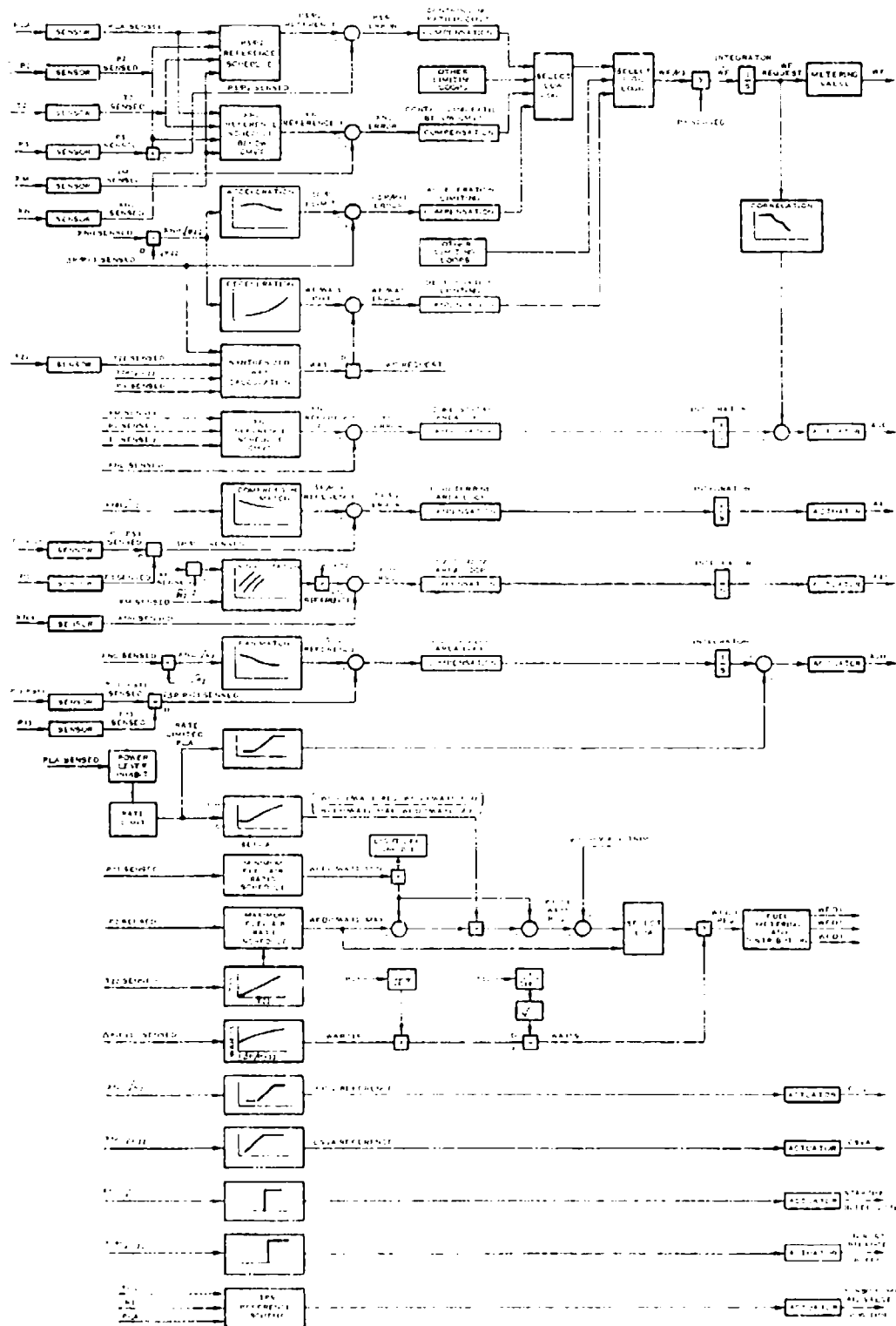
2.4.1 Basic Control Modes

A simplified mode logic block diagram shown in Figure 7 illustrates the basic control paths and the required input parameters.

Referring to the simplified logic block diagram, fan inlet guide vane angle (FIGV) and compressor stator vane angle (CSVA), are open-loop scheduled as a function of low and high rotor corrected speeds, respectively. With CSVA on schedule, high pressure turbine inlet area (A4) controls compressor discharge Mach number, which is characterized by the difference between total and static pressures divided by total pressure of the compressor discharge ($\Delta P/P_3$). Low turbine inlet area (A41) controls compressor corrected speed ($XNH/\sqrt{\theta_2}$) to set the match of the compressor. Similarly, with FIGV on schedule, core stream exhaust nozzle area (AJE) controls fan corrected speed ($XNL/\sqrt{\theta_2}$) and duct stream exhaust nozzle area (AJD) controls fan discharge Mach number, which is characterized by ($\Delta P/P_1$), to set the match of the fan during CMVT operation. The CMVT mode of operation maintains a constant airflow over a range of engine power settings. Gas generator fuel flow (WF) then controls engine pressure ratio (P5/P2 or EPR) to set power. A correlation schedule between the WFE and AJE loops provides rough scheduling of AJE to eliminate detrimental interaction between these two loops during rapid transients. Below breakpoint of CMVT operation, a loop transition is made so that WF controls low rotor speed to set power and AJE is held constant. A4 now maintains the desired compressor operating line and A41 maintains the desired relationship between low and high rotor corrected speeds.

This loop transition is accomplished with the first "Select Low Logic" block in the WF control loop. Below breakpoint power, engine pressure ratio reference (P5/P2 Reference) is scheduled to remain at the breakpoint value while low rotor speed reference (XNL Reference) is scheduled to decrease as a function of power lever angle (PLA) to correspond to part power operation. Thus, in the range below breakpoint power the compensated engine pressure ratio error (P5/P2 error) will always be a large positive number relative to the compensated low rotor speed error (XNL error) for steady state operation, and the XNL error path will be selected by the logic as the controlling error. Conversely, above breakpoint power, the low rotor speed schedule is raised up out of the way so that the engine pressure ratio path will be selected.

In addition to the variable geometry and fuel flow loops, the VCE gas generator control also includes logic for starting bleed and thrust balance bleed for safe engine control. The starting bleed is opened at starting conditions for stability accommodation and is closed at high power conditions to provide optimum compressor operation. The thrust balance bleed is used to change engine internal compartment pressure and maintain rotor thrust bearing load within allowable limits from startup to maximum power. Control logic for the



E-6160

FIGURE 7 SIMPLIFIED BLOCK DIAGRAM OF CONTROL MODE

augmentor turbopump was developed under this contract and is included in the gas generator control mode to ensure adequate hydraulic pressure for the engine actuation systems and duct augmentation fuel flow during operation of the duct heater.

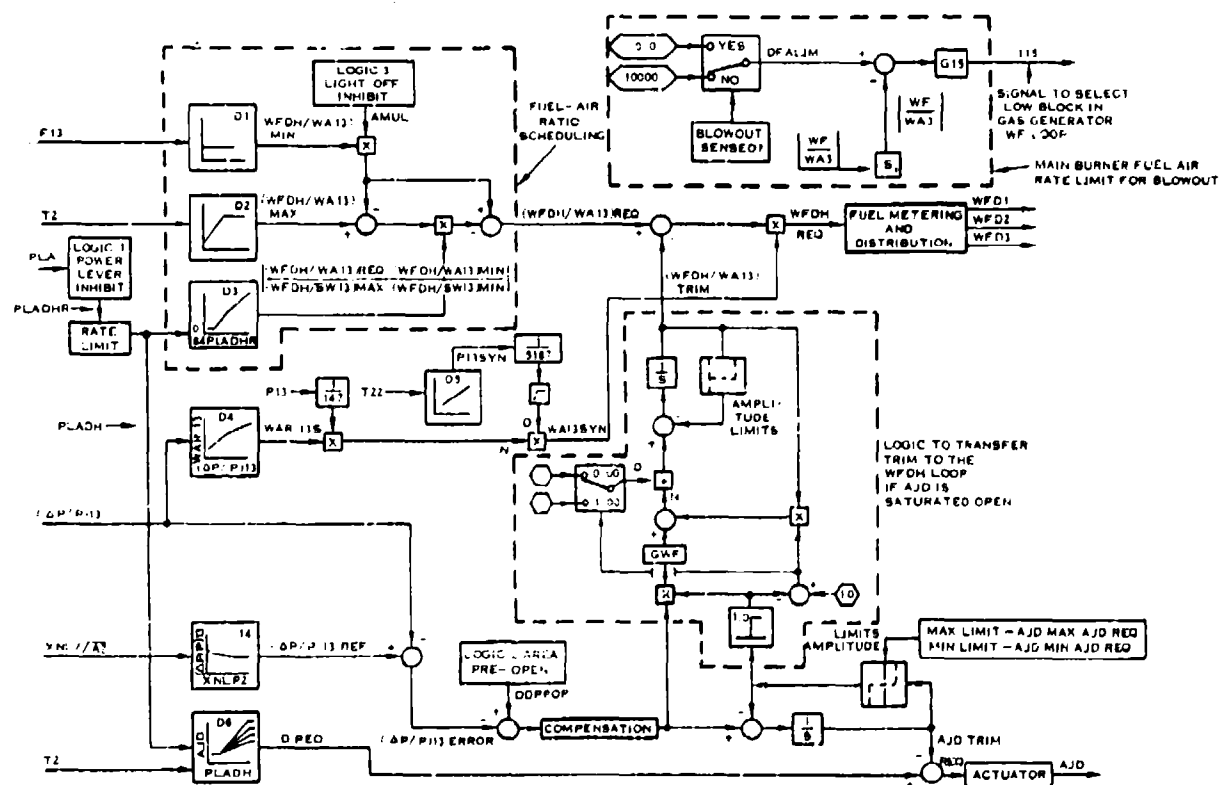
2.4.2 Augmentation Control Mode

The block diagram of the augmentation control mode is presented in Figure 8. A description of the sequence of events which occurs during a power excursion from intermediate to maximum follows.

As PLA is advanced above the intermediate power setting of 81 degrees, inhibit logic (LOGIC1) prevents the PLA signal to the duct augmentor control logic (PLADH) from increasing above 84 degrees until the engine is up to speed and the light-off detector (LOD) confirms light-off has occurred. Prior to the light-off, the duct nozzle is pre-opened (LOGIC2) by increasing the scheduled value of $(\Delta P/P)$ 13, thereby increasing fan surge margin to compensate for the duct pressure fluctuation, or "lighting spike", which occurs during light-off.

The quick-fill logic proceeds to slew the first segment metering valve to maximum travel and commands maximum pump capacity to maximize metering valve response characteristics and to fill the manifold as quickly as possible. The control monitors metering valve position feedback and uses the information along with stored dynamic characteristics for the system to predict the point in time where the metering valve must reduce flow in order to arrive at the scheduled light-off fuel flow without underfilling or overfilling the manifold. After establishing light-off, PLADH is released and ramps up to the requested PLA value. A similar sequence of events occurs on the subsequent segments which are timed approximately to ensure obtaining maximum thrust within 2 seconds (MIL-E-5007D requirement) after initiation of an intermediate-to-maximum PLA step.

During the transient, rough correlation between AJD and WFDH/WA13 is provided by the steady-state schedules versus PLADH. As noted above, the AJD trim integrator acts to maintain accurate control of $(\Delta P/P)$ 13. If the duct exhaust nozzle area should saturate wide open, either during transient or steady-state operation before the $(\Delta P/P)$ 13 error is reduced to zero, a further increase in WFDH/WA13 would cause an oversuppression of the fan. This is due to the decrease of effective area as exhaust temperature is increased with a constant flow area. To preclude transient fan surge or steady-state off-design operation of the fan, the integral trim action is transferred, by the logic shown in Figure 8, to the fuel-air path to decrease fuel-air as necessary in the event the area saturates open.



E 3463

FIGURE 8 VARIABLE CYCLE ENGINE CONTROL MODE- DUCT STREAM AUGMENTOR CONTROL BLOCK DIAGRAM

SECTION III CONTROLLER PRELIMINARY DESIGN

3.1 Introduction

The final RAEEC system design presented in this section is developed through a series of trade studies and analyses from a baseline system defined, essentially, by the U.S. Navy-sponsored FADEC program. Primary areas of concern in this study are requirements for improved reliability, maintainability and safety. Emphasis has been placed on Redundancy Management, coverage, and on self diagnostics and testing. A reliability analysis for both the baseline and final systems is presented as well as a flight safety model for the final system.

A detailed circuit level analysis of the RAEEC system is made here. Considerable effort has been devoted to presenting the alternatives examined for implementation of the various subsystems in the control. Based upon a concise matrix trade summary, a power/area/reliability sensitivity study is presented and a final RAEEC system design derived.

Finally, a thorough description of the mechanical design aspects of the control is given. Improvements over the baseline configuration are delineated, with primary emphasis placed upon the implementation of the control's modular construction to satisfy reliability and maintainability requirements. Of specific concern here, is the ability of the control package and contents to operate reliably in the projected thermal, vibratory, and acoustic environment to be encountered during actual service.

3.2 System Description

3.2.1 RAEEC Baseline System

The RAEEC baseline electronic unit provides all of the sensor signal conditioning, computation, and output signal processing functions necessary for controlling the variable cycle engine configuration as described in Section II. A simplified block diagram shown in Figure 9 illustrates the baseline control. The control unit employs two digital processors, redundant input and output circuitry, and two power supplies organized into primary and secondary controllers to provide secondary control capability.

The control loop computations, synthesizations, self-testing, and types of inputs and outputs processed within the primary and secondary portions of the electronic unit are listed in Table 3.

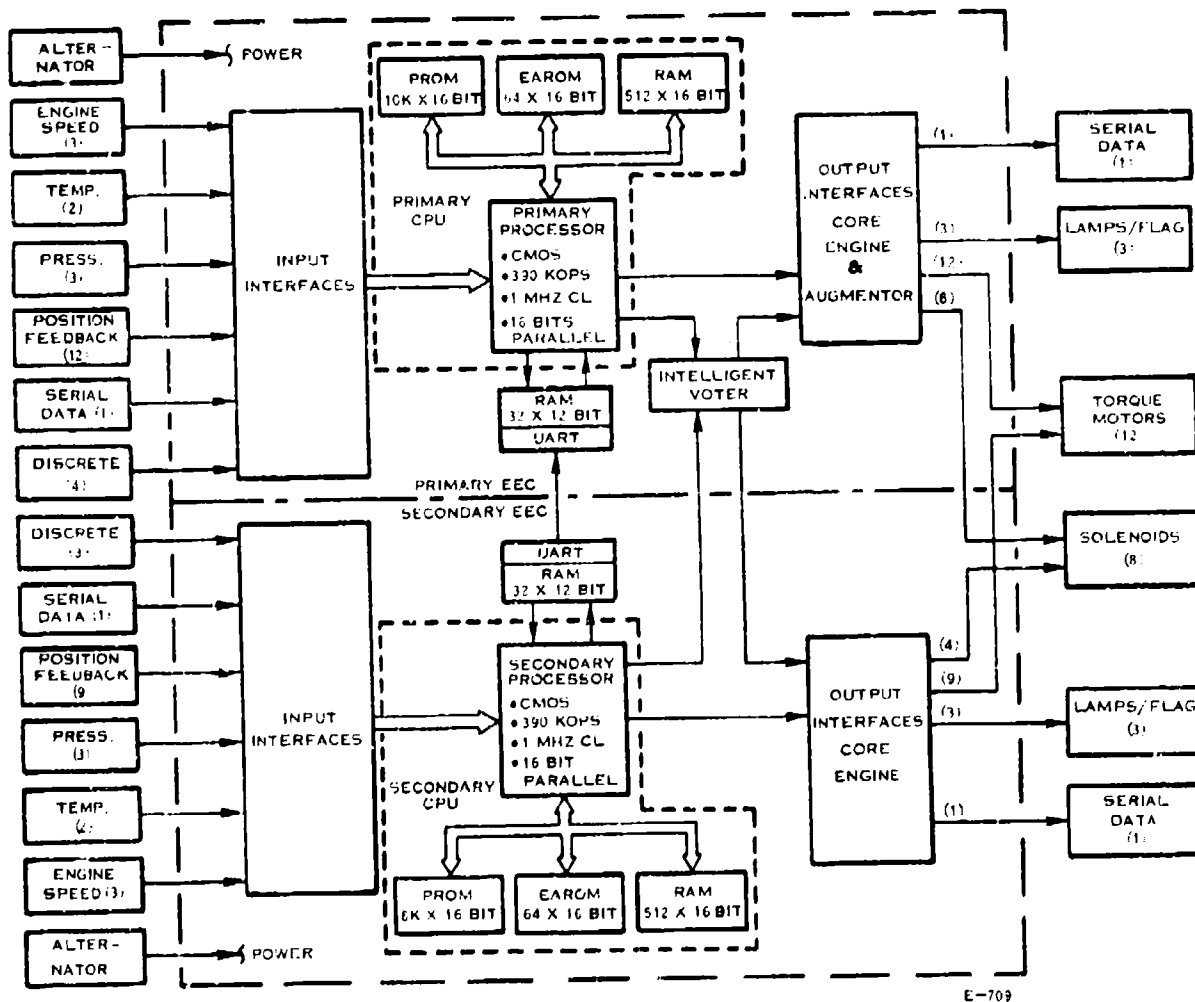


FIGURE 9 RAECC BASELINE SYSTEM SIMPLIFIED BLOCK DIAGRAM

TABLE 3 RAEC BASELINE SYSTEM DEFINITION

FUNCTION	PARAMETER	DEFINITION	NUMBER INCLUDED IN:	
			PRIMARY (1)	SECONDARY (1)
Power Supply	Alternator	Supplied From Dedicated Alternator Windings		
Input Signal Processing:	Engine Speed:	---	(3)	(3)
	TPS	Turbo Pump Speed	1	1
	NH	High Rotor Speed	1	1
	NL	Low Rotor Speed	1	1
	Temperature:	---	(2)	(2)
	T12	Fan Inlet Total Temp.	1	0
	T8T	Turbine Blade Temp.	1	1
	T22	Compressor Inlet Total Temp.	0	1
	Pressure:	---	(3)	(3)
	PT2	Fan Inlet Total Pressure	1	0
	PT3	Compressor Discharge Total Pressure	1	0
	$\Delta P13$	Fan Discharge Differential Pressure	1	0
	PT5	Low Pressure Turbine Discharge Total Pressure	0	1
	PT13	Fan Discharge Total Pressure	0	1
	$\Delta P3$	Compressor Discharge Differential Pressure	0	1
	Position:	---	(12)	(9)
	PLA	Power Lever Angle	1	1
	FIG V	Fan Inlet Guide Vane	1	1
	CSVA	Compressor Stator Vane Actuator	1	1
	A4	High Pressure Turbine Inlet Area	1	1
	A41	Low Pressure Turbine Inlet Area	1	1
	AJE	Core Stream Exhaust Nozzle Area	1	1
	AJD	Duct Stream Exhaust Nozzle Area	1	1
	WFEP	Gas Generator Primary Fuel Flow	1	1
	WFES	G.G. Secondary Fuel Flow	1	1
For Core Engine Control				

TABLE 3 RAECC BASELINE SYSTEM DEFINITION (Continued)

FUNCTION	PARAMETER	DEFINITION	NUMBER INCLUDED IN: PRIMARY	SECONDARY
For Augmentor Control	WFD1	Duct Augmentor Fuel Flow to Zone 1	1	0
	WFD2	Duct Augmentor Fuel Flow to Zone 2	1	0
	WFD3	Duct Augmentor Fuel Flow to Zone 3	1	0
For Core Engine Control	<u>Serial Digital Data Stream:</u>	---	(1)	(1)
	<u>Includes:</u>	---	---	---
	Air Inlet Control	---	---	---
	Flt. Control	---	---	---
	ECM	---	---	---
	Mission Computer	---	---	---
	<u>Discrete:</u>	---	(4)	(3)
	R.F.	Rocket Fire	1	1
	W.O.W.	Weight On Wheels	1	0
	Primary Enable	Pilot Switch Enables/Disables Primary EEC	0	1
For Augmentor Control	Secondary Enable	Pilot Switch Enables/Disables Secondary EEC	1	0
	LOD	Augmentor Light Off Detector	1	0
Output Drive:	<u>Torque Motor:</u>	---	(12)	(9)
For Core Engine Control	TPS	Turbo Pump Speed Control	1	1
	FIG V	Same as For Position	1	1
	CSVA	Same as For Position	1	1
	A4	Same as For Position	1	1
	A41	Same as For Position	1	1
	AJE	Same as For Position	1	1
	AJD	Same as For Position	1	1
	WFEP	Same as For Position	1	1
	WFES	Same as For Position	1	1

TABLE 3 RAECC BASELINE SYSTEM DEFINITION (Continued)

FUNCTION	PARAMETER	DEFINITION	NUMBER PRIMARY	NUMBER INCLUDED IN: PRIMARY SECONDARY
For Augmentor Control	WFD1	Same as For Position	1	0
	WFD2	Same as For Position	1	0
	WFD3	Same as For Position	1	0
For Core Engine Control	Solenoid:	---	(8)	(4)
	Start Bleed	---	1	1
	Staging	---	1	1
For Augmentor Control	Thrust Balance Bleed	---	1	1
	WFEP	Gas Gen. Primary Fuel Flow Shutoff Valve	1	0
	WFD1	Duct Zone 1 Fuel Flow Shutoff Valve	1	0
For Augmentor Control	WFD2	Duct Zone 2 Fuel Flow Shutoff Valve	1	0
	WFD3	Duct Zone 3 Fuel Flow Shutoff Valve	1	0
For Augmentor Ignitor Relay Lamps/Flags	Primary On	---	1	0
	Secondary On	---	(3)	(3)
	Primary Fault Flag (Latched)	Cockpit Lamp Indicates Primary EEC Enabled	1	0
For Annunciation	Secondary Fault Flag (Latched)	Cockpit Lamp Indicates Secondary EEC Enabled	0	1
	NOCs Fault Flag (Latched)	LRU Flag Indicates Primary EEC Fault	1	0
	Serial Digital Data Stream	LRU Flag Indicates Secondary EEC Fault	0	1
For Data Output	Same as For Input	Non-Operational Control System Fault Flag Located on ASP	1	1
		---	(1)	(1)

TABLE 3 RAECC BASELINE SYSTEM DEFINITION (Continued)

FUNCTION	PARAMETER	DEFINITION	INCLUDED IN:	
			PRIMARY	SECONDARY
Digital Data Processing	CPU	Central Processor Unit Implements EEC Channel Program	1	1
Control Loop Computation: For Core Engine Control	---	---	---	---
	WFEP & WFES	Gas Generator Primary and Secondary Fuel Flows	Yes	Yes
	AJE	Core Stream Exhaust Nozzle Area	Yes	Yes
	A4	High Pressure Turbine Inlet Area	Yes	Yes
	A41	Low Pressure Turbine Inlet Area	Yes	Yes
	AJD	Duct Stream Exhaust Nozzle Area	Yes	Yes
	FIG V	Fan Inlet Guide Vane Position	Yes	Yes
	CSVA	Compressor Stator Vane Actuator Position	Yes	Yes
	Start Bleed	Starting Bleed On/Off	Yes	Yes
	Thrust Balance	Thrust Balance Bleed On/Off	Yes	Yes
For Augmentor Control	TPS	Turbo Pump Speed Control	Yes	Yes
	WFD1, WFD2, & WFD3	Duct Augmentor Fuel Flows	Yes	NC
Synthesization* (See Figure 1C For Curves Used in Synthesizing Parameters)	NH	High Rotor Speed Synthesized From Curves 3, or 6	Yes	Yes
	TB1	Turbine Blade Temp Synthesized From Curve 3	Yes	Yes
	T22	Compressor Inlet Total Temp. Synthesized From Curve 1	Yes	Yes
	PT2	Fan Inlet Total Pressure Synthesized From Curves 2, or 4	Yes	Yes
	PT3	Compressor Discharge Total Pressure Synthesized From Curves 4, or 6	Yes	Yes

TABLE 3 RAECC BASELINE SYSTEM DEFINITION (Continued)

FUNCTION	PARAMETER	DEFINITION	INCLUDED IN:		
			PRIMARY	SECONDARY	
Synthesization (Continued)	PT13	Fan Discharge Total Pressure Synthesized From Curves 2, or 6	Yes	Yes	
	$\Delta P3$	Compressor Discharge Differen- tial Pressure Synthesized From Curve 5 Using Curves 7 and 8	Yes	Yes	
FUNCTION	PARAMETER	IN-FLY PRE-FLT TEST TEST	IMPLEMENTED BY:	INCLUDED IN:	
				PRIMARY	SECONDARY
Self Test	1: Input Range Limit Check	Yes	Yes	Software	Yes
	2: Parameter Correlation Check	Yes	Yes	Software	Yes
	3: Parameter Majority Logic Check	Yes	Yes	Software	Yes
	4: Read Only Memory Check	Yes	Yes	Software	Yes
	5: Computer Cycle Time Test	Yes	Yes	Hardware	Yes
	6: Output Wraparound Test	Yes	Yes	Hardware & Software	Yes
	7: Injected Input Test	No	Yes	Software	Yes
	8: Canned Output Computation	No	Yes	Software	Yes
	9: Loop Dynamic Check	Yes	Yes	Software	Yes
	10: Reference Signal Check	Yes	Yes	Hardware & Software	Yes
	11: Power Supply Test	Yes	Yes	Hardware	Yes
	12: Processor Instruction Test	Yes	Yes	Software	Yes
	13: Scratch Pad Memory Check	Yes	Yes	Software	Yes
	14: EOC Bit Not Detected	Yes	Yes	Software	Yes
	15: Hardware Parity & Code Verifier Checks	Yes	Yes	Hardware	Yes
	16: Clock Loss Detect Circuit	Yes	Yes	Hardware	Yes
	17: UART Sync Word Detected	Yes	Yes	Hardware	Yes

TABLE 3 RAEEC BASELINE SYSTEM DEFINITION (Continued)

FUNCTION	PARAMETER	DEFINITION	INCLUDED IN: PRIMARY	SECONDARY
Cross Talk	UART/Dual Port RAM	Universal Asynchronous Receiver Transmitter Combined With Dual Port RAM Provides Data Link Between Primary And Secondary CPU's For The Interchange of Input, Output, Parameter Synthesis, And Fault Data.	Yes	Yes
EEC Channel Switchover	Intelligent Voter	Provides Hard-wired Backup For UART/Dual Port RAM. Uses a preprogrammed PROM to select, on the basis of Fault Discretes received from both channels, The "Best Health" EEC. The other EEC is automatically disabled.		

Inputs are fed into each CPU via time multiplexed analog-to-digital converters (A/D), resolver to digital converters (R/D) and digital pulse counters. All of these interfaces are read into the CPU on a 3-state input/output (I/O) bus. CPU inputs are received as parallel 16-bit words.

Output signals for the Processor are handled similarly, with commands being sent out serially via the I/O bus to the digital-to-analog converters (D/A). The D/A's convert the digital word to a voltage level proportional to the magnitude of the command, providing control of the output drivers which power the effectors.

The flag outputs provide a means of communicating to ground personnel system fault conditions, as well as providing information as to which system, the primary or secondary is not operational.

The digital processor used in the primary portion of the control is duplicated in the secondary portion. The processor is capable of the following performance:

- 16 bit full parallel operation
- 2.0 microsecond addition time
- 12.0 microsecond multiply time
- 87 instruction repertoire
- 390,000 operations per second through-put
- 1.0 Megahertz clock rate

The primary processor services the following memory subsystems:

- 10K - 16 bit words of Programmable Read Only Memory (PROM)
- 384 - 16 bit words of Random Access Memory (RAM)
- 64 - 16 bit words of CPU - Alterable RAM

The secondary processor services the same complement of Random Access Memory but only 8K words of PROM, due to the elimination of augmentation fuel control logic in the backup mode.

3.2.2 Secondary Control Provisions, Self Test and Diagnostic System

The electronic secondary approach selected for the RAEEC baseline system employs dual path redundancy to provide a highly fault tolerant, nearly fail operational/failsafe, "self healing" system concept. A simplified schematic of this concept is illustrated in Figure 9. As shown in Figure 9, the electronic unit is organized into separate primary and secondary systems, each incorporating a digital processor and complement of input and output circuitry. Together they are able to provide full authority digital electronic control of all engine and augmentor functions and secondary control for gas generator functions through redundant circuit paths and alternate control modes. Self test and fault detection features are included to implement corrective action in the event of failures within the unit, external sensors or output devices (Table 3). The six pressure sensors required for control of the VCE are housed within the unit and are divided between the primary and secondary systems such that loss of either processor can be tolerated without jeopardizing safe engine operation.

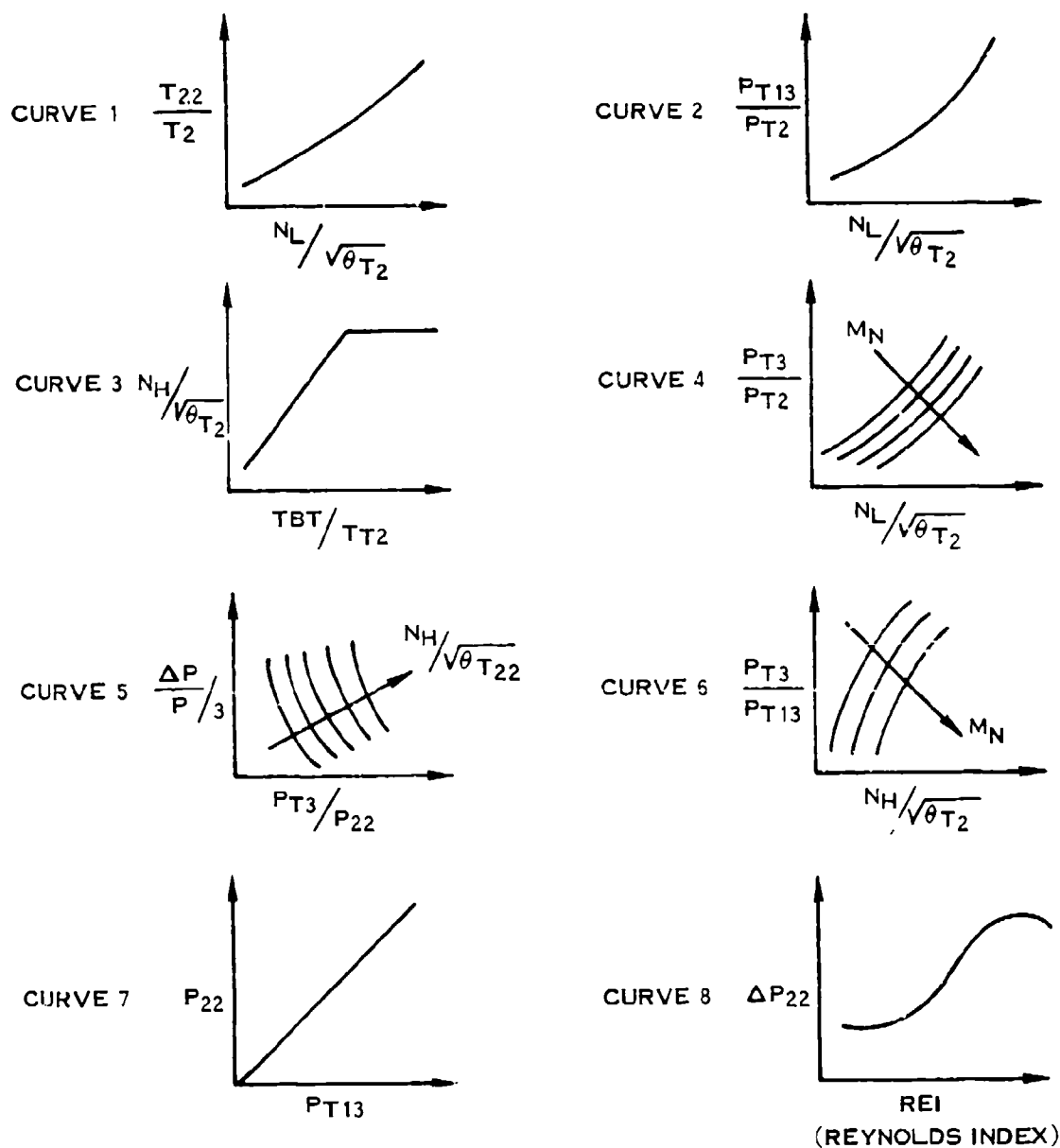
The primary and secondary processors communicate with each other in real time through a dual port RAM. Because of this communication capability, any failure of one system input parameter may be accommodated since the same parameter is available through interrogation of the other system with its redundant sensors.

Pressure inputs are nonredundant; however, four of the six pressure inputs can be synthesized by software from curves stored in the CPU PROMs. These synthesis curves are given in Figure 10, and are derived from the VCE model for engine response. These curves also provide for engine speed and temperature parameter synthesis as well as for pressure.

Synthesized parameters are somewhat less accurate than sensed parameters; however, their accuracy is sufficiently good to permit comparison checking with sensed parameters. The inclusion of parameter synthesis in both primary and secondary channels enables majority logic checks on those parameters for input sensor failure.

If a pressure sensor failure is detected by this means, the value of the synthesized parameter can replace the failed pressure sensor input in control loop calculations with some loss in engine performance; however, the pilot is still able to safely abort the mission. The failed sensor, of course, must be replaced before the start of the next mission.

In addition to the communication path provided by the dual port RAM, four discretes are transmitted from the primary to the secondary and vice versa. These discretes provide a hardwired backup information interchange system in the event that the previously described RAM communication is disabled. These four



NOTE:

FAIL 1 => CURVE 1

FAIL 2 => CURVE 2

ETC.

E-5656

FIGURE 10 FAILURE MODE SYNTHESIZATION CURVES

discretes provide multiple states of fault information to the other processor so that individual output loop switchover can take place under a multi-fault condition. Since each system is capable of providing all the engine control functions, with the exception of augmentation in the secondary system, it is desirable that the decision of which system is in control at a given time be validated by a third intelligence, or voter. A hardwired logic approach was utilized since a third processor would be a costly solution. This circuitry receives input signals, or discretes, from each of the two controls, and, based on a pre-defined state table, makes a decision as to which control is in the best health and should, therefore, be placed in command.

Note that provision is made not only for the capability to switch one system in to replace the other in the event of major malfunction, but individual output loops may also be switched in and out in the event of less significant malfunctions. Maximum flexibility is thus provided in response to any malfunction situation.

Information available for diagnostic system usage will consist of serial digital data, discrete type data and internal storage by means of EAROM (Electrically Alterable Read Only Memory) devices that are part of the EEC.

Serial digital data can be transmitted to any data retrieval system (such as the aircraft's mission computer) for any failure that occurs in the fuel control system and that is detectable by the EEC BIT (Built-in Test) system, i.e., input and outputs that are part of the EEC control loops, including the EEC itself. The EEC system has the capability to communicate with any other on-board system such as the Engine Condition Monitoring unit which could analyze all EEC generated data for trend or fault analysis.

EAROM devices, located in the EEC control, will be used to store any system malfunctions for later retrieval, either at the ground level by maintenance personnel or through post-flight checks made by an aircraft's mission computer. Maintenance personnel would be alerted through the pilot's log, reporting any cockpit information faults generated and subsequent observation of EEC fault flags or from a central mission computer that continually interrogates the EEC status.

One feature of the EAROM fault identification system is the detection and isolation of intermittent faults to the circuit level to assist maintenance personnel in fault diagnostics.

3.2.3 Self Test

-Automatic reversion to secondary control paths requires the ability to determine that a failure has occurred in a primary path. The RAEEC baseline provides self test techniques which detect failures and switches the control unit to an alternate control path allowing fail operational performance. A summary of the tests performed within the RAEEC baseline unit is shown in Table 3. As indicated in this Table, some of the tests are performed only during pre-flight ground check while the remainder are performed in flight as well. The pre-flight ground check is initiated by a command from the mission computer, with ground check continuing until signaled by the mission computer to enter the flight mode of control. The in-flight tests are performed on a continuous basis, independent of any externally generated command signals. A detailed description of each test listed in Table 3 follows.

3.2.3.1 Input Range Limit Test

The range limit test is a software BIT for detecting a failed computer input signal caused by a failure in the sensor, interconnecting cable, or input interface circuit. The range limit test is sensitive only to failures (open or short) which produce hardover signals. The range test program compares each input signal level with its normal operating range limits. Failure is indicated when the signal level exceeds its maximum or minimum limits for a given number of consecutive program cycles. The range limit test program also generates a digital failure status word indicating an input signal failure, however, it cannot identify the Line Replaceable Unit (LRU) in which the failure occurred, and can only indicate that the failure occurred somewhere in the system. The control system is switched to a redundant input signal.

3.2.3.2 Parameter Correlation Check

The parameter correlation check compares redundant parameter data words to determine if their difference in value falls within outside accuracy bounds. "Failure" in one of the two parameters is indicated when the accuracy bounds are exceeded for a given number of consecutive program cycles. However, the failed parameter channel is not isolated by this test alone. The redundant parameter data may be generated by hardware or by software synthesis.

3.2.3.3 Parameter Majority Logic Check

This is a comparison of triple redundant parameter data words to determine if their differences in value fall within outside accuracy bounds. Failure in one of the three parameters is indicated by excessive error between its value and that of the other two good parameters for a given number of consecutive program cycles. The error between the values for the two good parameter channels is, of course, within parameter accuracy limits. The failed parameter channel is

thereby identified by this test which generates a digital failure status word indicating the failed parameter channel; however, it cannot identify the LRU in which the failure occurred, and can only indicate the failure occurred somewhere in the system. The redundant parameter data may be generated either by hardware or by software synthesis. When failure is detected, the control is switched to a redundant input channel.

3.2.3.4 Read Only Memory (ROM) Check

The memory sum test is a software BIT for detecting a failed ROM. The test program sums each ROM location, and the sum total must equal a preset value for validity. An incorrect sum causes the program to recycle on the test thereby triggering a cycle time test failure. The memory sum test program also generates a digital failure status word indicating a ROM failure occurring in the ECU. The control system is switched to the backup control.

3.2.3.5 Computer Cycle Time Test

Computer cycle time is a hardware BIT for detecting a hung program. This test requires the completion of each program cycle within a maximum allowable time. A computer power on reset (POR) results when program cycle time exceeds the timing limit. The POR signal reinitializes the program once and also generates a digital failure status word indicating a hung program failure occurring in the ECU. The control system is switched to the secondary control when the test is failed on the next cycle.

3.2.3.6 Output Wraparound Test

Torque motor/solenoid outputs are electrically fed back as inputs to the processor for a check by the software to detect output D/A and torque motor/solenoid drive circuit failures. Resultant action would be to indicate an ECU failure and to switch control to a redundant output channel.

3.2.3.7 Injected Input Test

This is a pre-flight control test which is carried out on the ECU after engine start but prior to take off. The test is carried out under the control of the flight computer which exercises all of the ECU functions. Failure of the ECU to properly carry out each function is detected by the flight computer. Resultant action would be to indicate an LRU failure which must be repaired by an unscheduled "on line" service before the mission is dispatched.

3.2.3.8 Canned Output Computation

This is also a pre-flight control test except that the flight computer exercises the actuator loops. Failure of an actuator loop to respond within specifications to programmed commands is detected by the flight computer. Resultant action would be to indicate a system failure which must be repaired by unscheduled "on line" service before the mission is dispatched.

3.2.3.9 Loop Dynamic Check

The control loop error (command value minus measured value) is compared against programmed limits. Failure is indicated when the measured error exceeds the programmed error for a given number of consecutive program cycles. The loop dynamic check generates a digital failure status word indicating a failure in the control loop, but cannot alone identify in which LRU the failure occurred. When combined with the parameter correlation check, the two tests can isolate the failure to either the primary or backup ECU, or to the actuator.

3.2.3.10 Reference Signal Check

Input signals are supplied to multiplexer channels at preset levels, converted into digital data words, and transmitted to the CPU. In the CPU they are compared to reference levels stored in the memory. Failure is indicated when the reference signal data word exceeds the stored references for a given number of program cycles. The reference signal test program generates a digital failure status word indicating an input channel failure occurring in the ECU, and switches controls to a redundant input channel.

3.2.3.11 Power Supply Test

The purpose of this test is to monitor the supplies for in-tolerance operation. The power supply test is a hardware BIT in which positive and negative voltages are continuously compared with reference voltage levels. A failure signal is triggered when any supply voltage exceeds its preset tolerances. A failure signal generates a digital failure status word indicating power supply failure occurring in the ECU. The control system is automatically switched to the secondary control.

3.2.3.12 Processor Instruction Test

The processor instruction test is a software BIT for detecting a failed processor hardware instruction. The instruction test program operates on each instruction with a preset data word. It compares the data word at the end of the test with the preset data word. An incorrect answer causes the program

to recycle on test, thereby triggering a cycle time test failure. The instruction test program also generates a digital failure status word indicating an instruction failure occurring in the ECU. The control system is switched to the secondary control.

3.2.3.13 Read/Write (Scratch Pad) Memory Check

The scratch pad test is a software BIT for detecting a failed read/write memory. The scratch pad test program operates on each read/write memory location with a preset data word. The data word is entered into the read/write memory location and then read out. The output data word is then compared with the preset data word. An incorrect answer causes the program to recycle on test triggering a cycle time test failure. The scratch pad test program also generates a digital failure status word indicating a read/write memory failure occurring in the ECU. The control system is switched to the secondary control.

3.2.3.14 End of Conversion (EOC) BIT Not Detected

Failure of any digital converter to provide the processor with an EOC BIT after a preset time period following the start of data conversion indicates a hang-up and therefore, failed digital converter. The EOC test program generates a digital failure status word indicating which converter failed in the ECU, and switching the control to a redundant converter.

3.2.3.15 Hardware Parity and Code Verifier Checks

This is an automatic hardware test for detecting failure in the Serial Digital Data Transmission Link.

3.2.3.16 Clock Loss Detect Circuit

This is a hardware test which automatically detects failure in either of the redundant clock oscillators provided for the processor by comparing their cycle time period with the timing period of a one shot multivibrator. Failure of either oscillator generates a digital failure status word indicating a clock failure occurring in the ECU. The control switch is to the "good" clock for processor timing.

3.2.3.17 UART Sync Word Detected

This is an automatic hardware test of the UART cross talk channel providing communication between the primary and backup CPU. If the UART sync word is not detected by the receiving channel within a preset maximum time from the start of data transmission, a digital failure status word is generated indicating failure of the UART channel in the ECU and flagging a maintenance alert.

3.2.4 RAEEC Final System

3.2.4.1 Limitations of The Baseline System

The Advanced Full Authority Digital Electronic Control (FADEC) design study provided the baseline system for the RAEEC program. The design goal of FADEC was to implement the VCE control modes delineated in Section II in the VCE environment defined in Section IV, while providing high mission reliability. This goal is achieved by providing electrically independent primary and secondary channels with the primary fully functional, while the secondary provides backup for "major" functions whose loss can result in engine shutdown. Electronic functions required for Core Engine Control are classified "major" since the loss of Core Engine Control requires the pilot to shutdown the engine. All others are "minor" since their loss affects engine performance, but does not require shutdown. Electronic functions required for Augmentor Control only are classified "minor" since the loss of Augmentation limits the pilot to intermediate power, but allows him to safely abort the mission. For this reason, the FADEC (baseline) system secondary channel provides backup only for core engine control.

The FADEC ground rule for fault alerts is to flag every failure regardless of its effect on system performance and safety, i.e., FADEC does not permit deferred maintenance when failures occur.

The flagging of every failure in a system as complex as FADEC results in maintenance MTBF calculated as low as 3039 hrs (Section 3.3). FADEC achieves high mission reliability at the cost of frequent repairs which reduces availability.

The objective of the RAEEC program is to achieve 25,000 hrs maintenance MTBF while meeting all FADEC design goals including high mission reliability. At present, it is not feasible to meet such a stringent requirement by improvements in device reliability alone (i.e., single channel reliability). Redundancy Management (RM) techniques, as discussed in Section 3.3, must also be employed in the RAEEC program to extend maintenance MTBF. The FADEC ground rule, requiring every failure to be flagged, is incompatible with the application of RM techniques for the improvement of maintenance reliability. The FINAL RAEEC system, therefore, employs ground rules for flagging fault alerts which differ from FADEC by permitting deferred maintenance for failures providing they meet the following conditions:

- a) The failure must not cause any loss or curtailment of system performance.

- b) Mission reliability following the occurrence of the failure must not be any less than that of the FADEC (which is also the RAEEC baseline) system, i.e., a second like failure must not result in engine shutdown.

The application of RAEEC groundrules for flagging fault alerts to the baseline system described in Section 3.2.1 yields only an insignificant improvement in maintenance MTBF. This is because all major electronic functions are limited to dual redundancy while most minor functions are nonredundant. These limitations reflect the design goals of the FADEC system which is used as the baseline for the RAEEC program. An evaluation of Table 6 indicates that the only major function that need not be flagged for a first failure is N_H because parameter synthesization is available for this input as well as dual redundant sensors.

Similarly, several minor functions require no first failure alerts because they are inputs provided with dual redundant sensors. This analysis, therefore, suggests that effective use of RM technique for enhancing the maintenance reliability of the FINAL RAEEC system requires triple redundancy for major functions, and dual redundancy for minor functions. Parameter synthesis, where available, can be included as one of the redundant elements (except in the case of TBT).

3.2.4.2 RAEEC System Design Improvements

The application of RM techniques to enhance maintenance reliability provides the major impetus for the RAEEC final system design. Also significantly impacting system design is the application of "in-production" LSI devices (such as microcomputers) capable of generating higher electronic functions on a single chip, and the use of signaling modes such as "Pulse Width Modulation" (PWM) for output control. Both techniques substantially improve EEC reliability by reducing the number of circuit components, circuit complexity, and power dissipation.

Utilization of the above techniques for improving maintenance reliability requires substantial changes in system configuration partitioning, and CPU architecture. These changes are reflected in the simplified block diagram for the RAEEC final system shown in Figure 11, and in the RAEEC final system definition given in Table 4. Section 3.4 provides a detailed description of the RAEEC final system electrical design.

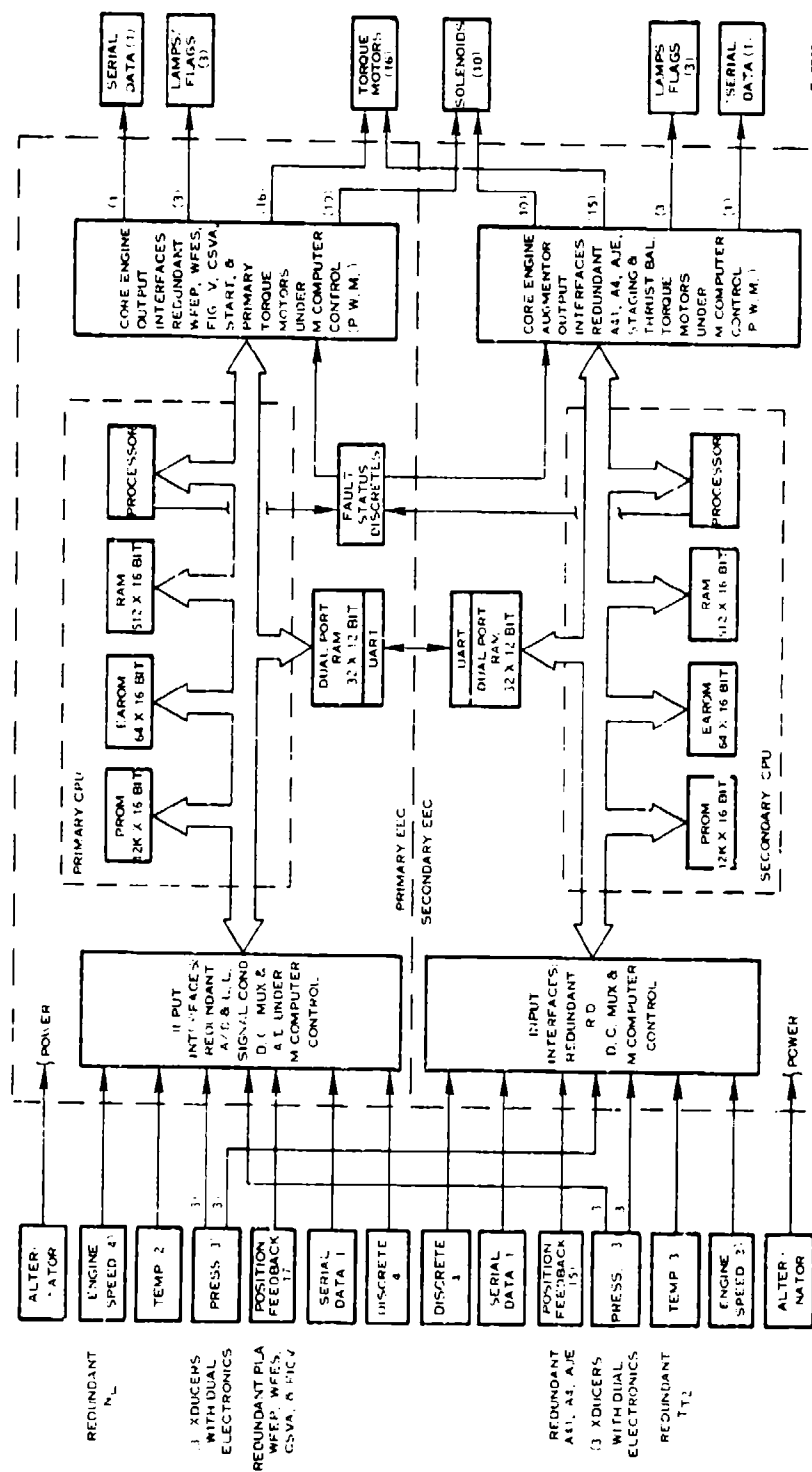


FIGURE 11 RAEEC FINAL SYSTEM SIMPLIFIED BLOCK DIAGRAM

TABLE 4 RAECC FINAL SYSTEM DEFINITION (Continued)

FUNCTION	PARAMETER	DEFINITION	NUMBER INCLUDED IN: PRIMARY	SECONDARY
For Augmentor Control	WFD1	Duct Augmentor Fuel Flow to Zone 1	1	1
	WFD2	Duct Augmentor Fuel Flow to Zone 2	1	1
	WFD3	Duct Augmentor Fuel Flow to Zone 3	1	1
For Core Engine Control	Serial Digital Data Stream Includes:	---	(1)	(1)
	Air Inlet Control	---	---	---
	Flt. Control	---	---	---
	ECM	---	---	---
	Mission Computer	---	---	---
	Discrete:	---	(4)	(4)
	R.F.	Rocket Fire	1	1
	W.O.W.	Weight On Wheels	1	0
	Primary Enable	Pilot Switch Enables/Disables Primary EEC	0	1
	Secondary Enable	Pilot Switch Enables/Disables Secondary EEC	1	1
For Augmentor Control	L0D	Augmentor Light Off Detector	1	1
Output Drive:	Torque Motor:	---	(16)	(15)
For Core Engine Control	TPS	Turbo Pump Speed Control	1	1
	FIG V	Same as For Position	2	1
	CSVA	Same as For Position	2	1
	A4	Same as For Position	1	2
	A41	Same as For Position	1	2
	AJE	Same as For Position	1	2
	AJD	Same as For Position	1	1
	WFEP	Same as For Position	2	1
	WFES	Same as For Position	2	1

TABLE 4 RAECC FINAL SYSTEM DEFINITION (Continued)

FUNCTION	PARAMETER	DEFINITION	NUMBER INCLUDED IN: PRIMARY	NUMBER INCLUDED IN: SECONDARY
For Augmentor Control	WFD1	Same as For Position	1	1
	WFD2	Same as For Position	1	1
	WFD3	Same as For Position	1	1
For Core Engine Control	Solenoid:	---	(10)	(10)
	Start Bleed	---	2	2
	Staging Thrust Balance Bleed	---	1	1
For Augmentor Control	WFEP	---	2	1
	WFD1	Gas Gen. Primary Fuel Flow Shutoff Valve	1	1
	WFD2	Duct Zone 1 Fuel Flow Shutoff Valve	1	1
For Augmentor Control	WFD3	Duct Zone 2 Fuel Flow Shutoff Valve	1	1
		Duct Zone 3 Fuel Flow Shutoff Valve	1	1
For Annunciation	Augmentor Ignitor Relay	---	1	1
	Lamps/Flags: Primary On	---	(3)	(3)
	Secondary On	Cockpit Lamp Indicates Primary EEC Enabled	0	1
For Annunciation	Primary Fault Flag (Latched)	Cockpit Lamp Indicates Secondary EEC Enabled	1	0
	Secondary Fault Flag (Latched)	LRU Flag Indicates Primary EEC Fault	0	1
	NOCS Fault Flag (Latched)	LRU Flag Indicates Secondary EEC Fault	1	1
For Data Output	Serial Digital Data Stream:	Non-Operational Control System Fault Flag Located on ASP	(1)	(1)
	Same as For Input	---		

TABLE 4 RAEEC FINAL SYSTEM DEFINITION (Continued)

FUNCTION	PARAMETER	DEFINITION	INCLUDED IN:	
			PRIMARY	SECONDARY
Digital Data Processing	CPU	Central Processor Unit Implements EEC Channel Program	1	1
Control Loop Computation:	---	---	---	---
	WFEP & WFES	Gas Generator Primary and Secondary Fuel Flows	Yes	Yes
For Core Engine Control	AJE	Core Stream Exhaust Nozzle Area	Yes	Yes
	A4	High Pressure Turbine Inlet Area	Yes	Yes
	A41	Low Pressure Turbine Inlet Area	Yes	Yes
	AJD	Duct Stream Exhaust Nozzle Area	Yes	Yes
	FIG V	Fan Inlet Guide Vane Position	Yes	Yes
	CSVA	Compressor Stator Vane Actuator Position	Yes	Yes
	Start Bleed	Starting Bleed On/Off	Yes	Yes
	Thrust Balance	Thrust Balance Bleed On/Off	Yes	Yes
	TPS	Turbo Pump Speed Control	Yes	Yes
	WFD1, WFD2, & WFD3	Duct Augmentor Fuel Flows	Yes	Yes
For Augmentor Control	NH	High Rotor Speed Synthesized From Curves 3, or 6	Yes	Yes
	TBT	Turbine Blade Temp. Synthesized From Curve 3	Yes	Yes
	T22	Compressor Inlet Total Temp. Synthesized From Curve 1	Yes	Yes
	PT2	Fan Inlet Total Pressure Synthesized From Curves 2, or 4	Yes	Yes
Synthesization: (See Figure 10 For Curves Used in Synthesizing Parameters)				

TABLE 4 RAEC FINAL SYSTEM DEFINITION (Continued)

FUNCTION	PARAMETER	DEFINITION	INCLUDED IN:			
			PRIMARY	SECONDARY		
Synthesization (Continued)	PT3	Compressor Discharge Total Pressure Synthesized From Curves 4, or 6	Yes	Yes		
	PT13	Fan Discharge Total Pressure Synthesized From Curves 2, or 6	Yes	Yes		
	ΔP3	Compressor Discharge Differential Pressure Synthesized From Curve 5 Using Curves 7 & 8	Yes	Yes		
FUNCTION	PARAMETER	IN-FLT/ PRE-FLT		IMPLEMENTED BY:	INCLUDED IN:	
		TEST	TEST		PRIMARY	SECONDARY
Self Test 1: 2: 3: 4: 5: 6: 7: 8: 9: 10: 11: 12: 13: 14: 15: 16: 17:	Input Range Limit Check	Yes	Yes	Software	Yes	Yes
	Parameter Correlation Check	Yes	Yes	Software	Yes	Yes
	Parameter Majority Logic Check	Yes	Yes	Software	Yes	Yes
	Read Only Memory Check	Yes	Yes	Software	Yes	Yes
	Computer Cycle Time Test	Yes	Yes	Hardware	Yes	Yes
	Output Wraparound Test	Yes	Yes	Hardware & Software	Yes	Yes
	Injected Input Test	No	Yes	Software	Yes	Yes
	Canned Output Computation	No	Yes	Software	Yes	Yes
	Loop Dynamic Check	Yes	Yes	Software	Yes	Yes
	Reference Signal Check	Yes	Yes	Hardware & Software	Yes	Yes
	Power Supply Test	Yes	Yes	Software	Yes	Yes
	Processor Instruction Test	Yes	Yes	Hardware	Yes	Yes
	Scratch Pad Memory Check	Yes	Yes	Software	Yes	Yes
	EOC Bit Not Detected	Yes	Yes	Software	Yes	Yes
	Hardware Parity & Core Verifier Checks	Yes	Yes	Software	Yes	Yes
	Clock Loss Detect Circuit	Yes	Yes	Hardware	Yes	Yes
	UART Sync Word Detected	Yes	Yes	Hardware	Yes	Yes

TABLE 4 RAEEC FINAL SYSTEM DEFINITION (Continued)

FUNCTION	PARAMETER	DEFINITION	INCLUDED IN:	
			PRIMARY	SECONDARY
Cross Talk	UART/Dual Port RAM	Universal Asynchronous Receiver Transmitter Combined With Dual Port RAM Provides Data Link Between Primary And Secondary CPU's For The Interchange of Input, Output, Parameter Synthesis, And Fault Data	Yes	Yes
EEC Channel Switchover	Fault Status	Provides Hardware Backup For UART/Dual Port RAM. Hardware Logic Supplied With Fault Discrites From Each EEC Determines Each Channel's Operating Status. Automatically Switches Control From Failed, Inoperative, EEC to Operative EEC.		

3.2.4.3 Design Implementation

The RAECC final system design features a dual redundant channel architecture with several distinctive characteristics as contrasted with a classical duplex system with one unit in standby.

Each channel in the RAECC final system is capable of independent operation, or "stand alone", because each channel has a full complement of sensor inputs, a computer and a full complement of function drive outputs. The computers are operated asynchronously. In addition, each channel has its own power system supplied by separate alternator windings. The two channels are also independent in that a failure in one channel cannot cause a failure in the other. Both channels are programmed to provide identical control modes, parameter synthesization, and self test routines.

Both channels are operated continuously to perform the in-line monitoring function for channel fault coverage and the cross-channel fault coverage function.

The cross-channel monitoring coverage is provided by having the primary and secondary channels communicate continuously with each other. This channel communication is accomplished by a Universal Asynchronous Receiver-Transmitter (UART). The UART is implemented to allow the primary channel and the secondary channel to address and read a dedicated portion of the opposing channel RAM. However, only the channel where the RAM is physically located may write into its own RAM. This design feature retains the integrity of the data in each RAM in the event of a fault in the other channel.

The UART-RAM communication provides an effective input sensor redundancy path while still maintaining channel independence from faults in the other channel. For example, if the primary channel PT2 pressure sensor input signal fails and the secondary PT2 pressure sensor input signal is still good, the primary channel processor can interrogate the secondary channel for the PT2 data. Upon receiving the proper data, the primary channel continues to process the data and retain control of its output functions. The input sensor is used in this example but the process can be applied to all input sensors.

In addition to the RAECC final system circuit redundancy and the UART-RAM data communication, a study was conducted to evaluate the possibility of using synthesized input sensor data in the event of faults with two like sensor input signals. The study indicated that eight input sensors could be synthesized in each channel by using data from other sensors and the schedules (Figure 10) stored in the processor memory. The functions which can be synthesized in each channel are:

- (1) Speed, NH
- (2) Temperature, TBT avg.
- (3) Temperature, TBT peak
- (4) Temperature, T22
- (5) Pressure, PT2
- (6) Pressure, PT3
- (7) Pressure, PT13
- (8) Pressure, P3

The accuracy of the data produced by the synthesization process is sufficient to be used for majority voting and also permits the pilot to safely abort the mission if both sensor input signals fail.

With data available from two sensor input signals (hardware) and similar data from two synthesizations (software) also available, the combination provides for an effective 4-way majority voting scheme for perfect coverage of a fault in one sensor input signal. When one of the redundant input sensor signals has already failed, the synthesis still provides for a 3-way majority voting scheme for perfect coverage of the remaining sensor signal.

By means of the RM techniques and design features described in Section 3.3, a dual channel engine control with additional selective redundancy in one channel can be developed for fault tolerant operation with excellent coverage for first and second failures. This type of redundant operation allows the engine control to operate at full performance and mission reliability with several dissimilar failures in the two channels. In many cases, the redundancy in the system also allows deferment of immediate maintenance actions to a later time without compromising effective engine control performance or mission reliability.

Since each system is capable of providing all engine control functions, it is desirable that a decision be validated as to which system should be in control at any given time. As in the baseline system, a third processor would be unjustifiable to perform just this function of a third intelligence, or voter. Therefore, a hardwired logic approach is used.

Selected fault discretés are hardwired between the two system processors to allow the status of each system to be transmitted to the other processor. This system operates even though two-way communication through the UART-RAM link is

inadvertently interrupted. The failure discretes provide up to eight states of fault information to be transmitted to the opposite control system so that a decision regarding which system should control the engine can be made. The three fault discretes for the two systems are:

- (1) Power Supply Condition (Power On Reset - POR)
- (2) Condition of Processor and I/O (System ON)
- (3) Pilot Enable Command (Manual Enable Switch)

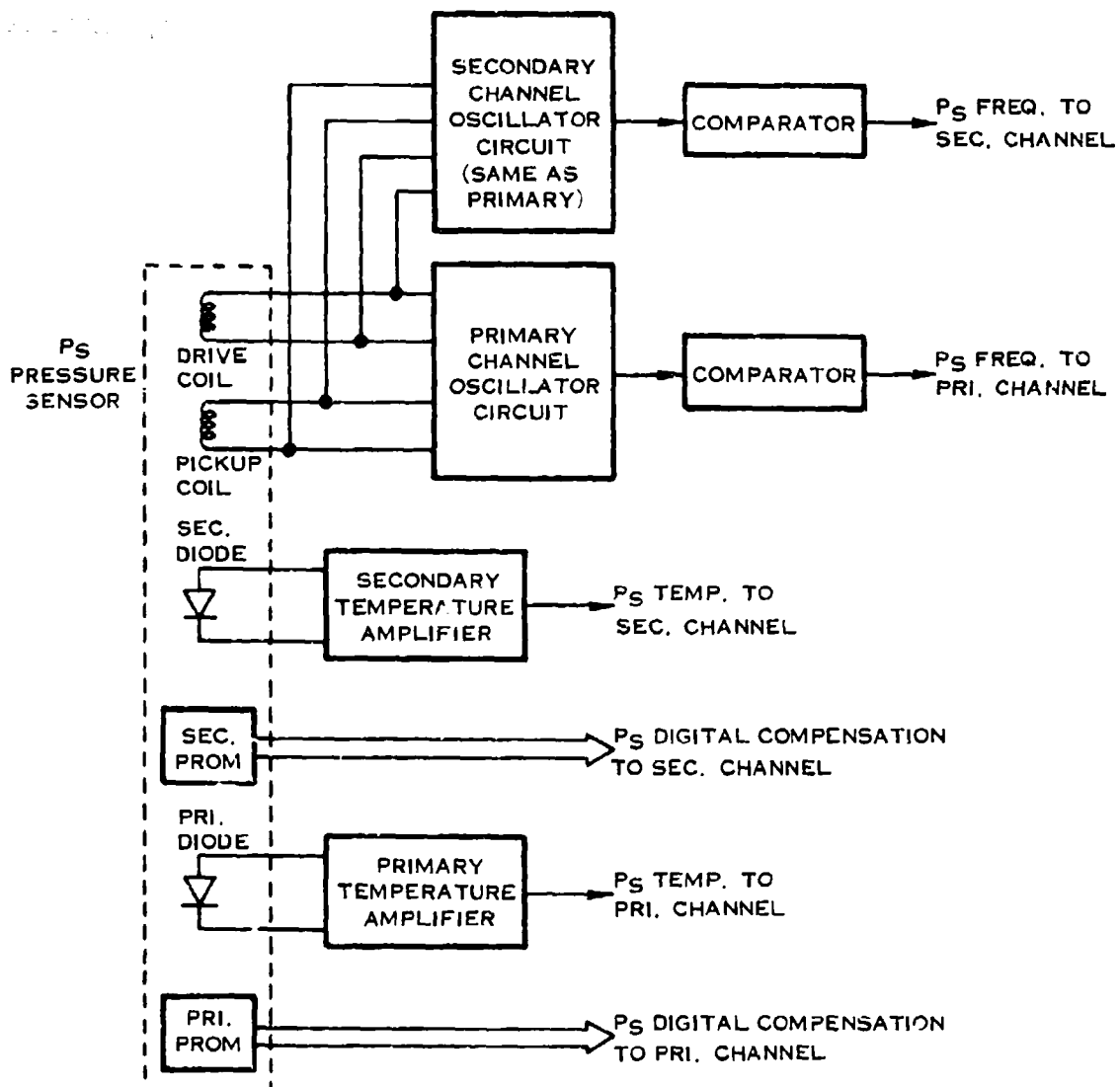
Based upon these six signals, or condition monitors, a decision is made as to which control is most capable of running the engine.

The output drivers of the two systems are interlocked so that only one system can control at a time. In no case can both systems be enabled to attempt simultaneous control. An additional design feature allows individual output loops to be switched in or out in the event of less significant system failures provided the UART-RAM link is operative. Thus, maximum control flexibility is provided to respond to all failure situations.

3.2.4.4 Quasi-Redundant Pressure Sensors

The FINAL RAEEC system configuration provides for fully redundant dual control channels and therefore, would theoretically require twelve single pressure sensors. However, twelve pressure sensors per control is not considered viable because of excessive size, weight, and cost. A trade off study of alternative pressure sensor configurations was carried out to determine if it is feasible to replace the twelve single pressure sensors with six quasi-redundant pressure sensor packages without significantly degrading RAEEC reliability. A quasi-redundant pressure sensor is characterized by a single (nonredundant) transducer assembly, with all or some of its electrical components redundant. The results of this analysis indicate that the most feasible configuration appears to be a pressure sensor with single cylinder and coils, but provided with dual redundant (parallel) oscillator circuits, PROMs, temperature sensors, and interface electronics.

Figure 12 is a block diagram of the selected quasi-redundant pressure sensor configuration. Separate temperature sensor diodes, PROMs, and pressure sensor output frequency signals are supplied to the primary and secondary channels. Primary and secondary components are independently excited by the primary and secondary power supplies respectively. The output signals from the pressure sensor components dedicated to the primary or secondary channel are converted to digital data words by the associated interface electronics and supplied to the channel CPU for compensation, self test, and control mode computation. It should be noted that the temperature sensing diode and PROM for each channel are matched to minimize errors due to temperature drift.



E-5777

FIGURE 12 PRESSURE SENSOR TRANSDUCER WITH DUAL ELECTRONICS

The baseline RAEEC self test routines are capable of detecting failures in the quasi-redundant pressure sensor. A fault which occurs in one channel but not the other will cause the RAEEC software to reject the pressure input data word from the failed channel, and continue computing with the input data word from the "good" channel; no hardware enable/disable switching is required. This type of fault is processed as a first failure and, therefore, "maintenance alert" is not signaled. A common mode fault, failing both channels identically, is detected either by input range limit testing or by a parameter majority logic check involving the average of both channel inputs, the pressure data word synthesized by the primary CPU, and the pressure data word synthesized by the secondary CPU. Common mode faults are processed the same as second like failures signaling "maintenance alert".

3.3 System Reliability Evaluation

3.3.1 Concepts

There are two methodologies concerning the reliability requirements for complex electronic engine controls. One approach is absolute in that a system works or it doesn't and a critical system failure is intolerable. The other approach is less severe in that a system must be tolerant towards single and multiple failures, but the system must not go down. There exists a middle ground between the absolute concept and the fault tolerant concept for present high reliability systems. The optimum approach for reliability attainment is to incorporate the best features of both methods. This study addresses the ways to increase the hardware reliability and to optimize the system configuration through redundancy.

The fault tolerant concept extends the period of trouble-free life and thus increases system availability. Fault tolerant systems do not eliminate the need for maintenance but they can reduce the frequency of unscheduled maintenance. These goals can be reached without significant sacrifice of inherent flight safety requirements. The design goal is to keep the system operational in spite of single and multiple hardware failures. As conceded earlier, failures can and will occur in any system. The problems are: What will happen and what can be done about it? As stated by Wulf (Reference 1), it is much more important to recover from failures than to prevent them since perfect reliability is not attainable.

The recovery concept cannot be precisely defined for all systems and designs. Recovery is most generally described as detecting, locating and automatically recovering from a hardware failure. Most reliability modeling assumes perfect detection and recovery from failures (Reference 2). Less-than-perfect detection and recovery from failures is defined by the concept of coverage (reference 3). Coverage C is the conditional probability that, given the

existence of a failure in the operational system, the system is able to recover and continue operation with no permanent loss of function. That is, $C = \text{Pr}(\text{System recovers}/\text{System fails})$. Therefore, reliability models must include coverage of failures as a design parameter.

The calculation of coverage values for each function is based upon the definition for system coverage. In the advanced system, coverage includes only those failure modes which degrade functional performance or coverage itself. Single failures having no effect on system operation, and not reducing the level of coverage for those failures which do degrade system performance, are called "non-functional" failure modes. The failure rates (λ_{NF}) associated with non-functional failure modes are subtracted from the total failure rate (λ_T) for the function. The remainder is the functional failure rate (λ_F). λ_F is therefore the sum of all failure modes which degrade performance and coverage. Functional failure modes which are undetectable by the in-flight BIT routines or cannot be isolated to one of the redundant elements, or cannot be repaired in flight, are called "uncovered". The sum of the failure rates associated with "uncovered" failure modes is called the uncovered failure rate (λ_u).

The coverage value (C) for each system function is the part of its functional failure rate (λ_F) derived from functional failure modes compatible with the requirements for coverage, i.e.,

$$C = \frac{\lambda_F - \lambda_u}{\lambda_F} = 1 - \lambda_u/\lambda_F = 1 - \frac{\lambda_u}{\lambda_T - \lambda_{NF}}$$

The coverage concept has introduced the idea of RM (Reference 4). The process of RM is directed at improving the coverage of failures with the purpose of making systems fault tolerant. As such, the goals of RM are synonymous with those of coverage in reliability modeling of system designs.

The basic reliability goals are modified when coverage of failures is considered as a system parameter. These specific reliability goals are stated as follows:

- (1) The ability to detect (almost) any failure in the system.
- (2) The ability to limit any system damage caused by a failure.
- (3) The ability to make failures transparent to system operation.
- (4) If unable to make failures transparent;

- (a) The ability to place the system in a consistent state so that recovery is possible and
- (b) The ability to report the failure to a higher level which can direct an intelligent system recovery thus making the failure transparent at higher levels.

The major contemporary redundancy techniques for developing fault tolerant systems are:

1. Shannon-Moore method (Reference 5).
2. Tryon method (Reference 6).
3. Von Neumann method (Reference 7).
4. Standby Redundancy (Reference 8).

Of these four methods, the standby redundancy method is perhaps the most basic and has been used for a long time. A system is configured with one subsystem operating and one or more subsystems "standing by" to take over operations if a fault is detected in the controlling subsystem. Depending on the number of standby units available, the above operation is continued until the last standby unit has failed.

The Von Neumann method which uses at least triple redundancy provides for majority voting logic and encourages continuous subsystem division and unit cross-strapping. With the advances in microelectronics, this method is most popular today.

The advanced system goals in this study were best satisfied by a combination of selective active standby redundancy and triplicate majority voting between the system channels.

3.3.2 Baseline System

3.3.2.1 Failure Effects

The baseline system shown in Figure 13 has secondary standby redundancy for engine critical functions that can affect flight safety. As such, the maintenance MTBF of 3039 hours is, by definition, a series summation of the failure rates so that repair actions are taken immediately to restore a high probability of flight safety. This system therefore, reflects a high repair rate which reduces its availability. In other words, maintenance and availability are sacrificed for flight safety. The effects of failures in this system are summarized in Table 5.



51

TABLE 5 FAILURE EFFECTS-BASELINE SYSTEM

Major Function (Gas Generator Associated)

<u>EVENT</u>	<u>MODE</u>	<u>PILOT ALERT</u>	<u>MAINT ALERT</u>
First Failure	Use Second Channel	Yes	Yes
Second Failure	Abort/ Shutdown	Yes	Yes

Minor Function (Augmentor Associated)

<u>EVENT</u>	<u>MODE</u>	<u>PILOT ALERT</u>	<u>MAINT ALERT</u>
First Failure	Abort	Yes	Yes

A summary of the effect of successive like failures on engine performance for the baseline system is shown in Table 5. A second failure for the gas generator associated functions causes an engine shutdown or a mission abort. These functions are redundant in the baseline configuration. The augmentor associated functions cause a mission abort because they are simplex in the baseline configuration.

3.3.2.2 Detail Failure Rate Sources

The rates for the various components are derived from over 250,000 hours field operating experience with an existing engine-mounted electronic fuel control. To compensate for the projected environment of the RAEEC system as compared to the JFC 90 environment, the techniques and adjustment factors set forth in MIL-HDBK-217B were used. The main factors used for this compensation were ambient temperature and component complexity.

The failure rates shown in Figure 13 are applied consistently in all of the reliability models discussed later in this report. That is, the total failure rate for a module or a system only changes by adding to or subtracting from the parts count because of design changes.

The parts failure rate summations for the various functions displayed in the models were rounded to simplify the many computations and to avoid a certain amount of "noise" in comparing values containing 2 or 3 decimals. Rounding up dominated over rounding down by using 0.4 rather than 0.5 as a dividing point to assure slightly pessimistic total values.

3.3.3 Reliability Groundrules

To balance the mission safety and availability, the following groundrules were established for the advanced system:

- (1) A completely failed channel must be identified to the crew. The purpose of this requirement is to enable the crew to identify a failed channel to (a) effect a repair before take off, or (b) abort the mission in flight, or (c) indicate during a mission that an engine shutdown can be imminent.
- (2) A warning is communicated to the crew when one additional like fault of a major function will cause a mission abort or an engine shutdown (catastrophic for single engine aircraft).

The purpose of this requirement is to decrease the failure likelihood of complete loss of engine control. This warning enables the crew to take appropriate action during flight based on complete knowledge of present and future system status.

- (3) A warning is communicated to the crew when a minor function has completely failed and there is a minor effect on engine control operations.

The purpose of this requirement is to alert the crew that (a) full engine performance is not available and (b) the augmentation function is not available if needed.

- (4) A Maintenance Alert is flagged when one additional like fault of a major function will cause mission abort. A Maintenance Alert is also flagged when a minor function has completely failed.
- (5) A channel with failed outputs must be inhibited from attempting any control functions.

The purpose of this requirement is to avoid transients in engine control output functions caused by the divergent command data being generated.

- (6) The failure of one channel should not cause failure of another channel.

The purpose of this requirement is to minimize the failure likelihood of the total system due to internal common mode failures.

- (7) The system shall not fail such that both channels are disabled.

The purpose of this requirement is to retain as much engine control as possible.

The application of the above groundrules to the baseline system demonstrates that a better balance between mission safety and availability can be achieved. There are now 50 first failure Maintenance Alerts for this modified baseline (Table 6) as compared to a Maintenance Alert on every first failure (58 first failure Maintenance Alerts).

3.3.4 RAEEC Final System

Several factors were considered in developing the techniques to satisfy the system groundrules listed above. One of the more significant considerations in the redundancy management design was fault detection, fault isolation and system recovery from faults having a catastrophic or major impact on engine operation.

Another important consideration was the amount of redundancy management resources needed to attain the excellent coverage required by a good fault tolerant system design. To minimize the need for special hardware dedicated to failure coverage, maximum use of computer software was indicated.

To reduce the possibility for control failures, the study evaluated the effects of applying selective triple redundancy for those functions having a significant impact on engine performance, and the effects of applying dual redundancy for functions having a minor impact. The effects of failures for a selectively redundant dual channel configuration are shown in Table 7.

To set the framework for the RM design, a study using the failure effects rules established the impact of various control system failures on engine performance. The results are tabulated in Failure Flag Action Table 8.

"Loss of Complete Function", indicates the impact of the function loss on engine performance. There are 14 functions where complete failure would cause the engine to shutdown. Also, there are 21 functions where control failures would have a major impact on engine performance. The loss of the remaining functions are designated as having a minor impact on engine performance.

TABLE 6. FIRST FAILURE FLAG ACTION MODIFIED BASELINE SYSTEM

	Function Identification	Loss of Complete Function	Elements	First Failure	
				Pilot Flag	Maint. Flag
I.	Power	Shutdown	2	Yes	Yes
II.	Speeds: TPS	Minor	2	No	No
	NH	Major	2 + S	No	No
	NL	Major	2	Yes	Yes
III.	Temperatures: TBT AVG	Minor	1 + (S)*	Yes	Yes
	TT2	Major	2	Yes	Yes
	TBT Peak	Minor	1 + (S)*	Yes	No
	T22	Major	1 + S	Yes	Yes
IV.	A/D Converter	Major	2	Yes	Yes
V.	Pressures: PT2	Major	1 + S	Yes	Yes
	PT3	Major	1 + S	Yes	Yes
	PT5	Minor	1	Yes	Yes
	Δ P13	Minor	1	Yes	Yes
	PT13	Minor	1 + S	Yes	Yes
	Δ P3	Major	1 + S	Yes	Yes
VI.	Resolvers: PLA	Shutdown	2	Yes	Yes
	Fig V	Major	2	Yes	Yes
	CSVA	Shutdown	2	Yes	Yes
	A4	Major	2	Yes	Yes
	A41	Major	2	Yes	Yes
	Aje	Major	2	Yes	Yes
	Ajd	Minor	2	No	No
	Wfep	Shutdown	2	Yes	Yes
	Wfes	Shutdown	2	Yes	Yes
	Wfd1	Minor	1	Yes	Yes
	Wfd2	Minor	1	Yes	Yes
	Wfd3	Minor	1	Yes	Yes
VII.	R/D Converter	Shutdown	2	Yes	Yes
VIII.	Signals: WOW	Minor	2	No	No
	Rf	Minor	2	No	No
	LOD	Minor	1	Yes	Yes
	ECU Enable	Major	2	Yes	Yes
	AIC Data	Minor	2	No	No
IX.	Pilot fault flag switch	Minor	1	Yes	Yes
X.	CPU	Shutdown	2	Yes	Yes
XI.	Crosstalk (CPU's)	Minor	1	Yes	Yes

TABLE 6 FIRST FAILURE FLAG ACTION MODIFIED BASELINE SYSTEM (Continued)

Function Identification		Loss of Complete Function	Elements	Pilot Flag	First Failure Maint. Flag
XII.	Torque Motors: TPS	Minor	2	No	No
	Fig V	Major	2	Yes	Yes
	CSVA	Shutdown	2	Yes	Yes
	A4	Major	2	Yes	Yes
	A41	Major	2	Yes	Yes
	Aje	Major	2	Yes	Yes
	Ajd	Minor	2	No	No
	Wfep	Shutdown	2	Yes	Yes
	Wfes	Shutdown	2	Yes	Yes
	Wfd1	Minor	1	Yes	Yes
	Wfd2	Minor	1	Yes	Yes
	Wfd3	Minor	1	Yes	Yes
XIII.	Solenoids: Start Bleed	Major	2	Yes	Yes
	Staging	Major	2	Yes	Yes
	Thr. Bal	Shutdown	2	Yes	Yes
	Wfep S.O.V.	Shutdown	2	Yes	Yes
	Wfd1	Minor	1	Yes	Yes
	Wfd2	Minor	1	Yes	Yes
	Wfd3	Minor	1	Yes	Yes
XIV.	Aug. Ign. Relay	Minor	1	Yes	Yes
XV.	Resolver Excitation: A	Shutdown	2	Yes	Yes
	B	Shutdown	2	Yes	Yes

S-Function has synthesis available.

** (S) - Function has synthesis available for BIT only.

TABLE 7. FAILURE EFFECTS - FINAL SYSTEM

Major Function (Gas Generator Associated)

<u>Event</u>	<u>Mode</u>	<u>Pilot Alert</u>	<u>Maint Alert</u>
First Failure	Use Second Channel	No	No
Second Failure	Use Third Channel	Yes	Yes
Third Failure	Abort/Shut-down	Yes	Yes

Minor Function (Augmentor Associated)

<u>Event</u>	<u>Mode</u>	<u>Pilot Alert</u>	<u>Maint Alert</u>
First Failure	Use Second Channel	No	No
Second Failure	Abort	Yes	Yes

TABLE 8. FIRST FAILURE FLAG ACTION FINAL SYSTEM

<u>Function Identification</u>	<u>Loss Of Complete Function</u>	<u>No. Of Elements</u>	<u>First Failure</u>	
			<u>Pilot Flag</u>	<u>Maint. Flag</u>
Power	Shutdown	2	Yes	Yes
Speed:				
TPS	Minor	2	No	No
NH	Major	2*	No	No
NL	Major	3	No	No
Temperatures:				
TBT Avg	Minor	2*	No	No
TT2	Major	3	No	No
TBT Peak	Minor	2*	No	No
A/D Converter	Major	3	No	No
Pressures				
PT2 Transducer	Major	1*	Yes	Yes
PT3 Transducer	Major	1*	Yes	Yes
PT5 Transducer	Minor	1	Yes	Yes
4P13 Transducer	Minor	1	Yes	Yes
4P3 Transducer	Major	1*	Yes	Yes
PT2 Electronics	Major	2*	No	No
PT3 Electronics	Major	2*	No	No
PT5 Electronics	Minor	2	No	No
4 P13 Electronics	Minor	2		No
PT13 Electronics	Minor	2*		No
4P3 Electronics	Major	2*		No
Resolvers				
PLA	Shutdown	3	No	No
Fig V	Major	3	No	No
CSVA	Shutdown	3	No	No
A4	Major	3	No	No
A41	Major	3	No	No
Aje	Major	3	No	No
Ajd	Minor	2	No	No
Wfep	Shutdown	3	No	No
Wfes	Shutdown	3	No	No

TABLE 8. FIRST FAILURE FLAG ACTION FINAL SYSTEM (Continued)

<u>Function Identification</u>	<u>Loss Of Complete Function</u>	<u>No. Of Elements</u>	<u>First Failure</u>	
			<u>Pilot Flag</u>	<u>Maint. Flag</u>
Resolvers (Continued)				
Wfd1	Minor	2	No	No
Wfd2	Minor	2	No	No
Wfd3	Minor	2	No	No
R/D Converter	Shutdown	3	No	No
Signals:				
WOW	Minor	2	No	No
RF	Minor	2	No	No
LOD	Minor	2	No	No
ECU Enable	Major	2	No	Yes
AIC Data	Minor	2	No	No
Fault Flag Switch	Minor	1	Yes	Yes
CPU	Shutdown	2	Yes	Yes
Cross talk (CPU's)	Minor	2	Yes	Yes
Torque Motors:				
TPS	Minor	2	No	No
FIGV	Major	3	No	No
CSVA	Shutdown	3	No	No
A4	Major	3	No	No
A41	Major	3	No	No
Aje	Major	3	No	No
Ajd	Minor	2	No	No
Wfep	Shutdown	3	No	No
Wfes	Shutdown	3	No	No
Wfd1	Minor	2	No	No
Wfd2	Minor	2	No	No
Wfd3	Minor	2	No	No

TABLE 8. FIRST FAILURE FLAG ACTION FINAL SYSTEM (Continued)

<u>Function Identification</u>	<u>Loss Of Complete Function</u>	<u>No. Of Elements</u>	<u>First Failure</u>	
			<u>Pilot Flag</u>	<u>Maint. Flag</u>
Solenoids:				
Start Bleed	Major	3	No	No
Staging	Major	3	No	No
Thr. Bal.	Shutdown	3	No	No
Wfep S.O.V.	Shutdown	3	No	No
Wfd1	Minor	2	No	No
Wfd2	Minor	2	No	No
Wfd3	Minor	2	No	No
Aug. Ign. Relay	Minor	2	No	No
Resolver Excit. A.	Shutdown	2	Yes	Yes
B.	Shutdown	2	Yes	Yes

* Parameter Synthesis Available

The significance of the added redundant functions can be evaluated by comparing Tables 5 and 7. The added redundancy has effectively inserted an additional tolerable function failure in the state paths from full performance to major system failure.

The impact on Maintenance Alert Requirements for the final system was evaluated. Between the baseline configuration and the final configuration, the system requires a Maintenance Alert on only 13 first failures as contrasted with a Maintenance Alert on every first failure (58) in the baseline system. If the same groundrules used for the final RAEEC system are applied to the baseline system, the situation changes very little. The baseline system now requires a Maintenance Alert on 50 first failures as compared to a Maintenance Alert on 58 first failures under the original groundrules. The final system is still significantly better.

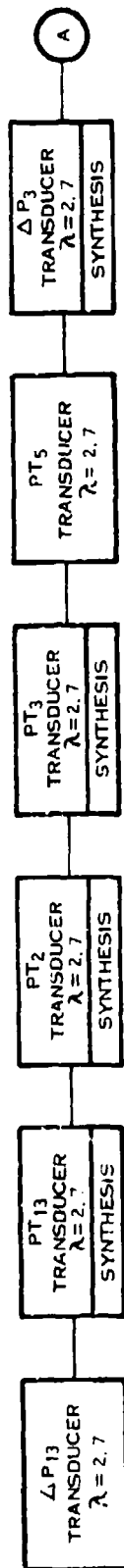
A description of the final system's dual channel redundancy implementation was presented in Section 3.2.4.3. Provisions have been made for cross-channel monitoring via the UART-RAM set-up, input sensor redundancy, input parameter synthesis, inter-channel, hardwired failure discretes, interlocked and inter-changeable output driver control. As a result of these features, maximum control flexibility is provided to respond to all failure situations.

The reliability block diagram for the final system is shown in Figure 14. The minimum operational MTBF of 7965 hours for the final RAEEC system was calculated with 2 computer programs. The arcs in Figure 14 illustrate the software cross-strapping of the various functions and the degree of failure allowed before a maintenance action is required while still maintaining minimum level of safety reliability.

3.3.5 System Coverage

Table 9 provides calculated coverage values for first and second like failures for each final RAEEC system function. Coverage is provided by:

1. The failure detection capability of the BIT applicable to each function is identified in Table 10. The table identifies the type of test and whether it is implemented by hardware or software.
2. The ability of the software to reject data from input channels in which failure is detected by the BIT, and to replace the failed data sources with data obtained from "good" redundant channels using, if necessary, the "cross-talk" data channel interlinking the primary and secondary CPU's.



E-5664

FIGURE 14 RELIABILITY BLOCK DIAGRAM -- FINAL SYSTEM (SHEET 1 OF 6)

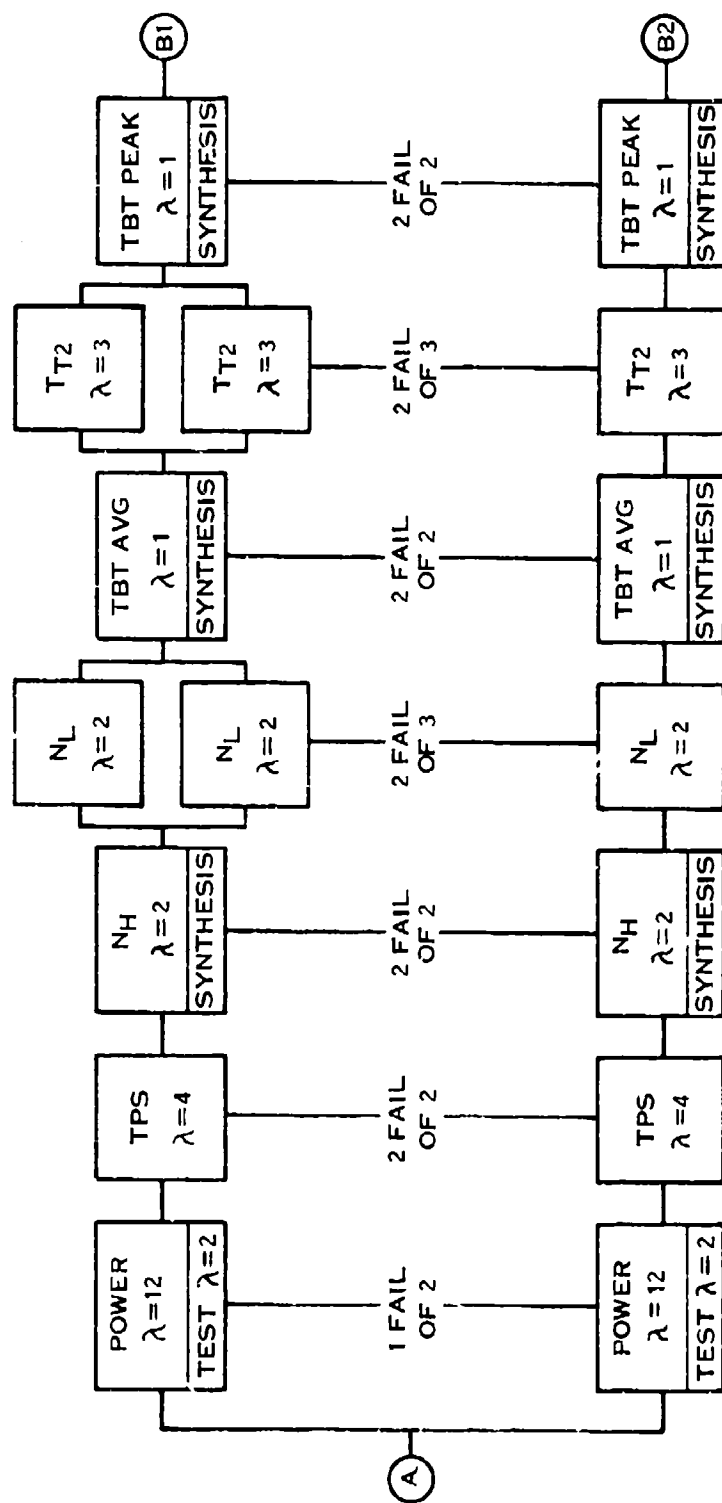


FIGURE 14 RELIABILITY BLOCK DIAGRAM - FINAL SYSTEM (SHEET 2 OF 6)

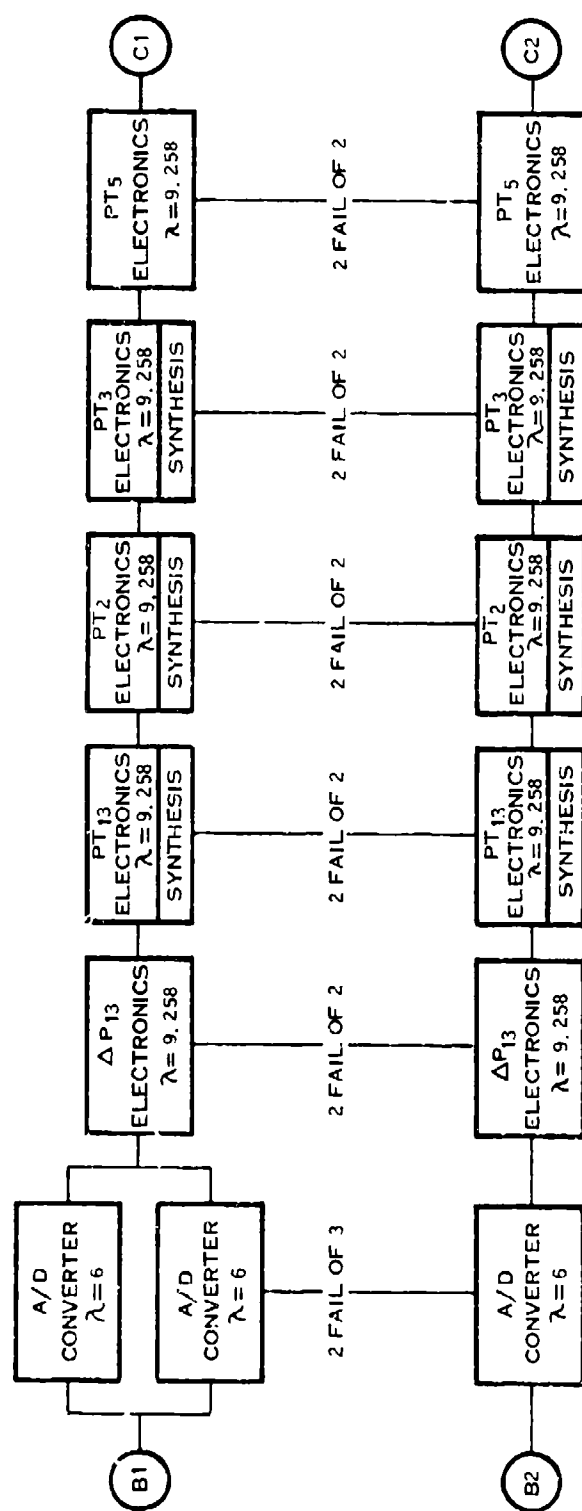


FIGURE 14 RELIABILITY BLOCK DIAGRAM — FINAL SYSTEM (SHEET 3 OF 6)

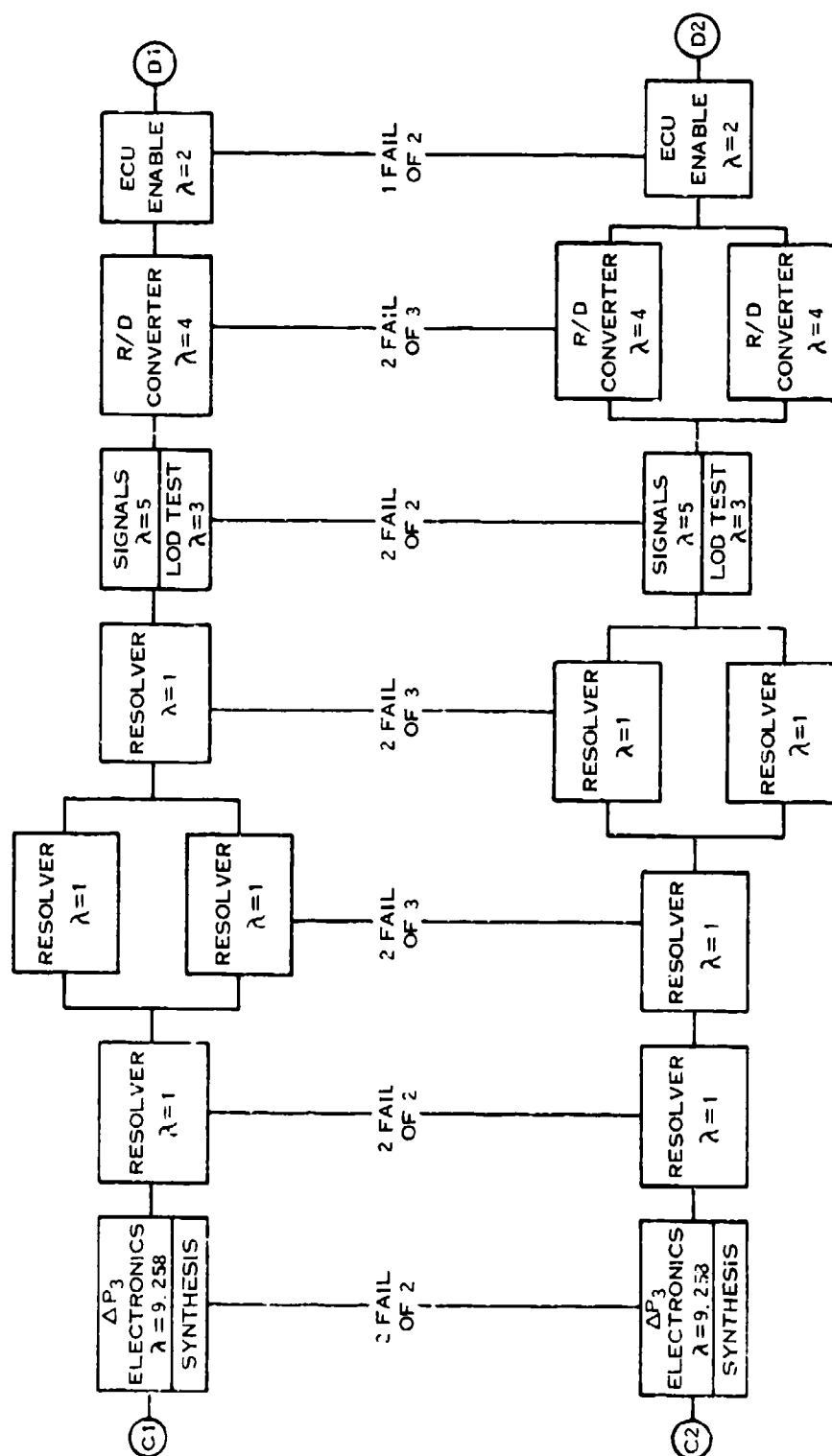


FIGURE 14 RELIABILITY BLOCK DIAGRAM — FINAL SYSTEM (SHEET 4 OF 6)

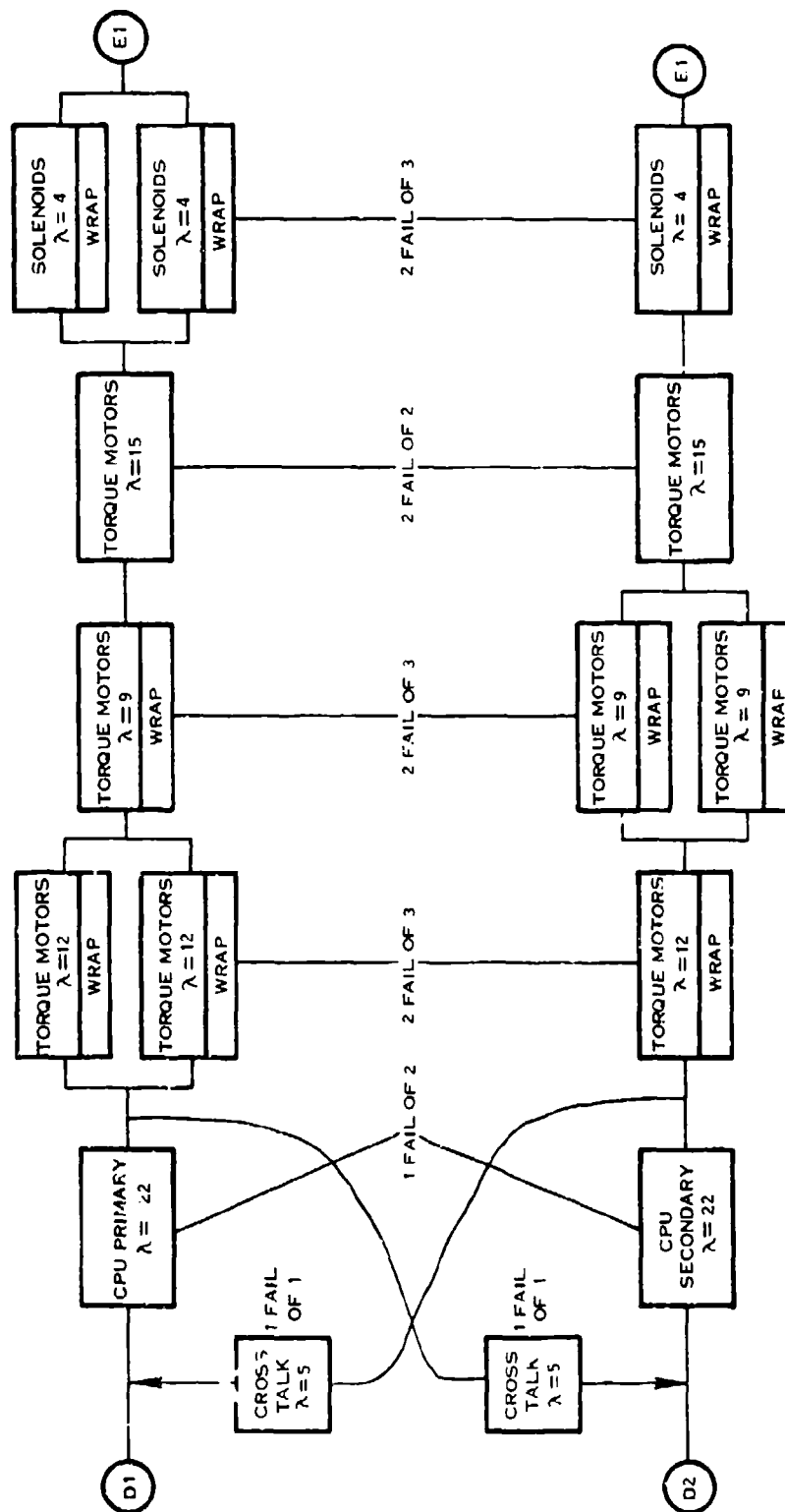


FIGURE 14 RELIABILITY BLOCK DIAGRAM -- FINAL SYSTEM (SHEET 5 OF 6)

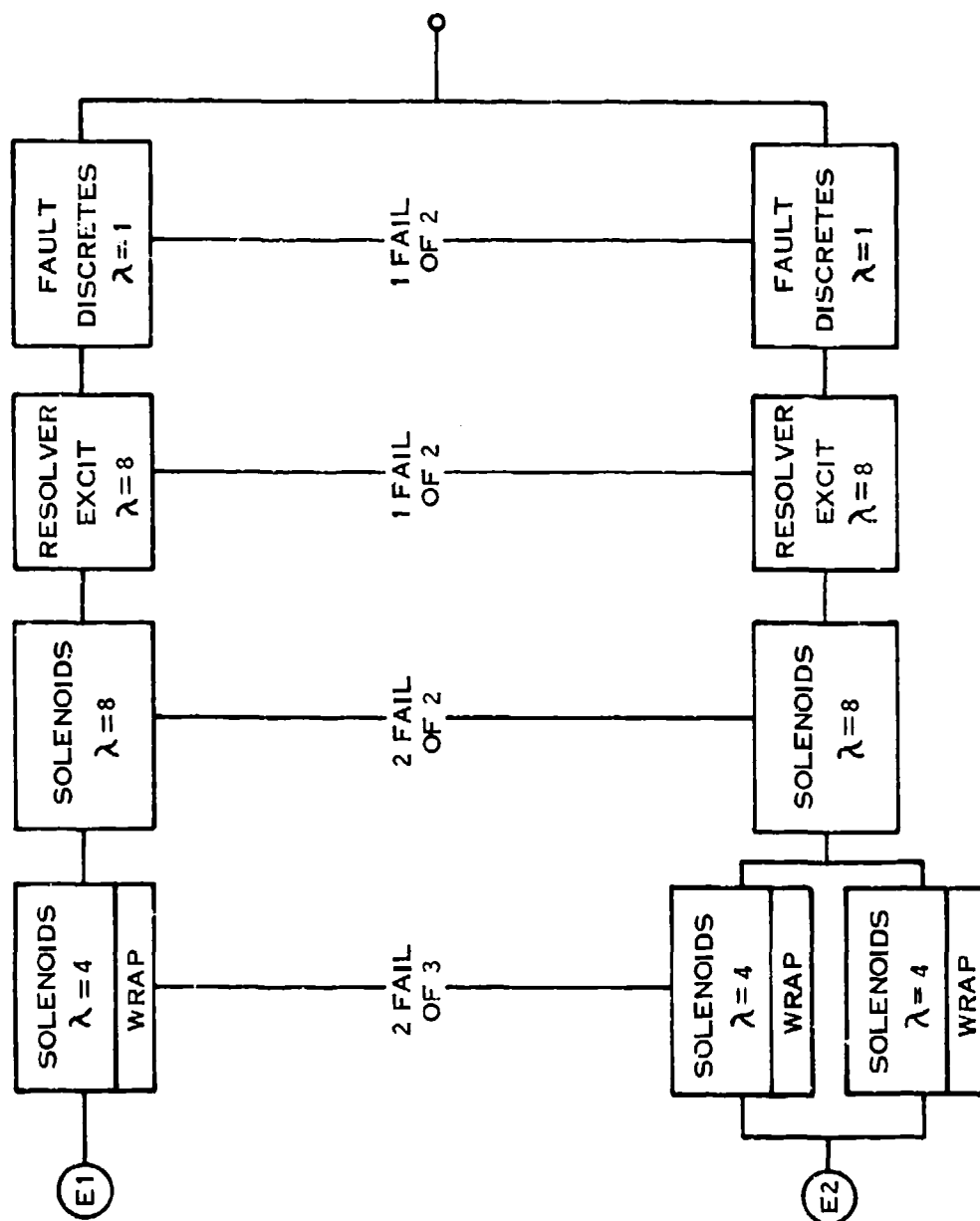


FIGURE 14 RELIABILITY BLOCK DIAGRAM - FINAL SYSTEM (SHEET 6 OF 6)

TABLE 9 FINAL RAECC SYSTEM COVERAGE

<u>Function Identification</u>	<u>No. Of Units</u>	<u>First Failure</u>		<u>Second Like Failure</u>	
		<u>Cov.</u>	<u>Test</u>	<u>Cov.</u>	<u>Test</u>
Power	2	.968	11	N/A	N/A
Speeds:					
TPS	2	.942	1,2,9,14	N/A	N/A
NH	2*	1.0	3	1.0	3
NL	3	1.0	3	.942	1,2,9,14
Temperatures:					
TBT Avg	2*	1.0	3	1.0	3
TT2	3	1.0	3	.929	1,2,9,10
TBT Peak	2*	1.0	3	1.0	3
A/D Converter	3	1.0	3	.976	1,2,9,10,14
Pressures					
PT2 Transducer	1*	1.0	3	N/A	N/A
PT3 Transducer	1*	1.0	3	N/A	N/A
PT5 Transducer	1	0	N/A	N/A	N/A
Δ P13 Transducer	1	0	N/A	N/A	N/A
PT13 Transducer	1*	1.0	3	N/A	N/A
Δ P3 Transducer	1*	1.0	3	N/A	N/A
PT2 Electronics	2*	1.0	3	1.0	3
PT3 Electronics	2*	1.0	3	1.0	3
PT5 Electronics	2	0.961		N/A	N/A
Δ P13 Electronics	2	0.961		N/A	N/A
PT13 Electronics	2*	1.0	3	1.0	3
Δ P3 Electronics	2*	1.0	3	1.0	3
Resolvers:					
PLA	3	1.0	3	.99	1,2,9,10
FIG V	3	1.0	3	.99	1,2,9,10
CSVA	3	1.0	3	.99	1,2,9,10
A4	3	1.0	3	.99	1,2,9,10
A41	3	1.0	3	.99	1,2,9,10
Aje	3	1.0	3	.99	1,2,9,10
Ajd	2	.99	1,2,9,10	N/A	N/A
Wfep	3	1.0	3	.99	1,2,9,10

TABLE 9. FINAL RAECC SYSTEM COVERAGE (Continued)

<u>Function Identification</u>	<u>No. of Units</u>	<u>First Failure</u>		<u>Second Like Failure</u>	
		<u>Cov.</u>	<u>Test</u>	<u>Cov.</u>	<u>Test</u>
Wfes	3	1.0	3	.99	1,2,9,10
Wfd1	2	.99	1,2,9,10	N/A	N/A
Wfd2	2	.99	1,2,9,10	N/A	N/A
Wfd3	2	.99	1,2,9,10	N/A	N/A
R/D Converter	3	1.0	3	.958	1,2,9,10 14
Signals:					
WOW	2	0	N/A	N/A	N/A
RF	2	0	N/A	N/A	N/A
LOD	2	.99	N/A	N/A	N/A
ECU Enable	2	0	N/A	N/A	N/A
AIC Data	2	.99	1.15	N/A	N/A
Fault Flag Switch	1	0	N/A	N/A	N/A
CPU 2	.996	4,5,12, 13,16	N/A	N/A	N/A
Crosstalk (CPU's)	2	.99	17	N/A	N/A
Torque Motors:					
TPS	2	.958	6	N/A	N/A
FIGV	3	.958	6	.958	6
CSVA	3	.958	6	.958	6
A4	3	.958	6	.958	6
A41	3	.958	6	.958	6
Aje	3	.958	6	.958	6
Ajd	2	.958	6	N/A	N/A
Wfep	3	.958	6	.958	6
Wfes	3	.958	6	.958	6
Wfd1	2	.958	6	N/A	N/A
Wfd2	2	.958	6	N/A	N/A
Wfd3	2	.958	6	N/A	N/A
Solenoids:					
Start Bleed	3	.958	6	.958	6
Staging	3	.958	6	.958	6
Thr. Bal	3	.958	6	.958	6
Wfep S.O.V.	3	.958	6	.958	6
Wfd1	2	.958	6	N/A	N/A
Wfd2	2	.958	6	N/A	N/A
Wfd3	2	.958	6	N/A	N/A

TABLE 9. FINAL RAEEC SYSTEM COVERAGE (Continued)

<u>Function Identification</u>	<u>No. of Units</u>	<u>First Failure</u>		<u>Second Like Failure</u>	
		<u>Cov.</u>	<u>Test</u>	<u>Cov.</u>	<u>Test</u>
Aug. Ign. Relay	2	.958	6	N/A	N/A
Resolver Excitation:					
A	2	.958	N/A		
B	2	.958	N/A		

<u>First Failure</u>		<u>Second Failure</u>	
<u>Coverage</u>	<u>Failure Rate</u>	<u>Coverage</u>	<u>Failure Rate</u>
1.0	135.98	1.0	84.98
.996	44.0	.99	6.0
.99	23.0	.976	18.0
.968	28.0	.958	99.0
.958	149.0	.942	6.0
.942	8.0	.929	9.0
.961	33.09		
0.0	15.4		

$$C_1 = \frac{\sum C_i \lambda_i}{\sum \lambda_i}$$

$$= \frac{411.75}{436.47}$$

$$= .943$$

$$C_2 = \frac{\sum C_i \lambda_i}{\sum \lambda_i}$$

$$= \frac{217.35}{222.98}$$

$$= .975$$

TABLE 10 BUILT-IN-TEST SUMMARY

<u>BIT Test Number and Name</u>	<u>In-Flt Tests</u>	<u>Pre-Flt Tests</u>	<u>Software (S) or Hardware (H)</u>
1 Input Range Limit Check	X	X	S
2 Parameter Correlation Check	X	X	S
3 Parameter Majority Logic Check	X	X	S
4 Read Only Memory (ROM) Check	X	X	S
5 Computer Cycle Time Test	X	X	H
6 Output Wraparound Test	X	X	H
7 Injected Input Test		X	S
8 Canned Output Computation		X	S
9 Loop Dynamic Check	X	X	S
10 Reference Signal Check	X	X	H
11 Power Supply Test	X	X	H
12 Processor Instruction Test	X	X	S
13 Read-Write (Scratch-pad Memory Check)	X	X	S
14 End of Conversion (EDC) BIT Not Detected	X	X	S
15 Hardware Parity and Code Verifier Checks	X	X	H
16 Clock Loss Detect Circuit	X	X	H
17 UART Sync Word Detected	X	X	H

3. The ability of the software to transfer output data from output channels in which failure is detected by BIT to "good" redundant channels using the cross-talk data channel interlinking the primary and secondary CPU's.
4. The ability of the software/hardware to electrically disable the primary channel entirely if it is inoperative, and to maintain system operation by electrically enabling the fully redundant secondary channel.

First failure coverage values given in Table 9 are calculated on the assumption that the system is initially failure free before failure occurs. Majority logic checks can therefore, be applied. Since the first failure in a three element function is reduced to a dual element function until scheduled maintenance takes place, in-line testing must be employed to provide coverage for a second like failure of the function. Coverage for the second like failure must be less than 100% because majority voting is not possible.

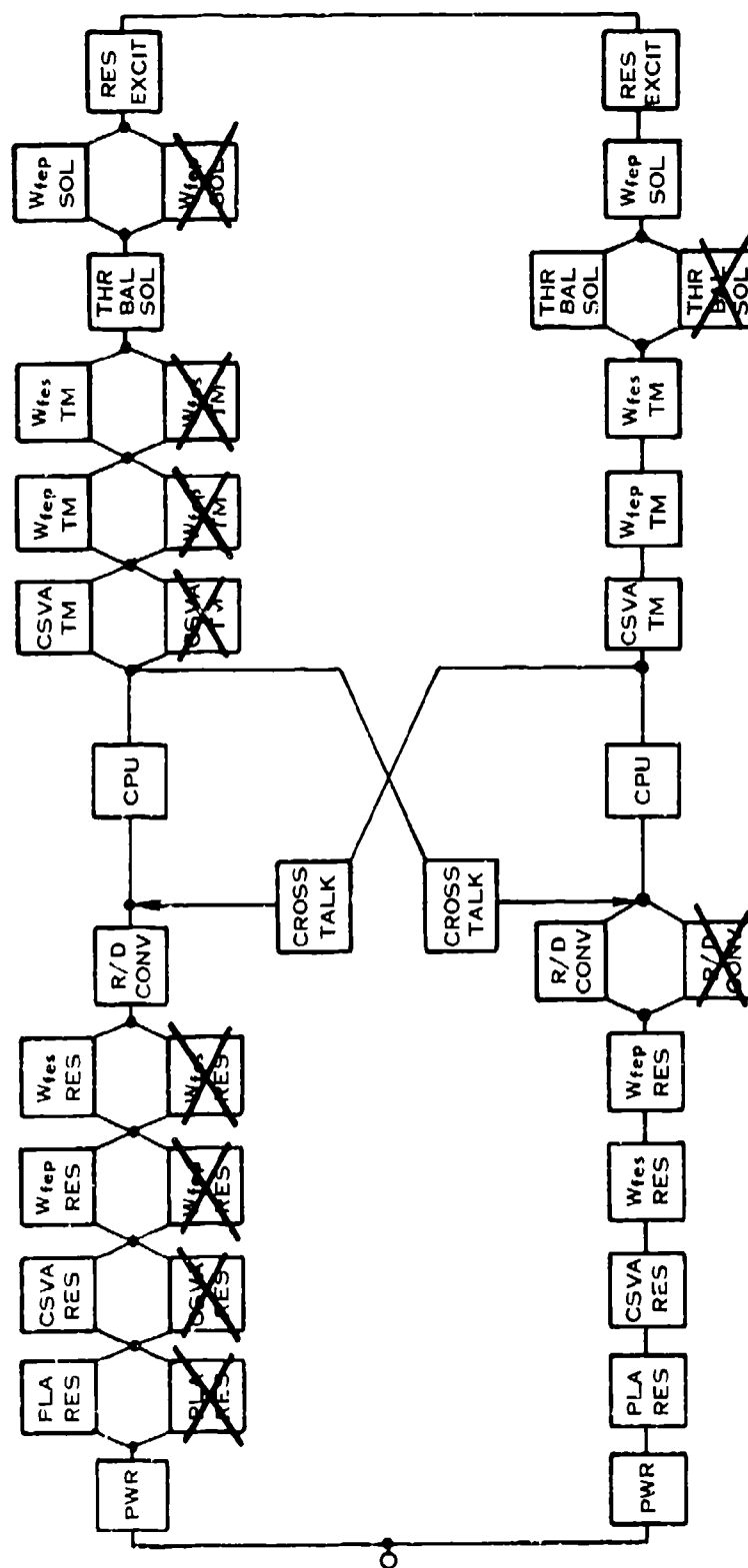
In the case of functions provided with two elements and software synthesis (in each CPU), the majority logic check can be applied to the second like failure because of the one remaining element and the software synthesis in each CPU. If the remaining single element is identified as the failed unit, it can be replaced for the remainder of the mission by the software synthesis. In this case, therefore, coverage for the second like failure remains near 100%.

For two element functions, first failure coverage is of course, less than 100%. Coverage for a second like failure is not applicable since recovery is not possible. However, the BIT effectiveness remains applicable since fault detection of second like failures in two element functions must be provided to flag a maintenance alert.

3.3.6 Final System Flight Safety Probability

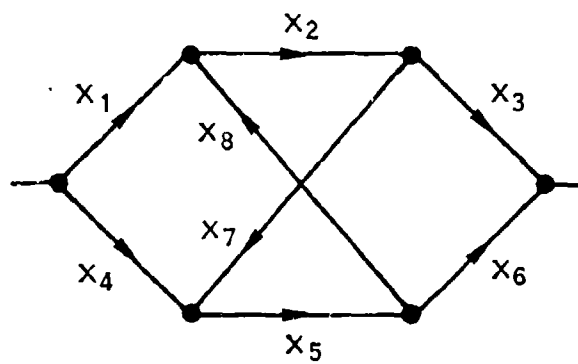
A flight safety model study was conducted using the classical reliability modeling and mathematical approach (Reference 9).

The model was developed by including all those engine control functions which can cause engine shutdown if they are not functioning and eliminating the other control functions. The safety model is shown in Figure 15 with failed units in the block diagram and can be represented by the reliability graph shown in Figure 16. This model is essentially the same architecture as the full final RAECC model except for the elimination of nonrelevant functions.



E-1157

FIGURE 15 FLIGHT SAFETY RELIABILITY BLOCK DIAGRAM



E-5661

FIGURE 16 SAFETY MODEL RELIABILITY GRAPH

The reliability of the system can be expressed in minimal tie sets of the graph.

$$R = \Pr (T_1 + T_2 + T_3 + T_4)$$

where the minimal tie sets are

$$T_1 = X_1 X_2 X_3$$

$$T_2 = X_4 X_5 X_6$$

$$T_3 = X_1 X_2 X_7 X_5 X_6$$

$$T_4 = X_4 X_5 X_8 X_2 X_3$$

All other tie sets are nonminimal.

In Figure 15, certain redundant elements have been crossed out to represent failure of that element. These "selected" failures for each channel reduce the system to a "worst case". Thus, they reflect the high degree of fault tolerance (hardware failure) not necessitating individual maintenance actions while still preserving mission safety critical functions. The model is defined as the minimal number of systems channel elements required for core engine operation.

With this reduced graph of flight critical components, the coverage value CT_n for each tie set is calculated using the data in Table 9 and the reliability equation. The tie set reliabilities with coverage are

$$T_1 = CT_1 (X_1 X_2 X_3)$$

$$T_2 = CT_2 (X_4 X_5 X_6)$$

$$T_3 = CT_3 (X_1 X_2 X_7 X_5 X_6)$$

$$T_4 = CT_4 (X_4 X_5 X_8 X_2 X_3)$$

where by symmetry $CT_1 - CT_2 = 0.975$

and $CT_3 = 0.981$

The equation for system probability is then expanded in terms of the joint tie set survival probabilities as

$$R = \sum_i \text{Pr} (T_i) - \sum_{ij} \text{Pr} (T_i T_j) + \sum_{ijk} \text{Pr} (T_i T_j T_k) \\ - \sum_{ijkl} \text{Pr} (T_i T_j T_k T_l)$$

Upon substituting the derived tie set data into the equation, the reliability of the safety model with coverage is 0.99999974 which is a failure likelihood of 2.26×10^{-7} .

3.4 Electrical Design

3.4.1 Introduction

The final RAEEC circuit design was derived from the baseline system through a series of trades study which are presented in Appendix A. The baseline, also described in Appendix A, is essentially a modified Full Authority Digital Electronic Control (FADEC). The final design choices are presented here for the fourteen circuit partitions studied.

(As a quick cross-reference aid the third digit of each paragraph dealing with a circuit partition is the same in this section and Appendix A.)

3.4.2 Analog-to-Digital Converter

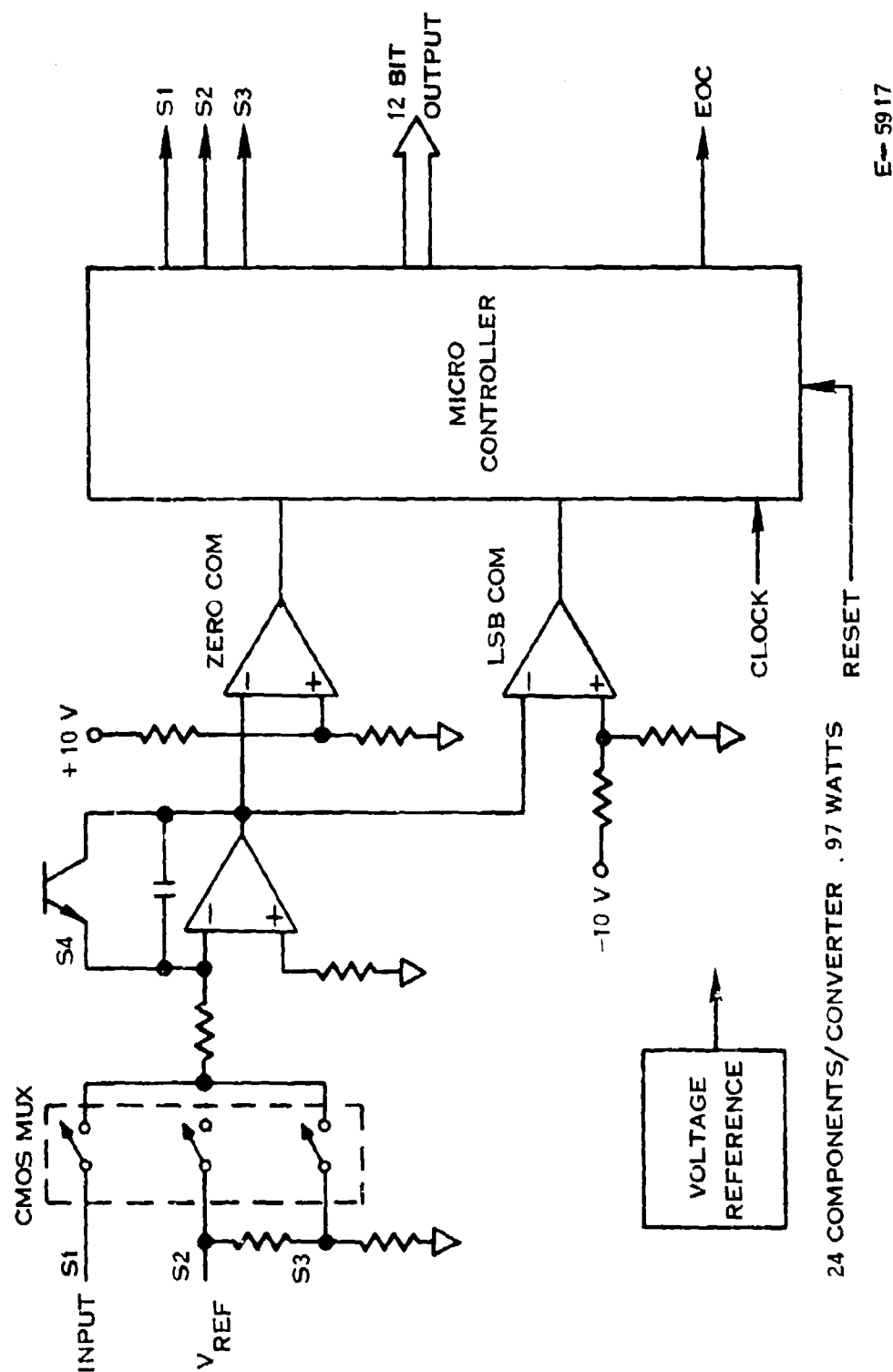
The "smart, multiple-ramp" analog-to-digital converter used in the RAEEC final design converts multiplexed high-level (0 to +10V) DC signals to a 12-bit binary number with a typical accuracy of 11 bits and with a maximum conversion time of 1.536 milliseconds. A microprocessor is used to perform the A/D control logic as well as its own signal multiplexing, input scaling, and range checks, in addition to fault isolation. The analog portion of the converter is comprised of an integrator with four multiplexed inputs, a zero comparator, and a least significant bit comparator. A simplified block diagram is shown in Figure 17.

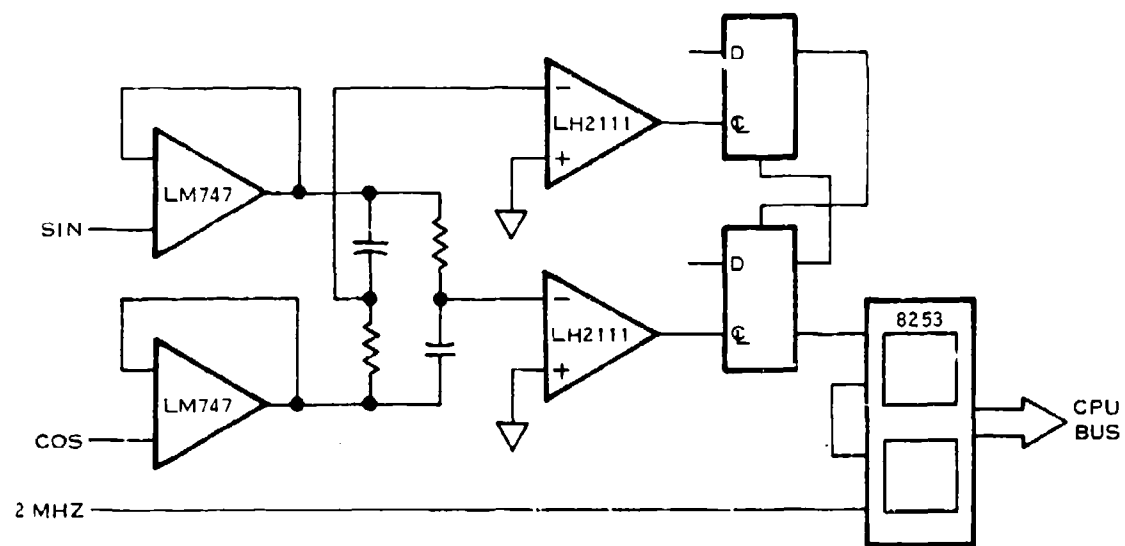
3.4.3 Resolver-to-Digital Converter

An R-C Bridge/Pulse Width to Digital R/D is incorporated in the final RAEEC design, which has superior reliability characteristics over other R/D circuits.

This 11-bit resolver to digital converter (Figure 18) comprises a pair of voltage followers, an R-C bridge, phase shift to pulse width comparators and logic, and a programmable interval timer and bus driver. The two, in phase, amplitude varying AC voltages from the output of the resolver mux (described in Section 3.4.9) carry resolver position (θ) information in the form of $\sin \theta$ and $\cos \theta$ which are converted in an R-C bridge to two constant amplitude, phase shifted voltages, whose phase difference in electrical degrees is equal to $2\theta - 90^\circ$. (Note that there is an electrical gain of two.) The two phase shifted voltages each drive their own zero-comparator whose output drives an equivalent dual-clocked flip-flop circuit, providing a logic-level pulse width proportional to twice the resolver mechanical angle. This single pulse width in turn, enables the programmable interval timer which can be addressed directly onto the data bus by the CPU.

The following lists the advantages and disadvantages of the R-C bridge resolver to digital converter:





E-5966

FIGURE 18 RESOLVER TO DIGITAL CONVERTER

ADVANTAGES:

1. All failure modes can be detected (if the total resolver movement is restricted to less than 90 mechanical degrees).
2. Provides a direct conversion of shaft angle; no transport delay delta between "SIN θ " and "COS θ " inputs.
3. With reference angle compensation, this interface is accurate to within 6 minutes.
4. Lends itself to multiplexing techniques.

DISADVANTAGES:

1. Precision R-C bridge required with good stability over temperature.
2. Accurate sine-wave generation required for resolver excitation. Converter is sensitive to odd harmonics.
3. Resolver movement should be restricted to less than 90°.

3.4.4 Resolver Excitation

The Resolver Excitation circuit used in the final RAEEC system, provides a precision 7 Vrms, 1.953 KHz sinewave for excitation of the engine fuel control resolvers. Although 400 Hz synchro excitation is available on most aircraft, this configuration for self excitation of fuel control feedback transducers is advantageous for the following reasons:

1. Loss of the 400 Hz bus would cause the engine fuel controls to lose feedback signals, causing engine shutdown.
2. A 400 Hz excitation system causes a long R/D conversion time, since the period of one sample would be 2.5 milliseconds, and a minimum conversion time of twice the excitation period is required for settling and conversion time.

This circuit, as shown in Figure 19, comprises five different functions which are described briefly as follows:

3.4.4.1 Transmission Gate Modulator

This circuit provides an amplitude modulated 1953 Hz squarewave, proportional to the error integrator output, which is fed to the tuned filter.

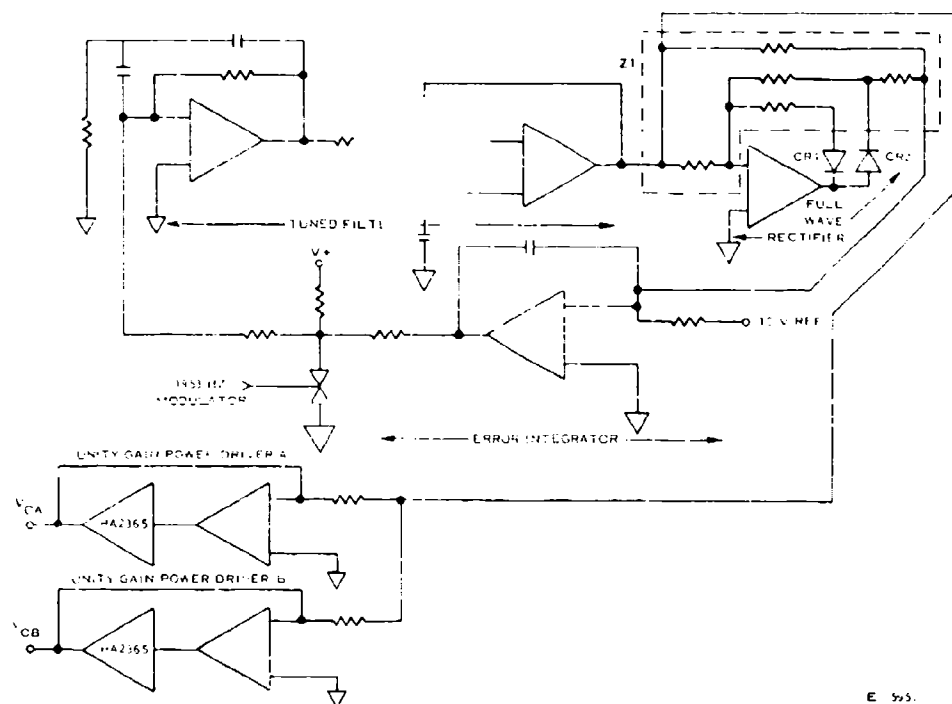


FIGURE 19 RESOLVER EXCITATION

3.4.4.2 Tuned Filter

The first stage of the active tuned filter section is a bandpass filter to attenuate the third harmonic of the square wave and also to block the DC component. The center frequency is at 1.953 KHz, the gain is 0 dbv, and the sensitivity is 10. The second stage is a low pass filter to further attenuate the third harmonic distortion. The center frequency is at 1.953 KHz; zeta is 0.1 resulting in a gain of 14 dbv at $f_0 = 1.953$ KHz.

3.4.4.3 Rectifier

Amplifier AR3 in conjunction with diodes CR1 and CR2 and network Z1 provide a gain of -1 for negative inputs and 0 for positive inputs. The offset error due to the diode is negated by the amplifier. The amplifier output is summed with the filter output through resistors with a 2:1 ratio producing a precise full wave rectified signal.

3.4.4.4 Error Integrator

To obtain the error signal necessary to produce a 6.8562 Vrms output, AR4 realizes a summing error integrator. The rectifier output current is summed with the current from the -10 VDC reference. If the currents are not equal, the integrator ramps up or down until they are. The sine wave input does not affect the DC voltage level of the integrator output because the average (or DC) value of the sine wave is zero. It does, however, produce a full-wave rectified current when summed with the half-wave rectifier output.

3.4.4.5 Power Stage

A monolithic power driver (HA2635) is used to obtain the necessary drive current for resolver excitation. The filter output is buffered with a 747 op-amp which supplies the drive for the HA2635. The feedback loop is unity gain and serves to reduce nonlinearity and crossover distortion of the HA2635.

The driver outputs are matched to the resolver impedance by a shunt R-C circuit, effecting a purely resistive load to the power booster. This reduced the required output power and subsequent dissipation in the HA2635. Matching, at this writing, is for six resolvers in parallel (per HA2635 driver) and can be adjusted where more resolvers are employed. Individual resolver impedance is $128 + j648$.

3.4.5 Torque Motor D/A's and Drivers

This circuit is capable of driving a torque motor with an average DC current of 40 milliamperes using a pulse width modulation technique. Positive or negative pulses of 40 msec at a frequency of 50 Hz drive the torque motor. The duty cycle can vary from 0 to 100% with a granularity of 256 increments. A microprocessor controls 8 torque motor driver circuits. The microprocessor's task is to turn "on" and "off" either a +14 volt switch or a -14 volt switch at 50 Hz at the proper pulse width. All inputs and outputs of the microprocessor are

buffered by latches because of the number of required I/O signals. The torque motor controller is a stand-alone circuit that is a slave to the central processor. (Figure 20.)

In addition, the microprocessor is part of a distributed processing system, which reduces the load on the CPU and enables self-error checking at the interface level.

3.4.6 Solenoid Drivers

Solenoid control data from the control CPU is stored in a TTL register (SN54LS164). This register will control 8 individual solenoids. When the output of the register is a logic "1" (5 volts), the solenoid will be activated by the power booster ULN-2804. The solenoid is powered by 20 preregulated volts from the power supply. The output state of the solenoid is monitored by a LM148 for fault detection. (Figure 21.)

It should be noted that although the circuit power dissipation is approximately 1 watt per energized solenoid, on an average, only three solenoids (and three drivers) will be energized.

3.4.7 Pressure Sensors and Circuitry

3.4.7.1 Hamilton Standard Pressure Sensor

The Hamilton Standard digital pressure transducer (Figure 22) is a precision device available to industry. The pressure transducer's pressure sensing element is a cylinder, excited by a magnetic driving circuit, which vibrates at its natural frequency. As the pressure to be measured increases, internal forces act to increase the stiffness of the sensing element causing the natural frequency to increase in proportion to the change in applied pressure. The inherent high accuracy and digital nature of this device make it ideally suited to computer controlled systems.

The physical parameters which may be measured with the greatest accuracy are time and frequency. Frequency does not lose its identity or precision by transmission and may always be measured with considerable accuracy.

The pressure transducer sensor is comprised of two concentric cylinders, an inner one and outer one, separated by an evacuated space, which becomes the absolute pressure reference. These cylinders, while separate at one end, share a common mounting base. The walls of the inner cylinder are caused to vibrate at their lowest natural frequency by force pulses from the magnetic field of a driver coil mounted internal to the inner cylinder.

Mounted in the same centerbody as the driver coil is the pickup coil which produces a voltage proportional to the frequency and amplitude of cylinder wall vibration. The pickup voltage is feedback to the driver coil through an operational amplifier so as to maintain a constant cylinder wall vibratory amplitude.

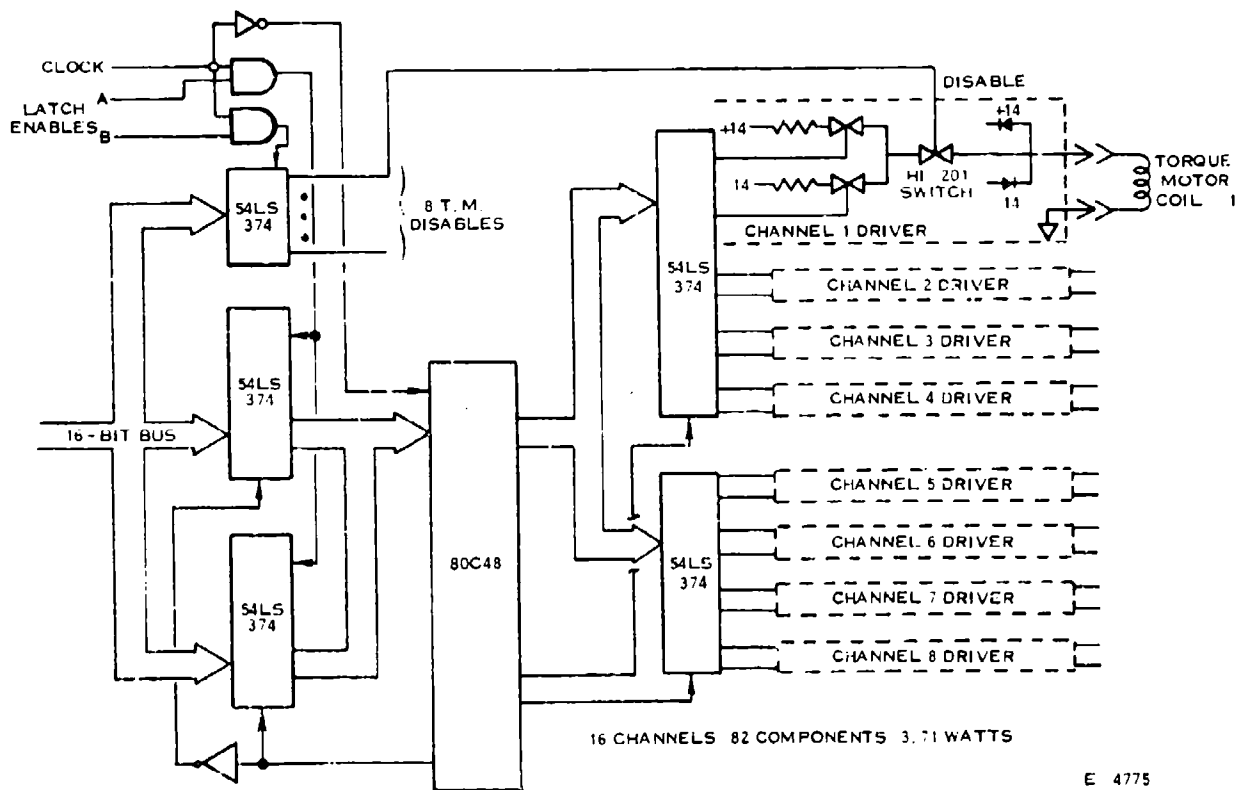


FIGURE 20 TORQUE MOTOR DRIVER

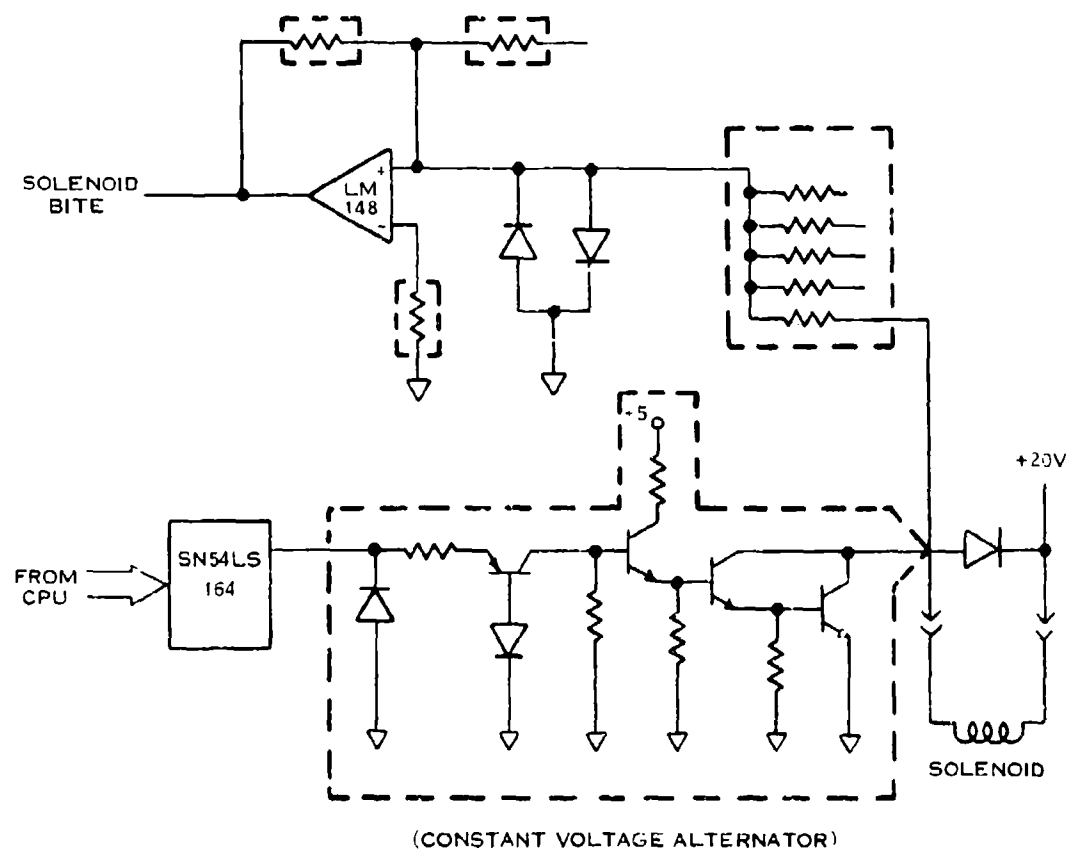
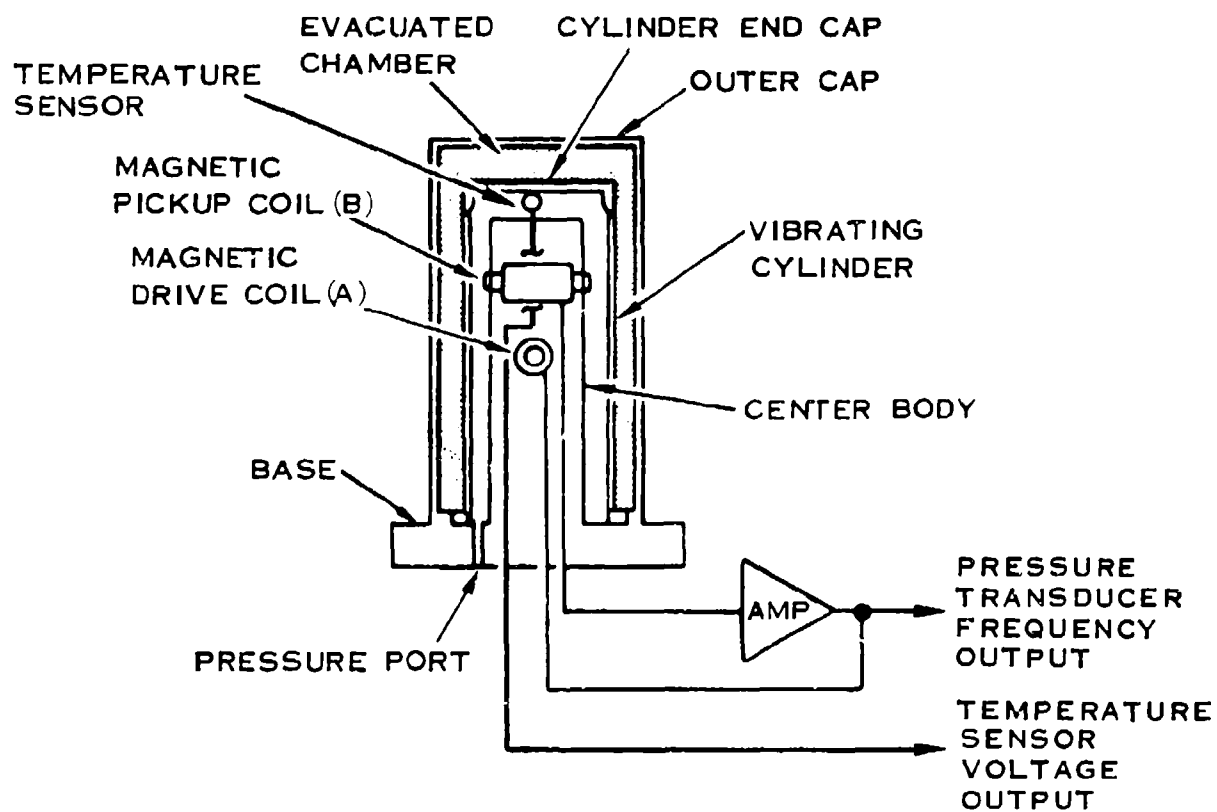


FIGURE 21 SOLENOID DRIVER



E-2014

FIGURE 22 SECTION VIEW OF PRESSURE SENSOR

When a pneumatic pressure is introduced into the inner (vibrating) cylinder, the wall elements are tensioned and the cylinder natural frequency increases. Hence, the natural frequency is dependent upon pressure in the nonlinear relationship:

$$\text{Pressure} = A + Bf_t + Cf_t^2 + Df_t^3 + Ef_t^4$$

where A, B, C, D, and E are calibration constants. Therefore, the transducer sensor converts sensed pressure into a 2 to 3 volt square-wave electrical signal whose frequency is a nonlinear function of the sensed pressure.

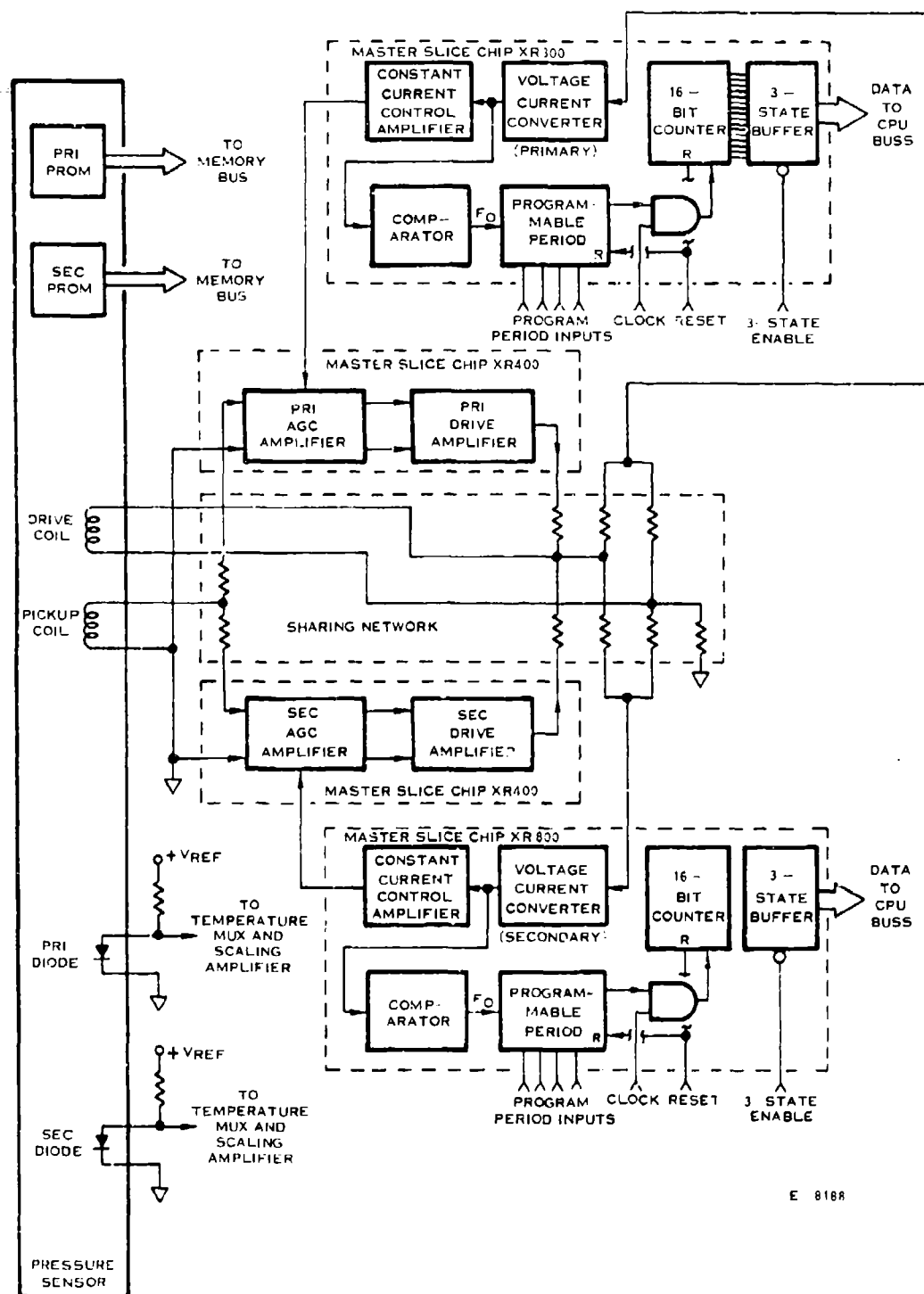
3.4.7.2 Circuitry

The pressure sensor electronics provide the necessary positive feedback for each transducer to sustain oscillation in its primary resonant mode. The pickup signal is amplified first by a variable gain stage and second by a fixed gain, bandpass amplifier. The filter elements in the second stage are chosen to provide the proper phase shift that will result in a loop phase shift of 360°. This gives maximum support to oscillation at the sensor's resonant frequency. Drive signal amplitude is controlled by sensing the AC drive current, precision rectifying it, and comparing the rectified signal to a DC reference. The resultant error signal is integrated and used to control the gain of the input variable - gain amplifier. The system frequency is sensed at the output drive by a comparator and converted to a logic level signal.

The selected pressure sensor concept utilizes two I²L devices per sensor channel, greatly reducing board area and number of interconnects. The custom concept also includes the frequency to digital converter. The circuit (primary and secondary channels) for one sensor is shown in block diagram form in Figure 23. Also included is the resistor network necessary for mating the redundant electronics to common drive and pickup coils on the sensor.

3.4.7.2.1 Temperature Sensor Circuit Because the natural frequency of the vibrating cylinder is a function of both pressure and the ambient temperature, a temperature sense circuit is provided to measure the temperature at the sensor and provide the information as an analog signal through the A/D to the processor. Placed at the top of the spool body is a diode, which is selected for its temperature coefficient.

3.4.7.2.2 Digital Correction PROM Each pressure sensor is packaged with specific compensating digital data. Raw data received from the sensor in an uncompensated form has variations in linearity with pressure level and temperature induced shifts. The calibration process to which each sensor is subjected establishes exactly how much compensation each sensor requires to accurately convert its frequency output to a precise digital number. This compensating data is then permanently programmed into a PROM Memory chip where it can be addressed by the computer each time the sensor is addressed. The determination of the normalization scale, cubic coefficients, adjusted counts, pressure and temperature maps are determined and converted from engineering units (volts,



E 8168

FIGURE 23 SENSOR CIRCUIT BLOCK DIAGRAM

psi, etc) to programmable binary information in PROM format by computer. Inputs to the computer are the data taken on each pressure sensor during calibration.

3.4.8 Low Level DC Interface

The low level interface (Figure 24) multiplexes four low level signals into a high impedance instrumentation amplifier. The signals are amplified to a 0-10V level and multiplexed along with the TBT signal into the analog-to-digital converter buffer. The buffer provides a higher current drive for the A/D converter. The circuitry is reduced by using multiplexers having internal protection. Note that the primary RAECC channel requires two of these interfaces, while the secondary requires only one.

3.4.9 Resolver Multiplexer

This resolver multiplexing scheme (Figure 25) employs an improved CMOS technology known as dielectrically isolated CMOS. The selected multiplexing devices have internal protection which makes possible the elimination of considerable external protective hardware.

3.4.10 Discrete Signal Conditioner Circuit

The discrete signal interface (Figure 26) inputs three discrete switch closures, a LOD detector, and a serial data stream transmitting the mach number. The discrete switch closures are conditioned with a diode resistor network that provides well defined logic levels to the I/O ports of the 8041 universal peripheral interface. The 8041 is also used to read the serial data stream and transfer the mach number to the main CPU. The LOD detector output is rectified and used to charge the capacitor which is monitored by the A/D converter to determine if a "light off" condition is present.

This approach utilizes a minimum amount of hardware and at the same time simplifies some of the CPU's tasks through distributive processing fault detection concepts.

3.4.11 Frequency to Digital Speed Interfaces

The speed circuit is an 8253 programmable counter to convert N_L and N_H frequency to digital information. The counter is configured as a divide by N counter which is used to enable a high frequency clock into a 16 bit counter also contained on the 8253. The signals are conditioned by using a quad comparator that converts to the proper logic levels internally. The comparators are provided with hysteresis to minimize the effects of noise on low frequency conversions. Diode protection is also provided to protect the comparator inputs from overvoltage transients (Figure 27).

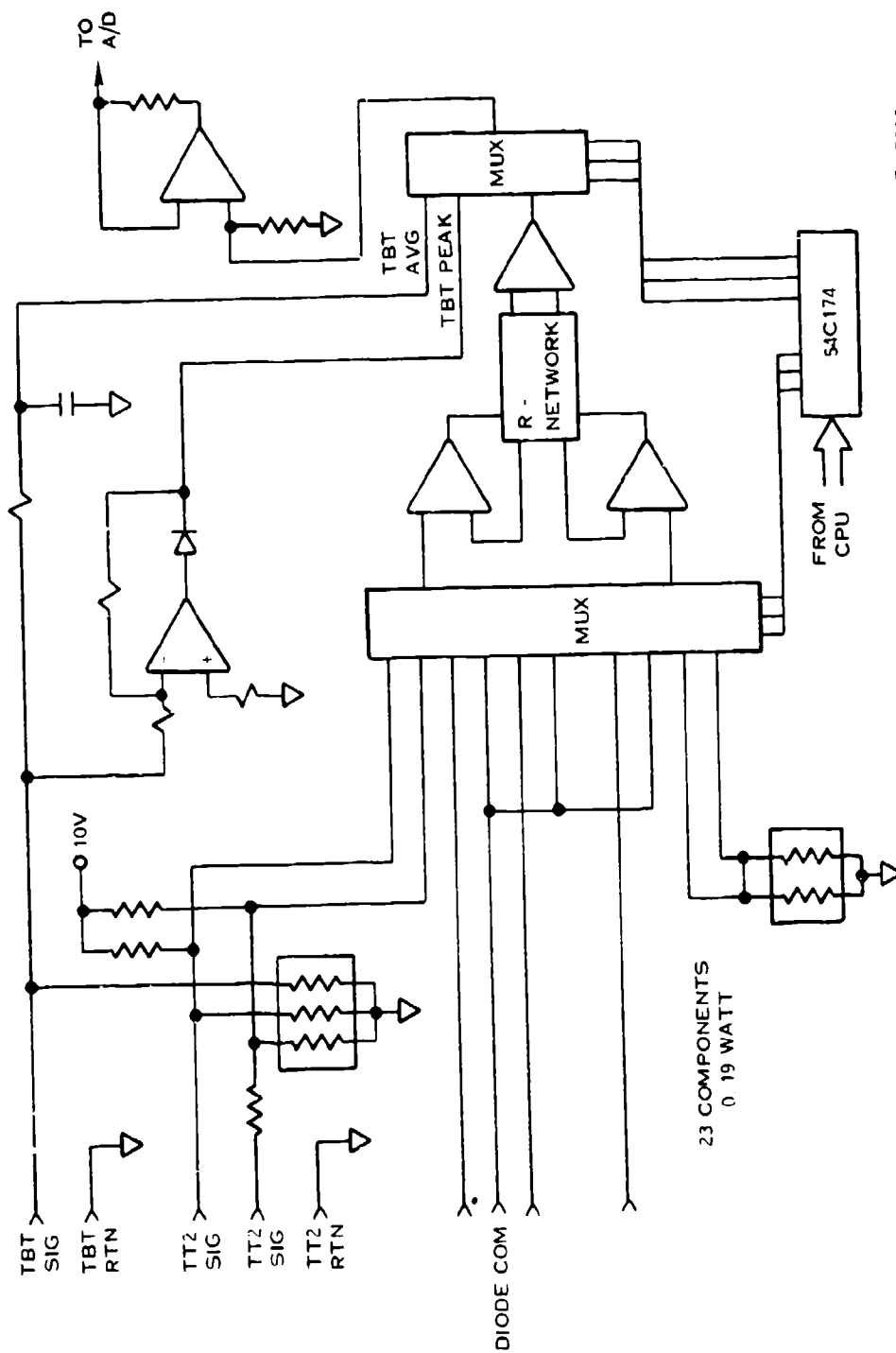
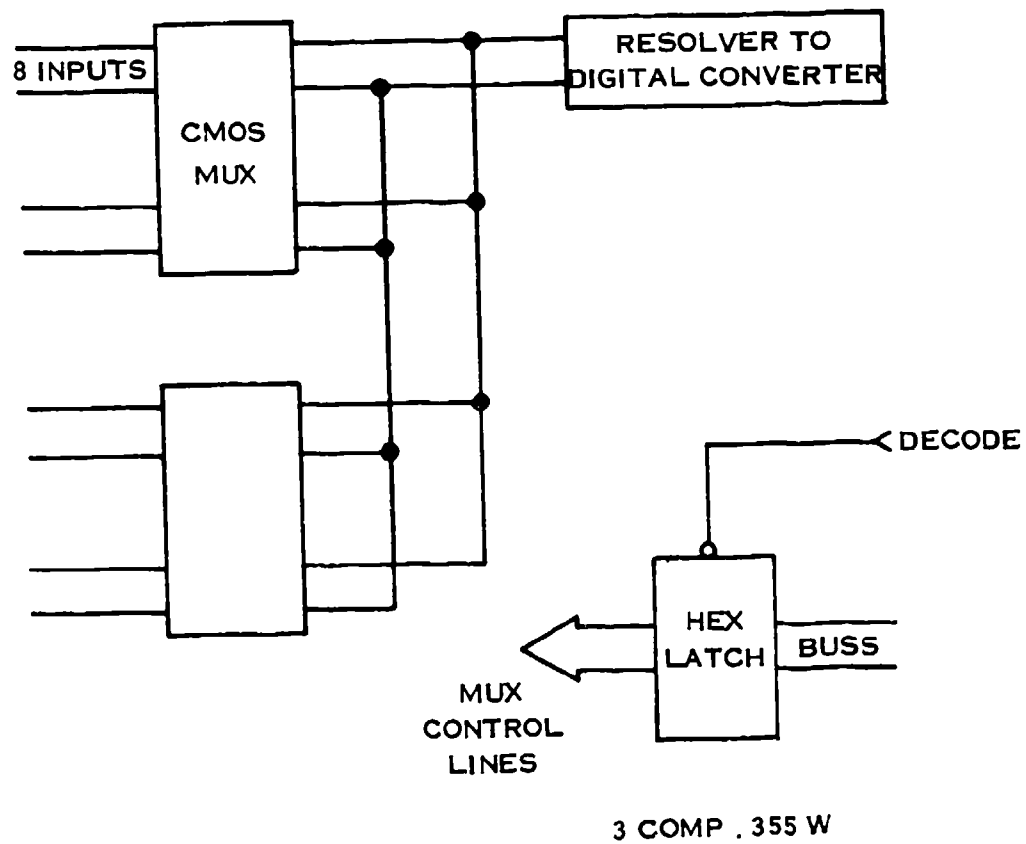


FIGURE 24 LOW LEVEL INTERFACE



E- 5821

FIGURE 25 RESOLVER MULTIPLEXER

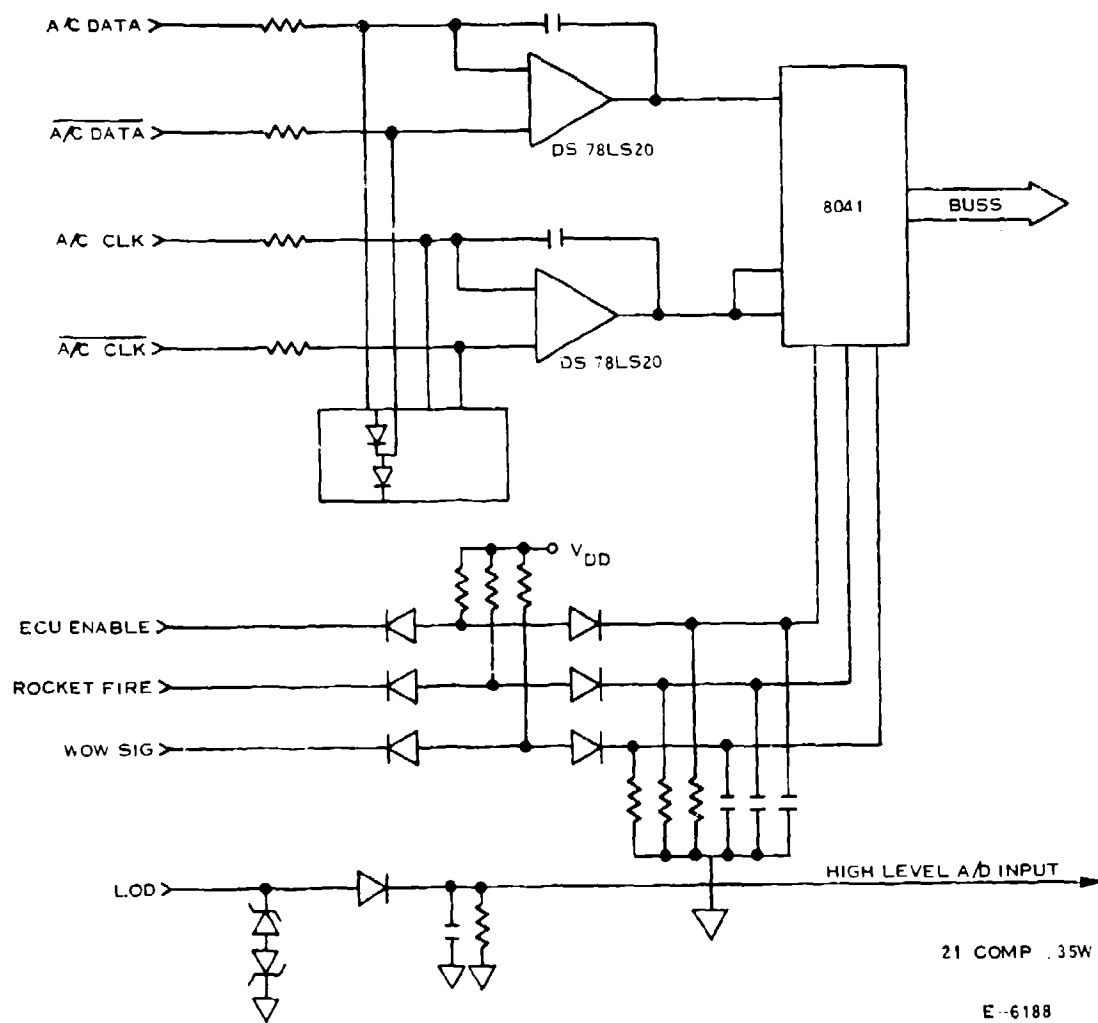


FIGURE 26 DISCRETE SIGNAL CONDITIONER

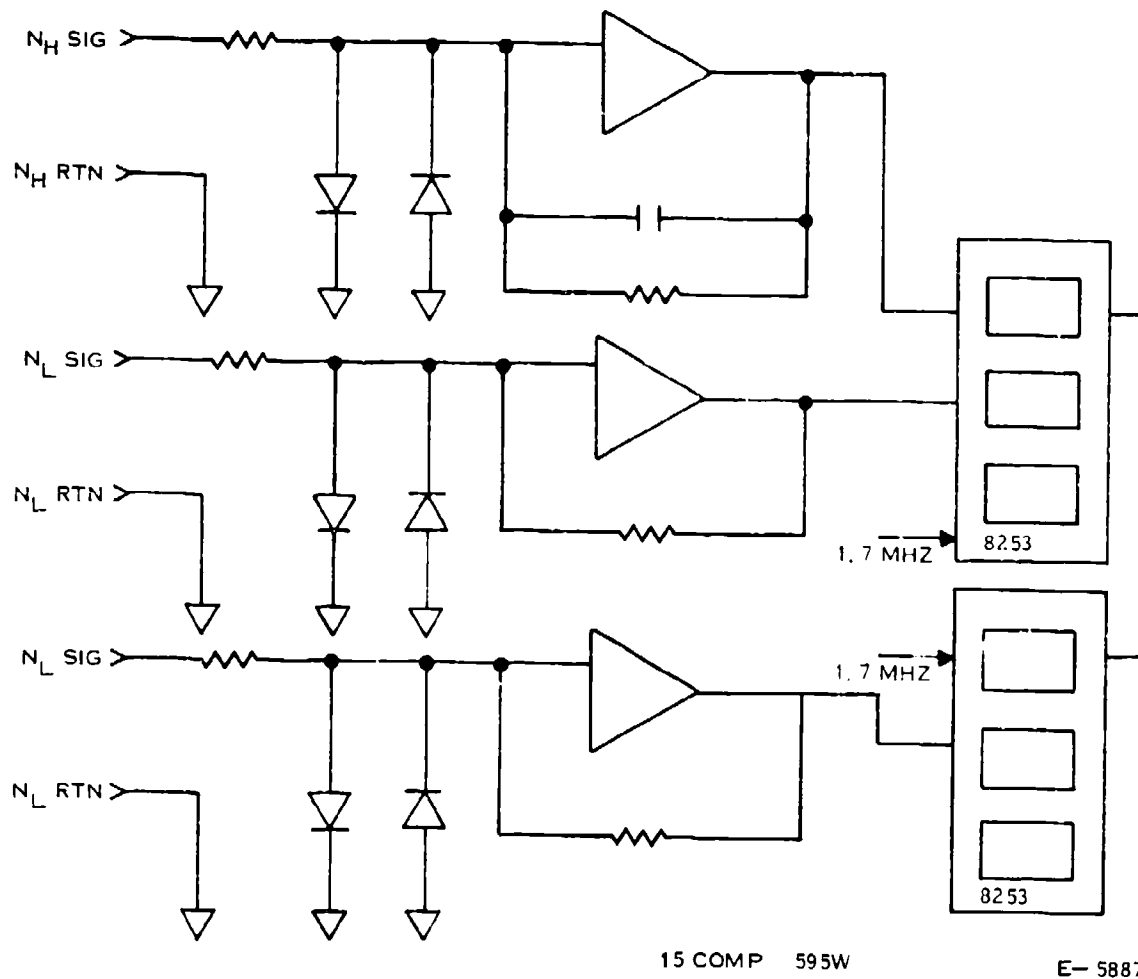


FIGURE 27 SPEED INTERFACE

3.4.12 Turbo Pump Speed Interface

The turbine pump speed interface inputs a pulse train from a magnetic pickup. The frequency of the pulses is proportional to the turbine pump speed. The pulses are converted to logic levels with a comparator and fed into a universal counter chip. This chip is programmed to count a specified number of periods and gate a high frequency clock into a self contained counter. The final count can be read by the CPU to determine turbine pump speed (Figure 28).

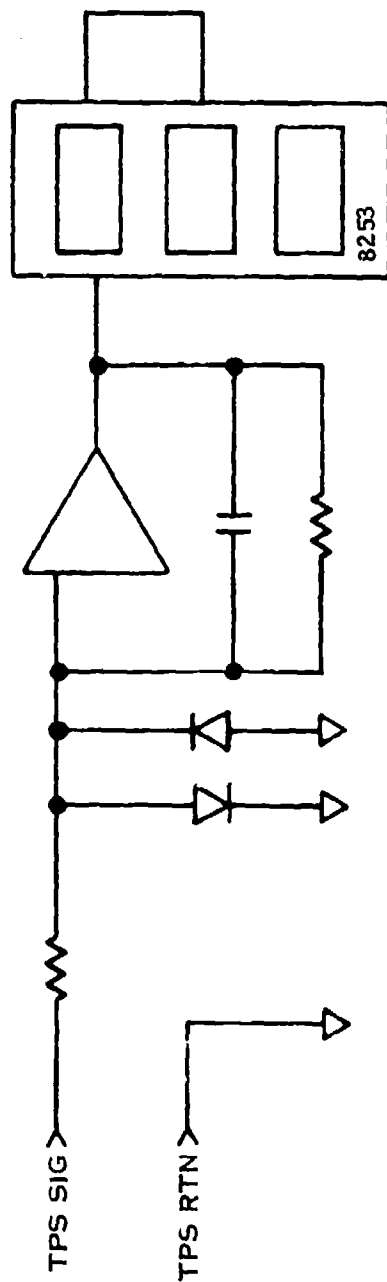
3.4.13 Fault Detection Logic

The primary channel receives four fault signals from the secondary channel. The secondary channel also receives four fault signals from the primary channel. A buffer and peripheral resistors are used for each signal path to interface the two channels. The fault signal paths for both channels are of a CMOS design with the constraint that no input signals can be present when the system is not energized. The power supplies from the two channels are OR'ed and then fed to both fault detection logic circuits. This ensures that both fault detection circuits will be powered if either channel is powered, thus satisfying the constraint that no input signals can be present when the system is not energized (Figure 29).

3.4.14 Power Supply System

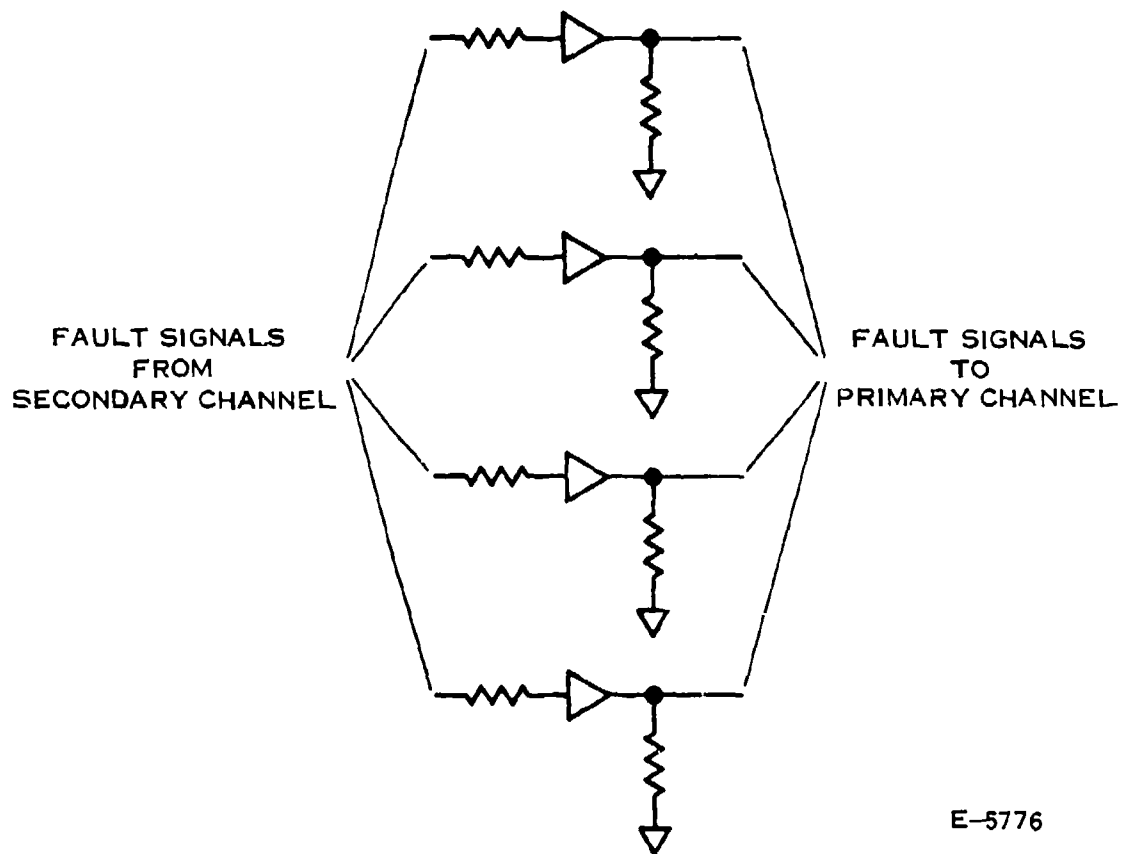
The power source is a voltage controlled "flux switching" type alternator. Input power is rectified and capacitor filtered. The rectified voltage (20 VDC) is sensed and compared with a reference. The resultant error signal is amplified and used to control the field of the alternator, thus maintaining a constant 20 VDC from the alternator. The +20V is used to power all solenoids, the +15V regulator and the +5V regulator. The +5V regulator is a pwm switching type regulator. The +5V powers all of the logic and memory circuits. The +15V regulator is a series monolithic regulator. The +15V supplies the positive rail for analog circuits and torque motors, the +10V reference, and an inverter from which negative voltages are developed. The inverter is operated in sync with the +5V switching regulator to preclude any beat effects. Inverting action is accomplished through a transformer with transistor push-pull drive. -15V, and any other negative voltages that may be desired, are derived from the transformer secondary. -15V supplies the negative rail for analog circuits and torque motors.

A comparator monitors +5 for overvoltage and has authority to decrease the +20V bus if an overvoltage condition is detected. Three additional comparators monitor +5 for low voltage and +10 for high or low voltage. All four comparators have authority to generate a power supply reset (PSR) signal if voltage is out of tolerance. (Figures 30 and 31, and Table 11.)



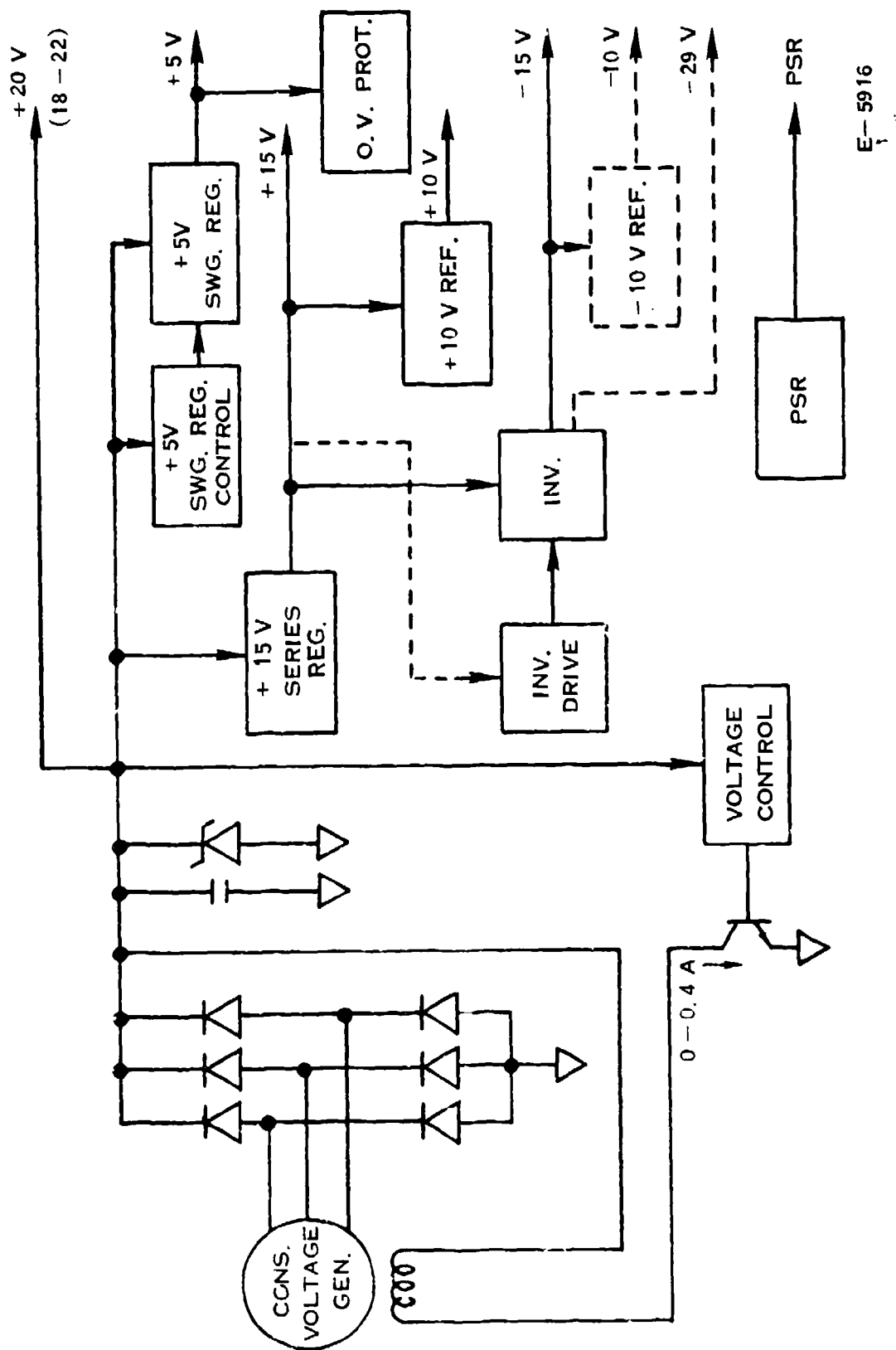
E-- 5868

FIGURE 28 TURBINE PUMP SPEED INTERFACE



NOTE: THE CIRCUIT IS REPEATED FOR THE OPPOSITE
DIRECTION (FROM PRIMARY TO SECONDARY)

FIGURE 29 FAULT DISCRETES



E-5916

FIGURE 30 POWER SUPPLY BLOCK DIAGRAM

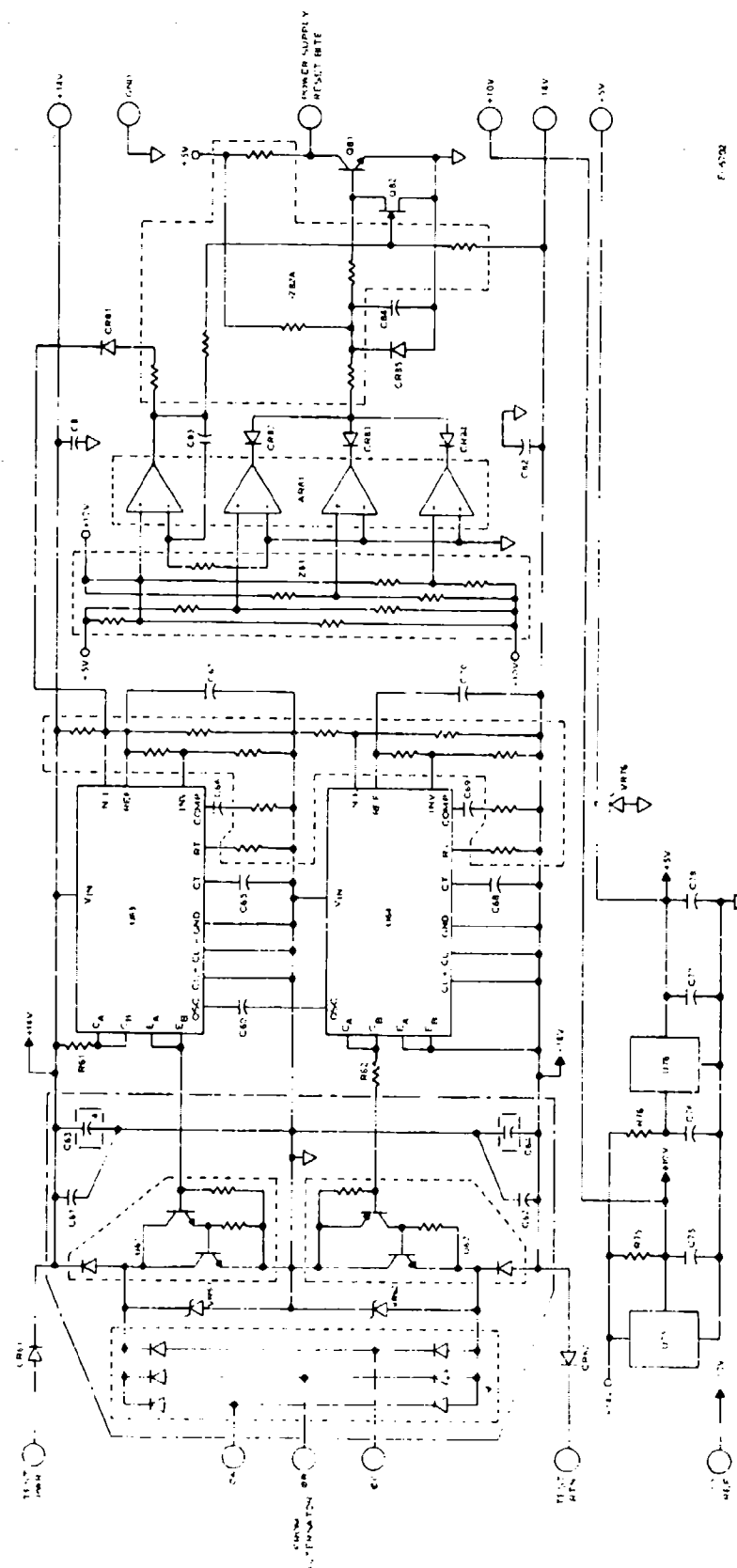


FIGURE 31 A/C INTERFACE, POWER SUPPLY SYSTEM

TABLE 11 POWER SUPPLY REQUIREMENTS

Power Supply Load Rating

<u>VOLTAGE</u>	<u>CURRENT</u>
+5V	.90A
+10V	.015A
+14V/+15V	.30A
-14V/-15V	.40A
+20V	3.10A

Typical Power Dissipation*

Prime	Input Bridge		3.40W
	Alt. Volt. Control Crt.		3.40W
	+15V Series Reg		4.68W
	Inverter & -15 Supply		1.50W
	+14V Shunt Reg		-
	-14V Shunt Reg		-
	+10V Reg		0.10W
	+5V Reg		1.75W
	PSR/OV		0.10W
	LOD in Standby		0.10W
	Power Supply Sub Total		15.53W
	EEC Digital	4.0	
	Analog	6.15	
	Drivers (Series Prop)	3.35	
	Total Non P/S		<u>13.50W</u>
	Total EEC		29.03W
Secondary			<u>29.03W</u>
	Total		58.06W

* Load Assumptions:

20V Solenoids @ .3A	3
Torque Motors .05A/.15A	+15V/-15V
Analog Load .2A/.2A	+15V/-15V
+10V Load	.015A
+5V Load	.8A

3.4.15 CPU Design

During the design phase of all the circuits involved in the trade study of Appendix A, it was realized that in several areas, it was more profitable both from a reliability improvement and a parts count reduction stand point, to use a single-chip microcomputer (like the 8048, for example) instead of all the discrete logic it replaced. When the studies were completed, the final RAECC design choice actually comprised six processors: the main CPU, and five I/O processors, as shown in Figure 32. This system became a distributive processing array, which simplified the task load on the main CPU. Since this system is actually a loosely-coupled parallel processing array, the resulting throughput is far in excess of what the simplex baseline design presented. As an example, the baseline CPU was responsible for all Built-In Test logic required to check itself and all interfaces; however, the final RAECC I/O processors will now be responsible for performing their own Built-In Test, relieving the main CPU for other tasks. Another example: in case of the untimely demise of the main CPU the Dual-Port Link Alive Processor will communicate with all surviving I/O processors, and then communicate the I/O data through the dual-port link to the other RAECC channel.

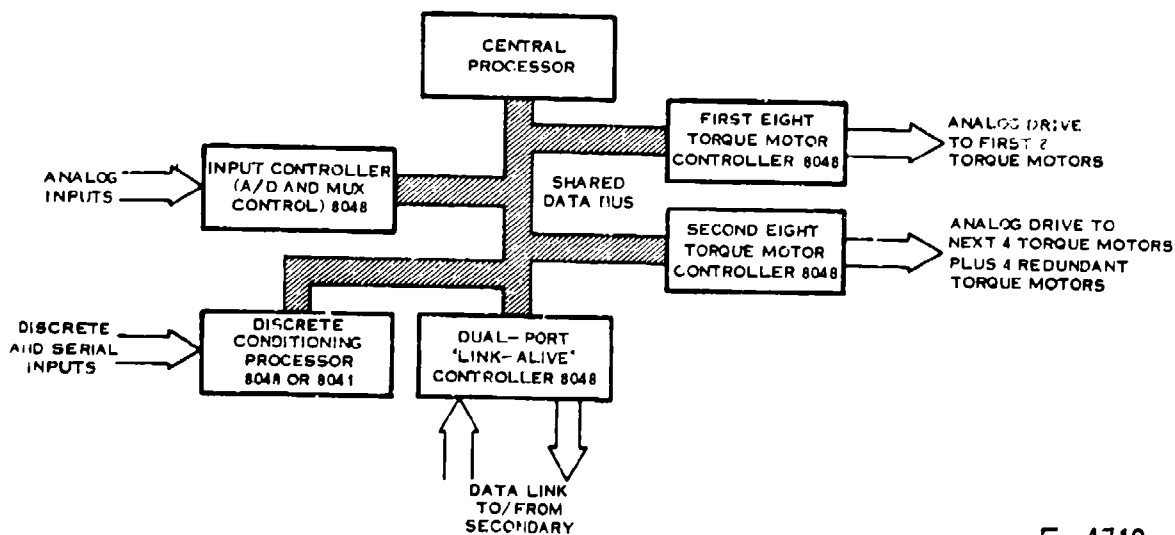
The computer architecture "Bottom-Line" is shown in Table 12. This summary presents the results of several complete CPU trades at a glance, including the final RAECC Single Instruction Single Data (SISD) design. The reader should note that the Design Recommendation Computer is only 2.4% better in reliability points than the Basic 2901 computer, but the final RAECC design recommendation computer also requires 24% less board area, and requires 391% less power. These other factors may have a larger effect than 2.4% on the final design than normally expected, since junction temperature (and reliability) will be a function of board area (final box size) and the power dissipation of surrounding components.

3.4.15.1 Processor Choice

The chosen processor is a 12 component 3 chip configuration which can be implemented in several semiconductor technologies and in either a semi-standard or custom manner. One configuration would use the CMOS/SOS HS 16/24. A second would use the same architecture but implemented with semi-standard gate arrays. The gate arrays would be made with either CMOS or T2L semiconductor technology. Selection of architecture which can be implemented several ways provides a freedom to select the final technology based on actual strength and availability of semiconductor sources rather than on projections of such sources.

The main CPU will be described as the CMOS/SOS HS 16/24 with the understanding that this might be implemented with CMOS or 12L gate arrays.

The processor was chosen only by the reliability score, (the exact same scoring system used on all other circuits), but could have been chosen on other merits as well.



E-4719

FIGURE 32 RAECC DISTRIBUTIVE PROCESSING

TABLE 12 COMPUTER ARCHITECTURE "BOTTOM-LINE"

COMPUTER ELEMENT	SISD OR SIMD MACHINE				MIMD MACHINE MULTIPLE OFF-THE-SHELF MICROPROCESSORS	FAULT TOLERANT "2900" TRD MACHINE
	BASELINE RAECC	FINAL RAECC	MOST "RADICAL" ALTERNATE	BASIC 2901 MACHINE		
PROCESSOR	24.4 in ² 0.79 w	5.13 in ² 0.32 w	5.13 in ² 0.32 w	12.39 in ² 11.65 w	7.51 in ² (For both) 3.88 w	51.00 in ² 47.96 w
RAM	9.94 in ² 0.24 w	2.20 in ² 1.62 w	1.98 in ² 0.10 w	2.20 in ² 1.62 w	3.24 in ² (For both) 3.2 w	2.20 in ² 1.62 w
ROM	27.3 in ² 6.62 w	4.01 in ² 0.87 w	3.72 in ² 0.31 w	4.01 in ² 0.87 w	3.58 in ² (For both) 1.2 w	4.01 in ² 0.87 w
TEST UART	5.5 in ² 0.09 w	2.38 in ² 0.09 w	2.38 in ² 0.09 w	2.38 in ² 0.09 w	1.95 in ² 0.51 w	2.38 in ² 0.09 w
I/O ADDRESSING	6.74 in ² 0.31 w	6.74 in ² 0.31 w	0.496 in ² 0.10 w	6.74 in ² 0.31 w	2.9 in ² (Incl. Bus Arbitration) 5.48 w	6.74 in ² 0.31 w
DUAL PORT	26.44 in ² 1.066 w	9.48 in ² 0.682 w	7.23 in ² 0.417 w	9.48 in ² 0.682 w	3.34 in ² 2.63 w	9.48 in ² 0.682 w
TOTAL	100.32 in ² * 9.116 watts	29.94 in ² 3.89 watts	20.94 in ² 1.337 watts	37.20 in ² 15.22 watts	22.52 in ² 16.90 watts	75.81 in ² 51.53 watts
RELIABILITY PICK	5	1	4	2	6	3

* CONVENTIONAL PACKAGES; DIPs, FLATPACKS, ETC.

E-2645

The main advantages of this processor over others considered are:

- Best reliability score
- Lowest power dissipation (320 milliwatts)
- Smallest board area
- Very good throughput (>666 KOPS)

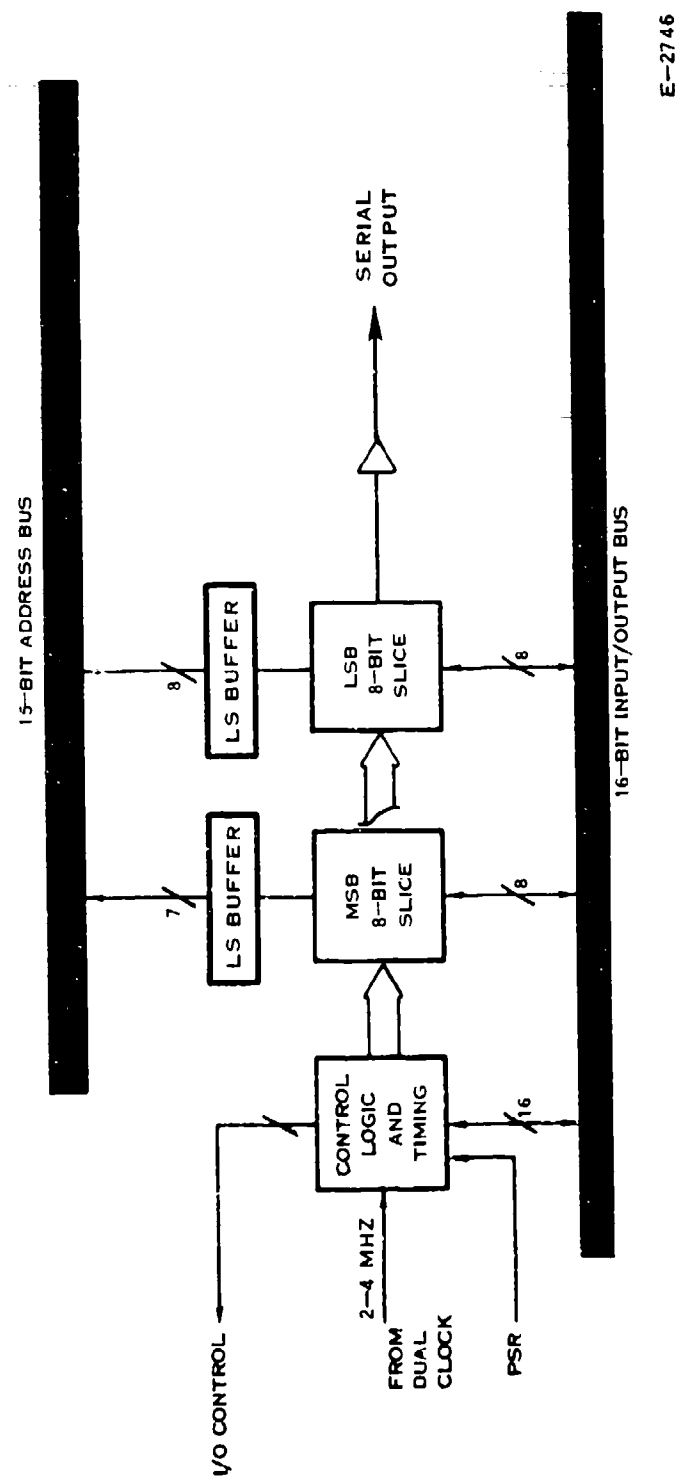
Custom Processor

Several system houses, including Hamilton Systems Division of Hamilton Standard, have been forced into the development of their own proprietary custom processors in order to provide a military, competitive, minimum component, low power machine with adequate performance. Hamilton Standard has designed its own CMOS Silicon-on-Sapphire processor to meet the system needs of the 1980's as shown in Figure 33. It is designated the SOS HS 16/24 since it can be configured as a 3-chip 16-bit machine, or as a 4-chip 24-bit machine. The custom chip set, when configured as a 16-bit parallel machine, comprises one "Control/Timing" chip and two "8-bit slice" chips, plus five standard SSI devices and four decoupling capacitors. These 12 components dissipate a total of 0.32 watts and will execute the fuel control instruction mix at 666 KOPS when configured with MOS RAM and ROM. This machine easily meets the "450 KOPS" minimum, and could therefore be slowed 30%; however, by the time that a RAEEC system flies, this extra capacity may be required for future tasks. Please refer to the summary shown in Table 13.

CPU Architecture

The HS 16/24 CPU is a flexible, controls-oriented, CMOS LSI, bit parallel, fractionally scaled two's complement, combinational logic, state machine. Designed initially for either 16- or 24-bit word lengths (16 bits for fuel controls and 24 bits for navigational computations), it may be operated with clock rates from 0 to 1 MHz (0 to 4 MHz clock input), supply voltages from 0 to -15 VDC, and temperatures from -55°C to +125°C. It is structured as shown in Figure 34 with six dedicated registers, a program incrementer, an arithmetic logic unit (ALU), all "hard-wired"* control logic and timing. The CPU's 37 instructions are designed to operate with a microinstruction controlled clock which can synchronously vary the microinstruction execution times between 500 nanosec and 2.0 microsec, allowing all instructions to be executed with maximum speed efficiency. Instruction execution times are also minimized via overlapped Fetch/Execute cycles, look-ahead carry in both arithmetic unit and register unit adders, and judicious selection of all register transfer paths to allow multiple register transfers to occur simultaneously.

- * A microprogrammable control store was designed for this machine, which unfortunately comprised some 20 components (including 5 ROMs), which were deemed far less reliable and slower than the hard-wired control logic which replaced them.



E-2746

FIGURE 33 THREE-CHIP HS 16/24 MACHINE

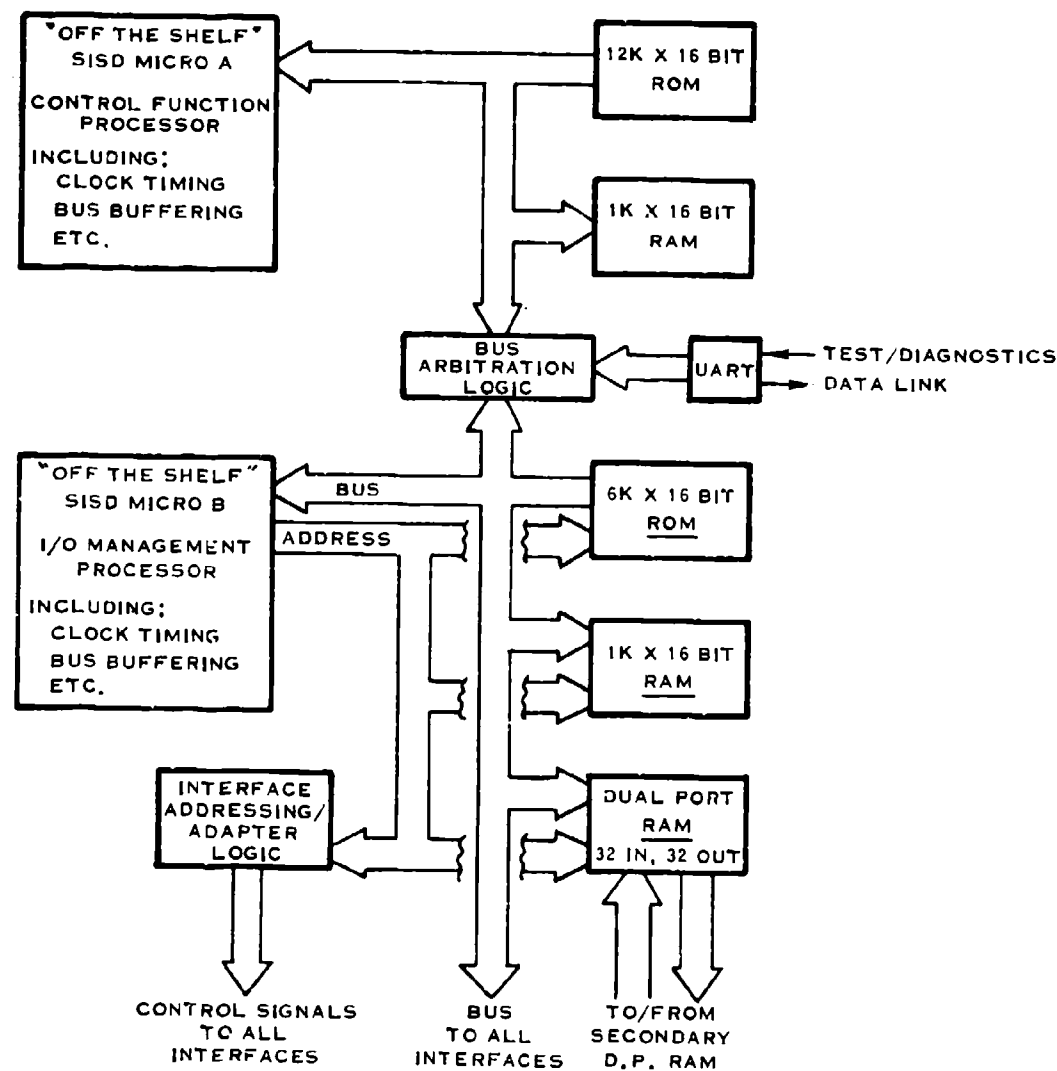
TABLE 13 SINGLE INSTRUCTION SINGLE DATA CPU

FEATURE	3-CHIP HS 16/24 IN DEVELOPMENT
# OF COMPONENTS	12
# OF SOLDER JOINTS	264
BOARD AREA (IN ²)	10.0 (5.13*)
CUSTOM LOGIC	YES
MAX THROUGH-PUT	>666 KOPS**
POWER DISSIPATION	.32 w maximum
RELIABILITY RATIO	226

* IMPROVEMENT USING LEADLESS CARRIERS

** ALTHOUGH MUCH HIGHER SPEEDS ARE OBTAINABLE (1 "MIP" FOR 2900 IS COMMON TODAY), THROUGHPUT IS LIMITED BY THE RELATIVELY LONG 300 ns MEMORY ACCESS TIME.

E-2646



E-2232

FIGURE 34 RAECC CPU BLOCK DIAGRAM (FOR A PARALLEL MULTIPLE INSTRUCTION MULTIPLE DATA MACHINE ARCHITECTURE)

CPU Hardware Implementation

The digital logic required to implement the HS 16/24 CPU design was partitioned into two different custom LSI types. A total of three of these LSI devices are required for the complete 16-bit processor design: one Control Logic/Timing CMOS SOS VLSI module (5E8065/10) and two 8-bit Register/ALU CMOS SOS VLSI modules (5E8065/09).

Register/ALU Description

The arithmetic logic unit performs the actual execution of all arithmetic and logic instructions. An arithmetic instruction always involves two operands that must be combined. One of the operands is specified in the address portion of the instruction word and comes from memory or an input device. The other operand is already in the A register of the arithmetic unit as a result of a previous instruction. The operation code portion of the instruction word specifies exactly how the two operands are to be arithmetically or logically combined.

There are six dedicated 16-bit parallel registers associated with the arithmetic and register units.

CPU Throughput

The performance of a processor may be measured in its throughput, or given a particular instruction mix, the maximum number of instructions that it will process in one second. While on the other hand, the figure of merit of a processor may be measured in its throughput per watt or kops/watt, where kops is thousands of operations per second. The instruction mix used in calculating throughput is derived from the actual program used in a recent breadboard designed for an engine fuel control. Based on this mix, the predicted throughput is 666 kops.

Watchdog Timer

The watchdog timer is a hardware built-in test circuit which is used to detect and either correct or flag a hung CPU condition. Its primary function is to eliminate any infinite looping that may occur as a result of a lightning discharge or other abnormal transient. This looping condition is quickly detected by the timer as the timer must be reset by the CPU after each CPU control loop. When the CPU is hung, the timer is not reset and the error is detected. A reset pulse is given to the CPU in an attempt to restart it. All output effectors are also reset at this time and, if the CPU does not recover, the LRU fault indicator is latched and the secondary is notified via the three emergency fault-status lines that it is now in full control.

3.4.15.2 Random Access Memory

The Random Access Memory chosen for the RAEEC is an all N-channel RAM. A 1024 word RAM block diagram is shown in Figure 35. Table 14 summarizes some of the RAM design features from the trade study of Appendix A.

3.4.15.3 Read Only Memory

All N-channel ROM was selected for the final RAEEC design. Among other things, this implementation enjoyed the highest reliability rating in the trade study of Appendix A (Table 15).

3.4.15.4 I/O Addressing Logic

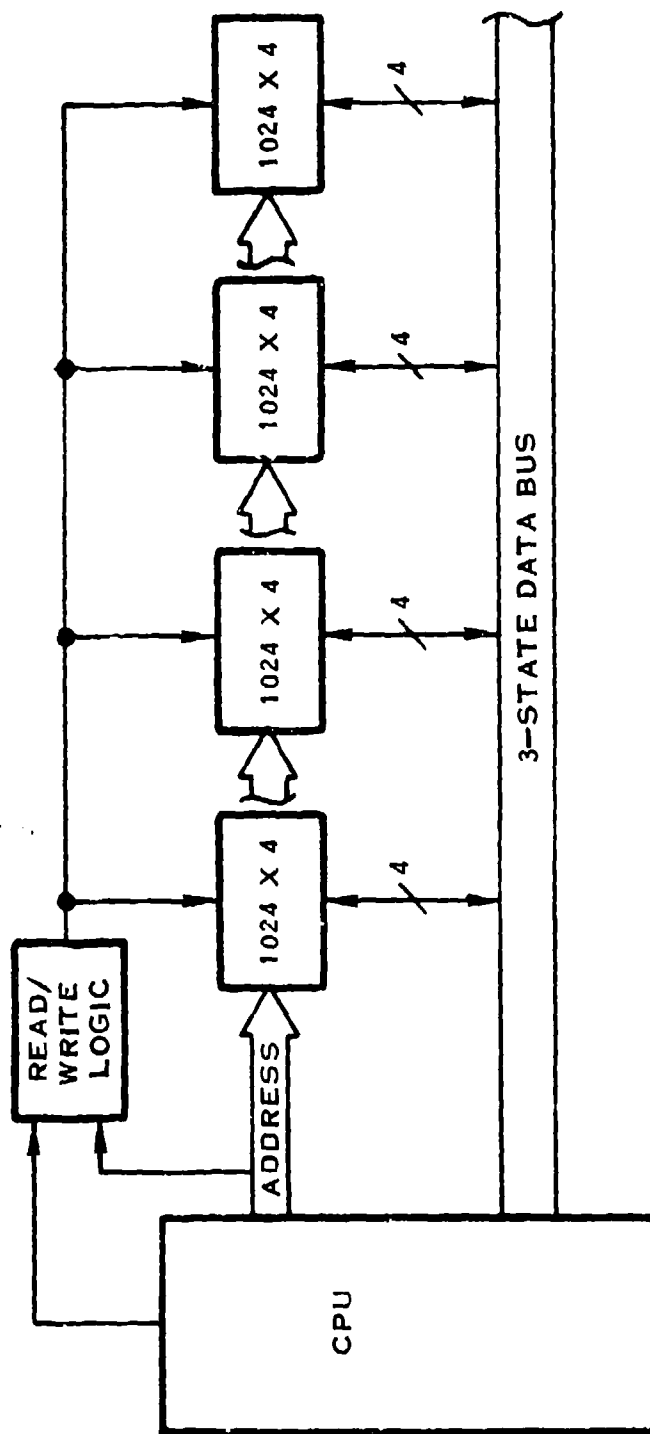
Every computer system requires a block of logic for special addressing functions, such as input/output interface enables, special memory enables, and special read/write signals. In small microprocessors, this logic might comprise a group of LSI chips known as "Peripheral Interface Adapters", plus a few SSI buffer chips.

The final RAEEC I/O design (Figure 36, Table 16) is the same as the baseline's (Appendix A). This combinational logic comprises 18 SSI and MSI components for implementing this function.

3.4.15.5 Dual-Port RAM

The "Dual-Port RAM" logic is possibly the most critical link to the success of the RAEEC program. This system must transfer information transparently between the two processor channels, and is therefore, referred to as a dual-port RAM system, since each processor has dual-port like access to the other's critical data. The actual "D-P RAM" interface design involved three individual trades; (a) method of data transmission between processors, (b) type of dual-port logic to be utilized, and (c) survivability of the data link in the event of a processor failure.

The transmission scheme selected in the trade study of Appendix A is serial transmission of word data. This system requires the fewest number of lines in each direction; one if single ended or two if the transmission is dual differential to avoid potential ambiguity. Since "UART" devices are relatively inexpensive, MIL-qualified and multiple sourced, and can simultaneously transmit and receive serial data, a UART was chosen for this purpose.



E-2612

FIGURE 35 1024 WORD RAM

TABLE 14 RAECC RAM DESIGN

FEATURE	RAECC ALL N-CHANNEL
# OF COMPONENTS	9.5
# OF SOLDER JOINTS	116
BOARD AREA (IN ²)	3.98 (2.20**)
POWER (WATTS)	1.62
MAX CYCLE TIME	450 ns
MAX ACCESS TIME	450 ns*
RELIABILITY RATIO	326

* THE CPU THRU-PUT WILL LIKELY BE REDUCED WITH THIS ACCESS TIME; A "WAIT-STATE" MAY BE REQUIRED.

** IMPROVEMENT USING LEADLESS CARRIERS

E-2648

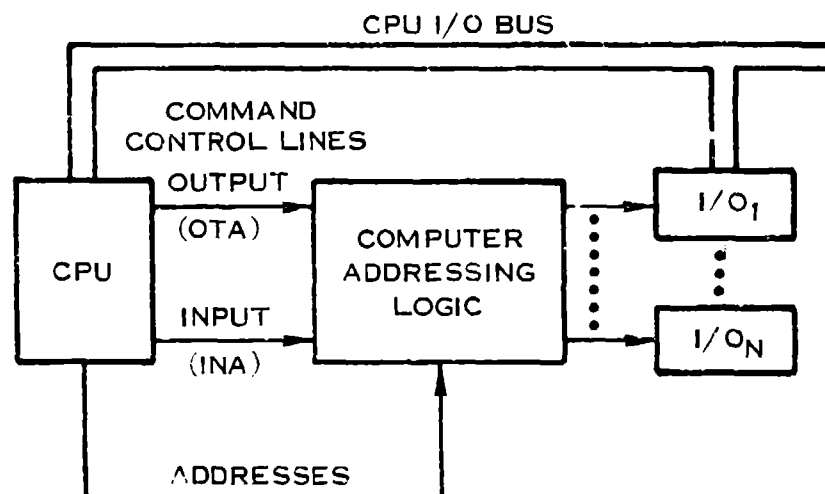
TABLE 15 RAEEC ROM DESIGN

FEATURE	ALL ROM (N-CHAN)
# OF COMPONENTS	14 1/6
# OF SOLDER JOINTS	210
BOARD AREA (IN ²) (1)/(2)	10.2/4.01
POWER (WATTS)	0.87
MAX ACCESS TIME	300 ns*/100 ns
CUSTOM MASK REQD?	YES (4)
PRODUCTION RECOMMENDATION	YES
RELIABILITY RATIO	212

(1) AREA USING CONVENTIONAL DIPS (2) AREA USING LEADLESS CARRIERS

- * "WAIT STATE MAY BE REQUIRED FOR MEMORY REFERENCED INSTRUCTIONS (POTENTIALLY REDUCING KOPS)
- ** SOS AND CMOS EXCITED WITH 5 VDC

E-2650



E-8185

FIGURE 36 I/O ADDRESSING

TABLE 16 RAECC I /O ADDRESSING

ITEM	FINAL SYSTEM
# OF COMPONENTS	18
# OF SOLDER JOINTS	180
BOARD AREA (IN ²)	5.74 (4.23*)
POWER (WATTS)	0.31
CUSTOM PARTS	NO
RELIABILITY RATIO	LCC DIP 307/302

* IMPROVEMENT USING LEADLESS CARRIERS

E-2651

D-P RAM Logic

Once the transmission medium was selected, the actual dual-port RAM logic was developed and studied. The five different approaches studied are described briefly below:

1. Real Time DMA (Cycle Steal)

This approach provides the fastest data access with the least data transport delay. However, it requires a very fast memory ($t_{\text{access}} < 100 \text{ ns}$) so that one machine isn't slowed by the one performing the DMA, and it requires full parallel access (all 16 bits of data) to prevent data change during a DMA cycle.

This concept has the advantage of being transparent to both CPU's.

2. DMA Block Transfer

This concept actually involves the halting of a machine for the time it takes to effect a complete transfer of data. Although fast, it runs the risk of an additional failure mode, whereby the transfer logic could paralyze a processor by holding it in a DMA mode.

3. Asynchronous Data Transfer, With Handshake

This concept requires a mail-box latch or "FIFO" (First-In, First-Out) approach, where either a flag is monitored or a data ready interrupt is generated. In either case, extra overhead for both CPU's is required to maintain the data transfer. (Refer to AM 2950 8 bit parallel I/O port, Appendix A.)

4. Virtual Dual-Port RAM

This concept requires that several off the shelf dual-port RAM's be tied together to make a large enough cache; however, this system provides a real time data transfer, without any possible interference between the two machines.

5. Simulated Dual-Port RAM

This concept provides the advantage of transparency between machines, but adds an additional data transport delay which is a function of the data transmission concept utilized. Data is accessed on a cycle-steal DMA basis and then sent serially to a second cycle-steal DMA interface, where the data is transparently placed into the second machines RAM.

This was the concept used in the baseline, which was improved in alternate design #1, shown in Figure 37 and Table 17, and chosen for the final RAEEC design.

Alternate Backup Modes For a Failed Processor in a Dual Channel System

An obvious multiple failure situation that could occur and would result in a completely inoperable system, if link operation were dependent on the CPU, is when a central processing unit (CPU) in one channel fails and any other functional block in the other channel fails.

The real choices can be reduced to a few obvious alternatives. These alternatives all consist of ways of providing a backup capability for the CPU to either provide full capability, partial capability, or conditional capability. By this it is meant that full capability implies that the backup system has the same level of performance as the prime. Partial capability implies that the backup system has a lesser level of performance than the prime. Conditional capability means that backup capability may or may not exist depending upon the mode of failure of the prime and, for this discussion, that if backup capability can be provided it's performance level will be less than that of the prime.

The tabulated choices include the following:

1. Full Capability Backup Using an Additional, Identical CPU

The advantages of this approach are that the task for the CPU remains the same and therefore, does not entail reconfiguration, redefinition, or alternate modes of operation which would involve extra firmware; it also allows operation with no degradation of performance. The backup system is also allowed to remain idle, with no power applied. Consequently, the backup is a "cold spare", which is more reliable having accumulated no operating time.

The disadvantages are that the approach is expensive in hardware, and consumes considerable space. See Figure 38.

This microcomputer, the "link-alive processor", is shown with the dual-port logic in Figure 37.

2. Conditional Capability Backup Using The "Failed" CPU at Reduced Performance Capability

The advantages of this approach are that the cost, power and space requirements are less than those of the first alternative. Switching is not involved except for PROM devices, and isolation of failed hardware is a software rather than a hardware function. This approach also encompasses memory failures (PROM) since a separate, reduced performance memory replaces the main memory after a failure.

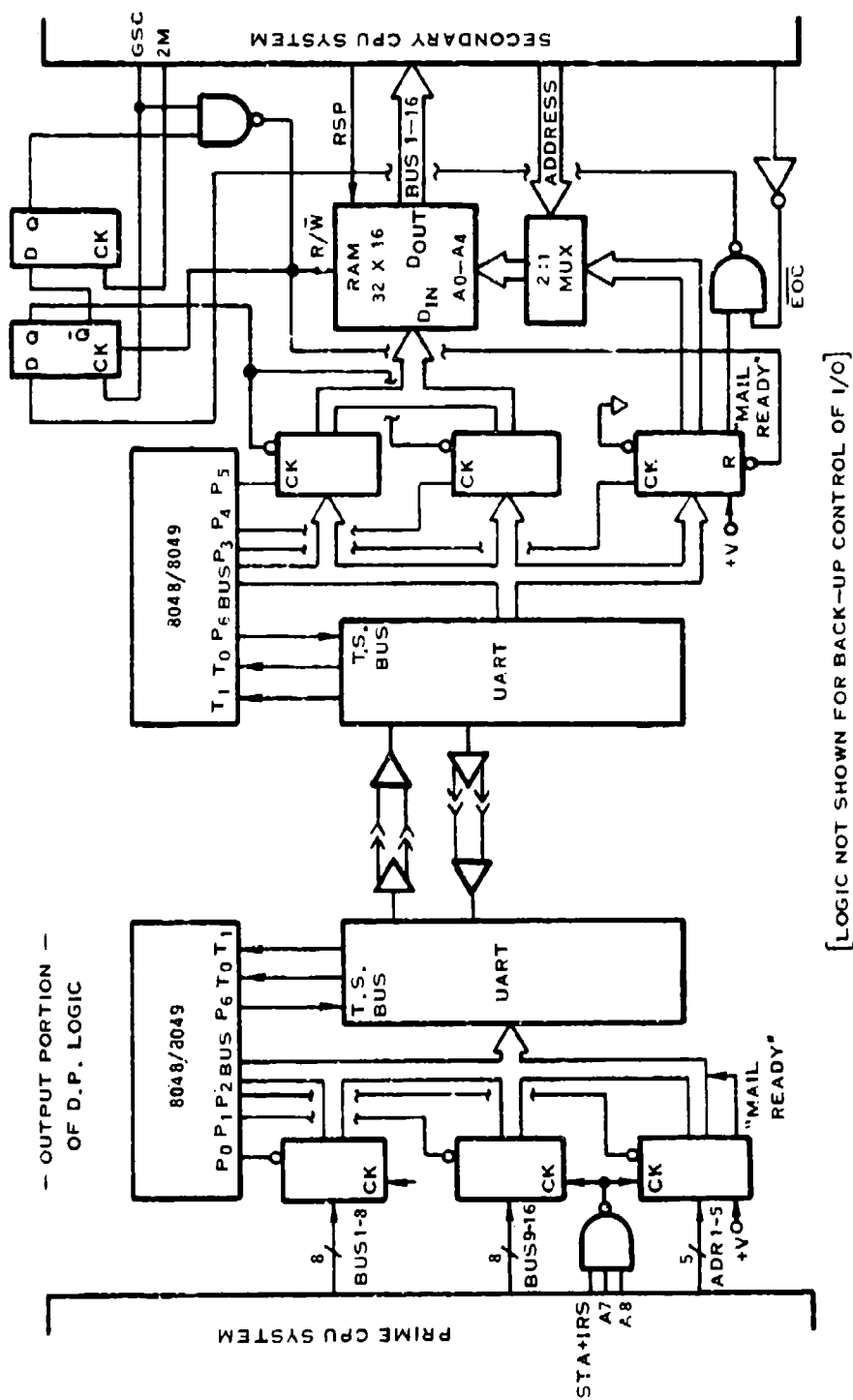


FIGURE 37 DUAL PORT RAM "IMMEDIATE TRANSFER"

TABLE 17 RAECC DUAL-PORT DESIGN TRADEOFFS

ARGUMENT	BASELINE D.P.	Alternate 1 (Final RAECC)	
		28	400
# OF COMPONENTS	42.66	37 1/3	28
# OF SOLDER JOINTS	624	477	400
BOARD AREA	26.44/12.27**	20.72/9.48**	17.58/7.23**
POWER (WATTS)	1.066/0.716*	0.682/0.332*	0.767/0.417*
CUSTOM LOGIC	YES (8048 PROGRAM)	YES (8048 PROGRAM)	YES (8048 PROGRAM AND CUSTOM LSI)
MAX TRANSPORT DELAY	5.6 ms (worst system delay 23.6)	0.728 ms per word - immediate - worst syst Δ = 18.728 ms	0.728 ms per word - immediate xfer - worst syst Δ = 18.728 ms
RELIABILITY RATIO	LCC DIP 205/195	219	210

NOTES: * LOWER POWER DISSIPATION IF INERSIL/RCA CMOS 8048 AVAILABLE

** IMPROVEMENT USING LEADLESS CARRIERS

E-2647

The disadvantages are that many failures will make the CPU completely inoperable rather than providing graceful degradation to a reduced performance mode. Software error detection schemes must be more sophisticated and therefore, consume more memory space.

By making certain assumptions, the last alternative yields the greatest increase in reliability for an incremental increase in redundancy and cost.

One of these assumptions is that the CPU's performance could be reduced to having the capability to do basic information transfers. Transfers such as inputting, outputting, register to memory and memory to register operations as well as a single conditional skip and a single jump operation. This rudimentary capability was assumed to be adequate for a minimum performance backup CPU. Another assumption is that error detection be limited to nonquantifying decisions so that any failure resulted in assuming performance capability degradation to the basic operations discussed. This last assumption yields a large pay back in the reduction of the sophistication of software, the amount of diagnostic software, the number of backup modes of operation, and the time necessary to achieve error detection.

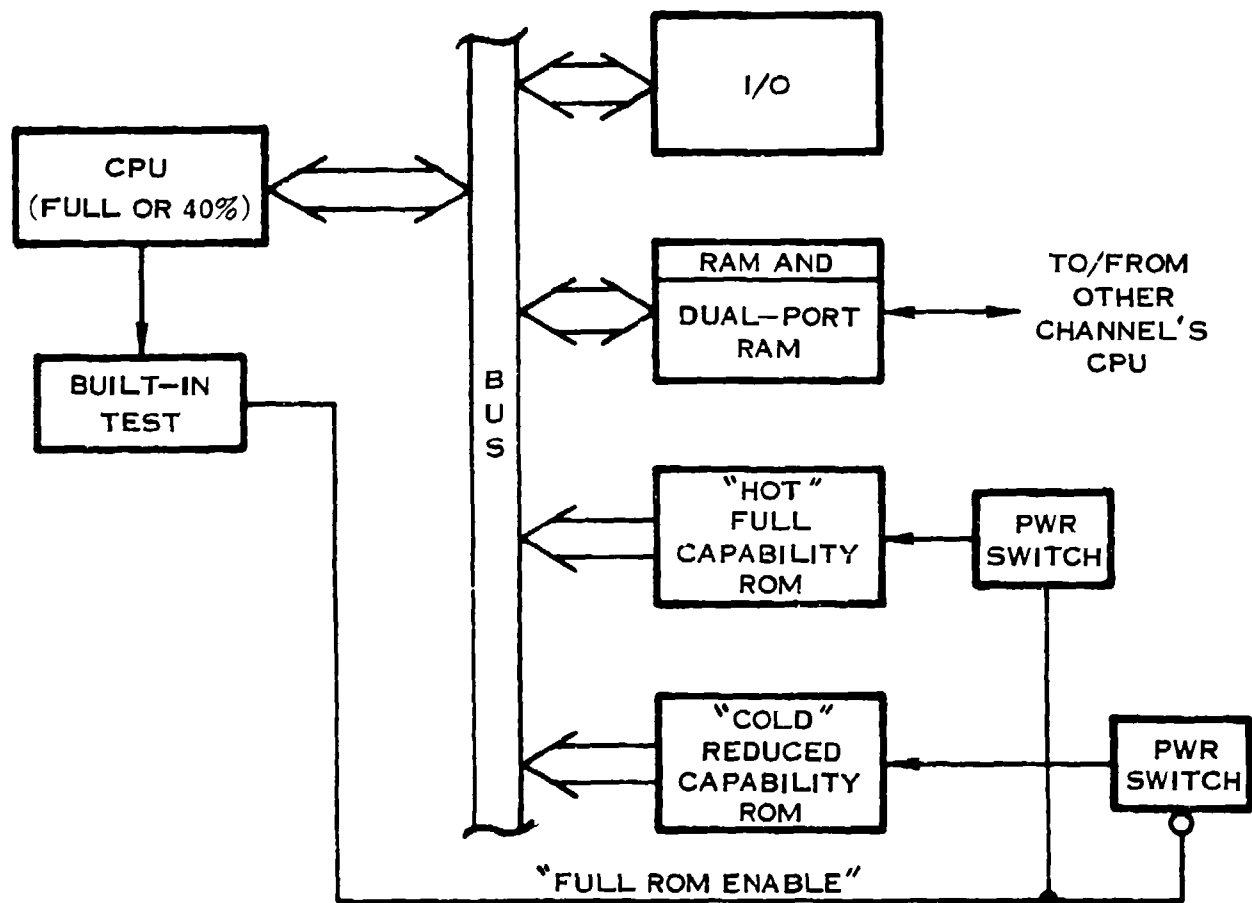
An investigation at the circuit level revealed that approximately 60% of the transistors on the chip could be stuck in either the high or low state (these were considered one at a time, not all at once) and an operable system could be maintained if limited to the discussed operations.

This approach requires that the failed CPU perform extensive diagnostics on itself, to determine which instruction has failed, and to branch to a backup I/O routine which does not contain the failed instruction. In this mode, the failed operable CPU provides I/O capability, via dual-port RAM, to the healthy CPU, thereby allowing additional/multiple I/O failures with no degradation in performance (Figure 39).

3. Partial Capability Backup Using a Single-Chip CPU

The advantages of this approach are that the system cost is less, power is less, and space requirements are less than the first, or second approach, while many of the good characteristics of both are retained. It should be understood that in this discussion the single-chip CPU includes its own RAM and ROM on the chip. And since the single-chip CPU is actually a stand-alone microcomputer it is only dependent on the main CPU's Built-In Test output for its operational mode; i.e., if the main CPU fails its instruction test, RAM diagnostic, or ROM sum check, or continuously watchdog times-out, then this backup CPU will take over control of the operation of the dual-port link.

This latter approach was the one chosen to maintain the data-link survivability, and in fact is referred to as the "link-alive" processor. Its two main functions are:



E-5693

FIGURE 39 CONDITIONAL CAPABILITY BACKUP USING THE FAILED CPU AT REDUCED PERFORMANCE CAPABILITY

- (1) To service the dual-port UART: to check word formatting, parity, etc., and to self-test the link.
- (2) In addition to the above, if the Built-In Test logic indicates a failure of the main CPU, this machine will communicate to all I/O, and format this information for the dual-port link.

3.4.15.6 Test UART

The Test UART is actually only used for ground test troubleshooting, and therefore, could fail and never cause any degradation in any flight mode. Since the baseline test UART already used a minimum of components, the only possible improvements would be to use leadless chip carriers and to use the 28 pin USART instead of the 40 pin UART in order to cut back on solder connections. This is the final RAECC choice. Refer to Figure 40 and the trade study summary shown in Table 18.

3.4.16 Low Voltage Circuit Derating

The baseline RAECC CMOS logic ran exclusively on the 10 volt power bus either to achieve adequate performance or to be compatible with CMOS which had to run at 10 volts. For example, the baseline processor, the SOS RAMs, all CMOS buffers, and the UARTs were operated at 10 VDC. Also, in the interface area, all discrete CMOS control logic, the six custom LSI chips (used for A/D, R/D, FREQ/D, and SERIAL/D), and the output shift registers were operated on the 10 volt power bus.

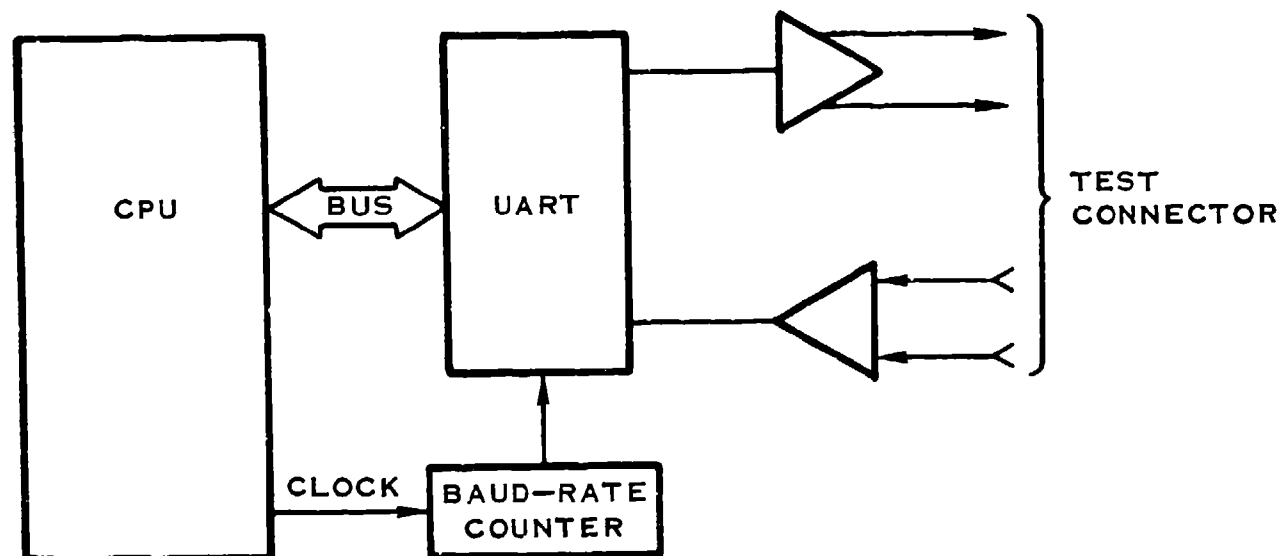
On the other hand, the final RAECC system contains no CMOS on the 10 volt bus except for the SOS HS 16/24 processor, which uses the 10 volts internally for high performance. The CMOS SOS HS 16/24 actually operates on two supply voltages; +10 VDC for internal performance and +5 VDC for TTL I/O compatibility. With this architecture, no CMOS anywhere in the system will be required to run on 10 VDC except for one 4050B (which is used as a clock buffer) and a single two-input NAND gate.

A comparison of derating factors used in the baseline and in the final RAECC systems is presented in Table 19. The design change from 100% CMOS operating on the 10 volt bus, to greater than 90% CMOS operating on the 5 volt power bus will result in a significant increase in RAECC CMOS logic reliability.

In the linear area, all the baseline RAECC design operational amplifiers were powered by the +14 volt and -14 volt power buses for two reasons:

The 14 volt supplies were convenient since the shunt regulators provided these buses.

Most analog signals were required to slew to either plus or minus 10 volts, which was only possible if the amplifier supplies were two to four volts greater than the range of operation.



E-2613

FIGURE 40 TEST UART

TABLE 18 RAECC TEST UART

ARGUMENT	BASELINE UART (CMOS)	(Final RAECC) 28 PIN UART (CMOS)
# OF COMPONENTS	9 3/4	9 3/4
# OF SOLDERJOINTS	106	94
BOARD AREA (IN)	5.5/2.49 *	4.7/2.38 *
POWER (WATTS)	0.09	0.09
CUSTOM PARTS	NO	NO
RELIABILITY RATIO	267/285	308

* IMPROVEMENT USING LEADLESS CARRIERS

E-2652

TABLE 19 CMOS STRESS DERATING IMPROVEMENT

Baseline Design

	<u>RATED VOLTAGE</u>	<u>OPERATING VOLTAGE</u>	<u>VOLTAGE STRESS</u>
5 Chip Processor	11V	10V	.91
6 Chip Interface	11V	10V	.91
Discrete CMOS	18V	10V	.56
RAM (SOS)	18V	10V	.56
ROM (TTL)	7V	5V	.71
UART (CMOS)	18V	10V	.56

Final Design

	<u>RATED VOLTAGE</u>	<u>OPERATING VOLTAGE</u>	<u>VOLTAGE STRESS</u>
3 Chip Processor	20V	10V	.50
N-Channel & 80C48	7V	5V	.71
Discrete CMOS	18V	5V	.28
RAM (N-Channel)	7V	5V	.71
ROM (N-Channel)	7V	5V	.71
UART (CMOS)	18V	5V	.28

However, there are CMOS operational amplifiers on the market today (manufactured by RCA and INTEL for example) which will slew rail to rail. If the + 10 volt reference supplies were made large enough to handle the additional (low power by the way) operational amplifier load, then the two 14 volt regulators could have been deleted. Also, if all op-amps were run on + 10 volts instead of + 14 volts, the voltage stress would decrease and there would be an accompanying increase in reliability. The scope of the program did not permit more study in this area, thus the 14 volt power buses were used.

3.5 Mechanical Design

3.5.1 General

The preliminary design of the Electronic Engine Control (EEC) developed under the RAEEC program meets the goals established for designing a highly reliable fuel control for operation on the projected Variable Cycle Engine (VCE). The controller design was developed using the baseline design with all the mechanical features upgraded in agreement with the established tradeoffs conducted. Results of the tradeoff studies are presented in Appendix B. The baseline RAEEC control features include: 1) a single vibration isolation system; 2) fuel cooling and external pin fins; 3) conventional printed circuit board/metal heat sink packaging techniques; and 4) conventional dip, flatpack and discrete components. The final RAEEC control employs: 1) a dual vibration isolation system; 2) fuel cooling; and 3) leadless chip carrier (LCC)/alumina ceramic packaging technology. All of the highest ranked features in terms of reliability, as determined by the numerous tradeoff studies, were utilized. Below is listed the reliability improvement goals for the various packaging features and how they compare to the actual improvement.

	<u>Goal</u>	<u>Actual</u>
Interconnects	1.3	2.15
Thermal Environment	2.3	2.6
Vibration Isolation	1.5	2.25

In addition to the established goals, gains were also made in the areas of maintainability, interconnect design, standardization, producibility, size, and weight. The modularization and standardization approach employed throughout the control facilitates testing and troubleshooting at key intervals of production, and also enhances product maintainability.

3.5.2 Configuration and Installation

External features of the control were designed for handling and installation using published human engineering guides and engine fuel control design experience. The external configuration of the control is shown in Figure 41. The final RAEEC control, which is actually two controls, has a basic rectangular size of 14.5 inches X 10.9 inches X 4.5 inches (a volume of 711 cubic inches), and weighs 26.1 pounds. As a comparison, the baseline control rectangular size is 17.1 inches X 9.75 inches X 4.92 inches, its volume is 800 cubic inches and it weighs 30.0 pounds. A complete weight breakdown is presented at the end of this section.

The control is mounted with four straight in bolts minimizing mounting tolerances. Connectors are oriented horizontally to the ground, when installed, to prevent contaminants from collecting in the backshell of the engine harness connector plugs.

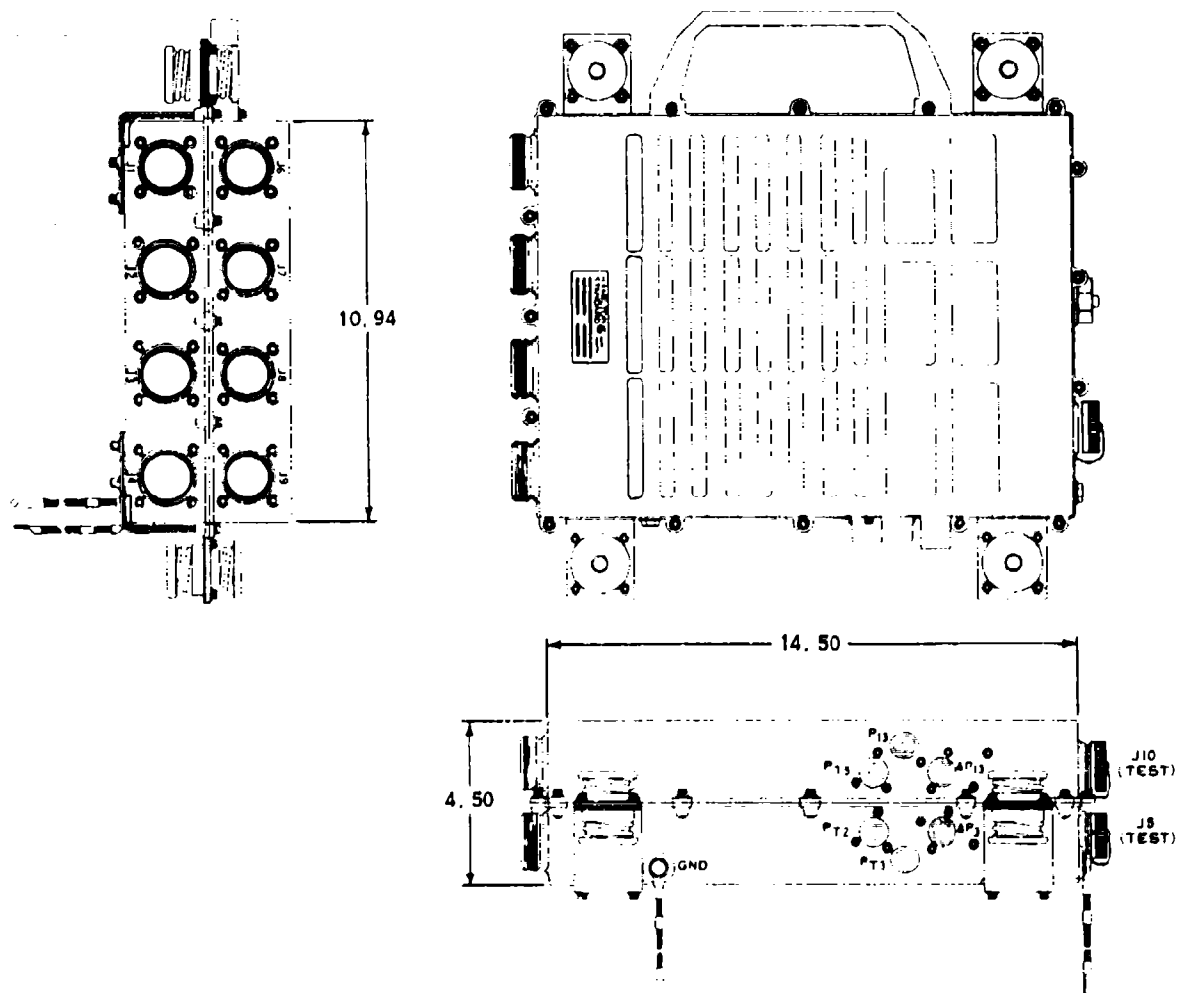
The pressure transducers are mounted on the side of the control with the pressure ports facing downward to prevent moisture ingestion. The control is equipped with eight electrical I/O connectors polarized to ensure proper mating with correct cables. Primary and secondary test connectors, located in the rear of the control, are equipped with protective caps for on engine protection. The six pressure transducer pneumatic lines and the fuel inlet and outlet hydraulic lines are polarized with the male insert which is normally installed by the engine manufacturer. The chassis is supplied with a bond strap in accordance with MIL-B-5087B, Class L, to provide effective grounding of the control against lightning.

The bond straps attach to the engine with #10-32 hardware. Installation and transport of the control is facilitated with the integrally cast handle provided. Fuel connections are made in the rear of the package.

Weight Breakdown:

Housings	9.10 lbs
Interconnect Modules	5.25 lbs
Basic Electronic Modules	7.00 lbs
Sensor Electronic Modules	0.80 lbs
Pressure Transducers	1.30 lbs
Power Supply Modules	0.65 lbs
Isolators	2.00 lbs

Controller Weight = 26.1 lbs



E-3557

FIGURE 41 RAECC PACKAGE OUTLINE

3.5.3 Physical Description

3.5.3.1 Modular Construction

The RAEEC Control employs modular construction throughout, as shown in Figure 42. Simplified to the fullest, all modules plug directly into a central Interconnect Printed Circuit Board Module. This modular design approach facilitates sequential testing of all subassemblies at critical stages throughout the build to assure a reliable end assembly. Each unique module has been standardized as much as the package restraints would allow. This feature is directed to the benefits of automated assembly techniques and attendant increased reliability.

3.5.3.2 Module Description

Separation of the housing yields two major modules identified as the Primary and Secondary Control Modules. Both of these modules are similar in configuration with slight differences due to the nature of the total system redundancy. The Primary and Secondary Control Modules are broken down into their unique sub-modules as follows:

<u>Sub-Modules</u>	<u>Primary</u>	<u>Secondary</u>
a. Electronic Module	14	14
b. Sensor Electronics Module	4	0
c. Pressure Transducer	3	3
d. Discrete Power Supply Module	1	1
e. Interconnect Module	1	1

The building and test stages of each unique sub-module are identified below, along with a description of each sub-module's detail parts and subassemblies. Room temperature bench testing of the controller in a closed or fanned-out condition is permissible without the need for supplementary cooling.

3.5.3.2.1 Electronic Module The configuration of a basic Electronic Module is shown with its mounting platform and detail parts in Figure 43. The heart of this module is the alumina(AL_2O_3) circuit substrate with a multilayer thick film interconnect system. The Electronic Modules were designed to use leadless chip carriers to carry the active circuit chips. Some of the major reasons for selecting this electronic packaging approach are: size and weight reductions; good repairability and component replacement; preassembly testing and burn-in capability; accelerated stress test capability; package ruggedness; improved thermal dissipating properties; and improved reliability. Reliability

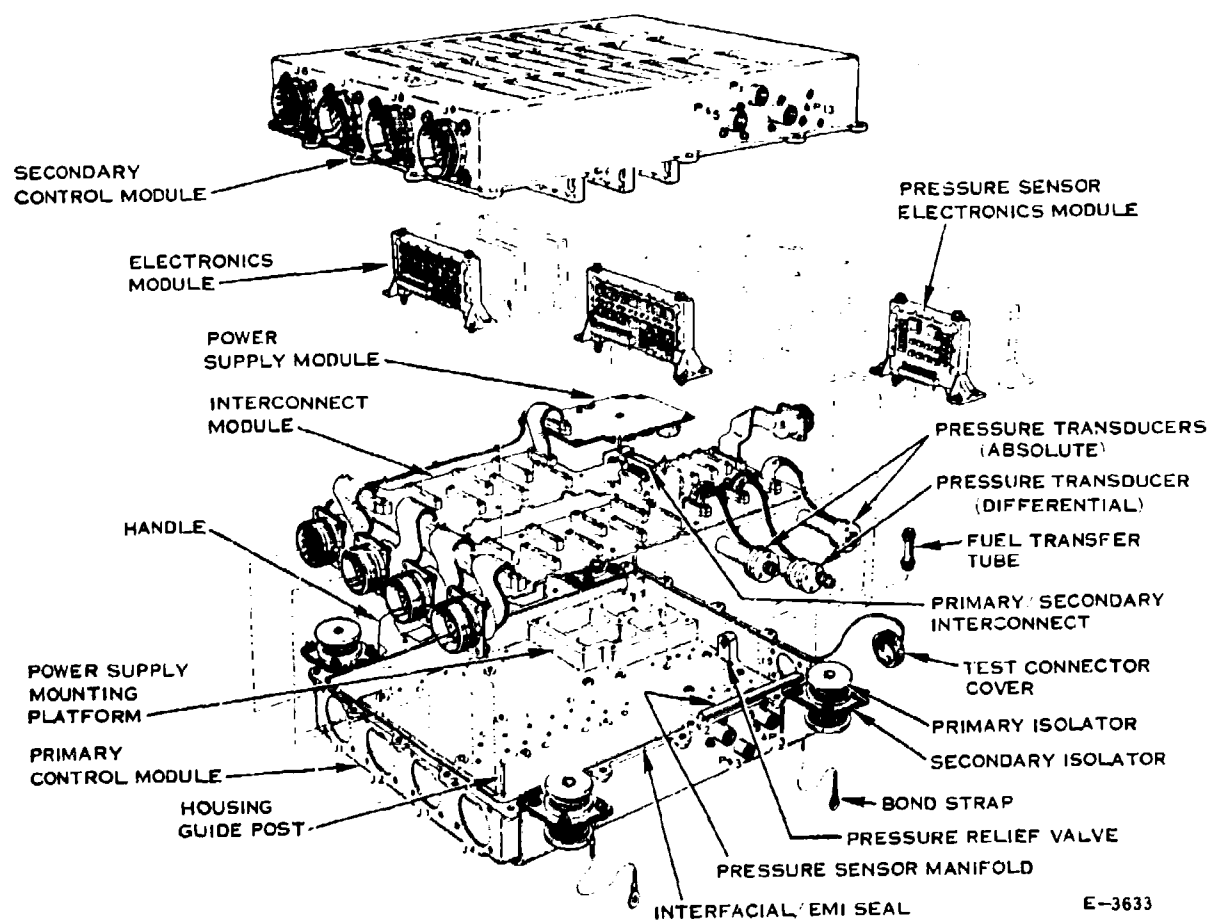


FIGURE 42 RAEEC PACKAGE CONFIGURATION

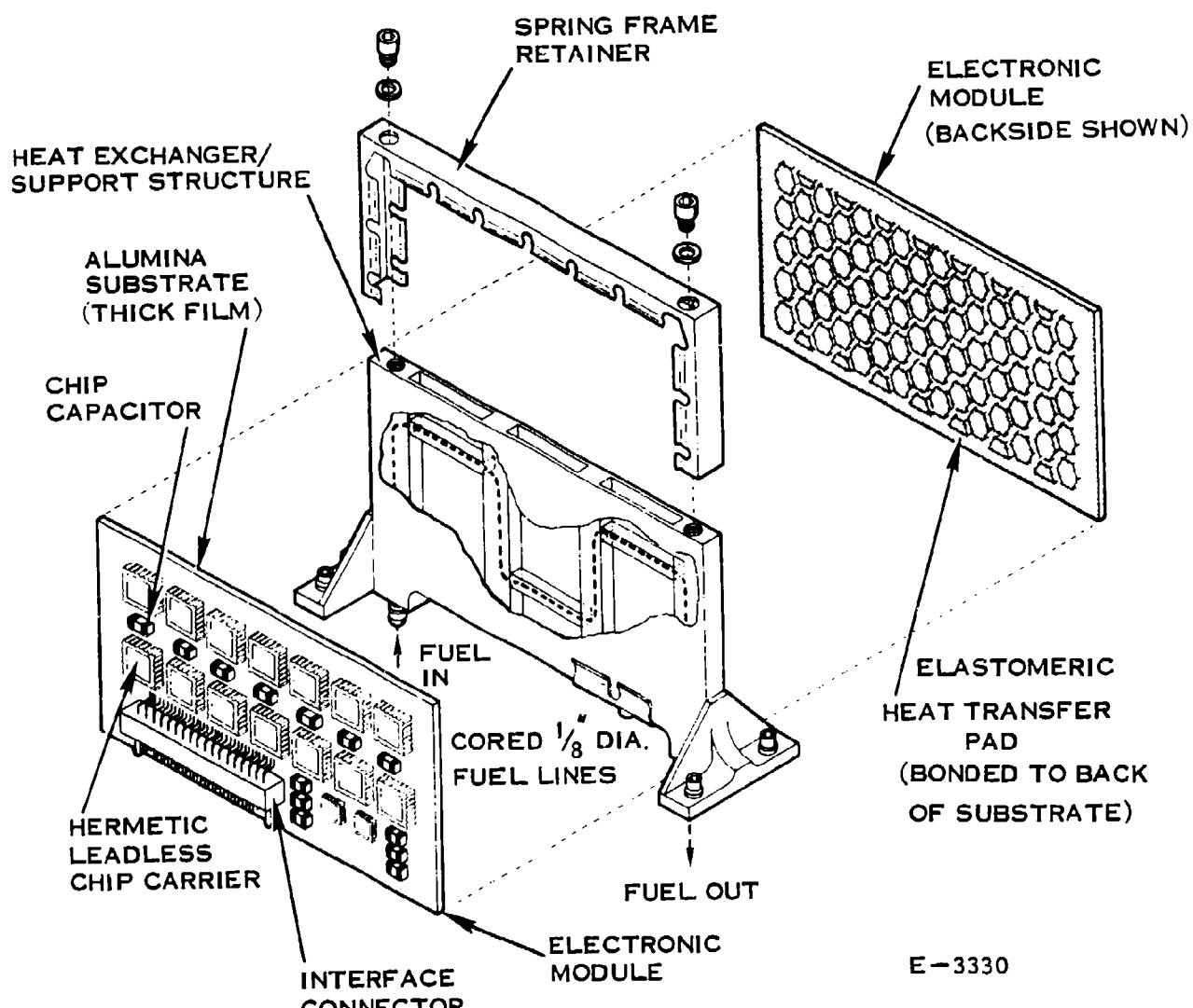


FIGURE 43 ELECTRONIC MODULE

is further enhanced by the capability of testing at both the component pre-assembly and post-assembly levels. Accelerated stress testing of an alumina ceramic module is also possible with the omission of the Module connector and the use of high temperature solder pastes to terminate the LCC packages.

The alumina substrate in the Electronic Module is one standard size (2.5 in. x 4.5 in.). The base substrate is 0.062 thick 96% Al_2O_3 available from a variety of manufacturers. Low substrate camber is required to obtain intimate contact between the substrate and LCC, as well as the substrate and aluminum heat exchanger. Camber is reduced prior to screening by a lapping or grinding operation. Camber due to screening can be reduced by using a low camber dielectrical material. The finished substrate is a composite, or multilayer, which is a ceramic substrate with electrically conductive patterns screen printed to the base substrate in layers. The layers are separated and insulated by high purity ceramic, and interconnected by conductive risers or vias wherever desired. The whole structure is sintered to form a monolithic unit that is strong, hermetic, chemically inert, dimensionally stable, and thermally conductive. Maximum component packaging density is achieved by restricting conductive lines to internal layers.

The LCC packages can be attached to the thick film alumina substrate circuit using a variety of techniques. Regardless of the heating method used, the chip capacitors and LCC packages are attached and interconnected by a reflow soldering process. Solder is applied to the ceramic circuit as a screen printed paste. The wet solder paste holds the LCC package in approximate position until the solder melts and floats it into place. Some of the heating methods used for reflow soldering are: 1) selective infrared heating; 2) special soldering tools now being developed; 3) conventional soldering irons; 4) localized hot air heating; and 5) vapor condensation. The thick solder pads on the LCC and ceramic substrate are of the same size and location which facilitates precise alignment of the LCC on the circuit pattern of the substrate. The solder wicks up the metallized patterns on the sides of the LCC packages and permits visual inspection of the electrical connection. The bottom surface of the LCC package will be metallized and soldered to the substrate for better mechanical attachment while providing a direct path for heat transfer. Nickel plated chip carriers and circuit substrates are very resistant to solder leaching so multiple repairs are possible with no solder dewetting. LCC packages can be reliably repaired up to 8-10 replacement cycles, which far exceeds the repair capabilities of conventional printed circuit board/dip packaging.

The module connector will be surface soldered in the same manner as the LCC's following high temperature stress testing. High strength, high temperature bonding mechanically fastens the connector to the substrate. Completed ceramic assemblies with the exception of the connector and test points are conformally coated with a two-part polyurethane system conforming to MIL-I-46058.

Electronic modules are mounted in pairs and clamped in place using a specially designed spring frame. Constructed of a phosphorous bronze material, the spring frame exerts only enough force on the ceramic substrate assembly to sufficiently secure it in the projected vibration environment, and to provide good heat transfer while minimizing the stresses in the ceramic itself. The spring frame slides over the two ceramic substrates and is held in place by two fasteners. An elastomeric heat transfer pad is molded to the back side of the ceramic substrate to optimize the thermal path from the ceramic substrate assembly to the module heat exchanger. The material hardness and pad size of the elastomer is designed to minimize the applied forces deflecting the ceramic substrate to a level consistent with the clamping forces of the spring retainer. An elastomeric material is used because with a minimum of pressure, it flows and fills the microsurface imperfections on the metal heat exchanger surface with a resultant minimal thermal resistance.

The module heat exchanger doubles as a module support structure. The basic supporting structure is a lightweight, cast aluminum heat exchanger with 1/8 inch diameter cored fuel passages. This structure provides the mechanical mounting accommodations used to secure the Electronic Module rigidly to the housing and connect it to the parallel fuel passages within, via two standard "O" ring sealed bosses.

3.5.3.2.2 Sensor Electronics Module The Sensor Electronics Module utilizes the same design approach as the basic Electronic Module, with the only difference being size. The alumina substrate size is a standard 2.5 inches x 3.0 inches for the four sensor substrate assemblies. These modules contain all of the pressure sensor electronics, including the redundant sensor characterization PROMs. The purpose of this remote location of the PROMs is to minimize the interconnects related to the miniature pressure transducers.

3.5.3.2.3 Pressure Transducers The RAEEC control contains six vibrating cylinder pressure transducers; four are absolute sensors with a vacuum reference and two are differential sensors. The design is similar to the Hamilton Standard miniature pressure transducer product line with some modifications. The modifications result from the redundancy features such as redundant temperature compensation diodes, redundant coil leads and redundant PROMs located on the Sensor Electronics Module.

The baseline control uses the larger standard size pressure transducers. A miniature transducer was developed under Navy contract based upon the Hamilton Standard larger size transducer design. Derivatives of this are presently used in HSD engine mounted hardware. Utilization of the miniature transducer

yields a 41% volumetric size improvement and a 38% weight improvement over the baseline transducer. The six transducers are mounted to the fuel cooled control housing and electrically interconnect to the adjacent Interconnect Module. The transducers utilize hard-wire harnessing and plug-in connectors which are equipped with jackscrews for ease of mating and separating without contact damage, while providing good mechanical retention. Severe engine control environments and strict accuracy requirements have limited the use of many types of pressure transducers whereas the vibrating cylinder type used in this design has demonstrated on-engine capability in a number of engine control applications.

3.5.3.2.4 Power Supply Modules The Primary and Secondary Control Modules contain identical Power Supplies, each comprised of two different module types. The components fall into three distinct categories: 1) LCC packages; 2) power discretes (large capacitors and resistors, TO-5 can, etc.); and 3) magnetics (chokes, transformers, etc.). The LCC components are packaged as a single Electronic Module, like the type described earlier, and are located adjacent to the Discrete Power Supply Module. The Discrete Power Supply Module contains all the remaining electronics associated with the power supply circuit. Conventional printed circuit board technology is utilized here because of the style of the power components presently available.

A high performance polyimide laminate is used for the power supply module multi-layer interconnect system. Polyimide ranked highest in the trade-off studies when compared to other circuit laminates. High glass transition temperature and good dimensional stability were the determining factors in that trade-off. Electronic components are physically and thermally mounted to a metal heat sink and electrically attached to the printed circuit board. The heat sink is etched aluminum, coated with a dielectric material and laminated to the printed circuit board.

3.5.3.2.5 Interconnect Module The Primary and Secondary Control Modules contain similar Interconnect Modules. All of the individual sub-modules contained within the control are interconnected by the Interconnect Module, the heart of which is a polyimide multilayer board. The Electronic Modules and Sensor Electronic Modules plug directly into the Interconnect Module using two-piece connectors equipped with *Hypertac[®] contacts which feature low contact insertion force, low contact resistance and assured electrical continuity under shock and vibration. The pressure transducers have a hard-wire harness and Hypertac[®] connector which mates with a corresponding connector on the Interconnect board. A flexible molded cable soldered to the Interconnect Module is provisioned with a Hypertac[®] connector mating it to the Discrete Power Supply Module. The mating halves of a larger Hypertac[®] two-piece connector, interconnected to each motherboard with flexible molded cables, provide the communications between the

* Hypertac[®] is a trademark of Industrial Electronic Hardware Corporation.

Primary and Secondary Control Modules. The I/O connector/cable assemblies include flexible molded cables terminated and potted to a severe environment resistant MIL-C-38999, series III, connector.

This design approach maximizes reliability by employing several important features. Only three terminations are required per signal: crimp connection at the I/O connector; soldered connection to a one piece molded connector; and a solder connection to the printed circuit board. Progressive strain relief is provided at both ends of the cable. A rigid epoxy and elastomeric fillet system is utilized at the back of the I/O connector and at the printed circuit board. No forces can be transmitted to any of the three terminations. The I/O connector is secured with four fasteners to the housing, and the one-piece connector is bolted with two fasteners to the printed circuit board. The I/O connector contact design provides multiple contact points assuring electrical continuity under high vibration. The individual I/O Connector/cable assemblies can also be fully tested prior to being soldered to the multilayer polyimide motherboard. The entire Interconnect Module, like all other modules in the RAEEC control, can be tested prior to being assembled in the control.

The alternator power and control lines are hard-wire twisted shielded triplets and twisted shielded pairs, respectively. These harnesses mate to the Power Supply Module thru its own plug-in, Hypertac[®] connector.

3.5.3.2.6 Housing Description Each major control module (Primary and Secondary) is packaged within its own housing. Both housings are similar one-piece castings with stiffening as required to minimize deflections, and with an integral, forced fuel heat exchanger in the outer walls to cool the internal electronics. The housing material is an AMS 4218 (A356-T6) premium strength structural investment casting having a MIL-A-8625, type 1, anodize finish. Where required for electrical continuity and EMC closure, machined surfaces are conversion coated per MIL-C-5541 class 3. Gun drilled fuel passages, sealed with pin plugs, are strategically located to optimize the cooling of the electronic modules, power supply modules and sensors. One housing's fuel passages are a mirror image of the others, utilizing a single transfer tube to transport fuel from the primary to the Secondary Control Module. This is the only fuel line separation required during normal maintenance. All other fuel containment is within drilled passages in the castings. A representation of the salient feature is shown in Figure 44.

Because these seals are involved in the normal maintenance cycle, the control is designed such that a failure of either or both seals will result in leakage which is routed through the drain point and is visible externally. In the event that one or both seals leak "slightly", leakage is directed overboard without filling the cavity. Thus no pressure build-up can occur which would force fuel between clamped housings into the unit.

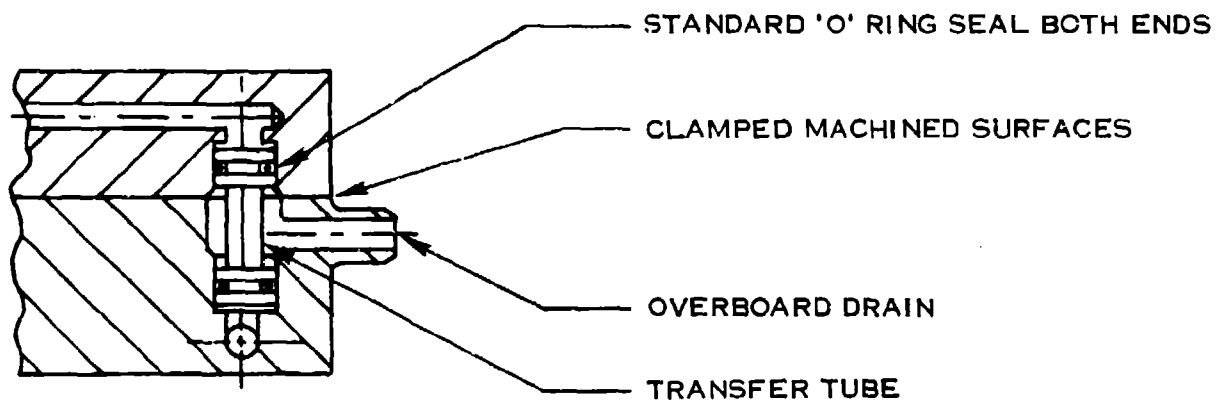


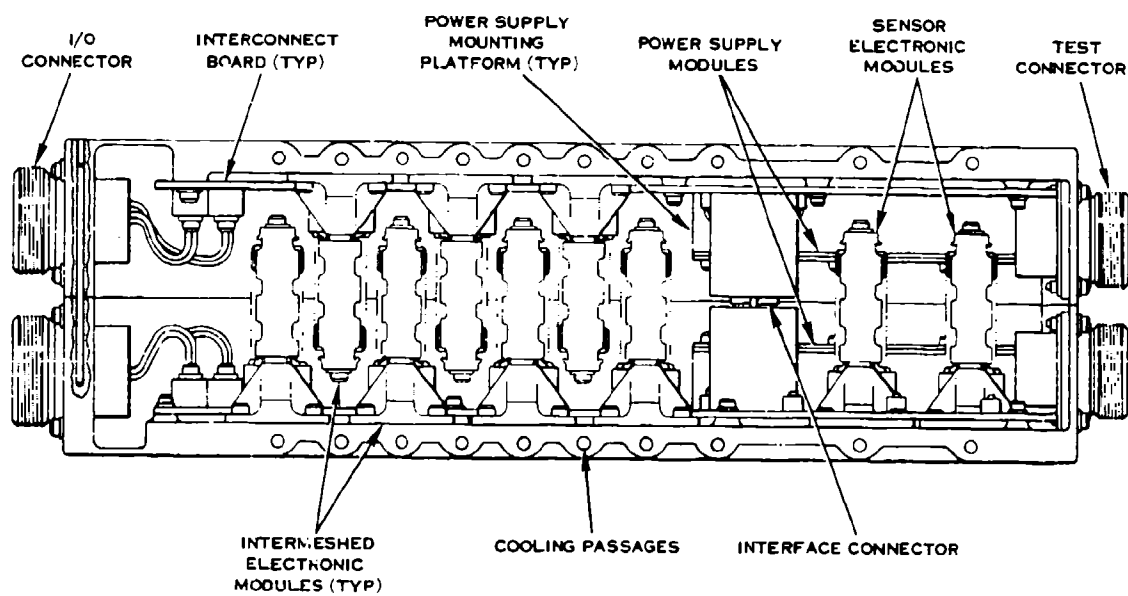
FIGURE 44 OVERBOARD DRAIN SCHEMATIC

E--6175

In the event that one or both seals fail completely (left out at assembly) the leakage rate into the cavity is limited by the annular clearance between the transfer tube and housings. The drain hole is sized to drain faster than the leak, thus precluding pressure build-up and forced leakage into the unit.

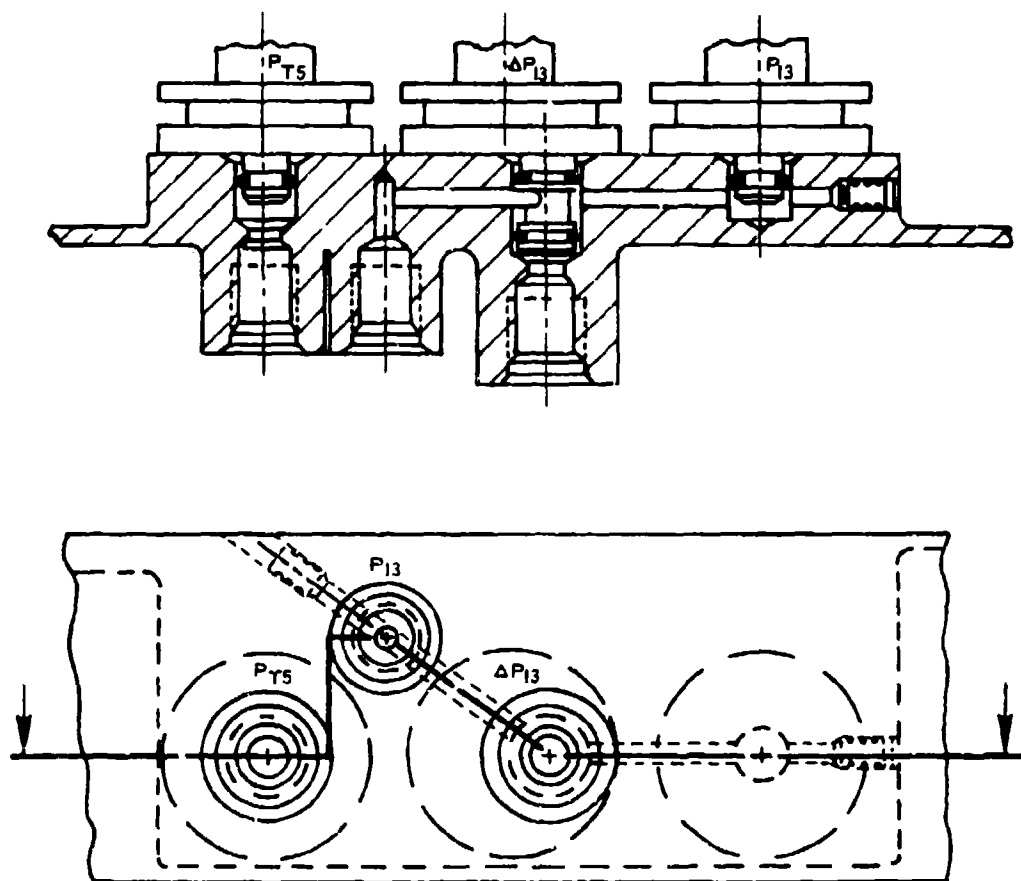
This is mainly a convenience feature during assembly and test, in that fuels or test fluids which enter the electronics area are of nuisance impact only. In service on the engine, fuels which might otherwise enter into the electronics do not constitute an immediate nor immanent failure threat. However, gross exposure to impure fuels, with temperature cycling and sufficient time for absorption, could eventually result in electrical degradation or failure, hence the desirability of overboard drain.

The mating surfaces of the housing guide posts are prepared with a single machine cut and seal groove and are included to guide the interwoven modules when mating the two control halves and to precisely align the guide pins of the interface connector. A cross-section of the control illustrating the need for these features is shown in Figure 45. Other housing features include internal mounting platforms for all modules, isolator mounting pads, fuel ports and raised cast letters for identifying all external interfaces. Also included are an integrally cast electrical bond lug, a sensor pneumatic manifold, and a handle for aiding installation and transportation. The sensor manifold shown in Figure 46 is an integrally cast part of the housing and provides the sensor mounting platform, drilled pneumatic lines and external pressure port bosses, which are machined in accordance with MS 33649.



E-3995

FIGURE 45 RAEEC CONTROL CROSS-SECTION



E-3982

FIGURE 46 PRESSURE SENSOR MANIFOLD

3.5.4 Maintainability

As mentioned in the modular design section of this report, the plug-in capability of each and every module has been a major contributor to the maintainability improvements of this control. Beyond interrogation of the external test connectors, the first step for maintenance requiring access to the unit interior is separation of the housing modules, or the Primary and Secondary Control Modules. The two modules are connected electrically by a rectangular connector which separates automatically upon separation of the housings. Guide pins are included with the connector to insure proper mating during reassembly. Guide posts are provided as part of the housing design to insure safe separation and assembly of the housing modules beyond the height of the internal electronic modules while also serving as a pre-guide to pick up the connector guide pins.

Disassembly of either housing module is performed in a similar manner. Any sensor or functional electronics module may be removed without disturbing any other module. There is no sequence required for disassembling these modules from the Interconnect board. Replacement of a ceramic module for component replacement can be accomplished simply by removing the spring retainer held in place by two fasteners, and disengaging the electrical connector. Any electronics module (basic or sensor) can be removed individually without disturbing any other feature. There is no need to ever remove an electronics module heat exchanger, except to facilitate replacement of an Interconnect Module. If necessary the heat exchangers can be taken out after removing the four mounting screws. Seals may be tested by plugging in the transfer tube and pressurizing the inlet. The Power Supply Module need only be removed if component replacement is required, since test points are accessible to permit testing without removal from the housing. If necessary, however, the power supply, can be removed by disengaging the electrical connector, secured by jackscrews, and removing the mounting fasteners securing it to the housing. Removal of a polarized Pressure Transducer can be done in a similar fashion. The Interconnect Module does not require removal under normal maintenance; only if replacement is necessary. It may be tested in place after removal of all the Basic and Sensor Electronic Modules, and separation of the Sensor and Power Supply connectors, and, if necessary, it may be removed and replaced. Removal of an Interconnect Module requires removal of its mounting fasteners, as well as the I/O connector fasteners.

3.5.5 Environmental Design

3.5.5.1 General

The RAEEC control package is designed to provide the electronic components with the most benign environment practicable for the projected service environment. Environmental investigations performed by both Pratt and Whitney Aircraft and Hamilton Standard were used for projecting the EMI, thermal, vibration, shock and acoustic environments. The basic package is designed as a sealed unit to protect the internal electronics from the short term and long term effects of humidity, salt and fluids.

A pressure relief valve is used in the design to avoid the significant weight penalty which would be incurred if sufficient rigidity had to be added to the module to enable it to survive the full differential ambient pressure range. The relief valve allows a maximum pressure differential of 1.2 psid between the inside and the outside of the module. The degree of moisture sealing is really dependent on the function of the pressure relief valve. This valve is presently being used on EECs for the F100 engine with no recognized moisture problems.

The housing's interfacial seal serves a dual purpose: in addition to environmentally sealing the control, it has built-in characteristics that protect the unit from the effects of EMC (electromagnetic compatibility).

3.5.5.2 EMC

In addition to circuit design, other features have been incorporated into the package for EMC protection. The housing seal mentioned previously, is an EMC O-ring gasket molded into the housing flange. Similar gaskets are provided at all I/O connector locations. The alternator power and signal lines inside the control are twisted and shielded to eliminate possible interference with electronics. Secondly, the I/O connectors are equipped with filter pin contacts since external cable shielding alone would not be adequate to prevent high frequency, short wavelength susceptibility. Finally, 3.5 inch maximum bolt spacing and 0.06 inch minimum wall thickness are being used to optimize EMC shielding.

3.5.5.3 Lightning

Bond straps, located at each end of the package, provide the control with suitable lightning protection. All bonding is done in accordance with MIL-B-5087B, Class L, and the bond strap design is in accordance with MS 25083-2B86.

The engine manufacturer must also terminate the bond strap to the engine in accordance with the surface preparation and hardware defined in MIL-B5087B, Class L. The bond strap is constructed of 12 AWG, stranded, tinned, copper wire rope to minimize vibration effects. It is fastened to an integrally cast bond lug at the controller, as well as to the engine case, with #10 fastener hardware.

3.5.5.4 Thermal Design

3.5.5.4.1 Environment The RAEEC control has been designed to operate at the highest reliability levels practicable for all cases described in Section IV, Controller Environment. Pertinent thermal environment data has been reproduced in Tables 20 and 21.

Mounted on the engine fan case inside the nacelle, the controller utilizes tank fuel for cooling the internal electronics. Figure 47 is a schematic representation of the fuel flow through the control. The maximum tank fuel temperature (159°F) occurs under extreme flight conditions. During a typical deep strike mission, the maximum fuel temperature is less (114°F). For design conservatism, the analysis presented later in this report was performed using 159°F tank fuel with a flow rate of 200 PPH, which is consistent with present system capability. The tank supplied cooling fuel may undergo a maximum temperature transient from 135°F to 0°F during air refueling.

For the present F-15 aircraft systems there exists a "no fuel" condition. Under this condition, nacelle air flow has to be used to convectively cool the control. The baseline control falls into this category, which is why pin fins were included to provide non-critical mounting attitude convective cooling. The F-16 and VCE systems, as well as the new F-15 systems, provide an assured supply of fuel. With a tank fuel sink, as in the RAEEC system, cooling to ambient is not required and the heat influx from ambient air is minimal. Therefore cooling fins prove ineffective and have been deleted.

3.5.5.4.2 Cooling Heat transfer to and from the exterior of the package is primarily by natural convection and radiation, with some effects of conduction through the mechanical interfaces. When considering convective cooling to and from the nacelle air, the effects of air temperature, pressure and velocity must be accounted for, but since the velocity is unknown, static air is assumed for conservatism. At flight points when the nacelle air temperature is high, the corresponding pressure is low, minimizing the effect ($\sqrt{P/14.7} = 0.26$). In addition, the duration at high temperature (180°F for battlefield interdiction and 307°F for deep strike mission) is short. Approximately 60% of the time the nacelle air will be cooling the package during a battlefield interdiction mission and about 90% of the time for a deep strike mission.

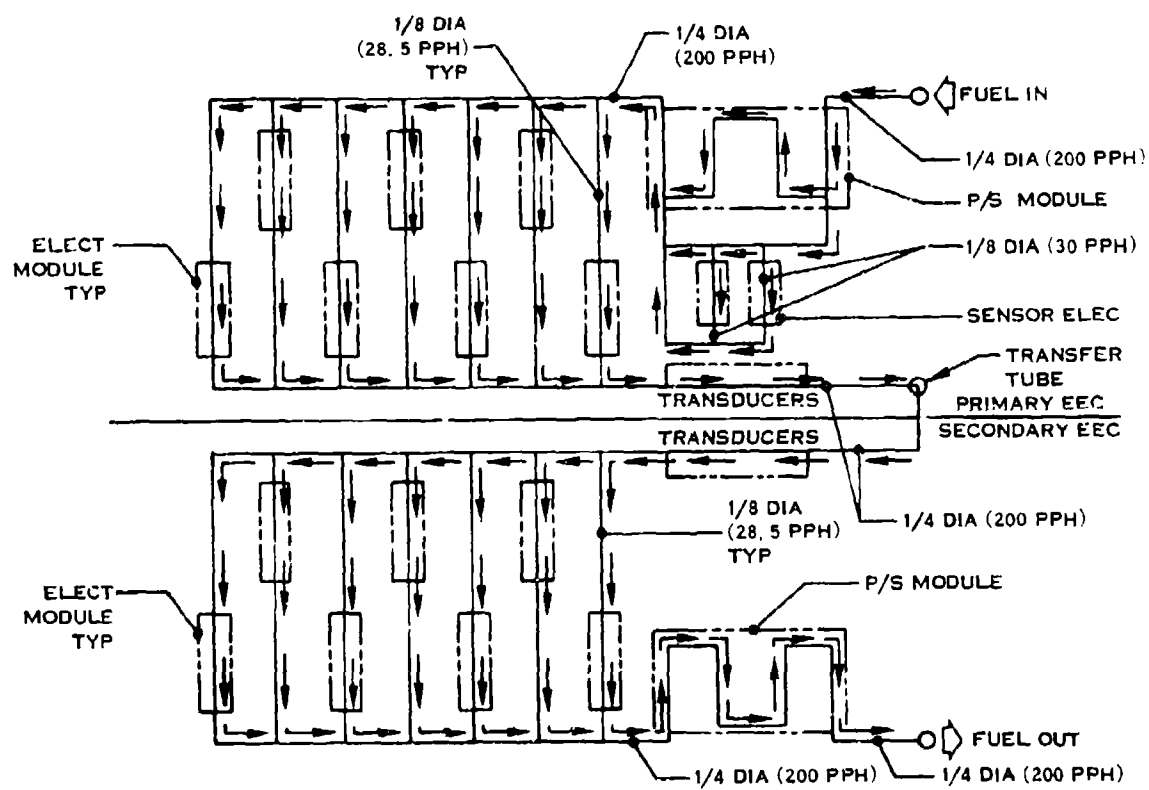
Other cooling paths include radiation to and from the engine case and nacelle metal, as well as conduction through the mounting, plumbing and wiring interfaces. While these paths are mostly beneficial, that is they tend to cool the package further, in those instances where heat is added to the control, it is directed to the fuel sink through the housing and thus negligible heat is transferred to the components. Internal cooling encompasses all three modes of heat transfer; conduction, the most dominant of the three, is heavily utilized. Effective conductive cooling has been achieved with every module

TABLE 20 TYPICAL ENGINE NACELLE THERMAL ENVIRONMENT - BATTLEFIELD INTERDICTION MISSION

[illegible]

TABLE 2: TYPICAL ENGINE NACELLE THERMAL ENVIRONMENT - DEEP STRIKE MISSION

Flight Point	Altitude (ft)	Mach No	Power Setting	Flight Condition	Duration (min)	Nacelle Pressure (psi)	Nacelle Airflow (lbm)	Nacelle Air Inlet Temperature (°F)	Aircraft Nacelle Metal Temperature (°F)	Maximum Case Temperature (°F)	Engine Case Temperature (°F)	Point A Fuel Tank Average Temperature (°F)	Point B Engine Fuel Inlet Average Temperature (°F)	Point C Boost Pump Discharge Average Temperature (°F)
26	0	0	Idle	Takeoff	30.0	14.7	0	59	54	95	361	80	200	228
27	0	0	Max	Takeoff	0.1	14.7	0	59	54	361	361	80	155	165
28	0	0.30	Fast Power	Climb	4.6	14.7	0	65	61	361	329	80	155	165
29	38,500	0.44	Part Power	Cruise	29.2	14.7	54	71	71	274	183	64	200	217
30	38,500	0.44	partial CR	Accl	2.8	14.7	54	71	71	267	227	64	187	201
31	56,100	0.70	partial CR	Cruise	10.4	14.7	55	80	70	440	437	83	197	212
32	56,100	0.70	Max	Cruise	4.6	14.7	55	80	70	440	437	83	197	212
33	61,000	0.74	partial CR	Cruise	11.1	14.7	55	80	70	440	437	114	200	217
34	61,000	0.74	partial CR	Cruise	11.1	14.7	55	80	70	440	437	94	200	221
35	0	0.32	Part Power	Land	10.0	14.7	0	69	69	142	170	90	200	222
36	0	0	Idle	Ground	10	14.7	0	59	54	95	361	100	200	226



E-3987

FIGURE 47 FUEL FLOW DIAGRAM

being directly tied to the central housing heat exchanger. Optimum thermal paths were attained by using individual, ceramic module, forced fuel, heat exchangers mated in parallel fuel paths with the housing heat exchanger. Also, each power supply module is supplemented with an aluminum alloy heat transfer plate mounted in direct contact with the main housing forced fuel heat exchanger. Components are strategically located to match the resultant thermal resistance with each component's power dissipation to minimize hot spots and maintain a close average temperature between components. The close proximity of the components to the fuel minimizes the thermal resistance, and consequently keeps the temperature rise from the component to the fuel low.

3.5.5.4.3 Power Dissipation Internal power dissipation for the RAEEC control totals 57.4 watts. This is a 2.48/1 reduction in the baseline control dissipation of about 200 watts. Power is first broken down by Electronic Modules and summarized in Table 22.

3.5.5.4.4 Thermal Analysis The thermal analysis conducted includes the determination of component operating temperature for the following cases: 1) LCC components (mounted on ceramic) located directly over a fuel line; 2) LCC components located centrally between two fuel lines; and 3) conventional power supply components mounted on an aluminum heat sink with fuel lines passing underneath. Figure 48 and the equivalent thermal resistance network that follows, describes the conductive heat transfer paths from the component junction to the fuel for a typical ceramic module.

Condition 1: Worst case fuel supply at 159°F

<u>Component Power</u>	<u>Case 1</u>	<u>Case 2</u>
0.002 watts (min)	159.04°F	159.11°F
0.100 watts (avg)	161.1 °F	163.3 °F
0.250 watts (max)	164.4° F	N/A

TABLE 22 POWER DISSIPATION

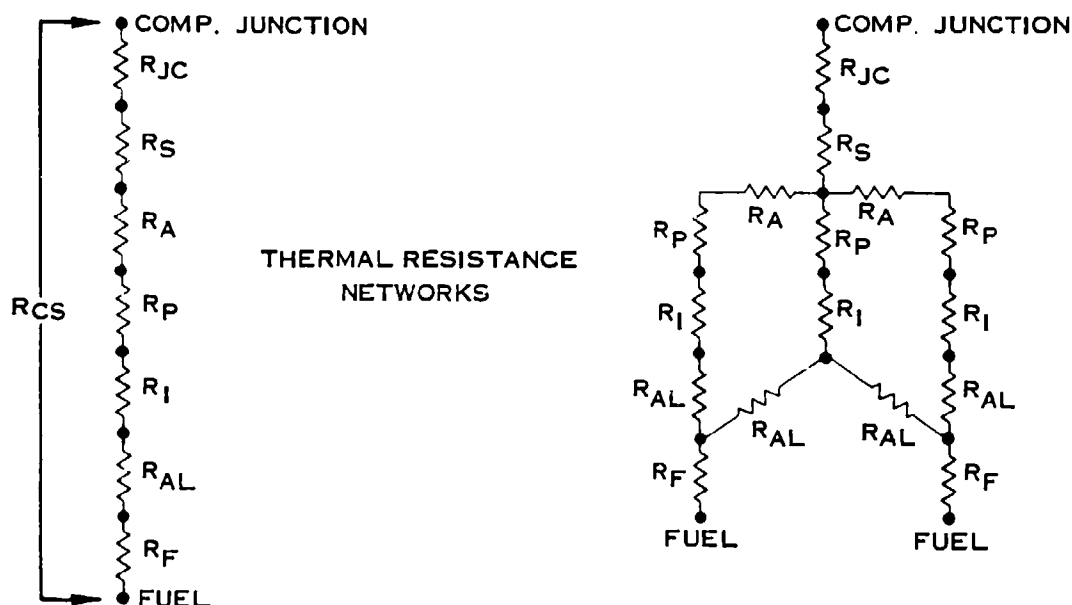
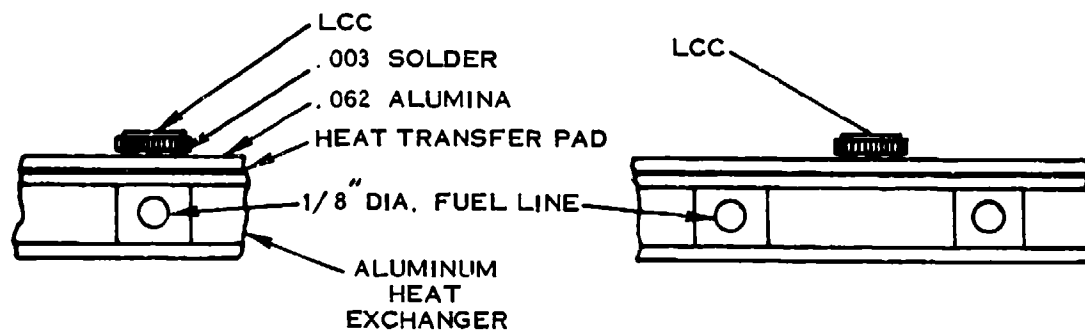
<u>Functional Circuit</u>	<u>Number of Ceramic Modules</u>	<u>Total Power Dissipation (watts)</u>
<u>Primary</u>		
Resolver	2	2.025
Low Level Interface	1	.380
A/D Converter	1	1.340
Speed	1	.681
Torque Motor Driver	2	3.712
Discretes	1	2.574
Power Supply	2	1.000
Processor	4	3.890
Total Primary	14	15.602 watts
<u>Secondary</u>		
Resolver	2	2.639
Low Level Interface	1	.190
A/D Converter	1	.670
Speed	1	.483
Torque Motor Driver	2	2.344
Discretes	1	.683
Power Supply	2	1.000
Processor	4	3.890
Total Secondary	14	11.899 watts

The controllers total power breakdown is as follows:

<u>Module</u>	<u>Quantity</u>	<u>Total Power (watts)</u>
<u>Primary</u>		
Basic Electronic Module	14	15.602
Sensor Electronic Module	4	3.000
Power Supply Module	1	13.450
Sub-total	19	32.052
<u>Secondary</u>		
Basic Electronic Module	14	11.899
Power Supply Module	1	13.450
Sub-total	15	25.349 watts
Total Controller	37	57.401 watts

CASE 1
(COMP. OVER FUEL LINE)

CASE 2
(COMP. BETWEEN FUEL LINE)



E-3986

Nomenclature

- R_{JC} - chip junction to case resistance
- R_S - eutectic solder resistance
- R_A - Alumina substrate resistance
- R_P - thermal pad resistance
- R_I - Interface resistance
- R_{AL} - Aluminum resistance
- R_F - fuel to housing resistance
- R_{CF} - total thermal resistance from component chip to fuel.

FIGURE 48 CONDUCTIVE HEAT TRANSFER PATHS

Condition 2: Average fuel supply at 77°F

<u>Component Power</u>	<u>Case 1</u>	<u>Case 2</u>
0.002 watts (min)	77.04°F	77.11°F
0.100 watts (avg)	79.10°F	81.30°F
0.250 watts (max)	82.40°F	N/A

N/A = Not applicable

There is one device on the Signal Interface circuit that dissipates 0.325 watts but was not considered a worst case condition because it is carried in a larger, 48 pad LCC package with a significantly lower R_{jc} than the 24 pad LCC package dissipating 0.25 watts. The latter was therefore chosen for analysis.

The Power Supply Module components are analyzed using conventional methods and the kinds of temperature rise and component operating temperatures are similar to present forced fuel cooled controls. Some typical high power components were analyzed and the results are summarized below.

Case 3

1/4" diameter fuel line

Fuel Temperature = 159°F max, 77°F avg.

*Fuel Flow Rate = 200 PPH (JP4)

Components mounted on heat sink directly attached to housing heat exchanger.

<u>Component type</u>	<u>Component temperature</u>	
	<u>Max fuel</u>	<u>Avg. fuel</u>
Transistor	176°F	94°F
30 Bridge	185°F	103°F
Capacitor	167°F	85°F
Sensors	187°F	105°F

* Because of the split in fuel flow, the secondary power supply gets 200 PPH but the primary power supply gets slightly less.

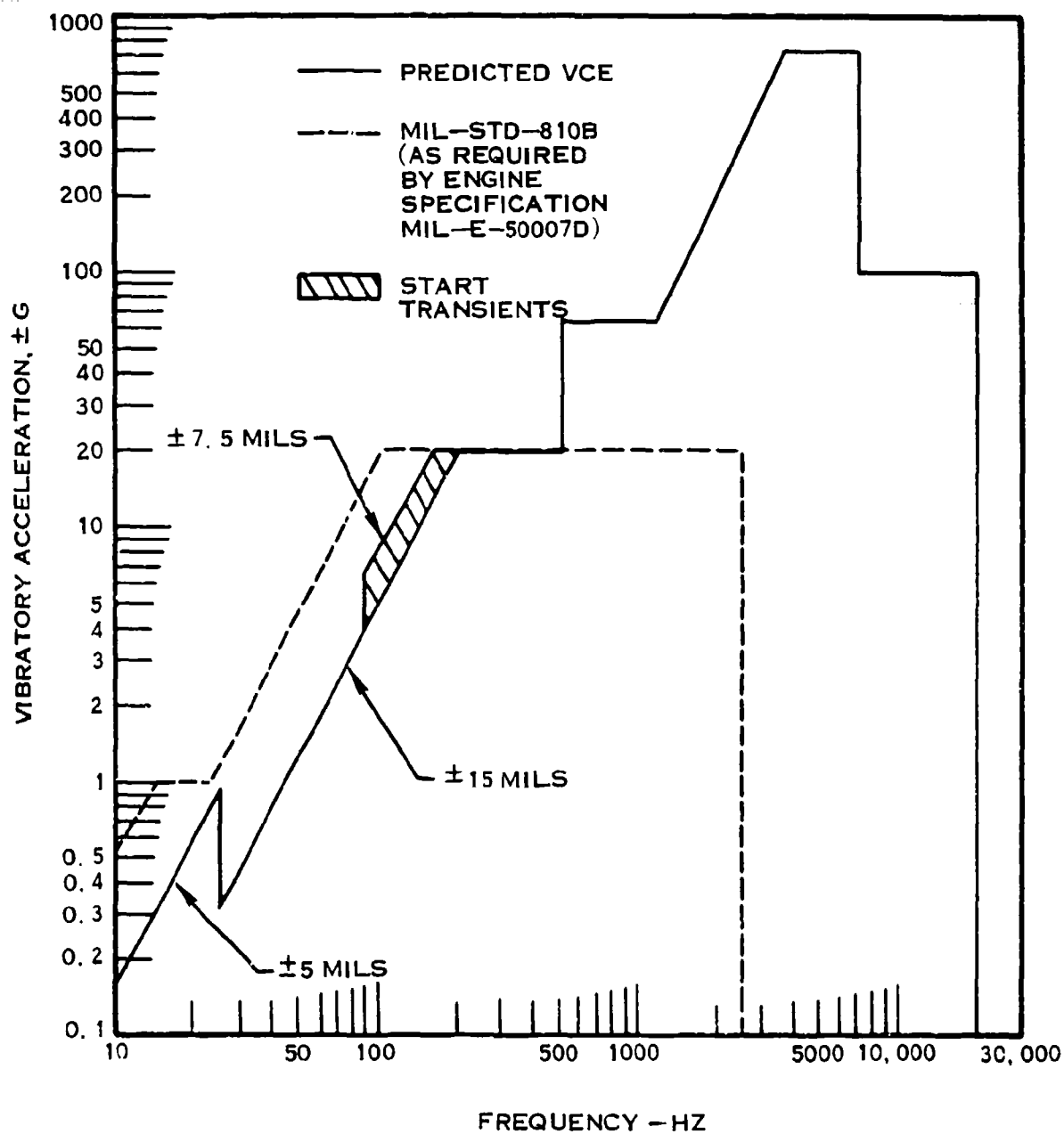
3.5.5.5 Vibration Design

3.5.5.5.1 Environment Engine test data shows that the general jet engine specification MIL-E-5007 and MIL-STD-810 are inadequate for the successful design of an electronic control. Based on the VCE fan design, using current engine test data as a reference, the VCE vibration levels in the 500 to 20,000 HZ range at the electronic control location are predicted to be above the military

specification, with respect to both amplitude and maximum frequency. The predicted vibration environment for the variable cycle engine is shown in Figure 49. The inputs shown on this curve are a combination of all worst case peaks at all speeds. The major sources of high vibration levels in the 500 to 20,000 Hz range are the fan blades. These levels vary considerably with axial location on the case. The electronic control receives vibration excitation from all contacts with the engine, including fuel and pneumatic plumbing, and electrical cables and the electronic control mounting brackets. There have been significant levels of vibration attributed to electronic control fuel plumbing connections which bypass the control mounting bracket isolation; but this problem can be substantially reduced in advanced engines by proper engine and plumbing design. The levels of vibration expected from aircraft fuel tank coolant source design is less than 10G and would occur at frequencies below 500 Hz. The vibration received from the electrical cables is inherently small because of the flexibility of construction. Discrete-frequency acceleration and displacement levels are identified in Figure 50 for fan (E_f) and high rotor (E_h) excitation orders. All of these frequency components appear simultaneously. At $20 E_f$, $24 E_f$ and $40 E_f$ the radial and tangential acceleration levels are 760 G, while the axial acceleration is only half that level. In the low-frequency range, displacement level is the more significant indicator. Additionally, on each engine design and in each position on the engine, some physical features are more influential than others.

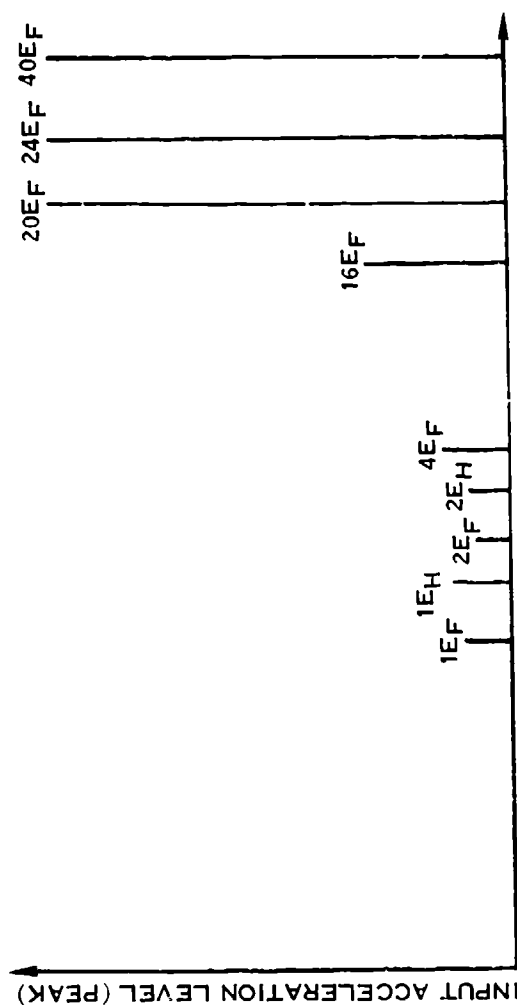
Vibration inputs to the control therefore are defined in a combined, maximum, overall form in Figure 49. The actual instantaneous vibration is more like the curve per Figure 51. Similar inputs occur at all engine speeds with frequency and peaks shifting with shaft speed.

3.5.5.5.2 Average overall response Data has been accumulated from the F100 testing. The worst case test engine data involving a JFC90 control was selected as an average response level for reliability calculations. It is difficult to express component responses as a generalization because response levels vary with input and with location within the control. While it is true that at the isolator frequency the control package is a rigid body mode and all components experience the same response as the housing, internal vibration must be considered since the internal design and location result in varying responses for different locations. This can best be shown in Figure 52.



E-3983

FIGURE 49 PREDICTED VIBRATION ENVIRONMENT FOR VARIABLE CYCLE ENGINE;
HIGHEST PEAKS IN FREQUENCY SPECTRUM AT OUTER ENGINE CASE
JUST UPSTREAM OF DUCT FLAMEHOLDER



ORDER	FREQUENCY RANGE (HZ)	DISPLACEMENT (M'LS)	ACCELERATION (G)
1EF	65 TO 175	.5	INSIGNIFICANT
1EH	150 TO 225	3.85	
2EF	130 TO 350	.1	
2EH	300 TO 450	.0.75	
4EF	260 TO 700	INSIGNIFICANT	
16EF	1040 TO 2800		
20EF	1300 TO 3500		
24EF	1560 TO 4200		
40EF	2600 TO 7000		

E-4024

FIGURE 50 PREDICTED VARIABLE CYCLE ENGINE INSTANTANEOUS VIBRATION SPECTRUM
AT THE ELECTRONIC CONTROL LOCATION

{
RADIAL 100%
TANGENTIAL 100%
AXIAL 50%

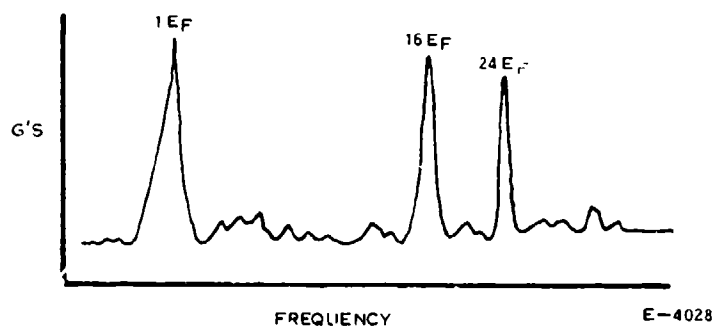


FIGURE 51 INSTANTANEOUS VIBRATION CURVE

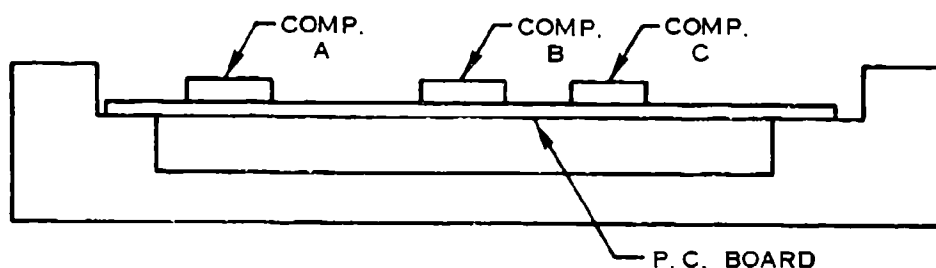


FIGURE 52 COMPONENT MOUNTING

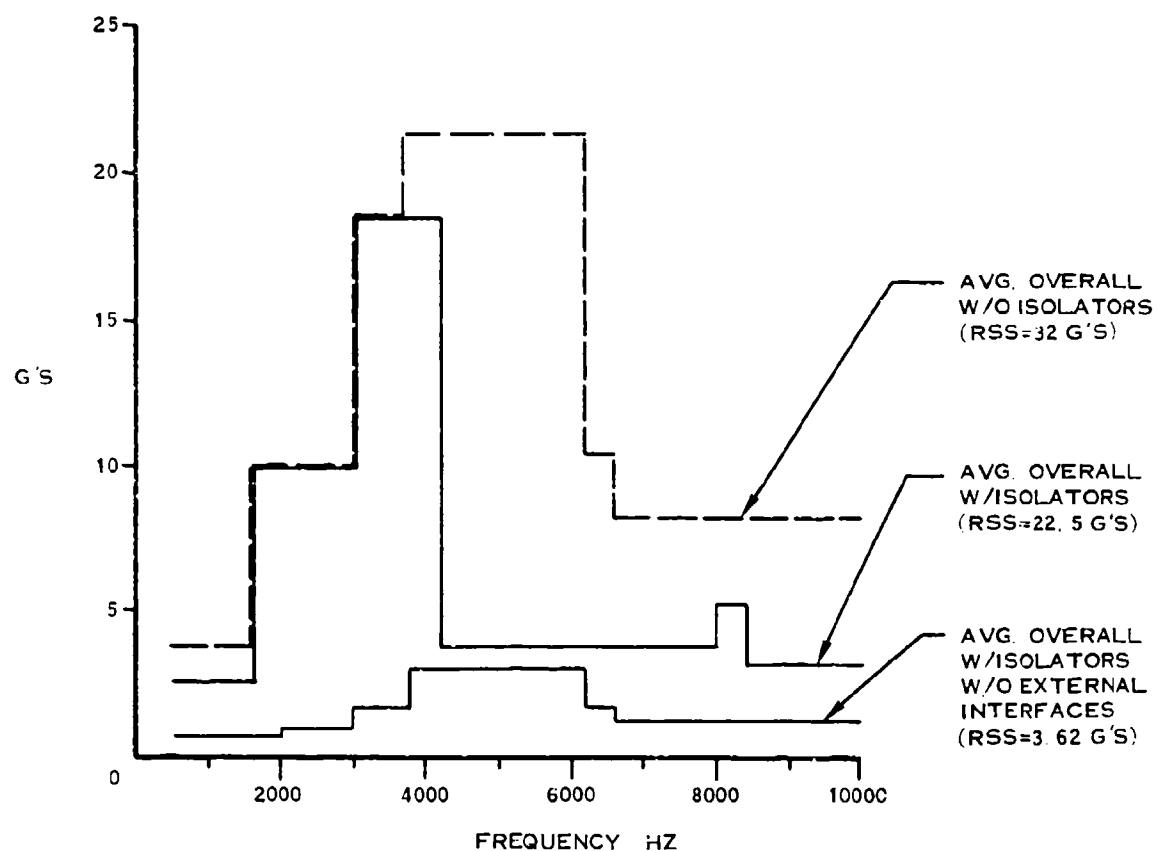
E-4029

At the printed circuit board resonances:

- Component B experiences the maximum amplification
- Component A experiences no amplification and is more affected by housing deflections
- Component C experiences an amplification somewhere in between

An approximation suitable for comparative purposes is obtained using an "average overall response", which is an RSS (root of sum of the squares) the combined worst case peak responses. Data was extrapolated from JFC testing and the average overall response for various mounting conditions are represented in Figure 53. As indicated on the curve, the JFC90 average overall response without isolators is 32 G while the average overall response with isolators is 22.5 G. The isolators that were added were only partially effective due to the influence of the plumbing interfaces which was not reduced by the isolators.

It is assumed that with a single isolation system, the RAECC control could duplicate the JFC 90 average overall response curve for single isolation without external interfaces, which is 3.62 G's. It is possible, but not probable according to P&WA, that the interface effects could be negligible. It is



E-3981

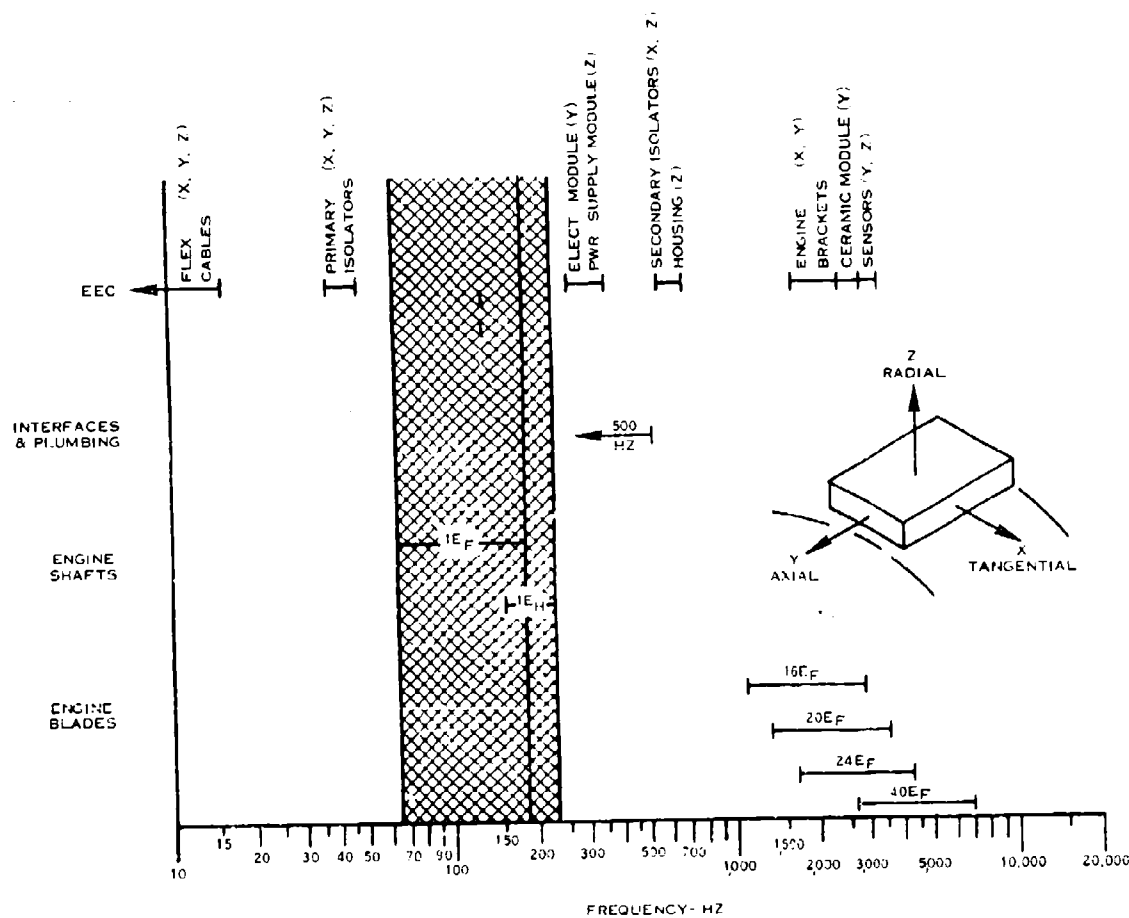
FIGURE 53 COMBINED MAX JFC90 INTERNAL COMPONENT RESPONSE TO ENGINE TESTS

therefore assumed for RAEEC that individual peak response levels will more realistically be about 50% greater. This means that the average overall response for the RAEEC control with single isolation is approximately 5.43 G's.

3.5.5.5.3 Secondary Isolation Secondary isolation is less effective than the primary because excitation levels are lower. The estimated average additional attenuation above 850 Hz is 2:1. Below 850 Hz an average amplification of 3:1 is realized. The resultant average overall response with the secondary isolation system is 3.53 G's. If it happens that the primary isolation system is less effective than anticipated and the attenuation of the secondary isolation system is 4:1, then the average overall response would be 2.6 G's.

3.5.5.5.4 Design Approach The ability of an electronic component to survive a severe vibration environment depends on: 1) component internal design; 2) component mounting configuration; 3) resonant frequency of the printed circuit board; and 4) acceleration forces. Component physical failures are usually the result of high cycle dynamic stresses that develop because of the relative motion of the component, its leads, and the printed circuit board. Relative motion is most severe during resonant conditions that can develop in the component part or the printed circuit board. There are only two variables that can be manipulated in controlling vibration response: frequency and amplitude.

Frequency tuning, the prime feature of the RAEEC vibration design, is carefully utilized to avoid frequency coupling via similar resonant frequencies. The result is minimized stresses and deflections. Figure 54 is a plot indicating all of the basic VCE engine resonant frequencies. The resonant frequency of each control feature is tuned outside the 35-175 Hz range of the fan and the 150-225 Hz range of the high rotor, since these are the most threatening due to the large displacements involved. As can be seen, not all of the engines frequencies can be avoided. The engine brackets and pressure sensors frequencies overlap the various blade passing frequencies. However, the displacements associated at these high frequencies are small and the isolators are at maximum attenuation. The flexible electrical cables and the primary isolator systems are designed with frequencies below those of the engine shafts. It is desirable to set these features below the turning speed so that vibration will only be experienced during start-up and shut-down. The secondary isolator frequency was selected between that of the external interferences/plumbing and the engine blades for maximum effect. All other features were frequency tuned based upon their inherent capabilities. The electronic modules are supported in the center of the printed circuit assembly. The ceramic substrates are relatively rigid and have a flexural modulus several times greater than most



E-3991

FIGURE 54 FREQUENCY TUNED SYSTEM

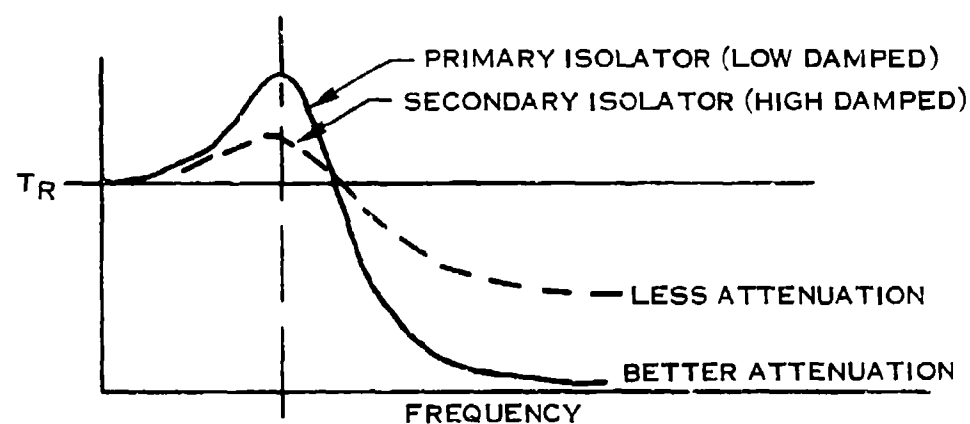
plastics. The results are that very low deflections and low dynamic stresses are exerted on the components. In addition, the leadless chip carrier packages themselves are considerably more capable of withstanding vibration than dips because of the inherent stiffness of the package and its mounting.

3.5.5.5.5 Isolation Design The primary isolator is a low damped, low frequency system designed for maximum attenuation of vibration inputs at engine frequencies (Figure 55). The higher amplification at natural frequencies is acceptable since it is only experienced at start up and shutdown. The isolator is a steel spring with wire mesh construction. The spring provides most of the spring rate with some added by the wire mesh. The wire mesh, however, provides all of the damping.

The secondary isolator is a high damped, high frequency system for minimum amplification at resonance with agreeable attenuation at higher frequencies (Figure 55). It is a laminated spring steel construction with viscoelastic inner layers. The secondary isolator system is designed to work only in the X and Z axis to reduce complexity. As mentioned earlier, the axial (Y-axis) inputs are only half those of the tangential (X-axis) and radial (Z-axis) input levels, therefore the benefits of a secondary isolation system in the Y-axis would be negligible.

3.5.5.6 Acoustics

Investigations of the F100 engine with a JFC 90 control indicated that acoustic excitations are high enough such that the response at the components may not be negligible. However, with proper controller design, the levels could be made insignificant relative to acoustically induced fatigue failures. As a comparison, the acoustic environment for the JFC 90 control and the baseline control is the same, but the peak vibration response at the printed circuit boards was reduced from 11 G's on the JFC 90 to 3.3 G's on the baseline by improved housing design. While the overall acoustic db level is higher for the final RAEEC control than for the baseline control, the acoustic vibration response at the components in the RAEEC control has been further reduced through improved housing design, the ceramic module mounting technique, and particularly through the inherent stiffness and damping characteristics of the ceramic substrate and heat transfer pad. The alumina substrate has a flexural modulus (or stiffness) 20 times the modulus of conventional printed circuit board laminates. In addition, the elastomeric heat transfer pad on the back of the substrate serves as a well damped elastic foundation for the substrate. As a result, the natural frequency of the ceramic substrate has been raised to 2500 Hz and higher. At the housing resonance, narrow band acoustics amplifies inside the package to an estimated maximum of 2 G's on the power supply boards, with little or no effect on the ceramic substrates. At the natural frequency of the ceramic substrate, acoustics is effectively attenuated by the housing such that the response at all component locations is negligible.



E-4027

FIGURE 55 ATTENUATION CHARACTERISTICS

SECTION IV CONTROLLER ENVIRONMENT

4.1 Variable Cycle Engine Simulation

A computer simulation of the VCE was used to define the physical environment for an engine-mounted electronic controller.

An advanced tactical fighter was selected for the analysis because it represents a typical application in which a VCE can be used. For this aircraft and typical mission profiles, a flight envelope was defined. The flight envelope was used to estimate the extreme environmental conditions which the controller would experience. The mission profiles were used to estimate environmental points during typical operation. This data will be used as the basis for the design and reliability assessment of the control.

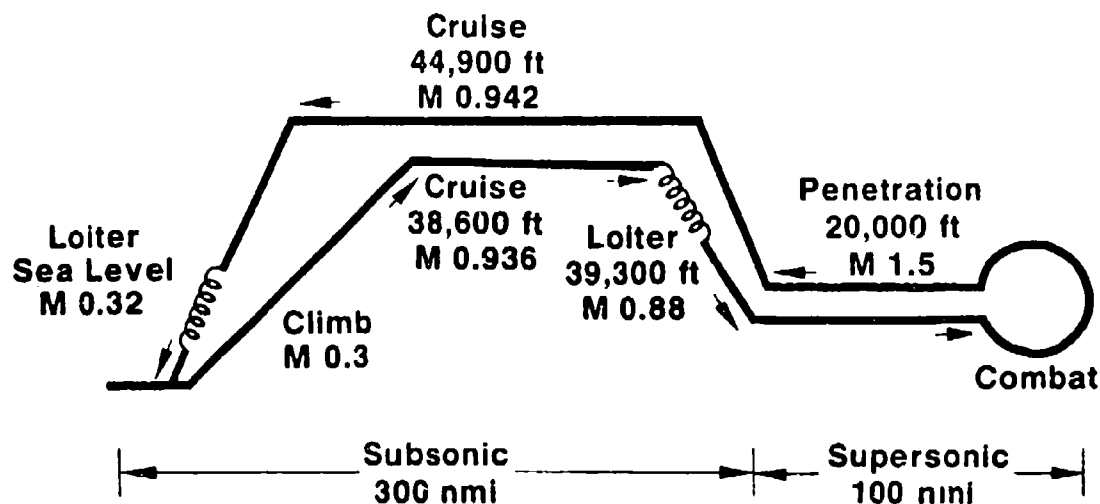
4.1.1 Aircraft and Engine Selection

An advanced tactical fighter was selected for the analysis because it represents a typical application for a VCE. Mission requirements for this type of aircraft generally include a significant amount of supersonic operation. A variable cycle engine can be designed for high performance at both subsonic and supersonic conditions. The cycle would be varied according to the flight condition to provide high performance at all flight conditions.

4.1.2 Mission Profile Selection

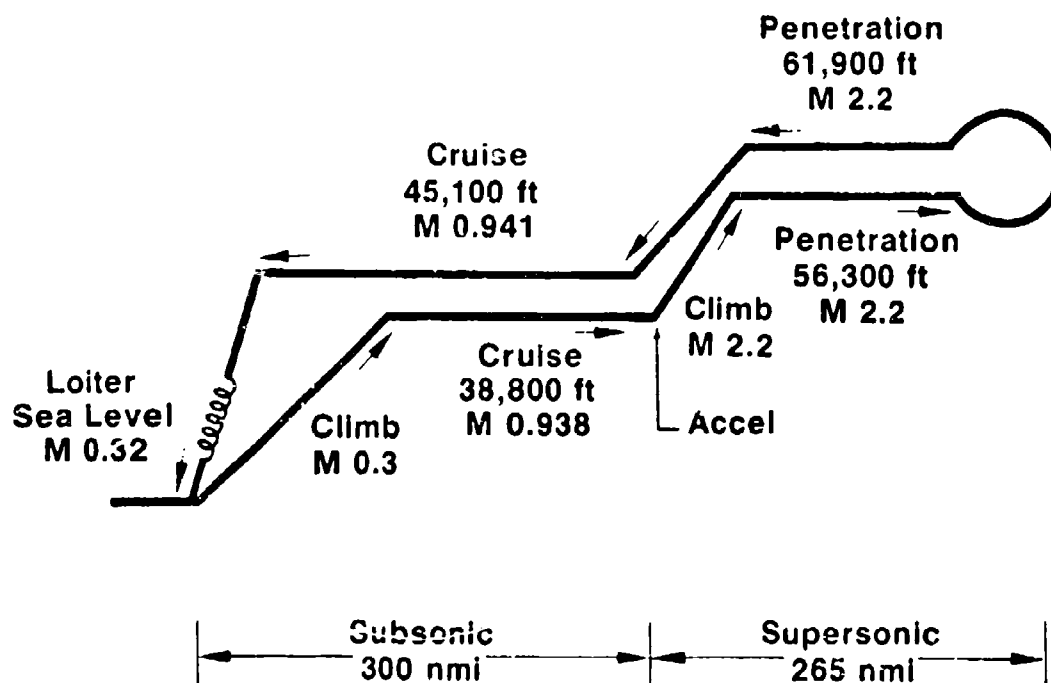
A battlefield interdiction mission (Figure 56) and a deep strike mission (Figure 57) are typical requirements for an advanced tactical fighter and are the basis of this study. Both missions have a 300-nmi subsonic radius which consists of takeoff, climb, and subsonic cruise, with a 30-min loiter at return to base. In addition, the battlefield interdiction mission has a 15-min high altitude loiter before penetration. The altitude and Mach number of the subsonic cruise out and back are optimized to provide maximum range per pound of fuel consumed.

The battlefield interdiction mission has a 100-nmi penetration radius at low altitude and low supersonic Mach number (20,000 ft, Mach 1.5). The deep-strike mission is directed at enemy supply lines, resulting in a greater penetration radius, approximately 265 nmi. After an acceleration to Mach 2.2, the aircraft climbs to an altitude that provides the maximum range per pound of fuel consumed. The altitude of the return leg at Mach 2.2 is also optimized for maximum range per pound of fuel.



E-4807

FIGURE 56 ADVANCED TACTICAL FIGHTER MISSION PROFILE (BATTLEFIELD INTERDICTION MISSION)



E-4808

FIGURE 57 ADVANCED TACTICAL FIGHTER MISSION PROFILE (DEEP STRIKE MISSION)

4.1.3 Flight Envelope Definition

From the mission requirements and engine design considerations, the flight envelope was defined (Figure 58). The maximum Mach number was selected to reflect the Mach number requirements of the deep strike mission, allowing some margin for the inlet and duct heater designs. The maximum altitude was selected to reflect typical combat requirements.

The flight envelope represents the extreme bounds of engine operation and all realistic operational points will lie within this envelope. Points 10, 11, and 12 help form these extreme bounds although they are outside the realm of realistic operation.

4.1.4 Simulation Methodology

To determine the worst operating environment that the controller would experience, the VCE simulation was executed over a full range of power settings at the extreme flight conditions defined by the flight envelope. The predicted controller operating environment, under these conditions, will be used by Hamilton Standard to define the controller design. The simulation was also executed at typical flight conditions defined by the battlefield interdiction and deep strike missions. The predicted engine operation at these conditions was used to determine the controller operating environment under normal usage. From the typical environment, the controller reliability will be determined.

Table 23 presents the predicted engine parameters for defining extreme environmental conditions that the controller could experience within the limits of the flight envelope. The flight points presented in Table 23 are also shown on the flight envelope in Figure 58. Flight points 3 through 9 and flight point 14 were used to define the vibrational loads. High rotor speeds, hence high vibration levels, are predicted for these flight conditions.

At these same conditions, high ram air temperatures and high duct flow temperatures are also predicted. This results in high thermal loads on the controller. A cooling scheme which uses fuel from the engine boost pump presents a problem at other flight conditions: At high altitudes, low Mach numbers, and low power settings, the fuel flow to the engine is low and its temperature is increased due to recirculation through the boost pump. This reduces its heat sink capability such that the thermal loads at these conditions (flight points 1, 2, 10, 11, 12, and 15) must be evaluated and reflected in the controller design.

Tables 24 and 25 present the predicted engine parameters at typical flight conditions. The tables contain these parameters for the battlefield interdiction and deep strike missions, respectively.

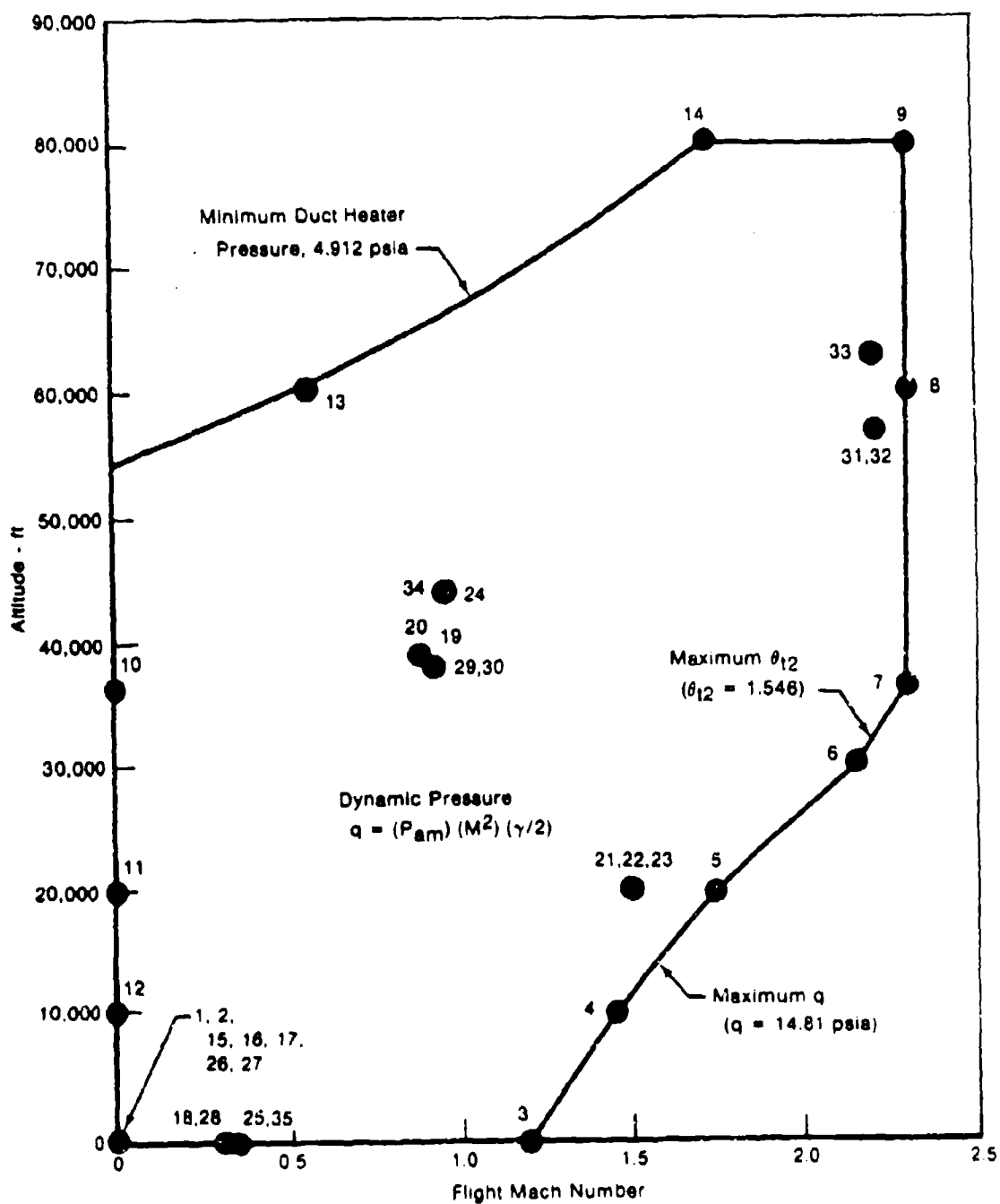


FIGURE 58 FLIGHT ENVELOPE AND FLIGHT POINTS FOR VARIABLE CYCLE ENGINE

TABLE 23 PREDICTED ENGINE OPERATING CONDITIONS AT EXTREME FLIGHT CONDITIONS

Flight Point	Altitude (ft)	Mach No.	Power Setting	Ambient Pressure, P _{amb} (psia)	Ambient Temperature, T _{amb} (°F)	Fan Inlet Total Pressure, P _{t2} (psia)	Fan Inlet Total Temperature, T _{t2} (°F)	Fan Duct Airflow Rate, M _{ad} (pps)	Fan Duct Total Pressure, P _{t4} (psia)	Fan Duct Total Temperature, T _{t4} (°F)	Low Rotor Speed, N ₁ (rpm)	High Rotor Speed, N ₂ (rpm)	Core Fuel Flowrate, W _{fc} (pph)	Duct Heater Fuel Flowrate, W _{hd} (pph)
1	0	0	Low	14.7	59.0	14.7	59.0	71.7	17.7	95.0	3,813	8,786	1,574	0
2	0	0	Low	14.7	59.0	14.7	90.0	69.6	17.7	128.1	3,925	9,045	1,588	0
3	0	1.20	Max	14.7	59.0	15.3	207.4	36.4	100.6	490.0	8,545	12,495	24,864	75,208
4	10,000	1.45	Max	10.1	23.0	31.5	275.2	310.1	92.5	502.8	8,527	12,540	22,176	68,687
5	20,000	1.77	Max	6.8	-12.6	15.1	267.5	317.3	90.1	534.6	8,491	12,652	20,152	66,032
6	30,000	1.98	Max	4.4	-48.3	40.9	341.7	321.1	94.1	592.7	8,284	12,845	18,587	66,824
7	36,000	2.30	Max	3.3	-70.0	16.7	341.7	287.4	84.1	592.7	8,275	12,840	16,599	59,793
8	60,000	2.30	Max	1.2	-73.0	1.6	341.7	83.0	26.0	587.3	8,151	12,779	5,000	18,519
9	80,000	2.30	Max	0.4	-62.2	4.5	357.2	31.4	9.2	595.7	7,757	12,647	1,595	6,536
10	36,000	0	Low	3.3	-70.0	3.3	-70.0	20.2	4.6	-18.4	3,367	8,253	568	0
11	20,000	0	Low	6.9	-12.6	6.8	-12.6	35.1	8.1	17.9	3,507	8,159	78.1	0
12	16,000	0	Low	10.7	-7.0	10.1	23.0	50.8	12.1	56.5	3,665	8,478	1,109	0
13	60,000	0.55	Low	1.0	-70.0	1.3	-46.2	9.9	2.0	28.7	4,611	9,004	249	0
14	20,000	1.71	Max	0.4	-62.1	1.9	164.5	18.6	5.0	422.0	7,973	12,018	1,124	3,879
15	0	0	Idle	14.7	125.0	14.7	125.0	66.2	16.1	147.9	3,570	8,802	1,287	0

TABLE 24 TYPICAL ENGINE OPERATING CONDITIONS - BATTLEFIELD INTERDICTION MISSION

[illegible]

TABLE 25 TYPICAL ENGINE OPERATING CONDITIONS - DEEP STRIKE MISSION

Flight Point	Altitude Hg.	Mach No.	Power Setting	Flight Condition	Duration min	Ambient Pressure, Psia (Std)	Ambient Temperature, °C (Std)	Fan Inlet Total Pressure, Psia (Std)	Fan Inlet Total Temperature, °C (Std)	Fan Duct Airflow Rate, GPM (Std)	Fan Duct Total Pressure, Psia (Std)	Fan Duct Total Temperature, °C (Std)	Low Rotor Speed, RPM (Std)	High Rotor Speed, RPM (Std)	Core Fuel Flowrate, Wg (ppm)	Core Fuel Flowrate, Wg (ppm)	Duct Heater Fuel Flowrate, Wg (ppm)
26	0	0	Idle	Ground	30.0	14.7	59.0	14.7	59.0	66.2	16.1	81.9	1,576	8,902	1,287	0	0
27	0	0	Max	Takeoff	0.1	14.7	59.0	14.7	59.0	219.7	56.7	360.6	9,015	12,747	18,021	45,720	0
28	0	0.10	Part Power	Climb	4.6	14.7	59.0	15.6	68.0	271.7	57.8	380.1	8,724	12,095	16,985	0	0
29	38,500	0.94	Part Power	Cruise	29.2	2.9	-70.0	5.2	-7.2	73.2	17.2	234.2	7,653	10,953	4,115	0	0
30	38,500	0.94	Partial O-M	Arce	7.6	2.9	-70.0	5.2	-7.2	42.5	14.9	269.7	8,519	11,597	7,130	14,545	0
31	54,100	2.20	Partial O-M	Cruise	10.5	1.2	-70.0	3.0	30.1	98.4	28.4	559.8	8,252	12,701	5,121	13,323	0
32	54,100	2.20	Max	Turn	4.8	1.2	-70.0	3.0	30.1	98.4	28.4	559.8	8,252	12,701	5,121	13,323	0
33	61,900	2.20	Partial O-M	Cruise	32.7	1.0	-70.0	9.2	30.1	74.5	21.5	557.4	8,197	12,676	4,316	10,784	0
34	45,100	0.94	Part Power	Cruise	33.3	2.1	70.0	3.9	-0.7	51.2	11.9	222.7	7,447	10,805	2,691	0	0
35	0	0.32	Part Power	Land	30.0	14.7	59.0	15.8	69.2	92.4	22.8	182.4	4,751	9,559	2,432	0	0
36	0	0	Idle	Ground	10	14.7	59.0	14.7	59.0	66.2	16.1	81.9	1,576	8,902	1,287	0	0

4.2 Thermal Environment

4.2.1 Thermal Environment Definition

For the thermal environment definition, the electronic control was assumed to be in an installation such as that shown in Figure 59. The control is mounted on the engine fan case inside the nacelle. Nacelle airflow enters through a scoop near the front of the engine, flows across the electronic control and other engine components, and exits near the exhaust nozzle. Mounted in this position, the electric control temperature is influenced by the temperature of the surrounding metal surfaces and by air temperatures.

The nacelle environment was predicted for the electronic control mounted downstream of the fan and upstream of the duct augmentor flame-holders. The thermal gradient in the nacelle is negligible between these two points. The temperatures of the nacelle wall metal, outer engine case metal, and nacelle air were calculated using the VCE simulation predictions of engine parameters. These calculations were derived by theoretical relationships and were based on current engine test data.

The predicted engine nacelle thermal data presented in table 26 were calculated for the same 15 flight points defined in Table 23. This data was tabulated to predict the extremes of the environmental conditions that would result from operating the engine at the limits of the aircraft flight envelope. Although the flight envelope sets the limits for which the engine may be operated. The use of an aircraft in the assumed mission profiles represents a more realistic range of operating conditions. The ambient environment resulting from operation of the engine at the mission-related conditions is tabulated in Tables 27 and 28. It should also be noted that the sea level ground idle point has been included as a mission point and is considered a realistic part of the aircraft mission.

The nacelle environments specified in the tables are for steady-state operation. Because of a transient thermal lag, the actual temperature levels at the higher Mach number points may be lower than the steady-state values shown in the tables.

The predicted engine case temperatures in the tables assume a titanium honeycomb construction. If the electronic control were mounted in an area of sheet and stringer structure, the maximum engine case temperatures shown in the preceding column would be used.

4.2.2 Cooling Methods

When the electronic control is mounted in the location assumed in this study, the elevated air temperatures and surrounding metal temperatures result in the requirement to cool the control. The use of fuel as a cooling medium is well established in current engine programs.

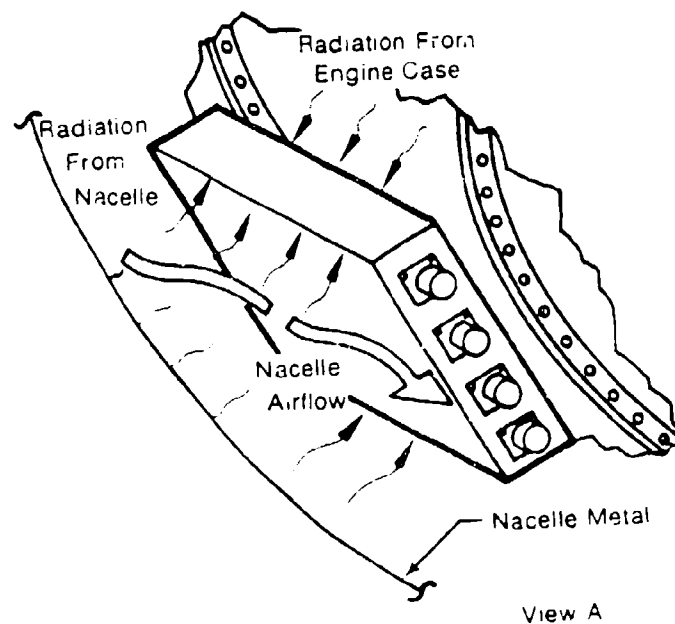
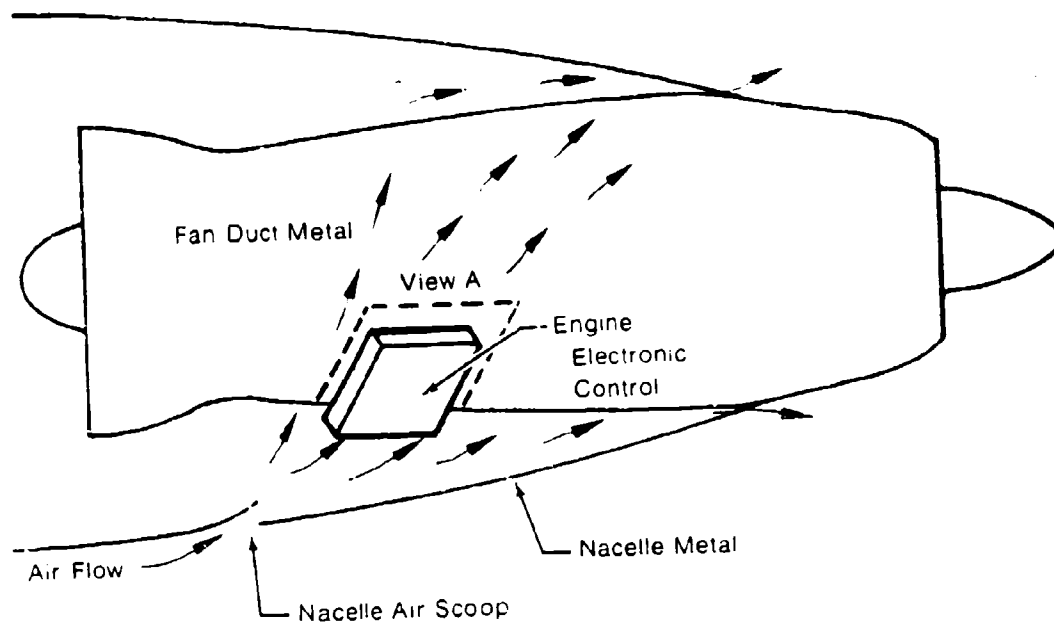


FIGURE 59 ELECTRONIC CONTROL MOUNTING CONFIGURATION

TABLE 26. PREDICTED ENGINE NACELLE THERMAL ENVIRONMENT AT EXTREME FLIGHT CONDITIONS

Figure 9

TABLE 27 TYPICAL ENGINE NACELLE THERMAL ENVIRONMENT - BATTLEFIELD INTERDICTION MISSION

Flight Point	Altitude (ft)	Mach No.	Power Setting	Flight Condition	Duration (min)	Nacelle Pressure (psi)	Nacelle Air Temperature (°F)	Nacelle Fuel Temperature (°F)	Engine Case Temperature (°F)	Point A Fuel Tank Average Temperature (°F)	Point B Engine Fuel (lb/hr) Average Temperature (°F)	Point C Nozzle Discharge Average Temperature (°F)
16	0	0	Idle	Ground	30	14.2	50	50	150	80	200	226
17	0	0	Idle	Ground	30	14.2	50	50	150	80	150	165
18	0	0	10	Partial Power	4.6	14.2	68	68	285	55	200	217
19	18,500	0.94	Partial Power	Cruise	23.8	14.2	100	100	300	55	200	218
20	19,100	0.94	Partial Power	Cruise	15.0	14.2	100	100	300	55	155	165
21	20,000	1.50	Partial Power	Cruise	6.8	14.2	100	100	300	55	155	165
22	20,000	1.50	Partial Power	Turn	0.9	14.2	100	100	300	55	155	165
23	20,000	1.50	Partial Power	Cruise	0.9	14.2	100	100	300	55	200	221
24	41,900	2.34	Partial Power	Cruise	3.0	14.2	100	100	300	55	200	227
25	0	0	Idle	Ground	30	14.2	50	50	150	80	200	226
26	0	0	Idle	Ground	30	14.2	50	50	150	80	200	226

TABLE 23 TYPICAL ENGINE NACELLE THERMAL ENVIRONMENT - DEEP STRIKE MISSION

Flight Point	Air Temp (°F)	Wing Mach	Engine Setting	Flight Condition	Nacelle Duration (min)	Nacelle Duration (hrs)	Nacelle Exit Temp (°F)	Nacelle Inlet Temp (°F)	Aircraft Nacelle Inlet Temp (°F)	Max Air Temp (°F)	Engine Case Temperature (°F)	Point A Fuel Tank Average Temperature (°F)	Point B Engine Case Inlet Average Temperature (°F)	Point C Boost Pump Case Inlet Average Temperature (°F)
16	0	0	Idle	Ground	30.0	0.5	0	0	0	0	0	0	0	0
17	0	0	Idle	Ground	30.0	0.5	0	0	0	0	0	0	0	0
18	0	0	Idle	Ground	30.0	0.5	0	0	0	0	0	0	0	0
19	0	0	Idle	Ground	30.0	0.5	0	0	0	0	0	0	0	0
20	0	0	Idle	Ground	30.0	0.5	0	0	0	0	0	0	0	0
21	0	0	Idle	Ground	30.0	0.5	0	0	0	0	0	0	0	0
22	0	0	Idle	Ground	30.0	0.5	0	0	0	0	0	0	0	0
23	0	0	Idle	Ground	30.0	0.5	0	0	0	0	0	0	0	0
24	0	0	Idle	Ground	30.0	0.5	0	0	0	0	0	0	0	0
25	0	0	Idle	Ground	30.0	0.5	0	0	0	0	0	0	0	0
26	0	0	Idle	Ground	30.0	0.5	0	0	0	0	0	0	0	0
27	0	0	Idle	Ground	30.0	0.5	0	0	0	0	0	0	0	0
28	0	0	Idle	Ground	30.0	0.5	0	0	0	0	0	0	0	0
29	0	0	Idle	Ground	30.0	0.5	0	0	0	0	0	0	0	0
30	0	0	Idle	Ground	30.0	0.5	0	0	0	0	0	0	0	0
31	0	0	Idle	Ground	30.0	0.5	0	0	0	0	0	0	0	0
32	0	0	Idle	Ground	30.0	0.5	0	0	0	0	0	0	0	0
33	0	0	Idle	Ground	30.0	0.5	0	0	0	0	0	0	0	0
34	0	0	Idle	Ground	30.0	0.5	0	0	0	0	0	0	0	0
35	0	0	Idle	Ground	30.0	0.5	0	0	0	0	0	0	0	0
36	0	0	Idle	Ground	30.0	0.5	0	0	0	0	0	0	0	0

For this study fuel temperatures were determined for three different cooling fuel access points. These access points are illustrated in Figure 60. In the first cooling method, fuel taken from access point A at the aircraft boost pump discharge upstream of the aircraft heat exchanger circulates through the electronic control and returns to the aircraft fuel tank. In the second method, fuel taken from access point B in the engine fuel supply line upstream of the engine boost pump, but downstream of the aircraft heat exchanger, circulates to the electronic control through a motive flow system using an ejector. The ejector motive flow is created by the pressure rise across the engine boost pump. Fuel pickoff point B must be located far enough in front of the boost pump to prevent fuel temperature elevations caused by fuel system recirculation flow to the boost pump. In the third method, fuel taken from point C at the engine boost pump discharge circulates through the electronic control and returns to the boost pump inlet.

Extended post-mission operation has been patterned after that experienced on the F-15 fighter aircraft. The bulk of ground operation is experienced in pre-flight checks (typically 30 minutes) as compared with the shorter post-flight time (10 minutes).

The fuel temperatures at these three fuel system points are presented for each flight point in Tables 26 through 28. It is evident that tank fuel, point A, is at a significantly lower temperature than point B or C fuel and does not vary appreciably from one flight condition to another as does point B and C fuel.

The method used to determine the fuel tank temperatures was developed during the Full Authority Digital Electronic Control study and was based on Air Force report AFAPL-TR-73-51, Aircraft Fuel Heat Sink Utilizations. This method evaluated the fuel temperature level and contributors to fuel temperature rise or decrease at each step of fuel handling or usage from ground bulk storage to engine combustor. Initial tank temperatures of 135°F for flight envelope conditions and 80°F for mission profile studies were assumed. Heating and cooling rates for the tank fuel over the flight envelopes and mission profiles were calculated using a time constant estimated from F-4C, F-5A, and F-111A aircraft inflight temperature profiles presented in report AFAPL-TR-73-51.

Point "A" maximum column reflects the maximum temperature of the fuel in the aircraft tank after a 12 minute duration at each flight condition in Table 26. The 12 minute duration was used to correlate the time at the extreme flight envelope temperature with the time duration expected at high Mach conditions in the mission requirements. At each flight condition given in Table 26, the initial tank temperature was assumed to be 135°F which is the maximum tank temperature recorded in current engine aircraft fuel tanks on the ground on extreme hot day conditions.

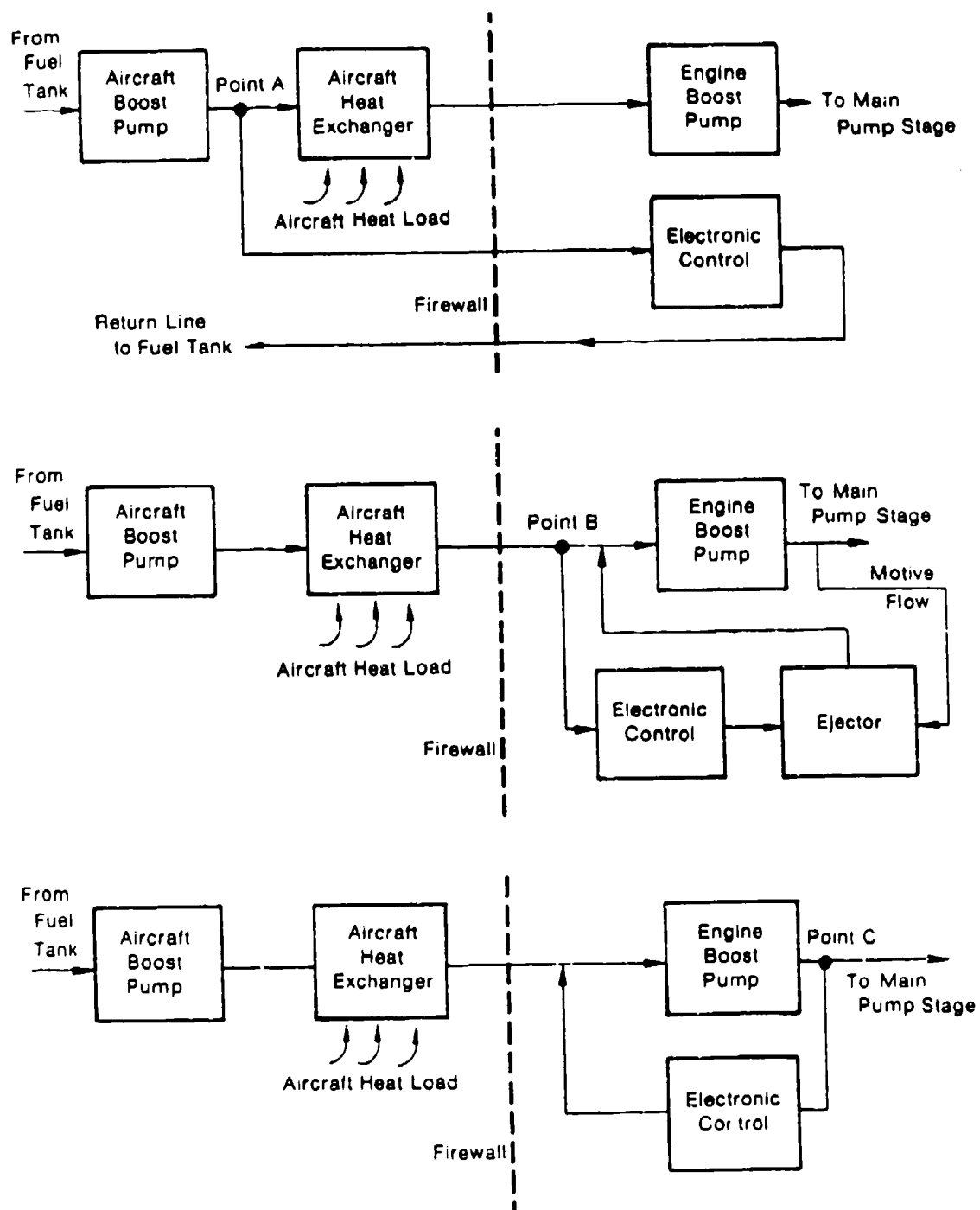


FIGURE 60 COOLING FUEL ACCESS POINTS

The Point "A" average column reflects the temperature of the fuel in the aircraft tank after a 12 minute duration at each flight condition in Table 26, assuming an initial temperature of 80°F as an average aircraft fuel tank temperature on the ground.

The tank temperature provided in Tables 27 and 28 for Point "A" are the temperatures existing in the fuel tanks as a result of operating the aircraft through the mission profiles used in the study.

For this study, it was assumed the shaft-power requirements of the aircraft were met with an engine-driven aircraft mounted gearbox (as in the F-15 and F-16). The heat rejected from that gearbox is imparted to the aircraft fuel through an aircraft mounted heat exchanger. This heat load that is recirculated by the aircraft fuel handling system is the major contributor to fuel temperature rise in the fuel tanks and to the elevation of fuel temperature between the fuel tank supply at Point "A" and the engine boost pump inlet Point "B".

The fuel temperature as supplied to the electronic control from access point B was based on the temperature of the fuel upstream of the engine boost pump. This fuel has a temperature elevated above that of the fuel tank supply temperature as a result of the addition of heat from the aircraft heat exchanger. This temperature is a function of climatic conditions, tank temperatures, mission points, and the extent to which the aircraft uses the fuel heat sink capability. The maximum temperature of this fuel supplied to the engine is a negotiated specification depending on engine-aircraft application and is controlled by the aircraft fuel management system. For this study, the maximum limit was set at 200°F based on current engine applications.

The temperatures tabulated for access point C boost pump discharge cooling fuel are elevated above the point B cooling loop by the temperature rise of the boost pump. This temperature rise is a function of fuel pump design (i.e., efficiency, flow curves, and pump bearing cooling flows). Since this study does not address pump design, the data for the engine boost pump temperature rise was based on existing test data for state-of-the-art pumps.

The mission profile environmental data reflects ambient air, metal, and fuel temperatures at steady-state engine operation at the specified flight condition. However, the tank supplied cooling fuel may undergo temperature transients during air refueling. The maximum change would be from 135° to 0°F. Engine supply fuel temperature transients of 200° to 180°F in 2.5 sec during power lever transients are typical. The total simultaneous ambient pressure and temperature changes may be as much as 6 psi/min and 10°F/sec.

The primary fuel used to cool the control will be fuel conforming to or having the variations in characteristics permitted by MIL-T-5624, Grade JP-4. Alternate fuels are:

- MIL-T-5624, Grade JP-5 (12 centistokes or less)
- ASTM Types A and B
- NATO Fuel No. F-40 and F-44 (equivalent to Grades JP-4 and JP-5, respectively).

These fuels may also contain anti-icing additive conforming to MIL-I-27686 and added in the same concentrations as specified for the primary fuel.

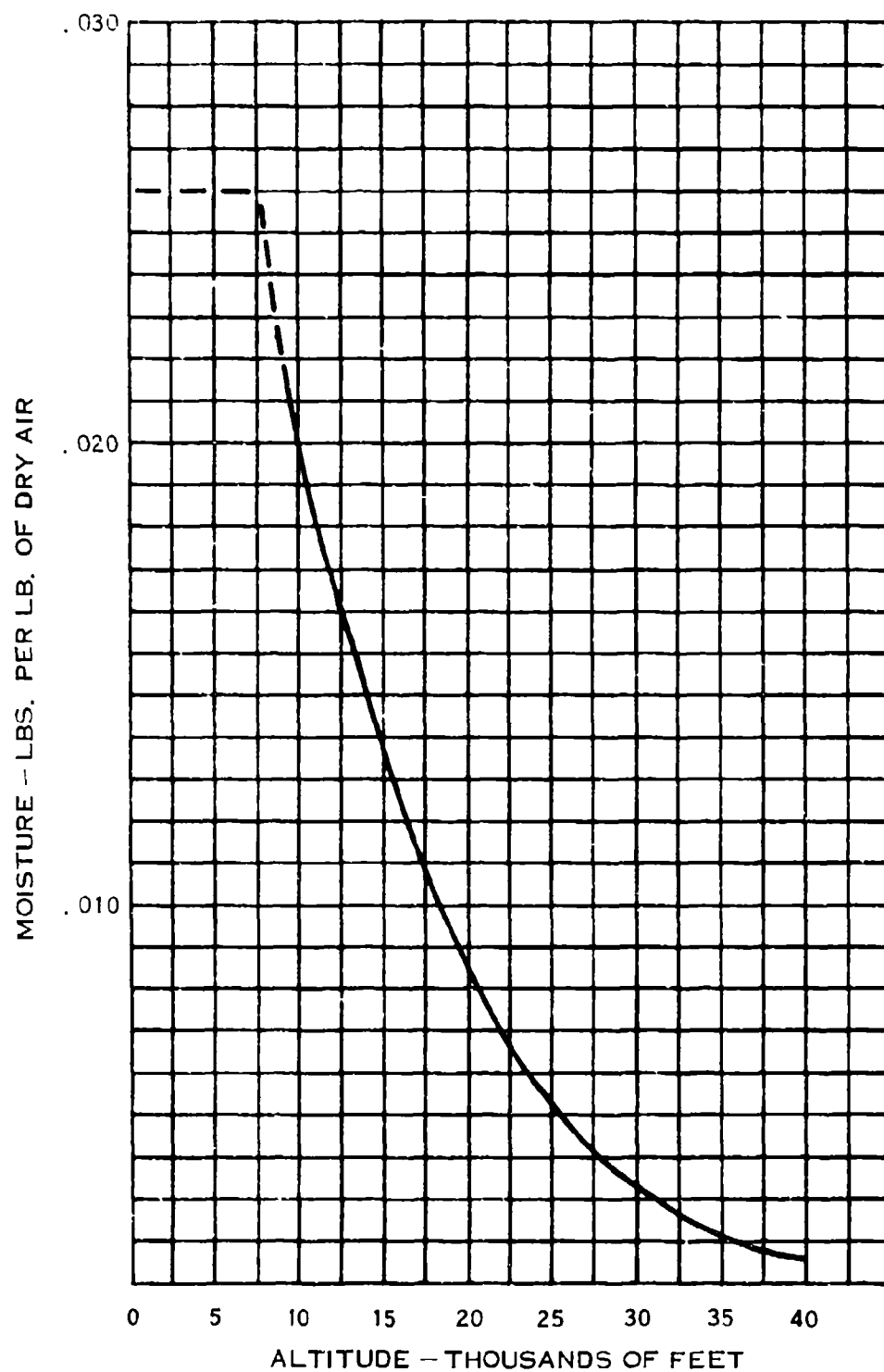
4.2.3 Moisture

The types of moisture which the electronic control would be exposed to are humidity, condensation and precipitation.

The humidity would affect the control during temperature changes which could condense the moisture out of the air and deposit it on the interior and exterior surfaces of the control. The most common occurrence of condensation would be in a humid tropical climate when the nighttime temperature drops the air temperature to the dewpoint causing condensation of the water vapor in the air. Typically on a 95°F day with a relative humidity of 75% the dew point would be reached by lowering the temperature to 85°F. At this point the air would have an absolute humidity of .026 lbs. of moisture/lb. of dry air which is about 13 grains per cu. ft.

The condensation of water vapor on the control and penetration into the control could also occur as a result of altitude change and temperature change of the air surrounding the EEC in the nacelle. The worst case temperature and altitude cycle during an aircraft mission would occur during take-off and landing in a tropical climate. Assuming a 95°F day with a relative humidity of 95% the air around the control has a specific humidity of .035 at 29.9 in. Hg. The aircraft would take-off and climb to an altitude of approximately 38,000 feet where the specific humidity would be less than .001 at a temperature of -1°F and pressure of 6.1 in. Hg. at cruise power. The specific humidity would vary with altitude during the climb as shown by Figure 61. During the remaining part of a mission, the aircraft would remain at high altitude conditions and low humidity. The aircraft would then complete the mission by landing during a 5 minute descent from the low humidity high altitude condition to the 95°F, 95 percent humidity condition assumed initially.

The above humidity cycle during normal operation and mission cycle does not consider the area of moisture due to precipitation. Since the aircraft must operate in most weather conditions, the area of rainfall must be considered. Although the control is located inside the airframe or nacelle, it is not completely sheltered from the moisture. The nacelles are typically purged with outside air by air scoops or an ejector system. For the worst case application we can assume that the liquid water content in the nacelle is the same as in the outside air.



E- 5918

FIGURE 61 MOISTURE DECREASE WITH ALTITUDE

Although the intensity of precipitation varies from storm to storm and within the same storm cell, models have been developed estimating the extremes in the tropics. These extremes were calculated by extrapolating surface climatological intensities with known probabilities, by employing recorded extremes aloft and by utilizing research information from meteorologists specializing in cloud physics and radar meteorology. These extremes are published by the Air Force Cambridge Research Laboratories (AFCRL) in Reference 4. Table 29, taken from the reference presents precipitation extremes at sea level and aloft that are exceeded with an average probability of 0.5 and 0.1 percent in the rainiest tropics during the rainiest months. In Table 29 the 0.5 percent surface precipitation range of 0.80 millimeters per minute and its corresponding 2.22 grams of water per cubic meter (g/m^3) of air was calculated using weather records for several locations in the rainy tropics. The 0.1 per cent probable extreme at the surface was calculated using the weather record for Cherapunji, India, the station with the world's greatest rainfall amount.

If an aircraft penetrates a 0.5% worst precipitation area "on the deck", it would experience a liquid water content of only 2.22 gm/m^3 by making the assumption that no clouds occur on the deck. At 1.5 kilometers, about 5,000 feet, it would experience 4.56 gm/m^3 (precipitation plus clouds). The moisture level would peak at about 4.5 to 6 kilometers (about 15,000 to 20,000 feet) at 5.47 gm/m^3 . The same type scenario can be made for the 0.1% probability area. It should be noted that the liquid water contents are lowest at sea level and above 20,000 feet.

The AFCRL data is summarized in Table 30 providing precipitation liquid water amounts in gm/m^3 and percent water to air by weight ratio.

Another source of moisture to the control would be in the form of cleaning solution used to wash down the engines. The engine and all the components are spray washed with a PD860 or PD880 petroleum distillate cleaning solution. This is done on a random basis as needed. During the engine wash down the control and associated connectors are completely wetted with the solution.

4.2.4 Fuel and Oil Resistance

The environment inside the Nacelle is normally purged by ducting outside air into the nacelle (See Figure 59). The airflow will keep the duct purged of fuel and oil vapors during engine operation. The electronic control and its electrical connectors will be operating in an area where engine fuel or oil spills could occur and therefore must be compatible with engine fuels (MIL-T-6625, JP-4 and JP-5) and lubricating oil (MIL-L-7808 and MIL-L-23699).

Lab analyses of deposits from outside cases of current engine electronic controls show trace amounts of petroleum distillates used in engine wash downs. The electronic control is completely wetted with these cleaning solutions and must therefore be designed to be compatible.

TABLE 29 LOW PROBABILITY MODELS OF PRECIPITATION RATES AND LIQUID WATER ALOFT

(SISSENWINE, AFCL-72-0369, 1972)

ALTITUDE		RATIOS		Exceeded With An Average Probability of .5 Per Cent				Exceeded With An Average Probability of .1 Per Cent			
				RATE		WATER PREC. CLOUD		RATE		WATER PREC. CLOUD	
				MM MIN	IN HR	g CU.M	g CU.M	MM MIN	IN HR	g CU.M	g CU.M
0	0	1.0	0	.80	1.9	2.22	0	3.13	7.2	8.35	0
1.5	4920	1.12	.83	.90	2.1	2.49	2.07	3.50	8.1	9.30	8.12
3	9840	1.24	.92	.99	2.3	2.73	2.30	3.88	8.9	10.28	9.00
4.5	14760	1.35	1.00	1.08	2.5	2.97	2.50	4.23	9.7	11.18	9.78
6	19680	1.35	1.00	1.08	2.5	2.97	2.50	4.23	9.7	11.18	9.78
9	29520	.75	.56	.60	1.4	1.68	1.44	2.35	5.4	6.32	5.53
12	39360	.44	.32	.35	.8	.97	.81	1.38	4.4	3.77	3.18
15	49200	.19	.14	.15	.4	.43	.35	.59	1.4	1.65	1.38
18	59040	.03	.02	.02	.1	.06	.05	.09	.2	.27	.21

TABLE 30 SUMMARY OF LIQUID WATER CONTENT AT ALTITUDE

(SISSENWINE, AFCL-72-0369, 1972)

ALTITUDE		THESE VALUES EXCEEDED AN AVERAGE PROB- ABILITY OF .5 PER CENT		THESE VALUES EXCEEDED WITH AN AVERAGE PROB- ABILITY OF .1 PER CENT	
KM	FEET	$\frac{g}{CU.M}$	$\frac{WW}{WA} \%$	$\frac{g}{CU.M}$	$\frac{WW}{WA} \%$
0	0	2.22	.18%	8.35	.88
4.5	14760	5.47	.5 %	20.96	2.69
6	19680	5.47	.83%	20.96	3.2
9	29520	3.12	.67%	11.85	2.53
15	49200	.78	.4 %	3.03	1.55

4.3 Vibration, Acoustic, and Impact Environment

4.3.1 Vibration Environment Definition

One area of the electronic control environment that has exhibited considerably more hostile conditions than were predicted by military specifications is the vibration environment. Engine test data shows that vibratory acceleration levels in the high-frequency range are significantly higher than specified in MIL-STD-810B. Based on the VCE fan design, using current engine test data as a reference, the VCE vibration levels in the 500 to 20,000 Hz range at the electronic control location are predicted to be well above the military specification, with respect to both amplitude and maximum frequency (See Figure 62). Vibratory acceleration in this range was determined from fan pressure ratio, fan blade numbers, and fan tip speed. The major source of high vibration levels in the 500 to 20,000 Hz range is the fan, and the VCE fan shows an increase in fan pressure ratio and fan tip speed over current engines. These fan-induced high-frequency vibration levels (Figure 62) are strongly influenced by axial location of the control on the engine case. Vibration levels in the 500 to 20,000 Hz range would be 20% higher if the control were located on the fan case and 30% lower than shown in Figure 62 if located in the immediate vicinity of the rear engine mount (Figure 63). The potential exists for localized vibration levels being reduced due to specific engine design. However, these reductions cannot be anticipated because the engine definition utilized for this study is effectively an aerodynamic/thermodynamic model.

Low-frequency vibration (10 to 500 Hz, Figure 62) is dominated by high rotor and low rotor excitations. Vibration acceleration level in this range is not a function of axial location along the engine case.

Discrete-frequency acceleration and displacement levels are identified in Figure 64 for fan (E_F) and high rotor (E_H) excitation orders; all of these frequency components appear simultaneously. At $20E_F$, $24E_F$, and $40E_F$ the radial and tangential acceleration levels are 760g, while the axial acceleration is only half that level. In the Low-frequency range, displacement level is the more significant indicator.

Figure 65 illustrates schematically the vibration definition with respect to the control mounting system. The schematic shows that the vibration defined for the engine in this study can be altered by the case structure, bracket structure, vibration isolators, and control packaging techniques.

The electronic control receives vibration excitation from all contacts with the engine, including fuel and pneumatic plumbing and electrical cables, as well as the electronic control mounting brackets. The vibration received from the electrical cables has been found to be small because of the flexible construction of the cable harness. There have been significant levels of vibration

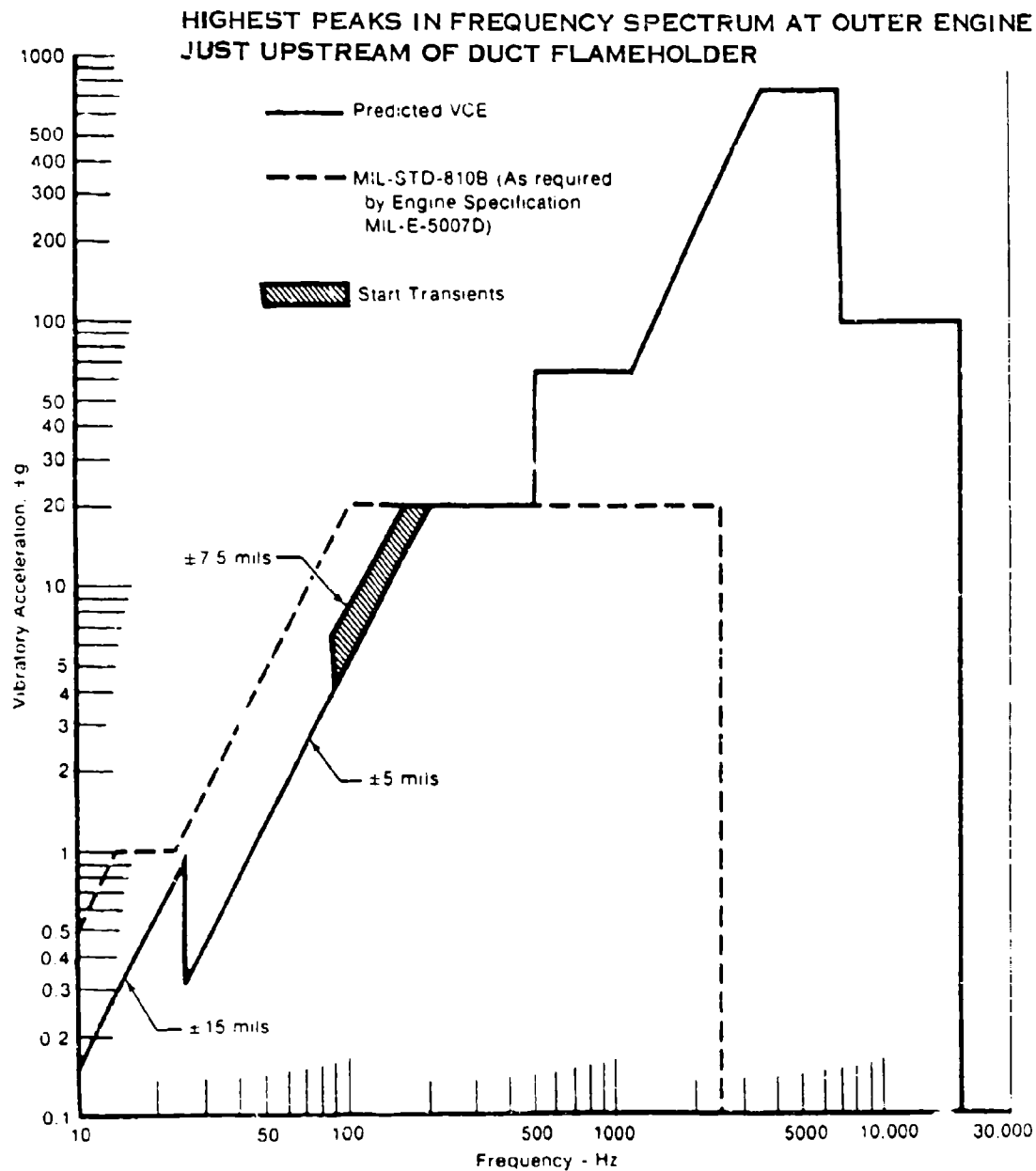


FIGURE 62 PREDICTED VIBRATION ENVIRONMENT FOR VARIABLE CYCLE ENGINE

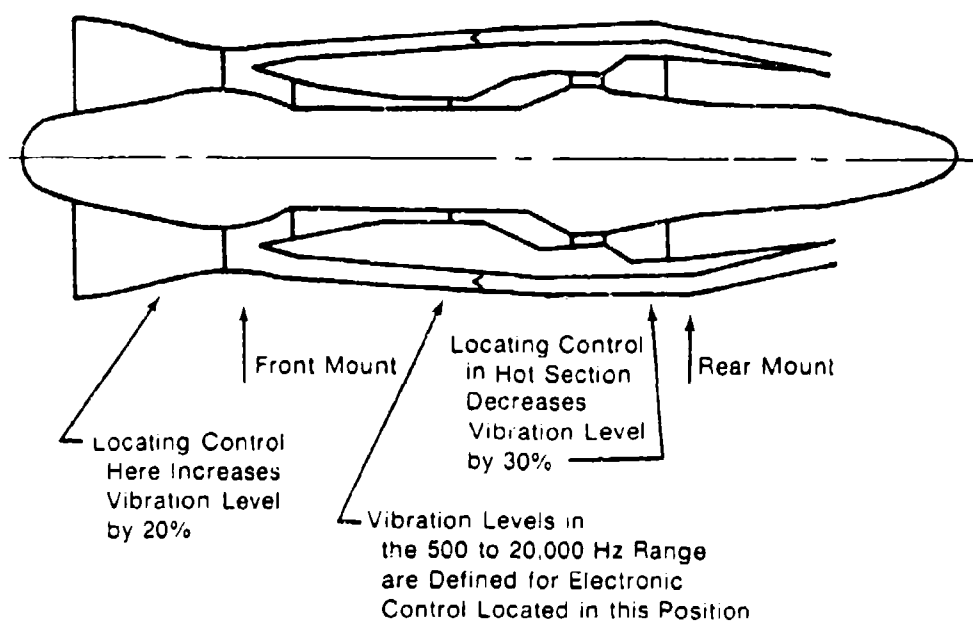
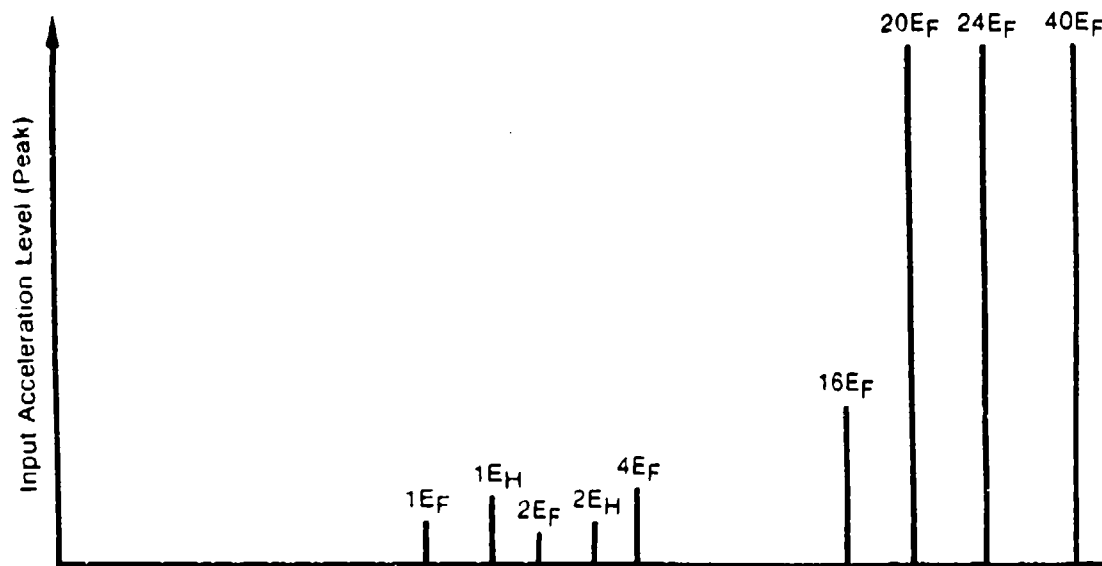


FIGURE 63 EFFECT ON VIBRATION ENVIRONMENT OF MOVING CONTROL LOCATION AXIALLY

Overall Displacement Level (70 Hz High Pass): ± 5 mils

Overall Acceleration Level (0 to 20,000 Hz): $\pm 1000g$



Highest Predicted Vibration Level (Maximum Peak)			
Order	Frequency Range (Hz)	Displacement (mils)	Acceleration (g)
1E _F	65 to 175	±5	Insignificant
1E _H	150 to 225	±3.85	↓
2E _F	130 to 350	±1	
2E _H	300 to 450	±0.75	
4E _F	260 to 700	Insignificant	±20
16E _F	1040 to 2800	↓	±100
20E _F	1300 to 3500		±760
24E _F	1560 to 4200		±760
40E _F	2600 to 7000		±760
			Radial 100%
			Tangential 100%
			Axial 50%

FIGURE 64 PREDICTED VARIABLE CYCLE ENGINE INSTANTANEOUS VIBRATION SPECTRUM AT THE ELECTRONIC CONTROL LOCATION

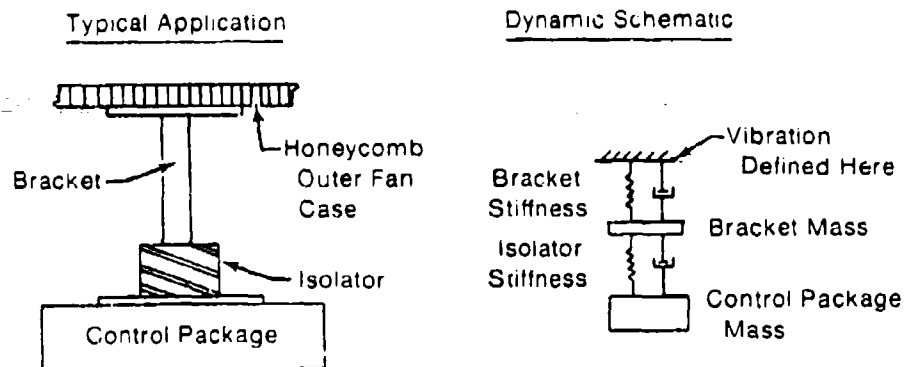


FIGURE 65 SCHEMATIC REPRESENTATION OF CONTROL MOUNTING WITH RESPECT TO VIBRATION

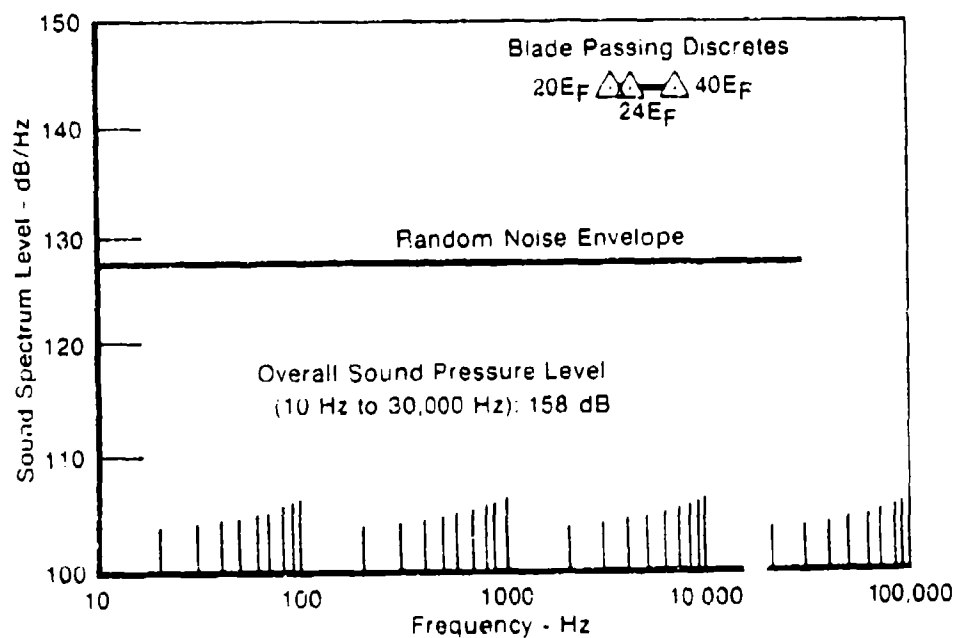


FIGURE 66 PREDICTED VARIABLE CYCLE ENGINE ACOUSTIC ENVIRONMENT

attributed to electronic control fuel plumbing connections which bypass the control mounting bracket isolation. This problem can be significantly reduced in advanced engines by proper engine fuel pump design techniques or by plumbing the control to the aircraft fuel tank. The levels of vibration expected from an aircraft fuel tank design would be less than 10g and would occur at frequencies less than 500 Hz.

The vibration associated with aircraft gunfire for the F-15 aircraft was reviewed and based on current fighter aircraft design practices there is no significant gunfire vibration passed thru the aircraft to the engine mounts.

4.3.2 Acoustic Environment Definition

The random noise portion of the acoustic environment was derived from current engine test data and predicted for the VCE, based on VCE burner pressure rise, and fan tip speed (Figure 66).

4.3.3 Impact Environment Definition

4.3.3.1 Impact Installed in Aircraft

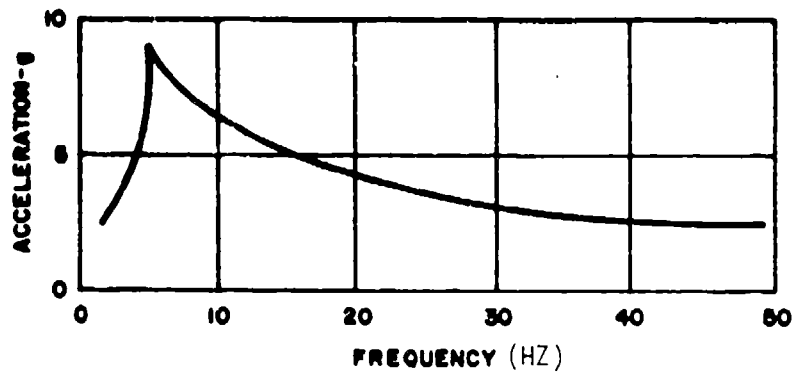
The impact shock loading associated with the engine electronic control is generated by aircraft landing or engine surge. Current engine applications of electronic controls have shown the shock load associated with landing or engine surge to be less than 10 g's.

4.3.3.2 Impact and Vibration During Transportation

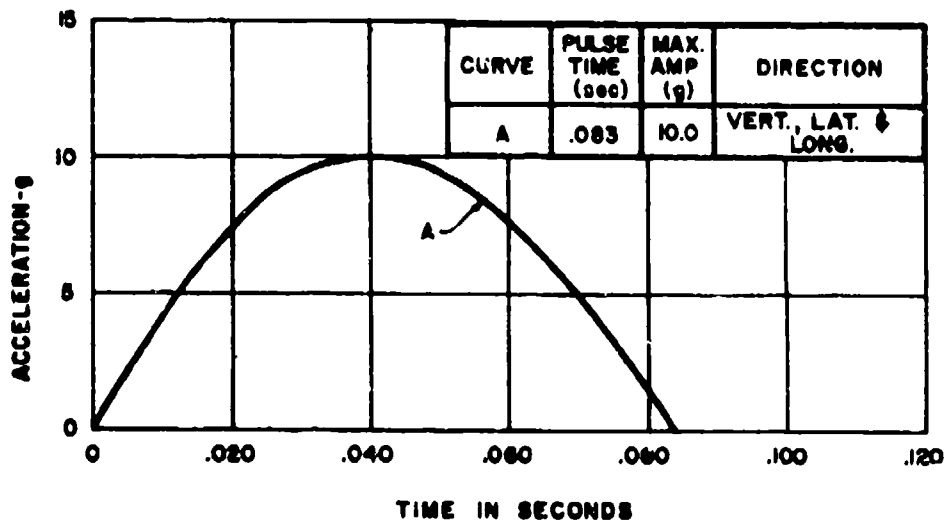
Engine Controls are shipped primarily by truck and by air transportation. Shock forces experienced during handling are probably the most severe that are encountered during the entire logistics cycle. Generally those forces are the result of the package being dropped. The amount of shock experienced by the package when dropped is directly affected by the pulse duration, or the shock rise time. The shock rise time is dependent on the yielding mass and is a function of its compressibility and elasticity. Other factors affecting shock rise time include the resiliency of the impact surface and the extent of the contact area, which may be a flat or curved surface, an edge, or a point.

Shock and vibration imparted by each mode of transportation are described below:

4.3.3.2.1 Truck Transportation The shocks and vibration encountered by transportation of material over the highway depend to some degree on the highway surface and on the characteristics of the transporting vehicle. Figure 67 shows the maximum shock in three planes and vibration in the vertical plane



- VIBRATION, VERTICAL -



- SHOCK -

FIGURE 67 CARGO ENVIRONMENTS FOR HIGHWAY TRANSPORT

obtained by the military for many types of road conditions and vehicles.

4.3.3.2.2 Air Transportation In-flight shock and vibration may be as high as 2 to 3 G's during normal operation of large commercial transport aircraft. The most damaging conditions are the shocks resulting from handling. Figure 68 shows the maximum shocks recorded during a test shipment in which two impact recorders were placed in a wooden box having a total weight of 73 pounds. The maximum acceleration experienced was 9G's due to handling.

Air transportation data from field studies of one of the military services is summarized in Figure 69. Envelopes of maximum values are recorded in three planes for vibration and in the vertical plane for shock. It is anticipated that data taken under emergency conditions would show accelerations that are somewhat higher.

4.4 Electrical Environment Definition

4.4.1 Summary

The lightning/EMI environment of a full authority electronic engine controller must be understood in order that adequate protective features can be provided in the controller design to prevent any harmful effects on the controller circuitry. This report describes the nature and magnitude of the assumed lightning/EMI environment.

4.4.2 General

The engine control when mounted on the VCE engine inside the engine nacelle is subjected to controlled amounts of high-frequency electromagnetic interference (EMI) energy from radar, communication, and navigation transmitters and to lower-frequency interference energy from lightning strokes.

Lightning is potentially capable of serious effects on both engines and controls. Protective features must prevent the effects of direct lightning strikes including the blasting, burning, direct coupling of voltage and currents, and structural deformation caused by direct lightning arc attachment as well as the high pressure shock waves and magnetic forces produced by the associated high currents. Indirect effects of lightning to protect against are the damage and malfunctions due to the large voltages and currents induced in the cables, wires, and circuits by the electromagnetic fields associated with lightning.

The electric field environment follows with the lightning environment first and then the environment due to electromagnetic interference from ground and airborne transmitters. In describing the lightning environment, information was compiled from References 23 through 35.

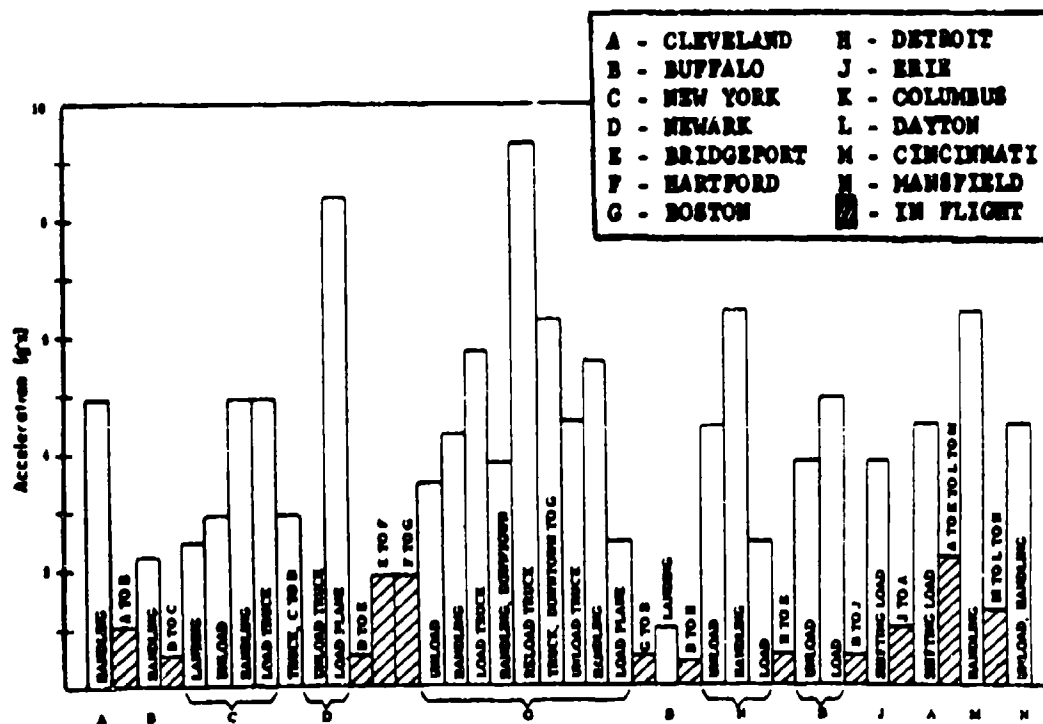
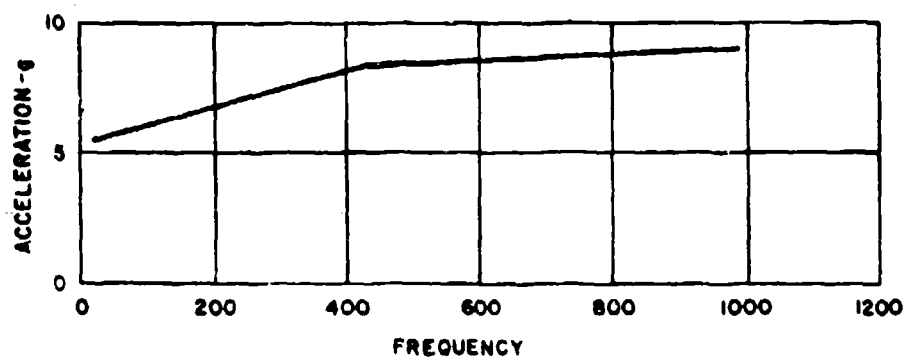
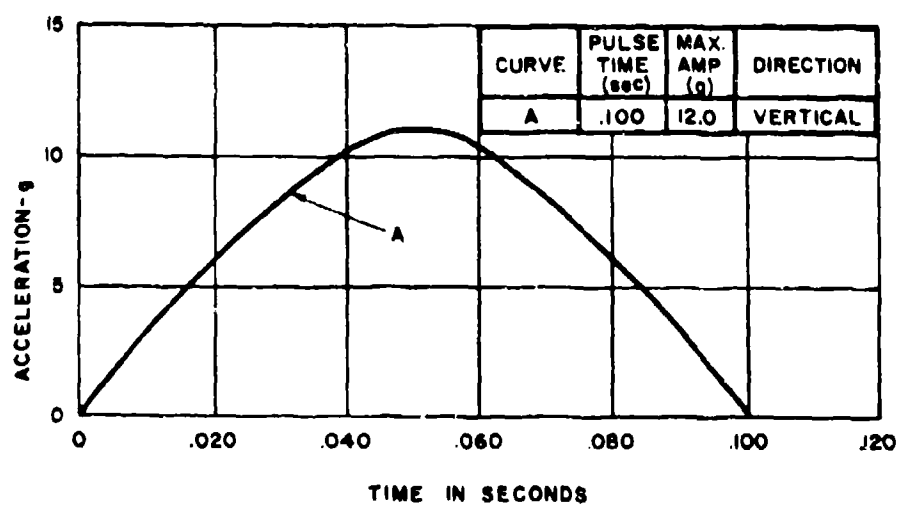


FIGURE 68 MAXIMUM SHOCKS RECORDED DURING AIRLINE TEST SHIPMENT



- VIBRATION, VERTICAL - LATERAL - LONGITUDINAL -



- SHOCK -

FIGURE 69 CARGO ENVIRONMENTS FOR AIR TRANSPORT

4.4.3 Lightning Environment

4.4.3.1 Lightning Strike Statistics

The Lightning and Transients Research Institute lightning-strike records indicate an average of about one lightning discharge for 2500 hours of flight time per commercial aircraft on domestic routes. This figure drops to a much lower value of about one strike per 10,000 hours for long-range flights in which the aircraft spends a much greater percentage of its time at altitude. These records also indicate that strikes to the engine nacelles are very infrequent, of the order of a few percent.

USAF experience for the years 1965 to 1969 indicates an average of 99,200 mean hours between lightning strikes for fighter aircraft. However, the strike experience in Europe is 10 times more frequent than in the U.S. and in most other parts of the world. RF-4C aircraft flying in Europe report 10.5 strikes per 100,000 hours, which rate is about 5 times greater than the world-wide exposure rate for these aircraft. For three different models of the F-4, a maximum of 8% of the strikes were to the fuselage. The higher lightning-strike exposure seems to result both from the level of lightning activity in Europe and from the political constraints placed on flight paths in this multinational region.

The various factors described which influence lightning-strike frequency indicate the care with which lightning-strike statistics must be approached. The following factors have been shown to be important, and their contributions must be assessed:

- a) Significant differences in reporting requirements.
- b) Commercial or military aircraft.
- c) Flight plans, including requirements to fly in all weathers.
- d) Flight paths, including opportunities for thunderstorm avoidance.
- e) Altitude.
- f) Weather conditions, including temperature, precipitation, and turbulence.
- g) Aircraft size and shape.
- h) Piston or jet engines.

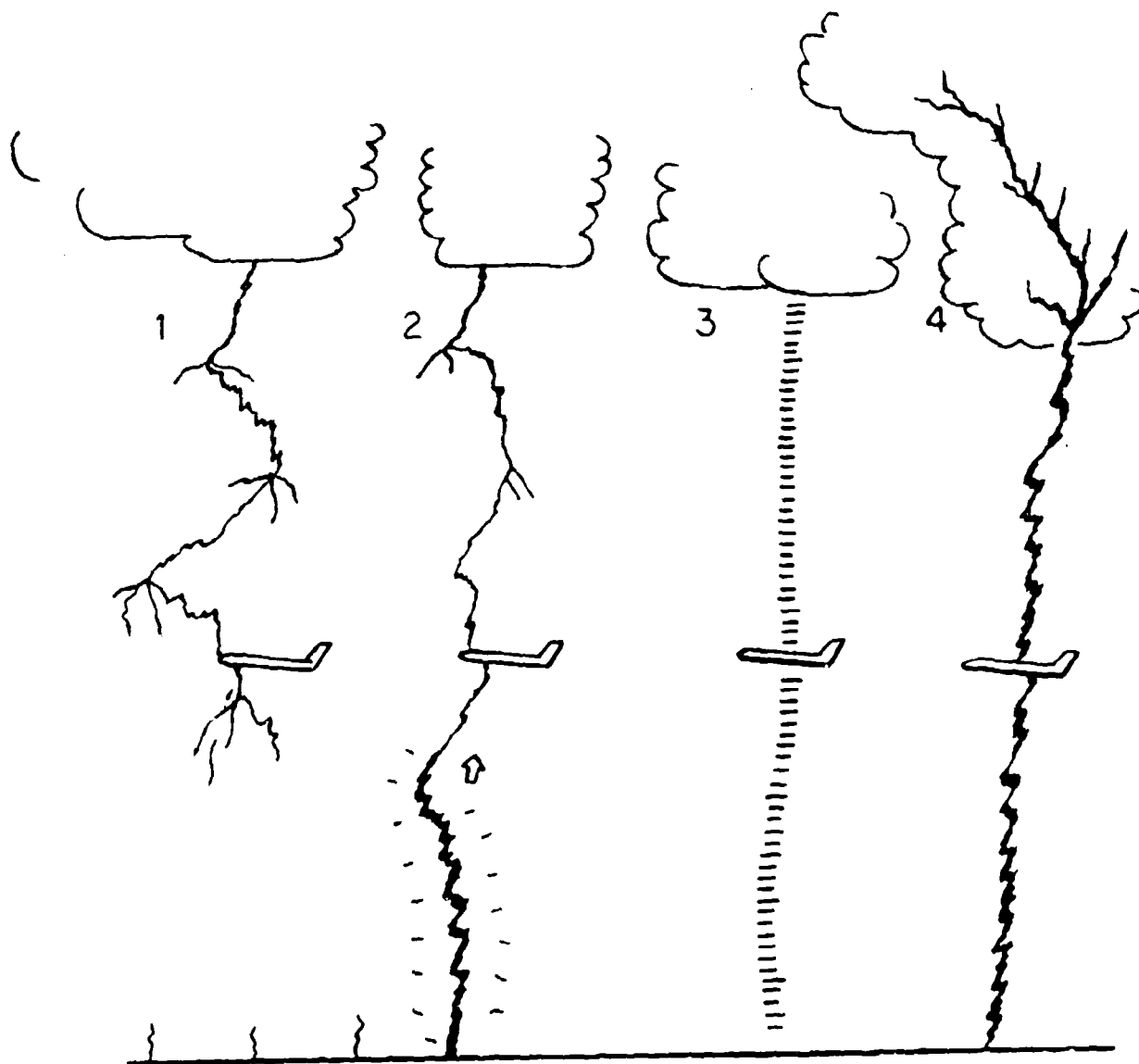
One important factor, which is not reflected in the current damage statistics is that aircraft are probably often struck with low current discharges which are not reported. A typical upper region intra-cloud discharge may be fairly low in current magnitude, of the order of a few thousand amperes, with low current rates of rise. This strike results in almost no noise and very little indication to the pilot, particularly with a strike to the aft portion of the aircraft. With all metal skins, the low amplitude discharges produce very minor pitting and the aircraft would have to be carefully examined over its entire outer surface after every flight to detect that a strike had occurred.

4.4.3.2 Lightning Strike Characteristics

It is useful to review briefly the basic mechanisms of stroke contact to an aircraft as illustrated in Figure 70. Natural lightning discharges initiate from a charged region in a cloud in the form of a "step leader" which advances in approximately 50 meter steps toward another charge region or toward the earth. In some cases, the aircraft triggers a lightning discharge which would not have occurred otherwise, and in some cases, it merely diverts the discharge slightly out of its normal path so that the stroke passes through the aircraft. As a step leader approaches an aircraft, the intense voltage existing between the tip of the step leader and the aircraft induces streamers, intense ionization, from all the external aircraft surfaces and particularly the extremities. This is illustrated in Figure 71 showing streamering from a model aircraft subject to intense cross fields in the laboratory. The step leader contacts one of the vehicle extremities through the streamer, and the vehicle potential is immediately raised to the extreme potential of the lightning discharge. Then additional streamering takes place from the opposite extremities of the vehicle to form the step leader for the continuation of the stroke paths to other charged regions or to the earth. Data indicate that jet-engine exhaust is only slightly more ionized than the ambient air and much less so than rocket exhaust with the result that jet exhaust has insufficient conductivity to initiate or attract a lightning leader.

When the step leader contacts the earth or another charged region, the existence of an ionized conducting path between the earth and the charged region (or the two oppositely charged regions) results in a large surge current, a kind of huge short circuit, in the form of an ionization wave which travels back up the step leader path to the initiating charge region in the cloud. This high current ionizing wave is referred to as the "return stroke". This phase is followed by an intermediate current, a long duration current of about 100 amps and sometimes one or more restrikes. (Note that in any case of significant damage to an aircraft, the discharge passed through the vehicle and did not initiate from it or terminate on it as is often indicated in strike reports). The different phases of the discharge are also illustrated in Figure 71 showing a triggered natural lightning discharge to the LTRI research vessel, Thunderbolt, triggered by firing a small rocket carrying a fine wire to an altitude of 300 to 1000 feet. The associated current waveform is shown in the oscillogram.

Lightning strokes thus generally consist of (a) an initial high current strike, (b) an intermediate current component, (c) a low current continuing component, and (d) multiple re-strikes with as many as 30 discharges in a single-stroke lasting for as long as three-quarters of a second. The time between re-strike is usually about 15 to 30 msec.



E-158

FIGURE 70 LIGHTNING STROKE MECHANISMS

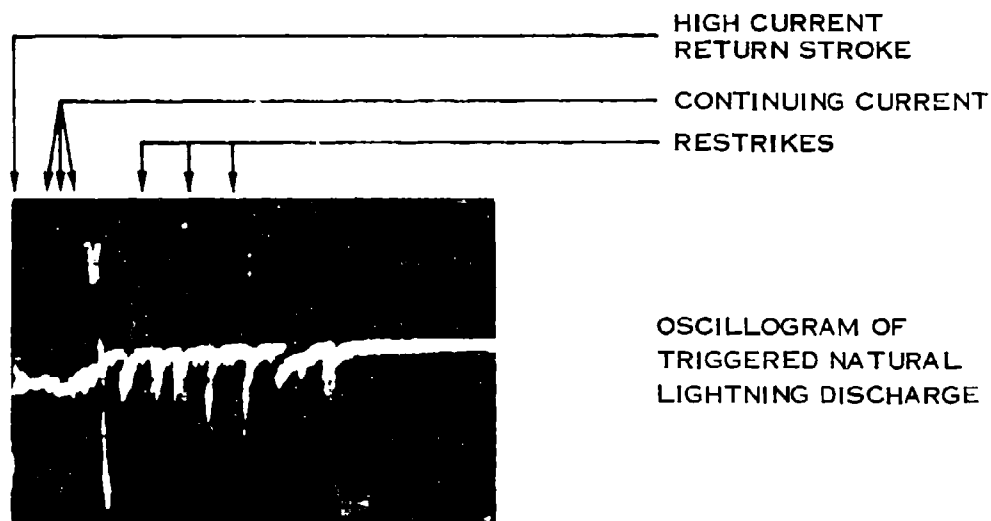
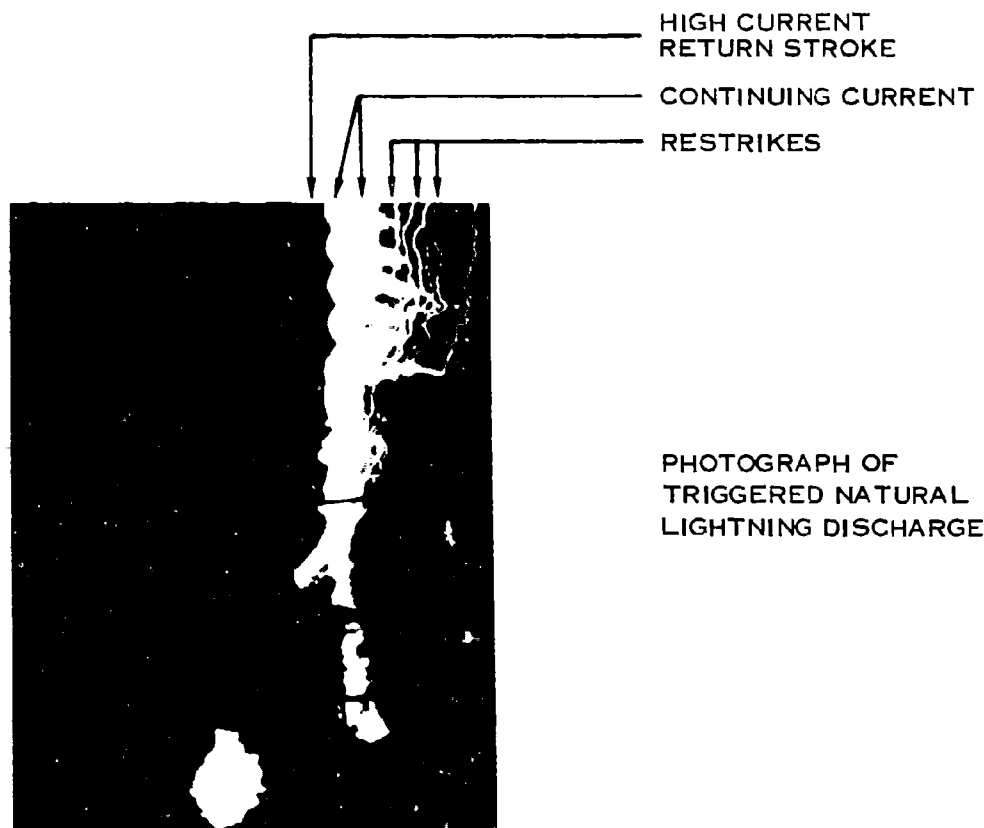


FIGURE 71 STREAMERING FROM AIRCRAFT PRIOR TO STRIKE

Because of motion of the aircraft past the relatively stationary lightning channel, the stroke may sweep backwards over the aircraft, permitting contact at nearly any point behind a major forward strike point, such as the nose. This means that initial attachment or hang-on of the flash may be expected at any section of an engine from the intake inlet, over the outside housing, to the exhaust nozzle at the rear. FAA advisory circular AC 20-53 defines the fuselage tail cone as being in zone 1, which includes points of direct stroke attachment. The task F subcommittee of the SAE Committee AE-4 on Electromagnetic Compatibility has defined the fuselage tail cone as being in zone 1B, which includes initial attachment points with high probabilities of flash hang-on. Assuming that the subject aircraft of this study has its engine exhaust nozzles projecting beyond the tail empennage, these nozzles will be within zones 1 or 1B.

4.4.3.3 Lightning Related Assumptions

Definition of the lightning/EMI solution is heavily dependent on the detailed form, configuration and materials content of the engine/nacelle design. In the absence of such detail for the VCE engine and installation, a few broad assumptions will be made in the event that they may be useful in a preliminary design.

4.4.3.3.1 Preferred Structural Path It is assumed that the airframe has been designed with lightning strikes in mind and that a preferred, continuous, metallic path is provided from the preferred point of lightning entry to the preferred exit point. The metallic path is assumed capable of conducting the peak and continuing currents of the lightning strike without damage and without jeopardizing the vehicle or crew safety. The metallic path consists of both internal structure and metal skin. The increasing use of boron-and graphite-reinforced composites to fabricate body panels is anticipated, particularly in the tail area and to a lesser extent in the forward fuselage. Because of heat problems and the intricate shape of body panels covering the engine, it is assumed that metal skin will continue to be used in the engine area. The preferred metallic path, including mated surfaces and bonds, is assumed to comply with the Class L requirements of MIL-B-5087B. The impedance between preferred-path extremities is assumed low enough so that a test current of 200kA peak, 20 μ s wide at 50% amplitude, and a risetime of 100kA/ μ s will cause a voltage drop in the path of 500V maximum. This impedance is also assumed to be retained for the life of the aircraft.

Boron-and graphite-reinforced plastics consist of filaments of these materials imbedded in a resin matrix. Because of the metal filaments, composites have some shielding effectiveness, but it is very low, and much less than an aluminum skin. Resistivities for typical boron and graphite composites are 2000 and 36 times respectively, that of aluminum, and for boron composites is dominated by the tungston filament on which the boron is deposited. Magnetic-

field attenuation provided by graphite composite 0.0375" thick varies from 15dB at 30MHZ to 30dB at 500MHZ. By comparison, aluminum of the same thickness has over 500dB of absorption loss at these frequencies. Composite panels usually require protection from overheating when carrying direct-strike currents, particularly zone 1 locations. Such protections include wire fabrics, aluminum foil, conductive paint, and flame-sprayed aluminum, all of which increase the shielding effectiveness of a composite panel so protected. However, magnetic-field shielding improvement is modest, being only 8.5dB for 1-mil aluminum foil and 5.2dB for flame-sprayed aluminum. Puncture-damage protectors such as diverter straps and foil strips do not significantly increase shielding effectiveness because of their narrowness and wide spacing. Test data for electric-field shielding effectiveness of composites are not available. However, data for the vacuum deposition of aluminum 0.030-mil thick on glass indicate a plane-wave shielding effectiveness of 45-60dB from 10kHz. Other data for flame-sprayed aluminum on Lexan foam show an electric-field shielding effectiveness of 65dB at 5MHZ falling to 13dB at 50MHZ. These data prompt some confidence that aluminum foil bonded to a composite panel will provide significant E-field shielding.

4.4.3.3.2 Cable Shields Cables are not a part of the subject study. However, it is assumed that all cables connecting to the EEC have an overall shield which is capable of carrying the heaviest direct or indirect current and is continuous without breaks or splices and which is solidly grounded at both ends with a bond whose resistance is less than 2.5 milliohms.

4.4.3.3.3 Lightning Stroke Model The detailed design of the VCE engine installation in an advanced tactical fighter is not available. However, in the event that preliminary calculations might be useful, a typical lightning-stroke model is assumed. The model is simplified in that it contains only two strokes whereas a natural lightning stroke may contain many. This simplification is realistic, however, because 50% of all flashes contain more than 2-3 strokes, whereas only 10% contain more than 5-6 strokes. Moreover, in magnitude the two strokes in the model are severe by comparison with natural strokes. Only 4% of 1st return strokes exceed 100kA, and only 4% of subsequent return strokes exceed 50kA.

Of the two model strokes, the first has a current peak of 100,000 amperes and a rate of change of 100,000 amps per microsecond. The second stroke is half the magnitude of the first. The model incorporates intermediate currents of several thousand amperes persisting for a few milliseconds, and a continuing current, comprised of two phases, of 700 amps average for 50 milliseconds followed by a 400 amp section for 300 milliseconds. The total charge transfer is less than 200 coulombs, 155 coulombs of which passes in the continuing current.

The currents flowing in a lightning flash to ground are conveniently separated into three categories:

- | | |
|--------------------------|--|
| a. Return stroke surges | Peak current on the order of up to 100,000 A or more. |
| b. Intermediate currents | Peak current on the order of up to 10,000 A or more.

Duration on the order of milliseconds. |
| c. Continuing currents | Peak current on the order of up to 1000 A.

Duration on the order of hundreds of milliseconds. |

Currents of types b and c are principally responsible for damages such as hole-burning, while currents of type a mainly produce explosive effects and undesirable coupling transients. The lightning model can also cause intra-aircraft problems even if it does not contact the aircraft directly but merely passes nearby. The ionized channel of the 1st return stroke is the source of high-intensity electromagnetic radiation. Within the channel an increase in field intensity from 5kV/M to over 100kV/M in a fraction of a microsecond is typical. This field radiates away from the channel, decreasing in intensity 60dB/decade of distance very close to the channel and 20dB/decade at greater distances. The field encompasses a broad frequency spectrum which can couple to the aircraft structure and cables within. The measured spectrum shows components from 3HZ to 1GHZ, and 10GHZ has been theoretically predicted. The various phases of the lightning stroke are responsible for different frequency ranges as shown below:

<u>Frequency Range</u>	<u>Source</u>
3HZ to 3kHz	Continuing current
3kHz to 20kHz	Return stroke
20kHz to 2MHZ	Return stroke, streamers, corona
2MHZ to 30MHZ	Streamers, corona
30MHZ to 1GHZ	Stepped and dart leaders

In the natural thundersorm environment, an aircraft is subjected to almost continuous, intense electromagnetic fields due to charge redistributions (lightning strokes) in adjacent areas. These EM fields, usually caused by intercloud discharges, are often referred to as cross-field transients. Since cross-field transients occur every time the aircraft is in the general area of a thunderstorm, exposure to them is orders of magnitude greater than

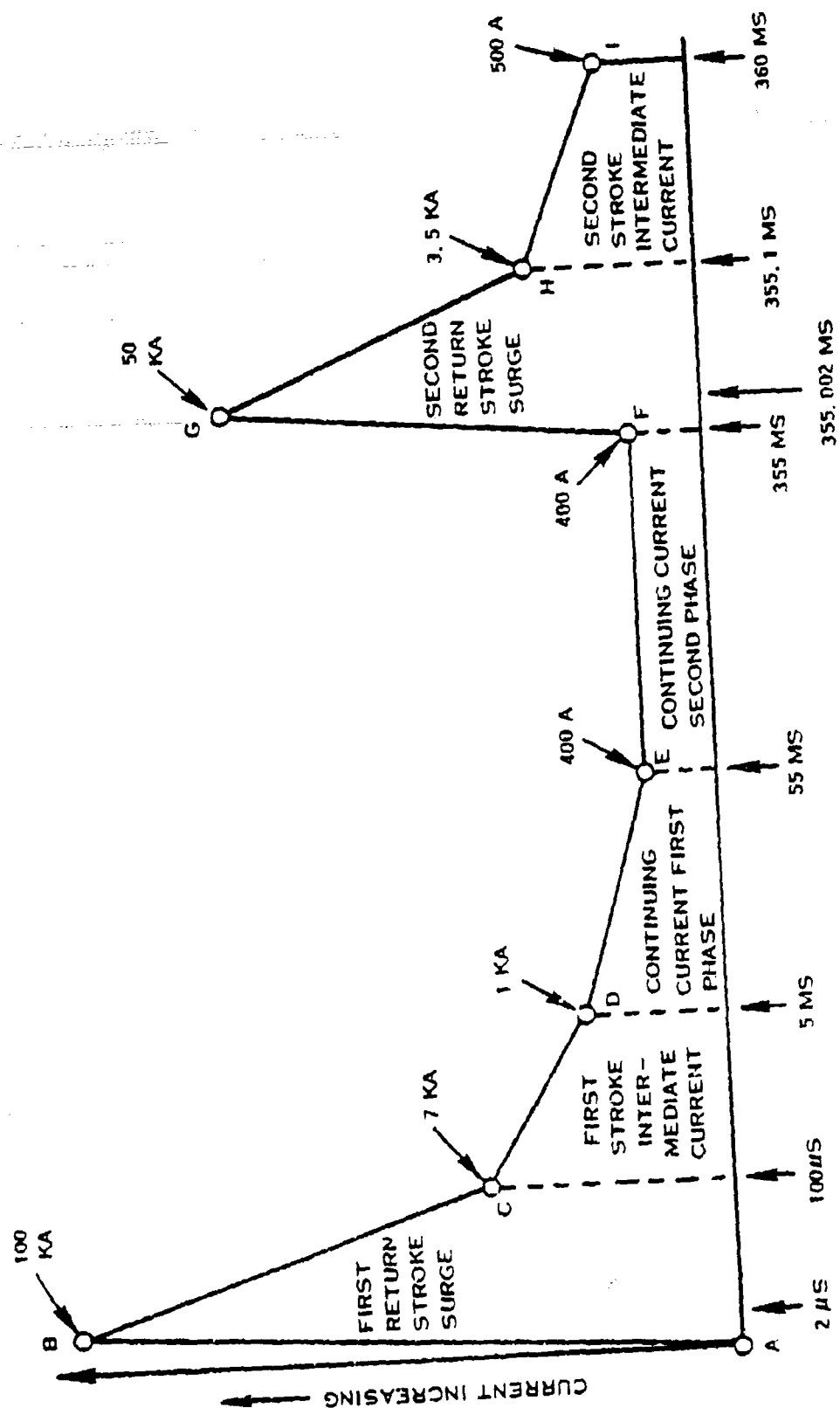
exposure to direct strikes. These EM fields have almost no effect on internal electronic systems in metal-skinned aircraft, but affect the aircraft interior in varying degrees with nonmetallic skins. The electric and magnetic field components produce entirely different effects on circuitry. Composite skin panels can result in induced streamering from thunderstorm E-fields of 10-100 amperes from terminal-board contacts even though the skin is not punctured. H-fields can induce large voltages in loop areas lying under the composite skin. Fortunately, the same types of protections against the infrequent EMP and lightning direct-strike occurrences are also effective against the more frequent cross-field transients.

In general, the time structure of lightning currents is less variable between individual strokes than are the amplitudes. It follows that severe lightning models are best developed first in terms of amplitudes, with subsequent secondary adjustments to the time structure in order to obtain overall physical reality. Furthermore, there is little connection within an individual discharge between the severity of the three categories of current; in other words, even if an initial return-stroke surge is severe, this has minimal influence on the severity of a following continuing current.

The current-time history for a model lightning stroke to ground is shown diagrammatically in Figure 72. The stroke is a very severe discharge. The model is formulated in terms of certain key points (A through I in Figure 72) at which specific values of current, i , and time, t , are attained. Between successive key points the current is assumed to change in a steady straight-line fashion with time.

The model consists of six current stages: a first return stroke including both a main-current surge and an intermediate current; a continuing current in two phases; and a second subsequent stroke again comprising a main surge succeeded by an intermediate current. The continuing current is modeled in two phases because material damage produced by continuing currents depends on actual time and current values and is not a function of charge transfer alone. It is possible that special types of damage could be produced by a subsequent stroke following a continuing current; hence the addition of the second stroke.

The model is essentially developed for applied purposes and it has consequently been simplified appropriately in both the analytical and physical respects. In physical reality, a severe discharge would have far more strokes and also, more phases of continuing current than indicated on Figure 108, however, the integrated effects of a very severe natural discharge and of the model are similar.



TIME INCREASING →

FIGURE 72 LIGHTNING STROKE MODEL

Intra-cloud discharges are less severe than flashes to ground largely because of the absence of the large sudden return-stroke surges. Thus, if material and equipment are unaffected by the severe ground-discharge model, material and equipment will also be immune to intra-cloud flashes.

4.4.3.4 Internal Environment of Aircraft Due to Lightning

4.4.3.4.1 External Current on Aircraft In the event of a direct strike, the attachment and exit points will be a reasonable facsimile of the lightning-current model. Some distortions will occur due to different surge impedances in air and in the aircraft. Reflections at the attachment and exit points will result in an oscillatory component in the current and a general slowing of risetime of the exit current. In the event of a near-miss lightning flash, the electromagnetic fields from the flash will excite a dipole response from the aircraft in a manner quite similar to EMP from a nuclear explosion. The current will be a damped oscillation with period proportional to aircraft length. Because the peak field intensities incident on the aircraft exterior are commensurate for EMP and a lightning near miss, the peak mid-fuselage current for a near miss is estimated at 5kA. Although the peak current excited by a near miss is much less than the peak current for a direct strike, its damage potential is not necessarily less, because it is more oscillatory in shape and more of its energy is concentrated in the higher frequencies which couple more tightly to interior circuits.

4.4.3.4.2 Field-Penetration Mechanisms For portions of the aircraft surrounded by a metal skin, the skin current immediately caused a magnetic field to surround the outside of the aircraft. For a typical fighter aircraft with a circumference of 5.5m just forward of the wing, the average field intensity at the skin surface for a current of 100kA is 18kA/m. Field intensity will be higher than the average in areas with small radii of curvature and lower than average for large radii. This H-field will in time diffuse to the aircraft interior. This diffusion is not instantaneous due to delays imposed by skin effect, eddy currents, and the counter H-fields generated by the eddy currents. As an example, a step-function H-field appearing at the outside surface of an aluminum skin 0.040" thick requires 12 μ s to reach 90% of its final value at the inside surface. This retardation has significance for coupling mechanisms to interior conductors which are functions of risetime. The final interior H-field for a skin of circular cross section is very small because of field cancellations due to symmetry. Diffusion through skin of elliptical cross section is more complicated. Buildup time may be much longer, and final interior H-fields will be much higher, particularly for ellipses of high eccentricity.

H-fields can couple instantaneously to the interior through apertures, such as canopies or composite panels. Risetime is not retarded as by diffusion, and a fast risetime will induce a higher voltage in a loop of given area than a slow risetime. Field strength decreases as the cube of the distance from aperture to the internal point of interest. As an example, for a 1M x 2M elliptical fuselage with a 0.1M x 0.2M elliptical aperture at its midline, 1000 amperes of fuselage current causes a field intensity of 80A/M at the aperture but only 0.1 A/M at 0.6M from the aperture. This suggests that H-field intensities are most troublesome in the immediate vicinity of the aperture, and that coupling to interior conductors can be minimized by locating conductors away from the aperture. For an engine controller, important apertures are the engine air scoops.

Electric fields propagate outwards from the ionized channel of a near miss, and may have any polarization relative to the aircraft. Penetration to the aircraft interior is principally through apertures, since the combined absorption and reflection losses for even a thin metal skin are quite high. The low shielding effectiveness of composite panels has been described, and such panels will behave as apertures to admit E-fields to the aircraft interior. Assuming an aperture with zero shielding effectiveness, the interior field intensity may reach kilovolts/meter for close flashes. Assuming a composite panel protected with aluminum foil or its equivalent, the interior field intensity will be reduced 20-60dB depending on frequency.

When directly struck, the outer surface of the aircraft assumes the electric potential of the flash, resulting in a maximum E-field intensity of approximately 100kV/M. This E-field is normal to the surface and will penetrate through apertures.

4.4.3.4.3 Voltage-Drop Mechanisms When the lightning-model current flows in an airframe path between attachment and exit points it causes a voltage drop which can couple capacitively to interior circuits. Assuming that the aircraft complies with the bonding requirements of MIL-B-5087B, this voltage drop is limited to 500V maximum between aircraft extremities, which forms an upper bound on the voltage which can be capacitively coupled. As a worst case, some or all of this voltage drop can be directly converted into a signal-mode voltage if a circuit uses the airframe as a signal return. This is a bad practice to be avoided in engine controllers.

4.4.4 Electromagnetic Interference (EMI) Environment

A severe EMI environment from ground and airborne transmitters across a wide frequency spectrum has been assumed. As previously described, the harmful effects of EMI can be positively prevented from affecting the performance of the engine control with the application of suitable protective material and

protective devices. In the future, the use of new communication technology such as fiber optics may influence the degree of such protection required. The degree of which EMI energy will penetrate the engine nacelles in the advanced tactical fighter is dependent on the detailed nacelle design configuration and materials (not available at this time). Aluminum nacelle skin affords more protection than composite nacelle skin. Composite skin is assumed for this study.

Figure 73 shows the peak values of the more powerful transmitters of EMI energy to which a tactical fighter is likely to be exposed. A navigation aid is assumed at 300 to 500 KHz, high frequency communications at 2 to 30 MHz and radars at 200 to 450 MHz and 1 to 40 GHz. In the absence of a detailed nacelle configuration, an assumption of the degree of attenuation that might be afforded by a graphite/epoxy nacelle skin has been used to reduce the external field, to the levels shown internal to the nacelle.

The resulting internal field will be further attenuated by the protective design of the engine control to levels that have no effect on control performance nor reliability.

4.5 Conclusions

The information necessary to define the environment for an electronic control on a variable cycle engine has been provided. From this information the following conclusions have been drawn:

- a. Fuel system point A (tank fuel) exhibits significantly lower fuel temperature levels than other fuel system points studied for electronic control cooling. In addition, since point A fuel temperature is not affected by engine power settings, rapid fuel temperature transients are avoided except during air refueling.
- b. The vibration levels predicted for the VCE are significantly higher than for current engines in the frequency range from 500 to 20,000 Hz because of higher levels of fan pressure and tip speeds. These higher levels of vibration will require additional effort in mounting and packaging the electronic control to meet the high reliability required in this program.
- c. The EMI/lightning electrical environment employed in this study is consistent with the latest information employed in the Space Shuttle Program and in the most advanced tactical fighter application.

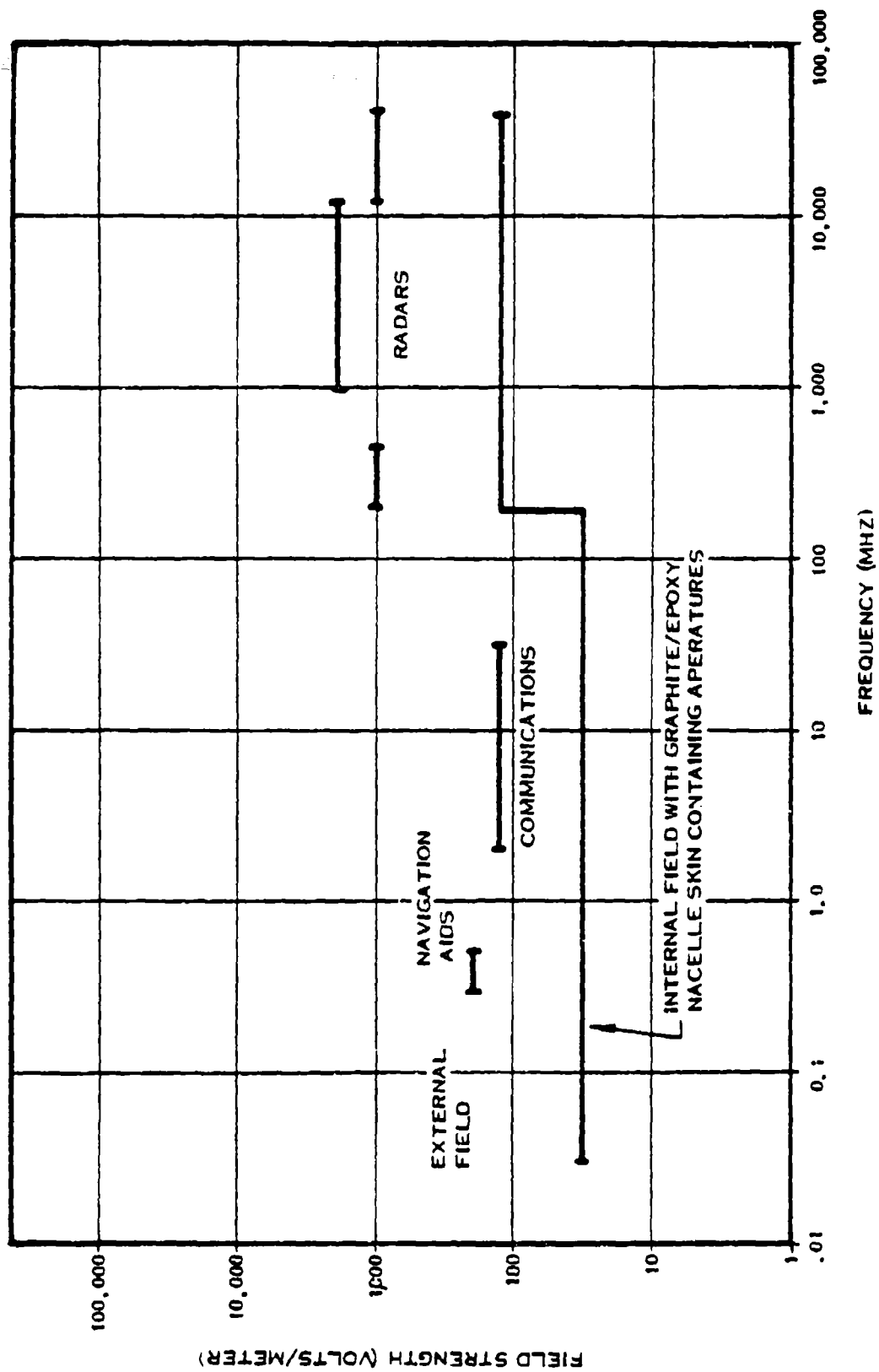


FIGURE 73 ASSUMED EMI FIELD OUTSIDE AND INSIDE ENGINE NACELLE

SECTION V COMPONENT BASELINES FOR RELIABILITY AND COST OF OWNERSHIP STUDIES

5.1 Baseline System Description, Functional

To properly evaluate, compare and measure the progress of the reliability analyses presented in this report, a brief description of the baseline configuration and its attendant features are set forth. (This is a summary of pertinent design information from Section III.)

A simplified block diagram of the baseline system configuration is shown in Figure 74. The system is composed of two channels which are designated the primary channel and the secondary channel. Each channel has its own set of input sensors and signals, a CPU, and a set of output function controls. The basic mode of operation for the controller is to establish function control by using the primary channel. If there is a detectable fault in the primary channel, the fault sense and switch device switches control of the output function(s) to the secondary channel. Memory-to-memory communication between the channels is provided by a UART data link and is necessary to effect channel switchover.

In the two channel baseline system, all input sensors and signals are redundant with the exception of the six pressure sensors and two temperature sensors.

The primary channel receives pressure sensor $\Delta P13$, Pt2 and Pt3 data and the secondary channel receives pressure sensor PT5, PT13 and $\Delta P3$ data. The secondary channel pressure data is forwarded from the secondary CPU by the UART. The reverse situation exists concerning the forwarding of the primary channel pressure sensor data to the secondary channel if it is in control. The two temperatures which are not redundant are Turbine Blade Temperature (TBT) peak value and average value. These values are also forwarded by the UART to the appropriate control channel.

The primary channel CPU has slightly more capability than the secondary channel CPU to provide for the augmentation function. The secondary channel in the baseline system does not have the augmentation function. This difference translates into the primary channel having slightly more ROM and RAM than the secondary. However, aside from this difference, the processor configuration and architecture in both channels is identical.

All output functions are redundant between channels with the exception of the augmentation function described above and a fault control. The fault control exception is caused by the uni-directional switching of control from the primary channel to the secondary channel.

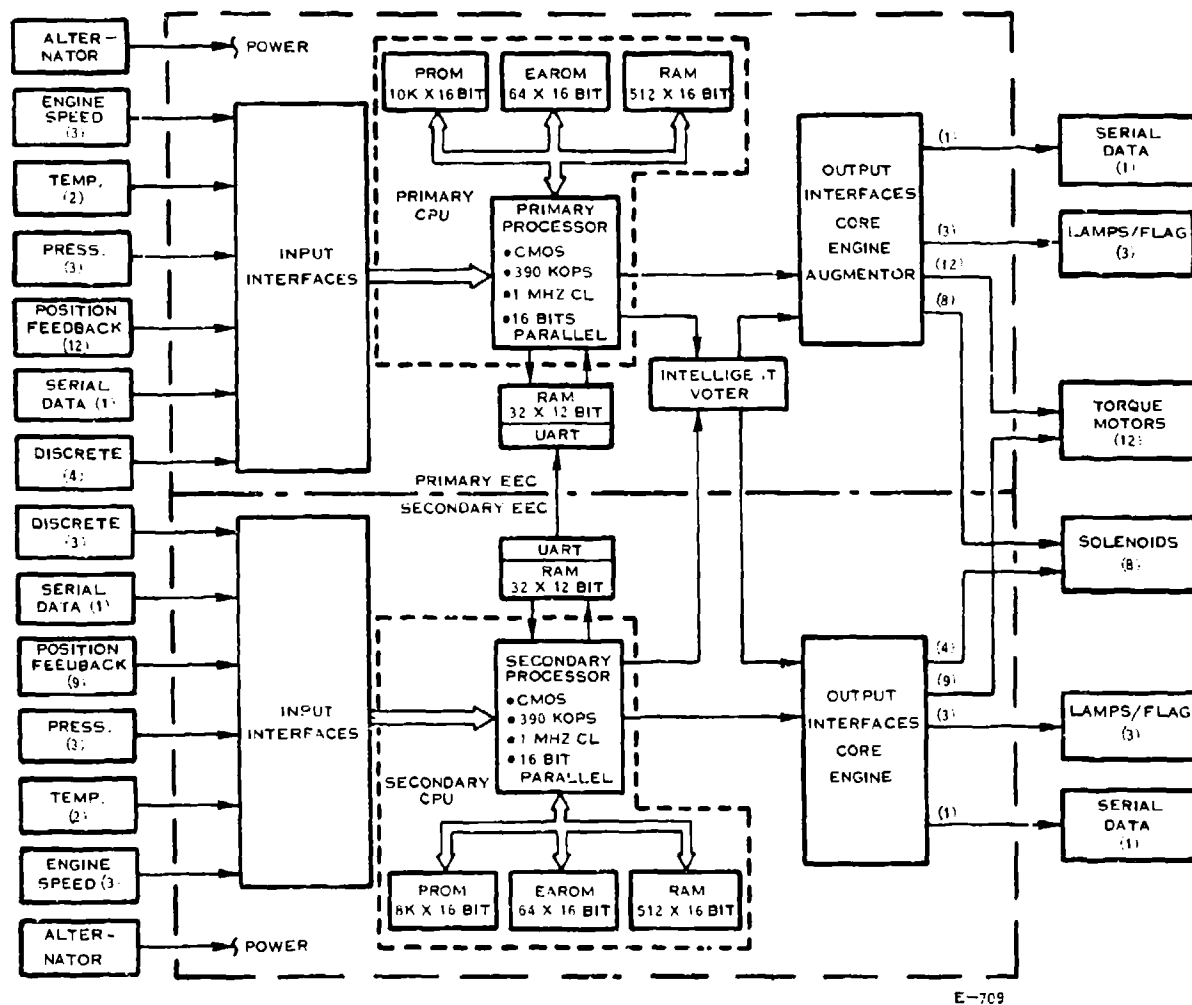


FIGURE 74 QUASI-REDUNDANT DUAL CHANNEL BASELINE SYSTEM

5.2 Baseline System Description, Mechanical

The printed circuit board assemblies are grouped by function to optimize the circuit design and to minimize the electrical interconnections between PCB assemblies. The functional partitioning of the printed circuit board assemblies is as follows:

- a. Processor and Memory Board
- b. Power Supply Board
- c. Sensor Board
- d. Input/Output Interface Board

Each printed circuit board is provided with an integrally bonded, chemically etched, aluminum heat sink plate. The heat sink provides both a thermal conductive path for the power dissipated by the components and a supportive structure whereby the combined panel natural frequency can be tuned to desired ranges for favorable vibration attenuation.

The electronic components are flow soldered to 6-8 layer epoxy laminate printed circuit boards. The components are placed on the heat sink side of the panels and the component leads are fed through the heat sink and soldered to the printed circuit boards. The components are bonded to the heat sink plate with epoxy or RTV adhesives as appropriate to enhance both the structural retention and the thermal sinking of the components. The components and panel assemblies are conformally coated to provide moisture protection for the electronics.

The assemblies are positioned in the control housing such that the high power dissipating components are placed closest to the cooling sink and the circuits with the highest quantity of components are packaged on the larger circuit boards. Access to the PCB assemblies requires removal of the cover panels, disassembly of the appropriate internal MIL-C-55302 qualified connector mates and removal of the retention fasteners. In the case of the sensor board, it is also necessary to remove the pressure sensor as well. The PCB panels are secured to the chassis at the brazed standoffs and are free from the exterior walls. The standoffs conduct internally dissipated power to the center deck and to the stainless steel tube heat exchanger. The standoffs are provisioned with self-locking threaded inserts for positive retention of the PCB panels.

The circuit boards are provisioned with test point pins and connectors in addition to the interconnect wiring to facilitate production acceptance testing, troubleshooting and fault isolation of individual board assemblies and the entire module as well.

The first line of interconnection, exclusive of those internal to the components themselves, is the printed circuit boards, which constitute the physical mounting platform for the components and interconnections via etched copper circuitry.

The PCB's are interconnected with flex tapes which terminate in solder connections at one end and separable printed circuit connectors at the other end. This makes each PCB an independent module. The pressure transducer is connected by hard wiring and soldered to terminals at the PCB end.

The two MIL-C-38999 I/O connectors are equipped with printed circuit interconnect boards which group and reduce the number of signals that connect to the PCB modules. Interconnection between the I/O connectors and the PCB's is accomplished with molded flexible cables having surface-soldered terminations with molded epoxy strain relief at the interconnect board and a separable MIL-C-55302 printed circuit connector at the PCB end. All wiring and flexible cabling is provided with appropriate strain relief for support both during handling and in service. The MIL-C-38999 I/O connectors provide excellent protection against water, dust and vibration. Electrically conductive materials or surface treatments are used at all points of mechanical interface between the coverplates, housing, connectors and transducer to provide complete continuity of the outer shell for electromagnetic compatibility and proper bonding at the ground strap lug.

The electrical I/O module consists of internal electrical harnesses which conduct the electrical signals from the engine/aircraft cables to the proper circuit board inside the unit. The harnesses are fabricated as a unit and pre-assembled into the chassis before the PCB panels are assembled. One important feature of the I/O circular connector selected for this application is the integral feedthrough EMI filters which form a part of the connector contact pins. Incorporation of the EMI filtering into the circular connector eliminates the need for intermediate compartments to house discrete filters. The effects of the discrete EMI filter approach would be to add volume, weight and increased complexity to the brazed aluminum chassis housing.

The pressure transducers are hard mounted to the chassis housing with the sensor pneumatic interface engaged into the pressure port. The sensors are thermally heat sunk to an extension of the stainless steel tube heat exchanger. The operating frequency range of the vibrating cylinder (greater than 5000 Hz) is much higher than the environmental vibratory range. The fragility levels of the transducer occur at frequencies greater than 3000 Hz and at chassis attenuated input amplitudes which greatly exceed anticipated levels by engine operation or qualification levels. The sensor has successfully qualified to MIL-STD-810 environmental requirements including shock, vibration, humidity, hot and cold temperature, salt, sand and dust, and fungus.

The baseline system embodies a thin wall, dipped brazed AMS4027 sheet metal chassis for high strength-to-weight relationship. The chassis is provisioned with a stainless steel heat exchanger to circulate tank supplied fuel for component cooling. The stainless steel tubing affords the fire resistance necessary to meet the fire safety hazard requirements. The piping is bonded to the chassis center deck to maintain close thermal contact between the chassis and the cooling medium.

The chassis design incorporates mounting standoffs to support the printed circuit board modules. These integrally brazed standoffs also afford a direct thermal path to the chassis from the PCB heat sink panels. All internal surfaces of the chassis have been coated with electrically conductive Alodine for both corrosion protection and electrical bonding. These surfaces provide EMI bonding at all external closure surfaces and grounding at all interfaces as appropriate.

The sheet metal covers are provisioned with elastomeric sealing gaskets to provide environmental protection. The thickness of the cover panel is such that acoustic noise is sufficiently attenuated so that PCB panel response levels are inconsequential.

5.3 Part Quality Levels

Part selection for engine and airframe mounted electronics must be made carefully with regard to types, supplier and procurement screening levels. All devices must usually meet the military temperature range requirements. All microcircuits and semi-conductors must be secured with hermetically sealed packages. Procurement of all devices must be controlled by drawings, specifications and Approved Vendor Lists (AVL) with 100% screening and appropriate hi-rel environmental screening. The part quality levels selected for the baseline are:

Semiconductors - JTX or Screened Equivalent

Integrated Circuits - MIL-STD-883, Class B

Passive Components - ER, Level S

SECTION VI RELIABILITY TECHNOLOGY TRANSFER

Hamilton Standard Division has developed and maintained effective liaison with several organizations which have demonstrated competence in the development of high reliability electronic systems and technology. The purpose of this contact was to obtain maximum benefit from the experience of others in order to assist Hamilton Standard in the attainment of the high MTBF goal established for the RAEEC program.

Reliability technology transfer discussions were held with:

- Bell Telephone Laboratories
- Rome Air Development Center
- Delco Electronics Division, General Motors Corporation
- U.S. Army Materiel Systems Analysis Activity
- Avionics Laboratory / Air Force Wright Aeronautical Laboratories
- U.S. Army Electronics Command

A sample documentation of one such relationship is presented in Appendix C.

SECTION VII RELIABILITY IMPROVEMENT MEASURES

7.1 General

In order to meet the goal of a 25,000 hour MTBF for an advanced electronic engine control, it is necessary to provide for reliability improvement in many key areas of design and production. For the RAEEC program the key areas targeted for an extensive reliability improvement effort were:

- Thermal Environment
- Redundancy
- Vibration Environment
- Interconnection Technology
- Component Technology
- Advanced Component Derating
- Component Screens
- Assembly Tests and Screens

The advanced FADEC design study provided the baseline system for the RAEEC program. Failure rates for the FADEC components were based on actual F100 EEC demonstrated reliability point estimates modified as follows:

- Where there have been no failures, 50% one-sided confidence level on zero failures was used.
- The EEC components were assumed to be 115°C.
- Failure rate adjustment due to complexity change was accomplished using MIL-HDBK-217B.
- All CMOS was assumed to be 2X failure rate of TTL based upon experience.

The failure rates for diode arrays, diode bridges, resistor networks, crystals and transformers were based on handbook or vendor data. The component failure rates were then summed to produce equipment failure rates. The equipment failure rates are then combined according to the arrangement determined by the fault flag policy. For the RAEEC baseline this resulted in an MTBF of 1321 hours.

7.2 Thermal Environment

One of the areas which can lead to increased reliability is an improvement in thermal environment. It is an accepted idea that lower component operating temperatures leads to reduced failure rates. In Appendix D, the failure rate

relationship with respect to operating temperature was explored. Through careful thermal design the operating temperature of the RAECC was reduced from the 115°C assumed for the baseline to 71°C. Using the failure rate/temperature graph in Appendix D, leads to a 2.6 factor of improvement in MTBF over the baseline control. Therefore the RAECC system now exhibits an MTBF of 3432 hours.

7.3 Redundancy

As detailed in Section III, the prime objective of the RAECC system is to maximize both Mission Reliability and System Availability. The major point highlighted in the section was the conflict which arises from attempting to maximize both reliability and availability. High levels of Mission Reliability requires several levels of redundancy while high availability is achieved through simplicity. This conflict was resolved through the application of Redundancy Management Techniques and Fault Tolerant Concepts.

In Section III, it was stated that the baseline MTBF was 3039 hours. This number was based on the tentative budgeted improvement factor of 2.3 for the improved thermal environment times the original MTBF of 1321 hours. After the application of the Redundancy Management Techniques and Fault Tolerant Concepts discussed in Section III, the MTBF of the RAECC system was 7965 hours. This corresponds to a redundancy improvement factor of 2.6.

Because the final improvement factor for improved thermal redundancy is larger than the tentative budgeted factor (2.6 vs. 2.3), the MTBF of the system before the Redundancy Techniques are applied, is not 3039 hours. Applying the redundancy improvement factor results in a system MTBF of 8923 hours.

7.4 Vibration Environment

One of the problems to be overcome with an engine mounted control is the extreme vibration environment encountered. The intuitive concept of high vibration levels adversely affecting reliability has gained much acceptance. Qualitatively, this concept is present in the use of Environmental Factors in MIL-HDBK-217B. Quantitatively, in Appendix D, an attempt is made to determine the relationship between vibration levels and failure rate levels.

In order to reduce the vibration impact upon reliability a comprehensive approach to vibration isolation and packaging, as detailed in Section III, Mechanical Design, will be necessary. This approach is expected to reduce the average overall vibration level from the 22.5 G's experienced by the F100 EEC to approximately 5.4 G's. Using the curve developed in Appendix D, the improvement factor is 2.25. This raises the RAECC MTBF from 8923 hours to 20,076 hours.

7.5 Interconnection Technology

The extreme vibration environment encountered by an engine mounted control impacts heavily upon interconnection technology. An intensive effort was made to reduce the failure rate contributions of the interconnections. (See Section III). Some of the techniques investigated include:

- Minimization of the number of interconnections
- Improved types of interconnectors
- Minimization of the number of separable terminations
- Adoption of flat packs and leadless chip carriers.

A trade study was conducted for various connectors, I/O cable assemblies, I/O cable terminations, etc., with respect to their inherent reliability and the quantity necessary to accomplish the function. The trade study indicated that the type of the interconnectors selected for use in the RAEEC program showed a 2.15 factor of improvement, in terms of reliability, over the baseline interconnectors. However, this improvement factor does not apply to the entire failure rate of the system, but only to the percentage of the failure rate attributed to the inter-connectors (20% of the system failure rate). This raises MTBF from 20,076 hours to 22,480 hours.

7.6 Component Technology

In order to meet the reliability goal for the RAEEC system, it will be necessary to choose the appropriate component technology based not only on functional implementation but also on the technology's inherent reliability. As detailed in the Development Guide Section XI, an alternative methodology to MIL-HDBK-217B was developed for evaluating the reliability of a design. This new methodology is based on historical data, Hamilton Standard's experience, and information obtained from industry surveys, seminars and technology transfer conferences. This method compares alternative circuits based on different component technologies for reliability maximization. Comparison is accomplished by the use of a relative index based on:

a. Active components

- Years in High Yield/High Volume Production
- Years to Industry Standard Compatibility
- Proven Space/Military Applications
- Accelerated Testing
- Component Functional Testability
- Inherent Technology Failure Rate

b. Functional Fabrication Level

- Number of Active Devices
- Number of Other Components
- Board Area Used
- Microcircuit Junction Temperature

The final RAECC design was chosen using this index after all the trade studies were completed (Appendix A). The improvement factor of 1.18 was calculated from the ratio of the final and the preliminary RAECC system indices. However, this improvement factor does not apply to the entire failure rate of the system but only to the percentage of the failure rate attributed to the electronic components (80% of the system failure rate). This raises the MTBF from 22,480 hours to 26,040 hours.

7.7 Advanced Component Derating

Recent studies have indicated that the application of derating principles with respect to the operating voltage for CMOS devices yields a substantial improvement in device failure rates. A recent study by RADC demonstrated that a 10:1 reduction in CMOS device failure rates is possible for devices specified at 18 volts and operated at 5 volts. Early results from two other ongoing studies (IBM & Intel) support the RADC findings. For operation at voltages between 5 volts and 18 volts, the improvement factor was assumed to vary linearly from 10 to 1, respectively.

As indicated in Section III, all of the final RAECC CMOS devices, with the exception of the SOS HS 16/24 processor and two other CMOS IC's, operate from the 5 volt bus instead of the 10 volt bus. The processor still operates from the 10 volt bus for improved performance. In the final design, the CMOS devices contribute 16% of the series summation system failure rate. Of this percentage of the series summation system failure rate attributed to CMOS devices, 71% is contributed by CMOS run from the 5 volt bus while 29% is contributed by CMOS run from the 10 volt bus. The additional failure rate reduction associated with this change in operating voltage (10 volt to 5 volt) will be a factor of 4.46. This was calculated as follows:

for 10 volt operation	failure rate reduction factor = 2.24
for 5 volt operation	failure rate reduction factor = 10.0
for 10 volt to 5 volt change	failure rate reduction factor = $\frac{10.0}{2.24} = 4.46$

This failure rate reduction factor applies only to the percentage (16.5%) of the system failure rate attributed to CMOS devices which changed from operating at 10 volts to operating at 5 volts. This raises the MTBF from 26,040 hours to 28,515 hours.

7.8 Component Screens

Reliability improvement factors attributed to additional screening of piece parts, above and beyond that available through military standards, are limited to those screens which can be directly traced to the elimination of infant mortality and the "freak" distributions. Infant mortality devices remaining in the population range from 0.05% to 0.3% while "freak" distribution devices comprise 2% to 10% of the population.

A comprehensive screening program as set forth in Section VIII will be necessary to ensure that the infant mortality and "freak" populations will be weeded out. The improvement factor of 1.5 was assigned based on the fact that the "freak" distribution devices, comprising 10% of the population, contribute more than 10% of the device failure rate, as experienced in use. A conservative estimate was made for the improvement factor. The literature in this area is non-committal in quantifying the improvement that can be expected due to additional component screens. This improvement factor is applicable to integrated circuits, semiconductors and tantalum capacitors (55% of system failure rate). Therefore, the RAEEC system now exhibits an MTBF of 35,201 hours.

7.9 Module Assembly Test and Screens

The module level of assembly represents the initial point in the fabrication cycle where piece parts are combined into functional circuit entities. Here, the assembly methods and manufacturing processes are brought to bear as well. From Section VIII, module testing affords an overall improvement to the performance of the system in the field both in customer acceptance and observed failure rates.

Assuming the functional entities to be independent from the constituent piece part on the basis of the different processes and methods involved, one can reason that a new set of failure mechanisms has been breached. Approaching the issue from the standpoint of the existence of an infant mortality and a freak distribution within the population permits the application of similar improvement factors based upon the stage of manufacture and the piece part compositions involved. Included are the failure mechanisms of that group of piece parts which has yet to be discussed namely, resistors, all nontantalum capacitors, magnetics and sensor mechanics which comprises 53% of the system failure rate at this stage. These parts will be subjected to accelerated screening at the module test level.

Ignoring the infant mortality contribution of less than 0.5%, the density of the freak population of 2% to 10% applies to both the "unscreened" parts and the functional entities, i.e., modules. Apportioning the improvement factor of 1.11 for the "unscreened" parts plus module entities and the lower limit of 1.02 for the "screened" parts to account for the effectiveness of the module screens results in an overall improvement factor of 1.07 bringing the MTBF of the system from 35,201 to 37,520 hours.

7.10 End Item Assembly Level Screening and Tests

As detailed in Section XIII the controller will undergo a thermal cycle and vibration screen plus a functional test at high temperature. The severity of the screen will disclose a set of failure mechanisms peculiar to end item level manufacture and functional interactions between modules. It may also unveil new module and/or part level mechanisms directly impacting the screening approach at those lower levels of assembly.

While an improvement factor resulting from end item testing but based upon piece part failure rates cannot be quantitatively substantiated (a 4:1 improvement in customer acceptance rate was established in the Development Guide), it is known that improvement in observed failure rate does occur as a direct result of end item screening. Our progression through the various improvement categories thus far has utilized the summation of piece part failure rates method to portray an MTBF improvement or enhancement. Retaining the same approach, thereby avoiding the contradiction that exists between the base of piece part failure rate summation and the base of rates of acceptance, the improvement factor applicable to end item testing is assumed to be 1.11. (See Summary for the discussion on interdependence.) This factor applies to 100% of the system failure rate raising the MTBF from 37,520 hours to 41,648 hours.

7.11 Summary

The analysis began with a determination of the MTBF for the RAEEC baseline using historical piece part data derived from the F100 EEC program. The inherent MTBF was modified to include the predicted reliability improvements resulting from the design and production philosophy for the RAEEC. The key areas of reliability improvement are:

- Thermal Environment (2.6)
- Redundancy (2.6)
- Vibration Environment (2.25)
- Interconnection Technology (2.15)

- Component Technology (1.18)
- Advanced Component Derating (4.46)
- Component Screens (1.5)
- Assembly Tests & Screens (1.11)

Overall Improvement Factor = 32

As can be seen in Figure 75, the MTBF of the RAECC starts at 1320 hours and climbs to approximately 42,000 hours after all the improvements are implemented.

It is important to note that the progression to 42,000 hours MTBF was calculated under the assumption that the predicted reliability improvement factors were independent. For example, it was assumed that an improvement resulting from component screens was totally independent to the improvement resulting from Final Assembly Screens. However, in the "real world", this assumption is not valid. An improvement in one area may have an impact, favorably or adversely, in one or more areas.

Because the improvement factors are not totally independent of one another, the RAECC MTBF of 41,648 hours must be considered an optimistic estimate. The greater the interdependencies of the improvement factors, the less the overall improvements.

It is estimated that 80% of each improvement is independent in every case establishing a realistic lower limit in overall improvement of $0.8 \times 41,648 + 1320$ or approximately 25. The two limits have been plotted in Figure 75.

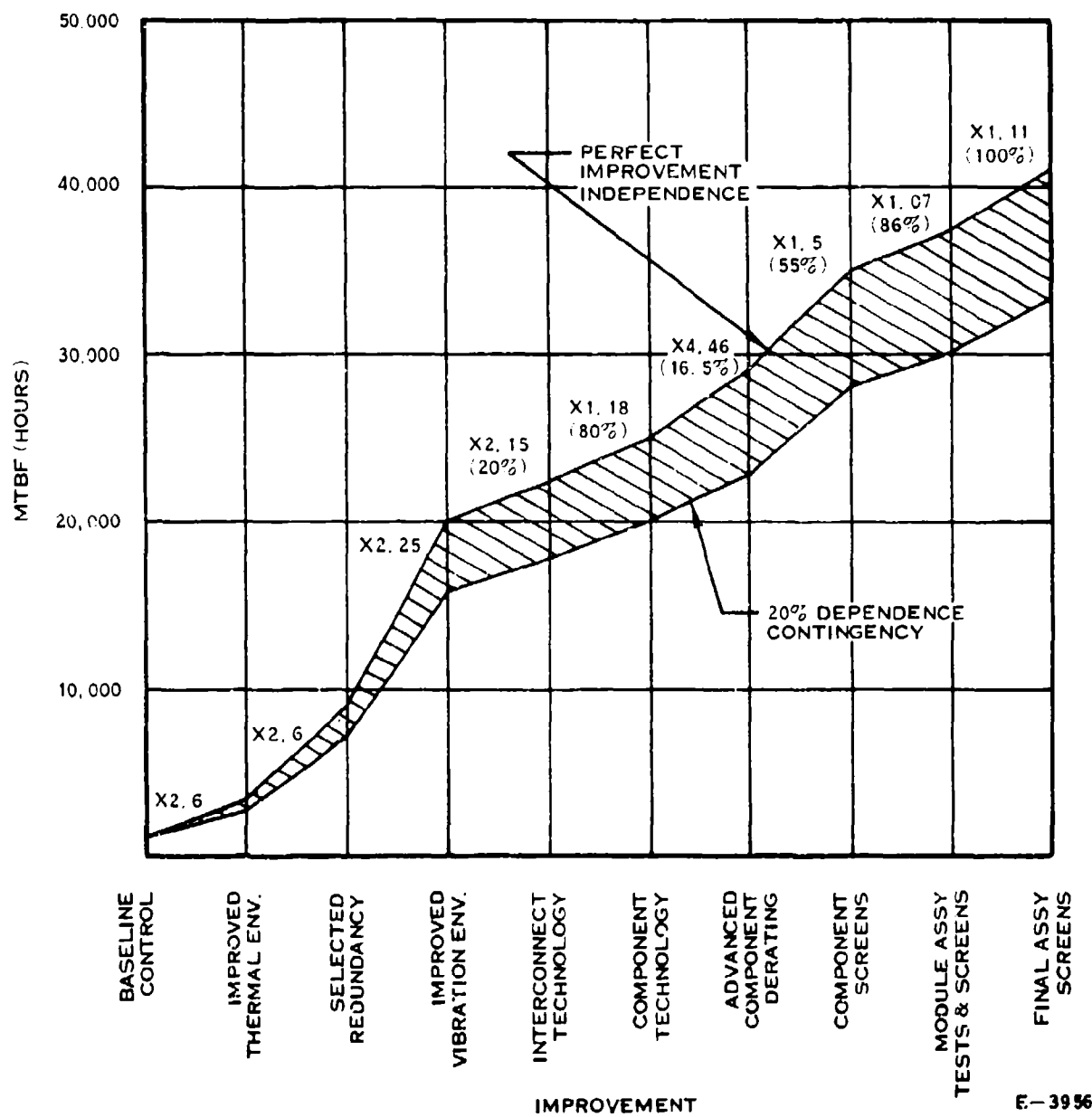


FIGURE 75 RELIABILITY ROADMAP

SECTION VIII TESTS TO ENHANCE RELIABILITY GROWTH

8.1 Introduction

This section of the Reliability Enhancement Study addresses the implementation of reliability tests and screens designed to enhance the reliability of electronic hardware intended for use in an environment identified as hostile due to its high vibration and temperature levels; conditions germane to an aircraft engine mounted application. The testing program structured herein emphasizes the performance of reliability tests at the key points of development and production cycles. Among the key points identified are the selection and screening of piece parts, fabrication and test of both polyimide and ceramic substrate multilayer printed circuit boards, subassembly or module level screening and end item level acceptance testing.

During the development, or preproduction, phase emphasis is placed upon the establishment of those screening and testing conditions which will be the most effective in ferreting out defect and/or marginal parts and assemblies during the production cycle. From various industrial reports on the subject of reliability testing, the single most effective screen at all levels of assembly is thermal cycling. All agree, however, that the optimum conditions of the thermal cycle screen (its rate of change, temperature range and number of cycles) are dependent upon the packaging and component mix of the equipment to be screened; the processes involved with its manufacture as well as the facilities where it is manufactured influence the behavior of the equipment to a degree sufficient to also affect the selection of thermal cycle parameters.

From reference 41 an approximation of the categories of failures detected in mature hardware through AGREE (Environmental Tester) testing is:

Design marginalities	5%
Workmanship and Process Related	33%
Faulty Parts	62%

It is further asserted that the temperature soak and low level vibration (usually 2 g's sinusoidal) portion of the AGREE test cycle play a minor role in screening effectiveness causing the AGREE test method to be "... essentially equivalent to a temperature cycling test dependent on the temperature range, the temperature rate of change, and the number of cycles."

Other reports, such as those prepared by Hughes Aircraft (Reference 42), General Dynamics (Reference 43), and Lockheed (Reference 44), contain summaries heralding the effectiveness of thermal cycling in enhancing the reliability of most any type

of electronic equipment. The Hughes Aircraft report, for example, cited results of thermal cycling which included "... a 50% reduction in failure rate due to board stress testing..." at the end item level, a "... 25% reduction at AGREE test...", and a "4 to 1 reduction in failure rate at customer receiving inspection."

The General Dynamics report concluded that "fifty percent overstress testing is 5 times more effective... than specification level testing", and "random vibration is 2 times more effective... than specification level testing", and "random vibration is 2 times more effective... than either high or low temperature testing."

Therefore, the following general rules were applied in the development of the test program defined herein.

A rational degree of flexibility must prevail throughout the test program commencing with the screening of piece parts and proceeding through the end item level acceptance test. Screens that produce no results should be discontinued while, at the same time those that continually produce meaningful results should be retained. As defect trends or failure modes are identified through testing and eliminated through follow-up recurrence control measures, it may be necessary to modify the conditions of the screen or impose an entirely different screen to assure reliability enhancement. The ability to alter the test program in a cost effective manner and essentially at will to the benefit of the ultimate customer in terms of equipment longevity and failure free operation should exist.

The worth of a set of screens at a given component or assembly level is to be measured and evaluated directly from test results at the next higher assembly level. This approach provides the degree of interaction between test levels necessary to allow the continuity and effectiveness of the overall test program to surface. The general idea is to screen defectives out at the lowest testing level possible.

The test program should be designed to increase, not measure, reliability. This means the test conditions should provide a stress of sufficient magnitude so as to isolate weak sisters and be performed on a 100% basis. Any consistently failure free test or screen is an immediate candidate for discontinuation. Further, the "test-in" reliability approach should require the shortest time feasible in order that the effectiveness of the overall program may be under constant appraisal. Measurement of reliability testing similar to that of MIL-STD-781 is extremely slow, very expensive, usually conducted on a minimum number of units and carries the stigma where, in the results, any failure poses a liability.

8.2 Piece Part Screening

The objective of 100% screening at the piece part level is to weed out infant mortality plus latent defects comprising the "freak" distribution defined in method 1016 of MIL-STD-883B. While the majority of infant mortality defects are screened out through the 100% process conditioning specified in Established Reliability procurement specifications (i.e., MIL-R-55182) and other military standards (i.e., MIL-STD-883), additional screening, generally accelerated, is required to adequately screen out those latent defects which manifest themselves at higher assembly level testing. Since these failure modes must first be identified, it is necessary to perform accelerated testing on samples of individual piece part types and families within types to establish the optimum accelerated conditions which will efficiently manifest those modes at the part screening level; i.e., through a 100% accelerated burn-in. The reliability of the balance of the lot, having been screened through these accelerated burn-in condition, is thereby greatly enhanced.

The following paragraphs address the recommended test programs per basic piece part (reference 41) type. It must be recognized, however, that the part manufacturer may have conducted similar tests on his devices. Once ascertained, the test results should be evaluated in terms of commonality and applicability to the programs outlined herein. Should the manufacturers data adequately satisfy the requirements stated, both quantitatively and statistically (i.e., variance analyses, goodness of fit, Arrhenius plots, Eyring equations, etc.), his accelerated test conditions should be incorporated in the interest of economy.

8.2.1 Integrated Circuits

Test guidelines pertaining to piece parts emanating from the NASA sponsored studies conducted by Martin-Marietta (reference 41) are listed below with some commentary.

Integrated Circuits

- "1. 100% electrical testing and burn-in for a minimum of 240 hours is mandatory for screening out defective devices. For programs requiring the highest reliability, consideration must be given to burn-in for longer than 240 hours, or at higher temperatures, because the internal elements of integrated circuits cannot be stressed to their rated capability."

It is their consideration to burn-in at higher temperatures that is of primary interest in this reliability enhancement study. As found in other independent studies (references 45 and 46) accelerated or high temperature burn-in is an

effective means of culling devices containing latent infant mortality related defects (termed "long term failure mechanisms") from a lot or lots of integrated circuits. Again, the rule that processes, facilities, etc., involved with its manufacture influence the reliability of the end item, here, a device, applied making it necessary to evaluate each device type and/or manufacturer contemplated for use in the production of a black box systems element.

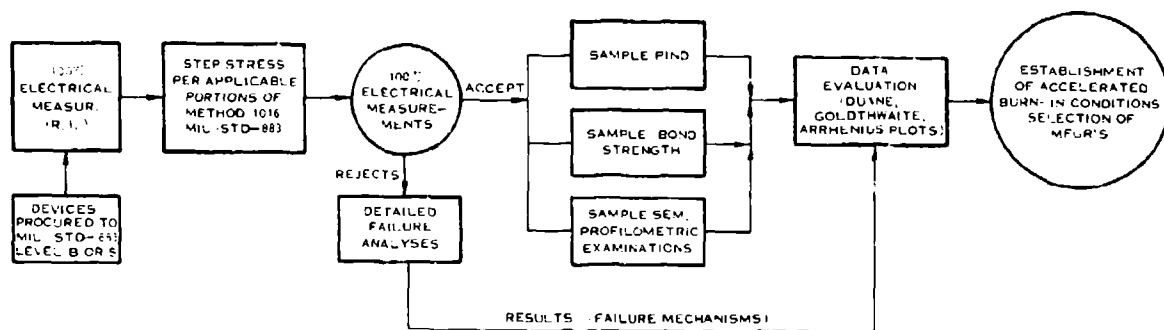
During the design and development phase, the accelerated screening criteria are to be developed on a per device level (Figure 76). Commencing with the procurement of integrated circuits screened to at least level B of MIL-STD-883, each device type is to be subjected to step stressing per applicable portions of method 1016 of MIL-STD-883 the stress conditions of which are to be selected as a function of device type/technology. The performance of PIND, Bond strength testing and Scanning Electron Microscope examinations on a sample basis plus detailed failure analyses on all step stress test rejects will identify problem manufacturers and device failure mechanisms. Collectively, these results including evaluation of step stress testing, are the tools with which the initial conditions of procurement, accelerated burn-in, and additional screening of detailed parts are to be structured for production builds.

The resulting screening program applicable to integrated circuits during the production phase of the program is depicted in Figure 77. The highlights of the screening program are the continuous evaluation of the screening against yield information derived from next higher level testing, and the flexibility of the screening program in responding to changes in requirements brought about by lot variations, change in sources, etc., usually during a long term production run.

- "2. 100% Pre-cap visual inspection to standards superior to that required by MIL-STD-883 is required to detect time-dependent failure mechanisms resulting from scratches, pin-holes, residues and improperly controlled processing."

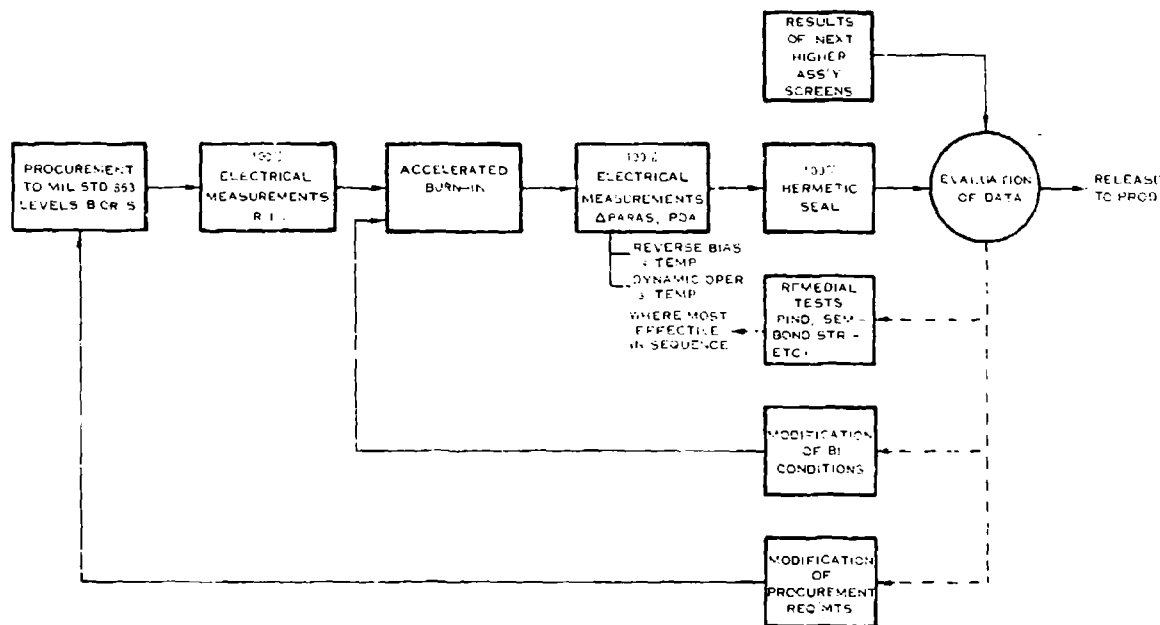
The latest issue of MIL-STD-883 contains a more stringent pre-cap visual inspection than the issue in existence during the preparation of the NASA study, however, the test condition applicable to level "S" is more rigorous than that of level "B". Depending upon program needs or in-house test results it may be necessary to impose condition "A" internal visual inspection requirements when procuring to MIL-STD-883 level "B" specifications.

- "3. 100% bond pull testing is currently quite controversial, but is recommended herein because it is being successfully performed by Autonetics, Fairchild, and others, and without evidence of the possible degradation postulated by the companies that have



E-5675

FIGURE 76 ESTABLISHMENT OF ACCELERATED BURN-IN CONDITIONS (DESIGN & DEVELOPMENT PHASE, FOR INTEGRATED CIRCUITS)



6-5704

FIGURE 77 100% SCREENING OF INTEGRATED CIRCUITS DURING PRODUCTION PHASE

not investigated and adopted this technique. Bond pull tests are needed since the acceleration and shock tests do not detect bad bonds because of the very small mass of the wire involved."

100% bond pull testing remains a controversial issue today and should be imposed only when considered remedial.

- "4. Submit a wafer sample from each metallization run to a detailed scanning electron microscope inspection to assure uniform and continuous metallization over window cuts and oxide steps, to avoid undercutting and water fall effects from oxide etch, to detect oversintering, and to verify mask alignment. Inspection at the wafer level is the most economical point in the process sequence for performance. Screening tests are not 100% effective in detecting these faults and further costly processing is avoided."

Not considered cost effective at the system manufacturing level due to the fact that a single order placed may be filled by integrated circuits from a number of different metallization runs. A more effective utilization of the SEM screen by the systems house would be to conduct SEM inspections on sampled devices as part of his part/manufacture evaluation program.

- "5. Submit a wafer sample from each metallization run to a profilometer test to verify metallization thickness and avoid electromigration problems."

Same observation as indicated for SEM above.

- "6. Perform the qualification tests of Group C in MIL-M-38510 in sequence on the same group of parts as opposed to performing the tests in parallel. This will impose the additive effects of environments that are more realistic to real life use. Also, the screening effectiveness can be evaluated."

As defined in MIL-M-38510, Group C is a periodic inspection not usually conducted on each lot. When conducted as part of the qualification procedure, the qualification approved status is valid for a period of 12 months, during which requalification is not required. Therefore, the value of performing the Group C tests in sequence as opposed to parallel is questionable when considering overall contribution. A further opposing argument is the limited availability and related high cost of fully qualified integrated circuit types. Systems manufacturers, due to these cost and availability considerations, tend to procure integrated circuits from reputable houses to industrial standards, process through MIL-STD-883 screening and qualify them by next higher assembly.

A more meaningful recommendation, or test guideline, would have been to include a more stringent thermal cycle test on each lot produced in light of the general finding of the study regarding the benefits of accelerated thermal cycling.

8.2.2 Discrete Semiconductors

- "1. A 100% nondestructive interconnect wire pull is recommended to eliminate defective wire bonds. Sound bonds will not be degraded."

While the worth of such a screen is undisputed, an alternate approach would be to impose both forward and backward instability shock tests as required for JANS devices, due to the rather high cost of performing 100% bond tests.

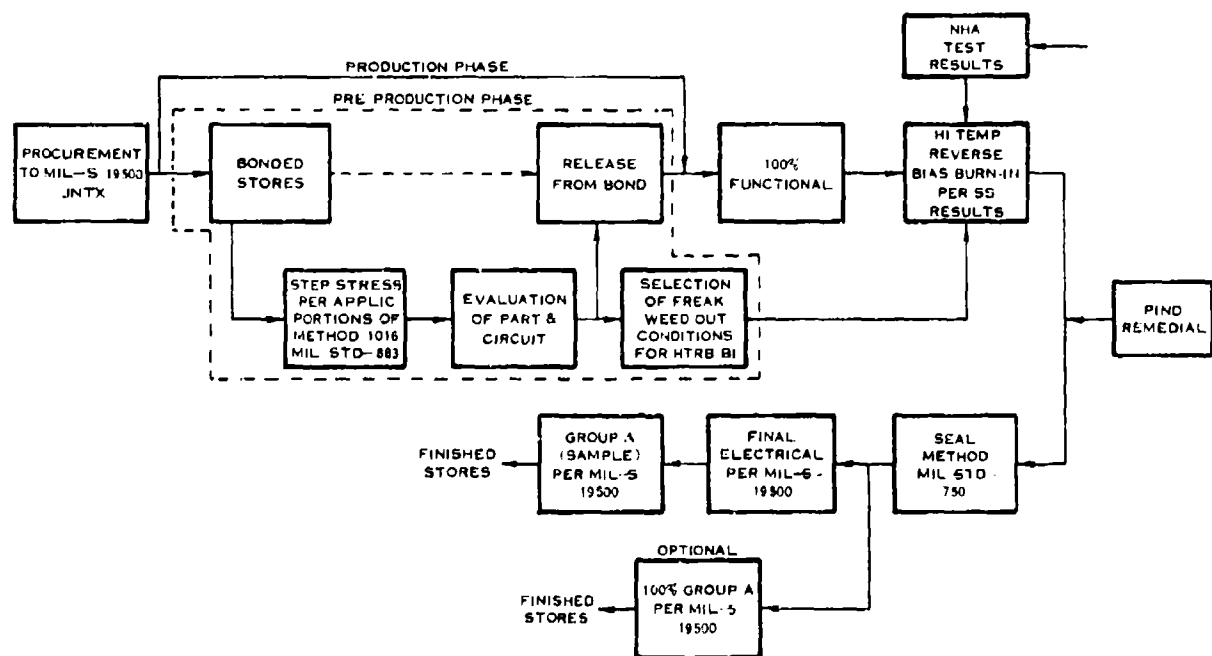
- "2. A rigorous pre-cap visual inspection of the die and header assembly is essential to eliminate common assembly defects. Perform die inspection (preferably at the wafer or die level) to eliminate defective die."

Procurement to either JANS or JNTXV levels of MIL-S-19500 would fulfill this requirement. Where reliability requirements warrant, the precap visual examination should be to MSFC 85M03924 criteria, incidentally, at any reliability level.

- "3. Screening tests on 100% of the parts, which include burn-in, HTRB, thermal cycling, mechanical shock, hermeticity, and parametric tests are essential to eliminate defective parts."

Procurement to JANS level of MIL-S-19500 fulfills the above; however, the above test series does not adequately address "freak" distributions, the elimination of which is essential for reliability enhancement. Figure 78 depicts the screening flow for discrete semiconductors during production and preproduction phases designed to weed out the "freak" distribution. Again, the screening conditions to be applied during the production phase are those identified through step stressing discretes during the preproduction phase. Results of next higher assembly (NHA) level testing, i.e., module, are to be factored into the high temperature burn-in conditions such that a high degree of efficiency may be maintained during the part screening exercise.

While procurement to JANS level of MIL-S-19500 fulfills the above requirements, cost and availability of level "S" devices may be prohibitive particularly since latent defects that may remain still must be screened out. Subjecting JNT devices to additional screening assures availability, lower initial cost, and control over the screening exercise.



E-5708

FIGURE 78 100% ACCELERATED SCREENING FLOW FOR DISCRETE SEMICONDUCTORS

8.2.3 Tantalum Capacitors

As stated in Reference 41, tantalum electrolytic capacitors are less reliable than other types. In the case cited therein, of 4622 capacitors used, the 6 failures involved only tantalum. No differentiation between solid and nonsolid electrolyte devices was made. The test guidelines included in Reference 41 are discussed below for both solid and nonsolid tantalum types where type designations are pertinent.

- "1. Tantalum capacitors should be qualified to the requirements of MIL-C-39003 or MIL-C-39006 level P, as a minimum. Additional program-peculiar requirements should be added as required."

Present QPL listings suggest level R requirements be selected as a minimum due to their availability; i.e., from more than one source. There are a few exceptions, however, where the minimum of level P would apply to avoid single sourcing.

QPL-39003 (Solid Tantalum)

Types CSR33

QPL-39006 (Nonsolid Tantalum)

Types CLR79

(Single sources only exist for the following types - CLR10, 14, 17, 69, 89 usage of which, therefore, is to be discouraged until second sources have qualified).

- "2. Radiographic inspection on 100% of the devices should be made in accordance with more comprehensive inspection criteria such as in MSFC-STD-355 to detect anomalies more effectively".

(Applies only to solid tantalum capacitors). The 100% radiographic examination criteria of MIL-C-39003 is considered adequate for aerospace programs excluding extended duration manned space expeditions. The implementation, however, of the more comprehensive radiographic inspection criteria of MSFC-STD-355 would be beneficial as a remedial action.

- "3. Burn-in should be increased to a minimum of 240 hours at rated voltage at 85 C with tight delta limit criteria. Stability is an indication of reliability and present durations are not sufficiently long to detect all parts with instabilities. Read and record measurements of capacitance, dissipation factor, and leakage

should be made before and after burn-in on 100% of the devices".

- "4. Accelerated tests are applicable to solid tantalum capacitors. Caution is required in applying these techniques to foil or wet slug capacitors as electrolyte breakdown may occur at relatively low voltages creating a new failure mechanism".

The burn-in criteria of current issues of MIL-C-39003 and MIL-C-39006 remain inadequate. But to improve the burn-in and then perform accelerated testing which ultimately reflects back to the burn-in criteria is less time efficient than conducting a component evaluation program employing step stress testing to arrive at an optimum burn-in.

The fact that low temperature (circa 182°C) solder is used in the manufacture of solid tantalum capacitors and the manganese dioxide layer is extremely sensitive to temperature, particularly above 125°C, dictates an acceleration of rated voltage in lieu of temperature. It also supports the demand for stringent controls over their circuit applications.

Shown in Figures 79 and 80 are step stress test programs for solid tantalum capacitors and nonsolid tantalum capacitors, respectively, designed to establish optimum burn-in criteria which would afford reliability enhancement at minimum expense and schedule impact.

The value of applied voltage is to be established as a function of case size and capacitance value. The values shown in Figure 79 are applicable to those case sizes requiring a minimum of 110% of rated DC voltage as an applied stress. This minimum value may not exceed 130% in which case the three step stress levels would be 110%, 120%, and 130%. Caution must be exercised in the application of the voltages in that the intended value should be reached through a gradual increase instead of through a step function.

For nonsolid tantalum capacitors, the restriction of maximum applied temperature is relaxed because low temperature solder is not employed. Therefore, as shown in Figure 80, the step stress is a function of temperature as opposed to voltage. The voltage to be applied during the step stress test is 100% of the 85°C rated value.

Once the optimum burn-in conditions and associated reject criteria have been established from results of the step stress testing, 100% of the tantalum capacitors should be subjected to the accelerated burn-in as defined in Figure 81. Hermeticity per standard methods should be performed following accelerated burn-in. Where acid electrolytes are used (normally in nonsolid devices) a litmus paper or thymol blue test should be added to the usual leak test (Reference 41).

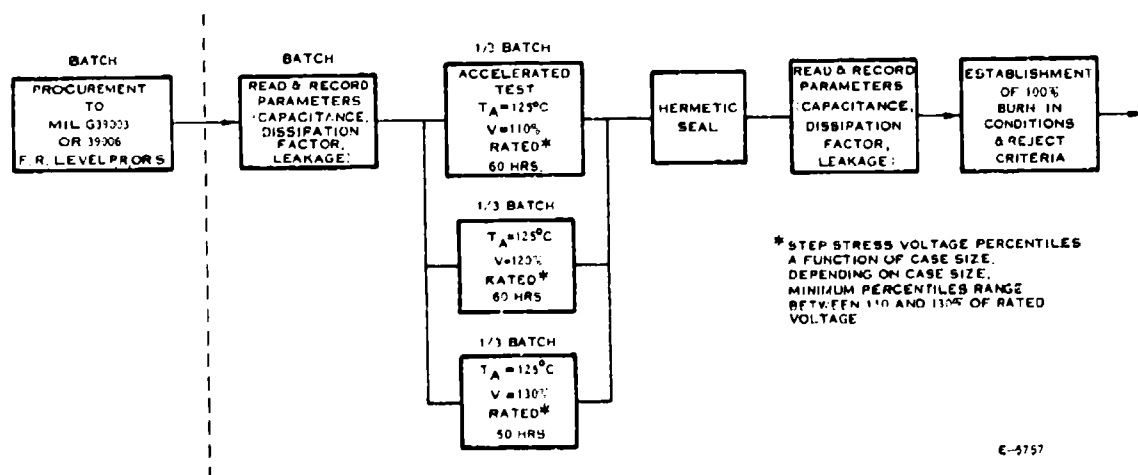


**FIGURE 79 STEP STRESS, TEST OF SOLID TANTALUM CAPACITORS
(PREPRODUCTION PHASE)**

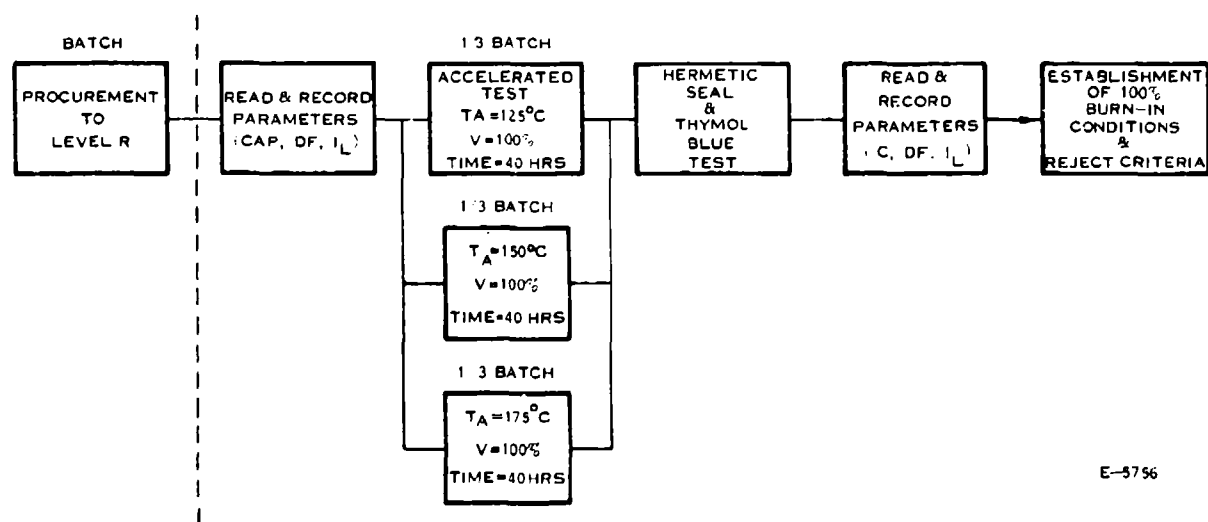
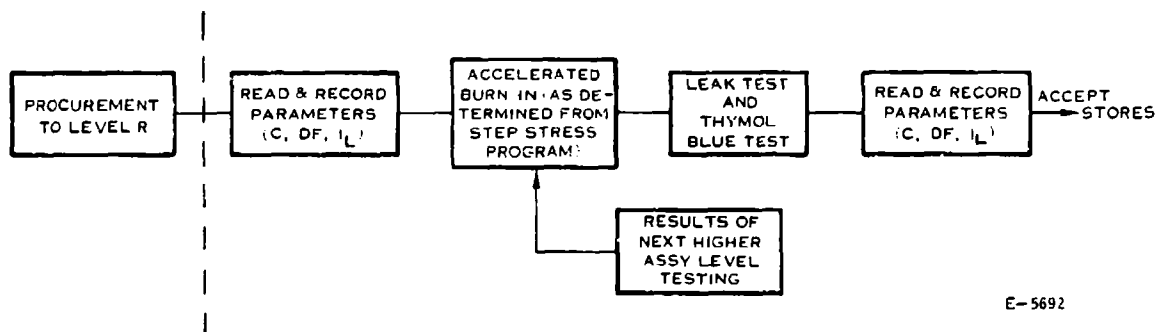


**FIGURE 80 STEP STRESS TEST OF NON-SOLID TANTALUM CAPACITORS
(PREPRODUCTION PHASE)**



E-5692

FIGURE 81 100% ACCELERATED SCREENING OF TANTALUM CAPACITORS (PRODUCTION PHASE)

The accelerated burn-in conditions should also be subject to alteration or refinement as a result of next higher level assembly screening.

8.2.4 Multilayer Epoxy or Polyimide Printed Circuit Boards

1. "A test coupon from each production board containing 80 to 100 plated-through holes, connected in series, should be temperature cycled between -65° and 110°C , and increased electrical resistance should be cause for rejection of the production boards.

For programs with a nominally mild temperature environment 50 temperature cycles are recommended. For more severe applications, 200 temperature cycles are recommended".

From the list of failure mechanisms germane to multilayer printed circuit boards, the mechanisms having the most impact on circuit functions are either short or open circuits. While the spectrum of short circuit causes cannot be completely eliminated through in-line inspection and process control measures, it can be substantially reduced. The same statement applies to the spectrum of open circuit causes but for one subtlety - open circuit failures are, by far, more time/temperature dependent.

The majority of open circuit failures, obviously, involves the plated through hole of the multilayer board. Failures are manifested by cracks or separations of the barrel of the hole from the terminal pads of one or more layers through which the barrel passes. (As stipulated in Reference 47 the primary factor affecting the long life of multilayer boards is the ductility of the copper.)

This failure mechanism also occurs during solder processing wherein the board and its plated through holes sustain the severe thermal shock associated with flow or wave soldering as well as hand soldering. In-house studies (ref. 48) have shown that a rather substantial improvement in reliability through the reduction of open circuit failures (based upon % rejects) results from the selection of polyimide/glass over epoxy/glass printed circuit board materials. While the use of polyimide over epoxy base material is encouraged, the 100% screening test outlined in Figure 82 would apply equally to either with a possible adjustment in number of thermal cycles.

A first article inspection to the criteria of MIL-P-55640 is recommended for each printed circuit configuration manufactured due to the fact that each board design is normally unique.

Test coupons should be specialized to best represent the complexity of the printed circuit board. A test coupon directly traceable to the board it represents and comprised of 80 to 100 plated through holes should be included.

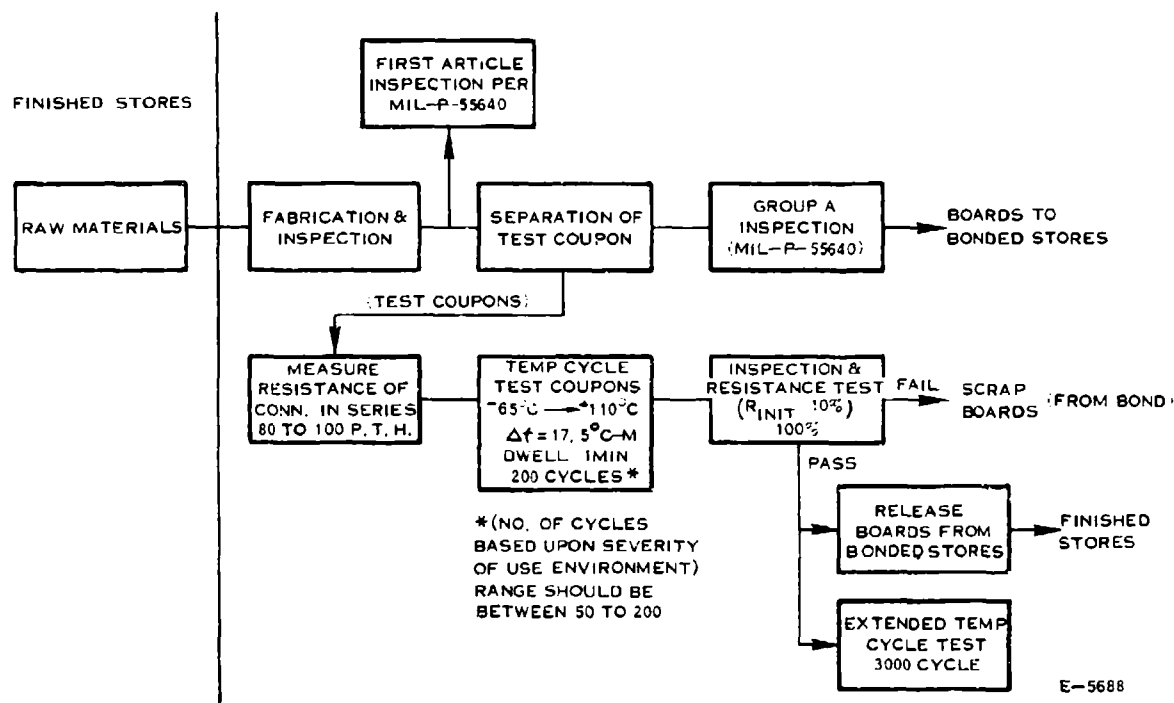


FIGURE 82 100% SCREENING OF MULTILAYER POLYIMIDE LAMINATE PRINTED CIRCUIT BOARDS PREPRODUCTION AND PRODUCTION

The plated through holes should be connected in series in such a manner that the connection of the pad of one layer to the pad of a different layer is made through the barrel of a plated through hole. In no case, should a conductor path on an individual layer be connected to more than 2 plated through holes at one time. (See Figure 83.)

The coupons containing the series connected plated through holes configured per the sketch should be subjected to from 50 to 200 temperature cycles depending upon the severity of the use environment. In the case of engine mounted hardware where temperature excursions are acute, 200 cycles are recommended. The suggested temperature extremes are -65°C to 110°C (reference 41). A thermal gradient of about 20°C per minute is adequate based upon module level testing conducted by Hughes (Reference 42). The selection of $175^{\circ}\text{C}/\text{minute}$ was based upon the gradient required to complete 200 thermal cycles in 72 hours with a minimum dwell at temperature extremes. (Note: the $17.5^{\circ}\text{C}/\text{minute}$ gradient is that to be experienced by the test coupon, not the temperature chamber volume).

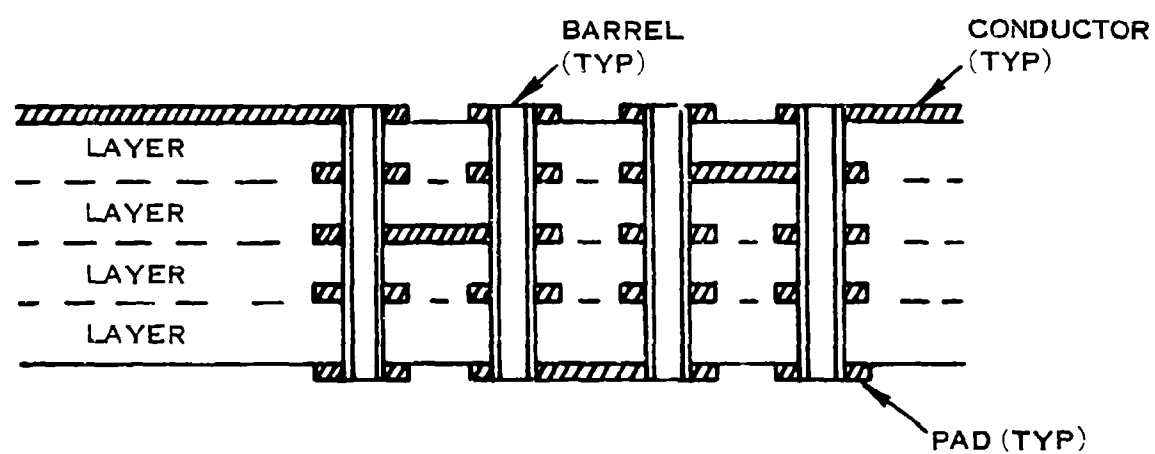
The accept/reject criteria to be applied is the delta resistance of the 80 to 100 plated through holes connected in series (R initial $+10\%$). Following an accept decision, the temperature cycle test should be continued for 3000 cycles simulating a 10 year life of the multilayer printed circuit board in normal aircraft usage.

2. "Acceptance tests should also include temperature shock tests simulating the wave, or the hand soldering operations, since thermal induced warping of the boards tends to cause cracks between the inner copper planes and the plated-through hole."

Group A inspection of MIL-P-55640 should be conducted on a tightened AQL, or better, 100% basis. In addition, thermal shock per method 107 of MIL-STD-202, test condition B should be performed.

8.3 Subassembly Level (Module) Screening

The effectiveness of a comprehensive screening program at the lower assembly level of a production run has been questioned for decades. The answer inevitably was that the measurably small improvement realized did not justify the cost of implementation. The principal reason for this lack of effectiveness was recently determined to be the rather benign environmental conditions utilized. The cost of module level test equipment falls out of the argument against subassembly screening because it has become an accepted program element, particularly, where the subassembly has a high density factor and circuit complexity.



E-5759

FIGURE 83 PRINTED CIRCUIT BOARD PLATED THRU HOLES

Numerous studies by independent firms (References 42, 43, 44) conducted on high volume production modules show a definite improvement in end item reliability attributable to subassembly thermal cycling and screening. Results indicate maximum screening effectiveness is achieved when the number of thermal cycles is between 20 and 40 and the rate of temperature change between 15 C and 25 C per minute. Complexity plays a major role in determining the most effective rate of change for a particular module; generally, the more complex modules require smaller rates of change. (Here we could define a complex module as being a multilayer polyimide printed circuit board containing 200 piece parts the majority of which being active parts, and 2000 solder joints).

8.3.1 Preproduction

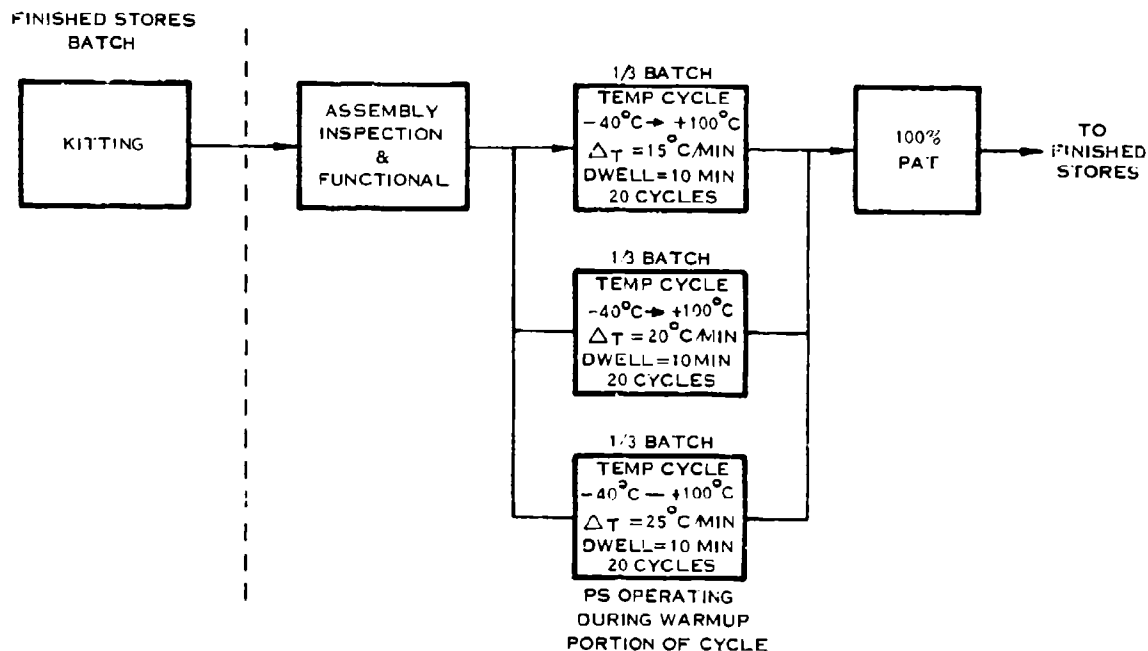
8.3.1.1 Polyimide/Glass Printed Circuit Board Assemblies

During the development phase of the program the determination of the stresses and levels which will provide optimum screening effectiveness (measured at the next higher assembly level) is to be accomplished. Figure 84 depicts the 100% screening of polyimide printed circuit board modules designed to establish the optimum rate of temperature change utilizing a fixed number of cycles and temperature ranges. These characteristics have been fixed at 20 and -40°C to +100°C, respectively, to reduce the number of variables. Additionally, these values are representative of the optimum conditions derived from the aforementioned industrial studies. The option to increase the number of cycles or the range between temperature extremes can be exercised depending upon design analysis, configuration/complexity, level of piece part screening as well as from results obtained from preproduction tests.

A preproduction batch of modules is divided into 3 equal sub-batches each of which is subjected to 20 thermal cycles differing only by the thermal gradient. (See Figure 85). Dwell time at temperature extremes should be less than 10 minutes.

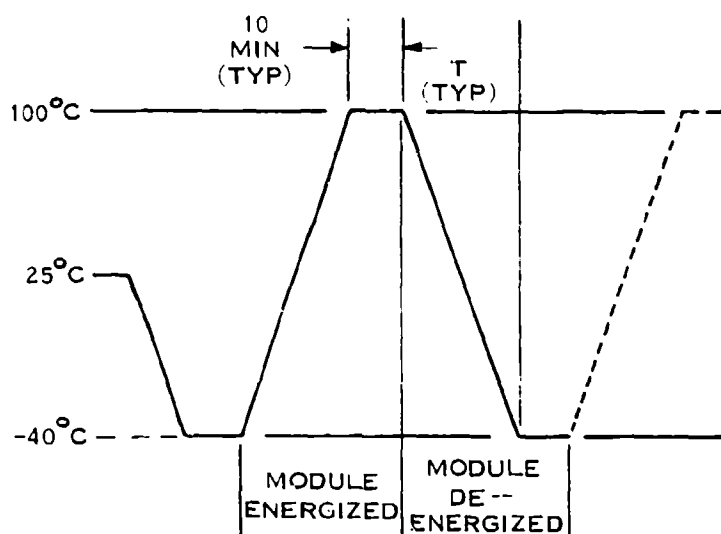
Assuming a dwell time of 10 minutes the length of test will range from 10.4 to 12.9 hours depending upon the thermal gradient employed. The traceability of a module to its thermal gradient sub-batch should be maintained through end assembly testing enabling the determination, from next higher assembly levels, of that thermal gradient which minimizes the failure occurrence of that module type. Once determined, the thermal gradient should be utilized during production testing.

The estimated yield through this subassembly level thermal screen will exceed 90% and through the end item level screening, approach 100%.



E-5687

FIGURE 84 100% SCREENING OF POLYIMIDE P.C. BOARD MODEL DURING PREPRODUCTION PHASE



$$\text{WHERE } T = \frac{\Delta T (^{\circ}\text{C})}{\theta}$$

$$\Delta T (^{\circ}\text{C}) = 140^{\circ}\text{C}$$

$$\text{FOR } \theta = 15^{\circ}\text{C/MIN, } T = 9.33 \text{ MIN}$$

$$\theta = 20^{\circ}\text{C/MIN, } T = 7 \text{ MIN}$$

$$\theta = 25^{\circ}\text{C/MIN, } T = 5.6 \text{ MIN}$$

E - 5775

FIGURE 85 TEMPERATURE EXTREMES AT DWELL TIME

8.3.1.2 Alumina Ceramic Modules

The alumina ceramic printed circuit board is a composite of ceramic insulating layers, interconnect patterns and a thick film alumina (Al_2O_3) substrate. The resulting monolithic unit is a sturdy, physically stable and thermally conductive device affording maximum device density and long term high reliability.

The physical properties of the alumina ceramic were taken into account when developing the 100% screening program shown in Figure 86 and related to a module comprised of leadless chip carriers (LCC) mounted on the alumina substrate board. Its high thermal stability and ease of rework characteristics, permit both the substrate and the LCC packs as a completed module assembly (less connector) to be thermal cycled concurrently.

The screening approach parallels that discussed earlier for polyimide printed circuit board modules except the temperature extremes have been increased to $-65^\circ C$ and $+150^\circ C$. The ceramic module minus the printed circuit board connector should be subjected to thermal cycling after which the connector is to be assembled, completing the ceramic module subassembly.

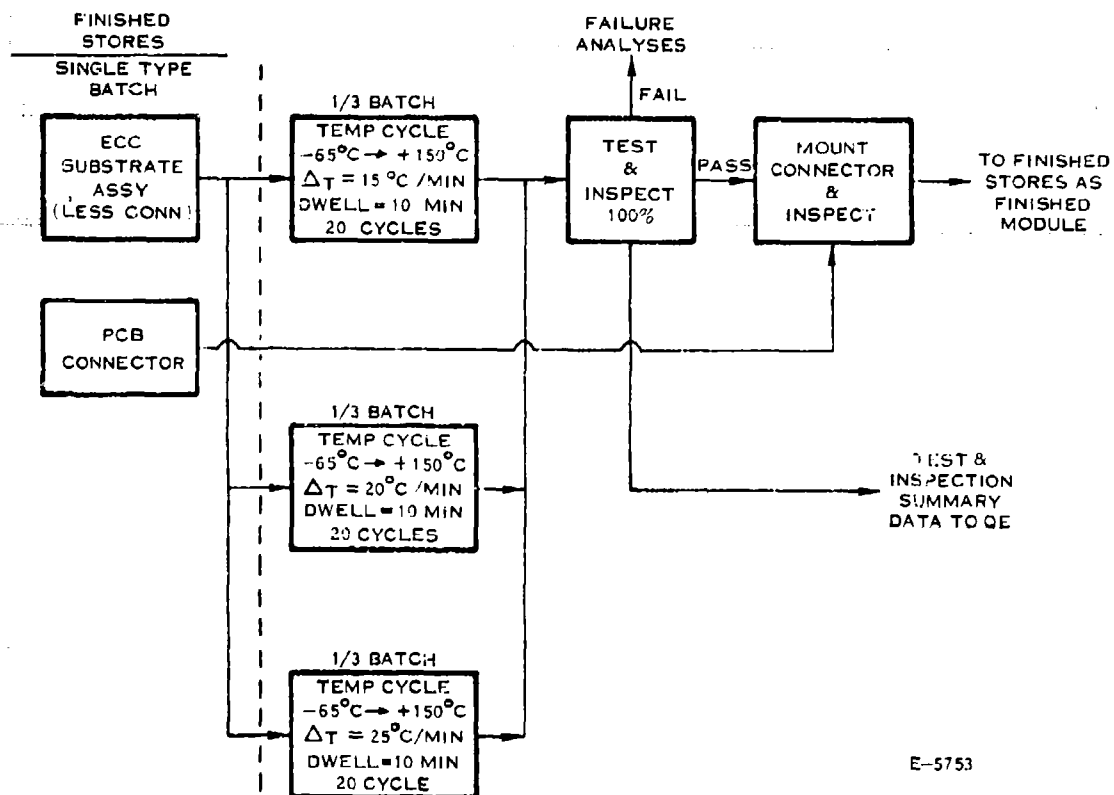
8.3.2 Production

That thermal cycle level of the three conducted on preproduction modules which manifests the most anomalies during module level screening but the least number of module failures of the same module at the next higher level screening level is to be selected as the production level module screen. That the screen levels selected over the family of module types may vary between types is to be anticipated.

The effectiveness of the selected screen should be monitored continuously at the next higher assembly screening level. In the event a new failure mechanism develops identified by an increase in module failures at the next higher assembly level, the screening program for the designated module type should be examined. Options are to vary the number of thermal cycles, the temperature range, or institute a pen test tailored to the detection of the specific anomaly. Varying the number of cycles should be avoided except as a last resort. The above is outlined in Figures 87 and 88.

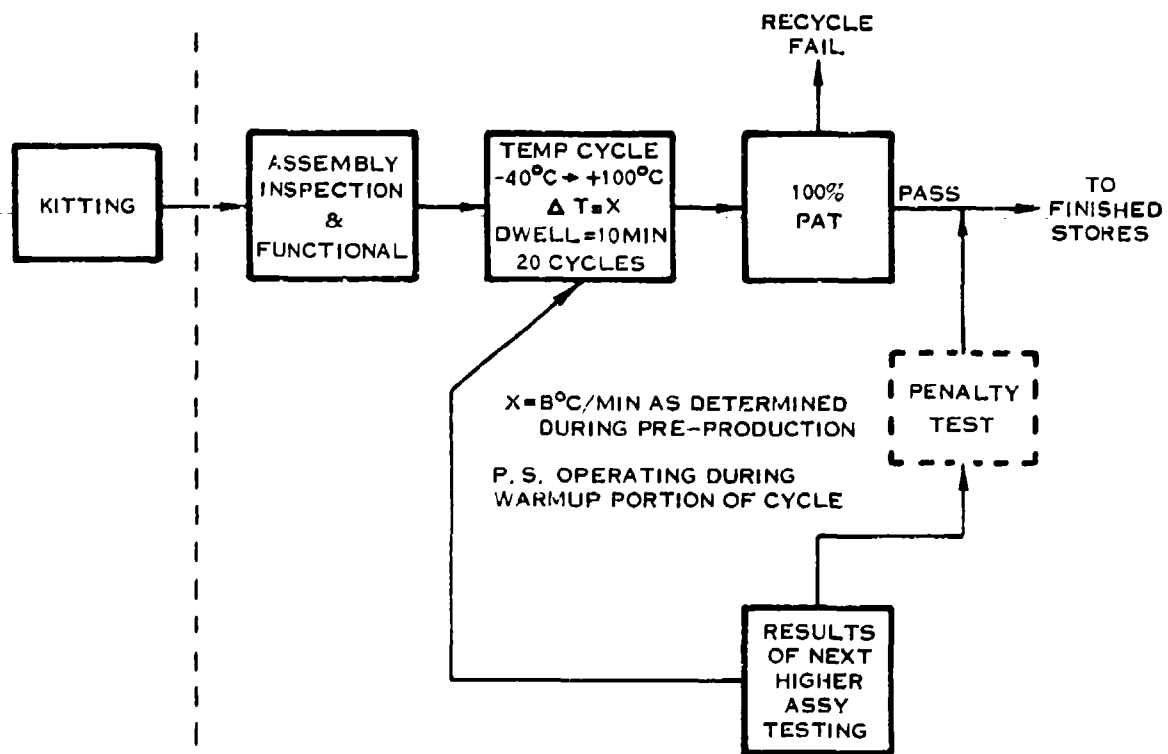
8.4 Final Assembly Level Screening

Our effort to compress the front end of the life cycle of a given equipment wherein failures usually identified as customer returns are corrected before initial shipment culminates at the final assembly screening level. Here, the effectiveness of module level screening is measureable permitting, also, an assessment of the module fabrication processes to be made. What remains is the proving of the fabrication processes related to end item level assembly and assurance testing the physical and functional interactions of the constituent modules and subassemblies.



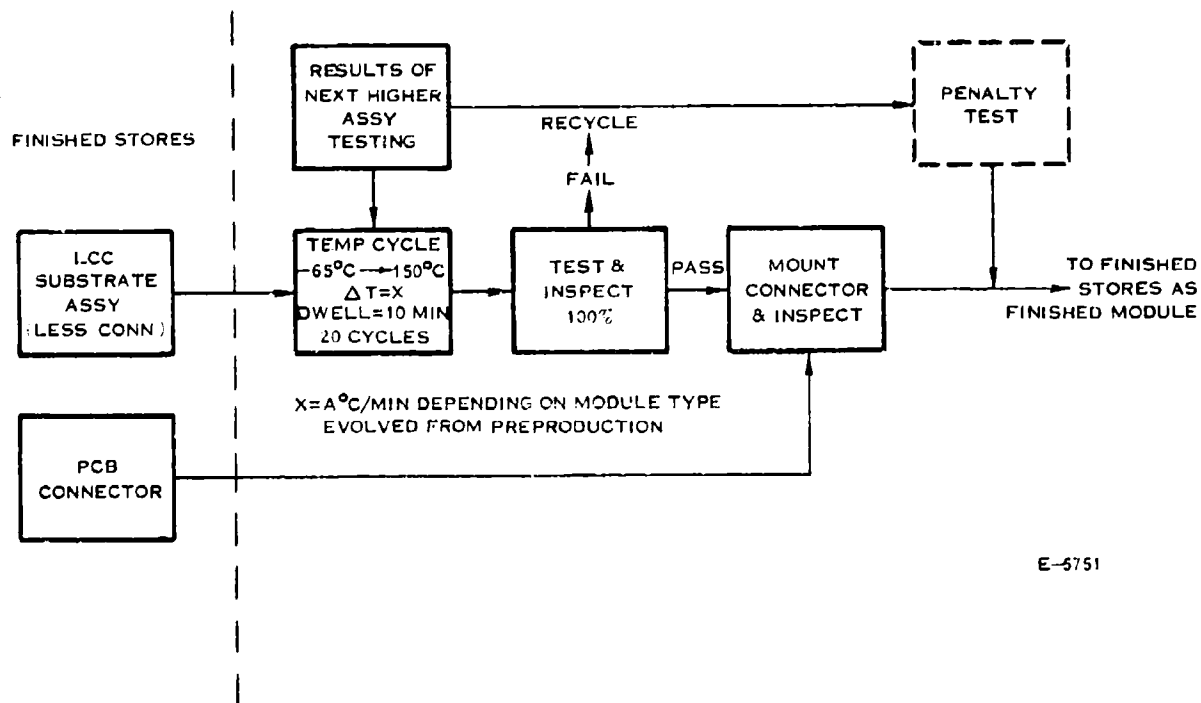
E-5753

FIGURE 86 100% PREPRODUCTION SCREENING OF MODULES INCORPORATING LCC AND CERAMIC SUBSTRATES



E-5752

FIGURE 87 100% SCREENING OF MODULES INCORPORATING POLYIMIDE P.C. BOARDS DURING PRODUCTION PHASE



E-5751

FIGURE 88 100% SCREENING OF PRODUCTION MODULES INCORPORATING LCC AND CERAMIC SUBSTRATES

The design of a high reliability assembly normally includes redundancy with the best form of redundancy being the physical and electrical separation of the redundant paths. Complete physical and electrical separation is usually unattainable in the pure sense due to package, control function and cost constraints. But in the practical sense, enough physical and electrical separation may exist when additional external interconnect or circuitry is incorporated in the test bed to permit each path to be exercised independently. Where the equipment design or program requirements do not lend themselves to optimally separate redundant paths, obviously, the conditions of the screening test conducted must be adjusted. The screening program shown in Figure 89 has been developed with consideration given to optimum physical and electrical separation between redundant paths. When this feature is too limited or non-existent the primary section path of the figure would apply.

The conditions for thermal cycling on end item assembly or equipment are dependent upon the parts mix, processes involved and the complexity of the end item. Taken from Reference 47 (page 11-16) is the graph entitled, "Generalized Temperature Cycling Failure Rate Curves as a Function of Equipment Complexity", shown herein as Figure 90 which represents the composite of their industry survey data normalized to show the typical relationship between complexity and number of required temperature cycles necessary to detect incipient failures. As can be seen, the more complex equipments require more cycles. From the same data the recommended number of thermal cycles for various complexity levels was derived as 1, 3, 6 and 10, respectively, for complexities of 100, 500, 2000 and 4000 electronic parts.

The credibility of having one cycle accomplish the intended result is questionable, particularly when another recommendation given was that the last cycle should be failure free. Re-examining the curve of Figure 90 in terms of net improvement of increasing the number of cycles to that number which more closely corresponds to the flat portion of the curve one can readily recognize an approximate 3 to 1 reduction in risk of a field failure for the case where complexity is 100 parts by increasing the number of cycles to 3. Improvement factors in the area of 2 to 1 for the other complexity levels are also recognizable at the cost of a few additional thermal cycles.

Following the guidelines given in Reference 47, as modified above, the number of cycles may be determined as a function of the equipment complexity per the following scale expanded in Figure 91 for extrapolation purposes.

<u>Number of Electronic Parts</u>	<u>Number of Cycles</u>
100	3
500	5
2,000	10
4,000	14

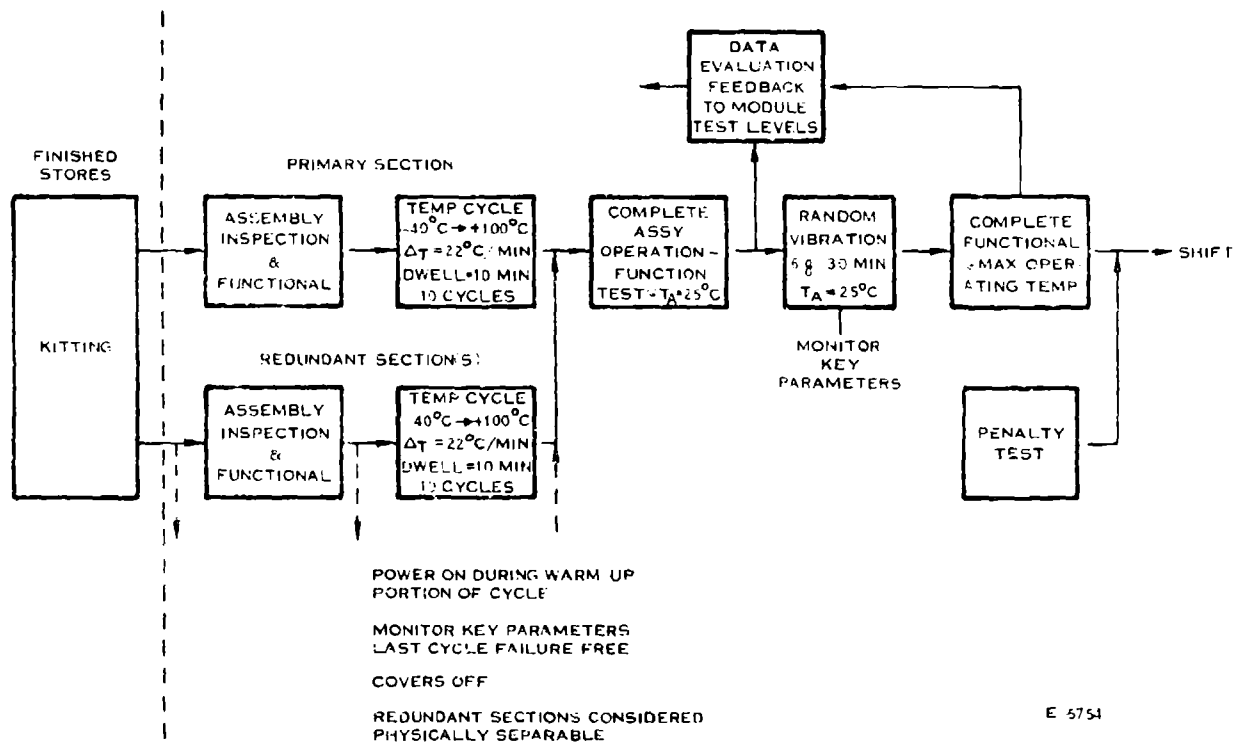


FIGURE 89 PRODUCTION ACCEPTANCE TEST OF END ITEM EQUIPMENT

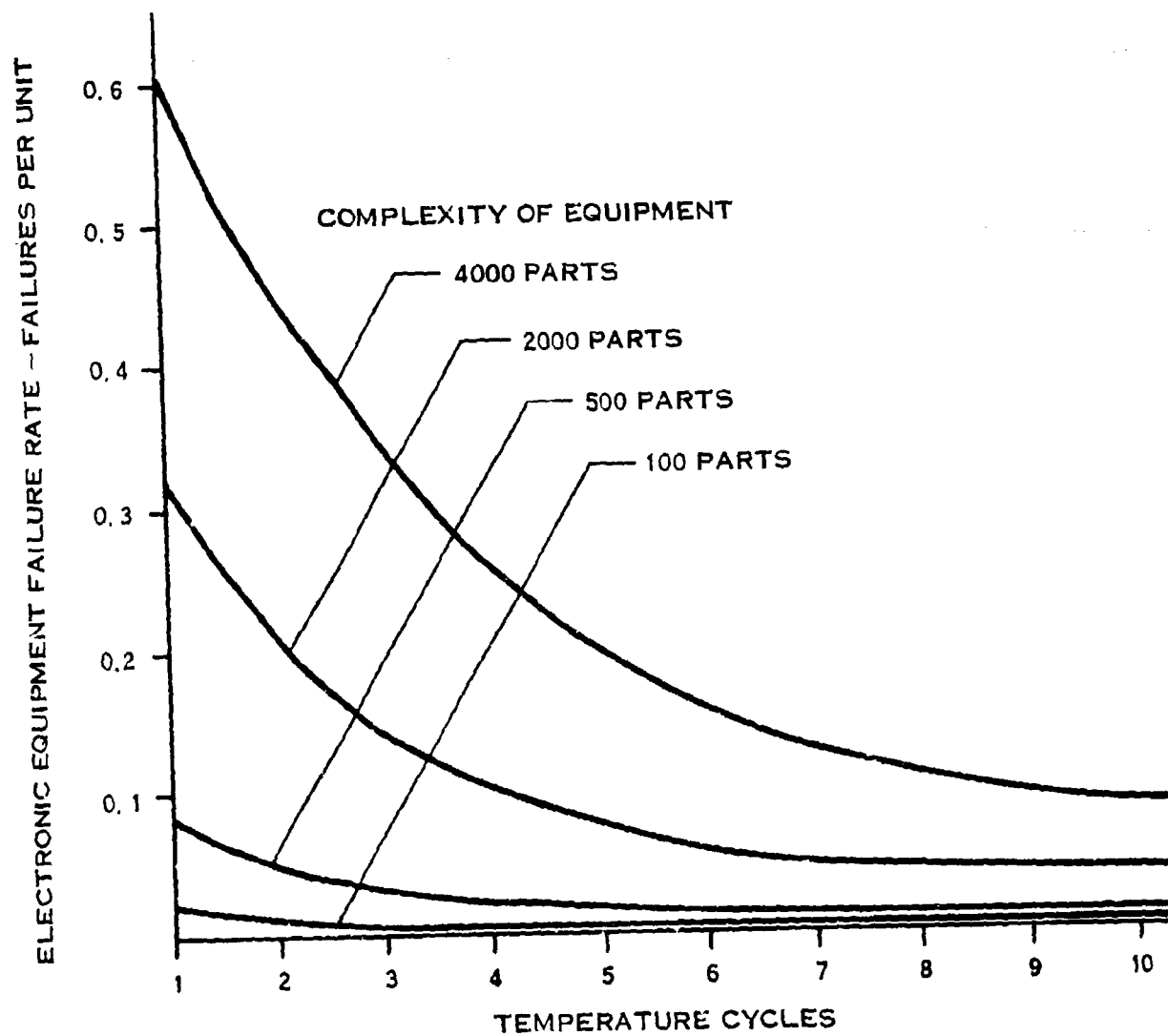
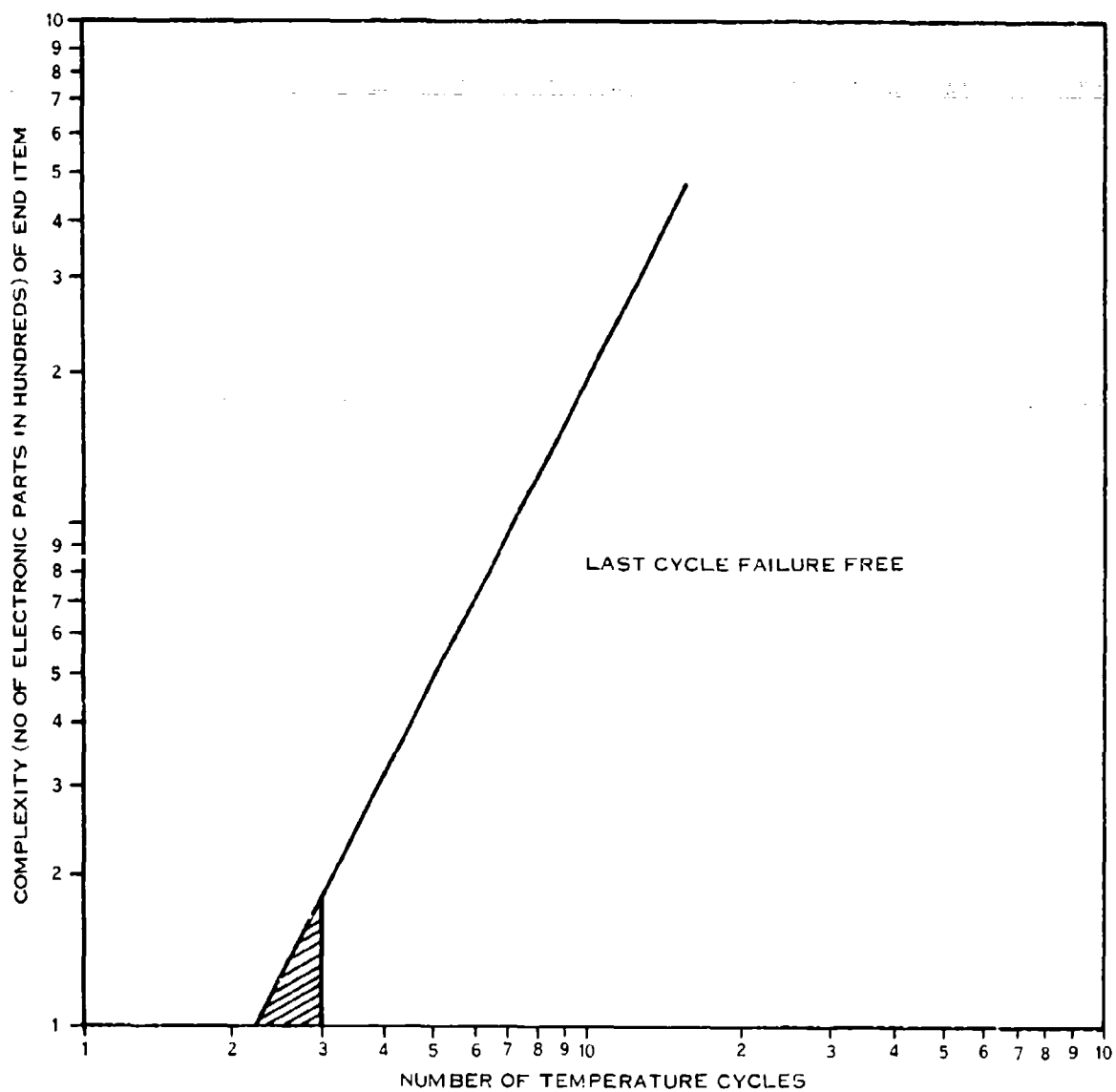


FIGURE 90 GENERALIZED TEMPERATURE CYCLING FAILURE RATE CURVES
AS A FUNCTION OF EQUIPMENT COMPLEXITY



E-5778

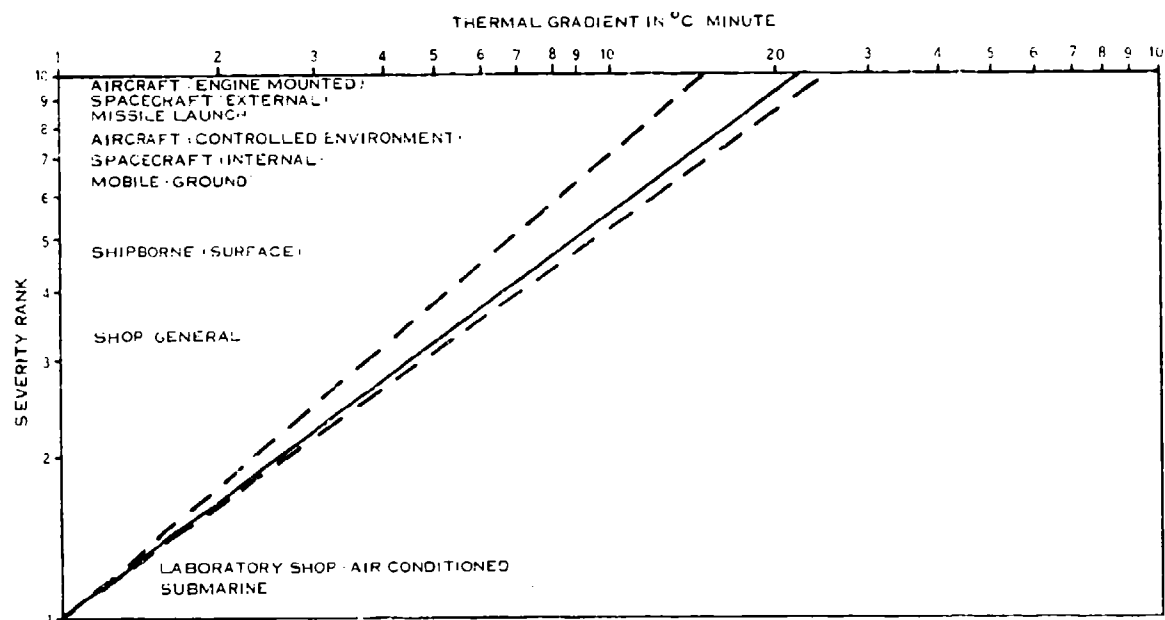
FIGURE 91 DETERMINATION OF NUMBER OF TEMPERATURE CYCLES
AS A FUNCTION OF EQUIPMENT COMPLEXITY

The thermal cycle screen shown in Figure 89 is based on an equipment complexity taken from the above for 2000 electronic parts corresponding to 10 thermal cycles (from Figure 91). The important aspects of the temperature range are (1) that there should be a delta of at least 160°F (71°C) between upper and lower extremes, and (2) that it should be representative of the use environment. Since in the equipment application being dealt with here, the temperature extremes normally are -40°C and +100°C, they were selected as the thermal conditions of the 100% screen. What will have the most effect in causing incipient failures to occur during the 10 cycles of thermal cycling is the temperature gradient.

The most effective thermal gradient for a given equipment will be that which best represents that found during its use environment. The normal range of thermal rates of change found should be between 1°C and 22°C and that the higher gradients are the most effective when utilized as a screen. The engine mounted environment in which hardware must provide continuous service over a number of years, normally can be considered to be one of the most severe. Design aspects built into the hardware such as externally supplied cooling and vibration isolation, tend to reduce the severity of the engine environment, however. In any case if one considers the range of use environments to be scaled from 1 to 10 with the most benign being 1, the most severe being 10, the engine mounted environment would be ranked in the vicinity of 10 (See Figure 92). The profile of the specified use environment, in other words, must be completely understood before an intelligent judgement in the selection of a thermal gradient intended as the rate of change in temperature during a thermal cycling test can be made. The enhancement of reliability at the end item screening level is dependent upon the ability, or effectiveness, of the screening process in isolating incipient failure mechanisms that would ordinarily occur early in the life cycle of the hardware. Having determined the severity level of the use environment as being between 8 and 10, the thermal gradient to be applied during the temperature cycle screen approximates 22°C/min in the worst case.

Dwell time, the final parameter to be established, should be between 1 and 10 minutes. From the various referenced publications, the general consensus is that temperature soak periods do little to enhance reliability. Therefore, it is necessary only to establish thermal stability at either extreme and continue cycle testing. But to assure maximum effectiveness of the thermal gradient, equipment should be turned off on the down trend and be turned on when the temperature upswing commences.

Equipment should be thermal cycled with covers off where mechanically feasible. Studies have shown that covers offer some insulation from the cooling medium to the inner parts and assemblies.



E-5705

FIGURE 92 TEMPERATURE RATE OF CHANGE OF EQUIPMENT IN ITS USE ENVIRONMENT BY SEVERITY RANK

While it may be cost prohibitive to perform functional testing, even on a limited scale, during the temperature cycling test, key output parameters should be monitored through some simplified means to alert test personnel of the occurrence of a fail condition. Special attention should be given to the determination of the condition of the key parameters during the last cycle, however, since this last cycle should be failure free. In the event a failure occurs during the thermal screen additional temperature cycles are to be conducted as a function of the complexity, ease, and quality of workmanship of the resulting repair action. Useful as a guide in making this determination is the following based upon excerpts of Reference 47.

Percentage of Total Parts Repaired/Replaced	Number of Final Consecutive Temperature Cycles Which must be survived by the Repaired/Replaced Portion of the Hardware*			
	4000 Parts (14 Cycles)	2000 Parts (10 Cycles)	500 Parts (5 Cycles)	100 Parts (3 Cycles)
0 to 0.1%	1	1	N/A	N/A
0.1% to 1%	2	1	1	N/A
1% to 5%	4	2	1	1
5% to 10%	6	4	2	1
*Additional cycles, as appropriate, should also be added when the repair cannot be easily and reliably performed.				

Finally, having completed the temperature cycle test, a complete standard functional test should be performed at ambient temperature to determine the integrity of the balance of the parameters. The resulting data in conjunction with the failure data emanating from the thermal cycle test is to be evaluated in terms of module sensitivity. From this evaluation the effectiveness of the module level screening is to be measured. In the ideal case, all module related failures have been isolated during module testing and what remains are end item assembly peculiar failure mechanisms. Should the analysis effort prove the existence of a module related failure mechanism, the module level screening conditions should be adjusted accordingly.

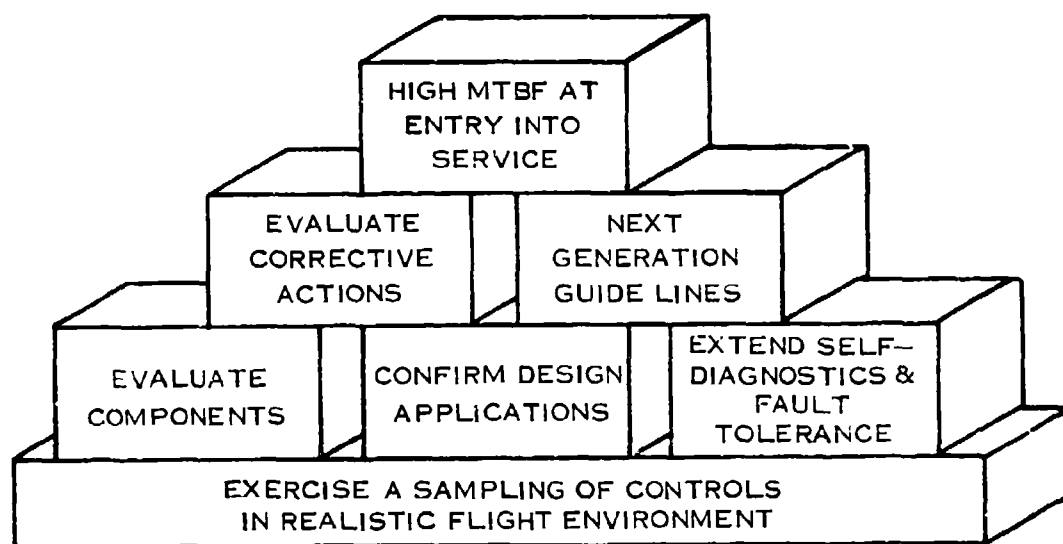
Returning to the production acceptance testing of the end item, from Figure 89 the next screen is random vibration. The extensive study and evaluation efforts referenced, conclusively show that sinusoidal vibration levels contained in MIL-STD-781B are ineffective. Experience at Hamilton Standard also echoes the conclusion reached. Support is given to random vibration for 30 minutes in each axis with equipment operating and of course monitored. The levels selected should be at least maximum specified values.

A complete functional test would follow the random vibration screen to ascertain that all parameters remain within specified limits. The temperature at which the final functional is to be conducted should be the specified maximum operating temperature, particularly during the development (preproduction) phase and should be conducted on enough hardware items to statistically prove the end item at that temperature. When the qualitative analysis supports the decision, reverting to the more simple ambient of 25°C could be done.

Penalty tests should be devised to screen any end item peculiar failure mechanisms on an as required basis depending upon screening results and/or customer returns. Again the penalty test incorporated at the end item level should be aimed at resolving process, assembly, or test problems germane to the end assembly. Where a failure mechanism can be isolated to a lower level of assembly, the incorporation of the penalty test should be at that level where economically feasible.

8.5 Reliability Development Testing

A significant contribution to accelerating the maturity of equipments can be attained by the employment of CERT (Combined Environmental Reliability Test) testing on electronic engine controls. CERT is a form of reliability test that is oriented toward "developing" reliability rather than "demonstrating fixed" reliability. The reliability development test process is particularly useful in the engine control area because comparable field experience is accrued at an extremely low rate, perhaps as low as 25 hours per month per aircraft. At this rate it could conceivably take years before MTBF values such as 25,000 hours can be substantiated. The cost of implementing corrective actions on user owned equipment is exorbitant, logistically difficult to administer, and reduces system availability. Thus, the overall purpose of CERT is to accumulate several thousand control operating hours in a simulated real world environment with early production units. The process objective then is to ensure theoretically and empirically that follow-on production controls will enter service with a high MTBF. This is illustrated in Figure 93.



E-5703

FIGURE 93 CERT OBJECTIVES

The CERT test facility provides sensor inputs and output loads for control operation. The environmental conditions which are obtained from actual flight profiles are applied in cycles and the performance of the controls monitored. Figure 94 illustrates a hypothetical reduction of real world conditions to CERT test conditions.

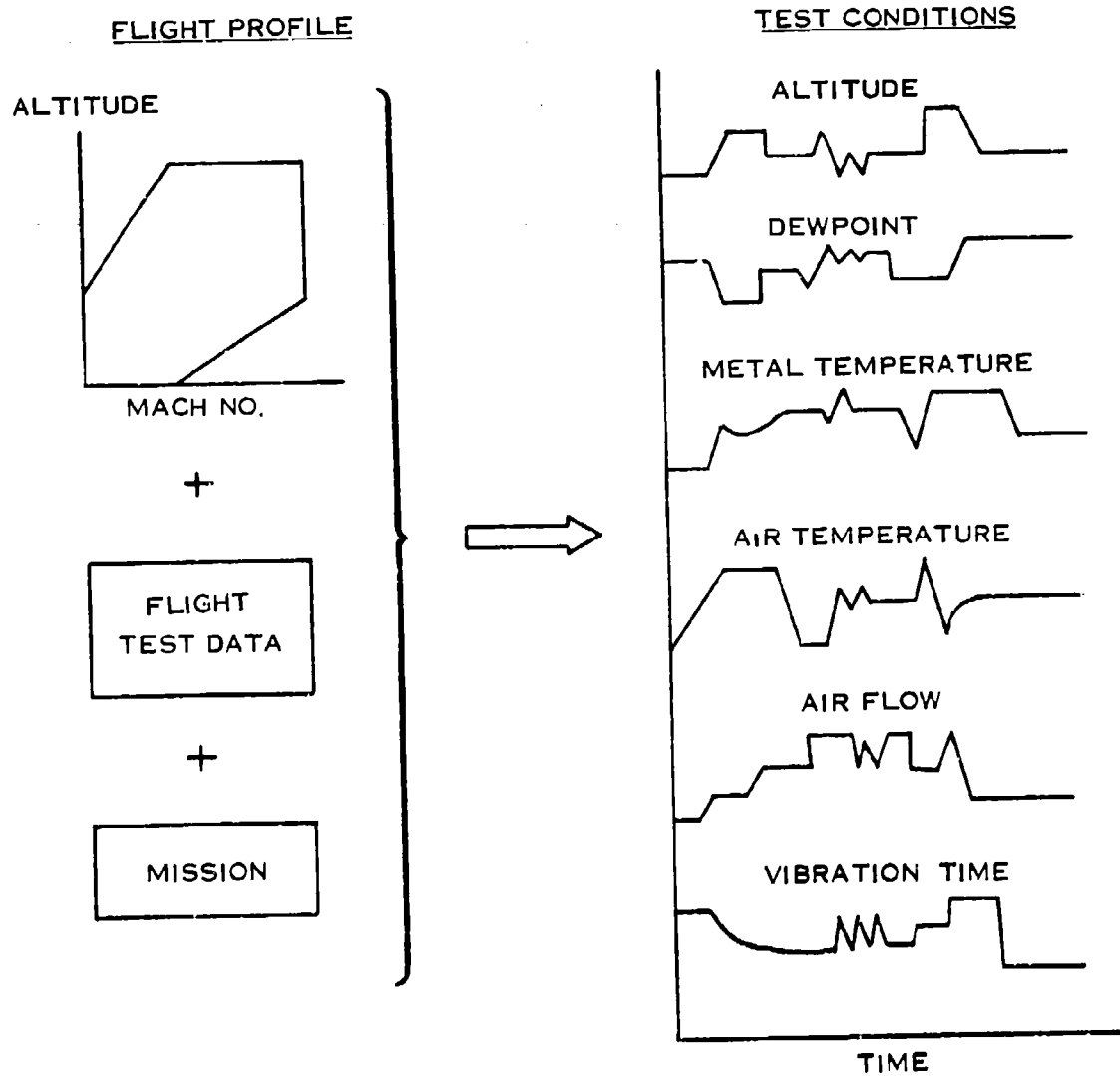
The CERT program should be operated in a test-fix-retest with delayed design fixes at three points. This is shown in Figure 95 as points F1, F2 and F3 on the time scale. The reliability of the control is expected to show growth during the test intervals with a jump expected at the time of the delayed fixes.

The increases in reliability at the time of delayed fixes occur as a result of a closed loop corrective action system. Each failure during the CERT test period is analyzed for cause. The cause of the failures are categorized and collected into general areas of responsibility such as components, workmanship, design, etc. A decision is made to fix immediately or delay the fix to the next milestone. Previous fixes are closely monitored from the time of incorporation for recurrence to evaluate the effectiveness of any changes made to the control.

The past practice of purging all failures associated with a failure mode that has theoretically been eliminated by a fix will not be followed when assessing reliability. This practice is an unnecessary and unacceptable procedure when applied to reliability assessment. With the recent advances in reliability growth procedures and mathematical modeling, purging is unnecessary because of the newer statistical methods to analyze data with changing failure rates.

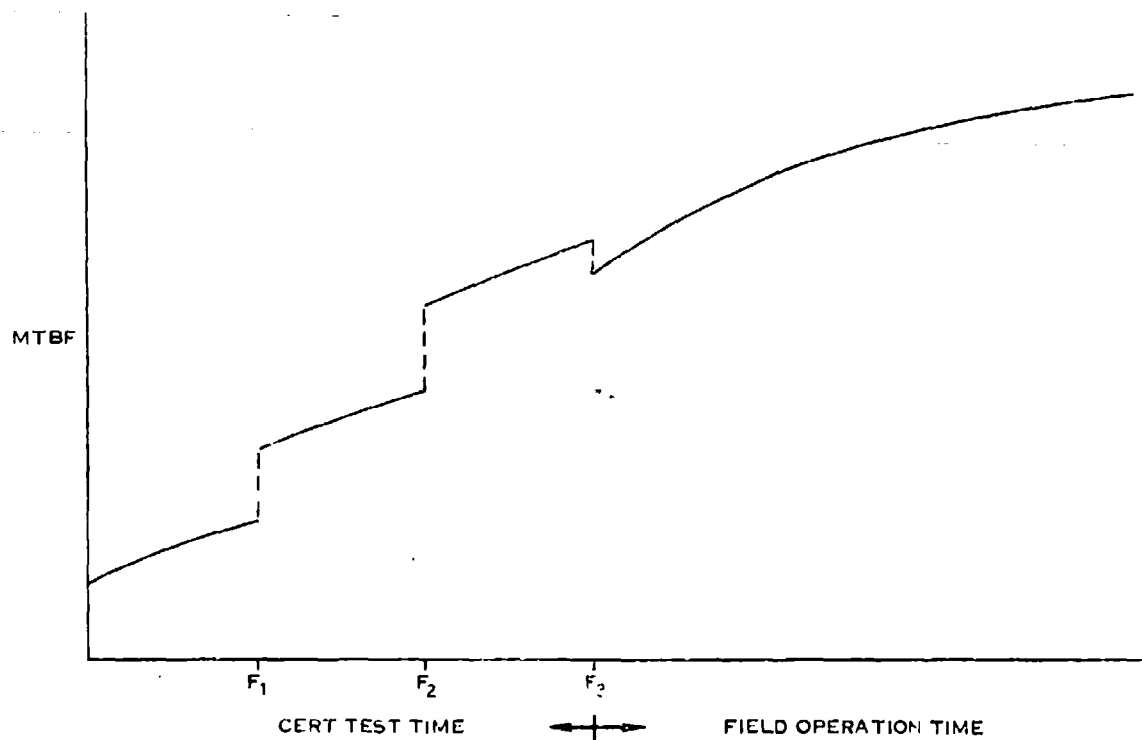
In the case for projecting reliability growth, it may be necessary to weight some of the failure modes based on a percentage of fix effectiveness when subsequent test data indicates a decrease in the failure rate for that mode.

At the conclusion of the CERT test phase of the program, the generalized growth curve in Figure 95 shows an initial drop in projected reliability. This drop is expected to offset the gains which could be anticipated for the last delayed fix. This lowered value of expected growth is caused by differences in actual versus simulated environments and field personnel unfamiliarity in handling and maintaining a new product. However, the reliability growth rate is expected to quickly resume the projected growth rate after a short shakedown period.



E-6214

FIGURE 94 CERT TEST CONDITIONS



E-5709

FIGURE 95 RELIABILITY GROWTH CYCLE

8.6 Reliability Growth Modeling

The development of designs and growth tests must be evaluated by sound mathematical techniques. The timely application and accuracy of these techniques is necessary to assure that:

- a. They will aid in the program planning so that milestones may be put into perspective with respect to the reliability goals.
- b. They will identify and quantify the impact of corrective actions.
- c. They will aid in allocation and reallocation of resources to achieve goals within the other program constraints.
- d. Optimization of the reliability growth process is achieved.

8.6.1 Generalized Statistical Analysis

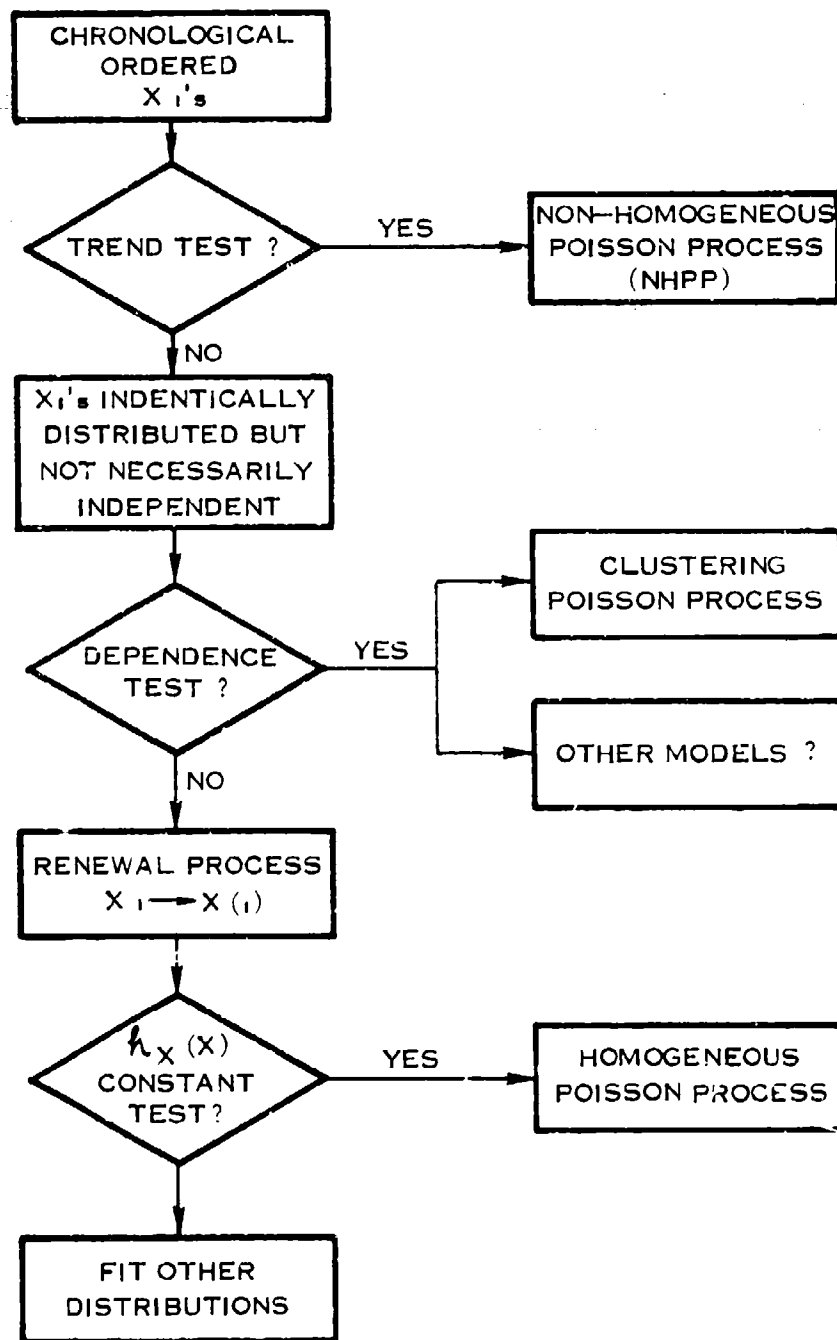
A Generalized Statistical Analysis Flow Chart is shown in Figure 96 which presents a summary of the basic notions on how a reliability growth analysis should be performed. There are a great number of details required to perform a specific analysis but broadly speaking, the flow chart shows the main steps in an analysis.

The reliability growth modeling presented in the remainder of this guide will primarily be concerned with the Non-homogeneous Poisson Process (NHPP) which is also known as the Army Material Systems Analysis Activity (AMSAA) reliability growth model.

8.6.1.1 Trend Testing

Trend tests, i.e., tests to determine whether there is a long term tendency for successive times between failures to become smaller (or larger) are discussed next. If a trend exists the Non-homogeneous Poisson Process is the simplest stochastic process which may be an adequate representation. It is possible that a more complex model may be required, but it has been shown no such model for repairable system reliability is really necessary from a statistical viewpoint.

The simplest way to perform a trend test is to plot cumulative number of failures versus cumulative operating time as in the upper part of Figure 97. If times-between-failures are tending to become smaller and smaller, a concave up shape will result as depicted in the figure. Conversely, if the times are getting larger, the plot will be concave down. An alternate procedure is to



E-5700

FIGURE 96 GENERALIZED STATISTICAL ANALYSIS FLOW CHART

estimate the average rate of occurrence of failures in three or more subintervals. In Figure 98, $P(t)$ is estimated for each subinterval by dividing the number of failures in that subinterval by $t_0/3$. Wearout (growth) is indicated if the successive estimates become larger (smaller). In extreme enough cases eyeball analyses of such plots will be adequate to disclose reliability growth or long term wearout. In most cases, however, quantitative tests will be necessary.

Under the null hypothesis of a homogeneous Poisson Process the T_i will be independent and uniformly distributed on $(0, t_0)$. Hence, for critical values corresponding to the 5% level of significance,

$$\left(\frac{\sum_{i=1}^n T_i}{n t_0} - \frac{1}{2} \right) (\sqrt{12n})$$

can be considered to be unit normal distributed, for n as small as 3, under the null hypothesis. This test has the following simple interpretation: under wearout (growth) the T_i will tend to occur after (before) the midpoint of the observed interval. Hence, under wearout (growth), n will

$$\sum_{i=1}^n T_i/n t_0$$

tend to be large (small). In other words, significantly large (small) values of the standardized variate

$$\left(\frac{\sum_{i=1}^n T_i}{n t_0} - \frac{1}{2} \right) (\sqrt{12n})$$

show significant evidence of wearout (growth). Since this test is so simple to implement and to interpret, it may appear to be "quick and dirty". Actually, however, it has been shown to be an optimum test against at least two plausible models by Cox (1955) and Bates (1955).

Laplace's test is not consistent against alternatives where the rate of occurrence of failure is non-monotone in such a way that $E(\sum T_i/n t_0) = 1/2$. In this case, a test developed by Hollander and Proschan (1974) is superior.

CUMULATIVE
FAILURES
 $N(T)$

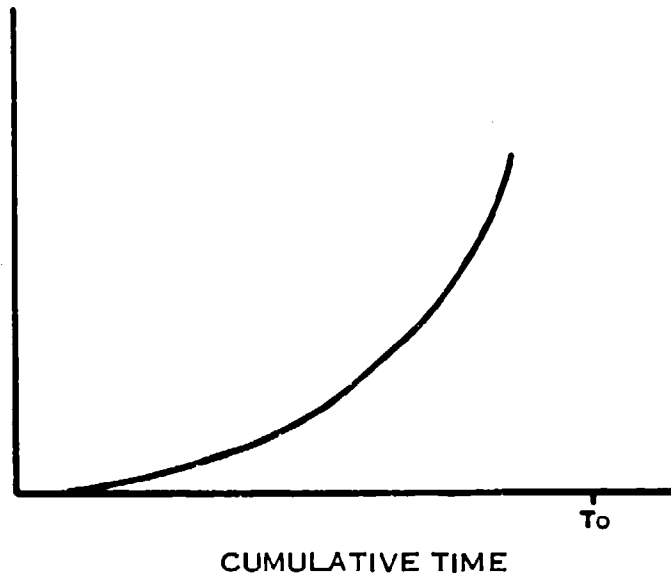


FIGURE 97 CUMULATIVE FAILURES

AVERAGE
FAILURE RATE
 $P(T)$

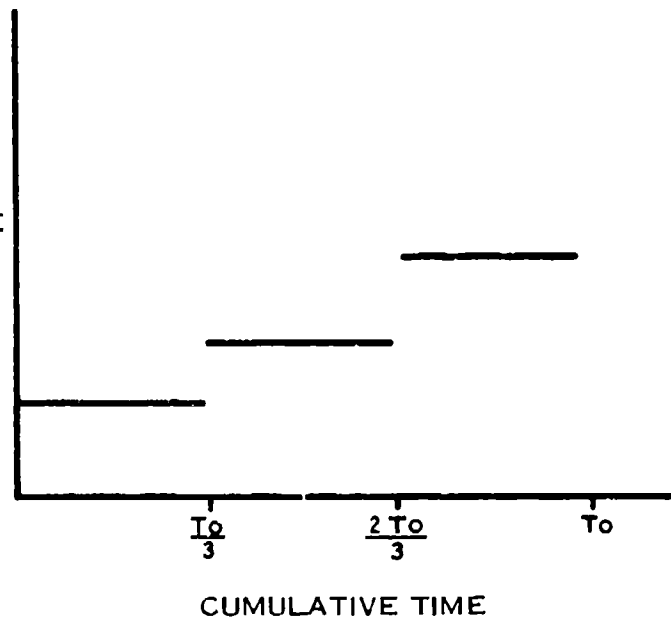


FIGURE 98 AVERAGE FAILURE RATE

8.6.1.2 AMSAA Reliability Growth Model

8.6.1.2.1 Basis of the model The US Army Material Systems Analysis Activity (AMSAA) employs a stochastic process to model reliability growth. This model adequately represents the improvement in reliability during development for a wide variety of systems. It is applicable to systems for which usage is measured on a continuous scale, for example, time in hours or distance in miles. For the sake of simplicity usage is referred to as time in the sequel. Duane (50) first observed that, for each of several systems, the number of failures accumulated at total operating time t could be approximated by λt^β , in which λ and β were positive parameters which varied from one system to another. The exponent must be less than one for representation of reliability growth. Historical data indicate that intensive reliability improvement programs are characterized by this parameter being in the range from .5 to .7.

8.6.1.2.2 Stochastic formulation Crow (Reference 51) formulated a statistical model to describe the pattern of reliability growth. This model provides that the average number of failures accumulated by time t is expressed as λt^β , but the actual number of failures observed to that time is a random variable described by the Weibull process. Other references on this process include Kempthorne and Folks (Reference 52), Englehardt and Bain (Reference 53), Bassin (Reference 54), Crow (Reference 55 and 56), Finklestein (Reference 57), and Lee and Lee (Reference 58). This development supplies methods for calculating statistically valid estimates of the mean time between failures which the system would exhibit if no further improvements are incorporated. This constitutes a means for monitoring reliability growth during the development process.

8.6.1.2.3 Cumulative number of failures The total number of failures, $N(t)$, accumulated on all test items in cumulative test time t is a random variable with the Poisson distribution. The probability that exactly n failures occur between the initiation of testing and total test time t is

$$P \{N(t) = n\} = \frac{m(t)^n e^{-m(t)}}{n!}$$

in which $m(t)$ is the mean value function; that is, the expected number of failures expressed as a function of test time. To describe the reliability growth process this function is of the form

$$m(t) = \lambda t^\beta$$

in which λ and β are positive parameters.

8.6.1.2.4 Number of failures in an interval The number of failures occurring in the interval from test time a until test time b is a random variable having the Poisson distribution with mean

$$m(b) - m(a) = \lambda(b^\beta - a^\beta).$$

The number of failures occurring in any interval is statistically independent of the number of failures in any interval which does not overlap the first interval. Only one failure can occur at any instant. The time history of the cumulative number of failures is said to be a non-homogeneous Poisson process or more precisely a Weibull process.

8.6.1.2.5 Intensity function The rate of change of the mean value function is called the intensity function of the process. For the reliability growth process the intensity function is

$$\rho(t) = \lambda \beta t^{\beta-1}$$

The probability of the occurrence of a failure between time t and time $t+h$ is approximately $\rho(t)h$ if the increment h is sufficiently small. The intensity function is sometimes called the failure rate; however, this concept is different from that of the failure rate or hazard rate of a life distribution.

Caution should be exercised so that the two ideas are not confused. The parameter λ is called a scale parameter because it depends upon the unit of measurement chosen for t . The parameter β is of prime importance because it characterizes the shape of the graph of the intensity function. If β is equal to one, the intensity function is constant. In that case the reliability of the system is not changing since the times between successive failures are independent identically distributed random variables with an exponential distribution with mean λ^{-1} . If β is not equal to one the times between successive failures are not identically distributed and do not have exponential distributions. For a development process during which the system improves the shape parameter β is less than one, and typically not less than .5. In this case the expected number of failures in an interval of fixed length decreases as its starting point increases. In a poorly managed reliability program improper design changes can result in degradation of system reliability. This situation is characterized by values of the shape parameter β greater than one. This indicates that the number of failures expected in a fixed increment of time is increasing with time.

8.6.1.2.6 Mean time between failures Parameters such as mean time between failures are used conventionally to represent the reliability performance of repairable systems. The use of these parameters to completely characterize reliability reflects the assumption that the times between failures are iden-

tically distributed. In particular, it is commonly assumed that these times come from the same exponential distribution. This corresponds to the special case of the reliability growth process in which the shape parameter is one. This special case is called a homogeneous Poisson process. It is proper to use the reliability growth model to predict a value of the mean time between failures for such a system. While it is in development the occurrence of failures follows the reliability growth process with a decreasing intensity function if the system is improving due to design changes. When production commences the design is fixed and therefore no further reliability improvement is assumed. The constant value of the intensity function for the production model should be approximately equal to the value of the intensity function at the end of development testing. Thus, the anticipated mean time between failures for the production model is equal to the reciprocal of the intensity function if the system is improving due to design changes. When production commences the design is fixed and therefore no further reliability improvement is assumed. The constant value of the intensity function for the production model should be approximately equal to the value of the intensity function at the end of development testing. Thus, the anticipated mean time between failures for the production model is equal to the reciprocal of the intensity function at the end of the development phase.

8.6.1.3 Reliability Growth Assessment

8.6.1.3.1 Graphical estimation Plots derived from the failure data provide a graphic description of test results. They furnish the analyst a means to examine the nature of the data. Graphical methods can also be used to obtain rough estimates of the reliability parameters of interest in the reliability growth process. Two types of graphs are described below. The first tells the analyst if growth is obviously demonstrated by the data. The second method goes further since it provides rough estimates of the two parameters in the expression for the intensity function.

8.6.1.3.2 Average failure frequency plots Construction of a plot of the average failure frequencies observed during testing yields a crude approximation of the intensity function. To construct such a plot divide the elapsed test time into at least three nonoverlapping intervals. These nonoverlapping intervals can be of unequal length. Next calculate the frequency of occurrence of failures within each interval by dividing the number of failures in the interval by its length. Plot the failure frequency as a horizontal line at the appropriate ordinate. The line should extend over the abscissas corresponding to time within the interval. Any significant increasing or decreasing trend in the intensity function should be apparent from this plot.

8.6.1.3.3 Cumulative failure plots A graph of the observed cumulative number of failures plotted against cumulative test time on full logarithmic paper furnishes crude estimates of the parameters which describe the intensity function. Taking logarithms in the expression for the mean value function yields the result

$$\ln m(t) = \ln \lambda + \beta \ln t$$

Therefore, the expression for the mean value function is represented by a straight line on full logarithmic paper. A line drawn to fit the data points representing the cumulative number of failures at the time of each failure occurrence is a suitable approximation of the true line. The ordinate of the point on the line corresponding to t equal to one is an estimate of λ . The actual slope of the line as measured with a ruler yields an estimate of the shape parameter β . Alternate methods include the plotting of the cumulative numbers of failures divided by cumulative test time or the reciprocal of that quantity. If either of those methods is used, the method for estimating the parameters is slightly more complicated.

8.6.1.3.4 Statistical estimation Modeling reliability growth as a non-homogeneous Poisson process permits the assessment of the demonstrated reliability performance by statistical procedures. The method of maximum likelihood provides estimates of the scale parameter λ and the shape parameter β . These estimates are used in estimation of the intensity function. The reciprocal of the current value of the intensity function is the mean time between failures that the system would exhibit in the absence of further improvements. Procedures for point estimation and interval estimation of mean time between failures are described below. The data employed in the estimation consists of a failure times from testing terminated at a given time or from testing terminated at the occurrence of a specified number of failures. The procedures vary slightly for these two types of tests. A goodness of fit test to determine whether the model is appropriate to describe the data is also described below. If the exact times of failure occurrence are unknown, it may still be possible to utilize the reliability growth model. This is the case when inspections are conducted to uncover hidden failures. Procedures to use in that instance are described by grouped data.

8.6.1.3.5 Time terminated testing The procedures described in this section are to be used to analyze data from tests which are terminated at a predetermined time or tests which are in progress with data available through some time. The required data consists of the cumulative test time on all systems at the occurrence of each failure as well as the accumulated test time. To calculate the cumulative test time of a failure occurrence it is necessary to sum the test time on every system at that instant. The data then consists of the N failure times X_1, X_2, \dots, X_N which occur prior to the accumulated test time T .

8.6.1.3.6 Point estimation The method of maximum likelihood provides point estimates of the parameters of the reliability growth process. The estimate of the shape parameter is

$$\hat{\beta} = \frac{N}{N \ln T - \sum_{i=1}^N \ln X_i}$$

Subsequently, the scale parameter λ is estimated by $\hat{\lambda} = N/T \hat{\beta}$. It follows that for any time t the intensity function is estimated by $\hat{\rho}(t) = \hat{\lambda} \hat{\beta} t^{\hat{\beta}-1}$. In particular, this holds for T , the accumulated test time. The reciprocal of $\hat{\rho}(T)$ provides an estimate of the mean time between failures which could be anticipated if the system configuration remains as it is at time T . If the reliability program is expected to continue without any shift in emphasis or environment, then the intensity function may be projected into the future to predict the benefit of continued attempts to improve reliability. Although the estimators use all failure occurrences, the model is effectively self-purging. The estimator $\hat{\rho}(T)$ can be written as $\hat{\beta}(N/T)$. Note that N/T would be the estimate of the intensity function for a homogeneous Poisson process. Hence, the fraction $(1-\hat{\beta})$ of the failures are effectively eliminated.

8.6.1.3.7 Interval estimation Interval estimates provide a measure of the uncertainty regarding the demonstration of reliability by testing. For the reliability growth process the parameter of primary interest is the mean time between failures that the system would exhibit after the initiation of production. The probability distribution of the point estimate of the intensity function at the end of the test is the basis for the interval estimate of the true value of the intensity function at that time. The values in Table 31 facilitate computation of confidence interval estimates for the mean time between failures. The table provides two-sided interval estimates on the ratio of the true MTBF to the estimated MTBF for several values of the confidence coefficient. If the number of failures is N and γ is the selected confidence coefficient, then the appropriate tabular values are L_N, γ and U_N, γ . The interval estimate of MTBF is

$$\frac{L_N, \gamma}{\hat{\rho}(T)} \leq \text{MTBF} \leq \frac{U_N, \gamma}{\hat{\rho}(T)}$$

Because the number of failures has a discrete probability distribution, these interval estimates are conservative, that is, the actual confidence coefficient is slightly larger than the stated confidence coefficient.

TABLE 31 CONFIDENCE INTERVALS FOR MTBF FROM TIME TERMINATED TEST

N \ y	.80		.90		.95		.98	
	L	U	L	U	L	U	L	U
2	.261	18.66	.200	38.66	.159	78.66	.124	198.7
3	.333	6.326	.263	9.736	.217	14.55	.174	24.19
4	.385	4.243	.312	5.947	.262	8.093	.215	11.81
5	.426	3.386	.352	4.517	.300	5.862	.250	8.043
6	.459	2.915	.385	3.764	.331	4.732	.280	6.254
7	.487	2.616	.412	3.293	.358	4.061	.305	5.216
8	.511	2.407	.436	2.991	.382	3.609	.328	4.539
9	.531	2.254	.457	2.750	.403	3.285	.349	4.064
10	.549	2.136	.476	2.575	.421	3.042	.367	3.712
11	.565	2.041	.492	2.436	.438	2.852	.384	3.441
12	.579	1.965	.507	2.324	.453	2.699	.399	3.226
13	.592	1.901	.521	2.232	.467	2.574	.413	3.050
14	.604	1.846	.533	2.153	.480	2.469	.426	2.904
15	.614	1.800	.545	2.087	.492	2.379	.438	2.781
16	.624	1.759	.556	2.029	.503	2.302	.449	2.673
17	.633	1.723	.565	1.978	.513	2.235	.460	2.584
18	.642	1.692	.575	1.933	.523	2.176	.470	2.503
19	.650	1.663	.583	1.893	.532	2.123	.479	2.432
20	.657	1.638	.591	1.858	.540	2.076	.488	2.369
21	.664	1.615	.599	1.825	.548	2.034	.496	2.313
22	.670	1.594	.606	1.796	.556	1.996	.504	2.261
23	.676	1.574	.613	1.769	.563	1.961	.511	2.213
24	.682	1.557	.619	1.745	.570	1.929	.518	2.173
25	.687	1.540	.625	1.722	.576	1.900	.525	2.134
26	.692	1.525	.631	1.701	.582	1.873	.531	2.098
27	.697	1.511	.636	1.682	.588	1.848	.537	2.068
28	.702	1.499	.641	1.664	.594	1.825	.543	2.038
29	.706	1.486	.646	1.647	.599	1.803	.549	2.008
30	.711	1.475	.651	1.631	.604	1.783	.554	1.980
35	.729	1.427	.672	1.565	.627	1.699	.579	1.870
40	.745	1.390	.690	1.515	.646	1.633	.599	1.788
45	.758	1.361	.705	1.476	.662	1.585	.617	1.723
50	.769	1.337	.718	1.443	.676	1.544	.632	1.671
60	.787	1.300	.739	1.393	.700	1.481	.657	1.591
70	.801	1.272	.756	1.356	.718	1.435	.678	1.533
80	.813	1.251	.769	1.328	.734	1.399	.695	1.488
100	.831	1.219	.791	1.286	.758	1.347	.722	1.423

For $N > 100$,

$$L = (1 + Z_{.5 + \frac{y}{2}} \sqrt{2N})^{-2} \quad U = (1 - Z_{.5 + \frac{y}{2}} \sqrt{2N})^{-2}$$

in which $Z_{.5 + \frac{y}{2}}$ is the $(.5 + \frac{y}{2})$ -th percentile of the standard normal distribution.

8.6.1.3.8 Goodness of Fit The null hypothesis that a nonhomogeneous Poisson process with an intensity function of the form $\lambda t^{\beta-1}$ properly describes the reliability growth of a particular system is tested by the use of a Cramer-von Mises statistic. An unbiased estimate of the shape parameter is used to calculate that statistic. This estimate of β is

$$\bar{\beta} = \frac{N-1}{N} \hat{\beta}$$

for a time terminated test with N failure occurrences. The estimate $\hat{\beta}$ is described as the point estimate. The goodness of fit statistic is

$$C_N^2 = \frac{1}{12N} + \sum_{i=1}^N \left[\left(\frac{X_i}{T} \right)^{\bar{\beta}} - \frac{2i-1}{2N} \right]^2$$

in which the failure times must be ordered so that $0 < X_1 \leq X_2 \leq \dots \leq X_N$. The null hypothesis is rejected if the statistic C_N^2 exceeds the critical value for the level of significance selected by the analyst. Critical values of C_N^2 for the .20, .15, .10, .05, and .01 levels of significance (α) have been computed and are in Table 32. The table is indexed by a parameter labeled M. For time terminated testing M is equal to N, the number of failures. If the test rejects the reliability growth model, an examination of the data may reveal the reason for the lack of fit. Possible causes of rejection include the occurrence of more than one failure at the same time or the occurrence of a discontinuity in the intensity function. In the first case, an appropriate procedure may be to group the data. In the latter case the data should be treated as a discontinuity.

8.6.1.3.9 Failure terminated testing The procedures described in this section are applicable to tests which are terminated upon the accumulation of a specified number of failures. The procedures are only slightly different from those used for time terminated testing. The data consists of the N failure times X_1, X_2, \dots, X_N expressed in terms of cumulative test time and arranged in nondecreasing order.

8.6.1.3.10 Point estimation The method of maximum likelihood furnishes point estimates of the shape parameter β and the scale parameter λ . The estimate of β is

$$\hat{\beta} = \frac{N}{(N-1) \ln X_N - \sum_{i=1}^{N-1} \ln X_i}$$

Note that this is equivalent to the estimate for time terminated testing with the test time equal to the time of occurrence of the last failure. The scale

TABLE 32 CRITICAL VALUES FOR CRAMER-VON MISES GOODNESS OF FIT TEST

$\alpha \backslash M$.20	.15	.10	.05	.01
2	.138	.149	.162	.175	.186
3	.121	.135	.154	.184	.23
4	.121	.134	.155	.191	.28
5	.121	.137	.160	.199	.30
6	.123	.139	.162	.204	.31
7	.124	.140	.165	.208	.32
8	.124	.141	.165	.210	.32
9	.125	.142	.167	.212	.32
10	.125	.142	.167	.212	.32
11	.126	.143	.169	.214	.32
12	.126	.144	.169	.214	.32
13	.126	.144	.169	.214	.33
14	.126	.144	.169	.214	.33
15	.126	.144	.169	.215	.33
16	.127	.145	.171	.216	.33
17	.127	.145	.171	.217	.33
18	.127	.146	.171	.217	.33
19	.127	.146	.171	.217	.33
20	.128	.146	.172	.217	.33
30	.128	.146	.172	.218	.33
60	.128	.147	.173	.220	.33
100	.129	.147	.173	.220	.34

For $M > 100$ use values for $M = 100$.

parameter λ is estimated by

$$\hat{\lambda} = \frac{N}{T \hat{\beta}}$$

as before. The intensity function and mean time between failures are estimated as before. For small sample sizes use of unbiased estimator $\bar{\beta}$ is advisable.

8.6.1.3.11 Interval estimation An interval estimate of the mean time between failures that the system would exhibit in the absence of further changes is also available for the case of failure terminated testing. Table 33 provides factors for the construction of two-sided interval estimates of the MTBF for several values of the confidence coefficient γ . The smaller number corresponding to the number of failures and desired confidence coefficient is divided by the point estimate of the intensity function at the end of the test to yield the lower limit of the interval. Division of the larger value by the intensity function estimate provides the upper limit.

8.6.1.3.12 Goodness of Fit The hypothesis that the AMSAA model is appropriate can be tested using a Cramer-von Mises statistic. It is important to note the difference in the calculations from those for time-terminated testing. An unbiased estimate of the shape parameter given by

$$\bar{\beta} = \frac{N-2}{N} \hat{\beta}$$

is used in calculation of the goodness of fit statistic. The parameter for indexing that statistic is M which is one less than N , the number of failures. The Cramer-von Mises statistic is then

$$C_M^2 = \frac{1}{12M} + \sum_{i=1}^M \left| \left(\frac{X_i}{X_N} \right)^{\bar{\beta}} - \frac{2i-1}{2M} \right|^2$$

Table 32 provides critical values for use in the test. The model is deemed inappropriate if the statistic C_M^2 exceeds the critical value for some specified level of significance α .

8.6.1.3.13 Grouped data It may happen that an event included within the scope of the definition of the term "failure" does not preclude the operation of the equipment. It is possible that such events are not uncovered until a thorough inspection is conducted. In this case the exact time of the failure is unknown; however, one can presume that it happened in the interval since the last inspection. The total number of failures in the interval between inspections

TABLE 33 CONFIDENCE INTERVALS FOR MTBF FROM FAILURE TERMINATED TEST

N	Y	.80		.90		.95		.98	
		L	U	L	U	L	U	L	U
2		.9065	33.76	.5552	72.67	.4099	151.5	.2944	389.9
3		.6940	3.927	.5137	14.24	.4054	21.96	.3119	37.60
4		.6601	5.328	.5174	7.681	.4225	10.65	.3368	15.96
5		.6568	4.000	.5290	5.424	.4415	7.147	.3603	9.995
6		.6600	3.321	.5421	4.339	.4595	5.521	.3815	7.568
7		.6656	2.910	.5548	3.703	.4760	4.595	.4003	5.963
8		.6720	2.634	.5668	3.294	.4910	4.002	.4173	5.074
9		.6787	2.436	.5780	2.989	.5046	3.589	.4327	4.469
10		.6852	2.287	.5833	2.770	.5171	3.286	.4467	4.032
11		.6915	2.170	.5979	2.600	.5285	3.054	.4595	3.702
12		.6975	2.076	.6087	2.464	.5391	2.870	.4712	3.443
13		.7033	1.998	.6150	2.353	.5488	2.721	.4821	3.238
14		.7087	1.933	.6227	2.260	.5579	2.597	.4923	3.064
15		.7139	1.877	.6299	2.182	.5664	2.493	.5017	2.921
16		.7189	1.829	.6367	2.114	.5743	2.404	.5106	2.800
17		.7234	1.788	.6431	2.056	.5818	2.327	.5189	2.695
18		.7278	1.751	.6491	2.004	.5888	2.259	.5267	2.604
19		.7320	1.718	.6547	1.959	.5954	2.200	.5341	2.524
20		.7360	1.688	.6601	1.916	.6016	2.147	.5411	2.455
21		.7398	1.662	.6652	1.881	.6076	2.099	.5478	2.390
22		.7434	1.638	.6701	1.848	.6132	2.056	.5541	2.333
23		.7469	1.616	.6747	1.818	.6186	2.017	.5601	2.281
24		.7502	1.596	.6791	1.790	.6237	1.982	.5659	2.235
25		.7534	1.578	.6833	1.765	.6286	1.949	.5714	2.192
26		.7565	1.561	.6873	1.742	.6333	1.919	.5766	2.153
27		.7594	1.545	.6912	1.720	.6378	1.892	.5817	2.116
28		.7622	1.530	.6949	1.700	.6421	1.866	.5868	2.083
29		.7649	1.516	.6985	1.682	.6462	1.842	.5912	2.052
30		.7676	1.504	.7019	1.664	.6502	1.820	.5957	2.023
35		.7794	1.450	.7173	1.592	.6681	1.739	.6158	1.905
40		.7894	1.410	.7303	1.538	.6832	1.660	.6328	1.819
45		.7981	1.378	.7415	1.495	.6962	1.606	.6476	1.747
50		.8057	1.352	.7513	1.460	.7076	1.562	.6605	1.692
60		.8184	1.312	.7678	1.407	.7267	1.496	.6823	1.607
70		.8288	1.282	.7811	1.367	.7423	1.447	.7000	1.546
80		.8375	1.259	.7922	1.337	.7553	1.409	.7148	1.499
100		.8514	1.225	.8100	1.293	.7769	1.353	.7334	1.431

For $N > 100$,

$$L = \left[1 - \sqrt{\frac{2}{N}} \left(2.5 + \frac{Y}{2} \right) \right]^{-1} \quad U = \left[1 - \sqrt{\frac{2}{N}} \left(2.5 - \frac{Y}{2} \right) \right]^{-1}$$

in which $2.5 + \frac{Y}{2}$ is the $(.5 + \frac{Y}{2})$ -th percentile of the standard normal distribution.

is therefore the sum of the number of failures detected at the time of occurrence and the number of failures found in the inspection. Such totals for each interval can be used to estimate reliability growth in accordance with the AMSAA model if there are at least three intervals.

8.6.1.3.14 Point estimation from grouped data The data consists of the total number of failures in each of K intervals of test time. The first interval starts at test time zero. The intervals do not have to be of equal length. Denote the number of failures in the interval from t_{i-1} to t_i by n_i . By convention t_0 is equal to zero. The maximum likelihood estimate of the shape parameter β is the value which satisfies

$$\sum_{i=1}^K n_i \left[\frac{t_i^{\hat{\beta}} \ln t_i - t_{i-1}^{\hat{\beta}} \ln t_{i-1}}{t_i^{\hat{\beta}} - t_{i-1}^{\hat{\beta}}} - \ln t_K \right] = 0,$$

in which $t_0 \ln t_0$ is defined as zero. This nonlinear equation can be easily solved by any of several iterative procedures. The scale parameter estimate is

$$\hat{\lambda} = \frac{\sum_{i=1}^K n_i}{t_K^{\hat{\beta}}}$$

which corresponds to the result for testing when all failure times are known with the exception that the estimate of β is calculated differently. Point estimates of the intensity function and the mean time between failures are calculated as explained for point estimates.

8.6.1.3.15 Goodness of Fit A chi-squared goodness of fit test can be used to test the hypothesis that the AMSAA reliability growth model adequately represents a set of grouped data. The expected number of failures in the interval from t_{i-1} to t_i is approximated by

$$e_i = \hat{\lambda} (t_i^{\hat{\beta}} - t_{i-1}^{\hat{\beta}})$$

Adjacent intervals may have to be combined so that the expected number of failures in any combined interval is at least five. Let the number of intervals after this combination be K and let the number of failures in the i -th interval be N_i . Furthermore, let e_i be the expected number of failures in the i -th new interval. Then the statistic

$$\chi^2 = \sum_{i=1}^K \left(\frac{N'_i - e'_i}{e'_i} \right)^2$$

is approximately distributed as a χ^2 random variable with $K-2$ degrees of freedom. The critical values for this statistic can be found in tables of the chi-squared distribution.

8.6.1.3.16 Discontinuities in the intensity function The simultaneous introduction of several design changes, a change in emphasis in the reliability program, or some other factor may cause an abrupt change in the intensity function. Such a jump should be detected by a departure from linearity in the full logarithmic plot of cumulative failures, a large change in the level of the average failure frequency, or rejection of the model by a goodness of fit test.

8.6.1.3.17 Location of discontinuity The cumulative test time at which a discontinuity has occurred can be determined by inspection from graphs of cumulative failures or average failure frequency. The methods presented above can then be used to estimate the intensity function by use of different parameters for the period before the jump and for the period after the jump. That is, if the discontinuity occurs at time T_J , then the intensity function is estimated by

$$\begin{aligned} \hat{\rho}(t) &= \hat{\lambda}_1 \hat{\beta}_1 t^{\hat{\beta}_1 - 1} & 0 < t \leq T_J \\ &= \hat{\lambda}_2 \hat{\beta}_2 (t - T_J)^{\hat{\beta}_2 - 1} & t > T_J \end{aligned}$$

in which λ_1 and β_1 are estimated only from failures on or before T_J and λ_2 and β_2 are estimated from those failures occurring after T_J . Only the second of these equations is needed to estimate the currently achieved value of the intensity function.

8.6.2 Early Reliability Growth Evaluation

The modeling of early reliability growth by using differential equations is a very useful technique for determining and reflecting known underlying failure mechanisms which are contributing to reliability growth.

The IBM differential equation growth model advanced by Rosner (Reference 59) is highly useful in that it is one of the few models addressing burn-in and screening effects. The model takes into account the nonlinearity of early growth and incorporates very plausible assumptions.

The IBM model assumes, explicitly, that: 1) there are random (constant intensity function) failures occurring at rate λ , and 2) there are a fixed but unknown, number of nonrandom design, manufacturing and workmanship defects present in the system at the beginning of testing. Let $N(t)$ be the number of nonrandom type defects remaining at time $t \geq 0$. This model makes the intuitively plausible assumption that the rate of change of $N(t)$ with respect to time is proportional to the number of nonrandom defects remaining at t . That is,

$$dN(t)/dt = -K_2 N(t)$$

and hence

$$N(t) = e^{-K_2 t + c}$$

Now if we denote the unknown number of nonrandom failures present at $t=0$ by K_1 then

$$N(t) = K_1 e^{-K_2 t} \quad t > 0, K_1, K_2 > 0$$

Defining $V(t)$ to be the expected cumulative number of failures up to time t then

$$V(t) = \lambda t + K_1 (1 - e^{-K_2 t})$$

Thus, the expected cumulative number of failures by time t is the expected number of random failures by time t plus the expected number of nonrandom failures removed by time t . It should be noted that $V(0) = 0$ as expected. Moreover, as $t \rightarrow \infty$, $V(t) \rightarrow \lambda t + K_1 \rightarrow \lambda t \rightarrow \infty$, as expected.

Because of the nonlinearity of the model, the estimation of λ , K_1 and K_2 must be evaluated by iterative methods. One method of solution is a nonlinear estimation computer program based on a methodology developed by G.E.P. Box.

There are some extremely nice features of this model. In addition to being "plausible", the most interesting feature is the ability of the model to predict the time when the system/equipment is "q" fraction debugged (i.e., q fraction of the original K_1 nonrandom failures have been removed, $0 < q < 1$). The number of nonrandom defects removed by time t is clearly

$$N(0) - N(t) = K_1 - K_1 e^{-K_2 t}$$

and hence the fraction (of K_1 initial nonrandom defects) removed by time t is

$$q = \frac{K_1 - K_1 e^{-K_2 t}}{K_1} = 1 - e^{-K_2 t}$$

Thus having estimated K_2 , say \hat{K}_2 , we can find the time at which $q = 0.95$ of the nonrandom defects have been removed by solving for $t_{0.95}$. That is,

$$t_{.95} = \frac{-\ln 0.05}{\hat{K}_2}$$

In general, for arbitrary q , $0 < q < 1$ the time by which the system/equipment is q fraction debugged is

$$t_q = \frac{-\ln (1-q)}{\hat{K}_2}$$

This equation is a powerful tool because it can be used to help determine the length of development testing, or, the debugging period.

Another important feature of the model is that the number of nonrandom failures remaining at time t can be estimated and of course is $K_1 e^{-K_2 t}$. The estimate of λ , say $\hat{\lambda}$, gives the estimate of the long-run achievable MTBF.

The differential equation model is used to develop reliability growth information on:

- a. Number of failures to be expected during any period of test or operating time.
- b. State and effectiveness of the CERT test phase in removing early failures.
- c. State and effectiveness of the production screening test phase in removing early failures.
- d. An estimated reliability for the control equipment during field operation.

SECTION IX ACCELERATED STRESS TESTING

9.1 Introduction

The accelerated stress testing of semiconductor devices is of paramount importance in that it provides the following:

- a. Information for the determination of device failure rates.
- b. Information necessary for devising a suitable, low cost, screening method to eliminate defective devices.
- c. Parameter characterization in life use to enable recognition of sensitive parameters for reliability predictions.
- d. Life testing data indicating median life, in order to obtain highly reliable parts.
- e. Information regarding the life-limiting failure modes and mechanisms for reliability studies.

Microcircuit life testing under electrical bias and at temperatures in excess of 150°C has been shown to be a valid means of both identifying life-limiting failure modes and relating those modes to their associated use-temperature lifetimes. This test plan was designed to identify failure modes and mechanisms in microcircuits in order to establish failure rates and median life, and to develop a screening method that could be used for the procurement of high reliability microcircuits for electronic engine fuel controls.

The program entailed various phases performed by several separate organizations. Hamilton Standard was responsible for procuring the test microcircuits from the device manufacturer. McDonnell Douglas Astronautics Company - St. Louis (MDAC-St. Louis) performed the bias circuit evaluation and the high temperature accelerated life tests. Hamilton Standard, in conjunction with United Technologies Research Laboratory, was responsible for detailed analysis of failed devices and Hamilton Standard was responsible for data reduction/analysis and final program documentation.

Guidance in test program definition and content was provided from the knowledge and experience of Bell Telephone Laboratories at Allentown (Mr. Conrad H. Fierdt, Jr.) and the Rome Air Development Center (Mr. Clyde Lane).

The cost of accelerated stress testing is dependent on non-recurring cost, capital equipment cost and recurring costs spread over the quantities of parts tested. For a quantity of 250 pieces the total cost of accelerated stress testing was approximately \$125/component. Recurring costs alone, for the quantities typically associated with electronic engine controls, are expected to fall in the ballpark of \$1.00 to \$1.50 per component.

9.2 Test Program

The Test Program flow and Sequence is shown in Figure 99.

The device used for the test plan was a Motorola MC14163B CMOS counter, processed in accordance with MIL-STD-883B, Method 5004 Class B. This device is a synchronous, programmable, 4 bit, binary counter with synchronous clear. It was selected for the following reasons:

- a. It possesses a circuit complexity representative of that contained in integrated circuits incorporated in the current state-of-the-art electronic fuel controllers.
- b. The generic family has been in production for an extended period attesting to the stability of the manufacturing process.
- c. It is adaptable for accelerated test conditions.

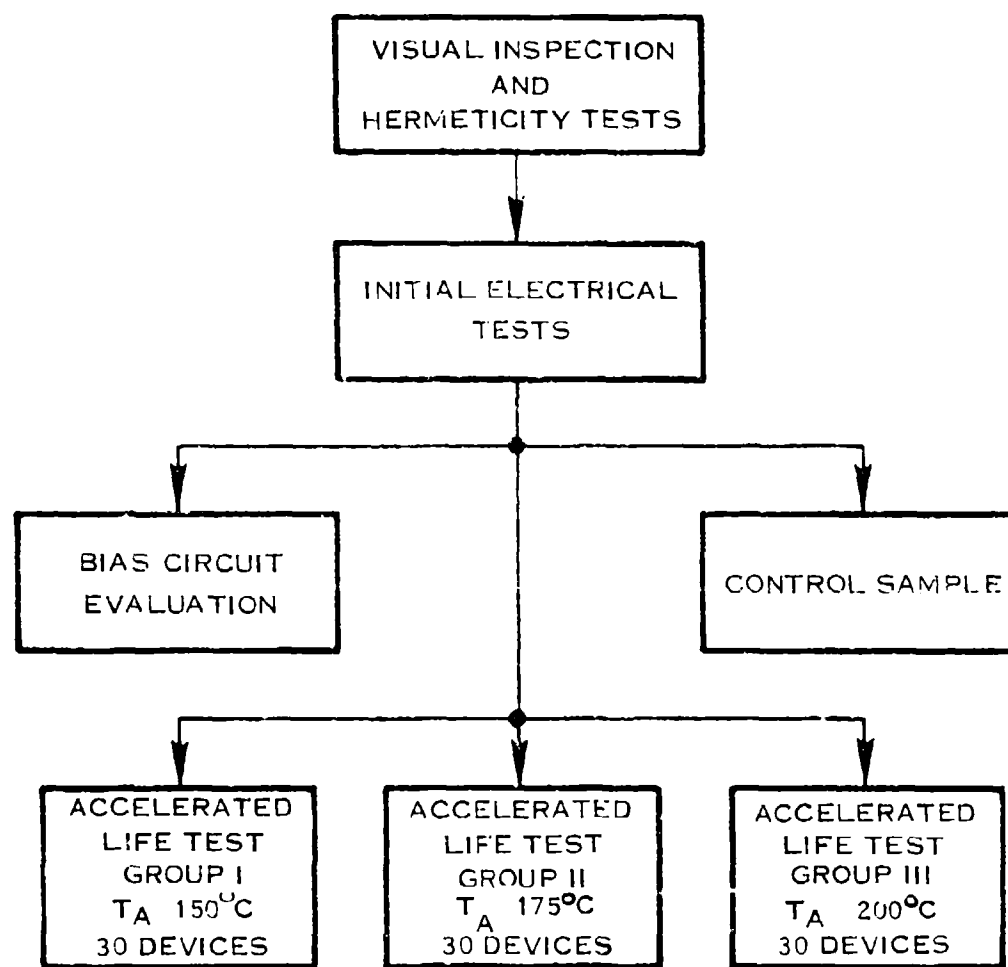
9.2.1 Facility Evaluation

MDAC - St. Louis was the facility chosen to perform the necessary testing for the following reasons:

- a. The facility possessed adequate equipment and lab facilities for high temperature testing.
- b. The personnel had demonstrated from previous work in this area that they had the technical expertise to perform all phases of the program.
- c. The personnel had demonstrated familiarization with the statistical nature of data obtained from accelerated tests from past experience in this area. This would be very instrumental in the correspondence of the necessary data and the reporting of results to Hamilton Standard.

Some of the equipment used at MDAC - St. Louis was:

- a. A Tektronix S3260 circuit tester for automatic testing with parametric printout. This tester was calibrated at regularly scheduled intervals and operated by personnel highly qualified and familiar with this device.
- b. Special circuit boards, connectors and sockets along with interconnecting wires and resistors to enable operation at temperatures in excess of 200°C.
- c. Special high temperature chambers that utilized rack mounting of assemblies containing the devices under test.



E-5681

FIGURE 99 TEST PROGRAM FLOW

9.2.2 Initial Inspections and Tests

Upon receipt at MDAC-St. Louis the Motorola MC14163B devices were subjected to a visual inspection performed per MIL-STD-883B, Method 2009.1. In addition, all devices were subjected to fine and gross leak tests per MIL-STD-883B, Method 1014.2, Conditions A1 and C2, respectively. The purpose of these examinations was the elimination of devices with shipment induced damage. No damage was observed in the visual inspection and all devices passed the hermeticity tests.

All devices were then subjected to initial electrical testing at 25°C using a Ilektronix S-3260 Automated Test System. The electrical tests were performed to establish a data base for the test program and to correlate the measurements obtained on the MDAC-St. Louis S-3260 test equipment with the manufacturer's test data. The electrical tests included both dc parametric tests and functional tests. Appendix I contains a description of the tests including test conditions, end point limits and the truth table for functional testing. No failures resulted from the initial electrical tests, and good correlation was noted between the MDAC-St. Louis and manufacturer provided parametric data.

9.2.3 Bias Circuit Evaluation

Prior to initiating the bias circuit evaluation, MDAC-St. Louis performed a construction evaluation. This was done to determine if the devices contained materials or construction features that would preclude their operation at the temperatures specified in the Test Plan. The results of this evaluation are summarized in Appendix F. They reveal no materials nor construction features that would limit testing below 250°C.

Following the construction evaluation, a bias circuit evaluation was performed to determine the suitability of the selected bias circuit, shown in Figure 136, for high temperature accelerated life tests. This evaluation was accomplished in three parts. First, a preliminary bias circuit evaluation was performed. Next, the formal bias circuit evaluation, in compliance with the Test Plan, was conducted. Finally, the formal bias circuit evaluation was continued at higher ambient temperatures to obtain additional data.

The preliminary bias circuit evaluation utilized two test devices. This was done to limit the number of devices that would be destroyed in the event of a catastrophic failure mode at the temperatures of interest. The devices were operated at ambient temperatures from 150°C to 250°C, in 25°C increments, for approximately 30 minutes at each temperature. No problems were found that would have required a test plan change. This evaluation demonstrated that the devices remained functional at ambient temperatures up to 250°C.

The formal bias evaluation was subsequently performed in accordance with the Statement of Work. Five devices were operated in the Figure 100 bias configuration at each of the three specified ambient temperatures (150°C, 175°C, and 200°C). The power supply current and the sum of the six high input currents were monitored and recorded when the devices reached the ambient temperature, 15 minutes thereafter and at 1 hour, 2 hours and 4 hours. In addition, the outputs of each device were monitored periodically with an oscilloscope. The results of this testing are included in Table 34, Bias Circuit Evaluation Summary. All devices remained functional and none exceeded the specified supply current limit of 600 μ A, or the input current limit of 1.0 μ A. With the exception of the data points noted, the Table 34 results indicate good device stability after thermal equilibrium is reached. The devices were cooled-down under bias after each 4 hour step and underwent electrical testing. This testing indicated that the selected bias circuit was non-destructive at the specified ambient temperatures and was suitable for the high temperature accelerated life tests.

The bias circuit evaluations were continued at higher ambient temperatures until an ambient temperature was reached at which the devices would not function properly. Five devices were operated at 225°C, five at 250°C, and five at 275°C. The results of the 225°C and 250°C steps are included in Table 34. At 275°C the output signals were severely degraded and the evaluation was discontinued. Although all devices remained functional at the 225°C and 250°C ambient temperatures, three devices at 225°C, and all five at 250°C, exhibited a supply current in excess of the specified 600 μ A while the input currents remained within the 1 μ A limit. Subsequent electrical parametric and functional testing indicated negligible device degradation.

Based on the results of the bias circuit evaluation, it was concluded that the long term (2,000 hour) accelerated life tests could be safely conducted at the specified ambient temperatures of 150°C, 175°C and 200°C. It was also concluded that life testing could be safely conducted at ambient temperatures as high as 250°C. After a review of the device characteristics with the manufacturers, and through correspondence with our technology transfer agents, it was discovered that a potential latch-up problem, and possibly others, would occur above 200°C. The 200°C maximum test temperature was determined to be adequate for the test and it insured that no test induced failure mechanisms would result.

9.2.4 High Temperature Accelerated Life Tests

The high temperature accelerated life tests were performed at the three selected ambient temperatures (150°C, 175°C, and 200°C) for 2,000 hours. Each test cell contained thirty devices which were biased in the Figure 100 configuration. Periodically during the life tests the devices were cooled-down under bias for interim electrical testing. The interim electrical tests were the same as the initial electrical tests and are described in detail in Appendix E.

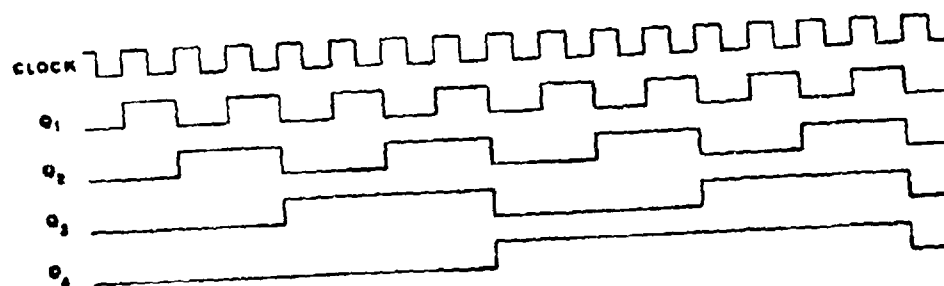
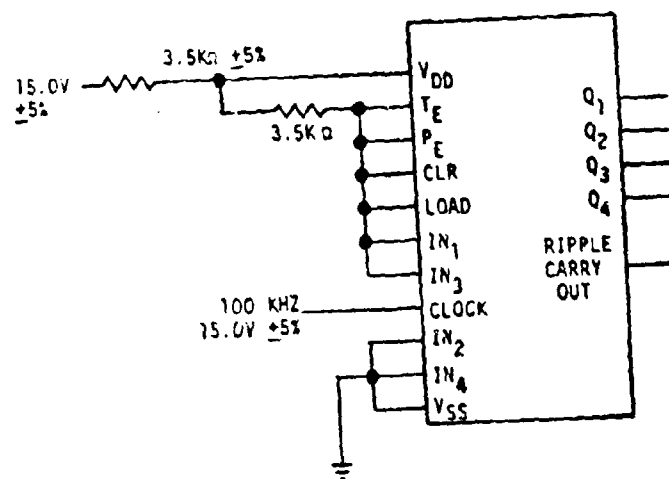


FIGURE 100 MC14163B BIAS CIRCUIT

TABLE 34 BIAS CIRCUIT EVALUATION SUMMARY

Temperature	Readout Time	Supply Current (μ A) (1)	Input Current (nA) (1)
150°C	0	67 (2)	4
	15 MINUTES	145	4
	1 HOUR	146	4
	2 HOURS	147	5
	4 HOURS	147	5
175°C	0	161	18
	15 MINUTES	171	30
	1 HOUR	175	31
	2 HOURS	175	32
	4 HOURS	175	32
200°C	0	269	97
	15 MINUTES	278	100
	1 HOUR	282	101
	2 HOURS	282	99
	4 HOURS	284	99
225°C	0	647	194
	15 MINUTES	586	262
	1 HOUR	596	268
	2 HOURS	597	269
	4 HOURS	598	272
250°C	0	1490	480
	15 MINUTES	1720	527
	1 HOUR	1750	533
	2 HOURS	1750	535
	4 HOURS	1750	395 (3)

NOTES:

- (1) Average of five devices
- (2) An adjustment in the V_{DD} and clock high level voltage was required following this measurement accounting for this low reading
- (3) This reading is in error due to an offset voltage shift in the DVM. Subsequent electrical testing indicated no input degradation.

The interim electrical test times were 4, 8, 16, 32, 64, 128, 256, 512, 1,000 and 2,000 hours. A control sample of ten devices was also tested at each interim readout to verify the long term stability of the automated test equipment.

No device failures were generated by any of the accelerated life tests. In addition, no device exhibited parametric change that would indicate device degradation, as shown in Table 35.

9.3 Conclusion and Results

The interim electrical test data was reviewed throughout the high temperature accelerated life tests to identify both failed devices and specific parameters that exhibited drift. As an additional data evaluation tool, summaries of the parametric data were generated for each test group and at each interim readout. The data included means, standard deviations, and maximum and minimum values for each parameter. Those measurements that were performed on several inputs or outputs were combined for this evaluation. The initial and final means and the standard deviations for the device parameters in the three test groups are included in Table 46. The initial values were computed using the specific initial data of the devices which comprise the various test groups. It can be seen that no important changes were observed as a result of the life tests. A single device (S/N 52) in the 175°C group exhibited a large I_{SS} ($\approx 12\mu A$) when measured at $V_{DD} = 15.0$ V, resulting in a high mean and sigma value for that group. This measurement was high when initially tested by MDAC-St.Louis as well as when the manufacturer tested the device. This current remained relatively constant throughout the life test and was well within the specified end point limits.

The failures versus time data was instrumental in determining the median life and reliability level of the devices tested. No failures were obtained for up to 2,000 hours @ 200°C. This data was indicative of a highly reliable lot of devices.

In applying the failure data obtained to the lognormal distribution and Arrhenius curves, the following relationships apply.

- a. The median life of the devices under test is greater than the time obtained. With no failures to 2,000 hours, at 200°C, this extrapolates to no failures in approximately 4×10^9 hours at 25°C using a 1.0 eV slope on the Arrhenius curves (characteristic of CMOS devices). The median life is greater than 4×10^9 hours at 25°C as no failures were obtained at this point.

TABLE 35 PARAMETRIC TEST SUMMARY

PARAMETER	150°C Group				175°C Group				200°C Group			
	INITIAL		2,000 HOURS		INITIAL		2,000 HOURS		INITIAL		2,000 HOURS	
	MEAN	SIGMA	MEAN	SIGMA	MEAN	SIGMA	MEAN	SIGMA	MEAN	SIGMA	MEAN	SIGMA
15V, I_{SS} (nA)	106.7	46.07	104.2	47.69	480.8	2060	484.2	2073	95.83	13.82	97.5	10.90
15V, I_{IL} (nA)	-1.359	3.950	-1.554	3.816	-1.139	0.7806	-1.320	0.8510	-1.141	0.7507	-1.311	0.8495
15V, I_{IH} (nA)	3.163	1.031	6.413	1.224	3.091	1.032	6.048	1.212	3.052	0.9818	7.072	1.280
V_{OHD} (μV)	-325.3	163.6	-304.0	159.2	-330.0	172.9	-300.0	187.3	-283.0	158.7	-342.7	163.3
V_{OL} (μV)	1055	83.54	951.3	86.39	1054	88.31	944.0	87.54	1064	81.26	962.3	82.85
15V, I_{OH} (mA)	-8.877	0.3052	-8.904	0.3028	-8.817	0.3023	-8.839	0.2974	-8.790	0.2825	-8.784	0.2736
15V, I_{OL} (mA)	9.951	0.5584	10.24	0.5577	9.997	0.4854	10.46	0.4913	9.871	0.7057	10.37	0.7030
10V, I_{SS} (nA)	88.33	30.78	92.5	22.03	91.67	30.51	88.33	32.10	82.50	32.69	75.00	40.31
10V, I_{OH} (mA)	-2.441	0.08473	-2.451	0.08277	-2.426	0.08645	-2.428	0.08301	-2.417	0.07506	-2.413	0.07602
10V, I_{OL} (mA)	2.533	0.1528	2.634	0.1566	2.549	0.1280	2.686	0.1412	2.507	0.1905	2.664	0.1983
5V, I_{SS} (nA)	80.00	35.59	90.83	26.6	74.17	40.30	81.67	32.87	70.83	42.12	88.33	27.94
5V, I_{OH} (mA)	-4.459	0.1778	-4.468	0.1757	-4.404	0.1810	-4.407	0.1780	-4.398	0.1397	-4.375	0.1406
5V, I_{OL} (mA)	1.000	0.06880	1.026	0.06395	0.998	0.07020	1.030	0.07390	0.996	0.09246	1.030	0.09711
I_{NSAT} (mA)	2.805	0.2470	2.819	0.2450	2.792	0.3267	2.807	0.3312	2.823	0.3924	2.839	0.4023
I_{PSAT} (mA)	-5.330	0.2304	-5.346	0.2286	-5.260	0.2350	-5.267	0.2354	-5.255	0.1800	-5.224	0.1840

- b. The failure distribution of the devices can be obtained by further analysis. The standard deviation (σ) parameter was not obtained as a result of the lack of failures. However, using an assumed σ that is characteristic of CMOS devices, the median life and failure distribution can be obtained after only a few percent of failures. The slope of the lognormal cdf curve corresponding to σ will also provide the 50% median life point and other failure points. The 50%, or greater, failures data is needed to fully determine the exact values of median life and σ of each group of devices. At 125°C, the extrapolated value of 2,000 hours at 200°C is 2.5×10^5 hours.

The accelerated tests and resultant data indicated that the CMOS devices used were highly reliable. Other characteristics of these devices are indicated by the values of the parameters that were actually obtained. In particular, the values of the leakage currents (approximately 100 nA @25°C) were far below the maximum specified value of 5.0 μ A by the manufacturer. The amount of drift of this parameter was small as indicated in Table 35. The low values for leakage currents correspond to the values that would be used in MIL-M-38510 for CMOS devices.

In closing, it was found that accelerated stress testing has demonstrated that reliable CMOS devices are obtainable and the data obtained is useful for screening processes and reliability indicators.

SECTION X COST OF OWNERSHIP STUDY FOR RELIABILITY ADVANCEMENT OF ENGINE ELECTRONIC CONTROLLERS

10.1 Introduction

A limited Cost-of-Ownership Study of Candidate Preliminary Designs was performed as part of a digital electronic control system design study to determine guidelines for Reliability Advancement of Electronic Engine Controller (RAEEC). The scope of this cost study was guided by the program directive that primary emphasis shall be given to achievement of the controller MTBF goal recognizing that cost, performance, weight and volume limits must be observed. Therefore, the cost of ownership study represents a small part of the total program and indicates trends and guidelines based on the analysis of "preliminary designs."

A fundamental reason for Cost-of Ownership Investigation during the design of weapon systems, subsystems and equipment is to influence the decision process to insure the production of hardware which will satisfy reliability and operational requirements for the lowest total cost of ownership. The program described herein estimates the expected support costs that may be incurred by adopting a particular design. The model is also used to compare and discriminate among design alternatives where relative cost difference and cost trend is an important figure of merit.

The input for the Cost-of-Ownership Study was based on the controller reliability improvements evolved by the RAEEC study. This study identified reliability improvements in eight categories. The overall controller mean time between unscheduled removal (MTBUR) was assessed for the addition of each reliability improvement feature. The acquisition cost was also incremented to show the cost effect of the reliability improvement along with the specific cost-to-repair information. This input was then modeled with the life cycle cost (LCC) computer deck to evaluate the overall Cost-of-Ownership effect.

10.2 Objective

The specific objective of the Cost-of-Ownership Study was the determination of advanced controller life cycle costs for various degrees of increased reliability. Previous studies of controller improvement have indicated cost benefits derived from the "Self-Trim" aspect of advanced controllers. Cost savings resulting from the "Self-Trim" feature are primarily in the area of reduced engine spare parts costs and an increase in the engine flight hours to operating hours ratio. (See Appendix F). The present study examines degrees of increasing cost-effectiveness resulting from increased reliability, until an optimum point is reached.

10.3 Summary

Current engine controllers, with little inherent redundancy, exhibit reliability values of about 1500 hr operating time between failures (repairs). In this study, incremental increases in reliability are predicted for specific improvements in

component technology and operating philosophy for several advanced controllers. Each of these improvements involves an initial acquisition cost increase but results in decreased support costs over the useful life of the controller. The cumulative effects of increased reliability result in decreasing total LCC due to fleet-wide reductions in the frequency of removal and repair of controllers. However, a point of diminishing returns is generally seen in any attempt to continually increase the reliability aspects of each type of controller.

In general, reliability improvement to a level of about ten thousand (10,000) hours between controller repair is seen to result in a significant decrease in operating and support costs over a 15-yr operational life, with a relatively small increase in acquisition cost. The greatest decrease in support cost, and consequently total cost, occurs as reliability improvement approaches the 10,000 hr level. This encompasses essentially the first five incremental reliability improvements of the eight levels of improvement under consideration. Beyond that point of reliability achievement, the considered reliability improvements (selected redundancy, component and assembly screens) indicate a three-fold increase in hours between unscheduled control removal (30,000 + hr), but produce diminishing support cost reductions which do not offset the increased acquisition cost for the specific improvements. The total LCC therefore increases with introduction of these latter improvements.

The diminished benefits of increased reliability take on increased significance when viewed in relation to the usefulness of the increase to total engine life. As reliability of the particular controller increases beyond the useful life of the engine on which it is utilized, the value of increased reliability through incremental improvement is not cost-effective as total cost of additional reliability increases.

10.4 Approach

10.4.1 Ground Rules

The advanced controller Cost-of-Ownership Study was based on incorporation of controls into an F-15 type of aircraft powered by two engines. This system was chosen as a baseline for the study because of availability of engine and airframe LCC data, particularly engine maintenance costs.

Specific ground rules used in the study include:

- 729 total aircraft, 540 operational
- 1674 engines, including spares
- Each operational A/C flies 25 hr/month for 15 years

- Organizational and intermediate level labor rate is \$16.25 per man-hour; depot rate is \$26.00, unless otherwise specified
- Fuel cost is \$0.45 per gallon
- Current Tactical Air Command maintenance concepts
- Constant 1978 dollars

These criteria were utilized as baseline input to the engine LCC model, which collects all major cost elements of controller operation for proper assessment of reliability increase within the control. (See Figure 101). The model produces cost projections for fleet-wide incorporation of particular control configurations at specified reliability levels.

10.4.2 System Configurations

The LCC model was exercised for four advanced control configurations which differ in degree of redundancy utilized in controller design. The four controls under consideration are:

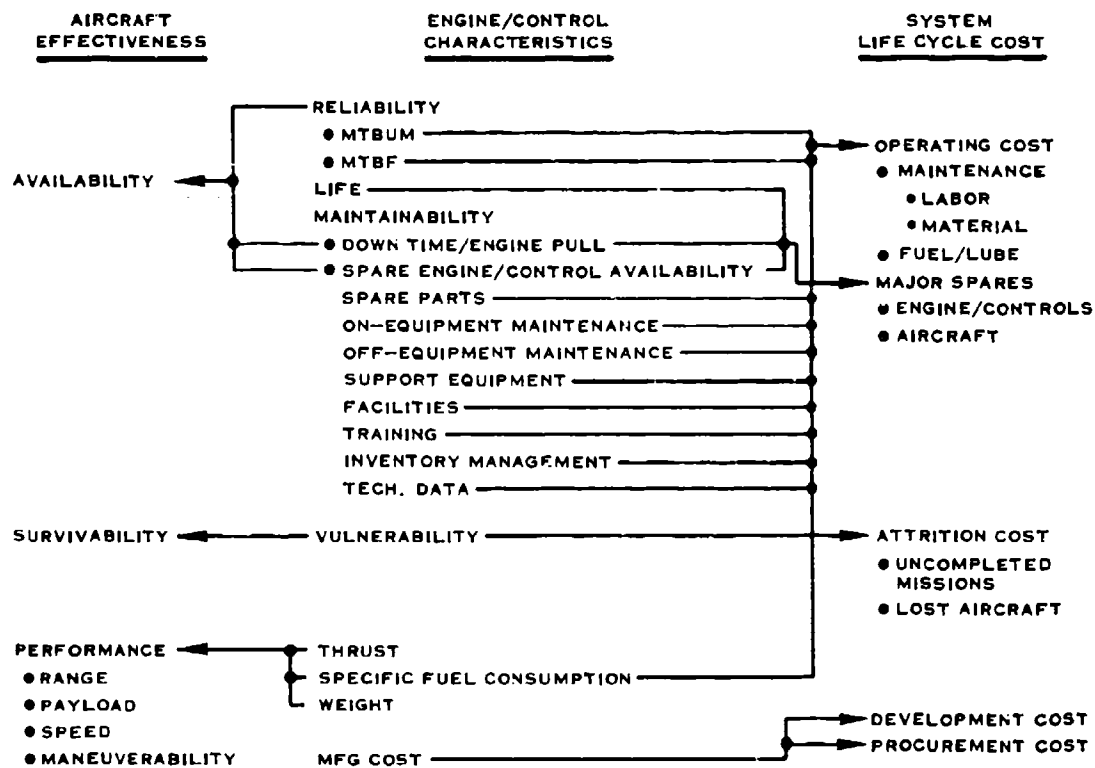
- a) Nonredundant (Simplex)
- b) Duplex control
- c) RAEEC Control - Primarily Duplex with selected Triplex functions
- d) Triplex control

All these control systems have the design capability to control an advanced variable cycle engine and operate with a "self-trim" mode.

Each control type is evaluated for the cost of eight specific reliability improvements, each representing an incremental increase in reliability from the baseline configuration.

Each control was first configured with baseline technology which was that of the Full Authority Digital Electronic Control (FADEC). The controls were then redesigned utilizing the following eight reliability improvement technologies:

- a) Reduced Voltage CMOS
- b) Improved Thermal Packaging
- c) Improved Vibration Isolation
- d) Improved Component Technology
- e) Reduction of Interconnects
- f) Selected Redundancy



E-2032

FIGURE 101 LIFE CYCLE COST ELEMENTS

- g) Component Screening
- h) Assembly and Test Screening

In addition to the reliability improvement measure, all controls were packaged with a modular construction. This packaging change was implemented with the improved thermal package. This change resulted in a significant difference in maintenance philosophy because 90% of the control maintenance could now be accomplished at the intermediate level. This has been reflected in the repair costs by reducing maintenance man-hours to repair, increasing cost of parts to repair, and reducing overall support equipment costs. This maintenance philosophy was then held constant for the remainder of the reliability improvements.

10.4.3 Major Cost Elements

The LCC of any system is normally divided into three major elements: Research and Development (R&D), Acquisition, and Operations and Support (O&S). R&D costs for the subject program were estimated based on actual R&D costs from the electronic engine control for the JT9-D engine. Additions were made to account for the greater complexity of the basic control due to the greater number of control loops and control functions as well as the effect of redundancy on the R&D costs.

Acquisition costs were estimated from parts and material lists generated for the subject program. Recurring manufacturing costs were augmented by the costs of special tooling and test equipment to build the design described in the report section describing control packaging.

Operating and Support Costs were calculated using the Air Force Logistics Command (AFLC) Logistic Support Cost Model (reference 60). The support model equation elements are listed in Figure 102. This study was directed at only those cost elements affected by the control. These are equations (1, 2, 3, 6, and 7) and are shown in Figures 103 thru 107. Equation 5 for costing support equipment was replaced with a total cost for support equipment supplied by Hamilton Standard. Equations 4, 8, 9, and 10 were deleted from the study.

The terms used in the LSC model equations are defined in Table 36. Values for terms which were held constant in the equations are also defined in this table. The items which were input parameters are defined in Table 37 along with numerical values for these parameters.

The overall electronic control reliability factor, MTBUR, and associated cost were supplied by Hamilton Standard for each control configuration. These inputs, coupled with specific maintenance and support costs were utilized by the Model in Equation 1 (Figure 103) to determine the differences in spare

Equation	Cost Element	Drivers
①	Pipeline Spares	MTBF, Cost, Flt hr
②	On-Equipment Maintenance	MTBF, Flt hr, Labor Rates
③	Off-Equipment Maintenance	MTBF, Flt hr, NRTS, Labor Rates
4	Inventory Management	Deleted - Not Impacted by Study Variables
5	Support Equipment	Replaced With HSD Cost Data
⑥	Personnel Training	MTBF, Flt hr, Repair Time
⑦	Technical Data	MTBF, Flt hr, No. Pages
8	Facilities	
9	Fuel	Deleted-Not Impacted by Variables in this Study
10	Spare Engines	

○ = Equations Used in this Study

FD 178424

FIGURE 102 USAF LOGISTICS SUPPORT COST MODEL

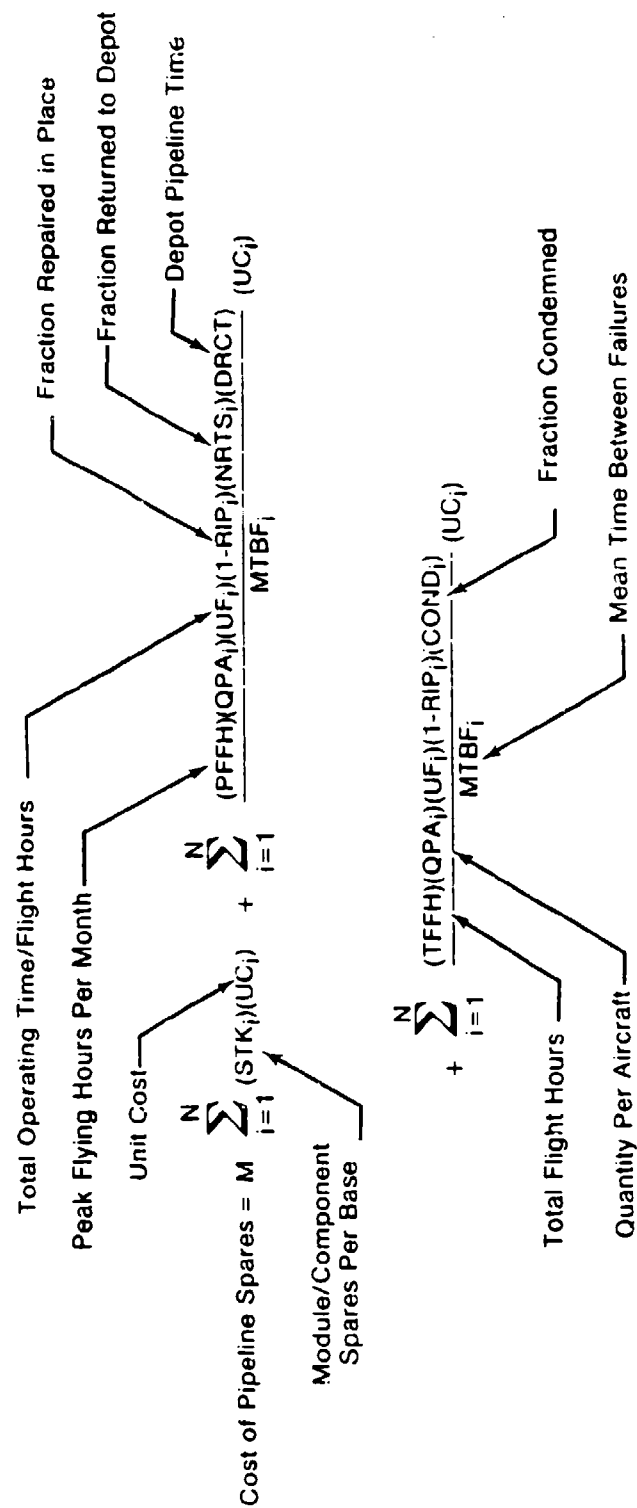
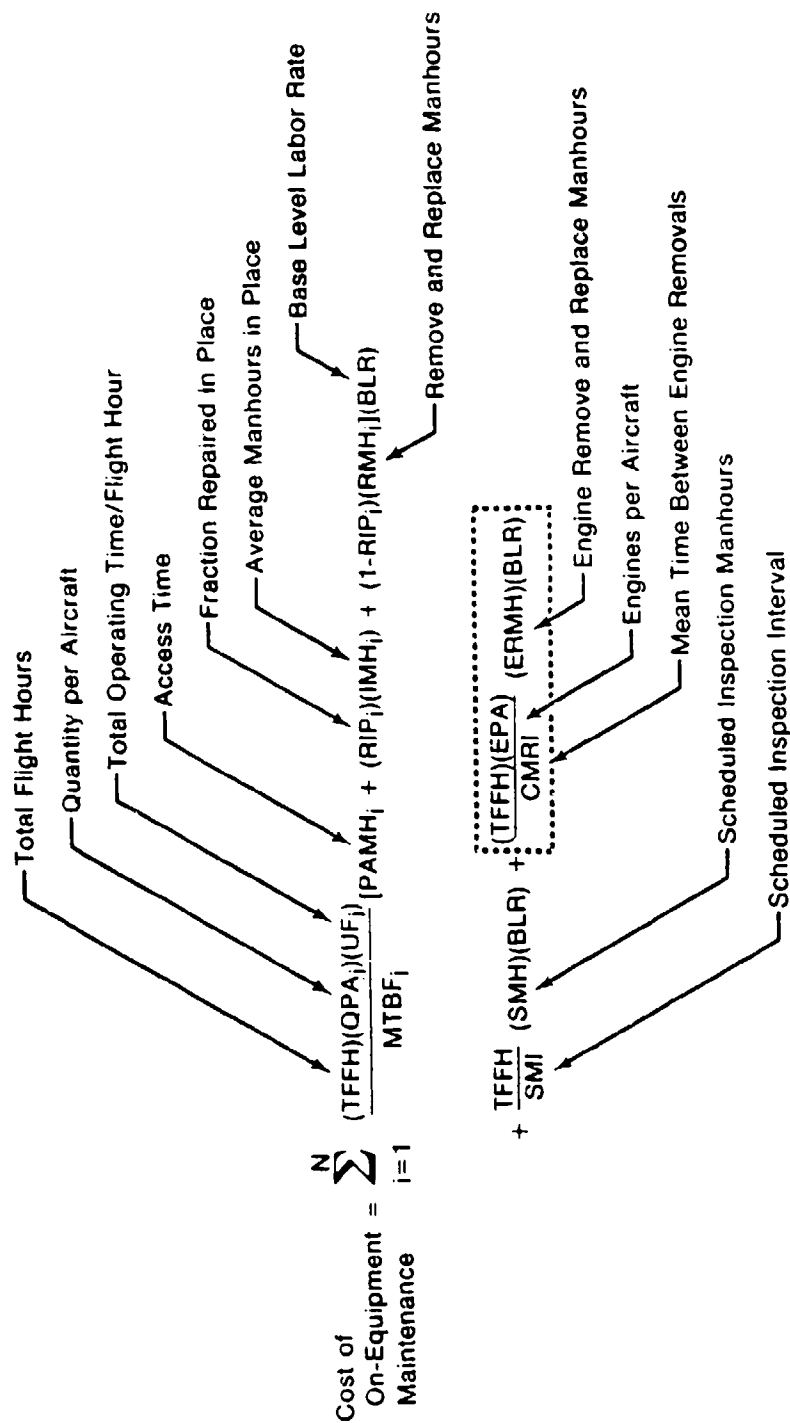


FIGURE 103 EQUATION 1 - PIPELINE SPARES



FD 175331

FIGURE 104 EQUATION 2 - ON-EQUIPMENT MAINTENANCE

$$\begin{aligned} \text{Cost of Off-Equipment Maintenance} &= \sum_{i=1}^N \frac{(\text{TFFH}) (QPA_i) (UF_i) (1 - \text{RIP}_i)}{\text{MTBF}_i} \\ &\quad + \frac{[(\text{BCMHI}_i) (\text{BLR}) + \text{RTS}_i \{(\text{BMH}_i) (\text{BLR} + \text{BMR}) \\ &\quad + (\text{BMC}_i) (UC_i)\} + \text{NRTS}_i \{(\text{DMH}_i) (\text{DLR} + \text{DMR}) + (\text{DMC}_i) (UC_i)\}]}{\text{Depot Labor Rate}} \\ &\quad + \frac{[(\text{BCMHI}_i) (\text{BLR}) + \text{RTS}_i \{(\text{BMH}_i) (\text{BLR} + \text{BMR}) \\ &\quad + (\text{BMC}_i) (UC_i)\} + \text{NRTS}_i \{(\text{DMH}_i) (\text{DLR} + \text{DMR}) + (\text{DMC}_i) (UC_i)\}]}{\text{Depot Consumable Material Rate}} \\ &\quad + \frac{[(\text{BCMHI}_i) (\text{BLR}) + \text{RTS}_i \{(\text{BMH}_i) (\text{BLR} + \text{BMR}) \\ &\quad + (\text{BMC}_i) (UC_i)\} + \text{NRTS}_i \{(\text{DMH}_i) (\text{DLR} + \text{DMR}) + (\text{DMC}_i) (UC_i)\}]}{\text{Average Base Material Cost, Fraction of UC}} \\ &\quad + \frac{[(\text{BCMHI}_i) (\text{BLR}) + \text{RTS}_i \{(\text{BMH}_i) (\text{BLR} + \text{BMR}) \\ &\quad + (\text{BMC}_i) (UC_i)\} + \text{NRTS}_i \{(\text{DMH}_i) (\text{DLR} + \text{DMR}) + (\text{DMC}_i) (UC_i)\}]}{\text{Average Depot MMH}} \\ &\quad + \frac{[(\text{BCMHI}_i) (\text{BLR}) + \text{RTS}_i \{(\text{BMH}_i) (\text{BLR} + \text{BMR}) \\ &\quad + (\text{BMC}_i) (UC_i)\} + \text{NRTS}_i \{(\text{DMH}_i) (\text{DLR} + \text{DMR}) + (\text{DMC}_i) (UC_i)\}]}{\text{Average Intermediate MMH}} \\ &\quad + \frac{[(\text{BCMHI}_i) (\text{BLR}) + \text{RTS}_i \{(\text{BMH}_i) (\text{BLR} + \text{BMR}) \\ &\quad + (\text{BMC}_i) (UC_i)\} + \text{NRTS}_i \{(\text{DMH}_i) (\text{DLR} + \text{DMR}) + (\text{DMC}_i) (UC_i)\}]}{\text{Base Consumable Material Rate}} \\ &\quad + \frac{[(\text{BCMHI}_i) (\text{BLR}) + \text{RTS}_i \{(\text{BMH}_i) (\text{BLR} + \text{BMR}) \\ &\quad + (\text{BMC}_i) (UC_i)\} + \text{NRTS}_i \{(\text{DMH}_i) (\text{DLR} + \text{DMR}) + (\text{DMC}_i) (UC_i)\}]}{\text{Fraction of UC}} \\ &\quad + \frac{[(\text{BCMHI}_i) (\text{BLR}) + \text{RTS}_i \{(\text{BMH}_i) (\text{BLR} + \text{BMR}) \\ &\quad + (\text{BMC}_i) (UC_i)\} + \text{NRTS}_i \{(\text{DMH}_i) (\text{DLR} + \text{DMR}) + (\text{DMC}_i) (UC_i)\}]}{\text{Shipping Weight}} \\ &\quad + \frac{[(\text{BCMHI}_i) (\text{BLR}) + \text{RTS}_i \{(\text{BMH}_i) (\text{BLR} + \text{BMR}) \\ &\quad + (\text{BMC}_i) (UC_i)\} + \text{NRTS}_i \{(\text{DMH}_i) (\text{DLR} + \text{DMR}) + (\text{DMC}_i) (UC_i)\}]}{\text{Shipping Cost, US}} \\ &\quad + \frac{[(\text{BCMHI}_i) (\text{BLR}) + \text{RTS}_i \{(\text{BMH}_i) (\text{BLR} + \text{BMR}) \\ &\quad + (\text{BMC}_i) (UC_i)\} + \text{NRTS}_i \{(\text{DMH}_i) (\text{DLR} + \text{DMR}) + (\text{DMC}_i) (UC_i)\}]}{\text{Fraction Deployed Overseas}} \\ &\quad + \frac{[(\text{BCMHI}_i) (\text{BLR}) + \text{RTS}_i \{(\text{BMH}_i) (\text{BLR} + \text{BMR}) \\ &\quad + (\text{BMC}_i) (UC_i)\} + \text{NRTS}_i \{(\text{DMH}_i) (\text{DLR} + \text{DMR}) + (\text{DMC}_i) (UC_i)\}]}{\text{Fraction of Engine Repaired at Org and Int}} \end{aligned}$$

FIGURE 105 EQUATION 3 - OFF-EQUIPMENT MAINTENANCE

Base Personnel Turnover Rate

$$\text{Cost of Personal Training} = \frac{[1 + \frac{(PIUP-1)(TRB)]TCB}{(PIUP)(FMB)} \left[\sum_{i=1}^N \frac{(TFFH)(QPA_i)(UF_i)}{MTBF_i} \right] + PAMH_i + (RIP_i)(IMH_i)}{\text{Available Mannours/Man/Year, Base Level}}$$

Training Cost, Base

$$+ (1-RIP_i)(RMH_i + BCMH_i + (RTS_i)(BMH_i)) + \frac{TFF_i}{SMI} (SMH_i)$$

Depot Personnel Turnover Rate

$$+ \left[\frac{(TFFH)(EPA)}{CMRI} (ERMH_i) \right]$$

$$+ \frac{[1 + \frac{(PIUP-1)(TRD)] TCD}{(PIUP)(PMD)} \left[\sum_{i=1}^N \frac{(TFFH)(QPA_i)(UF_i)}{MTBF_i} \right] (1-RIP_i)(NRTS_i)(DMH_i)}{\text{Available Mannours/Man/Year, Depot}}$$

Training Cost, Depot

+ TE

FD 175333

FIGURE 106 EQUATION 6 - PERSONNEL TRAINING

$$\begin{aligned} \text{Cost of} \\ \text{Technical Data} = & \sum_{i=1}^N \frac{(TFFH)(QPA_i)(UFI_i)}{MTBF_i} [MRO + (1-RIP_i)(MRF + SR + TR)] BLR \\ & \quad \text{On-Equipment Records Manhours} \quad \text{Off-Equipment Records Manhours} \\ & \quad \text{Supply Records Manhours} \quad \text{Transportation Records Manhours} \\ & + \frac{TFFH}{SMI} [MRO + 0.1(SR + TR)] BLR + TD(JJ + H) \\ & \quad \text{Original Cost Per Page} \quad \text{Pages of Org and Int Manuals} \quad \text{Pages of Depot Manuals} \end{aligned}$$

FD 175324

FIGURE 107 EQUATION 7 – TECHNICAL DATA

TABLE 36 DEFINITION OF TERMS IN LSC MODEL EQUATIONS

<u>Equation</u>	<u>Value</u>	<u>Description</u>
BCMH	Variable	Average man-hours to perform a shop bench check, screening and fault verification on a removed FLU prior to initiating repair action or condemning the item.
BLR	16.25	Base labor rate.
BMC	Variable	Average cost per failure for a FLU repair at base level for stocking and repair of lower level assemblies expressed as a fraction of the FLU unit cost.
BHM	Variable	Average man-hours to perform intermediate-level (base stop) maintenance on a removed FLU, including fault isolation, repair, and verification.
BMR	3.19	Base consumable material consumption rate.
CMRI	400	Combined maintenance removal interval. Average engine operating hours between removals of the whole engine.
COND	0.0	Fraction of removed FLU's expected to result in condemnation at base level.
DLR	26.00	Depot labor rate.
DMC	Variable	Same as BMH except refers to depot repair actions
DMH	Variable	Same as BMR except refers to depot-level maintenance.
DMR	5.19	Same as BMR except refers to depot-level maintenance.
DRCT	1.48	Weighted average depot repair cycle time in months.
EOH	0.0	Average cost per overhaul of the complete engine at the depot expressed as a fraction of the engine unit cost.
EPA	2.0	Number of engines per aircraft.
ERMH	0.0	Average man-hours to remove and replace a whole engine including engine trim and run-up time.

TABLE 36 DEFINITION OF TERMS IN LSC MODEL EQUATIONS (Continued)

<u>Equation</u>	<u>Value</u>	<u>Description</u>
ERTS	0.8	Return rate for engines; fraction of removed whole engines which are returned to service by base maintenance.
EUC	0.0	Expected unit cost of a whole engine.
IMH	0.0	Average man-hours to perform corrective maintenance of the FLU in place or on-line without removal, including fault isolation, repair, and verification.
M	7.0	Number of intermediate repair locations (operating bases).
MTBF	Variable	Mean time between failures in operating hours of the FLU in the operational environment.
N	1.0	Number of different FLU's within the system.
NRTS	0.1 or 0.9	Fraction of removed FLU's expected to be returned to the depot for repair.
OS	0.0	Fraction of total force deployed to overseas locations.
PAHM	1.0	Average man-hours expended in place on the installed system for preparation and access for the FLU.
PFFH	27,000	Peak force flying hours - expected fleet flying hours for one month during the peak usage period.
PSC	0.59	Average packing and shipping cost to CONUS locations.
PSO	1.22	Average packing and shipping cost to overseas locations.
QPA	1.0	Quantity per application.
RIP	0.0	Fraction of FLU failures which can be repaired in place or on-line without removal.
RMH	7.0	Average man-hours to fault isolate, remove, and replace the FLU on the installed system and verify restoration of the system to operational status.

TABLE 36 DEFINITION OF TERMS IN LSC MODEL EQUATIONS (Continued)

<u>Equation</u>	<u>Value</u>	<u>Description</u>
RTS	0.0	Fraction of removed FLU's expected to be repaired at base level.
SMH	12.0	Average man-hours to perform scheduled periodic or phased inspections on the system.
SMI	300.0	Flying hour interval between scheduled periodic or phased inspections on the system.
STK	0.0	Required for each base to fill the base repair pipeline, including a safety stock to protect against random fluctuations in demand.
TFFH	4,860,000	Expected total force flying hours over the program inventory usage period.
UC	Variable	Expected unit cost of the FLU at the time of initial provisioning.
UF	1.5	Ratio of operating hours to flying hours for the FLU (Use Factor).
W	Variable	FLU unit weight in pounds.

TABLE 37 WEAPON SYSTEM INPUT PARAMETERS

<u>Term</u>	<u>Value</u>	<u>Description</u>
EBO	0.10	Standard established for expected back orders - the expected number of unfilled demands existing at the lowest echelon (bases) at any point in time.
IMC	46.60	Initial management cost to introduce a new line item of supply (assembly or piece part) into the Air Force inventory.
M	7.00	Number of intermediate repair locations (operating bases).
MRF	0.24	Average man-hours per failure to complete off-equipment maintenance records.
MRO	0.08	Average man-hours per failure to complete on-equipment maintenance records.
NSYS	1.00	Number of systems within the weapon system.
OS	0.0	Fraction of total force deployed to overseas locations.
OST	0.394	Weighted average Order and Shipping Time in months. The elapsed time between the initiation of a request for a serviceable item and its receipt by the requesting activity.
PFFH	27,000	Peak Force Flying Hours - expected fleet flying hours for one month during the peak usage period.
PIUP	15 yrs	Operational service life of the weapon system in years. (Program Inventory Usage Period).
PMB	1704	Direct productive man-hours per man per year at base level (includes "touch time", transportation time, and setup time).
PMD	1788	Direct productive man-hours per man per year at the depot (includes "touch time", transportation time, and setup time).
PSC	0.59	Average packing and shipping cost to CONUS locations.
PSO	1.22	Average packing and shipping cost to overseas locations.

TABLE 37 WEAPON SYSTEM INPUT PARAMETERS (Continued)

<u>Term</u>	<u>Value</u>	<u>Description</u>
RMC	104.20	Recurring management cost to maintain a line item of supply (assembly or piece part) in the wholesale inventory system.
SA	36.59	Annual base supply line item inventory management cost.
SR	0.25	Average man-hours per failure to complete supply transaction records.
TD	220.00	Average cost per original page of technical documentation. The average acquisition cost of one page of the reproducible source document.
TFFH	4,860,000	Expected Total Force Flying Hours over the Program Inventory Usage Period.
TR	0.16	Average man-hours per failure to complete transportation transaction forms.
TRB	0.129	Annual turnover rate for base personnel.
TRD	0.10	Annual turnover rate for depot personnel.
ARBUT	0.30	Engine Automatic Resupply and Buildup Time in months.
BP	0.20	Base engine repair cycle time in months.
CMRL	400.0	Combined Maintenance Removal Interval. Average engine operating hours between removals of the whole engine.
CONF	0.90	Confidence factor reflecting the probability of satisfying a random demand for a whole engine from serviceable stock to replace a removed engine.
DP	2.9	Depot engine repair cycle time in months.
FC	0.45	Fuel cost per unit.
FR	0.0	Fuel consumption rate of one engine in units per flying hour.

TABLE 37 WEAPON SYSTEM INPUT PARAMETERS (Continued)

<u>Term</u>	<u>Value</u>	<u>Description</u>
LS	15.0	Number of stockage locations for spare engines.
BCA	0.0	Total cost of additional items of common base shop support equipment per base required for the system.
BAA	168.0	Available work time per man in the base shop in man-hours per month.
BLR	16.25	Base labor rate.
BMR	3.19	Base consumable material consumption rate. Includes minor items of supply (nuts, washers, rags, cleaning fluid, etc.) which are consumed during repair of items.
BPA	0.0	Total cost of peculiar base shop support equipment per base required for the system which is not directly related to repair of specific FLU's or when the quantity required is independent of the anticipated work load (such as overhead cranes and shop fixtures).
BRCT	0.33	Average Base Repair Cycle Time in months. The elapsed time for a RTS item from removal of the failed item until it is returned to base serviceable stock (less time awaiting parts).
CS	1.0	Cost of software to utilize existing Automatic Test Equipment for the system.
DCA	0.0	Total cost of additional items of common depot support equipment required for the system.
DAA	168.0	Available work time per man at the depot in man-hours per month.
DLR	26.0	Depot labor rate.
DMR	5.19	Same as BMR except refers to depot-level maintenance.
DPA	0.0	Same as BPA except relates to depot support equipment.

TABLE 37 WRAPON SYSTEM INPUT PARAMETERS (Continued)

<u>Term</u>	<u>Value</u>	<u>Description</u>
DRCT	1.48	Weighted average Depot Repair Cycle Time in months. The elapsed time for a NRTS item from removal of the failed item until it is returned to depot serviceable stock. This includes the time required for base-to-depot transportation and handling and the shop flow time within the specialized repair activity required to repair the item.
FB	0.0	Total cost of new base facilities (including utilities) to be constructed for operation and maintenance of the system, in dollars per base.
FD	0.0	Total cost of new depot facilities (including utilities) to be constructed for maintenance of the system.
FLA	0.0	Total cost of peculiar flight-line support equipment and additional items of common flight-line support equipment per base required for the system.
H	4150	Number of pages of depot-level technical orders and special repair instructions required to maintain the system.
IH	0.0	Cost of interconnecting hardware to utilize existing Automatic Test Equipment for the system.
JJ	1700	Number of pages of organizational and intermediate level technical orders required to maintain the system.
N	1.0	Number of different FLU's within the system.
SMH	12.0	Average man-hours to perform a scheduled periodic or phased inspection on the system.
SMI	300.0	Flying hour interval between scheduled periodic or phased inspection on the system.
SYSNOUN		Name of the system - up to 60 alphanumeric characters.

TABLE 37 WEAPON SYSTEM INPUT PARAMETERS (Continued)

<u>Term</u>	<u>Value</u>	<u>Description</u>
TCB	9500	Cost of peculiar training per man at base level including instruction and training materials.
TCD	7000	Cost of peculiar training per man at the depot including instruction and training materials.
TE	240,000	Cost of peculiar training equipment required for the system.
XSYS	2300	System identification. The assigned five-character alphanumeric Work Unit Code of the system.

control requirements resulting from the changes in MTBUR. The model determines the base and depot facility pipeline spares supply required to ensure with 90% confidence that no out-of-stock situation will occur. The operating and support cost equations 2, 3, 6 and 7 from the LSC model were then used to calculate the remaining O&S costs.

10.5 Results

The total life cycle cost for each control configuration is plotted against controller maintenance reliability (mean time between unscheduled removals).

Figure 108 is related to only one portion of the reliability study, namely, maintenance reliability. Maintenance reliability is the characteristic for which a formal goal was established in the subject RAEEC program. However, another very important reliability characteristic is mission reliability. The importance of mission reliability has been recognized but credible cost data could not be assembled within the time and money framework of the subject program.

The results shown in Figure 108 relating to the maintenance reliability portion of the cost of ownership story are indications of the trends associated with various redundancy levels. The tendency to select the lowest cost "Simplex" controller configuration must be tempered with the mission reliability and flight safety requirements of a real-life aircraft application. A "simplex" control with its inherent lack of fault tolerance cannot approach levels of reliability desired for mission and flight safety requirements of a full-authority electronic engine controller. A degree of redundancy will doubtless be required and the cost trades associated with several types of redundancy are indicated in Figure 108.

If very high operational readiness and/or mission reliability levels are found to be necessary the additional cost of achieving the associated higher MTBUR levels appears modest.

As MTBUR is increased in Figure 108 costs diminish rapidly for the RAEEC and duplex systems to a minimum at about the 5000 hour point, followed by rising costs as MTBUR increase to the 10,000 to 30,000 hour level. The sharp drop in cost as MTBUR increases to 5000 hours is due to a reduction in Operation and Support Cost. Further reduction in Operation and Support cost coupled with increases in acquisition cost are present as MTBUR increases beyond 5000 hours. This consideration is responsible for the slow increase in life cycle cost beyond 5000 hours.

A comparison of the life cycle costs for duplex and duplex/triplex RAEEC (selected triple redundancy) shows a comparable level of life cycle cost for each at values of MTBUR below 4000 hours. This is made possible by the cost effective selection of parts to be triplicated. The added level of redundancy in selected locations of the RAEEC control makes voting possible with resulting improved coverage and opportunities for more effective fault detection resulting in higher reliability and lower operating and support costs while achieving levels of maintenance and mission reliability not possible with a duplex system.

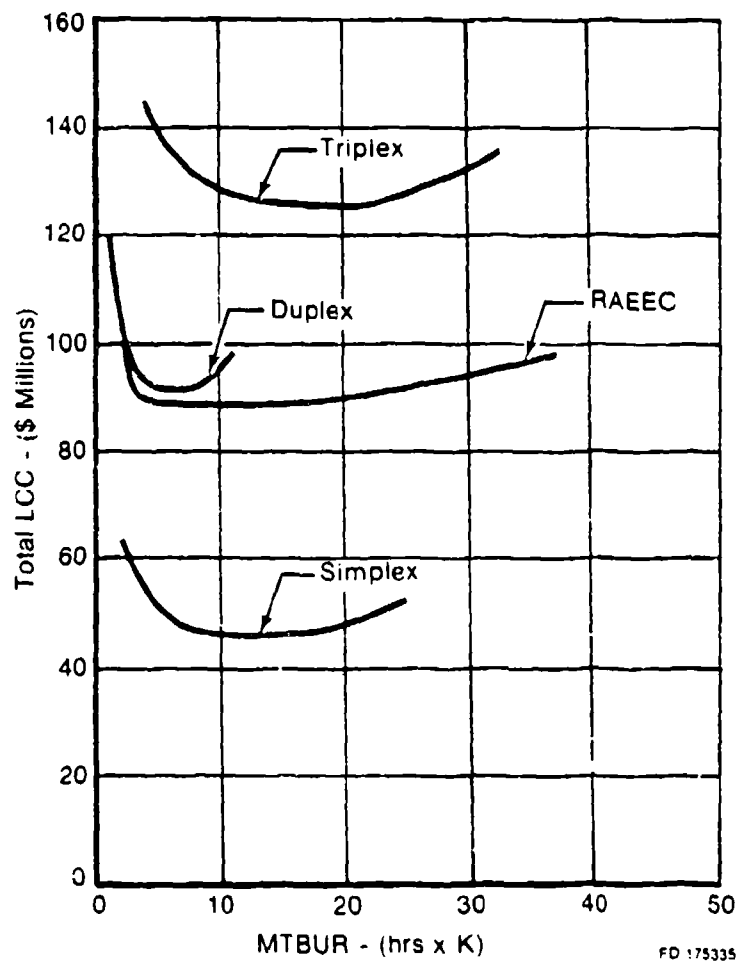


FIGURE 108 ELECTRONIC ENGINE CONTROLLER COST COMPARISON

The four curves of Figure 108 labeled Simplex, Duplex, RAECC and Triplex are different in life cycle cost by a substantial amount. This is due primarily to large differences in redundancy being reflected in substantial differences in acquisition cost.

It should be noted in Figure 108 that the Duplex curve increased in overall LCC at a steep rate after approximately 8000 hours. This was caused by the fact that the "fly with faults" philosophy was not introduced for the Duplex system, but was introduced for the triplex channels of the RAECC and Triplex systems. Figure 144 also shows that adding redundancy can extend the MTBUR to extremely high numbers but at a significant increase in overall LCC.

10.6 Conclusion

The Cost-of-Ownership study was conducted for the Reliability Advancement Study for Electronic Engine Controllers. The objective was to evaluate the overall effect on cost of ownership of significantly increased electronic controller reliability. This was accomplished by defining eight reliability improvement measures and their associated acquisition cost and maintenance data. These acquisition costs and maintenance data were then input to the Air Force Logistics Command Logistics Support Model to evaluate the LCC. The results were tabulated and the following conclusions were made:

- a) Increasing electronic controller reliability does decrease the cost-of-ownership of the controller by decreasing operating and support costs up to a given point. At this point the effect on operating and support cost diminishes and is offset by increasing acquisition cost, which causes an increase in total LCC.
- b) The addition of redundancy results in a significant increase in controller life cycle cost. The increase to acquisition cost caused by duplicating and triplicating the control parts overrides the payback from reducing O&S costs with the increased MTBUR. It should be noted, however that there were no cost savings considered for the improved mission reliability which would result from the redundancy.
- c) Incorporation of the modular design concept produced a large improvement in LCC. This can be attributed to allowing the maintenance to be moved to the intermediate level from the depot level, thus reducing the number of spare controls required for the pipeline and reducing the cost to repair the units.

SECTION XI DEVELOPMENT GUIDE

Based on the material presented in this "Final Report", a "Guide for Development of High Reliability Electronic Engine Controllers", AFWAL-TR-80-2063, Vol II, has been prepared. This is a comprehensive document which specifies procedures, practices, concepts, measures, testing, quantitative measures of λ , etc., for use by any future developer of said controllers. Emphasis has been placed on areas essential to the achievement of very high reliability goals.

SECTION XII CONCLUSIONS

The projected use of electronic technology in the full authority control systems of future high performance aircraft engines has required the subject investigation of means to improve the reliability potential of electronic engine controllers such that at maturity no reliability penalty need attend their use on military aircraft engines. In order that the reliability of electronic controllers approach the reliability level of mature hydromechanical controls, a variety of reliability improvements have been investigated in this study. It is significant that the selected reliability improvements do indeed show the potential to meet and even exceed the 25,000 hour MTBF goal for a mature control. And further that substantial reliability improvements can be achieved with reasonably cost-effective changes in the design/manufacturing process.

Specific conclusions are:

- No single reliability improvement measure will result in a highly reliable controller. The best reliability improvement measure examined resulted in a reliability improvement of 2.6.
- A family of reliability improvement measures, employing design procurement and manufacturing disciplines can result in a full-authority EEC with a maintenance reliability many times greater than the overhaul period of the engine it controls. The RAECC control studied showed a reliability improvement of 28. As it improved from a MTBUR of 1320 hours to 37,000 hours.
- Redundancy is one of the most effective and one of the most expensive ways to increase reliability. Therefore, redundancy should only be used to achieve the exceptional levels required by high mission reliability. RAECC with duplex/triple redundancy achieved a mission failure likelihood of 2×10^{-7} .
- Mission reliability is not likely to be justified on a cost basis and must be required by factors such as human life and strategic value of mission completion. Weapon system requirements must realistically balance maintenance and mission reliability.
- Reductions in maintenance cost diminish to small levels when maintenance reliability exceeds 10,000 - 15,000 hours MTBF.
- Accelerated stress screening of components is the only economic method of removing the premature component failures from semiconductor lots when history shows a lot to lot variation of 3-5 to 1 in acceptable units.
- Reliability growth modeling methodologies described by Dr. L.R. Crow and others can be correlated directly with CERT reliability development testing.

- Optimum engine controller reliability can only be achieved using several different component technologies; e.g., bi-polar, N-MOS etc.
- Semiconductor voltage derating is one of the most cost-effective reliability improvements. Voltage reductions of 3:1 produced a 6:1 improvement for CMOS components.
- Package design should emphasize small repetitive blocks which lend themselves to automated/semiautomated manufacture.
- Package design improvements to minimize the flow of failed units to the repair depot can cause a 2:1 reduction in handling and spares cost in the repair pipeline.
- Interconnect systems must force the bulk of the connections into the most environment-tolerant and controlled-process form; e.g., connections within highly complex semiconductors and within leadless chip carriers and hybrids. Reductions of 2:1 in the less reliable connections were possible in RAEEC.

SECTION XIII RECOMMENDATIONS

During the course of the study, new materials and methods of controller construction, and new methods of cost-effective screening at the subassembly level were discussed. Only limited experience exists in the application of these construction and screening techniques to electronic engine controllers. In addition, lightning protection is an extremely vital issue in the construction of reliable full authority electronic controllers. 99% assurance of lightning protection based on paper design without the 100% certainty of testing appears inadequate. Therefore, several recommendations are presented for consideration:

- Construct and test several typical ceramic/metal fuel cooled modules to mature and optimize the assembly and repair techniques.
- Further investigate the potential for accelerated stress testing at the subassembly level. Build, test, and evaluate some simple test pieces.
- Design, build and evaluate a simple dedicated power system which can be made redundant at low cost.
- Design, build and test a lightning protection system for a full-authority electronic control.

APPENDIX A
ELECTRICAL DESIGN: BASELINE
and TRADE STUDIES

A.1 Introduction

This appendix presents an extensive description of the baseline RAEEC design and related trade studies on fourteen major circuit partitions. The final RAEEC design is based upon the results of these trades.

A.2 Baseline Design

A.2.1 Baseline/FADEC Relationship

This portion of the report provides a detailed description of the RAEEC baseline system, which is actually a modified Full Authority Digital Electronic Control (FADEC). The baseline RAEEC modifications to FADEC are:

1. Addition of a redundant A/D in primary.
2. Addition of a redundant R/D in secondary
3. Addition of a "Link Alive" dual-port communications processor
4. Addition of redundant torque motor drivers
5. Addition of redundant solenoid drivers.
6. Addition of a redundant low level DC interface in the primary.

The FADEC hardware, on which this baseline is made, successfully demonstrated dual-channel full-authority electronic control capability in the high altitude test chamber at the NASA LEWIS Cleveland test facility on a Pratt & Whitney F401 Navy engine. The FADEC electronic unit provided all of the sensor signal conditioning, computation, and output signal processing functions necessary for controlling the variable turbine engine. The control unit was organized into primary and secondary sections, shown in Figure A-1 each with its own digital processor, memory, and complement of input and output signal conditioning circuitry. Both the primary and secondary sections are capable of operating the engine from start up to intermediate power. The primary also incorporates circuitry necessary for controlling augmentation control functions. Each section includes power regulation circuitry supplied by separate primary and secondary windings in the alternator. The primary electronic unit houses three vibrating cylinder type pressure transducers P_2 , P_{13} and ΔP_{13} for the Advanced Technology Demonstration Engine (ATDE). The secondary unit for ATDE, provide highly accurate measurement with a digitally compatible frequency output signal. Three pressure transducers feed into each digital processor, and are organized such that parameter synthesization provides for continued safe operation of the engine should one processor and/or power supply malfunction.

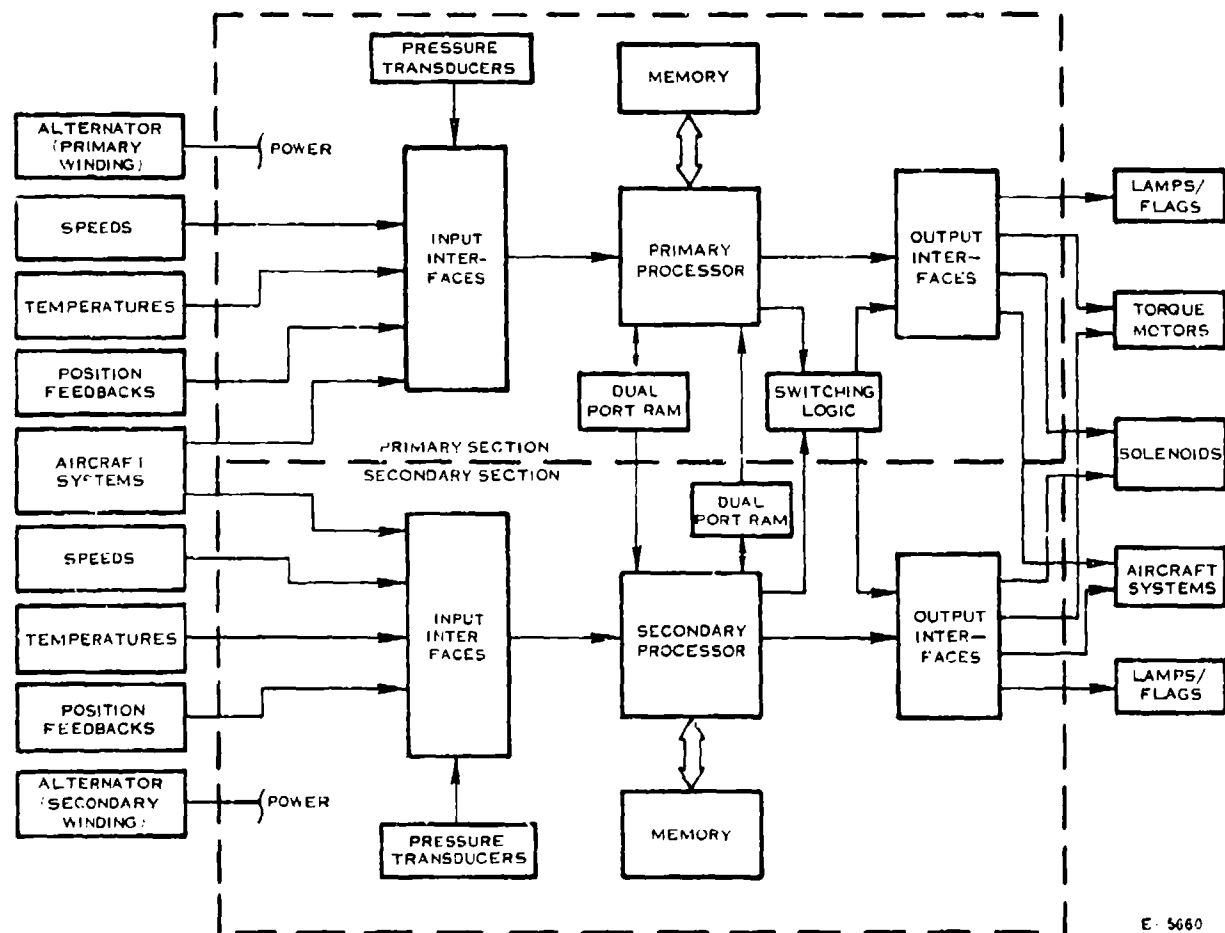


FIGURE A-1 FADEC ELECTRONIC UNIT ORGANIZATION

Serial digital communication between the primary and secondary processors is provided using a dual port RAM arrangement. The electronic unit incorporates comprehensive built-in test software and hardware features to identify malfunctions both within itself and other system components for facilitating maintenance and for implementing redundancy management.

A.2.2 Analog-to-Digital Converter

The "multiple-ramp" analog-to-digital converter used in the RAEEC baseline, converts multiplexed high-level (0 to +10 V) DC signals to a 12-bit binary number with a typical accuracy of 11 bits, and with a maximum conversion time of 1.536 milliseconds.

The A/D control logic and data registers are contained in three custom CMOS LSI devices, which also contain registers and control logic for two frequency to digital converters, and one serial data link. Furthermore, the analog portion of the A/D comprises an integrator with four multiplexed inputs, a zero comparator, and a least significant bit comparator. (Figure A-2.)

In order to understand some of the advantages of a "multi-ramp" converter, the following theory of operation is presented.

At the beginning of the conversion cycle, the integrator is shorted by switch S4 (Figure A-3). Thus, the output of the integrator at t_0 is

$$V_0(t_0) = 0$$

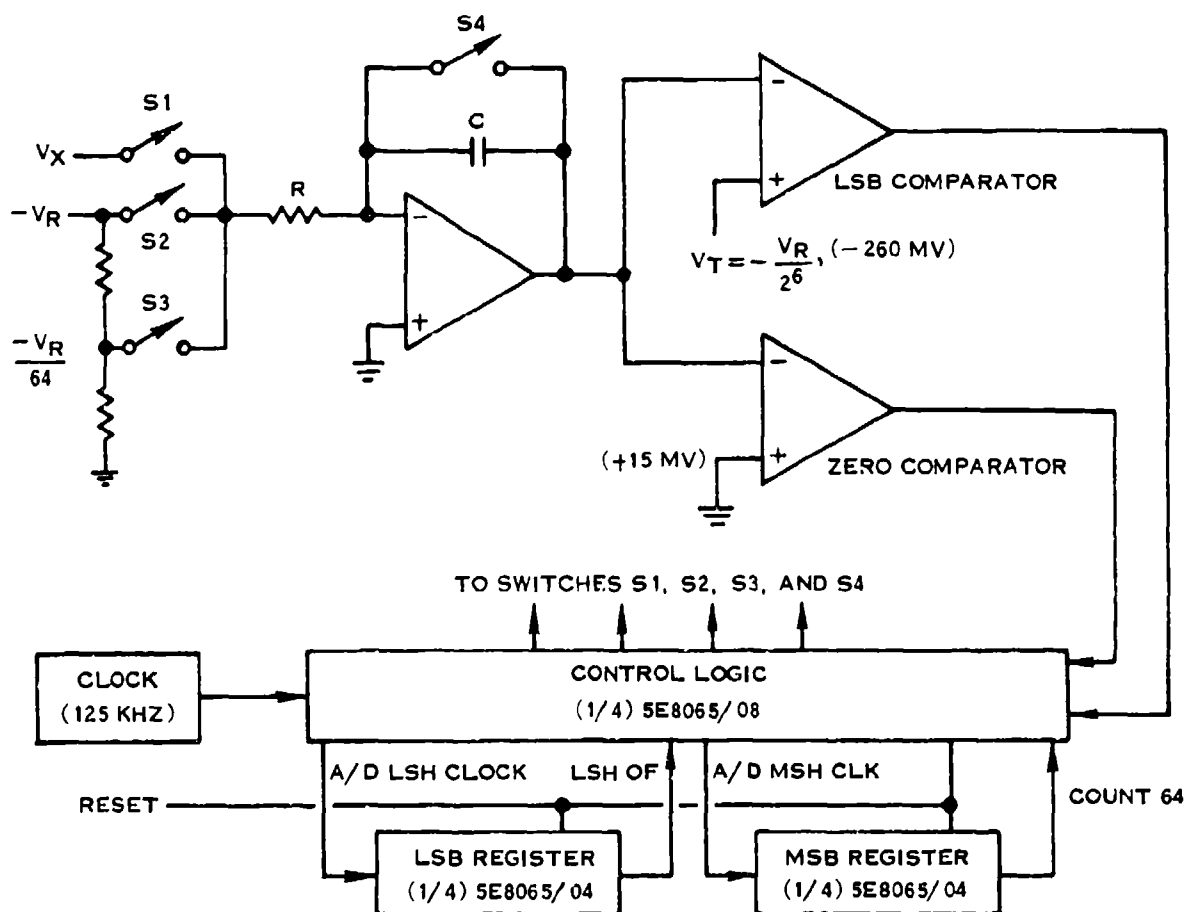
At t_0 , S4 is turned off and S1 is turned on and the input signal to be measured (V_X) is integrated for a fixed time interval, $t_1 - t_0$ (ramp 1). The output voltage of the integrator at t_1 is,

$$V_0(t_1) = - \frac{V_X}{RC} (t_1 - t_0)$$

The time interval $t_1 - t_0$ is equal to

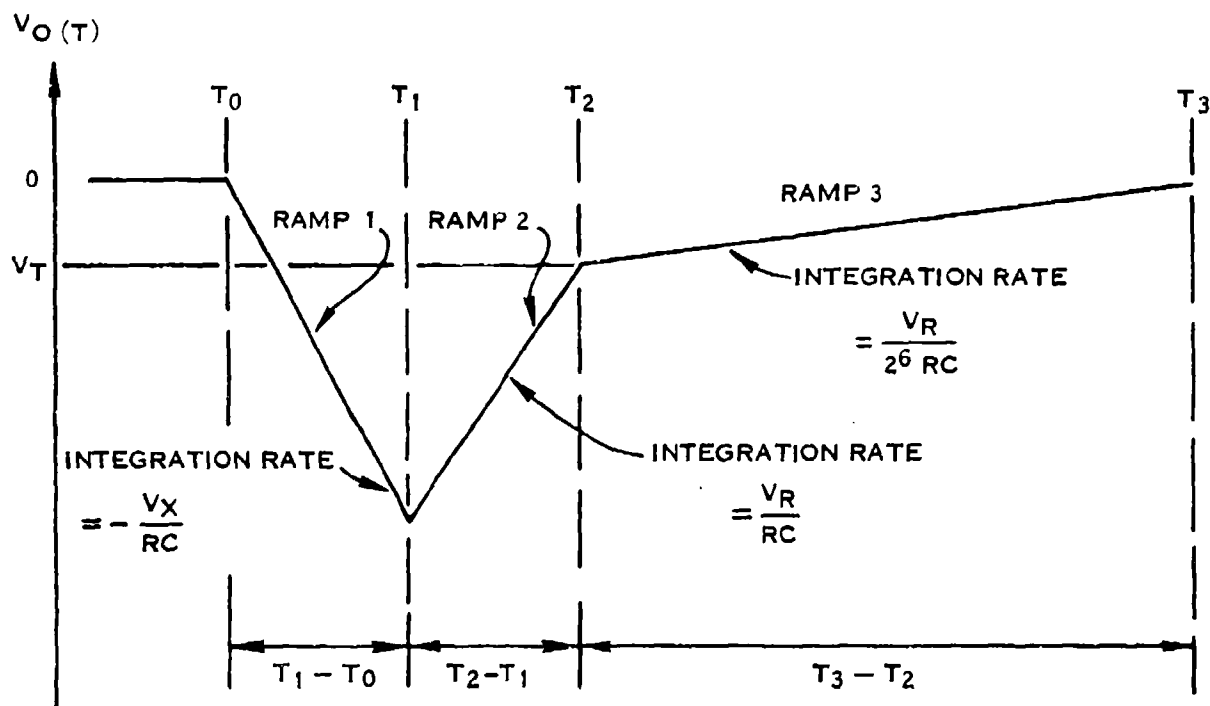
$$(t_1 - t_0) = 2^6/f_c$$

where f_c is the clock frequency.



E-5658

FIGURE A-2 BLOCK DIAGRAM MULTIPLE RAMP CONVERTER



E-5659

FIGURE A-3 IDEAL MULTIPLE RAMP TIMING DIAGRAM

At t_1 , S1 is turned "off" and ramp 2 is turned on by S2. The reference voltage V_R , is then integrated until the first clock pulse after the LSB comparator is tripped. The bias voltage, V_t , is slightly less than $-V_R/2^6$ which ensures the LSB register will accumulate a full count if the LSB comparator is tripped simultaneously with a clock edge.

The output voltage at the end of ramp 2 at T_2 is,

$$V_0(t_2) = \frac{-V_X}{RC}(t_1 - t_0) + \frac{V_R}{RC}(t_2 - t_1)$$

During ramp 2, the MSB register is accumulating clock pulses. Thus, the number of counts accumulated in the MSB register, N_2 , is

$$N_2 = 2^6(t_2 - t_1)fc$$

Notice, because the clock pulses are clocked into the MSB register, each clock pulse is weighted by a factor of 2^6 . The time interval of ramp 2 is

$$(t_2 - t_1) = \frac{N_2}{2^6fc}$$

At t_2 , S2 is turned off and ramp 3 is turned on by switch S3. The reference voltage $V_R/2^6$ is integrated until zero comparator is tripped. The output voltage of ramp 3 at t_3 is,

$$V_0(t_3) = \frac{-V_X}{RC}(t_1 - t_0) + \frac{V_R}{RC}(t_2 - t_1) + \frac{V_R}{2^6RC}(t_3 - t_2) \quad (18)$$

During ramp 3, the LSB register is accumulating clock pulses. Thus, the number of counts accumulated in LSB register (N_1) during ramp 3 is

$$N_1 = (t_3 - t_2)fc$$

If there are any counts in excess of 2^6-1 the LSB register will overflow into MSB register. The time interval of ramp 3 is

$$(t_3 - t_2) = \frac{N_1}{fc}$$

The zero comparator detects when the integrator crosses zero volts, thus, $V_0(t_3)$ is equal to zero volts. Therefore, $V_0(t_0) = V_0(t_3) = 0$ and can be reduced to,

$$\frac{V_X}{RC} (t_1 - t_0) = \frac{V_R}{RC} (t_2 - t_1) + \frac{V_R}{2^6 RC} (t_3 - t_2)$$

Substituting for equations

$$\frac{V_X 2^6}{RC f_c} = \frac{V_R N_2}{RC 2^6 f_c} + \frac{V_R N_1}{2^6 RC f_c}$$

cancellation of common terms,

$$V_X 2^6 = \frac{V_R N_2}{2^6} + \frac{V_R N_1}{2^6} = \frac{V_R}{2^6} N$$

where N is the total number of counts in the register.

N is equal to,

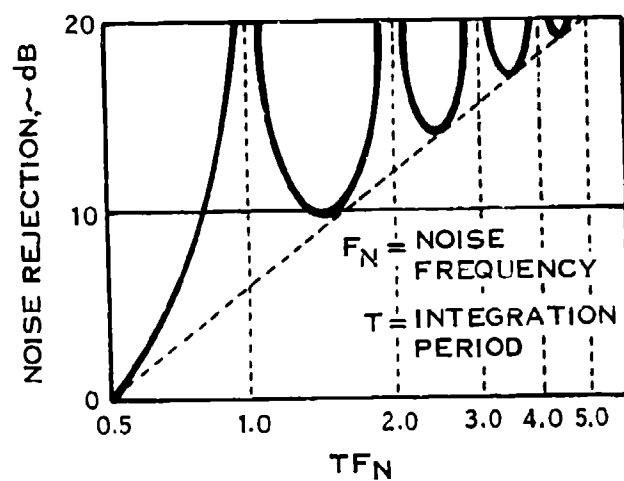
$$N = \frac{V_X}{V_R} 2^{12}$$

This is the basic equation of any multiple ramp converter. The number of counts in the register is simply a ratio of the input voltage to the reference voltage. Because of this, the accuracy is directly proportional to the reference voltage. The frequency of the converter and the gain of the integrator have no effect on the output, and thus, have no effect on error. Moreover, if the input signal (V_X) is ratioed with the referenced voltage V_R , ideally there will be no converter error.

The following lists the advantages and disadvantages of a multiple Ramp A/D Converter.

ADVANTAGES:

1. Input signal is precisely averaged over ramp 1 time.
2. No sample/holds - another source of error/jeopardy.
3. A/D method with inherent filtering, Figure A-4, which is totally compatible with input multiplexing techniques.
4. Inherently monotonic due to integration and counting technique.



E-5683

FIGURE A-4 A/D FILTERING CHARACTERISTICS

DISADVANTAGE:

Slower conversion speed than the successive approximation converter (1.536 ms vs. 12 μ s). However, even though there are other converters which have shorter conversion times, a faster converter isn't required for the application, since all critical DC inputs are converted during each control cycle.

A.2.3 Resolver to Digital Converter

The baseline 11-bit resolver to digital converter comprises a pair of voltage followers, an R-C bridge, phase shift to pulse width comparators and logic, and a custom LSI counter and bus driver (Figure A-5). The two, in phase, amplitude varying AC voltages from the output of the resolver mux (described in Section A.2.9) carry resolver position (θ) information in the form of $\sin \theta$ and $\cos \theta$ which are converted in an R-C bridge to two constant amplitude, phase shifted voltages, whose phase difference in electrical degrees is equal to $2\theta - 90^\circ$. (Note that there is an electrical gain of two.) The two phase shifted voltages each drive their own zero-comparator whose output drives an equivalent dual-clocked flip-flop circuit, providing a logic-level pulse width proportional to twice the resolver mechanical angle. This single pulse width in turn, enables the 4.0 MHz precision clock into two 8-bit registers. These registers are contained in two custom CMOS LSI chips (which also contain the data registers for three additional converters) which can be addressed directly onto the data bus by the CPU.

The bridge is trimmed such that the impedance R_B exactly equals that of the C_B at the excitation frequency of 1953.125 Hz, and the same holds true for R_A and C_A . Since these components are matched, and with the excitation frequency shift less than 50 ppm, the following identities hold true:

The voltage V_1 solved for using node equations is;

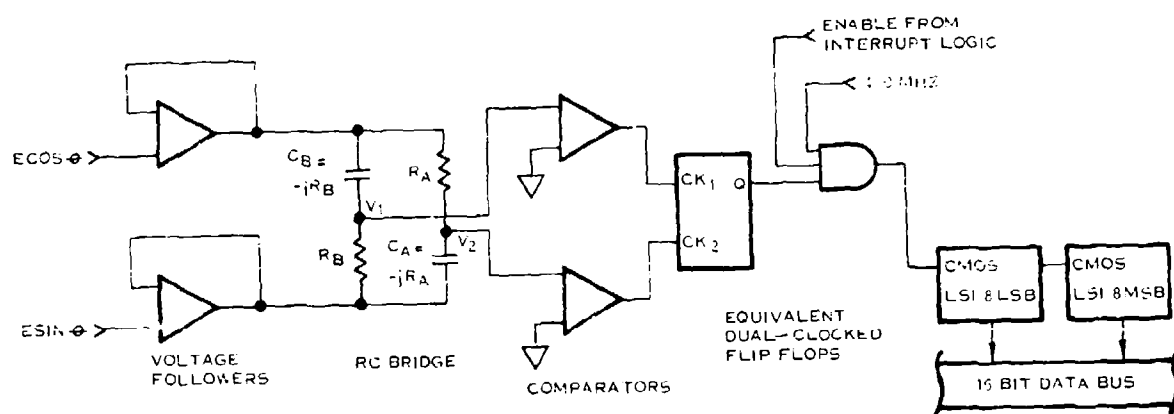
$$\frac{V_1 - E \cos \theta}{-j R_B} + \frac{V_1 - E \sin \theta}{R_B} = 0$$

$$R_B (V_1 - E \cos \theta) = j R_B (V_1 - E \sin \theta)$$

$$V_1 (1 - j) = E \cos \theta - j E \sin \theta$$

$$V_1 = \frac{E (\cos \theta - j \sin \theta)}{1 - j} = \frac{E \angle -\theta}{\sqrt{2} \angle -45^\circ}$$

$$V_1 = \frac{1}{\sqrt{2}} E \angle 45^\circ - \theta$$



E - 5964

317 COMP @ 33 WATTS

FIGURE A-5 RESOLVER TO DIGITAL CONVERTER (BASELINE)

Solving for V_2 in a similar manner:

$$\frac{V_2 - E \cos \theta}{R_A} + \frac{V_2 - E \sin \theta}{-j R_A} = 0$$

$$j R_A (V_2 - E \cos \theta) = R_A (V_2 - E \sin \theta)$$

$$V_2 (j - 1) = j E \cos \theta - E \sin \theta$$

$$V_2 = \frac{E (\cos \theta + j \sin \theta)}{1 + j} = \frac{E \angle \theta}{\sqrt{2} \angle 45^\circ}$$

$$V_2 = \frac{1}{\sqrt{2}} E \angle \theta - 45^\circ$$

Solving for ϕ , the phase difference between V_1 and V_2 :

$$\phi = (\theta - 45) - (45 - \theta) = 2\theta - 90^\circ$$

The following lists the advantages and disadvantages of the R-C bridge resolver to digital converter:

ADVANTAGES:

1. All failure modes can be detected (if the total resolver movement is restricted to less than 90 mechanical degrees).
2. Provides a direct conversion of shaft angle; no transport delay delta between "SIN θ " and "COS θ " inputs.
3. With reference angle compensation, this interface is accurate to within 6 minutes.
4. Lends itself to multiplexing techniques.

DISADVANTAGES:

1. Precision R-C bridge required with good stability over temperature.
2. Accurate sine-wave generation required for resolver excitation. Converter is sensitive to odd harmonics.
3. Resolver movement should be restricted to less than 90°.

A.2.4 Resolver Excitation

The Resolver Excitation circuit used in the RAEEC baseline system, provides a precision 7 Vrms, 1.953 KHz sinewave for excitation of the engine fuel control resolvers. Although 400 Hz synchro excitation is available on most aircraft, this configuration for self excitation of fuel control feedback transducers is advantageous for the following reasons:

1. Loss of the 400 Hz bus would cause the engine fuel controls to lose feedback signals, causing engine shutdown.
2. A 400 Hz excitation system causes a long R/D conversion time, since the period of one sample would be 2.5 milliseconds, and a minimum conversion time of twice the excitation period is required for settling and conversion time.

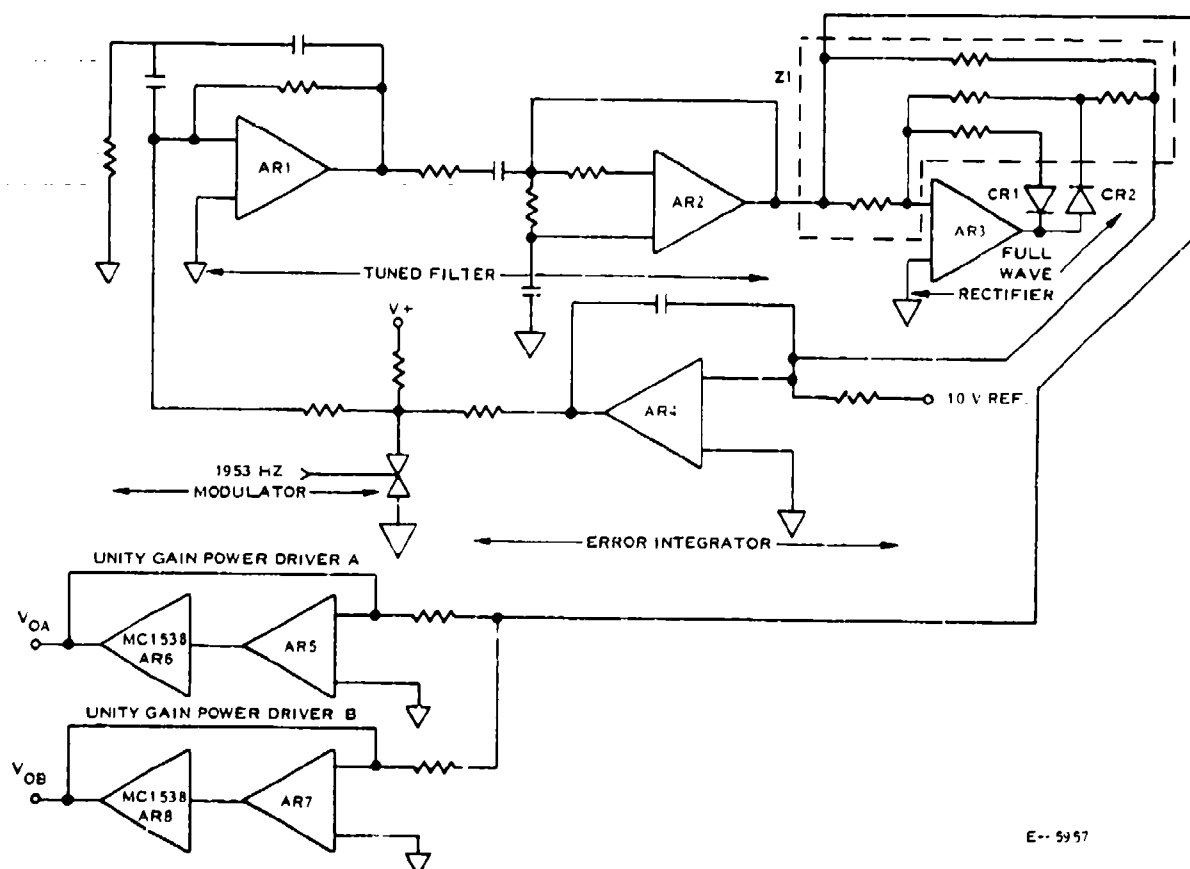
This circuit, as shown in Figure A-6, comprises five different functions which are described briefly as follows:

A.2.4.1 Transmission Gate Modulator This circuit provides an amplitude modulated 1953 Hz squarewave, proportional to the error integrator output, which is fed to the tuned filter.

A.2.4.2 Tuned Filter The first stage of the active tuned filter section is a bandpass filter to attenuate the third harmonic of the square wave and also to block the DC component. The center frequency is at 1.953 KHz, the gain is 0 dbv, and the sensitivity is 10. The second stage is a low pass filter to further attenuate the third harmonic distortion. The center frequency is at 1.953 KHz; zeta is 0.1 resulting in a gain 14 dbv at $f_0 = 1.953 \text{ KHz}$.

A.2.4.3 Rectifier Amplifier AR3 in conjunction with diodes CR1 and CR2 and network Z1 provide a gain of -1 for negative inputs and 0 for positive inputs. The offset error due to the diode is negated by the amplifier. The amplifier output is summed with the filter output through resistors with a 2:1 ratio producing a precise full wave rectified signal.

A.2.4.4 Error Integrator To obtain the error signal necessary to produce a 6.8563 Vrms output, AR4 realizes a summing error integrator. The rectifier output current is summed with the current from the -10 VDC reference. If the currents are not equal, the integrator ramps up or down until they are. The sine wave input does not affect the DC voltage level of the integrator output because the average (or DC) value of the sine wave is zero. It does, however, produce a full-wave rectified current when summed with the half-wave rectifier output.



E-- 5957

FIGURE A-6 RESOLVER EXCITATION (BASELINE)

A.2.4.5 Power Stage A Motorola MC1538R Power Booster is used to obtain the necessary drive current for resolver excitation. The filter output is buffered with a 747 op-amp which supplies the drive for the MC1538R. The feedback loop is unity gain and serves to reduce nonlinearity and crossover distortion of the MC1538R.

The driver outputs are matched to the resolver impedance by a shunt R-C circuit, effecting a purely resistive load to the power booster. This reduces the required output power and subsequent dissipation in the 1538R. Matching, at this writing, is for six resolvers in parallel (per MC1538 driver) and can be adjusted where more resolvers are employed. Individual resolver impedance is $128 + j648$.

A.2.5 Torque Motor D/A's and Driver

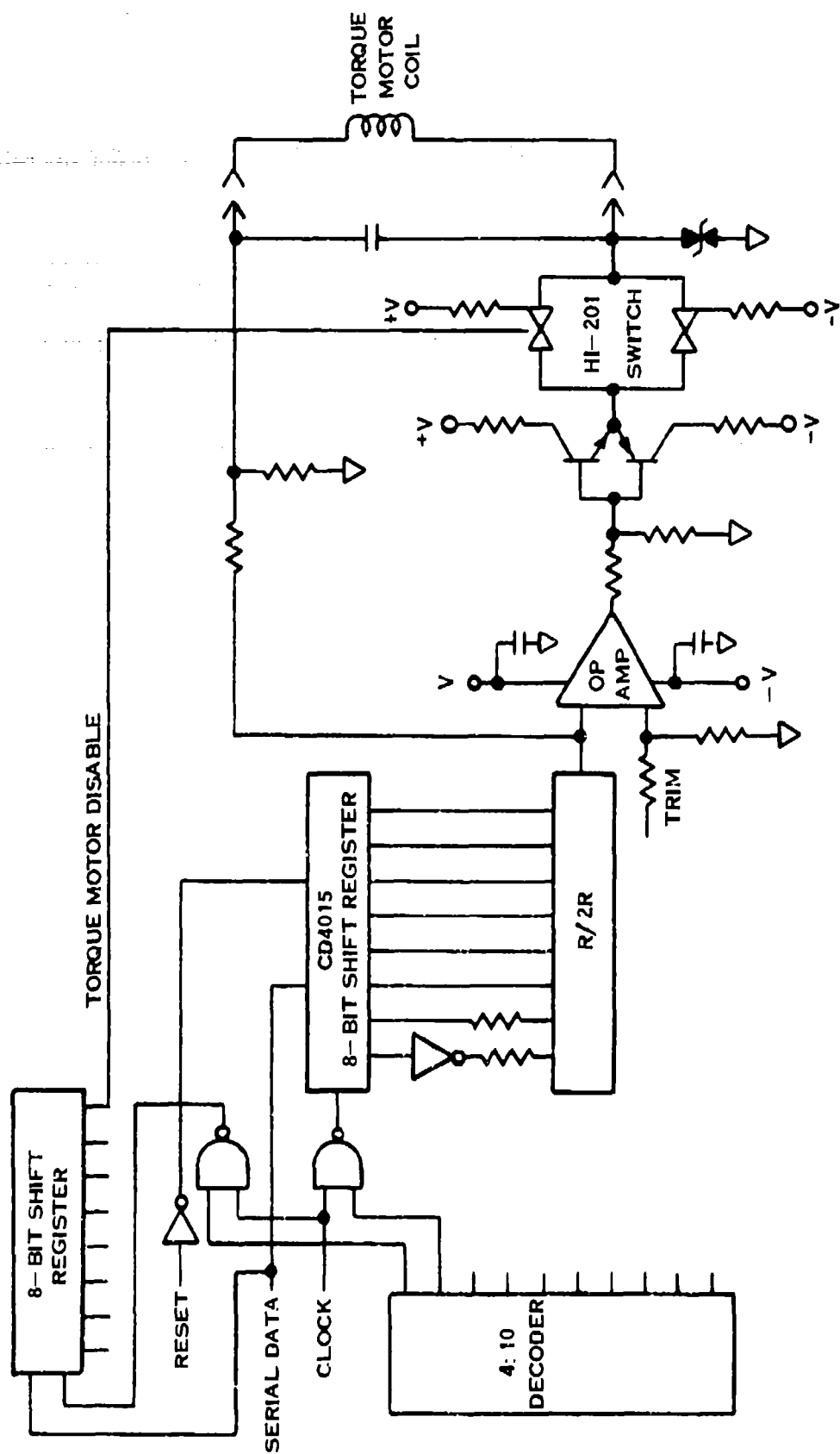
This circuit is capable of driving a torque motor with a DC current of 40 milliamperes. Control information from the central computer is fed into a shift register in a serial format. The output of this register controls a R/2R ladder network. Changing the binary input to the R/2R ladder will change the current through the torque motor. A LM148 is used as the circuit amplifier and a complimentary transistor pair as a voltage follower. The granularity of the torque motor's current will be ± 128 increments. In the event of a circuit failure, the torque motor may be turned off by the central processor with a CMOS switch. (Figure A-7).

A.2.6 Solenoid Drivers

Discrete solenoid data is loaded into a CMOS register (CD4015) from the central CPU. This register will store the control data for 8 solenoids. The output of the CD4015 drives a power amplifier, via the 2N2907A (buffer). This power amplifier has the feature of built-in short circuit protection. The output voltage of the amplifier is monitored by the LM148 for the purpose of fault detection. (Figure A-8).

A.2.7 Pressure Sensors and Circuitry

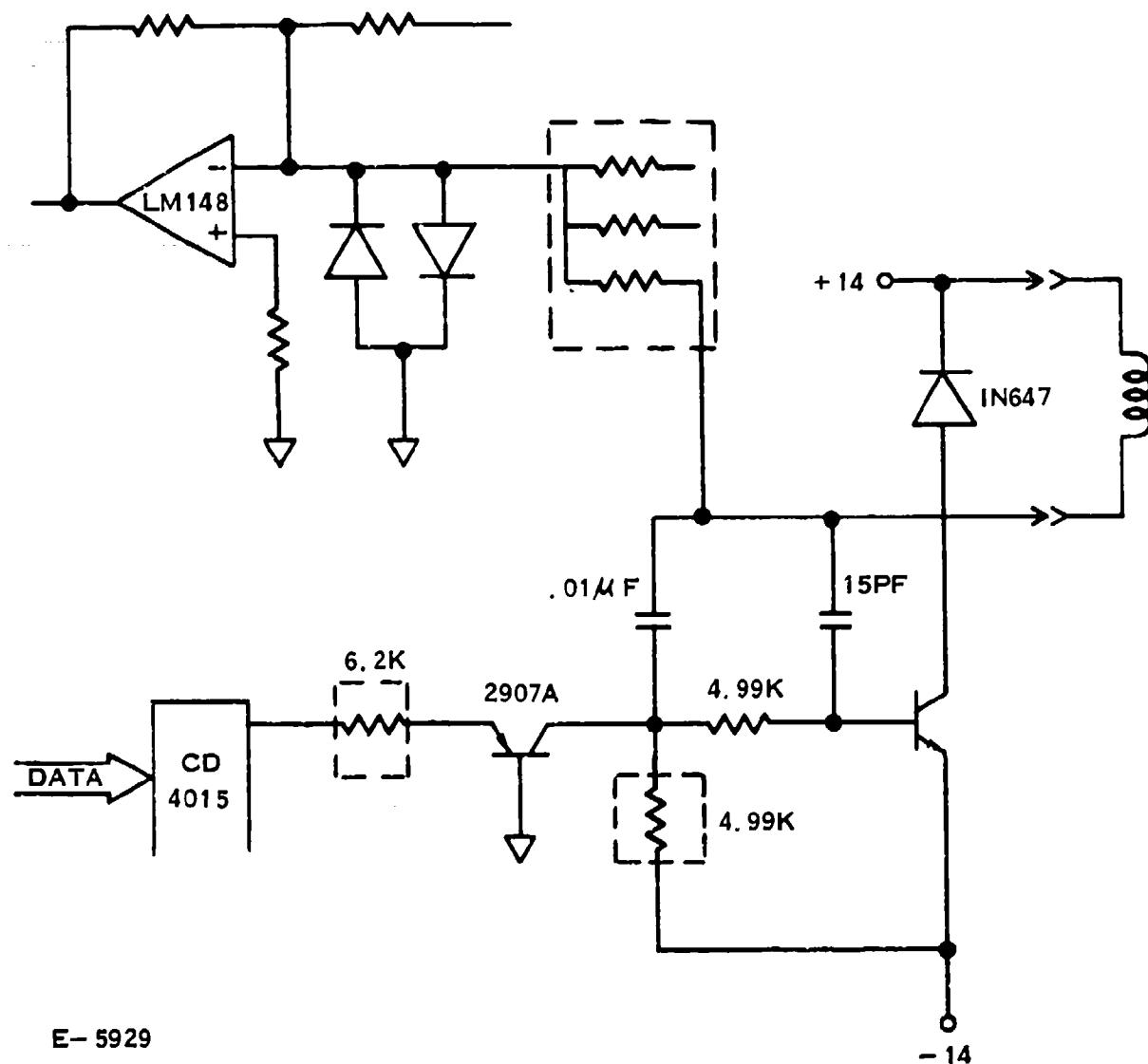
The Hamilton Standard digital pressure transducer is a precision device available to industry. The pressure transducer's pressure sensing element is a cylinder, excited by a magnetic driving circuit, which vibrates at its natural frequency. As the pressure to be measured increases, internal forces act to increase the stiffness of the sensing element causing the natural frequency to increase in proportion to the change in applied pressure. The inherent high accuracy and digital nature of this device make it ideally suited to computer controlled systems. (Figure A-9).



E-4776

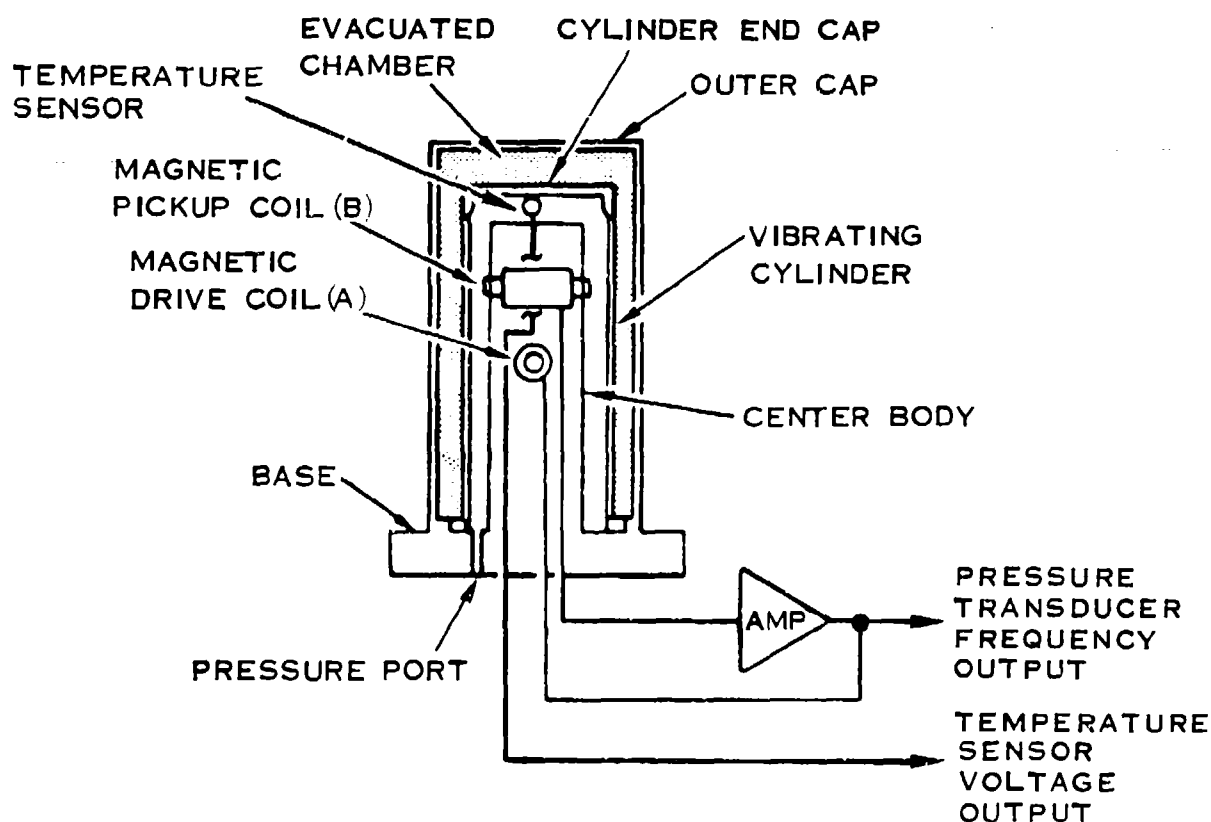
16 CHANNELS 175 COMPONENTS 7.48 WATTS

FIGURE A-7 TORQUE MOTOR DRIVER (BASELINE)



E-5929

FIGURE A-8 SOLENOID DRIVER (BASELINE)



E-2014

FIGURE A-9 SECTION VIEW OF PRESSURE SENSOR

The physical parameters which may be measured with the greatest accuracy are time and frequency. Frequency does not lose its identity or precision by transmission and may always be measured with considerable accuracy.

The pressure transducer sensor is comprised of two concentric cylinders, an inner one and outer one, separated by an evacuated space, which becomes the absolute pressure reference. These cylinders, while separate at one end, share a common mounting base. The walls of the inner cylinder are caused to vibrate at their lowest natural frequency by force pulses from the magnetic field of a driver coil mounted internal to the inner cylinder.

Mounted in the same centerbody as the driver coil is the pickup coil which produces a voltage proportional to the frequency and amplitude of cylinder wall vibration. The pickup voltage is feedback to the driver coil through an operational amplifier so as to maintain a constant cylinder wall vibratory amplitude.

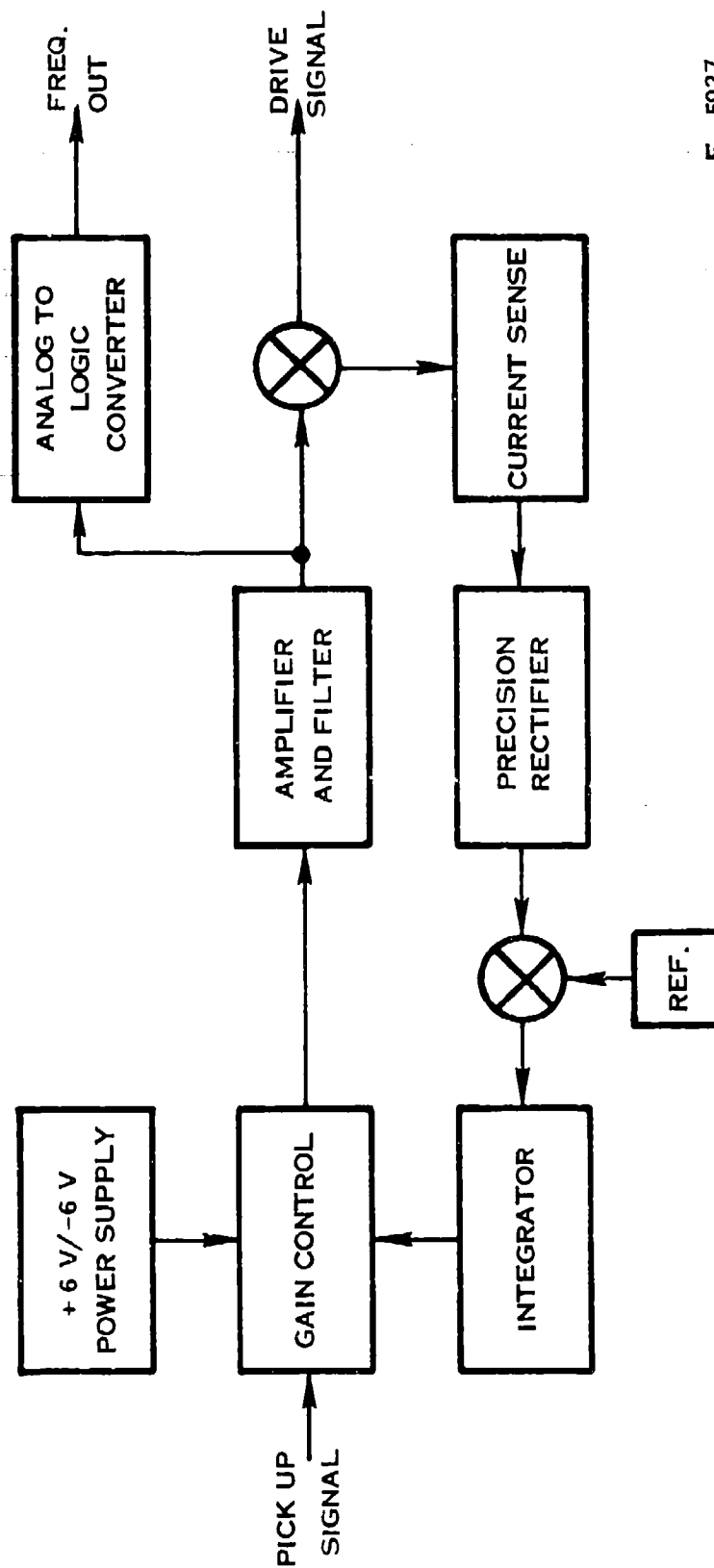
When a pneumatic pressure is introduced into the inner (vibrating) cylinder, the wall elements are tensioned and the cylinder natural frequency increases. Hence, the natural frequency is dependent upon pressure in the nonlinear relationship:

$$\text{Pressure} = A + Bf_t + Cf_t^2 + Df_t^3 + Ef_t^4$$

where A, B, C, D, and E are calibration constants. Therefore, the transducer sensor converts sensed pressure into a 2 to 3 volt square-wave electrical signal whose frequency is a non-linear function of the sensed pressure.

A.2.7.1 Pressure Sensor Drive System The pressure sensor electronics provide the necessary positive feedback for each transducer to sustain oscillation in its primary resonant mode. The pick-up signal is amplified first by a variable gain stage and second by a fixed gain, bandpass amplifier. The filter elements in the second stage are chosen to provide the proper phase shift that will result in a loop phase shift of 360°. This gives maximum support to oscillation at the sensor's resonant frequency. Drive signal amplitude is controlled by sensing the AC drive current, precision rectifying it, and comparing the rectified signal to a DC reference. The resultant error signal is integrated and used to control the gain of the input variable - gain amplifier. The system frequency is sensed at the output drive by a comparator and converted to a logic level signal (Figure A-10).

The circuit is repeated for each of 12 pressure sensors. The circuits share a common + 6 volt power supply required by the variable - gain stage. The balance of the circuit utilizes analog +14/-14V power.



E-5927

FIGURE A-10 PRESSURE SENSOR ELECTRONICS - BLOCK DIAGRAM (BASELINE)

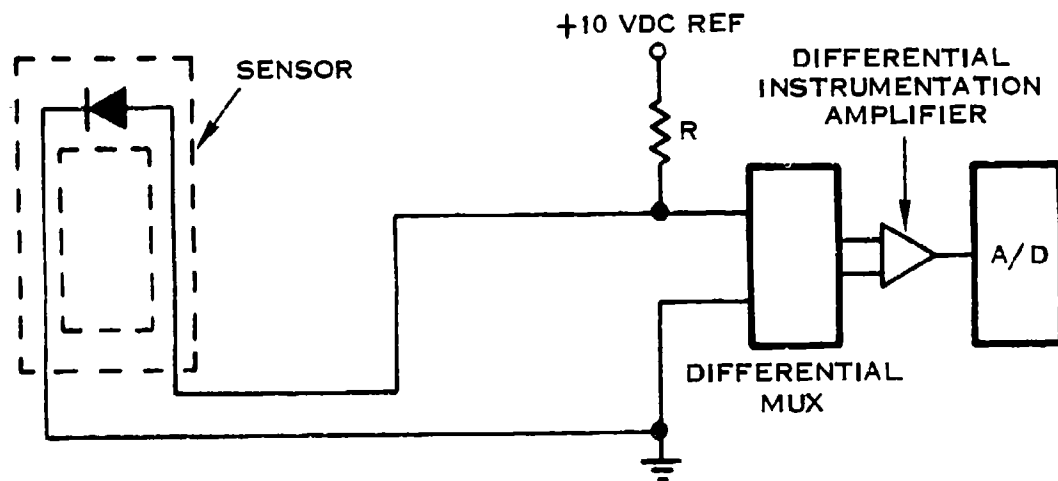
A.2.7.2 Temperature Sensor Circuit Because the natural frequency of the vibrating cylinder is a function of both pressure and the ambient temperature, a temperature sense circuit is provided to measure the temperature at the sensor and provide the information as an analog signal through the A/D to the processor. Placed at the top of the spool body is a diode, which is selected for its temperature coefficient. The actual "circuit" comprises a precision resistor as indicated in the circuit shown in Figure A-11.

A.2.7.3 Digital Correction PROM Each pressure sensor is packaged with specific compensating digital data. Raw data received from the sensor in an uncompensated form has variations in linearity with pressure level and temperature induced shifts. The calibration process to which each sensor is subjected establishes exactly how much compensation each sensor requires to accurately convert its frequency output to a precise digital number. This compensating data is then permanently programmed into a PROM Memory chip where it can be addressed by the computer each time the sensor is addressed. The determination of the normalization scale, cubic coefficients, adjusted counts, pressure and temperature maps are determined and converted from engineering units (volts, psi, etc) to programmable binary information in PROM format by computer. Inputs to the computer are the data taken on each pressure sensor during calibration.

A.2.7.4 Sensor Frequency to Digital Converter The baseline system sensor frequency to digital conversion is performed in custom CMOS LSI. Two sensor frequency outputs are multiplexed under processor control into a custom chip which counts a predetermined sensor period count. The output of this period counter is a pulse width which enables a precision 2 MHz clock into two custom LSI 8-bit counter chips. The resulting 16-bit counter is tri-stated onto the computer bus under CPU control. Since the three LSI devices mentioned are designed to handle five 16-bit digital conversions, only 1/4 of 3 LSI chips are used for this process, or roughly 185 logic gates for each sensor pair (Figure A-12).

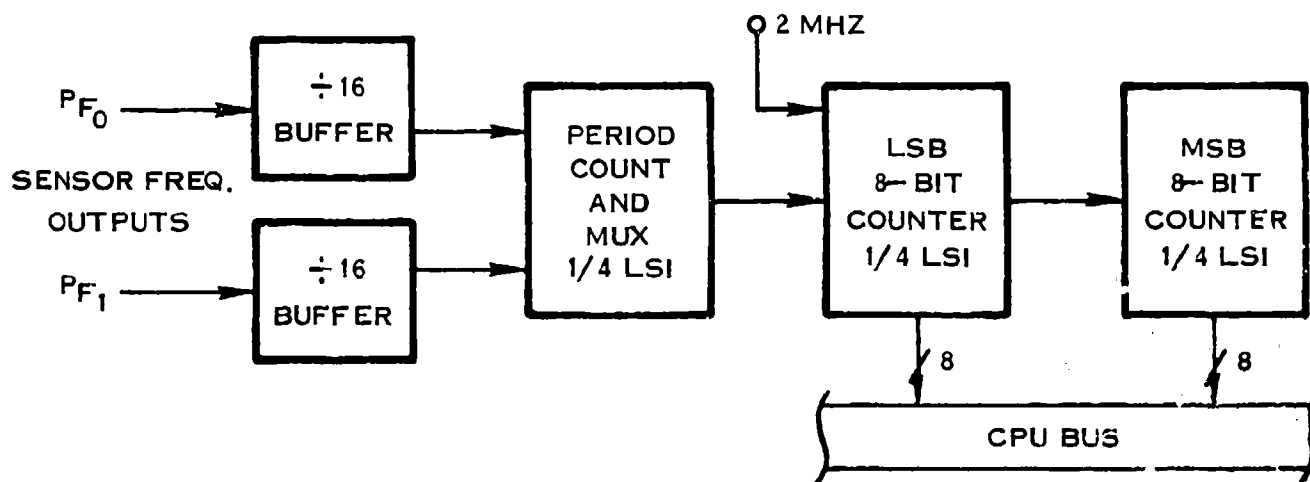
A.2.8 Low Level DC Interface

The baseline system inputs four low level signals and one high level signal. The low level signals are multiplexed into an instrumentation amplifier which provides a high level signal for multiplexing into the analog-to-digital converter. The high level signal is buffered with a separate instrumentation amplifier which is also multiplexed into the A/D. The multiplexer is followed by a buffer stage to provide higher drive capability for the A/D converter (Figure A-13).



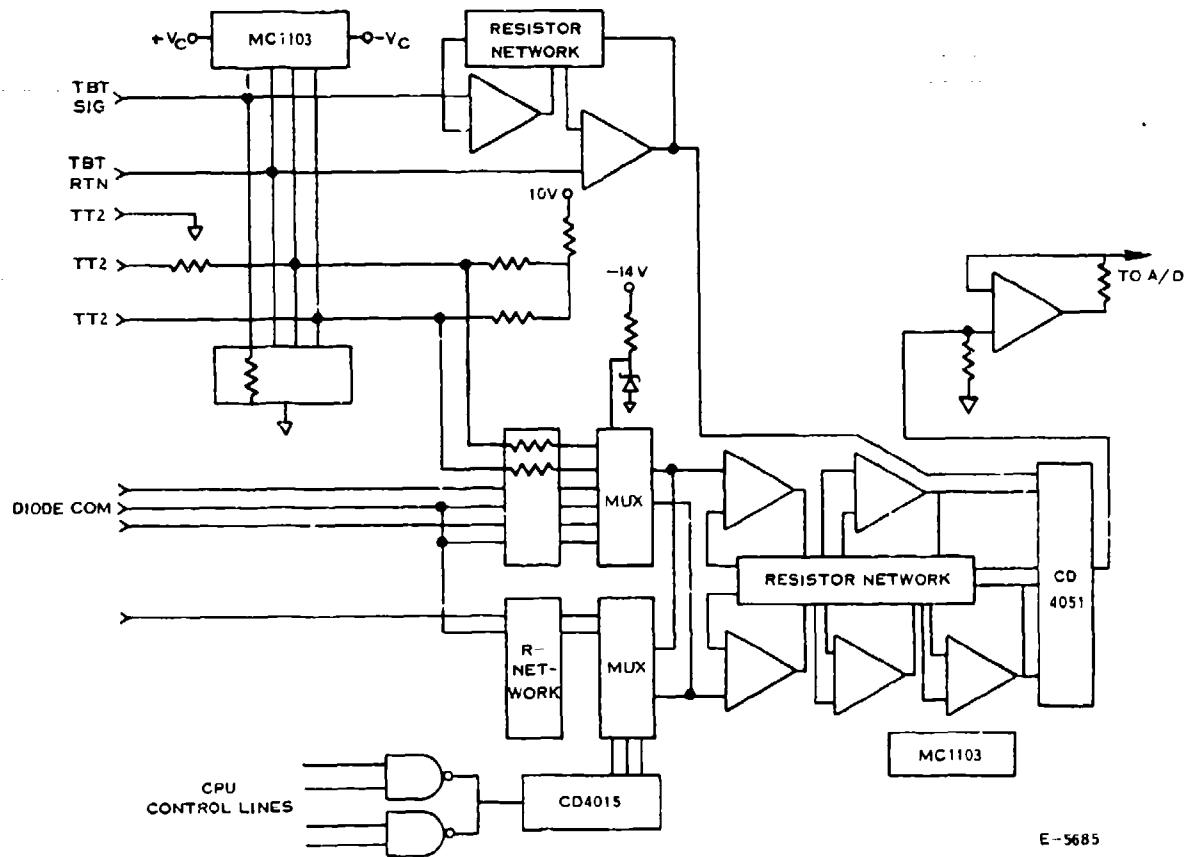
E-5680

FIGURE A-11 TEMPERATURE SENSOR CIRCUIT



E-5678

FIGURE A-12 SENSOR FREQUENCY TO DIGITAL CONVERSION



E-5685

FIGURE A-13 LOW LEVEL INTERFACE (BASELINE)

A.2.9 Resolver Multiplexer

The resolver inputs are presently multiplexed into the resolver to digital converter. The multiplexing is accomplished by using CMOS multiplexers. The CMOS multiplexers require protection from voltage transients which could damage them. This protection is accomplished with a diode voltage clamp and a series impedance on each channel (Figure A-14).

A.2.10 Discrete Signal Conditioner Circuits

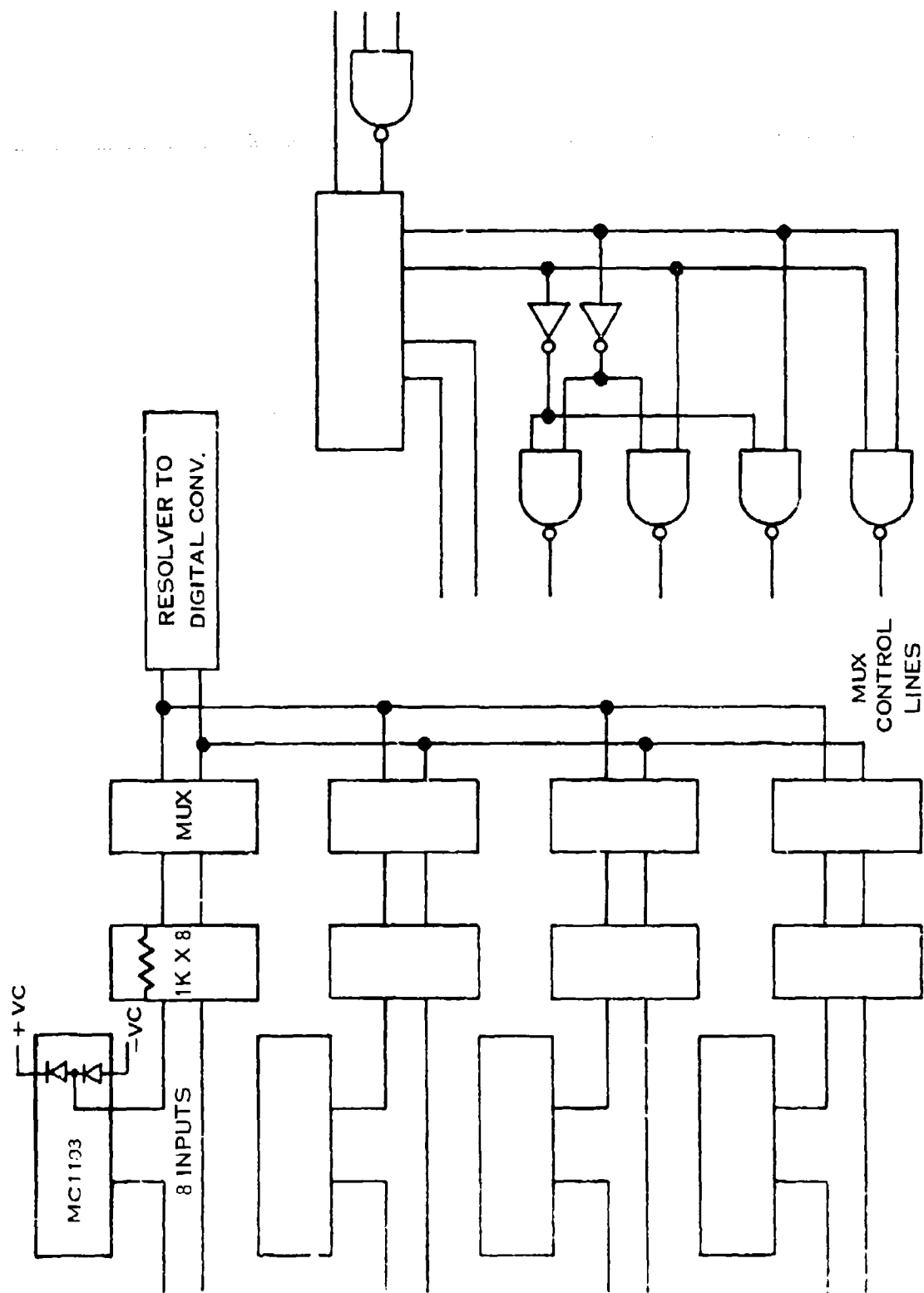
The baseline signal interface provides circuitry to condition and input signals from three discrete switch closures; a LOD Detector, and a Serial Data Stream transmitting the mach number. The discrete switch closures are conditioned with a diode resistor protection network to protect the CMOS devices from voltage transients which may be coupled on to the external signal lines. The information is input to the processor by enabling a bus driver. The LOD detection is accomplished by gating the frequency into a counter for a known period of time. The resulting count is read by the processor and compared to a fixed limit. The mach number serial data stream is received with its corresponding clock with a differential line receiver. The resulting signal is shifted into a register which is read by the processor. (Figures A-15 and A-16).

A.2.11 Frequency to Digital Speed Interface

The baseline speed interface uses custom LSI chips to perform the frequency to digital conversion. The signal conditioning is accomplished by using a quad operational amplifier as a comparator. The output of the amplifier requires level shifting to CMOS logic level. Additional gating is provided to allow for variable frequency division of the signal prior to digital conversion. The LSI chip contains tristate bus drivers for communication with the CPU. (Figures A-17 and A-18).

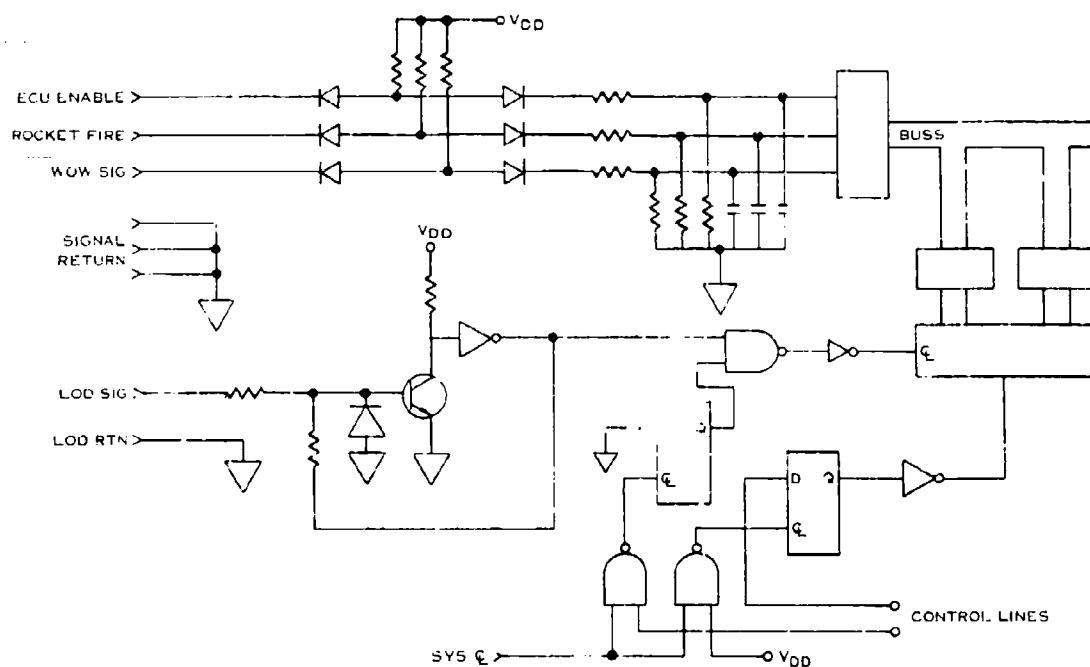
A.2.12 Turbo Pump Speed Interface

The baseline turbine pump speed circuit inputs a pulse train where the frequency of the incoming pulses is proportional to the pump speed. The pulses are conditioned with an operational amplifier and converted to logic levels with a diode and CMOS buffer. The signal is then fed into a custom LSI period counter which gates a high frequency clock into a counter. The counter can be read by the CPU to determine the pump speed (Figure A-19).



E-5819

FIGURE A-14 RESOLVER MULTIPLEXER (BASELINE)



E 5845

FIGURE A-15 SIGNAL INTERFACE (BASELINE)

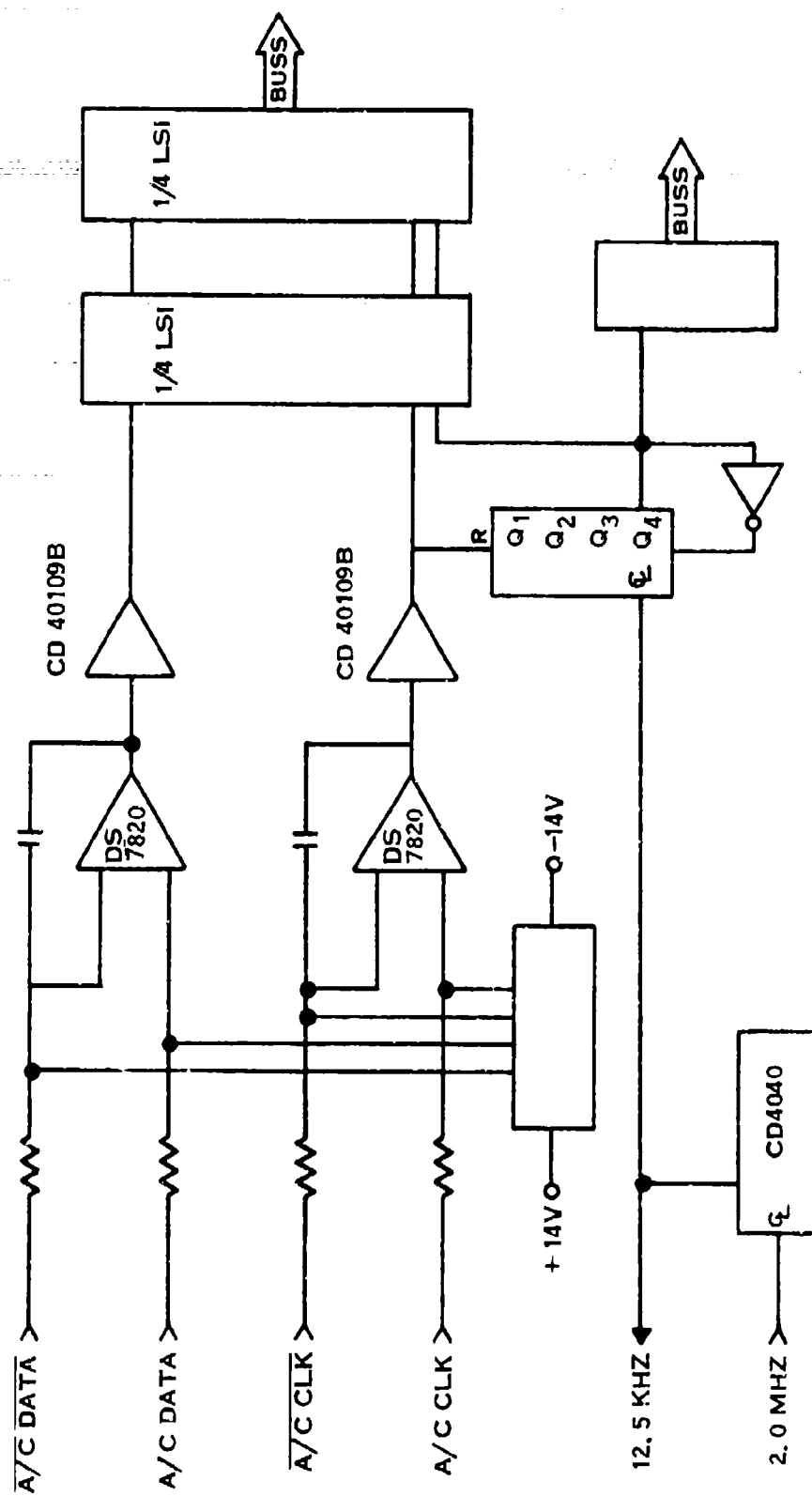
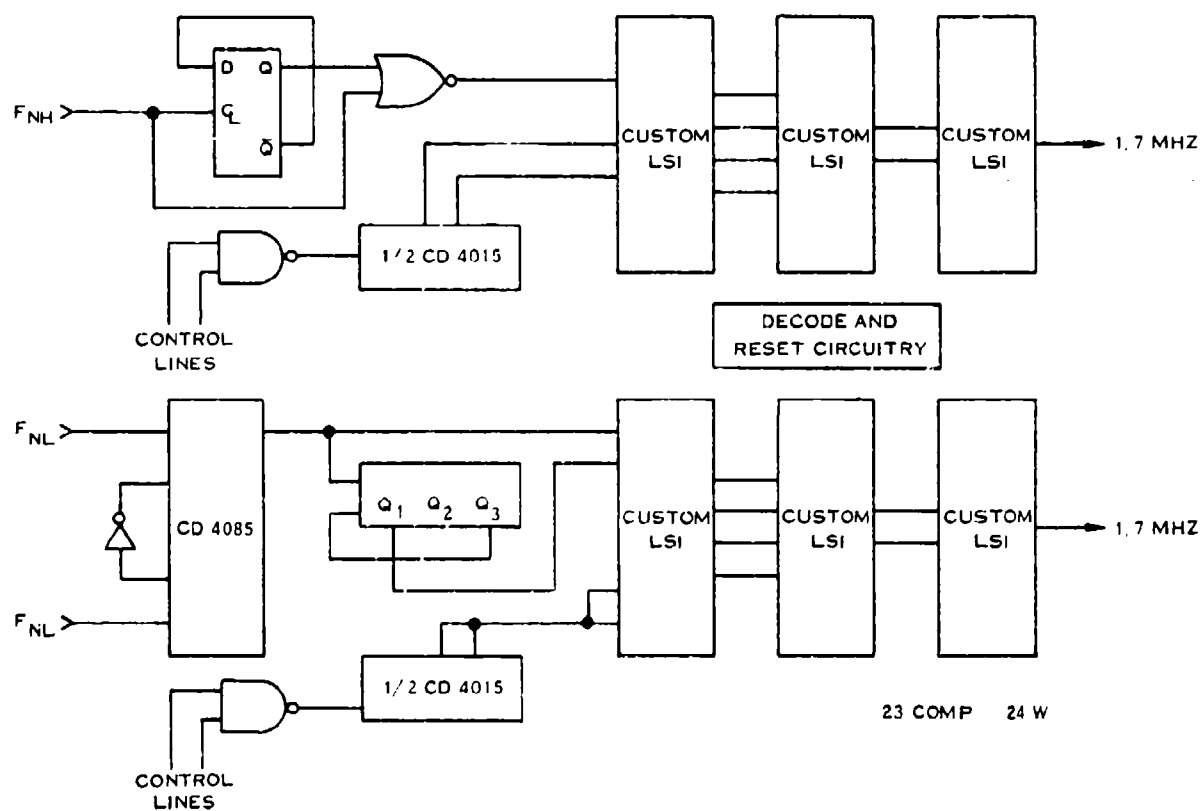
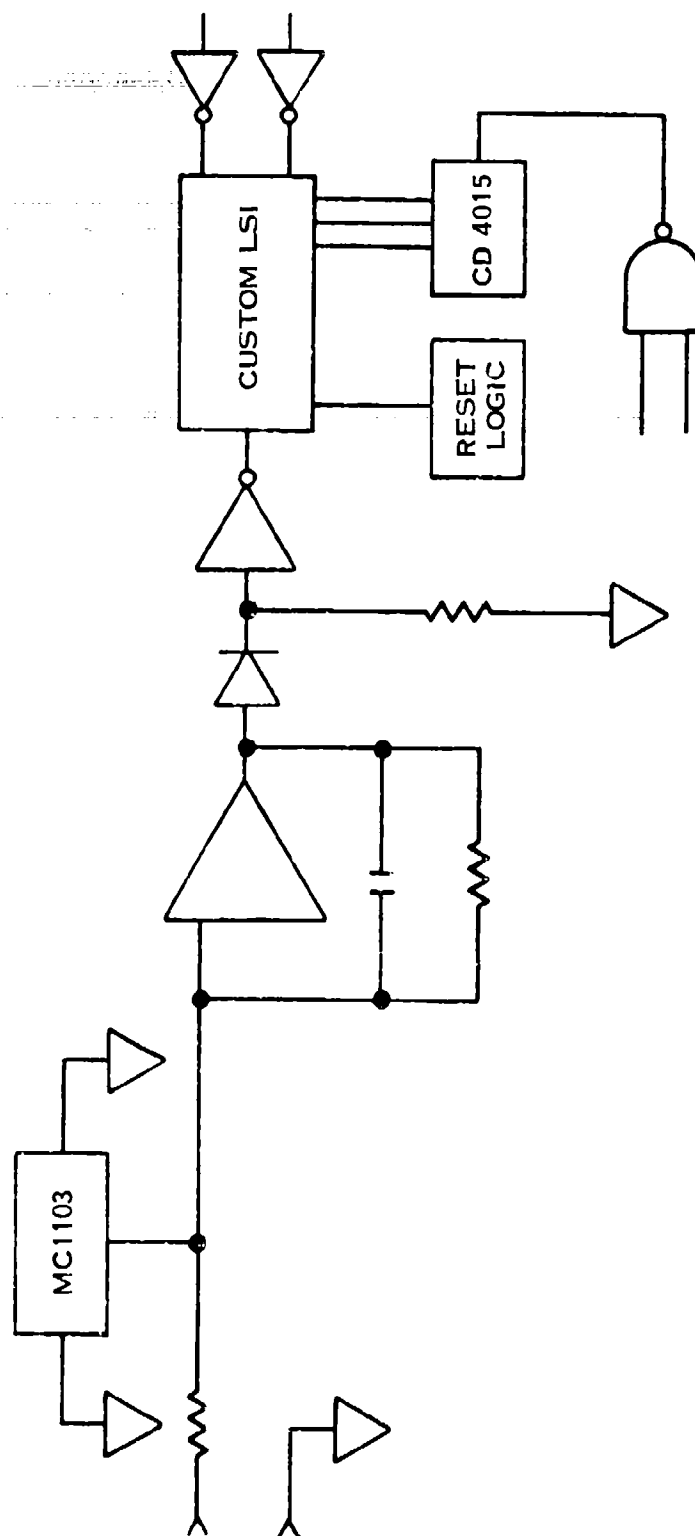


FIGURE A-16 SIGNAL INTERFACE (BASELINE)



E-5915

FIGURE A-17 SPEED INTERFACE (BASELINE)



E-5866

FIGURE A-19 TURF NE PUMP SPEED (BASELINE)

A.2.13 Fault Detection Logic

Four fault discretes are signal conditioned by a Quad voltage comparator. Each input is current transient protected by a series resistor and voltage protected by clamping diodes. The capacitor on all inputs will act as a filter to all high frequency noise and prevent false triggering. The buffer protects the primary BUS from uncontrollable power sequencing. A separate power supply is used to power this circuitry and also the voting logic (not shown). This supply has voltage diode ORing at the input and is capable of driving a load of 100 ma (Figure A-20).

A.2.14 Power Supply System

A.2.14.1 Baseline Power Supply Summary The power source is a 3Ø permanent magnet, constant current alternator. Input power is rectified, capacitor filtered, and converted to two constant voltages (+14 and -14) by two shunt regulators. Input current is 3.3 to 4.0 ADC. Current not required by the effectors and electronic circuits must be absorbed by the shunt regulators and dissipated as power. +14V is utilized by the effectors and analog circuits. +5V for the logic and memory circuits is derived by a monolithic series regulator powered off the +14V bus. +10V for logic and analog circuits is also derived from +14V by means of a series regulator. Two comparators monitor +5 and +10 for overvoltage and decrease the +14V regulator if overvoltage is detected. Two additional comparators monitor +5 and +10 for undervoltage and generate a "power supply reset" (PSR) if low voltage is detected. Finally, a drive circuit to provide excitation to the Light Off Detector is included. This circuit includes on/off logic, level shifting (+10 logic to -14) and push-pull power switching with inherent current limiting. The circuit is repeated for a LOD test channel (Figure A-21 and Table A-1).

A.2.14.2 Permanent Magnet Alternator (Constant Current Alternator) The Permanent Magnet Alternator consists of a multipole permanent magnet rotor and a multitooth stator. The rotor is constructed of alternating polarity rare earth magnets positioned radially around the circumference of the rotor. The magnets are retained by nonmagnetic materials and a thin nonmagnetic sleeve which yields a smooth, low-friction surface. The output windings are wound in segments around the stator teeth and connected for a 3Ø output. The number of teeth is 1.5 times the number of magnet poles in a 3Ø machine.

The permanent magnet alternator is particularly attractive for airborne use because of its simplicity, lightweight and absence of an exciter, a commutator, slip rings, brushes, and a field winding.

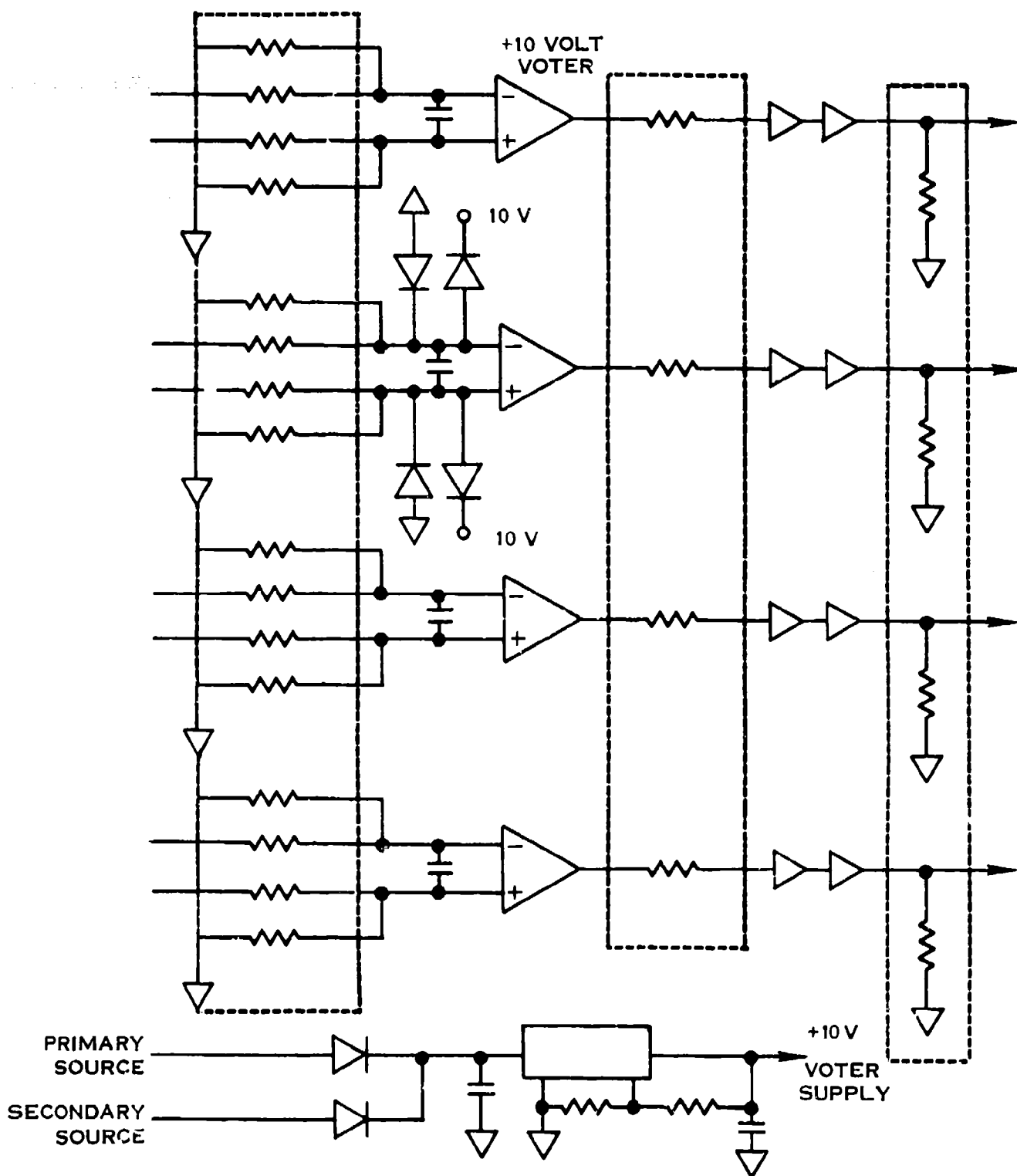


FIGURE A-20 FAULT DISCRETES (BASELINE)

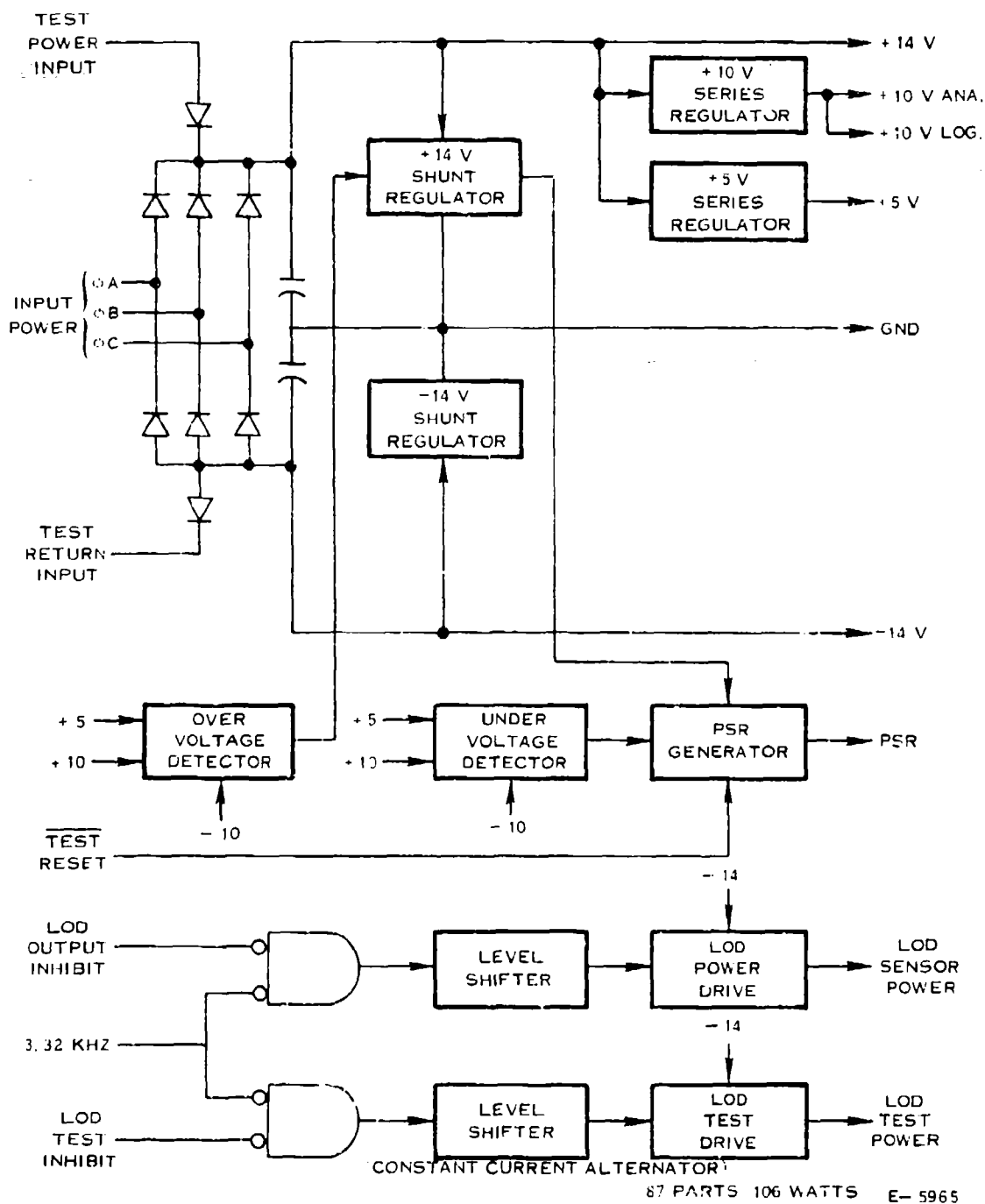


FIGURE A-21 POWER SUPPLY BLOCK DIAGRAM (BASELINE)

TABLE A-1 POWER SUPPLY LOAD RATING

+ 5V	.65 A
+ 10V	.45 A
+ 14V/+ 15V	1.90
- 14V/- 15V	3.00 A
+ 20V	-----

TYPICAL POWER DISSIPATION*

	Input Bridge	7.00 W
	Alt. Volt. Control Ckt.	-----
	+ 15V Series Reg	-----
	Inverter & -15 Supply	-----
	+ 14V Shunt Reg	35.50 W
	- 14V Shunt Reg	41.30 W
	+ 10V Reg	1.60 W
	+ 5V Reg	5.20 W
	PSR/OV	.10 W
Prime	L00 In Standby	
	Power Supply Subtotal	<u>90.70 W</u>
	EEC Digital	6.1
	Analog	5.95
	Drivers (Series Drop)	<u>3.0</u>
	Total Non P/S	15.05 W
	Total EEC	<u>105.75 W</u>
	Secondary	<u>105.75 W</u>
	Grand Total	211.50 W

* Assumptions used in Typical Power Dissipation above:

14V Solenoids @ .4A	1
20V Solenoids @ .3A	0
28V Solenoids @ .2A	2
Torque Motors .05A/.15A	+14V/-14V
Analog Load .2A/.2A	+14V/-14V
+10V Load	.35A
+5V Load	.55A

Characteristically, open circuit voltage increases proportionately with speed, while short circuit current remains relatively constant. Hence, the permanent magnetic alternator may be referred to as a constant current generator. For a fixed load, the alternator parameters may be chosen to provide relatively constant current over a wide speed range.

A.2.15 Central Processor

This portion describes the RAECC baseline Central Processor which comprises the five-chip CPU, the 12K word PROM, the RAM, the EAROM, and the Dual-Port RAM. Although the EAROM is presented in this discussion, it was not considered in the trade studies since it is not flight critical, and is used only to keep track of fault words.

A.2.15.1 Central Processor Unit The five-chip (CPU) implemented in the baseline unit is a technology improved version of the 11 LSI-chip, ion-implanted bulk-CMOS, HS 16/24 SISD, bit-parallel processor used in the EEC102 and JFC 106 engine-mounted fuel controls. The five chips comprise two custom very large scale integration (VLSI) CMOS silicon-on-sapphire (SOS) devices, and three custom ion-implanted CMOS devices. Features of the parallel HS 16/24 SOS/CMOS parallel processor are:

1. Low Power: 0.5 watt at 4 MHz, 10 VDC
2. High Speed: 1.0 microsec register and Immediate, 2.0 microsec Memory Ref. Inst.
3. Excellent noise immunity
4. Full MIL Spec: -55°C to +125°C, 5E8065 (based on MIL-M-38510, Class B)
5. Technology: Very high density, 2600 FET, static CMOS SOS VLSI; 4 to 10 nanosec delay per gate at 25°C
6. Addressing: Direct to 2048 words; indirect to 32K words
7. Priority interrupt structure
8. Hardware Multiply: 17.0 μ s absolute max at 4 MHz, (13.5 μ s based on arithmetic mean)
9. Hardware Divide: 17 μ s

10. 87 Instructions: 14 Memory Reference, 2 Input/Output, 17 Shift, 1 Load Immediate, 13 Skip with 53 Combinations
11. Integral Test Hardware: Single-step Run/Halt, DMA, External Diagnostic Memory and Terminal Interface provided via test connector
12. TTL Compatible Inputs: No buffers required on input bus
13. TTL Compatible Serial Outputs: No buffers required on Serial or Parallel Outputs

CPU Architecture

The HS 16/24 CPU is a flexible, controls-oriented, CMOS LSI, bit parallel, fractionally scaled two's complement, combinational logic, state machine. Designed initially for either 16- or 24-bit word lengths (16 bits for fuel controls and 24 bits for navigational computations), it may be operated with clock rates from 0 to 1 MHz (0 to 4 MHz clock input), supply voltages from 0 to +15 VDC, and temperatures from -55°C to +125°C. It is structured as shown in Figure A22 with six dedicated registers, a program incrementer, an arithmetic logic unit (ALU), all "hard-wired" control logic and timing. The CPU's 87 instructions are designed to operate with a microinstruction controlled clock which can synchronously vary the microinstruction execution times between 500 nanosec and 2.0 microsec, allowing all instructions to be executed with maximum speed efficiency. Instruction execution times are also minimized via overlapped Fetch/Execute cycles, look-ahead carry in both arithmetic unit and register unit adders, and judicious selection of all register transfer paths to allow multiple register transfers to occur simultaneously.

CPU Hardware Implementation

The digital logic required to implement the HS 16/24 CPU design was partitioned into two different custom LSI types. A total of three of these LSI devices are required for the complete 16-bit processor design: one Control Logic/Timing CMOS SOS VLSI module (5E8065/10) and two 8-bit Register/ALU CMOS SOS VLSI modules (5E8065/09).

- * A microprogrammable control store was designed for this machine, which unfortunately comprised some 20 components (including 5 ROMs), which were deemed far less reliable and slower than the hard-wired control logic which replaced them.

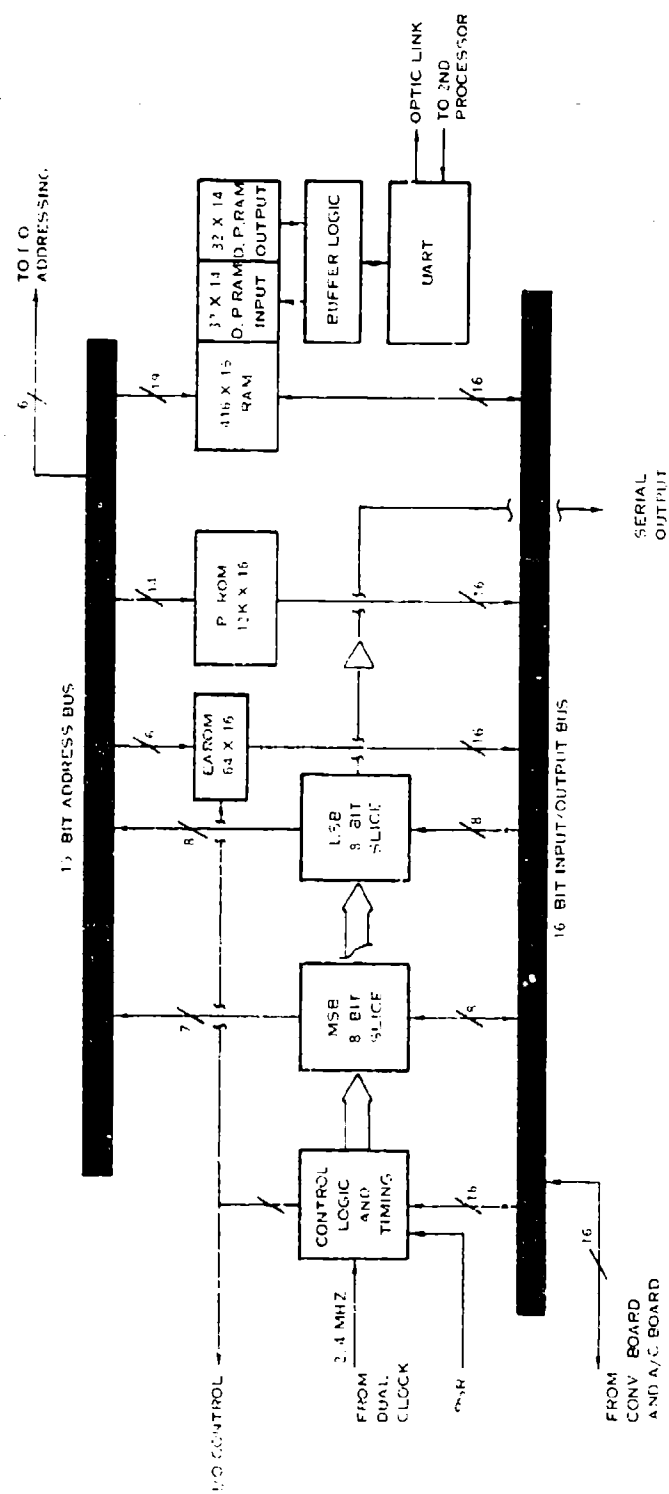


FIGURE A-22 CPU BLOCK DIAGRAM – BASELINE

Register/ALU Description

The arithmetic logic unit performs the actual execution of all arithmetic and logic instructions. An arithmetic instruction always involves two operands that must be combined. One of the operands is specified in the address portion of the instruction word and comes from memory or an input device. The other operand is already in the A register of the arithmetic unit as a result of a previous instruction. The operation code portion of the instruction word specifies exactly how the two operands are to be arithmetically or logically combined.

There are six dedicated 16-bit parallel registers associated with the arithmetic and register units.

CPU Throughput

The performance of a processor may be measured in its throughput, or given a particular instruction mix, the maximum number of instructions that it will process in one second. While on the other hand, the figure of merit of a processor may be measured in its throughput per watt or kops/watt, where kops is thousands of operations per second. The instruction mix used in calculating throughput is derived from the actual program used in a recent breadboard designed for an engine fuel control. Based on this mix, the predicted throughput is 390 kops and the performance throughput per watt is 780 kops/watt (based on 0.5 watt for the five-chip CPU system).

Watchdog Timer

The watchdog timer is a hardware built-in test circuit which is used to detect and either correct or flag a hung CPU condition. Its primary function is to eliminate any infinite looping that may occur as a result of a lightning discharge or other abnormal transient. This looping condition is quickly detected by the timer as the timer must be reset by the CPU after each CPU control loop. When the CPU is hung, the timer is not reset and the error is detected. A reset pulse is given to the CPU in an attempt to restart it. All output effectors are also reset at this time and, if the CPU does not recover, the LRU fault indicator is latched and the secondary is notified via the three emergency fault-status lines that it is now in full control.

A.2.15.2 Programmable Read-Only Memory The programmable read-only memory is the main-program read-only memory for this fuel control and is specifically designed to:

- a. Minimize memory parts count and printed circuit board (PCB) area by using high density, internal power strobed, 8K-bit (2048 X 4), compact 18-pin DIP-package, PROM integrated circuits.

- b. Reduce memory power dissipation through the use of self-power strobed, bipolar PROM's.
- c. Provide maximum development flexibility at low cost through use of programmable ROM (PROM) devices.
- d. Access 256 words of PROM from each pressure sensor by externally quadruplexing 1024 X 4 bit PROMs into 256 X 16-bit words, (in the A/C card).

In the primary, 12K words of memory are made up of 24 8K integrated circuit (IC) packages. As the 1024 words of page zero of memory can be addressed directly from any other memory page, its locations are extremely valuable and must be used efficiently. The 416 words of RAM and 64 words of DPCTRAM (32 words primary plus 32 words secondary) therefore, reside in the top half of this page with PROM contained in the lower half. The half-page zero PROM's displaced by RAM memory, however, are not wasted, as these locations can be accessed through memory page 16.

Pressure sensor calibration data, usually 32 words per absolute sensor plus 224 words of additional program memory, is available in each of three pressure sensor calibration PROM's. This memory is implemented with 1024 X 4 PROM IC's but is accessed using a CPU wait state which allows it to be quadruplexed into full 16-bit words. The wait state adds only 1.0 microsecond to the instruction execution time and greatly off-loads the CPU by not requiring the assembly of the otherwise four separate 4-bit nibbles into 16-bit words.

A.2.15.3 Random Access Memory The Random Access Memory scratch pad is specifically designed to: (1) provide up to 416 X 16-bit words of directly addressable (page zero) scratch pad memory for the CPU and (2) reduce power dissipation through the use of CMOS RAM IC's.

The CMOS RAM can be accessed by the CPU at full speed, no wait states are required. All 416 words of RAM memory can be directly addressed from any other page of memory such that indirect references are not required. It should be pointed out that only 416 words of RAM can be accessed; 64 words are permanently disabled to enable the 32 word dual-port cross-talk RAM, allowing the most judicious organization of the 1024-word base-page, as mentioned above under Programmable Read-Only Memory.

A.2.15.4 Electrically Alterable Read-Only Memory Module The EAROM is a hybrid module which contains two - 32 words by 16 bits - EAROM chips and the CMOS address latches, output buffers, and logic control circuits necessary to interface with the baseline system.

This EAROM device differs from RAM devices in two ways; it is essentially non-volatile, but it requires milliseconds to perform either its ERASE or WRITE functions. It therefore requires multiple commands to perform either function, each requiring 100ms delay loops.

The EAROM memory itself uses MNOS P-Channel technology to realize electrically alterable memory with unpowered, nonvolatile storage for ten years at 70°C. Data retention is a minimum of 2×10^{11} read cycles/word before refresh is required. READ access time is 4.0 microseconds with ERASE WRITE requiring a minimum of 50 milliseconds. Data is stored by applying negative writing pulses.

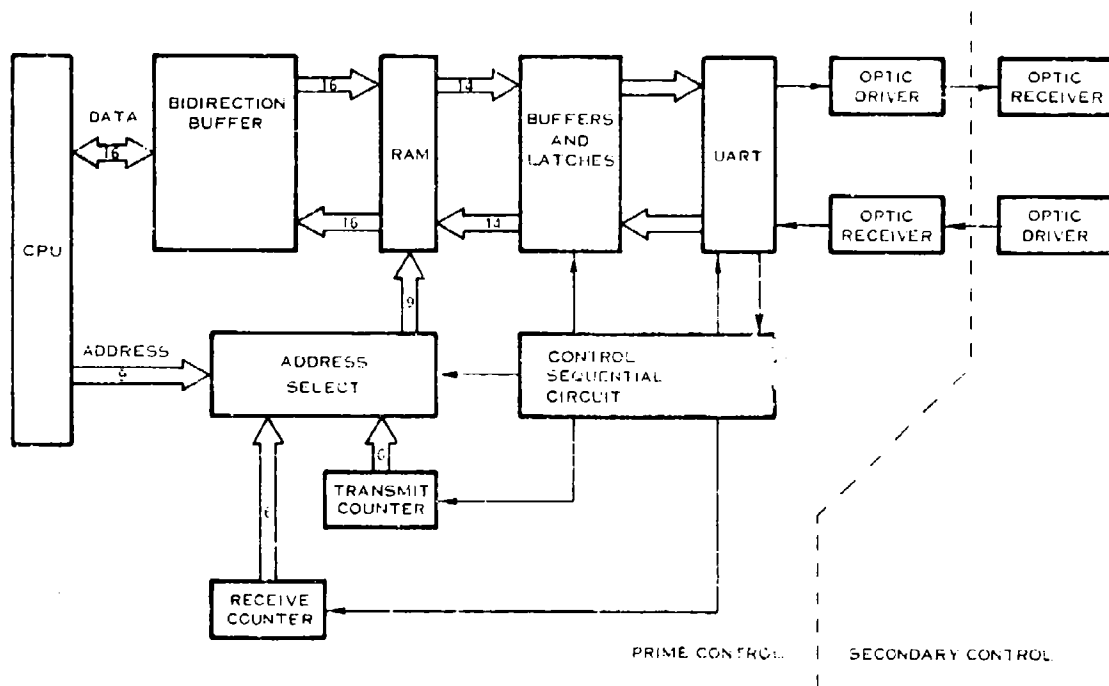
The EAROM module is program controlled with I/O Commands being utilized as read clock, address and function control, write inhibit, and data strobes. A programmed sequence is generated to accomplish the READ and ERASE/WRITE tasks.

Special care must be taken in two areas to ensure proper operation of the EAROM hybrid. First, the read clock must have a pulse width greater than 20 microseconds and less than 40 microseconds. This clock should only be active when an actual READ of data is desired and is not to be a constant input frequency. Secondly, the design of the EAROM hybrid is such that one of the two EAROM chips is always enabled and, therefore susceptible to any changes of the C1 and C2 control signals. It is therefore recommended that these signals be changed one at a time and that address be changed only when C1 and C2 are in the read modes.

The baseline system initializes C1, C2 to the READ/HOLD mode, sets EAROM clock low, and inhibits writing when the system is activated with Power-On-Reset (POR). These states should be returned to at the end of any READ, ERASE, or WRITE cycle.

A.2.15.5 Dual-Port Cross-Talk RAM A dual-port cross-talk RAM is required in each baseline primary and secondary subsystem to provide a "real-time" data access link between processors (Figure A-23).

It should first be clarified that a dual-port RAM is a device with dual independent data and address buses which allows simultaneous asynchronous access to two different data words. Possibly the best hardware example is the Advanced Micro Device AM 29705 16-word X 4-bit dual port RAM, which allows access from either A or B ports, but allows data writing only through the B port, which in this case would be dedicated to the primary control. Since CMOS dual-port RAMs of high enough density do not yet exist, 64 14-bit words of the total 512 RAM words are partitioned with data mux and latches to act like D.P. RAM. A UART coupled with a dedicated receiver and transmitter interface, continuously and simultaneously sends and receives data to/from a UART on the second processor's D.P. RAM at a 125 KHz bit rate.



E-5972

FIGURE 1-13 DUAL-PORT CROSS-TALK RAM BLOCK DIAGRAM

Receiver

The CPU cannot write into locations 1700g through 1777g, which are reserved for the dual-port receiver. A single jumper change will allow the CPU to write into these locations. All received words contain data in the 14 most significant bits and zeros in the 2 least significant bits. The dual-port receiver is wired for reception of up to 32 words. A single jumper change will allow up to 64 words to be received. While the receiver can accept a flexible number of words, the transmitter circuitry constrains the dual-port to operation of blocks of 32 words or 64 words only. The sync word, 17774g, will be found at the most significant location, 1737g for the 32 word case and 1777g for the 64 word case.

Transmitter

All 16 bits of all words in the transmitter portion of the dual-port RAM are readable by the CPU as well as writable. The two least significant bits are not transmitted. The circuit is connected for transmission of RAM locations 1600g through 1637g. A single jumper change will allow transmission of addresses 1600g through 1677g. The transmit circuitry is completely independent of the sync word, outputting either blocks of 32 or 64 words depending upon a single jumper position. Continuous transmission occurs with or without the presence of a sync word in the transmitted block of words.

Any location may contain the sync word, 17774g, where the two least significant bits are don't care bits. However, additional software constraints are required for error free dual-port operation. After power-on-reset there is an immediate write into the UART transmitter of the contents of location 1600g. This occurs before the CPU has a chance to write into the scratch pad memory. Since this may result in an initial inadvertent sync word transmission, however unlikely, initial acceptance of dual-port data as valid data must depend on reception of a second sync word at the proper position in the received block of words. That is, dual port data is not to be considered valid until the most significant dual port receiver word contains the sync word. The transmitter must position the sync word in scratch pad memory as the most significant word to be transmitted.

The dual-port UART is wired for selection of an 8 bit word followed by an odd parity bit and one stop bit. Since there are 10 transmitted bit periods per output word, plus a stop bit period, at a 125K baud rate, a complete half word is transmitted every 88 μ s. The most significant data bit is the most significant word half indicator to the receiver circuit. This bit is not available to the CPU.

Dual-Port RAM Addressing

There are 3 sources of address to the RAM integrated circuits: CPU address, dual-port receiver address, and dual-port transmitter address. To accomplish address selection from the 3 sources, TTL tri-state drivers are used to establish an address bus which is pulled-up to Vdd with resistors to provide the logic high voltage required by the RAM integrated circuits operating at 10 volts. The address drivers are capable of operating with the outputs pulled up to 10 volts and can also operate with their inputs at 10 volts. The latter requirement is imposed because the receiver and transmitter addresses are sourced by CMOS counters operating at Vdd. Normally the tri-state buffers are in the high impedance state. The scratch pad memory (SPM) address decode enables CPU address to the bus. The sequential circuits associated with the dual-port receiver and transmitter can supply address from their respective counters during the time toggle 1 MHz is at a logic high state. This is only allowed during a gated system clock period in which the CPU does not use RAM (the scratch pad memory address decode is not asserted). Since the RAM address bus is driven by TTL devices, the logic high state is achieved by passive pull-up. The time required to go from a low state on the address bus is approximately one time constant since the TTL driver actively drives the address to 3.5 volts. Thus, it takes 2.0K ohm times 120 pf or 240 ns to attain a valid logic high level.

Detailed Receiver Operation

The UART is the heart of both the receiver and transmitter circuitry. The UART receives serial data from the optic interface and, once a word is assembled in the parallel receiver buffer register within the UART, a high Data Ready flag is provided on UART pin 19. This flag is synchronized to Gated System Clock by a flip-flop. The output of this flip-flop enables data to the inputs of the RAM integrated circuits if the CPU does not access SPM during that clock period. The writing of data into the RAM occurs only if a most significant word half has been received, that is if the most significant received bit is a logic high. The signal that enables dual-port write into RAM is clocked into a flip-flop which causes a counter to increment, thus preparing the receiver for the reception of the next word.

When the least significant half of a dual-port word is received, those 7 data bits are latched for subsequent deposit into RAM upon the reception of the most significant half of that dual-port word. Thus, an entire 14 bit word is changed in RAM simultaneously.

The receiver is synchronized by reception of 177 octal followed by reception of 377 octal. This causes the reset of the error flip-flop, which allows the sync word and subsequent words to be written into the dual-port RAM, and also

causes the receiver address counter to be reset to zero. A flip-flop stores the occurrence of a write into the receiver dual port RAM so that the receiver counter can be incremented after each write. Incrementation of this counter above the set number of words will cause the error flip-flop to set, preventing further writing into the dual-port receiver RAM until a new sync word is received.

Detailed Transmitter Operation

The UART Transmit Buffer Register Empty signal, TBRE, from pin 22 goes high to initiate the reading of the Dual-Port RAM and then transmission of that word. The word taken from the RAM is 14 bits long, with 7 bits written into the UART and 7 bits stored in a holding register. The MSB's, the stored 7 bits, are transmitted upon issuance of the next TBRE signal. Upon the serial transmission of a byte the Transmit Register Empty signal, UART pin 24 goes high and increments the transmit address counter. The least significant bit of this counter is the most significant word half indicator, TMSH. The remaining bits of this counter are used as address bits to the RAM.

The RAEEC CPU board contains a serial transmission link that is used to communicate with a similarly equipped CPU. The transmission link is interfaced with the RAEEC CPU through Direct Memory Access (abbreviated DMA). That is, the RAEEC CPU merely sends data to a portion of its scratch pad memory to output data; received information appears in another block of scratch pad memory.

A.3 RAEEC Circuit Trade Study

A.3.1 Introduction

This section of the report provides detailed descriptions of the various circuitry considered in the RAEEC circuit trade study. The trade studies considered any application of any technology in production as of 1979, with specific regard to the salient features, drawbacks, circuit board area, and power dissipations of each design. The final summary of these trades is presented in Section 3.4.3. Also refer to the Reliability Diagram (Figure A-24).

(Information on the derivation of the Reliability Figures used in this section is contained in the "Guide for Development" referred to in Section XI.)

A.3.2 Analog to Digital Converter

There are several well known analog to digital conversion techniques which include the following:

- a. The two-ramp A/D

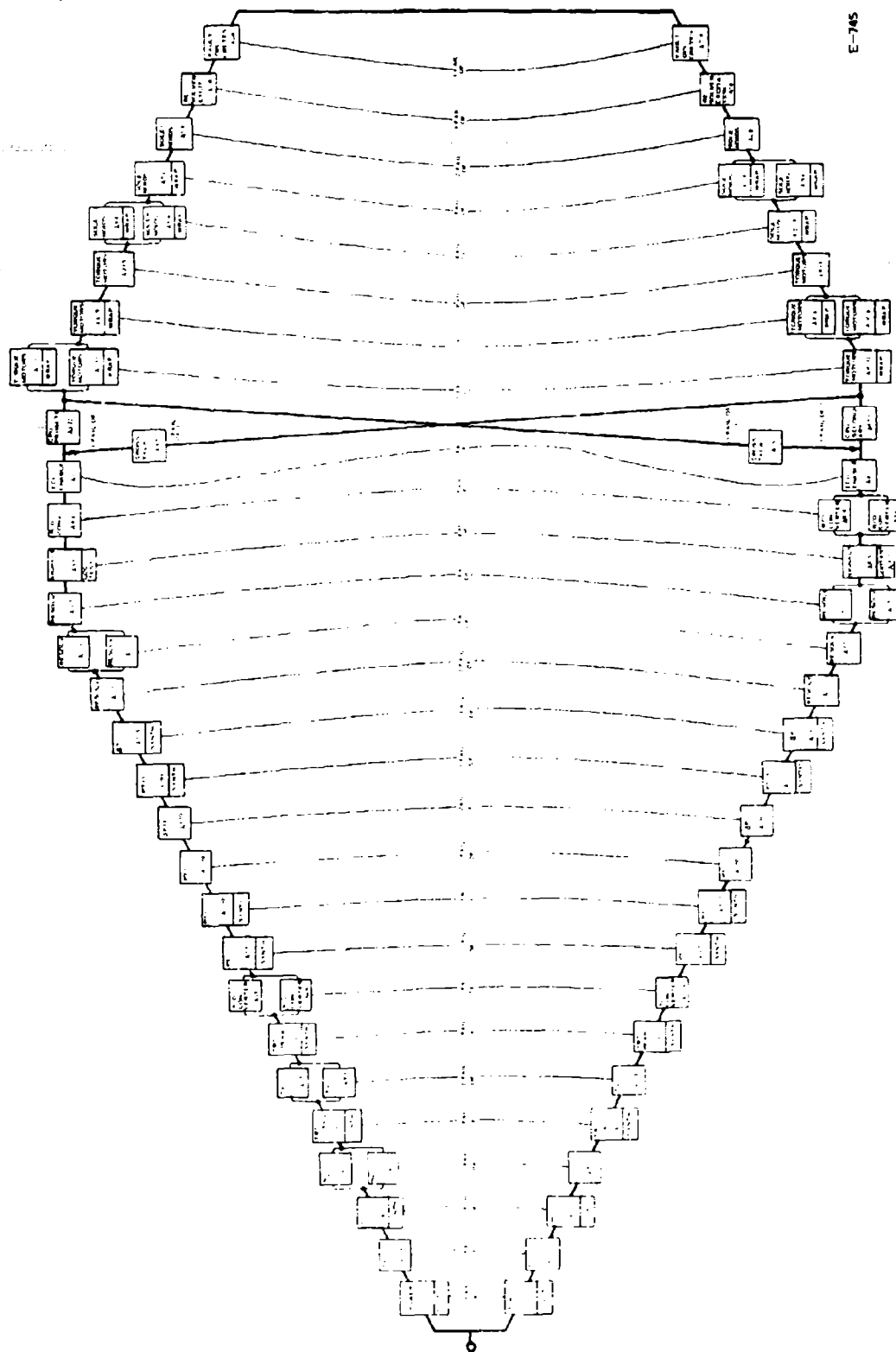


FIGURE A-24 RAEEC SYSTEM RELIABILITY BLOCK DIAGRAM COMPLETED CIRCUIT TRADEOFFS

- b. The multi-ramp A/D (3-ramp, quad slope, etc.)
- c. Successive approximation A/D (SAC)
- d. A/D doubling converter
- e. Video speed comparator/bit A/D

Of the five A/D's mentioned above, only the "multi-ramp A/D" and the "SAC A/D" were considered in these trades, since only they can perform a full 12 bit conversion in under 1.5 milliseconds over the full military temperature range, at a competitive price. A summary of the A/D trades is shown in Table A-2.

A.3.2.1 Multi-Ramp A/D Converter It has been successfully demonstrated at Hamilton Standard, that a "smart multi-ramp A/D" can be fabricated using a microprocessor in place of the control logic. Because this A/D uses a microprocessor, it can be programmed to perform the logic sequence described in Paragraph A.2.2, but also can perform its own input signal multiplexing, input scaling, range checks, in addition to fault isolation. A simplified block diagram is shown in Figure A-25.

A.3.2.2 Successive Approximation A/D The successive approximation type of analog-to-digital converter can be used to convert the analog signals to a digital format. This type of converter requires a sample and hold unit to maintain a constant input amplitude during the conversion. The conversion can be made very rapidly, typically less than $50\mu\text{sec}$. There are two drawbacks to using this type of conversion scheme in a control environment. A successive approximation converter is very sensitive to noise on the input signal, requiring dedicated filtering on all input channels. Filtering complicates the dynamics of the system by adding lags which must be compensated for in the control scheme. Additional software filtering is usually necessary which affects software overhead and required processor capability. It should be pointed out that although this converter is "off the shelf", monolithic, and faster than the multi-ramp type converter, the additional sample hold circuitry, filtering circuitry, and software filtering makes this system less attractive. A simplified block diagram is shown in Figure A-26.

A.3.3 Resolver to Digital Converter

A few possible resolver conversion concepts are presented for review:

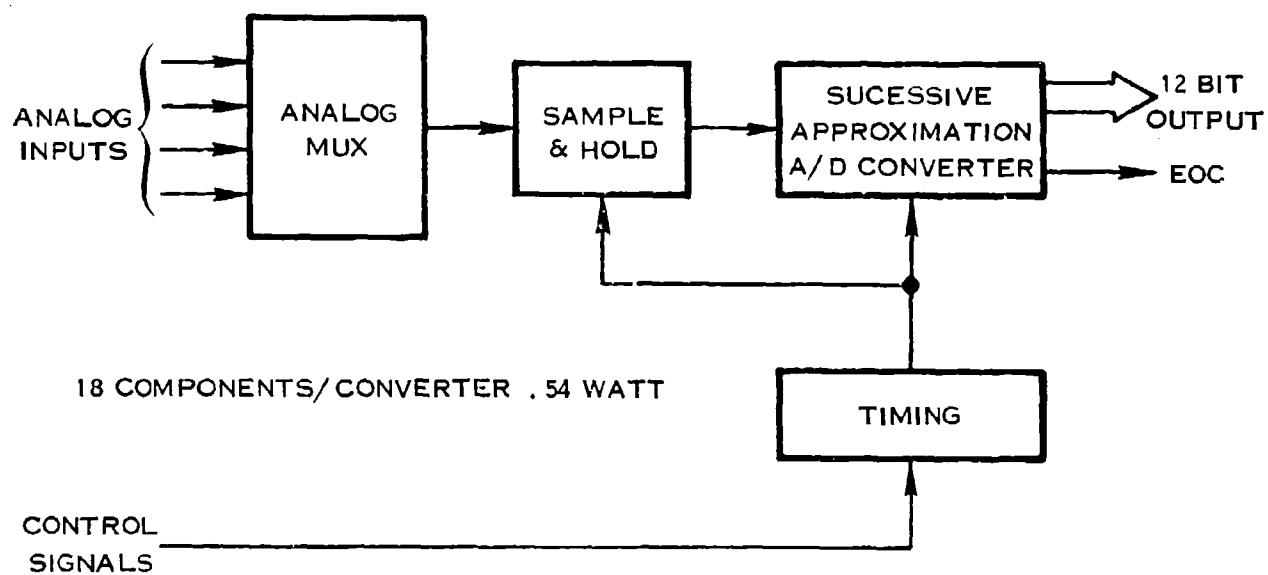
- a. R-C bridge to pulse width to UC to digital via A/D.
- b. R-C bridge to pulse width to digital.

TABLE A-2 SUMMARY A/D CONVERTER

	BASELINE TRIPLE RAMP	ALT # 1 TRIPLE RAMP N-CHANNEL	ALT # 2 SUCCESSIVE APPROX.
# Of Components	27	24	18
# Of Solder Joints	109	170	100
Board Area (In ²)	6.89/5.15*	6.45/3.96*	5/2.78*
Power (Watt)	.89	.97/.67**	.54
Custom I.C. Required	Yes	No	No
Digital Scaling	No	Yes	No
Mux Addressing	No	Yes	No
Self Test	No	Yes	No
Drift Correction	No	Yes	No
Range Check	No	Yes	No
Inherent Filtering	Yes	Yes	Yes

* Improvement with leadless carriers.

** Power reduction using CMOS μ Processor.



E- 5967

FIGURE A-26 SUCCESSIVE APPROXIMATION A/D ALTERNATE DESIGN #2

c. SIN θ and COS θ synchronous demodulation to DC followed by A/D.

d. SIN θ and COS θ precision rectification to DC followed by A/D.

Of the four conversion techniques mentioned above, the second and fourth were considered in these trades, since they will meet the six minute accuracy requirement with minimum hardware. A summary of the R/D trades is presented in Table A-3 at the end of this section.

A.3.3.1 R-C Bridge/Pulse Width to Digital R/D The operation of this resolver to digital converter is identical to the baseline RAEEC design described in Section A.2.3 with one exception: instead of the resulting pulse width gating precision 2 MHz clocks into a custom LSI chip, a standard programmable interval timer, LSI 8253, is used. This concept is referred to as alternate design #1 and is shown in Figure A-27.

A.3.3.2 Precision Rectification R/D This type of R/D converter is shown as alternate design #2 in Figure A-28. The resolver sine and cosine inputs are time multiplexed through a voltage follower, and then converted to a "0 to 10 Vdc" signal by a precision rectifier. This DC output is then converted to digital by an A/D, which in this case is the "Smart TripleRamp" A/D. This smart A/D has the advantage over other A/D's in that it can control its own resolver input multiplexing, perform its own built-in test, provide offset error correction if required, and provide fault isolation.

A.3.4 Resolver Excitation

In the alternate design trade studies, two concepts for resolver 7 Vrms sine-wave excitation were considered:

a. Custom monolithic design of the baseline excitation circuit.

b. State-of-the-art improvements to the baseline design.

Since only one or possibly two of these circuits are used per channel, it was considered uneconomical to convert this circuit to a custom chip. National Semiconductor is manufacturing commercial monolithic devices which with the addition of a few resistors and capacitors can be made into bandpass, band elimination, butterworth, etc., filters. It is conceivable that one of these components would replace the two stage tuned filter in the 1980's, once it became a militarized component.

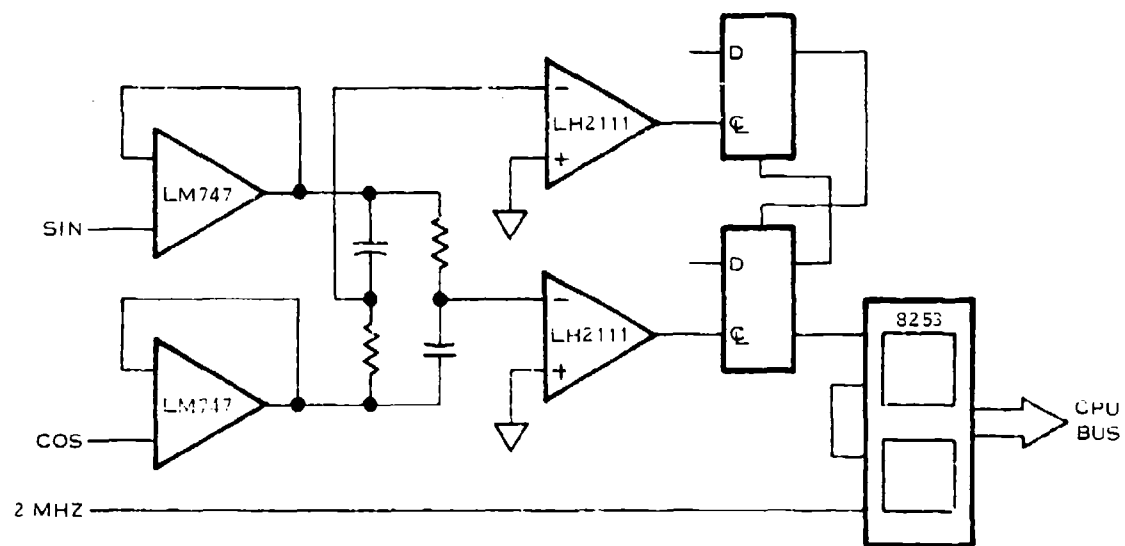
The only improvement which was feasible in the RAEEC time-frame was to replace the Motorola hybrid MC1538 with a monolithic Harris HA2635 driver as shown in Figure A-29.

TABLE A-3 SUMMARY R/D CONVERTER

	BASLINE RESOLVER TO DIGITAL CONVERTER	ALTERNATE # 1 R/D CONVERTER	ALTERNATE # 2 R/D CONVERTER
# Of Components	32	26	29
# Of Solder Joints	195	102	225
Board Area (In ²)	8.36 In ² /5.94*	5.00/4.12 In ² *	9.71/4.69 In ²
Power (Watt)	.33	.415	1.08/.8*
Custom I.C. Required	Yes	No	No
Drift Correction	No	No	Yes
Range Check	No	No	Yes
Digital Scaling	No	No	Yes
Mux Addressing	No	No	Yes
Self Test	No	No	Yes

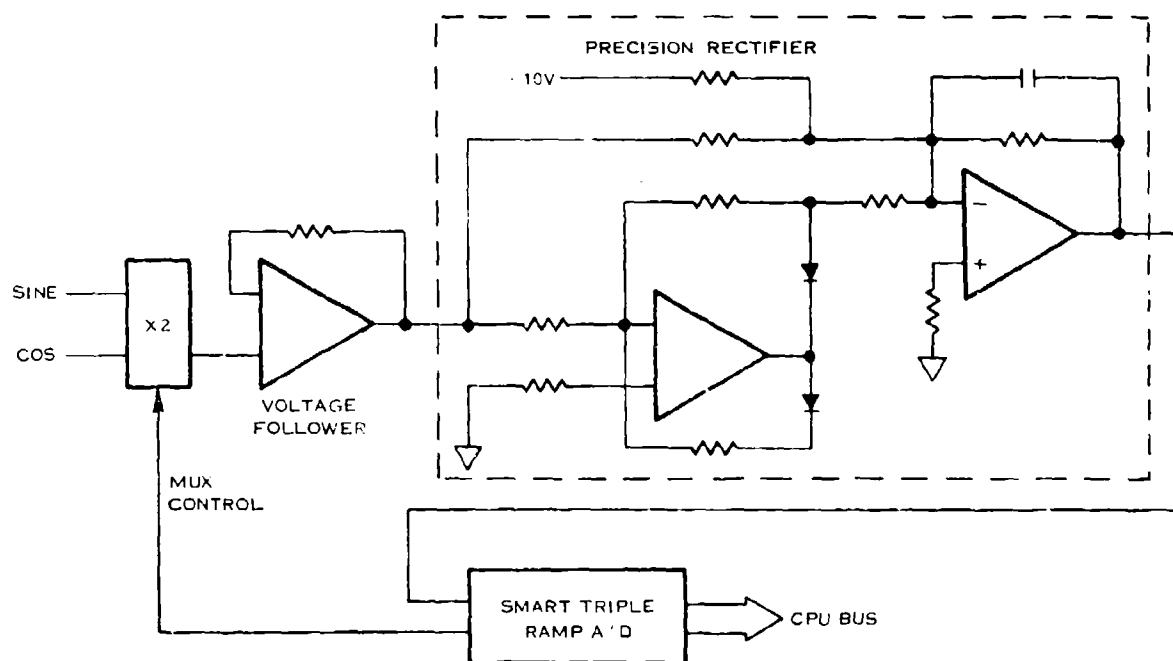
* Improvement using leadless carriers.

** Improvement using CMOS.



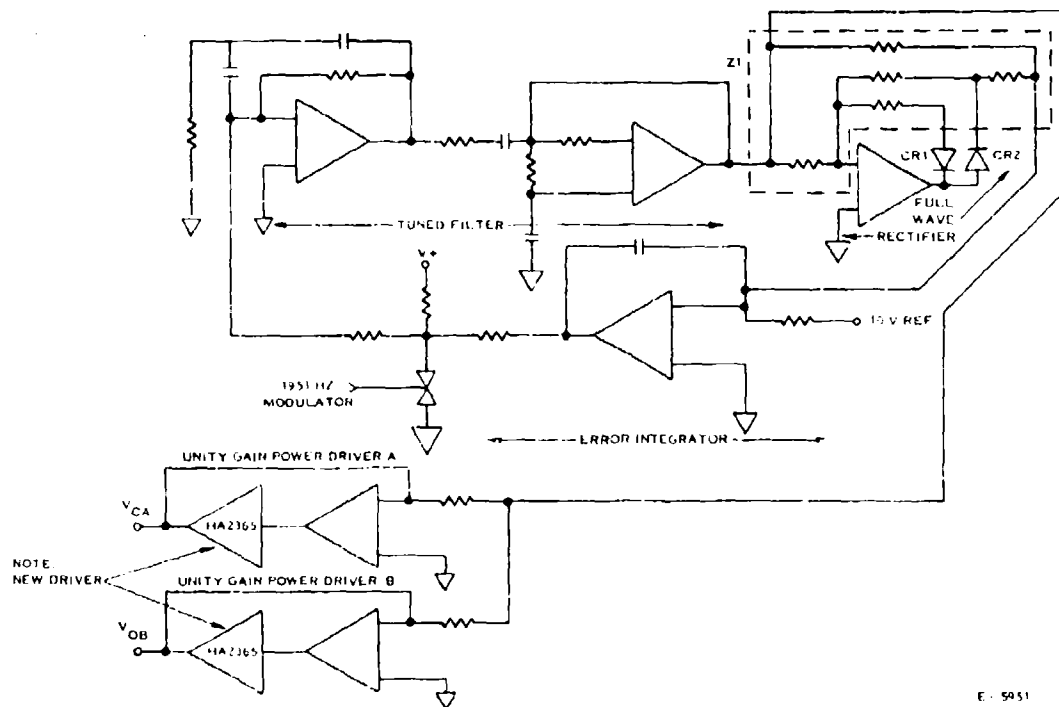
E-5966

FIGURE A-27 RESOLVER TO DIGITAL CONVERTER (ALTERNATE DESIGN #1)



E-6080

FIGURE A-28 RESOLVER TO DIGITAL CONVERTER (ALTERNATE DESIGN #2)



E-5951

FIGURE A-29 RESOLVER EXCITATION

A.3.5 Torque Motor D/A's and Drivers

This circuit is capable of driving a torque motor with an average DC current of 40 milliamperes using a pulse width modulation technique. Positive or negative pulses of 40 msec at a frequency of 50 Hz drive the torque motor. The duty cycle can vary from 0 to 100% with a granularity of 256 increments. A microprocessor controls 8 torque motor driver circuits. The microprocessor's task is to turn "on" and "off" either a +14 volt switch or a -14 volt switch at 50 Hz at the proper pulse width. All inputs and outputs of the microprocessor are buffered by latches because of the number of required I/O signals. The torque motor controller is a stand-alone circuit that is a slave to the central processor (Figure A-30 and Table A-4).

A.3.6 Solenoid Drivers

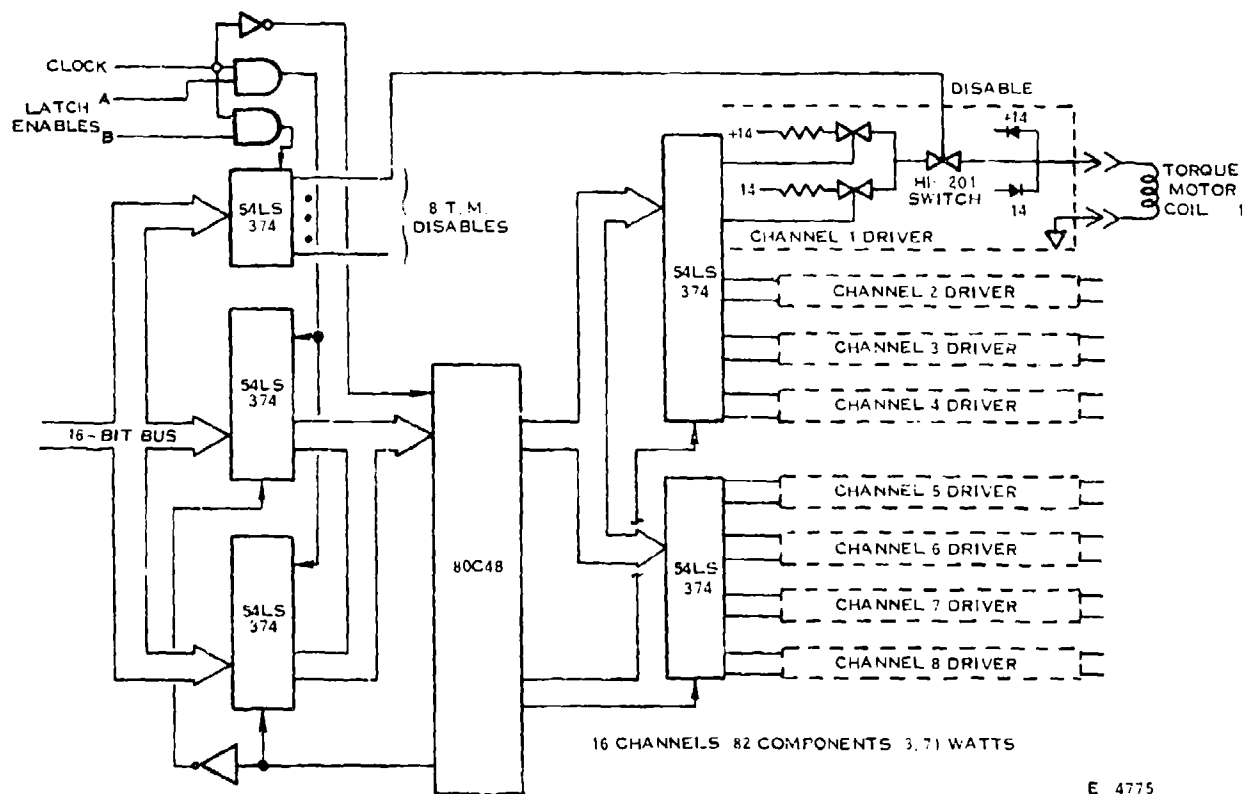
There are two alternate solenoid driver designs; alternate #1, corresponds with the "constant voltage alternator", and alternate #2 corresponds with the "constant current alternator" power system.

A.3.6.1 Alternate Design #1 Solenoid control data from the control CPU is stored in a TTL register (SN54LS164). This register will control 8 individual solenoids. When the output of the register is a logic "1" (5 volts), the solenoid will be activated by the power booster ULN-2804. The solenoid is powered by 20 preregulated volts from the power supply. The output state of the solenoid is monitored by a LM148 for fault detection (Figure A-31).

A.3.6.2 Alternate Design #2 Solenoid control data is loaded from the main CPU into a TTL holding register (SN54LS164). This register is capable of controlling 8 individual torque motor circuits. The output of the register controls a CMOS switch (HI-201). This switch applies current to the power amplifier, LM195, which activates the solenoid. The LM148 op-amp provides solenoid state information for fault detection (Figure A-32).

A.3.7 Pressure Sensors and Circuitry

As explained in Section 3.2.4.4, a full duplication of pressure sensors would not be practical from a reliability enhancement standpoint. A tradeoff study was carried out to determine if it is feasible to replace the twelve single pressure sensors with six quasi-redundant pressure sensor packages without significantly degrading RAEEC reliability. The most feasible configuration appears to be a pressure sensor with single cylinder and coils, but provided with dual oscillator circuits, PROMs, and temperature sensors. This study is described in Section 3.2.4.



E 4775

FIGURE A-30 TORQUE MOTOR DRIVER ALTERNATE DESIGN #1

TABLE A-4 SUMMARY TORQUE MOTOR DRIVERS

	BASELINE TORQUE MOTOR DRIVER	ALT # 1 TORQUE MOTOR DRIVER
# Of Components	175	82
# Of Solder Joints	1302	741
Board Area (In ²)	43.08/30.5*	32.8/12.8*
Power (Watt)	7.48	5.78/3.712**
Self Test	No	Yes

* Area saving by use of leadless carriers.

** Power saving by use of CMOS.

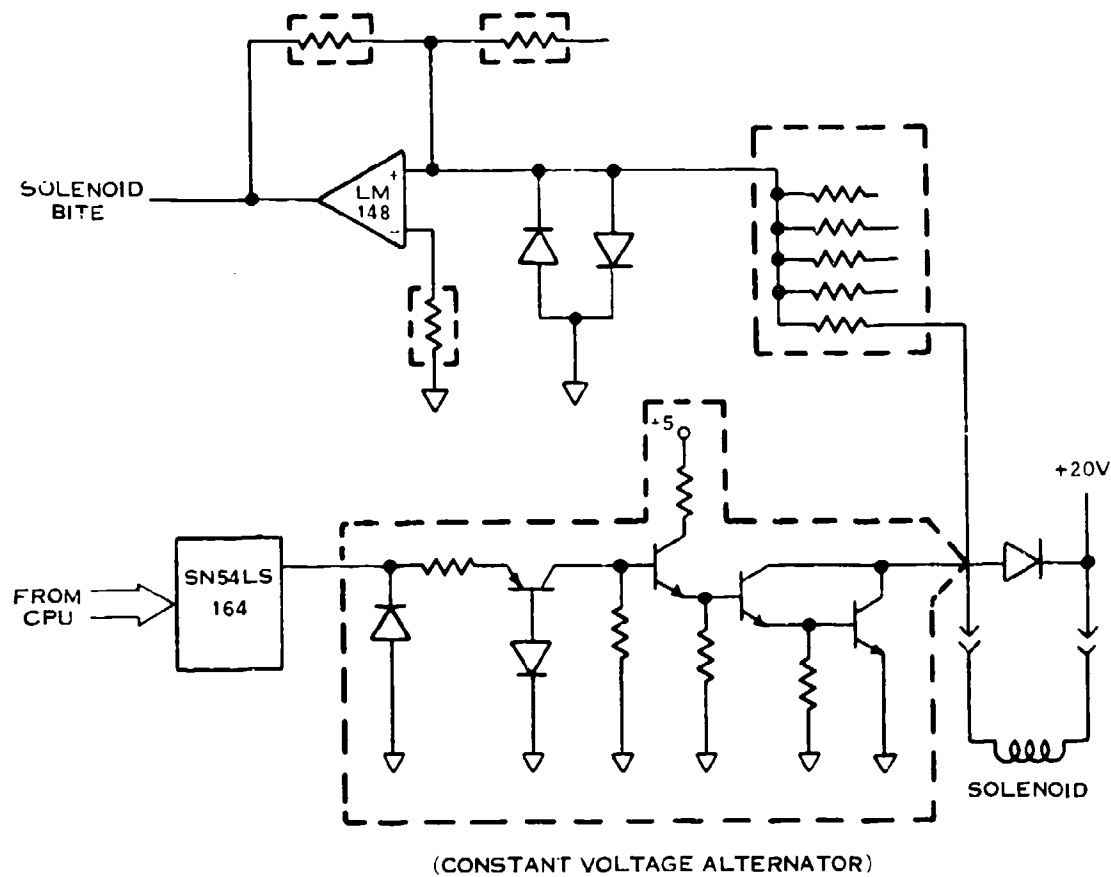
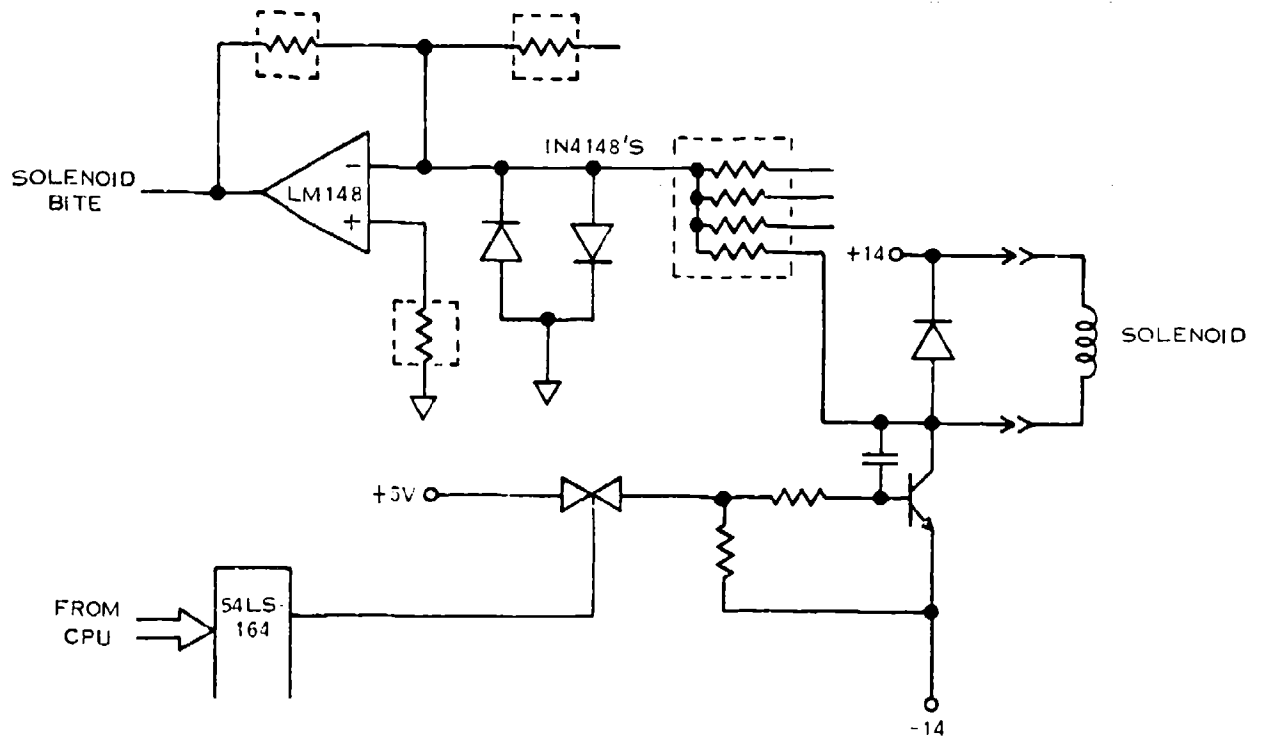


FIGURE A-31 SOLENOID DRIVER ALTERNATE #1



(CONSTANT CURRENT ALTERNATOR)

E-5684

FIGURE A-32 SOLENOID DRIVER ALTERNATE #2

The trade studies involved five oscillator circuit configurations which perform identically as described in Section A.2.7, with one exception; since six sensors are utilized by two RAEEC channels, each sensor and electronics now comprise:

1. Two independent 1N4850 diodes.
2. Two independent sensor characterization PROMs.
3. Dual, independently powered, fault tolerant, oscillator circuitry.

The concept of dual oscillator electronics is shown in Figure A-33. Note that with the isolation resistors (R) and capacitors (C), the surviving oscillator circuit will maintain proper sensor oscillations.

A.3.7.1 Oscillator The six different oscillator circuits are summarized in Table A-5. They employ varying degrees of thick film resistor networks, quad op-amps, discretes, and custom monolithic circuitry.

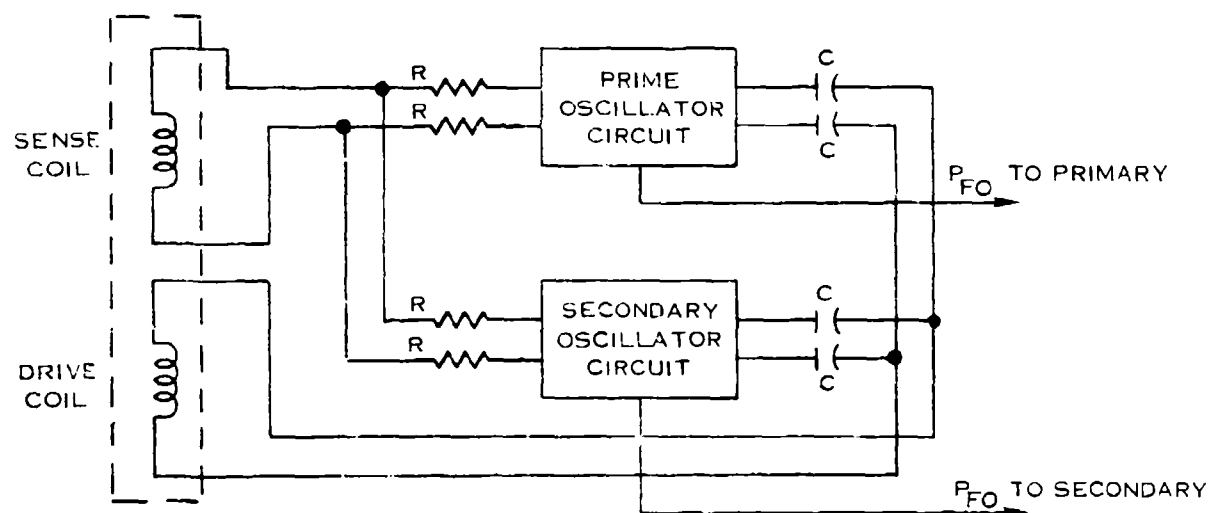
A.3.7.2 Sensor Frequency to Digital Converter The proposed frequency to digital conversion circuitry for the pressure sensors requires two thirds of a universal counter chip and one digital multiplexer. The multiplexer will gate one of two channels to the universal counter chip. The universal counter chip will be configured as a divide by N period counter which will be used to gate a high frequency clock into another sixteen bit counter, also contained on the N-channel counter chip (Figure A-34).

A.3.8 Low Level DC Interface

The proposed low level interface multiplexes four low level signals into a high impedance instrumentation amplifier. The signals are amplified to a 0-10V level and multiplexed along with the TBT signal into the analog-to-digital converter buffer. The buffer provides a higher current drive for the A/D converter. The circuitry is reduced by using multiplexers having internal protection (Figure A-35). Note that the primary RAEEC channel requires two of these interfaces, while the secondary requires only one.

A.3.9 Resolver Multiplexer

This resolver multiplexing scheme employs an improved CMOS technology known as dielectrically isolated CMOS. The selected multiplexing devices have internal protection which makes possible the elimination of considerable external protective hardware (Figure A-36).



E--5677

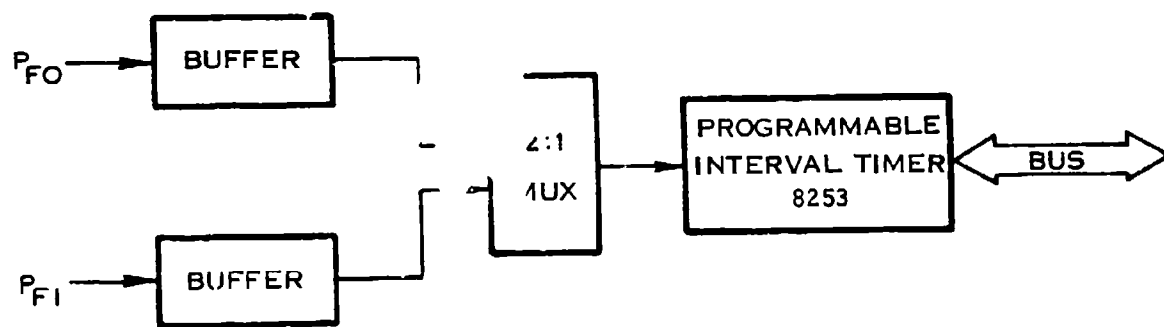
FIGURE A-33 PRESSURE SENSOR CIRCUITRY

TABLE A-5 RAEEC SENSOR TRADES

(PER SENSOR)

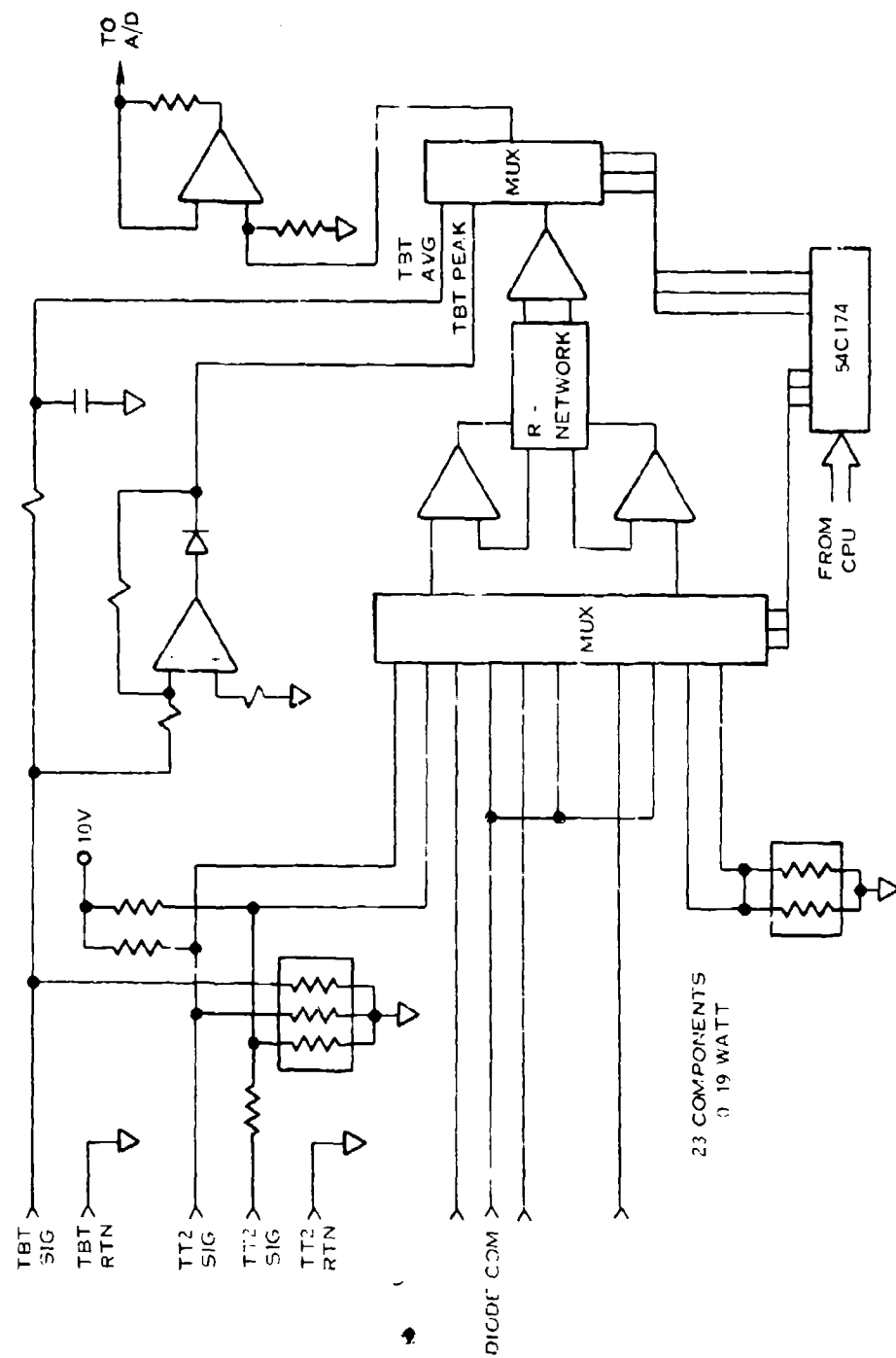
CIRCUIT DESIGN	# PARTS	POWER	AREA	RELIABILITY SCORE
Baseline	32 + 5.5 (37.5)	0.578	7.63	246
Navy ΔP Sensor Alt 1	21 + 3.65 (24.65)	0.555	3.73	300
EPR Sensor Alt 2	19 + 3.65 (22.65)	0.555	3.57	300
Custom Sensor I ² L Alt 3	9 + 0	0.500	1.89	264
Hybrid Navy ΔP Sensor Alt 4	8.5 + 3.65	0.555	2.44	215
Hybrid Gate Array I ² L Alt 5	1 Hybrid 2 Caps (40 Pin Pkg)	0.500	3.83 (No LCC)	205

NOTE: Discrete diodes cannot be grouped into one common package.



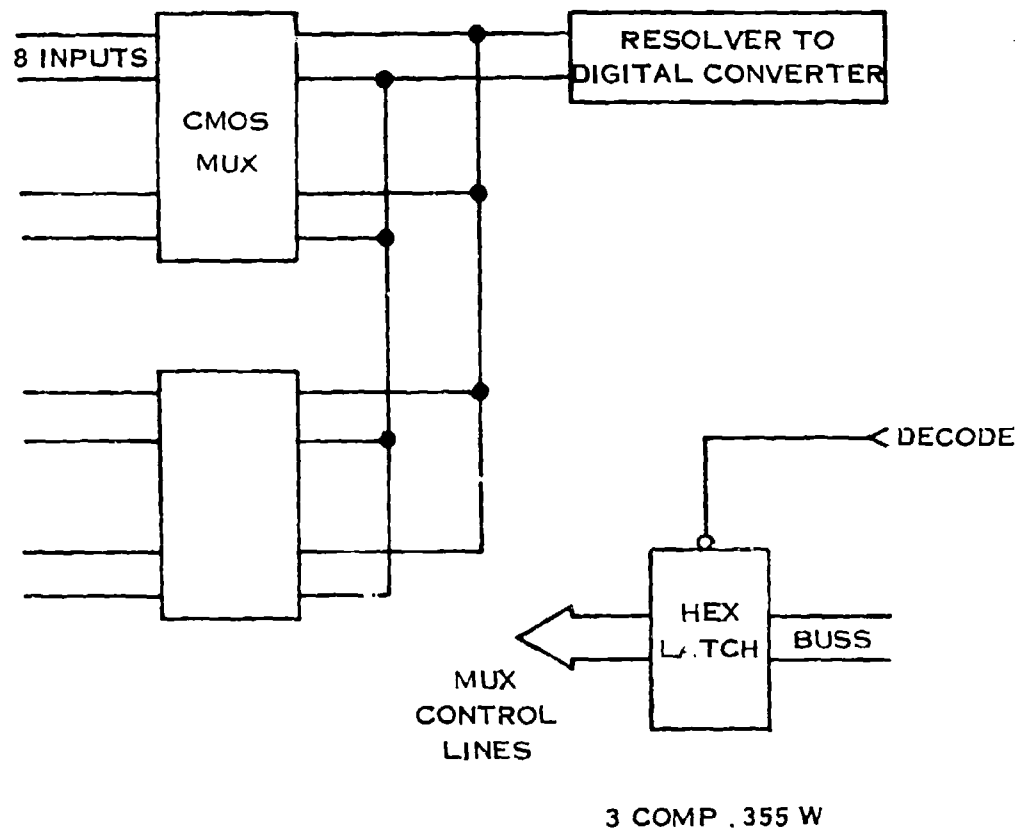
E-5679

FIGURE A-34 SENSOR FREQUENCY TO DIGITAL CONVERSION



E-5682

FIGURE A-35 LOW LEVEL INTERFACE



E- 5821

FIGURE A-36 RESOLVER MULTIPLEXER

A.3.10 Discrete Signal Conditioner Circuit

The proposed signal interface inputs three discrete switch closures, a LOD detector, and a serial data stream transmitting the mach number. The discrete switch closures are conditioned with a diode resistor network that provides well defined logic levels to the I/O ports of the 8041 universal peripheral interface. The 8041 is also used to read the serial data stream and transfer the mach number to the main CPU. The LOD detector output is rectified and used to charge a capacitor which is monitored by the A/D converter to determine if a "light off" condition is present (Figure A-37).

A.3.11 Frequency to Digital Speed Interfaces

The proposed speed circuit is an 8253 programmable counter to convert N_L and N_H frequency to digital information. The counter is configured as a divide by N counter which is used to enable a high frequency clock into a 16 bit counter also contained on the 8253. The signals are conditioned by using a quad comparator that converts to the proper logic levels internally. The comparators are provided with hysteresis to minimize the effects of noise on low frequency conversions. Diode protection is also provided to protect the comparator inputs from overvoltage transients (Figure A-38).

A.3.12 Turbo Pump Speed Interface

The proposed turbine pump speed interface inputs a pulse train from a magnetic pickup. The frequency of the pulses is proportional to the turbine pump speed. The pulses are converted to logic levels with a comparator and fed into a universal counter chip. This chip is programmed to count a specified number of periods and gate a high frequency clock into a self contained counter. The final count can be read by the CPU to determine turbine pump speed (Figure A-39).

A.3.13 Fault Detection Logic

The primary channel receives four fault signals from the secondary channel. The secondary channel also receives four fault signals from the primary channel. A buffer and peripheral resistors are used for each signal path to interface the two channels. The fault signal paths for both channels are of a CMOS design with the constraint that no input signals can be present when the system is not energized. The power supplies from the two channels are OR'ed and then fed to both fault detection logic circuits. This ensures that both fault detection circuits will be powered if either channel is powered, thus satisfying the constraint that no input signals can be present when the system is not energized (Figure A-40).

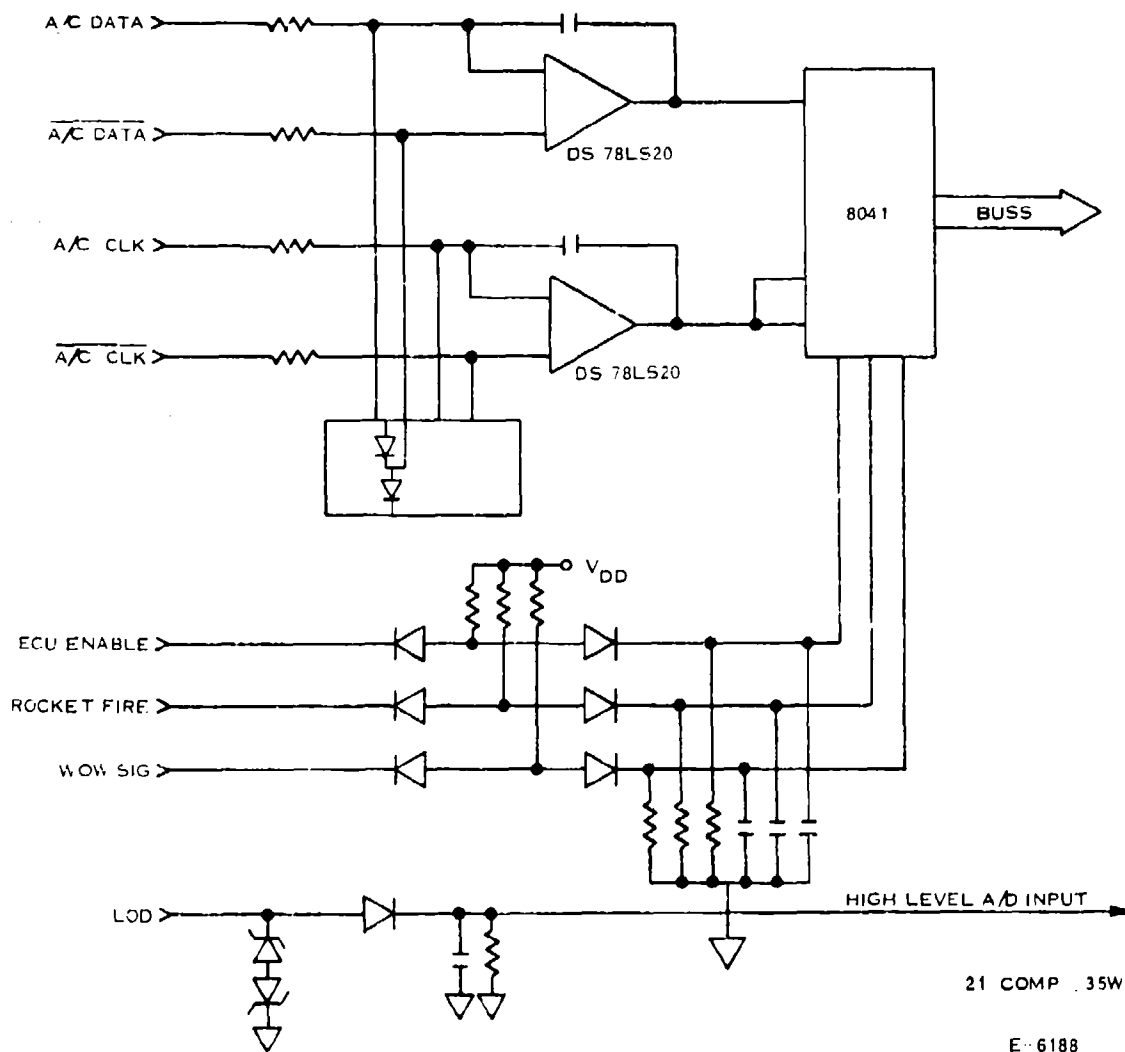


FIGURE A-37 DISCRETE SIGNAL CONDITIONER

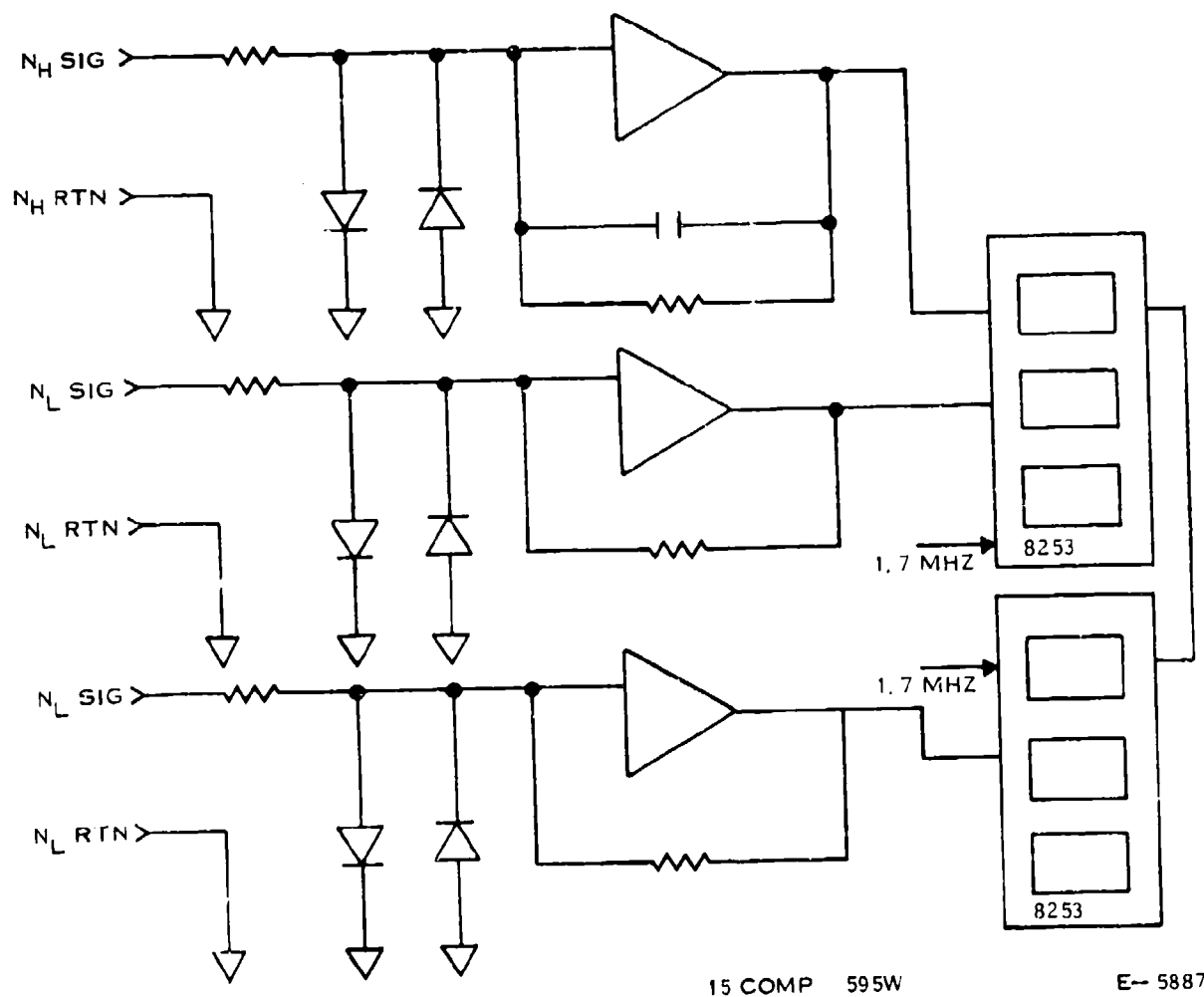
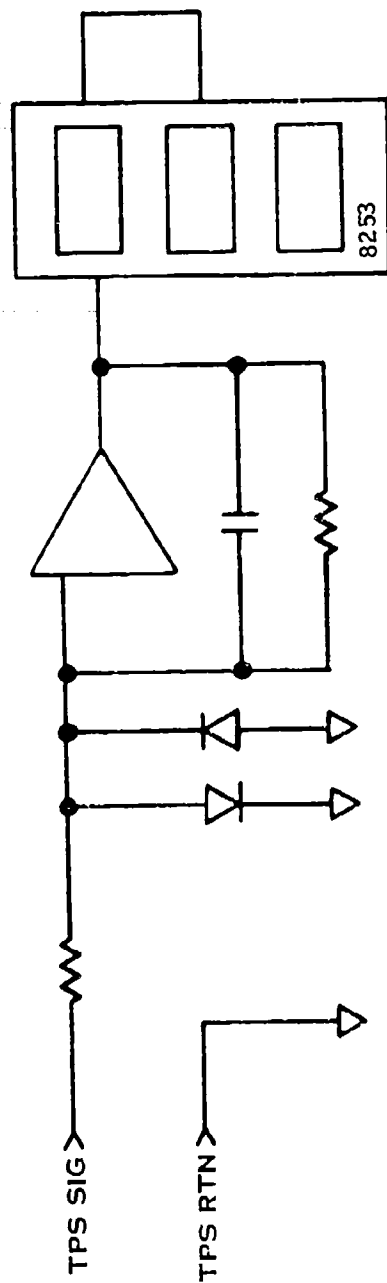
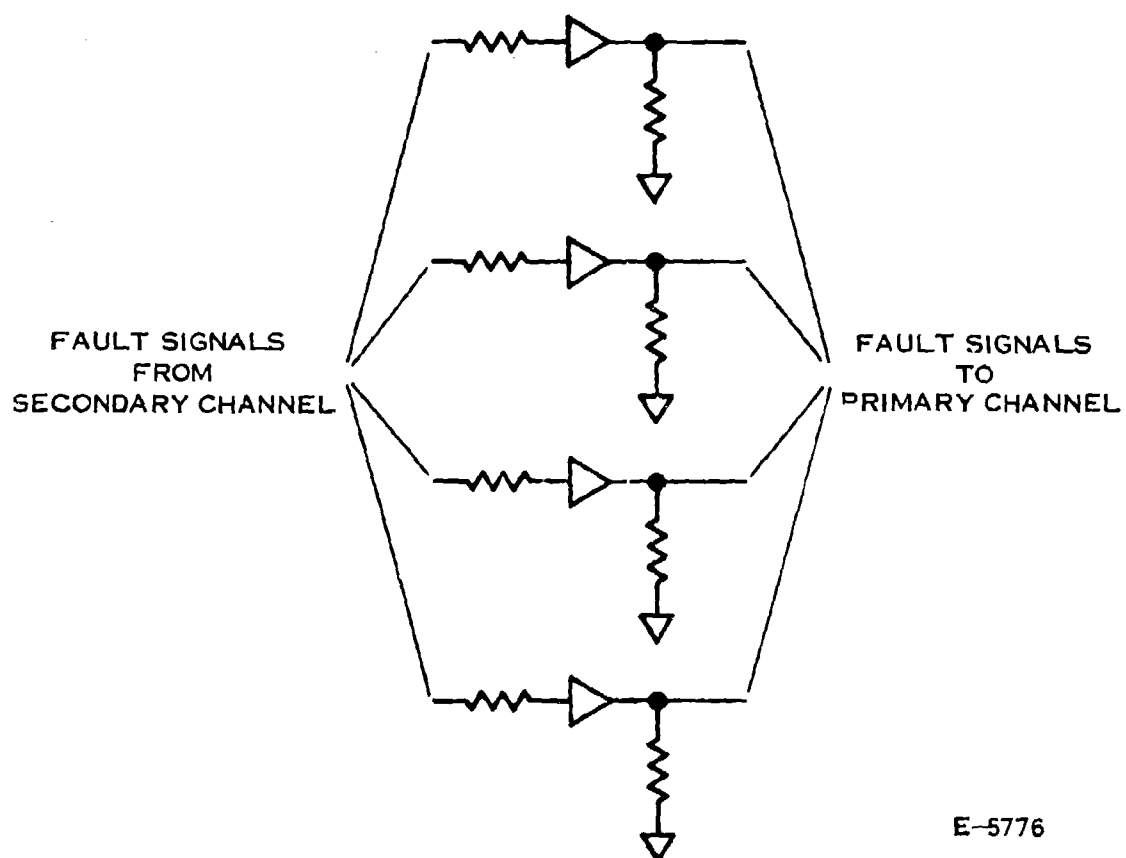


FIGURE A-38 SPEED INTERFACE



E-5868

FIGURE A-39 TURBINE PUMP SPEED INTERFACE



E-5776

NOTE: THE CIRCUIT IS REPEATED FOR THE OPPOSITE DIRECTION (FROM PRIMARY TO SECONDARY)

FIGURE A-40 FAULT DISCRETES

A.3.14 Power Supply System

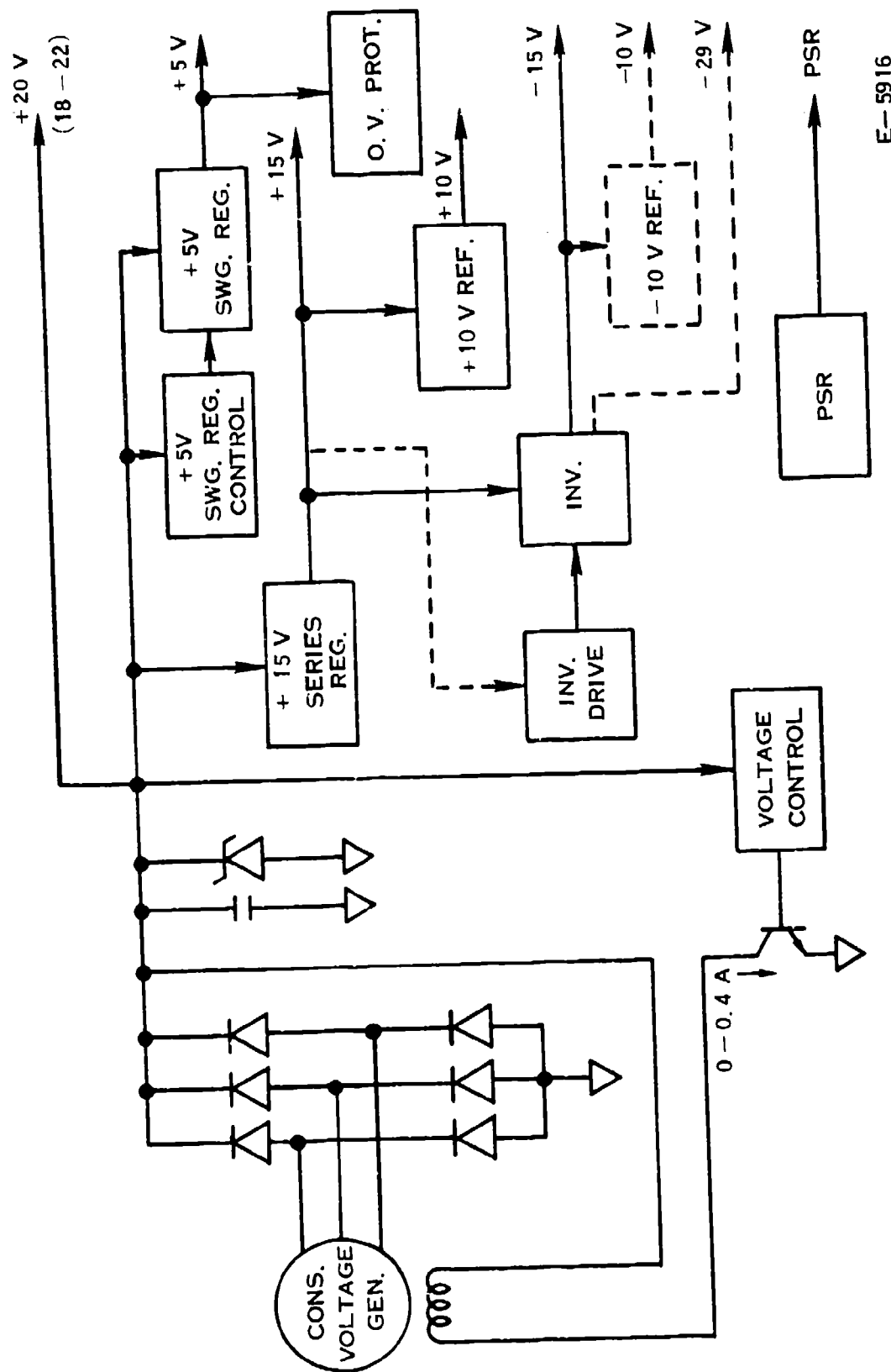
A.3.14.1 Alternate #1 The power source is a voltage controlled "flux switching" type alternator. Input power is rectified and capacitor filtered. The rectified voltage (20 Vdc) is sensed and compared with a reference. The resultant error signal is amplified and used to control the field of the alternator, thus maintaining a constant 20 Vdc from the alternator. The +20V is used to power all solenoids, the +15V regulator and the +5V regulator. The +5V regulator is a pwm switching type regulator. The +5V powers all of the logic and memory circuits. The +15V regulator is a series monolithic regulator. The +15V supplies the positive rail for analog circuits and torque motors, the +10V reference, and an inverter from which negative voltages are developed. The inverter is operated in sync with the +5V switching regulator to preclude any beat effects. Inverting action is accomplished through a transformer with transistor push-pull drive. -15V, and any other negative voltages that may be desired, are derived from the transformer secondary. -15V supplies the negative rail for analog circuits and torque motors.

A comparator monitors +5 for overvoltage and has authority to decrease the +20V bus if an overvoltage condition is detected. Three additional comparators monitor +5 for low voltage and +10 for high or low voltage. All four comparators have authority to generate a power supply reset (PSR) signal if voltage is out of tolerance (Figures A-41 and A-42 and Table A-6).

A.3.14.2 Alternate #2 The power source is a 3Ø permanent magnet, constant current alternator. Input power is rectified and converted to two constant voltages (+14 and -14) by two switching shunt regulators. These are "nondissipative" regulators. They control the voltage by pulse-width modulating the current. Input current is 3.3 to 4.0 ADC. Current not required by the load is switched to ground (shorted out). A bank of four capacitors supplies the load while the input is shorted. When the short is removed, the capacitors are recharged through a clamp diode.

+ 14V is utilized by the effectors and analog circuits. +5V for the logic and memory circuits is derived by a monolithic series regulator powered off the +14V bus. +10V for the analog circuits is developed from +14V by means of a precision reference device.

A comparator monitors +5 for overvoltage and has authority to decrease the +14V regulator if an overvoltage condition is detected. Three additional comparators monitor +5 for low voltage and +10 for high or low voltage. All four comparators have authority to generate a power supply reset (PSR) signal if voltage is out of tolerance (Figure A-43 and Table A-6).



E-5916

FIGURE A-41 POWER SUPPLY BLOCK DIAGRAM ALTERNATE #1

TABLE A-6 POWER SUPPLY REQUIREMENTS

<u>Power Supply Load Rating</u>				
	<u>Baseline Design</u>	<u>Alternate #2</u>	<u>Alternate #1</u>	
+5V	.65A	.90A	.90A	
+10V	.45A	.015A	.015A	
+14V/+15V	1.90	2.08A	.30A	
-14V/-15V	3.00A	3.00A	.40A	
+20V	-	-	3.10A	
<u>Typical Power Dissipation*</u>				
	<u>Baseline Design</u>	<u>Design #2</u>	<u>Design #3</u>	
Input Bridge	7.00W	7.00W	3.40W	
Alt. Volt. Control Crt.	-	-	3.40W	
+15V Series Reg	-	-	4.68W	
Inverter & -15 Supply	-	-	1.50W	
+14V Shunt Reg	35.50W	4.40W	-	
-14V Shunt Reg	41.30W	4.40W	-	
+10V Reg	1.60W	0.10W	0.10W	
+5V Reg	5.20W	7.20W	1.75W	
PSR/OV	.10W	.10W	0.10W	
LOD in Standby	0	.10W	0.10W	
Power Supply Sub Total	<u>90.70W</u>	<u>23.30W</u>	<u>15.53W</u>	
EEC Digital	6.1	4.0	4.0	
Analog	5.95	5.75	6.15	
Drivers (Series Prop)	3.0	3.0	3.35	
Total Non P/S	<u>15.05W</u>	<u>12.75W</u>	<u>13.50W</u>	
Total EEC	<u>105.75W</u>	<u>36.05W</u>	<u>29.03W</u>	
Secondary	<u>105.75W</u>	<u>36.05W</u>	<u>29.03W</u>	
Grand Total	211.50W	72.10W	58.06W	

*Assumptions used in typical power dissipation above:

TABLE A-6

Typical Power Dissipation* (Continued)

	<u>Baseline Design</u>	<u>Alternate #2</u>	<u>Alternate #1</u>
14V Solenoids @.4A	1	1	0
20V Solenoids @.3A	0	0	3
28V Solenoids @.2A	2	2	0
Torque Motors .05A/.15A	+14V/-14V	+14V/-14V	+15V/-15V
Analog Load .2A/.2A	+14V/-14V	+14V/-14V	+15V/-15V
+10V Load	.35A	.015A	.015A
+5V Load	.55A	.8A	.8A

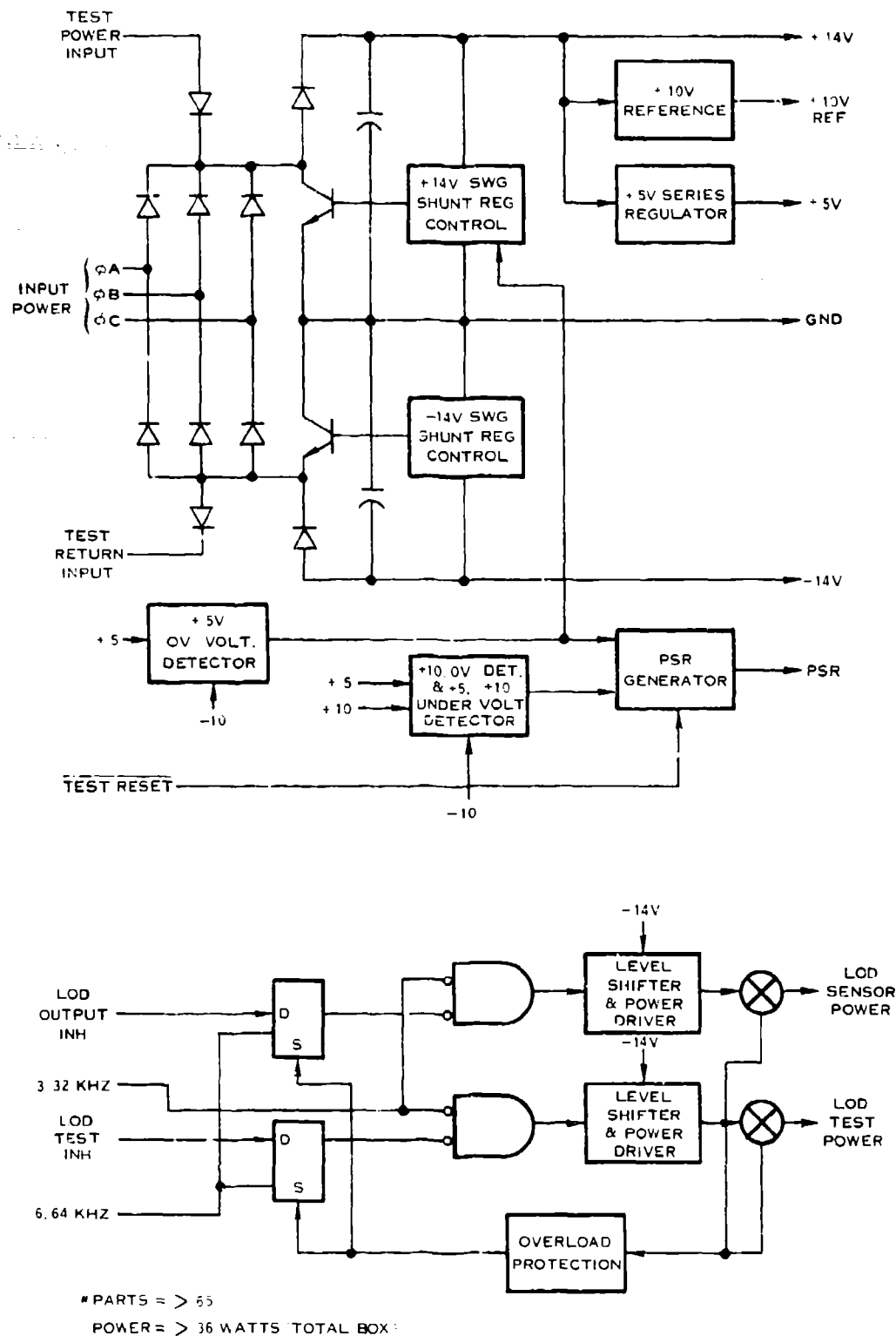


FIGURE A-43 POWER SUPPLY BLOCK DIAGRAM ALTERNATE #2

E-5758

A.3.15 Central Processor

The RAECC Central Processor is seen as a complex function comprising the Processor, the RAM, the ROM, the test UART, and the Dual-Port RAM. The following paragraphs describe the detailed trade studies performed on each of the aforementioned five functions.

A.3.15.1 Processor Trades The study was divided into detailed studies of three different computer architectures which could be designed into fuel controls. They are:

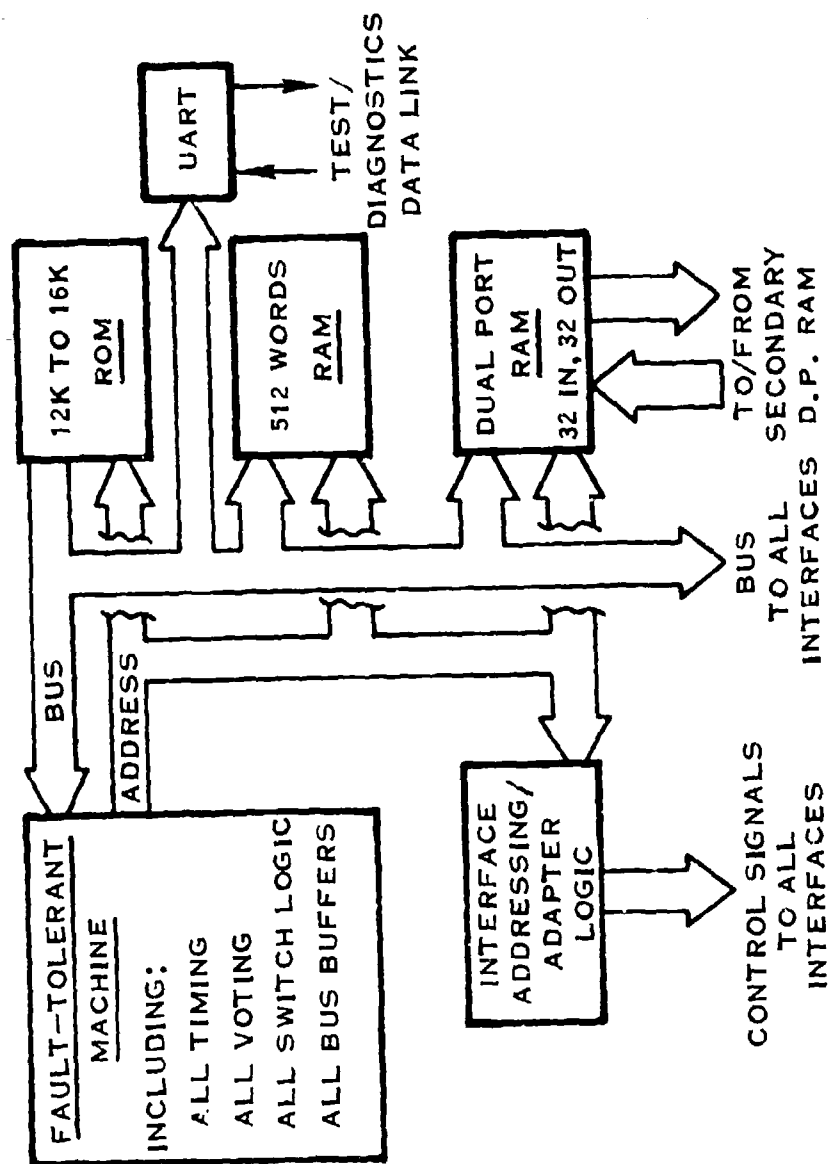
- a. A fault-tolerant "SISD" machine (Figure A-44).
- b. A "Multiple Instruction Multiple Data" (MIMD) parallel processing machine comprising two or more off-the-shelf 16-bit microprocessors, each μ -processor with its own RAM and ROM (Figure A-45).
- c. A "Single Instruction Single Data" (SISD) or "Single Instruction Multiple Data" (SIMD) simplex machine. (Figure A-46).

It was first determined that each of the above architectures met the instruction throughput requirements of at least 450 thousand operations per second (450 KOPS). This benchmark was generated from a "Fuel Control Instruction Mix" (based on Hamilton experience), operating at a 18 millisecond loop update time, with 2.7ms spare.

A detailed parts list was generated for each of the "blocks" of the three block diagrams so that area, power dissipation, number of components and reliability improvement could be traded off on a block by block basis.

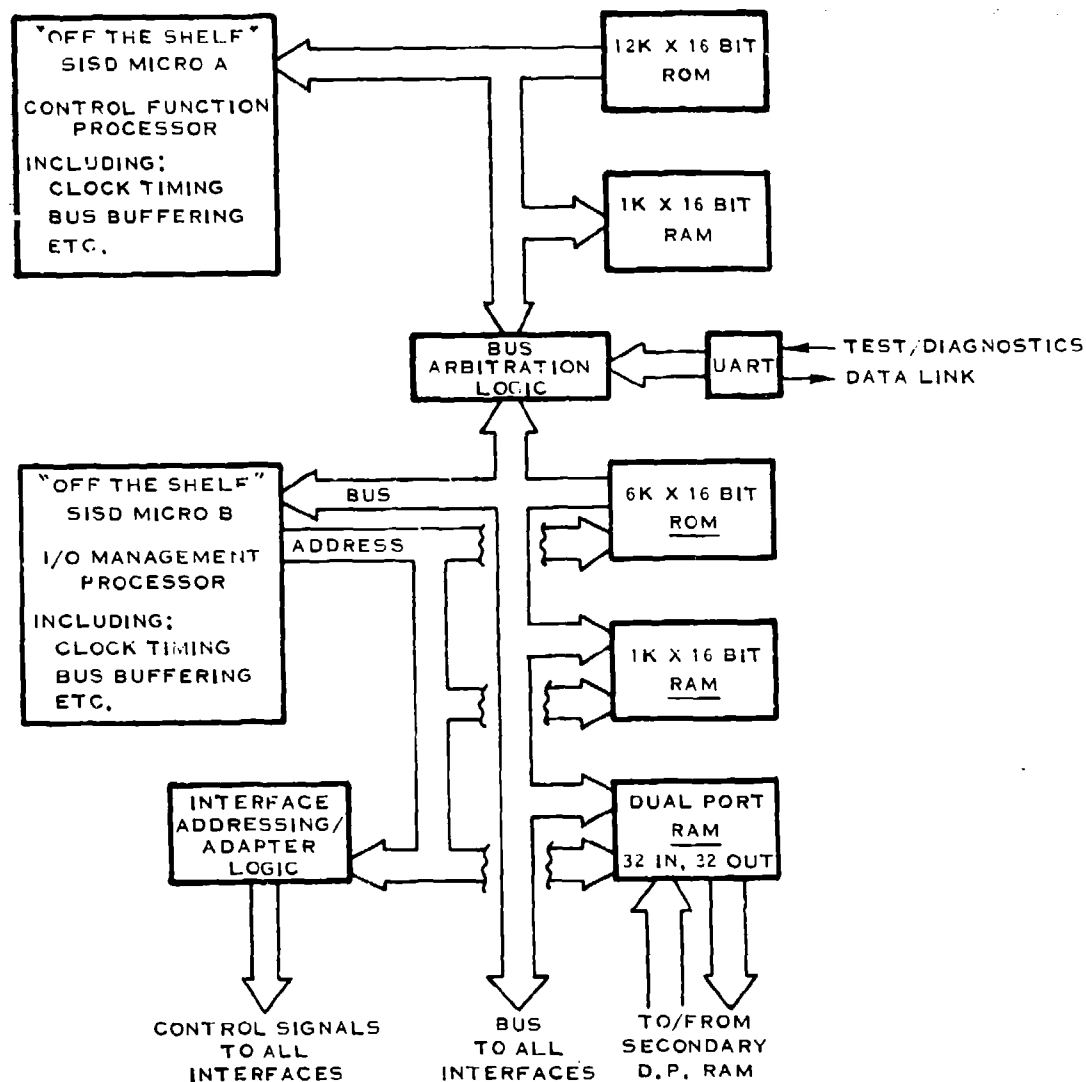
Triple Redundant Machine Architecture

The fault-tolerant TRD machine architecture shown in Figure A-47 is based on the "2901" bit slice, since the "2901" is well known in the military arena. In order to provide a parts list for this system, a design for a simple-simplex 2901 machine was generated and then scaled up by a factor of 4.12. This ratio was determined from the 210 components utilized by the G.E. self diagnosing fault tolerant microprocessor (Reference 10) (SDFTP), divided by 51 components required for a simple-simplex "2901" machine; i.e., $210/51 = 4.12$. In this way, a 12.39 in² 11.65 watt simplex machine was ratioed into a 51 in² 47.96 watt TRD machine.



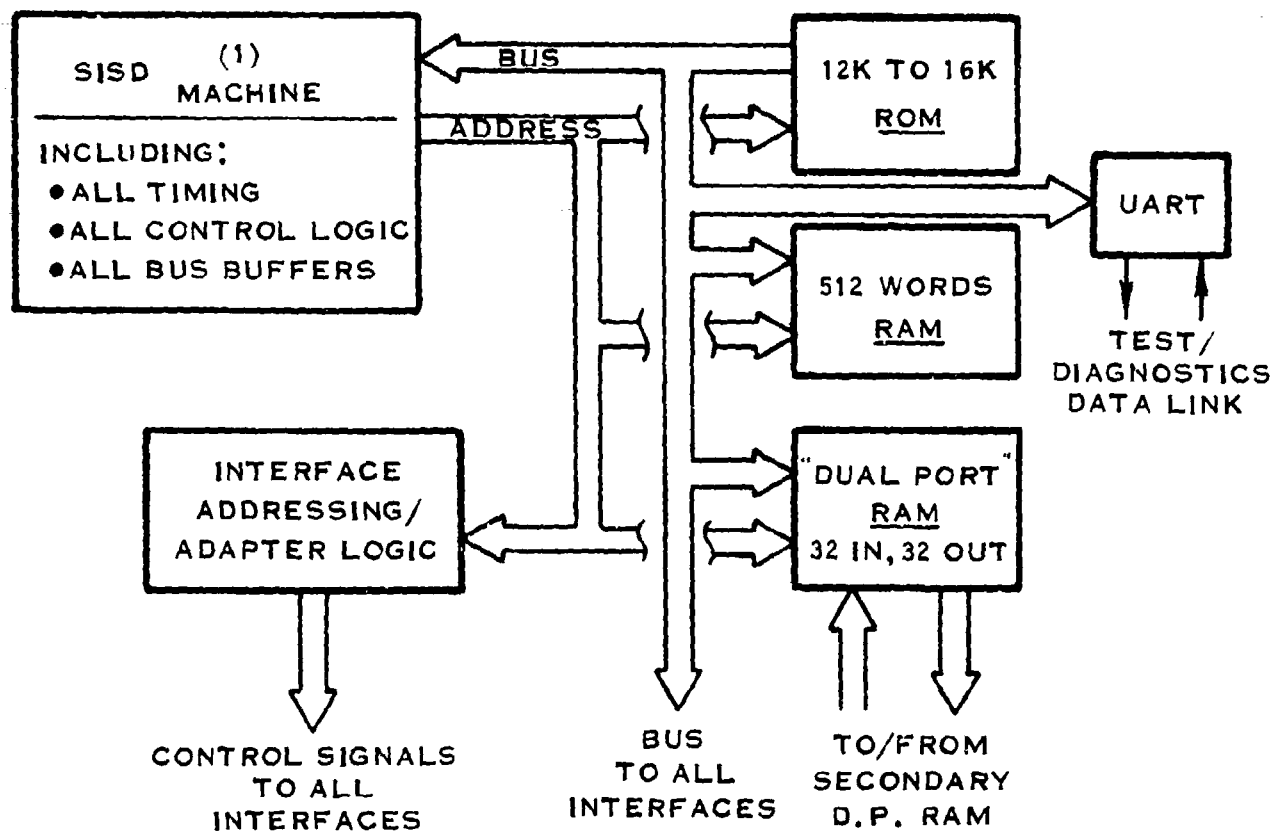
E-2235

FIGURE A-44 RAEEC CPU BLOCK DIAGRAM (FOR FAULT-TOLERANT MACHINE ARCHITECTURES)



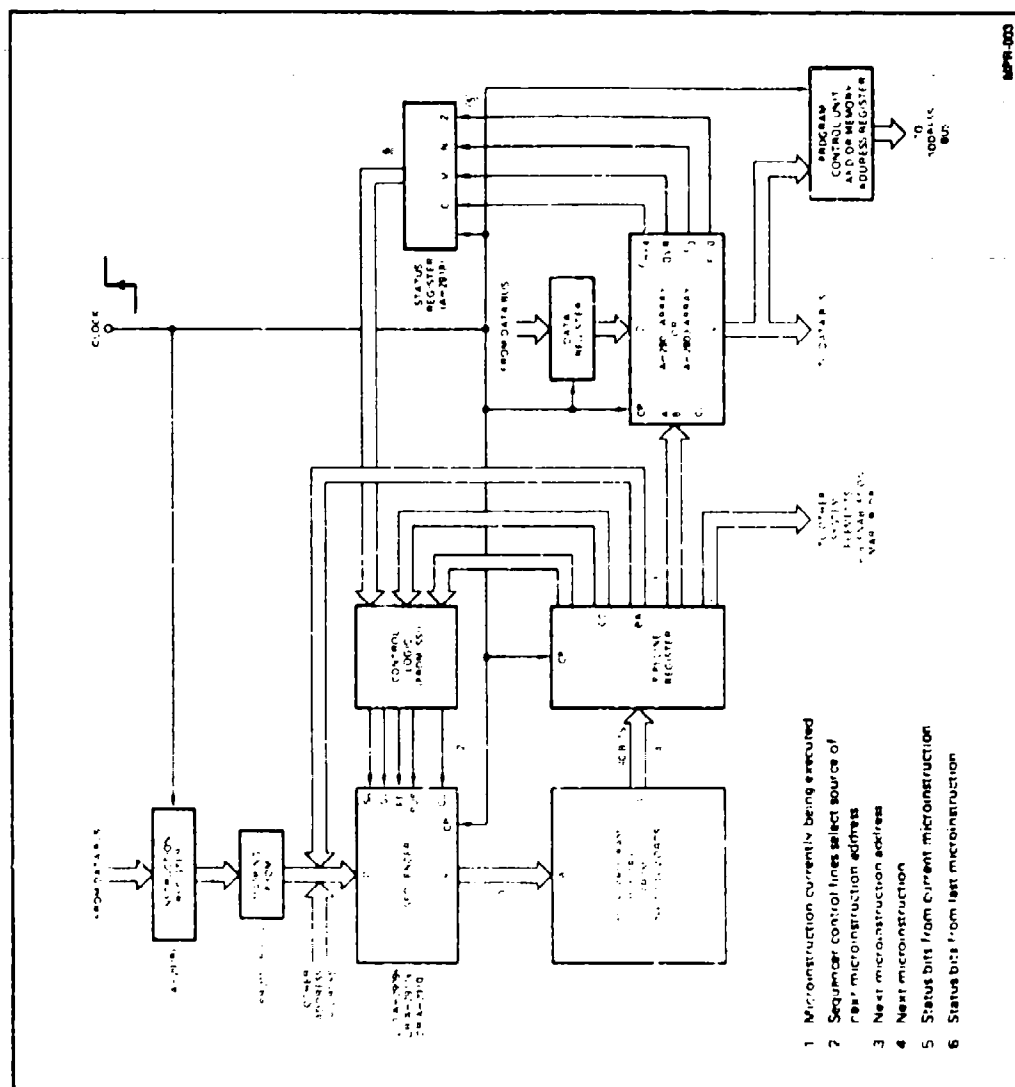
E-2232

FIGURE A-45 RAECC CPU BLOCK DIAGRAM (FOR A PARALLEL MULTIPLE INSTRUCTION MULTIPLE DATA MACHINE ARCHITECTURE)



E-2233

FIGURE A-46 RAEEC CPU BLOCK DIAGRAM (FOR SINGLE INSTRUCTION SINGLE DATA OR "SINGLE INSTRUCTION MULTIPLE DATA" MACHINE ARCHITECTURE)



**FIGURE A-47 FAULT TOLERANT 2900 IS 4.11 TIMES THE MINIMAL
AMD 2900 BIT-SLICE MACHINE**

E-2641

Another fault tolerant machine worthy of mention is the "USAF Fault Tolerant Computer" which was presented at the 1978 Government Microcircuits Applications Conference (GOMAC). This machine, shown in Figure A-48, comprises four processors, two of which are power strobed off, one which is running the system control task, and one which is monitoring the controlling processor. Even though this "machine" chose low power SOS CMOS for its technology (which provided a RAD-hard process), it wasn't seriously considered for the RAEEC task, due to its high parts count and relatively slow 200 KOPS instruction rate. (This rate might be substantially higher for a fuel control instruction mix, however).

Multiple Processor Architecture

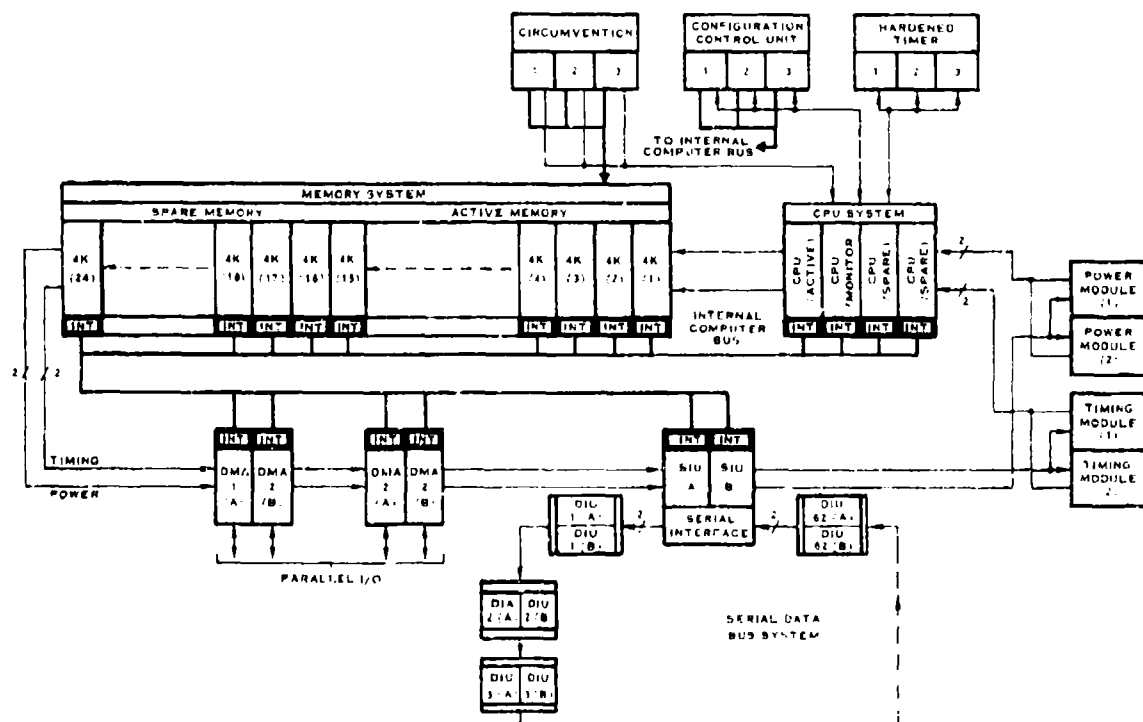
The multiple processor, "Multiple Instruction Multiple Data" architecture shown in Figure A-45, is seen as an extremely viable alternative to systems houses which are unable to locate a military single chip processor with enough throughput. The parts lists for this system were based on two Intel 8086 16-bit machines, since it is expected that the 8086 will eventually become full-MIL-Spec devices, (preliminary test data shown in Figure A-49 indicates full mil possibilities). It can be shown that an 8086 executing a fuel control instruction mix, will conservatively execute at approximately 325 thousand operations per second. Since approximately 40% of the fuel control program is dedicated to I/O handling, it appears that one good architecture partition is: A dedicated I/O processor handling 40% of the total task, and a dedicated control processor handling 60% of the total task. (This architecture is also known as "loose coupled parallel processing".) In order to indicate the effective performance of two 16-bit μ -processor, the following scenario is developed:

Desired throughput goal: 450 KOPS and 18ms loop update time, which allows 8100 words to be executed in 18 milliseconds.

If there is a 40/60 split in task, plus an overhead of 100 words for intra- μ -processor communications, then $I/O = 8100 \times .4 + 100 = 3340$ words for the I/O processor. $Control = 8100 \times .6 + 100 = 4960$ words for the controls processor. Since most of the I/O software comprises "LOAD", "ADD", "STORE" and "MOVE" instructions, it can be assumed that a "GIBSON-MIX" of instructions will be executed, and for the sake of argument let us assume that this " μ -P" can execute this mix at a 400 KOP rate. Then an I/O cycle can be executed in $3340/400$ KOPS or 8.35 milliseconds.

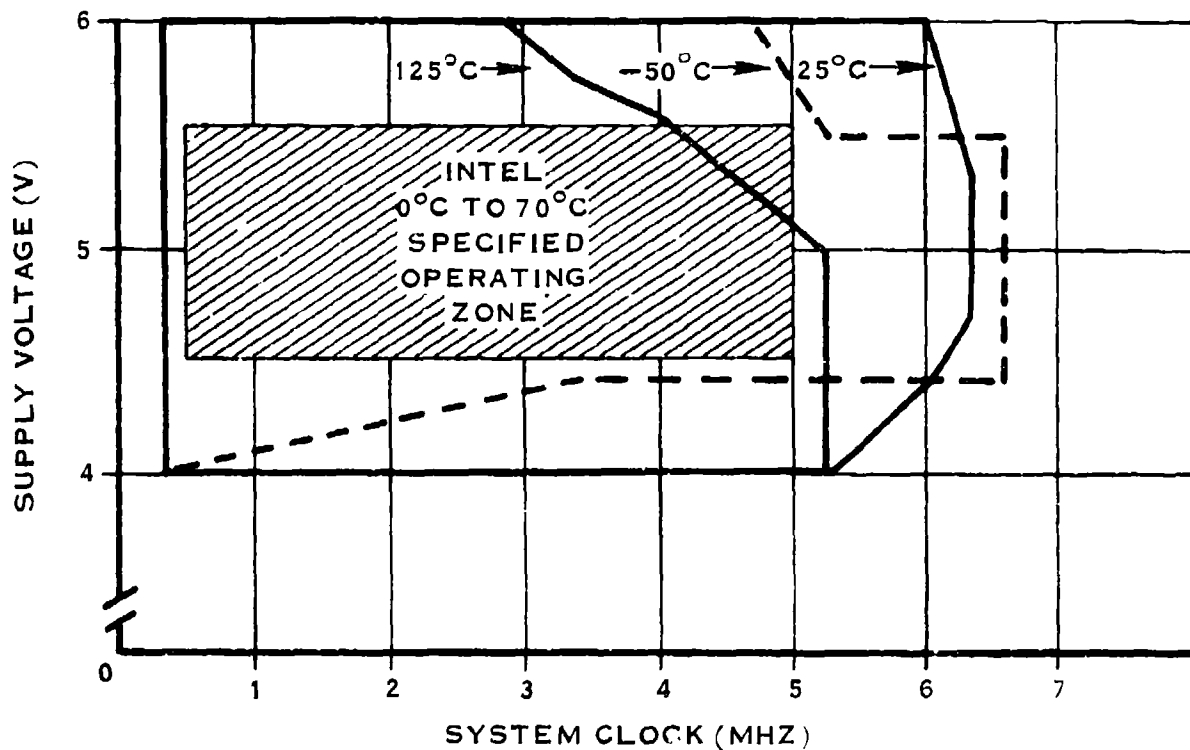
It is expected that the controls portion of the fuel control program will look more like the NASA mix of 80% short instructions, and 20% multiply, divide and other long instructions. Again for the sake of argument let us say that this " μ -P" can execute this mix at a 300 KOP rate. Then a control cycle can be executed in $4960/300$ KOPS or 16.53 milliseconds.

TYPE	GENERAL-PURPOSE, STORED PROGRAM, PARALLEL, DIGITAL COMPUTER
DATA FORMATS	FIXED POINT 32-BIT BINARY 2 S COMPLEMENT INTEGER FLOATING POINT 24-BIT BINARY 2 S COMPLEMENT MANTISSA 8-BIT BINARY 2 S COMPLEMENT EXPONENT 95, INCLUDING, INTEGER, FLOATING POINT AND VECTOR
ADDRESS MODES	REGISTER-REGISTER INDEXED AUTO INCREMENT DIRECT IMMEDIATE INDEXED AUTO DECREMENT DIRECT DIRECT INDEXED DIRECT INDIRECT INDEXED INDIRECT
CONTROL REGISTERS	CENTRAL MICROPROGRAMMED CONTROL UNIT EIGHT GENERAL-PURPOSE 32-BIT REGISTERS THAT SERVE AS ACCUMULATORS, INDEX REGISTERS, OR ADDRESS POINTERS
INTERRUPTS	10 INTERRUPT LEVELS
MEMORY	UP TO 60K WORDS OF ADDRESSABLE PROGRAM MEMORY
THROUGHPUT	200K OPERATIONS PER SECOND (SPECIFIED MIX)



E-2649

FIGURE A-48 FAULT TOLERANT SPACEBORNE COMPUTER (FTSC) CHARACTERISTICS AND BLOCK DIAGRAM



E-267 5

FIGURE A-49 8086 TEST DATA VOLTAGE-FREQUENCY-TEMPERATURE CHARACTERISTIC

In the above discussion, it was shown that two microprocessors could perform their tasks in parallel in under 18 milliseconds; i.e., the I/O machine can perform its task in 8.35ms, and the controls machine in 16.53ms. In order for 16.53ms to become the worst case loop delay, the I/O machine must be synchronized to the controls machine, otherwise the worst case loop delay could result in the sum of the two processing loops, 16.53 plus 8.35 = 24.88. If the I/O μ -processor is properly synchronized, then the resulting effective throughput could be 8100 words/16.53 or 490 thousand operations per second.

The "Full-Up" twin 8086 parts list indicated that the two processors only dissipated approximately 6 watts; however, in order to achieve the required performance, several high power LSI and MSI devices were necessary to make the processor complement of RAM, ROM, bus controllers, etc., operate properly. A second design was then completed which had the objective of minimizing support LSI, and maximizing the utilization of CMOS and low power Schottky MSI. Table A-7 indicates the results of these two trades; the utilization of off the shelf low power logic resulted in a reliability improvement, but unfortunately, also resulted in a marked degradation in performance.

SISD Processor

The field of Single Instruction Single Data (SISD) military 16-bit microprocessors which meet the 450 KOPS throughput requirements at the time of this writing are limited to the three known bit-slice machines, and to the special purpose, system house proprietary, custom machines.

Bit-Slice Processor

Of the three well known bit slice machines (Intel 2-bit slice, MMI 4-bit slice and AMD's 4-bit slice), the most widely accepted and multiple sourced is the AMD 2900 4-bit slice family. The "minimal" machine shown in Figure A-50 comprises 51 components and dissipates approximately 11.7 watts, but easily meets the 450 KOPS throughput requirement. In fact, this machine will probably execute a fuel control instruction mix in excess of 700 KOPS in this minimal configuration, utilizing MOS RAM and ROM. Please refer to the summary shown in Table A-8.

Custom Processor

Several system houses, including Hamilton Systems Division of Hamilton Standard, have been forced into the development of their own proprietary custom processors in order to provide a military, competitive, minimum component, low power machine with adequate performance. Hamilton Standard has designed its own CMOS Silicon-on-Sapphire processor to meet the system needs of the 1980's as

TABLE A-7 RAECC MIMD TRADES

	TWIN 8086			TWIN 8086		
	FULL SPEED/SCHOTTKY	MIN POWER W/CMOS		WATTS	AREA	REL
	WATTS	AREA	REL	WATTS	AREA	REL
PROCESSORS	3.88	7.51	112	3.88	7.51	112
RAMS	3.2	3.24	305	.2	2.55	305
PROMS	1.2	3.58	166	1.2	3.58	166
TEST UART	.51	1.95	286	.07	2.06	282
I/O ADDRESSING/BUS ARBITRATION	5.48	2.90	206	1.37	3.48	266
DUAL PORT	2.63	3.34	172	.48	4.63	228
TOTALS	16.9 WATTS	22.52 IN ²	1247	6.0 WATTS	23.81 IN ²	1359

NOTE: THE TWIN 8086 WITH CMOS (6 WATT TOTAL) MUST RUN 15% SLOWER AND IS THEREFORE DISQUALIFIED, SINCE IT WILL NOT MEET THE 450 KOP MINIMUM

TABLE A-8 SINGLE INSTRUCTION SINGLE DATA CPU DESIGN TRADEOFFS

ARGUMENT	BASELINE 5 CHIP HS 16/24	3-CHIP HS 16/24	MINIMAL "2900" BIT SLICE MACHINE
# OF COMPONENTS	22 1/4	12	51
# OF SOLDER JOINTS	427	264	826
BOARD AREA (IN ²)	24.4 (8.14*)	10.0 (5.13*)	31.2 (12.39*)
CUSTOM LOGIC	YES	YES	NO (u-prog in proms)
MAX THROUGH-PUT	390 KOPS	>666 KOPS**	>700 KOPS**
POWER DISSIPATION	.79 w maximum	.32 w maximum	11.65 w typical
RELIABILITY RATIO	*160/145	226	186

* IMPROVEMENT USING LEADLESS CARRIERS

** ALTHOUGH MUCH HIGHER SPEEDS ARE OBTAINABLE (1 "MIP" FOR 2900 IS COMMON TODAY), THROUGHPUT IS LIMITED BY THE RELATIVELY LONG 300 ns MEMORY ACCESS TIME.

E-2646

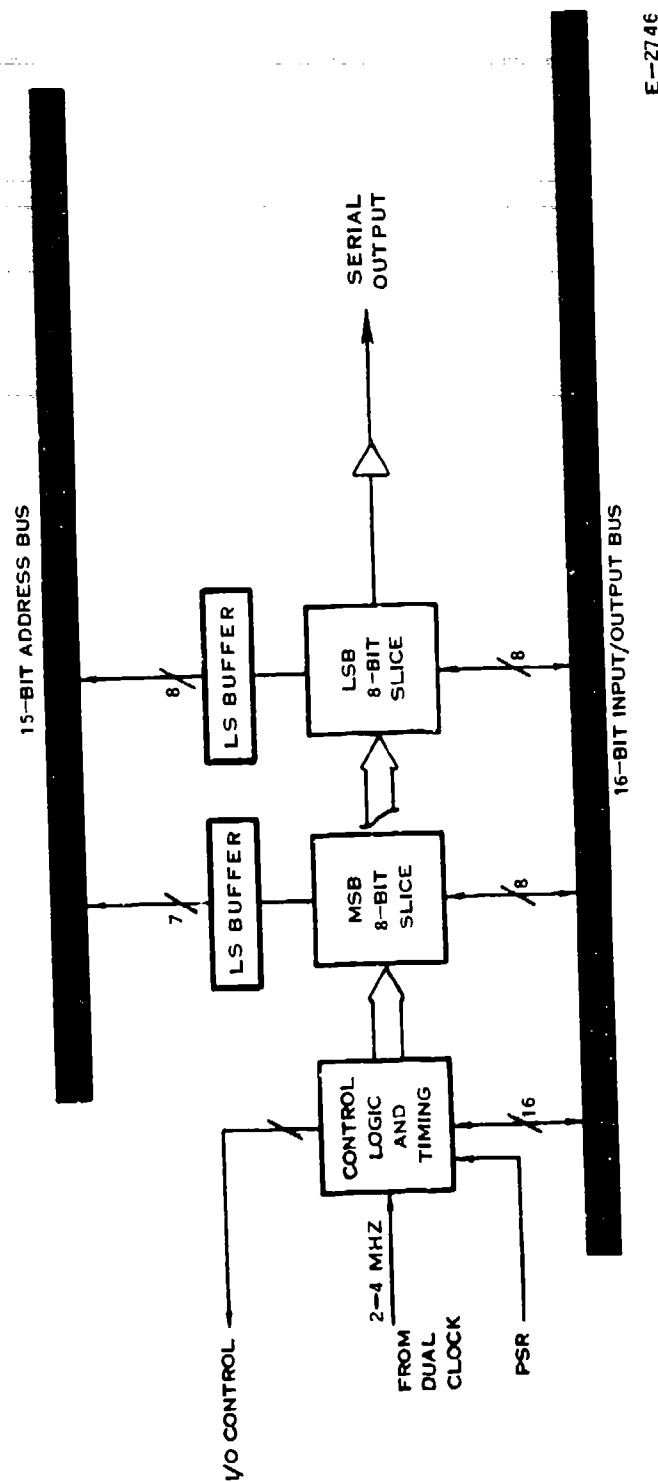
shown in Figure A-51. It is designated the SOS IIS 16/24 since it can be configured as a 3-chip 16-bit machine, or as a 4-chip 24-bit machine. The custom chip set, when configured as a 16-bit parallel machine, comprises one "Control/Timing" chip and two "8-bit slice" chips, plus five standard SSI devices and four decoupling capacitors. These 12 components dissipate a total of 0.32 watts, and will execute the fuel control instruction mix at 666 KOPS when configured with MOS RAM and ROM. This machine easily meets the "450 KOPS" minimum, and could therefore be slowed 30%; however, by the time that a RAEEC system flies, this extra capacity may be required for future tasks. Please refer to the summary shown in Table A-8.

A.3.15.2 Random Access Memory Trades The three configurations of RAM studied were the baseline RAM, all N-channel RAM, and all CMOS RAM. A 1024 word RAM block diagram is shown in Figure A-52. The number of components required is less than ten, since four 1024 x 4 RAM devices comprise the memory and the other six devices comprise the read/write control logic buffering, and decoupling capacitors. Please refer to the trade summary shown in Table A-9.

Error correction techniques were also studied in order to attempt the realization of a more reliable RAM system. However, in order to take advantage of Hamming code error correction techniques, four 1024 X 1 RAMs should be used in place of each 1024 X 4 RAM because of the possibility of an undetectable 4-bit failure. Because of the 21 bit word length required for single error correction and dual error detection, twenty-one 1024 X 1 RAMs plus error correction logic would be required to replace the four 1024 X 4 RAMs. Since this error correction scheme resulted in a large increase in power dissipation and board area, and a large decrease in reliability, it is not presented in Table 19.

A.3.15.3 Read Only Memory Trades In addition to the Baseline ROM, four different ROM architectures were studied: All 16K words Ultra-Violet (U-V) erasable; all N-channel ROM; all CMOS SOS ROM; and half U-V half N-Channel ROM as indicated in Figure A-53. The obvious advantage to using U-V erasable ROMs is that they can easily be erased and reprogrammed during the development phase of a program, and can be replaced with a pin for pin compatible N-channel ROM in the production phase. The penalty for using U-V ROM is a possible speed jeopardy due to its relatively slow 400ms access time, and its uncertain data retention when operating at temperatures above 100°C.

The baseline PROM (Fuse-link Programmable Read Only Memory) enjoyed the advantage of fast turnaround during the development phase, after a suitable burn-in, but suffered from a high parts count, and high power dissipation when compared to the all-ROM or half-UV approaches.



E-2746

FIGURE A-51 THREE-CHIP HS 16/24 MACHINE

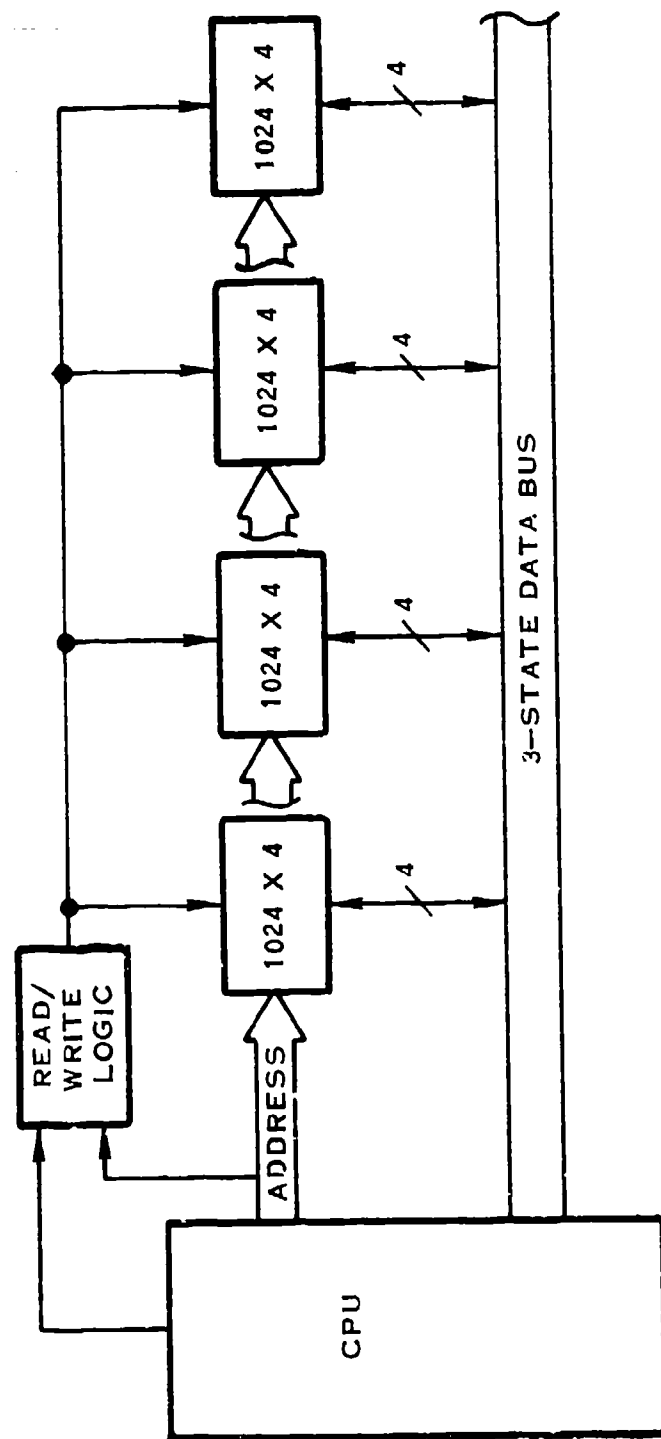


FIGURE A-52 1024 WORD RAM

E-2612

TABLE A-9 RAECC RAM DESIGN TRADEOFFS

ARGUMENT	BASELINE RAMS	ALL N-CHANNEL	ALL CMOS
# OF COMPONENTS	17 1/2	9.5	7.5
# OF SOLDER JOINTS	257	116	97
BOARD AREA (IN ²)	9.94 (4.52**)	3.98 (2.20**)	3.6 (1.98**)
POWER (WATTS)	0.24	1.62	0.10
MAX CYCLE TIME	200 ns @ 10 V	450 ns	420 @ 5 V
MAX ACCESS TIME	200 ns @ 10 V	450 ns*	320 @ 5 V
RELIABILITY RATIO	267/262	326	299

* THE CPU THRU-PUT WILL LIKELY BE REDUCED WITH THIS ACCESS TIME; A "WAIT-STATE" MAY BE REQUIRED.

** IMPROVEMENT USING LEADLESS CARRIERS

FROM CPU

ADDRESS BUS ($ADR_1 \rightarrow ADR_{13}$)

2364 ROM
8K X 8

2732 U-V
4K X 8

2732 U-V

16-BIT DATA BUS

EXTERNAL TEST BUS

2:1 MUX

TO CPU

THE CPU SPEED-UP PERFORMANCE THROUGH-PUT MAY BE SEVERELY LIMITED DUE TO THE RELATIVELY LOW ACCESS TIME OF THE U-V BUS. THE "WAIT-STATE" TIME MAY BE REDUCED BY CUTTING OFF THE U-V "WAIT-STATE" OR A SLOW-DOWN MODE WHEN FEEDBACK FROM U-V MEMORY. }

FIGURE A--53 8K WORD ROM & 8K WORD U-V MEMORY

As was discussed in Paragraph A.3.15.2, Hamming-Code error correction techniques were studied for single-bit ROM error correction and dual error detection. However, since ROMs today are configured as a byte wide (8 bits), the code would have to also detect the failure of eight bits stuck either high or low in the event of a ROM chip failure. Because more than a 5-bit correction code would be required to detect 8-bit failures, the error correction concept was configured with an additional 16K X 8 memory, requiring a total ROM of 16K X 24 bits. When the final parts-list was studied, it was realized that the extra Hamming Code parity detection, bit correction logic was less reliable than the original four ROMs, and for this reason is not detailed in this study.

Please refer to the ROM tradeoff summary shown in Table A-10.

A.3.15.4 Input/Output Addressing Each and every computer system requires a block of logic for special addressing functions, such as Input/Output interface enables, special memory enables, and special read/write signals. In small microprocessors, this logic might comprise a group of LSI chips known as "Peripheral Interface Adapters", plus a few SSI buffer chips.

Figure A-54 indicates what the I/O addressing logic would look like if implemented with either "Programmable Logic Arrays" (PLA), or "Programmable Array Logic" (PAL) devices. The advantage to using these devices is that they replace several discrete SSI decoders and gates and can easily be programmed for each I/O application. The only disadvantage to using these devices is their relatively low reliability score since they do not enjoy the high volume production that bipolar PROMs do.

Another design approach to the I/O addressing problem is to design a semi-custom gate-array LSI chip to perform all the decoding and special timing logic. Obviously if this LSI chip were designed in a CMOS gate array, it would then require only a single decoupling capacitor, for a total parts count of two, and a power dissipation of only 100mw, as opposed to the 18-component 310mw baseline configuration. The corresponding disadvantage to this custom approach is the relatively high-cost of a one-per-system LSI device. Please refer to the I/O addressing trade summary shown in Table A-11.

A.3.15.5 Dual-Port RAM The "Dual-Port RAM" logic is possibly the most critical link to the success of the RAEEC program. This system must transfer information transparently between the two processor channels, and is therefore, referred to as a dual-port RAM system, since each processor has dual-port like access to the other's critical data. The actual "D-P RAM" interface design involves three individual trades; (a) method of data transmission between processors, (b) type of dual-port logic to be utilized, (c) survivability of the data link in the event of a processor failure.

TABLE A-10 RAECC ROM DESIGN TRADEOFFS

ARGUMENT	BASELINE PROMS	ALL U-V	PARTIAL U-V	ALL ROM (N-CHAN)	ALL ROM (SOS)**
# OF COMPONENTS	55	20	17 1/3	14 1/6	14 1/6
# OF SOLDER JOINTS	816	314	259	210	226
BOARD AREA (IN ²) (1)/(2)	27.3 / 14.55	16.4/4.93	13.4/4.53	10.2/4.01	10.4/3.72
POWER (WATTS)	6.62	2.09	1.72	0.87	0.31
MAX ACCESS TIME	100 ns	400 ns	400 ns	300 ns*/100 ns	125 ns
CUSTOM MASK REQD?	NO	NO	YES (2)	YES (4)	YES (4)
PRODUCTION RECOMMENDATION	YES	NO	NO	YES	YES
RELIABILITY RATIO	220/210	104	179	212	141

(1) AREA USING CONVENTIONAL DIPS (2) AREA USING LEADLESS CARRIERS

* WAIT STATE MAY BE REQUIRED FOR MEMORY REFERENCED INSTRUCTIONS (POTENTIALLY REDUCING KOPS)

** SOS AND CMOS EXCITED WITH 5 VDC

E-2650

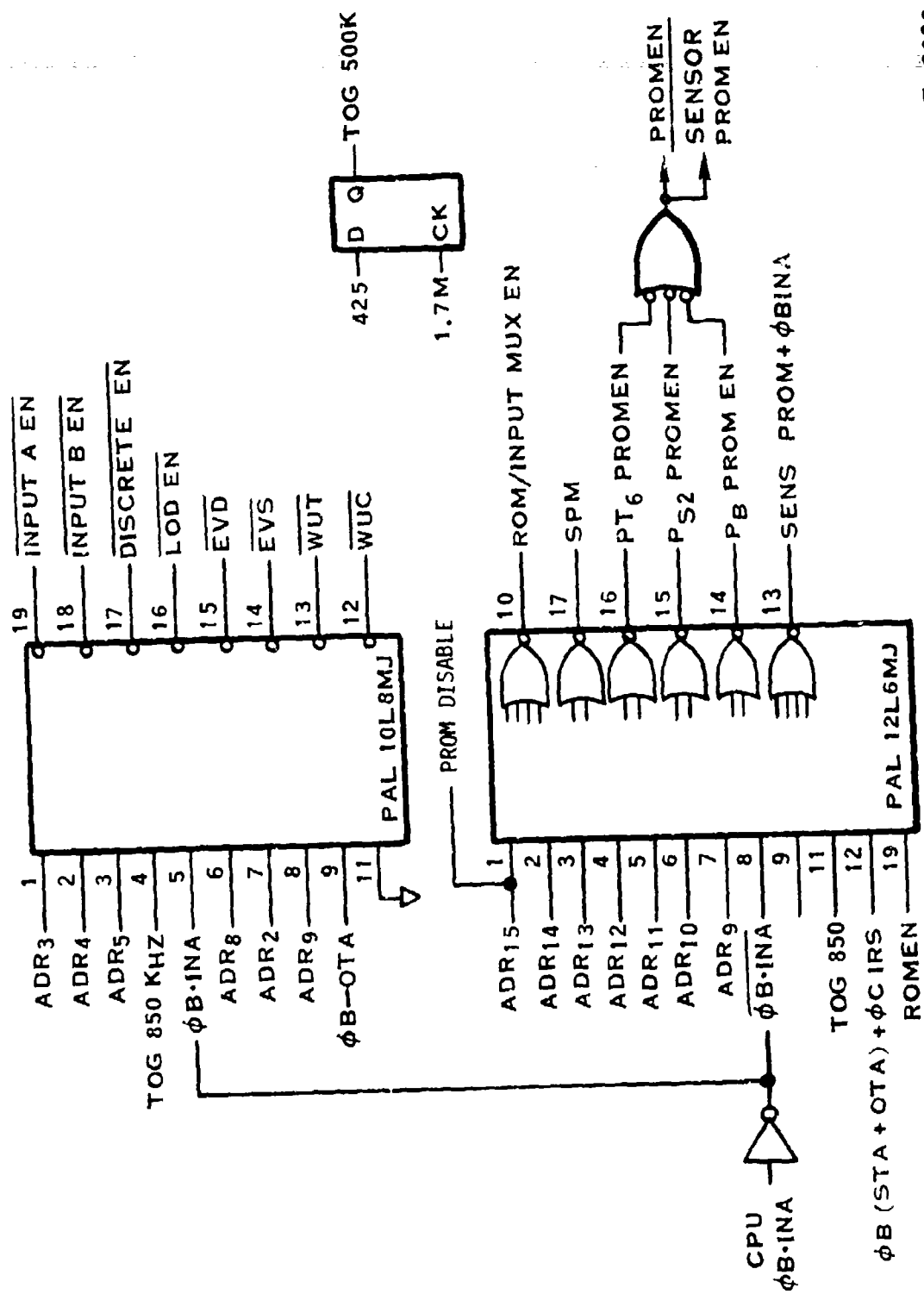


FIGURE A-54 I/O ADDRESSING (SIMPLEX MACHINE) PLA APPROACH

E-2620

TABLE A-11 RAECC I/O ADDRESSING

ARGUMENT	PRESENT ADDRESSING	PLA ADDRESSING	LSI ADDRESSING
# OF COMPONENTS	18	5	2
# OF SOLDER JOINTS	180	59	30
BOARD AREA (IN ²)	6.74 (4.23*)	2.96 (1.59*)	1.84 (0.496*)
POWER (WATTS)	0.31	0.57	0.10
CUSTOM PARTS	NO	NO (PROGRAMMED PLA)	YES, GATE ARRAY
RELIABILITY RATIO	LCC DIP 307/302	233	276

* IMPROVEMENT USING LEADLESS CARRIERS

E-2651

D-P RAM Data Transmission

One technique of data transmission between the two RAEEC channels is the "full parallel word transfer". This would involve 16 data lines, 6 data address lines and a pair of control lines. Since none of these lines can be shared between the two systems because of possible common failure modes, 48 data and control lines would be required if this transmission concept were used.

Another technique which could be used is the byte transfer, where three successive bytes would transfer 16 bits of data and 6 bits of data address. If this scheme were selected, only 20 lines would be required between the two channels, 10 in each direction.

The transmission scheme selected in this sub-study is serial transmission of word data. This system requires the fewest number of lines in each direction; one if single ended or two if the transmission is dual differential to avoid potential ambiguity. Since "UART" devices are relatively inexpensive, MIL-qualified and multiple sourced, and can simultaneously transmit and receive serial data, a UART was chosen for this purpose.

D-P RAM Logic

Once the transmission medium was selected, the actual dual-port RAM logic was developed and studied. The five different approaches studied are described briefly below:

a. Real Time DMA (Cycle Steal)

This approach provides the fastest data access with the least data transport delay. However, it requires a very fast memory ($t_{\text{access}} < 100 \text{ ns}$) so that one machine isn't slowed by the one performing the DMA, and it requires full parallel access (all 16 bits of data) to prevent data change during a DMA cycle.

This concept has the advantage of being transparent to both CPU's.

b. DMA Block Transfer

This concept actually involves the halting of a machine for the time it takes to effect a complete transfer of data. Although fast, it runs the risk of an additional failure mode, whereby the transfer logic could paralyze a processor by holding it in a DMA mode.

c. Asynchronous Data Transfer, With Handshake

This concept requires a mail-box latch or "FIFO" (First-In, First-Out) approach, where either a flag is monitored or a data ready interrupt is generated. In either case, extra overhead for both CPU's is required to maintain the data transfer. (Refer to AM 2950 8 bit parallel I/O port).

d. Virtual Dual-Port RAM

This concept requires that several off the shelf dual-port RAMs be tied together to make a large enough cache; however, this system provides a real-time data transfer, without any possible interference between the two machines.

e. Simulated Dual-Port RAM

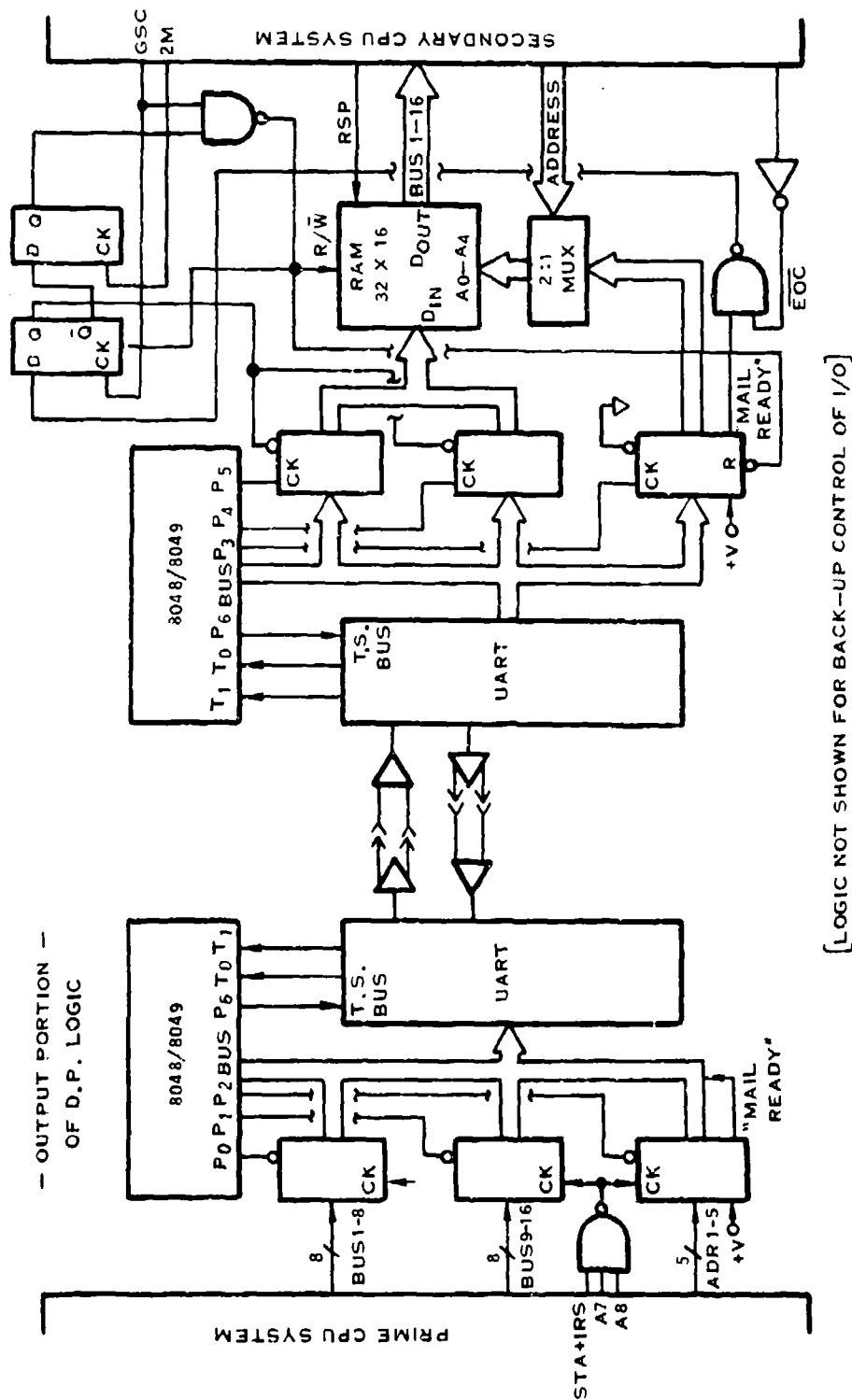
This concept provides the advantage of transparency between machines, but adds an additional data transport delay which is a function of the data transmission concept utilized. Data is accessed on a cycle-steal DMA basis and then sent serially to a second cycle-steal DMA interface, where the data is transparently placed into the second machines RAM.

This was the concept used in the baseline, which was improved in alternate design #1 shown in Figure A-55. Alternate design #2 assumes the design of a custom CMOS dual-port RAM, which reduced the parts count from 37 1/3 to 28, as indicated in the trade summary shown in Table A-12.

Alternate Backup Modes for a Failed Processor in a Dual Channel System

An obvious multiple failure situation that could occur and would result in a completely inoperable system, if link operation were dependent on the CPU, is when a central processing unit (CPU) in one channel fails and any other functional block in the other channel fails.

The real choices can be reduced to a few obvious alternatives. These alternatives all consist of ways of providing a backup capability for the CPU to either provide full capability, partial capability, or conditional capability. By this it is meant that full capability implies that the backup system has the same level of performance as the prime. Partial capability implies that the backup system has a lesser level of performance than the prime. Conditional capability means that backup capability may or may not exist depending upon the mode of failure of the prime and, for this discussion, that if backup capability can be provided it's performance level will be less than that of the prime.



E-2622

FIGURE A-55 DUAL PORT RAM "IMMEDIATE TRANSFER" ALTERNATE 1

TABLE A-12 RAEEC DUAL-PORT DESIGN TRADEOFFS

ARGUMENT	BASELINE D.P.	ALTERNATE 1	ALTERNATE 2
# OF COMPONENTS	42.66	37 1/3	28
# OF SOLDER JOINTS	624	477	400
BOARD AREA	26.44/12.27**	20.72/9.48**	17.58/7.23**
POWER (WATTS)	1.066/0.716*	0.682/0.332*	0.767/0.417*
CUSTOM LOGIC	YES (8048 PROGRAM)	YES (8048 PROGRAM)	YES (8048 PROGRAM AND CUSTOM LSI)
MAX TRANSPORT DELAY	5.6 ms (worst system delay 23.6)	0.728 ms per word - immediate - worst syst Δ = 18.728 ms	0.728 ms per word - immediate xfer - worst syst Δ = 18.728 ms
RELIABILITY RATIO	LCC DIP 205/195	219	210

NOTES: * LOWER POWER DISSIPATION IF INERSIL/RCA CMOS 8048 AVAILABLE

** IMPROVEMENT USING LEADLESS CARRIERS

E-2647

The tabulated choices include the following:

a. Full Capability Backup Using an Additional, Identical CPU

The advantages of this approach are that the task for the CPU remains the same and therefore, does not entail reconfiguration, redefinition, or alternate modes of operation which would involve extra firmware; it also allows operation with no degradation of performance. The backup system is also allowed to remain idle, with no power applied. Consequently, the backup is a "cold spare", which is more reliable having accumulated no operating time.

The disadvantages are that the approach is expensive in hardware, and consumes considerable space (Figure A-56).

This microcomputer, the "link-alive processor", is shown with the dual-port logic in Figure A-55.

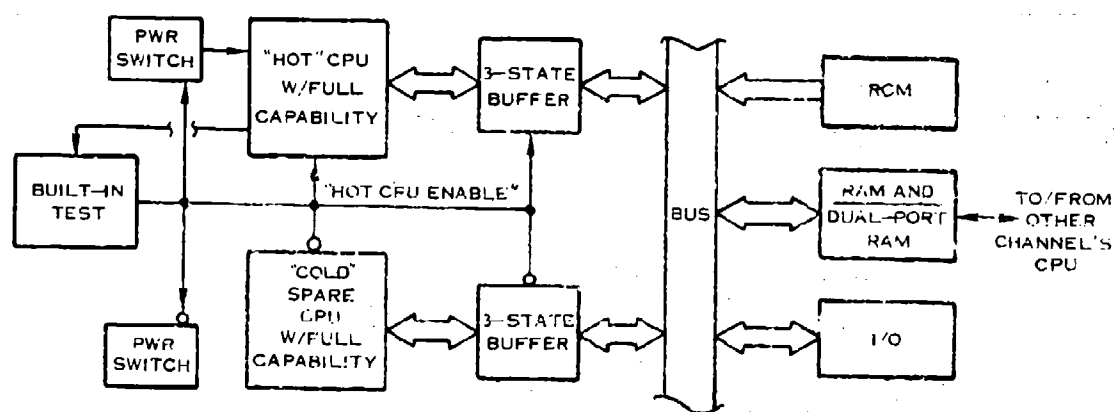
b. Conditional Capability Backup Using The "Failed" CPU at Reduced Performance Capability

The advantages of this approach are that the cost, power and space requirements are less than those of the first alternative. Switching is not involved except for PROM devices, and isolation of failed hardware is a software rather than a hardware function. This approach also encompasses memory failures (PROM) since a separate, reduced performance memory replaces the main memory after a failure.

The disadvantages are that many failures will make the CPU completely inoperable rather than providing graceful degradation to a reduced performance mode. Software error detection schemes must be more sophisticated and therefore, consume more memory space.

By making certain assumptions, the last alternative yields the greatest increase in reliability for an incremental increase in redundancy and cost.

One of these assumptions is that the CPU's performance could be reduced to having the capability to do basic information transfers. Transfers such as inputting, outputting, register to memory and memory to register operations as well as a single conditional skip and a single jump operation. This rudimentary capability was assumed to be adequate for a minimum performance backup CPU. Another assumption is that error detection be limited to nonquantifying decisions so that any failure resulted in assuming performance capability degradation to the basic operations discussed. This last assumption yields a large pay back in the reduction of the sophistication of software, the amount of diagnostic software, the number of backup modes of operation, and the time necessary to achieve error detection.



E-5691

FIGURE A-56 FULL CAPABILITY BACKUP USING AN ADDITIONAL, IDENTICAL CPU

An investigation at the circuit level revealed that approximately 60% percent of the transistors on the chip could be stuck in either the high or low state (these were considered one at a time, not all at once) and an operable system could be maintained if limited to the discussed operations.

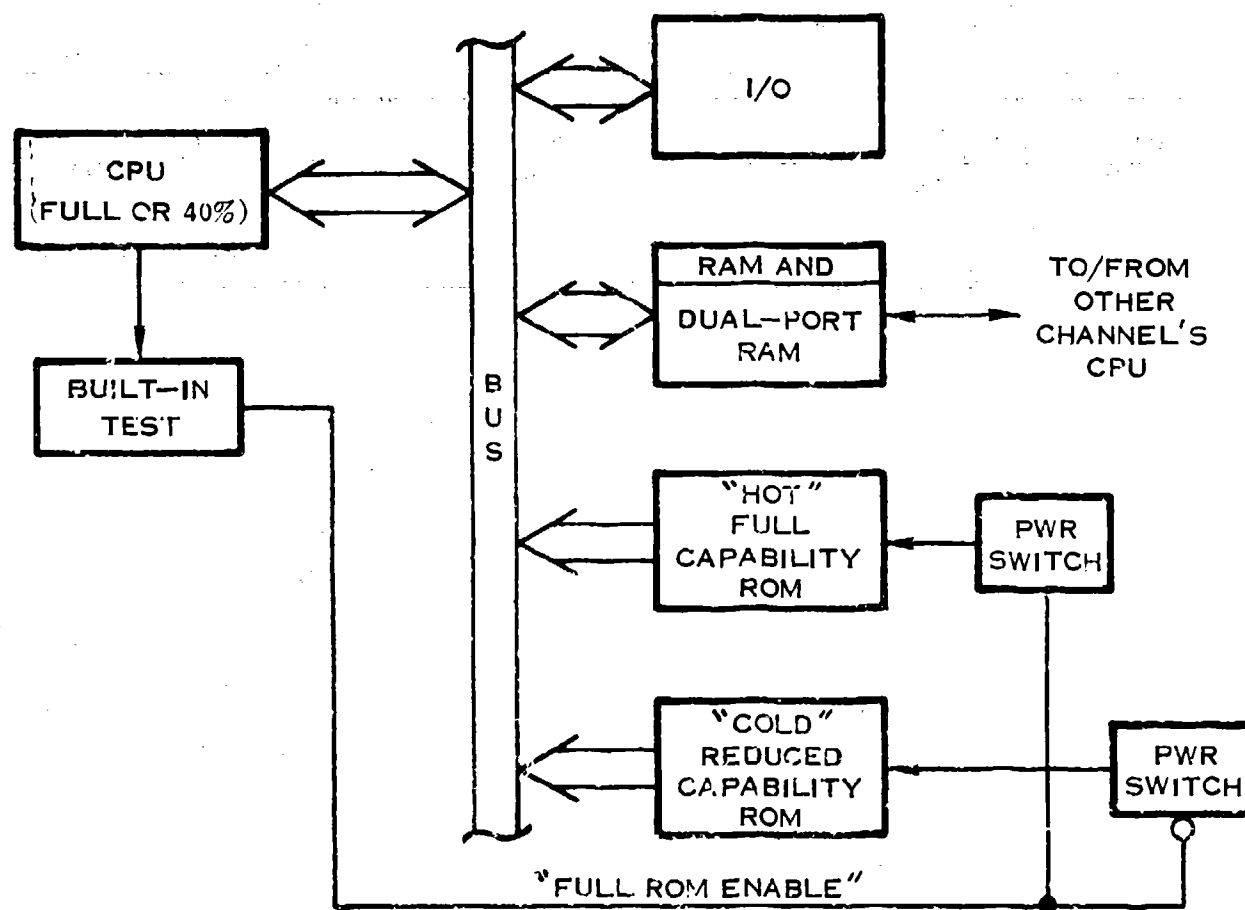
This approach requires that the failed CPU perform extensive diagnostics on itself, to determine which instruction has failed, and to branch to a backup I/O routine which does not contain the failed instruction. In this mode, the failed operable CPU provides I/O capability, via dual port RAM, to the healthy CPU, thereby allowing additional/multiple I/O failures with no degradation in performance (Figure A-57).

c. Partial Capability Backup Using a Single-Chip CPU

The advantages of this approach are that the system cost is less, power is less, and space requirements are less than the first, or second approach, while many of the good characteristics of both are retained. It should be understood that in this discussion the single-chip CPU includes its own RAM and ROM on the chip. And since the single-chip CPU is actually a stand-alone microcomputer it is only dependent on the main CPU's Built-in test output for its operational mode; i.e., if the main CPU fails its instruction test, RAM diagnostic, or ROM sum check, or continuously watchdog times-out, then this backup CPU will take over control of the operation of the dual-port link.

This latter approach was the one chosen to maintain the data-link survivability, and in fact is referred to as the "link-alive" processor. Its two main functions are:

- (1) To service the dual-port UART: to check word formatting, parity, etc., and to self-test the link.
- (2) In addition to the above, if the Built-in test logic indicates a failure of the main CPU, this machine will communicate to all I/O, and format this information for the dual-port link.



E-5693

FIGURE A-57 CONDITIONAL CAPABILITY BACKUP USING THE FAILED CPU AT REDUCED PERFORMANCE CAPABILITY

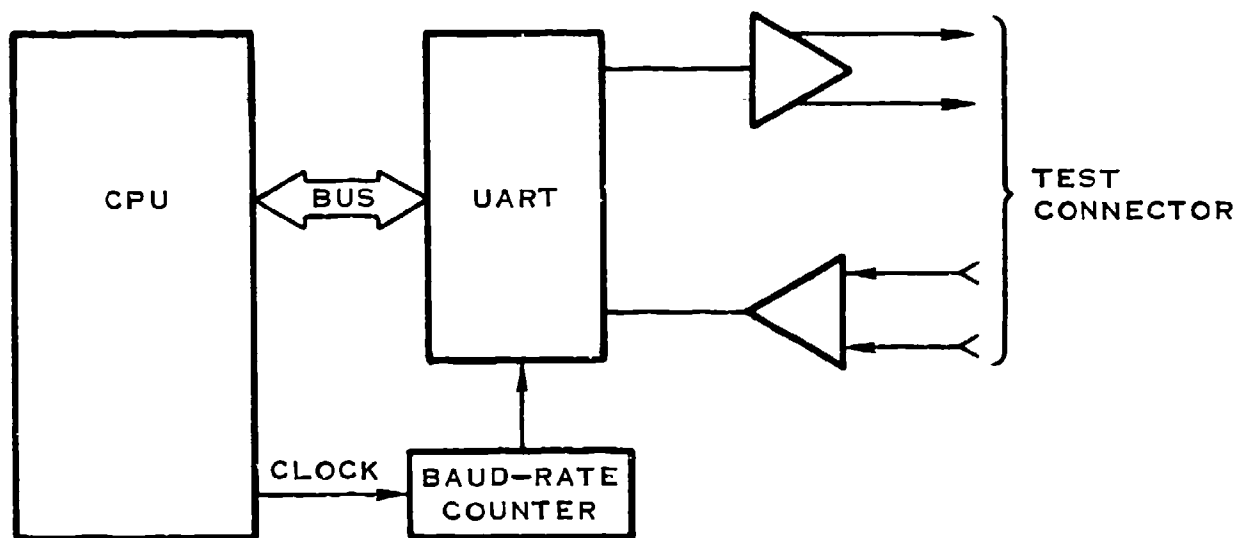
A.3.15.6 Test UART The Test UART is actually only used for ground test troubleshooting, and therefore, could fail and never cause any degradation in any flight mode. Since the baseline test UART already used a minimum of components, the only possible improvements would be to use leadless chip carriers and to use the 28 pin USART instead of the 40 pin UART in order to cut back on solder connections. Refer to Figure A-58 and the trade study summary shown in Table A-13.

A.4 Matrix Trade Summary: Alternatives

The tables provided in this section present a concise summary of the important parameters associated with each of the fourteen circuit partitions. Table A-14 presents the power dissipation, leadless chip carrier (LCC) printed circuit board area, and reliability weighting factor associated with the different circuits studied for the RAEEC primary channel. Table A-15 provides basically the same information as Table A-14 except that the RAEEC secondary channel presented has one less "A/D", one more "R/D", one less "low level interface", and 15 torque motor drivers instead of the primary's 16.

With the information provided in the above tables, a power/area/reliability sensitivity study was summarized in Table A-16. The objective of this summary was to indicate the total effect on an electronic fuel control if all electronics were selected for (1) minimum power dissipation, or (2) minimum printed circuit board area, or for (3) maximum reliability. Although the numbers in the Reliability columns are really representative of each circuit's "Reliability Figure of Merit" (as explained in the Reliability section of the Development Guide), it was realized that although they were dimensionless, they could be summed to find the relative reliability ratios of each RAEEC concept with respect to the "RAEEC Baseline".

Table A-16 indicates that if an RAEEC control were designed for maximum reliability, it would enjoy an improvement in reliability of 19% over baseline system. However, the most reliable design would also dissipate 10.4% more power than a minimum area type design. It should be pointed out to the reader that although the "Min Power" and "Min Area" designs resulted in a lower overall reliability ratio, it is conceivable that additional iterative trades on each circuit in the "Max Rel" column could result in less power and less area, which would in turn reduce junction temperature, increasing the overall reliability improvement ratio well above the present 19% mark. Because of the system complexity of RAEEC, and its complex heat flow calculations, each design improvement iteration is quite costly since it involves all design disciplines, and further design iterations were outside the scope of this program.



E-2613

FIGURE A-58 TEST UART

TABLE A-13 RAECC TEST UART

ARGUMENT	PRESENT UART (CMOS)	28 PIN USART (CMOS)
# OF COMPONENTS	9 3/4	9 3/4
# OF SOLDERJOINTS	106	94
BOARD AREA (IN)	5.5/2.49 *	4.7/2.38 *
POWER (WATTS)	0.09	0.09
CUSTOM PARTS	NO	NO
RELIABILITY RATIO	287/285	308

* IMPROVEMENT USING LEADLESS CARRIERS

E-2652

TABLE A-14 PRIME RAEEC SUMMARY

CIRCUIT	BASELINE RAEEC			ALTERNATE 1			ALTERNATE 2			ALTERNATE 3		
	POWER	AREA	REL	POWER	AREA	REL	POWER	AREA	REL	POWER	AREA	REL
CENTRAL PROCESSOR	9.116	100.32/46.2	1446	3.89	29.72	1583	1.34	20.94	1460	16.9	22.52	1256
(2) A/D CONV	1.78	13.78/11.09	231	1.94	15.56/8.74	265	1.34	15.56/8.74	265		10/5.56	306
R/D CONV	0.33	8.36/5.94	256	0.52	5/4.12	299	1.25	9.71/4.69	230			
RESOLVER EXCIT	1.25	8.96/7.82	311	1.25	8.48/7.34	351						
(16) TORQUE M. DRIVER	7.04	44.51/22.6	333	5.44	33.94/13.48	353	3.712	33.94/13.48	353			
(9) SOLENOID DRIVER	9.07	13.57/12.03	281	9.22	5.13/1.48	309	9.22	3.57/1.38	364			
(6) PRESSURE SENSORS	3.47	57.36/45.78	246	2.50	30.24/22.38	300						
(2) LOW LEVEL INTF	0.42	17.5/13.03	298	0.38	12.38/8	317						
RESOLVER MUX	0.10	11.69/5.14	248	0.36	4.9/1.05	330						
DISCRETE SIGNALS	0.09	8.39/5.73	238	0.35	6.47/2.7	350						
SPEED INTERF	0.24	17.62/6.7	201	0.60	2.86/0.10	342						
T.P.S.	0.09	8.84/3.47	298	0.20	3.72/1.63	278						
FAULT DET	0.32	5.26/4.12	277	0.11	3.84/1.16	310						
POWER SUPPLY	75.05	40.9/35.14	193	19.2	22.56/20.47	259	14.45	23.32/20.85	284			
TOTALS	105.99	356.96/236.79	4857	N/A			N/A			N/A		

E-2655

TABLE A-15 SECONDARY RAECC SUMMARY

CIRCUIT	BASELINE RAECC		ALTERNATE 1		ALTERNATE 2		ALTERNATE 3	
	POWER	AREA	REL	POWER	AREA	REL	POWER	AREA
CENTRAL PROCESSOR	9.116	100.32/46.2	1446	3.89	29.94	1586	16.9	22.52
(1) A/D CONV	0.87	6.89/5.55	231	0.97	7.78/4.37	265	0.67	5/2.78
(2) R/D CONV	0.66	12.72/12.54	256	1.03	10/8.48	299	2.50	10/8.48
RESOLVER EJECT	1.25	8.96/7.82	311	1.25	8.48/7.34	341		9.71/4.69
(15) TORQUE M. DRIVER	6.6	41.63/30.48	373	5.1	31.74/12.61	353	3.48	31.74/12.61
(9) SOLENOID DRIVER	9.07	13.57/12.03	281	9.22	5.13/1.48	309	9.22	3.57/1.38
(6) PRESSURE SENS	3.47	57.36/45.78	246	2.50	30.24/22.38	300		
(1) LOW LEVEL INTF	0.21	8.7 /6.52	298	0.19	6.19/4.0	317		
RESOLVER MEZ	0.10	11.69/5.14	248	0.36	4.9/1.05	330		
DISCRETE SIGNALS	0.09	8.39/5.73	238	0.35	6.47/3.7	350		
SPEED INTF	0.24	17.62/6.7	201	0.60	2.86/2.10	342		
T. PUMP SPEED	0.09	8.84/3.47	298	0.20	3.72/1.63	278		
FAULT DET	0.32	5.26/4.12	277	0.22	3.84/1.16	310		
POWER SUPPLY	75.05	40.9/35.14	193	19.2	22.56/20.47	259	14.45	23.32/20.85
TOTALS	104.76 watts	342.85/229.22 sq. inches	4957 points		N/A			N/A

E-2654

TABLE A-16 RAECC PICKS CHOICES

CIRCUIT	MINIMUM POWER			MINIMUM AREA			MAXIMUM REL			FINAL CHOICE		
	PWR	AREA	REL	PWR	AREA	REL	PWR	AREA	REL	PWR	AREA	REL
CENTRAL PROCESSOR	1.34	20.94	1460	1.34	20.94	1460	3.89	29.72	1583	3.89	29.72	1583
(2) A/D CONV	1.34	7.92	265	1.94	7.92	265	1.08*	5.56	306	1.34	7.92	265
R/D CONV	0.33	5.94	256	0.42	4.12	299	0.42	4.12	299	0.42	4.12	299
RESOLVER EXCIT	1.25	7.34	341	1.25	7.34	341	1.25	7.34	351	1.25	7.34	351
TORQUE M. DRIVER	3.71	13.48	353	5.44	13.48	353	5.44	13.48	353	3.71	13.48	353
SOLENOID DRIVER	9.07	12.03	281	9.22	1.38	364	9.22	1.38	364	9.22	1.38	364
PRESSURE SENSOR	2.50	22.38	300	2.50	22.38	300	2.50	22.38	300	2.50	22.38	300
LOW LEVEL INTF	0.19	8.0	312	0.19	8.0	312	0.19	8.0	312	0.19	8.0	312
RESOLVER MUX	0.10	1.05	248	0.36	1.05	330	0.36	1.05	330	0.36	1.05	330
DISCRETE SIGNALS	0.09	5.73	238	0.35	3.7	350	0.35	3.7	350	0.35	3.7	350
SPEED INTF	0.24	6.7	201	0.60	2.1	342	0.60	2.1	342	0.60	2.1	342
T. PUMP SPEED	0.09	3.47	298	0.20	1.63	278	0.09	3.47	298	0.09	3.47	298
FAULT DET	0.11	1.16	310	0.11	1.16	310	0.11	1.16	310	0.11	1.16	310
POWER SUPPLY	14.45	20.85	284	19.10	20.47	259	14.45	20.85	284	14.45	20.85	284
TOTALS	34.81	136.99	5147	43.02	115.67	5563	38.43	124.31	5787	38.22	126.67	5741
MEDIAN	1.06 : 1			6.16 : 6			1.49 : 6			1.88 : 6		

* INCOMPATIBLE INTERFACE

E-2653

It must be pointed out that the "final choice" is actually identical to the "Max Rel" configuration, except for the choice of the A/D converter. Although it is obvious that a successive approximation converter with a rel-merit number of 306 is more reliable than the "Smart A/D" with a number of 265, the additional factors which influenced the choice of the "Smart A/D" are:

- a. Unloading of CPU resulting in increased throughput
- b. Reduction of CPU memory, since digital filtering not required
- c. Reduction of filtering in the "low level" dc interface

In actuality, the "Max Rel" design should have been penalized by the above factors, which might have lowered its improvement ratio below that of the final choice. Unfortunately it was beyond the scope of this program to reiterate the other circuit designs due to the actual total impact caused by the utilization of a successive approximation converter.

Table A-17 indicates the total influence on reliability if the 2901 bit slice processor were used, since it was the second most reliable processor in the processor trade studies. The reader should note that although all the other circuits were held constant, the power supply had to be redesigned to carry the additional 11 watts of power required. This design concept resulted in a 48.7% increase in power dissipation, a 9.7% higher board area, and a 1% worsening in reliability as compared to the "Final Choice". However, if the 2900 approach were chosen, it would have been realized after a detailed thermoanalysis that the junction temperatures of all circuits would have risen substantially, causing a worse merit ratio below the 17% mark.

In summary, the "Final Choice" represents an 18% increase in reliability over the baseline RAEEC, and although the summary is shown for the "primary", the tabulation of the "secondary" provides the identical results.

A.5 Final RAEEC Design Choice

A.5.1 Introduction

This portion of the report provides a description of each of the fourteen circuit partitions chosen in the design choice as a result of the reliability trade study. Also included in this section is the rationale used in making these selections. As a quick cross-reference aid to the reader, the third digit of each circuit's paragraph number in this section corresponds directly to its baseline description in Section A.2.X and its corresponding circuit trade study in Section A.3.X.

TABLE A-17 RAECC SENSITIVITY SUMMARY II

CIRCUIT	MINIMUM POWER			MINIMUM AREA			2900 APPROACH			FINAL CHOICE		
	PWR	AREA	REL	PWR	AREA	REL	PWR	AREA	REL	PWR	AREA	REL
CENTRAL PROCESSOR	1.34	20.94	1460	1.34	20.94	1460	15.22	37.2	1548	3.89	29.72	1586
(2) A/O CONV	1.34	7.92	265	1.94	7.92	265	1.34	7.92	265	1.34	7.92	265
R/D CONV	0.33	5.94	256	0.42	4.12	299	0.42	4.12	299	0.42	4.12	299
RESOLVER EXCIT	1.25	7.34	341	1.25	7.34	341	1.25	7.34	351	1.25	7.34	351
TORQUE M. DRIVER	3.71	13.48	353	5.44	13.48	353	3.71	13.48	353	3.71	13.48	353
SOLENOID DRIVER	9.07	12.03	281	9.22	1.38	364	9.22	1.38	364	9.22	1.38	364
PRESSURE SENSOR	2.50	22.38	300	2.50	22.38	300	2.50	22.38	300	2.50	22.38	300
LOW LEVEL INTF	0.19	8.0	312	0.19	8.0	312	0.19	8.0	312	0.19	8.0	312
RESOLVER MUX	0.10	1.05	248	0.36	1.05	330	0.36	1.05	330	0.36	1.05	330
DISCRETE SIGNALS	0.09	5.73	238	0.35	3.7	350	0.35	3.7	350	0.35	3.7	350
SPEED INTF	0.24	6.7	201	0.60	2.1	342	0.60	2.1	342	0.60	2.1	342
T. PUMP SPEED	0.09	3.47	298	0.20	1.63	278	0.09	3.47	298	0.09	3.47	298
FAULT DET	0.11	1.16	310	0.11	1.16	310	0.11	1.16	310	0.11	1.16	310
POWER SUPPLY	14.45	20.85	284	19.10	20.47	259	21.85	25.68	264	14.45	28.85	284
TOTALS	34.81	136.99	5147	43.02	115.57	5563	56.86 ⁽¹⁾	138.98 ⁽²⁾	5686	38.22	126.67	5744
MERRIT #	1.06:1			1.16:1			1.17:1			1.18:1		

NOTES
 (1) 48.7% HIGHER POWER DISSIPATION
 (2) 9.7% HIGHER BOARD AREA

E-2653
 MODIFIED

A.5.2 Analog-to-Digital Converter

The result of the A/D design trade was the selection of the "Smart, Multiple-ramp, A/D Converter". As converters go, the successive approximation A/D is a monolithic chip which dissipates less power, uses less board area and performs conversions faster than the multiple ramp type (See Table A-2). However, the above factors do not reflect the actual savings provided by the "Smart multiple ramp converter", which are:

- a. Reduction in CPU memory; no digital filtering required.
- b. Reduction of CPU tasks and memory; analog multiplexing task moved to A/D
- c. Reduction of filtering on low level DC interface

The resulting "bottom line" when the total system is reviewed is that the "Smart A/D" provides some degree of distributed processing which reduced overall hardware when compared to a "S.A.C. A/D" based system.

A.5.3 Resolver to Digital Converter

The "R-C Bridge/Pulse Width to Digital" R/D as described in Paragraph A.3.3.1 was chosen in the final design choice due to its superior reliability. The reader should be reminded that the primary RAEEC channel contains one R/D, while the secondary contains two.

A.5.4 Resolver Excitation

The "Alternate #1" resolver excitation circuit described in Paragraph A.3.4 was chosen in the final design choice due to its superior reliability. This improved circuit uses a monolithic power driver (HA2635) instead of the hybrid (MC1538), which resulted in the reliability improvement.

A.5.5 Torque Motor D/A's and Drivers

The circuit choice could have been successfully made on merits of number of interconnects, or number of components or power dissipation reduction, but the microprocessor based pulse width modulated (P.W.M.) torque motor driver concept was a clear "winner" in the trade studies. Based on the summary presented in Table A-4, the P.W.M. concept dissipated half the power of the baseline circuit, used half the components, and used half the number of interconnects. In addition, the microprocessor became part of a distributed processing system, which reduced the load on the CPU, and allowed self-error checking at the interface level.

A.5.6 Solenoid Drivers

The solenoid driver circuits chosen were those described in Paragraph A.3.6 for the constant voltage alternator. It should be pointed out that although the circuit power dissipation is approximately 1 watt per an energized solenoid, on an average, only three solenoids (and three drivers) will be energized.

A.5.7 Pressure Sensors and Circuitry

The selected pressure sensor concept utilizes two I²L devices per sensor channel, greatly reducing board area and number of interconnects. The custom concept also includes the frequency to digital converter. The circuit (primary and secondary channels) for one sensor is shown in Block Diagram form in Figure A-59. Also included is the resistor network necessary for mating the redundant electronics to common drive and pickup coils on the sensor.

A.5.8 Low Level DC Interface

The low level DC interface chosen in the final RAEEC design choice is the alternate design described in Section A.3.8. Two of these interfaces are designed into the prime, and one into the secondary.

A.5.9 Resolver Multiplexer

The resolver multiplexer chosen in the final RAEEC design choice is the alternate design described in Paragraph A.3.9.

A.5.10 Discrete Signals Conditioner Circuits

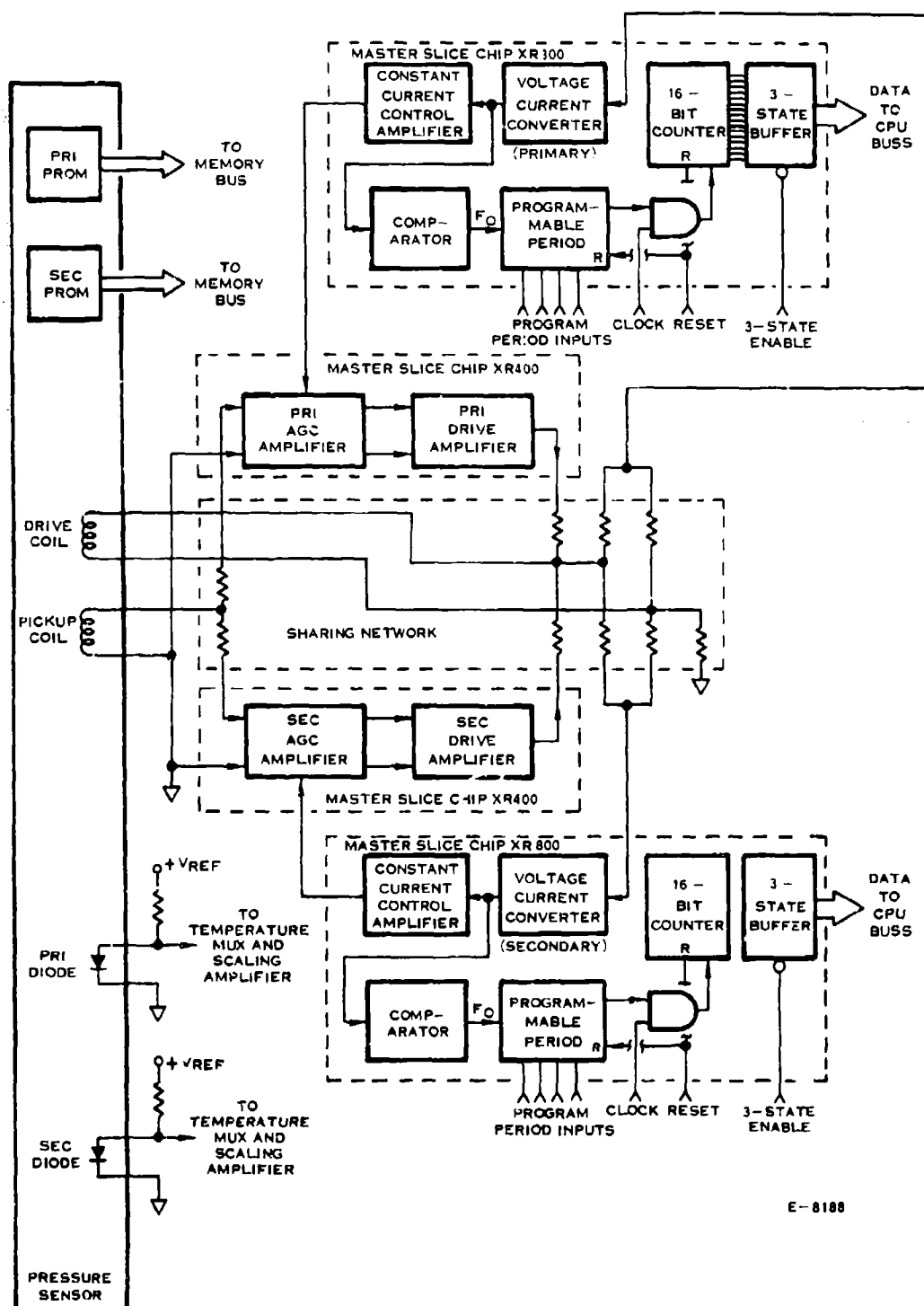
The discrete signal conditioner circuit's approach chosen is described in Paragraph A.3.10. This approach not only saved hardware, but simplified some of the CPU's tasks through distributive processing fault detection concepts.

A.5.11 Frequency to Digital Speed Interfaces

The frequency to digital speed interface chosen in the final RAEEC design choice is described in Paragraph A.3.11. This system eliminates the need for custom LSI devices, and allows better conversion accuracy over the full speed range since the period counter is CPU programmable.

A.5.12 Turbo Pump Speed Interface

The turbo pump speed interface described in Paragraph A.3.12 was chosen since it eliminates the need for custom LSI devices and allows better conversion accuracy over the 0-11 pump speed range, since the 8253 is CPU programmable.



E-8100

FIGURE A - 59 SENSOR CIRCUIT BLOCK DIAGRAM

A.5.13 Fault Detection Logic

The fault detection logic circuit choice is described in Paragraph A.3.13.

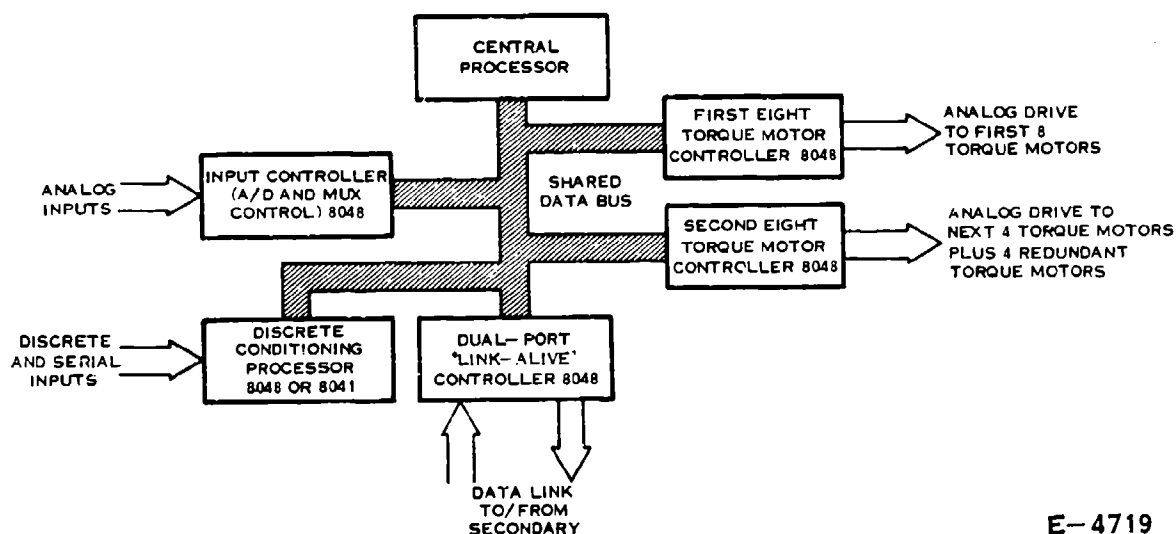
A.5.14 Power Supply System

The power supply system chosen for the final RAEEC design is the constant voltage power system described in Paragraph A.3.14. Although the constant current alternator power system required fewer parts, the reduced power dissipation realized in the constant voltage system, reduced junction temperatures significantly, resulting in a system with highest reliability.

A.5.15 CPU Design Pick

During the design phase of all the circuits involved in the trade study, it was realized that in several areas, it was more profitable both from a reliability improvement and a parts count reduction stand point, to use a single-chip microcomputer (like the 8048, for example) instead of all the discrete logic it replaced. When the studies were completed, the final RAEEC design choice actually comprised six processors: the main CPU and five I/O processors, as shown in Figure A-60. This system became a distributive processing array, which simplified the task load on the main CPU. Since this system is actually a loosely-coupled parallel processing array, the resulting throughput will be far in excess of what the simplex baseline design presented. As an example, the baseline CPU was responsible for all Built-In Test logic required to check itself and all interfaces; however, the final RAEEC I/O processors will now be responsible for performing their own Built-In Test, relieving the main CPU for other tasks. Another example: in case of the untimely demise of the main CPU, the Dual-Port Link Alive Processor will communicate with all surviving I/O processors, and then communicate the I/O data through the dual-port link to the other RAEEC channel.

The computer architecture "Bottom-Line" is shown in Table A-18. This summary presents the results of several complete CPU trades at a glance, including the final RAEEC design recommendation. The reader should note that the Design Recommendation Computer is only 2.4% better in reliability points than the Basic 2901 computer, but the final RAEEC design recommendation computer also requires 24% less board area, and requires 39% less power. These other factors may have a larger effect than 2.4% on the final design than normally expected, since junction temperature (and reliability) will be a function of board area (final box size) and the power dissipation of surrounding components.



E-4719

FIGURE A-60 RAECC DISTRIBUTIVE PROCESSING

TABLE A-18 COMPUTER ARCHITECTURE "BOTTOM-LINE"

COMPUTER ELEMENT	SISD OR SIMD MACHINE				MIMD MACHINE MULTIPLE OFF-THE-SHELF MICROPROCESSORS	FAULT TOLERANT "2900" TRD MACHINE
	BASELINE RAECC	RECOMMENDATION	MOST "RADICAL" ALTERNATE	BASIC 2901 MACHINE		
PROCESSOR	24.4 in ² 0.79 w	5.13 in ² 0.32 w	5.13 in ² 0.32 w	12.39 in ² 11.65 w	7.51 in ² (For both) 3.88 w	51.00 in ² 47.96 w
RAM	9.94 in ² 0.24 w	2.20 in ² 1.62 w	1.98 in ² 0.10 w	2.20 in ² 1.62 w	3.24 in ² (For both) 3.2 w	2.20 in ² 1.62 w
ROM	27.3 in ² 6.62 w	4.01 in ² 0.87 w	3.72 in ² .31 w	4.01 in ² 0.87 w	3.58 in ² (For both) 1.2 w	4.01 in ² 0.87 w
TEST UART	5.5 in ² 0.09 w	2.38 in ² 0.09 w	2.38 in ² .09 w	2.38 in ² 0.09 w	1.95 in ² 0.51 w	2.38 in ² 0.09 w
I/O ADDRESSING	6.74 in ² 0.31 w	6.74 in ² present 0.31 w	0.496 in ² 0.10 w	6.74 in ² 0.31 w	2.9 in ² (Incl. Bus Arbitration) 5.48 w	6.74 in ² 0.31 w
DUAL PORT	26.44 in ² 1.066 w	9.48 in ² 0.682 w	7.23 in ² 0.417 w	9.48 in ² 0.682 w	3.34 in ² 2.63 w	9.48 in ² 0.682 w
TOTAL	100.32 in ² * 9.116 watts	29.94 in ² 3.89 watts	20.94 in ² 1.337 watts	37.20 in ² 15.22 watts	22.52 in ² 16.90 watts	75.81 in ² 51.53 watts
RELIABILITY PICK	5	1	4	2	6	3

* CONVENTIONAL PACKAGES; DIPs, FLATPACKS, ETC.

E-2645

A.5.15.1 Processor Choice The processor was chosen only by the reliability score, (the exact same scoring system used on all other circuits), but could have been chosen on other merits as well. This chosen machine, was the 12 component 3-chip SOS HS 16/24 which dissipates only 320 milliwatts. The processor with the second highest score was the Basic 2901 machine. The following presentation outlines summarize the relative merits and disadvantages of each of the processors discussed previously:

RAEEC HS 16/24

a. Advantage

- Best reliability score
- Lowest power dissipation
- Smallest board area
- Very good throughput (> 666 KOPS)

b. Disadvantage

- Not an off-the-shelf standard processor

RAEEC Fault-Tolerant Approach

a. Advantage

- Good CPU reliability

b. Disadvantages

- Excessive board area required
- Excessive power requirements and large impact to power supply
- Total reliability points not as good as simplex approach

RAEEC Twin 8086 Approach

a. Advantage

- Small board area

b. Disadvantages

- High power dissipation
- Marginal throughput and high programming jeopardy
- High variety of new components
- Lowest reliability points

RAEEC Simplex 2900 Approach

a. Advantages

- All components available in high volume from multiple vendors
- Good reliability points

b. Disadvantages

- Relatively high number of components and interconnects
- Relatively high power dissipation, with corresponding impact and decrease in reliability of power supply
- Reliability points not as good as low power HS 16/24 approach

A.5.15.2 RAM Choice The Random Access Memory chosen for the RAEEC is the N-channel RAM presented as Alternate 1 in Paragraph A.3.15.2 which had the best reliability score.

A.3.15.3 ROM Choice The Read Only Memory chosen for the RAEEC is the All N-channel ROM presented as Alternate 3 in Paragraph A.3.15.3 which had the best reliability score of all alternatives presented.

A.5.15.4 I/O Addressing Logic Choice The I/O Addressing Logic chosen for the RAEEC is the baseline circuit as described in paragraph A.3.15.4. Although the other alternatives required less components than the baseline design, the baseline provided the best reliability score since all the components used were standard, off the shelf low-power schottky.

A.5.15.5 Dual-Port RAM Choice The Dual-Port RAM circuitry chosen for RAEEC is Alternate 1 as presented in detail in Paragraph A.3.15.5 which had the best reliability score.

A.5.15.6 Test UART Choice The Test UART circuitry chosen for RAEEC is Alternate 1 as presented in Paragraph A.3.15.6 which had the better reliability score.

However, there are CMOS operational amplifiers on the market today (manufactured by RCA and INTEL for example) which will slew rail to rail. If the + 10 volt reference supplies were made large enough to handle the additional (low power by the way) operational amplifier load, then the two 14 volt regulators could have been deleted. Also, if all op-amps were run on + 10 volts instead of + 14 volts, the voltage stress would decrease and there would be an accompanying increase in reliability. The scope of the program did not permit more study in this area, thus the 14 volt power buses were used.

A.6 Design Comparison Summary

Table A-19 presents a comparison of 12 system functions for the baseline and final RAEEC designs. Each channel is considered separately.

TABLE A-19. COMPARISON OF BASELINE AND FINAL RAECC SYSTEMS

Channel	Function	Baseline System	Final System
Primary	Power Supply	Raw power from alternator primary winding	Same
	Pressure Sensors	PT2, PT3, Δ P13 each with single cylinder and single electronic input to primary channel	PT2, PT3, Δ P13 each with single cylinder and redundant electronic inputs; on each chanr
	All other core engine inputs	All inputs are non-redundant	Selective redundancy provided for some inputs.
	Augmentor inputs	All inputs are non-redundant	Same
	Input interfaces	Non redundant interface electronics under direct CPU control	Selective redundancy provided for low level signal conditioning A/D conversion. D.C. multiplexing and A/D conversion under microcomputer control.
	CPU	-16 bit parallel processor -10K x 16 bit PROM -512 x 16 bit RAM -64 x 16 bit EAROM	Same except for 12K x 16 bit PROM

TABLE A-19. COMPARISON OF BASELINE AND FINAL RAEEC SYSTEMS (Continued)

Channel	Function	Baseline System	Final System
Primary (Cont)	Interchannel Data Link	<ul style="list-style-type: none"> -UART with 32 X 12 bit RAM interlinking Primary with second-ary CPU -Intelligent Votor (hardwired smart PROM backup for selecting best of two channels) 	<ul style="list-style-type: none"> -UART with 32 x 16 bit dual port RAM interlinking prim-ary and secondary CPU -Fault status dis-cretes (hard-wired circuit backup for switch-over to secondary when primary channel is inop-erative)
	Output Interfaces	Nonredundant interface electronics under direct CPU control	<p>Selective redundancy provided for some output signals.</p> <p>Torque motors under microcomputer pulse width modulation control</p>
	Core engine outputs	Each output connected to one winding of dual winding effector	Outputs provided with selective redundancy con-nected to two windings of triple winding effector
	Augmentor Outputs	Each output connected to one winding of dual winding effector	Same

TABLE A-19. COMPARISON OF BASELINE AND FINAL RAECC SYSTEMS (Continued)

Channel	Function	Baseline System	Final System
Secondary	Power Supply	Raw power from alternator secondary winding	Same
	Pressure Sensors	PT5, PT13, ΔP_3 each with single cylinder 4 single electronic input to secondary channel	PT5, PT13, ΔP_3 each with single cylinder and dual redundant inputs; one to each channel
	All other core engine inputs	All inputs are non- redundant	Selective redundancy provided for some inputs
	Augmentor inputs	None provided	All inputs are non- redundant
	Input Interfaces	Non-redundant interface electronics under direct CPU control	Selective redundancy provided for R/D conversion. D.C. multiplexing and A/D conversion under microcomputer control
	C.P.U.	-16 bit parallel processor - 8 K x 16 bit PROM -512 X 16 bit RAM -64 X 16 bit EAROM	Same except for 12K x 16 bit PROM
	Interchannel Data Link	UART with 32 X 16 bit RAM interlinking secondary with primary C.P.U.	UART with 32 x 16 bit Dual port RAM interlinking secondary with primary CPU
	Output Interfaces	Nonredundant interface electronics under direct CPU control	Selective redund- ancy provided for some output signals. Torque motors under microcomputer pulse width modulation control

TABLE A-19 , COMPARISON OF BASELINE AND FINAL RAECC SYSTEMS (Continued)

Channel	Function	Baseline System	Final System
Secondary (Cont)	Core Engine Outputs	Each output connected to one winding of dual winding effector	Outputs provided with selective redundancy connect- ed to two windings of triple winding effector
	Augmentor	None provided	Each output con- nected to one winding of dual winding effector

APPENDIX B
MECHANICAL DESIGN TRADE STUDIES

MECHANICAL DESIGN TRADE STUDIES

Summarized in this Appendix are: 1) circuit board reduction studies; 2) technology comparisons; and 3) various trade-off studies. This information was used as a guide for selecting the various package features, materials and technologies that make up the final RAEEC high reliability design. This Appendix serves as a reference so that the reader may have a better understanding of how the final design was derived.

Figure B-1 is a review of circuit board reduction studies, and shows the relative improvement in reducing: 1) the total printed circuit board area; 2) component quantity; and 3) carrier-to-substrate terminations, as the design progressed from the baseline configuration (phase 1) to the final RAEEC configuration (phase 3) using leadless chip carriers.

The RAEEC design concluded with phase 3 for the following reasons:

1. Although phase 4, which requires mounting leadless chip carriers on both sides of the substrate, is a viable approach to further reducing the circuit board area, it was not used because of its incompatibility with the HCC module design. It was determined that it was more advantageous to provide optimum thermal design than to further reduce the circuit board area.
2. Although phase 5 was not included as part of the RAEEC study, it is still an area for future consideration since the multichip carrier approach can yield substantial benefits in reducing circuit board area, component count and carrier-to-substrate terminations. Because of the uncertainty involved, and the effect it may have on test capability and package standardization, it was not introduced at this time.

Table B-1 is a summary of the technology selected for the RAEEC Control and represents the results of the various trade-offs presented in Figures B-2 through B-4 and Tables B-3 through B-7. Table B-1 also compares the RAEEC technological improvements to that of old technology, which is representative of the baseline control. The points shown for the old technology were chosen arbitrarily and the points shown for the RAEEC technology were determined based on the relative improvement in reliability over the old technology. The reliability factor (R_f) was based primarily on the quantity of each feature contained in the controller design. Table B-2 illustrates how R_f was determined.

Figures B-2 through B-4 and Tables B-3 through B-7 represent all the trade-offs that were performed for each of the package features. Figure B-2 indicates how many I/O connectors should be used to optimize reliability and maintainability.

Tables B-3 through B-7 and Figures B-3 and B-4 are all based on a similar approach. A list of rating criteria was generated for each package feature. The various designs were then assigned a weighting factor (WF) and a rating factor (RF). The weighting factor is based on the relative importance in terms of reliability; the rating factor is a measure of how good that particular characteristic is. The product of the two (i.e. $RF \times WF$) is the overall rating for that feature. The totals of all of the individual feature ratings are then used to show the relative magnitude of improvement in design and to serve as a guide for selection.

Below is a list of abbreviations used in the following tables and figures.

Assy	Assembly
BD	Board
Conn	Connector
Flex	Flexible
PC	Printed Circuit
PTH	Ploated Thru Hole
Term	Termination
T.I.	Texas Instruments

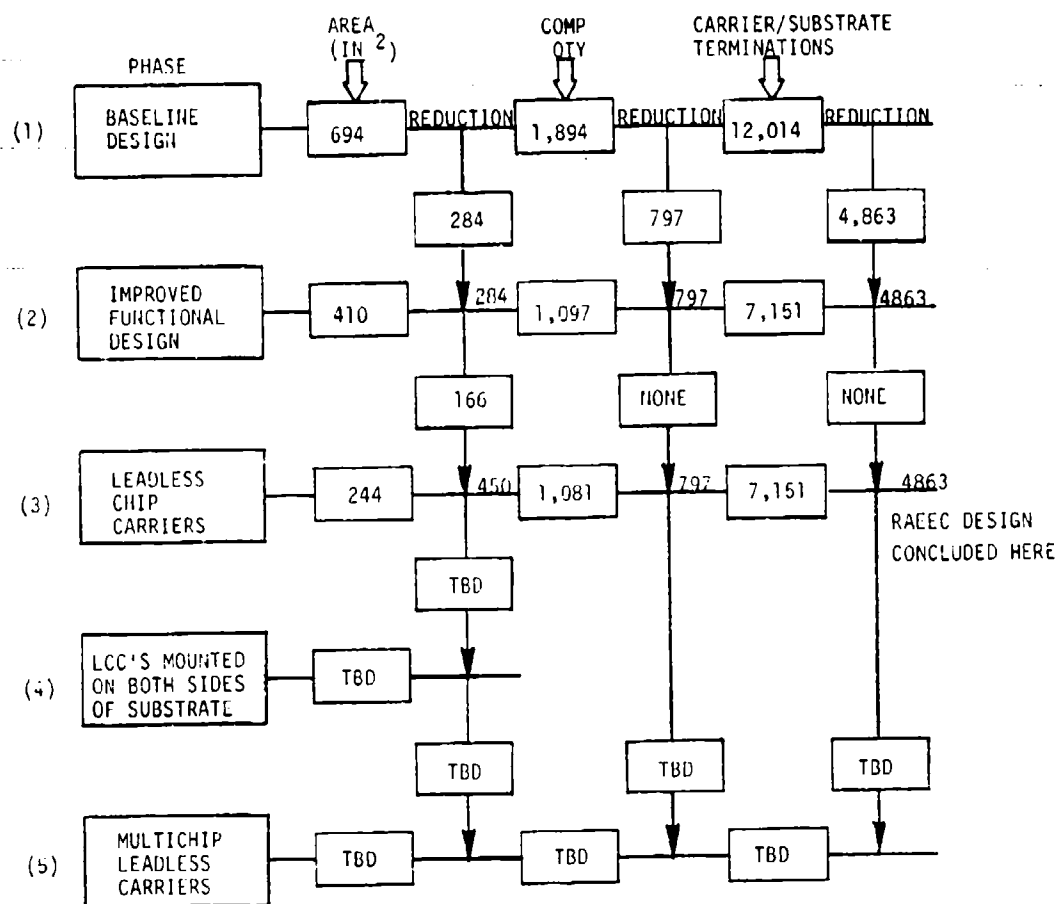
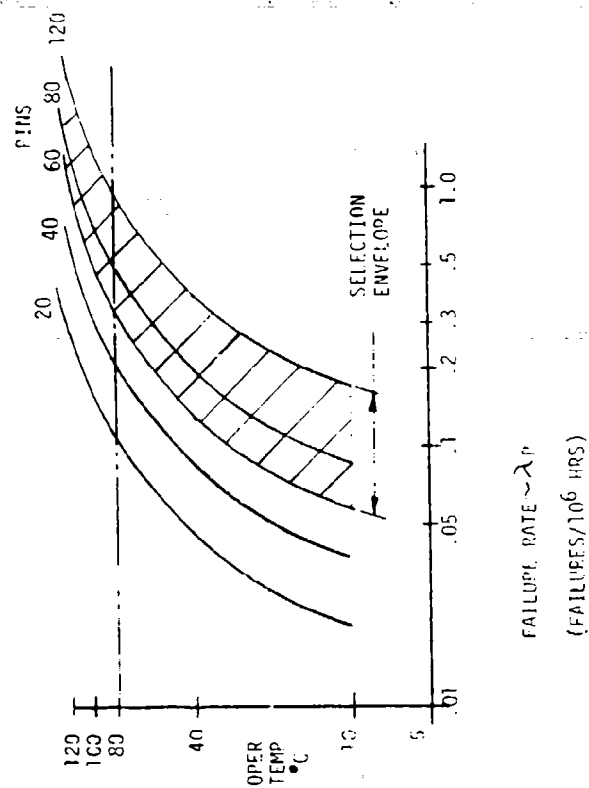


FIGURE B-1 REDUCTION STUDIES

TABLE B-1 RAECC PACKAGE FEATURES

FEATURE	OLD TECHNOLOGY				RAECC TECHNOLOGY				PERCENT IMPROVEMENT
	COMMENT	POINTS	Rf	TOTAL POINTS	COMMENT	POINTS	Rf	TOTAL POINTS	
I/O Conn.	6 Conn. 60 Pins Ea.	300	5	1,500	8 Conn. 60 Pins Ea.	1,344	3	4,032	2.69:1
I/O Cable Assembly	Flex Ckt. w/P.C. Pin Term. (≈ 12 Cables)	419	5	2,095	Molded Flex Cable w/Potted S/R Both Ends (≈ 16 Cables)	638	5	3,160	1.51:1
I/O Cable Term.	Soldered To P.C.B. w/Some S/R. (≈ 240)	1,157	1	1,157	Soldered TD P.C.B. w/Good S/R. (≈ 240)	1,300	1	1,300	1.12:1
P.C. Substrate	Epoxy (694 in ²)	343	2	686	Polyimide/AL203 (244 in ²)	518	6	3,108	4.53:1
80-80 Cable	Flex Ckt. (≈ 180 Term.)	345	3	1,035	Molded Flex Cable (≈ 100 Term.)	468	5	2,340	2.26:1
TOTAL				6,473				13,940	2.15:1
Elect. Comp.	Dip/Flat Pack	282	3	846	LCC	405	5	2,025	2.39:1

RF = Reliability Factor Based On Quantity



PRIMARY I/O PINOUTS	220
SECONDARY I/O PINOUTS	220

PROJECTED CONNECTOR PIN QTY MIX

CONN QTY	# PINS	TOTAL PINS	51/ RADC REVISED FAILURE RATES		MIL-HDBK-217B PREDICTED FAILURE RATES	
			λ_{ea}	λ_{total}	λ_{ea}	λ_{total}
4	60	240	.33	1.32	1.48	5.92
3	80	240	.49	1.47	2.12	6.36
2	120	240	.96	1.92	4.25	8.5

51/ G.F. GUTH, MARTIN MARIETTA CORP. "DEVELOPMENT OF NON-ELECTRONIC PART CYCLIC FAILURE RATES" (RADC-TR-77-417, DEC. '77)

FIGURE B-2 RAECC I/O CONNECTOR SIZE SELECTION

WEIGHTING FACTOR: MOST IMPORTANT = 10
 (WF) VERY IMPORTANT = 8
 IMPORTANT = 5
 SOMEWHAT IMPORTANT = 3
 NOT IMPORTANT = 1

RATING FACTOR: EXCELLENT = 10
 (RF) VERY GOOD = 8
 GOOD = 5
 FAIR = 3
 UNACCEPTABLE = 1

ITEM	DIE AND WIRE BONDING		BEAM LEAD		FLIP CHIP		TAB	
	WF	RF	WF X RF	RF	WF X RF	RF	WF X RF	RF
AVAILABILITY	10	10	100	3	30	3	80	8
HEAT TRANSFER TO CASE	10	8	80	3	30	5	80	8
MULTICHIP CAPABILITY	10	10	100	3	30	3	30	3
INSPECTABILITY	10	9	90	5	50	1	90	9
DURABILITY	9	7	63	7	63	5	72	8
AUTOMATED ASSEMBLY	8	8	64	5	40	8	64	8
EXPERIENCE	8	9	72	8	64	4	48	6
COST	2	7	14	3	6	8	16	8
TOTAL			585		313		277	
								480

FIGURE B-4 CHIP TO CARRIER TERMINATION

TABLE B-2 RAECC PACKAGE FEATURES - RELIABILITY FACTOR (Rf)

I/O CONNECTORS:	QTY	Rf	ELECT. COMP. CONNECTIONS:	QTY	Rf
	1 - 2	7		< 1,000	7
	3 - 4	5		1,000 - 5,000	5
	5 - 6	3		5,000 - 10,000	3
	7 - 8	1		10,000 - 15,000	1
	9 - 10	0		15,000 - 20,000	0
	> 10			> 20,000	
I/O CABLE ASSY:	QTY	Rf	P.C. SUBSTRATE:	AREA (in ²)	Rf
	1 - 4	7		< 100	8
	5 - 9	5		100 - 199	6
	10 - 16	3		200 - 399	4
	17 - 20	0		400 - 599	2
	> 20			600 - 799	0
				> 799	
I/O CABLE TERMINATION	QTY	Rf	BD-BD INTERCONNECT:	QTY	Rf
	< 60	7		< 60	7
	60 - 100	5		60 - 100	5
	101 - 160	3		101 - 160	3
	161 - 200	1		161 - 200	1
	201 - 260	0		201 - 260	0
	> 260			> 260	

TABLE B-3 I/O CONNECTOR TERMINATION COMPARISON

RATING CRITERIA	(WF)	TERMINATION					
		MECHANICAL			THERMAL		
		(RF)	OVERALL RATING (WF X RF)	(RF)	OVERALL RATING (WF X RF)	(RF)	OVERALL RATING (WF X RF)
Resistance to Environments	High Temp	9	90	6	60	5	50
	Low Temp	9	90	8	80	9	90
	Thermal Shock	8	80	7	70	8	80
	Vibration	9	90	3	30	6	60
	Salt & Humidity	8	80	6	60	9	90
	Aging	8	80	8	80	9	90
	Hemetic	10	100	1	10	10	100
Mechanical Properties	Pull Off Force	9	54	8	48	9	54
	Low Creep	9	54	7	42	9	54
	Strength	9	54	7	42	9	54
Electrical Properties	Low Resistance	9	45	9	45	9	45
	Res. Stability	9	45	9	45	10	50
	Low Voltage	9	45	9	45	9	45
Accessibility in Assembly	High Currents	9	45	2	40	8	40
	Little Space						
	Req'd Ease Of	9	27	8	24	8	24
Applicability to These Conductors	Stranded	9	27	7	24	8	24
	Insulated	10	80	0	0	9	72
	Wire Component	10	80	9	72	6	48
Joining Wire To:	Wire	9	27	-	0	10	30
	Component	8	24	8	24	10	30
	Separable Connector	9	27	7	21	9	27
TOTALS			1254		839		1157

Weighting Factors: Most Important = 10 Rating Factor: Most Applicable = 10
 (WF) Important = 5 (RF) Acceptable = 5
 Not Important = 0 Not Recommended = 0
 62/ No. Applicable = -

62/ Donald F. Cottrell and Thomas E. Kirejczyk, Martin Marietta Corp.
 "Crimp Connection Reliability" (RADC-TR-78-15, Jan. '78)

E-6215

TABLE B-4 PRINTED CIRCUIT BOARD CONNECTORS

FEATURE CONTRIBUTING TO HIGH RELIABILITY	RELIABILITY WEIGHTING FACTOR (WF)	2-PIECE CONNECTOR (MIL-C-55302)	RELATIVE RATING FACTOR (RF)	OVERALL RATING (WF X RF)	1-PIECE CONNECTOR (MIL-C-21097)	RELATIVE RATING FACTOR (RF)	OVERALL RATING (WF X RF)
Positive Contact Alignment	10	Jackscrews Line Up Mating Contacts	10	100	Groove In Conn. Aligns In One Direction Only	8	80
Mating/Remating W/O Contact Loading	10	Positive Alignment Minimizes Contact Loading	8	80	Spring Leaf Contacts W/Applied Load	0	0
Mechanical Retention Of Mated Connector Pair	10	Jackscrews Retain Connector Pair Preventing Damaged Contacts	8	80	Fastener Hardware Could Be Used	5	50
Strair Relief	10	Not Provided But Can Be Added	5	50	Not Provided But Can Be Added	5	50
Quality Control Of Plug And Receptacle	5	Connector Mfg. Makes Both Connector Halves	8	40	Connector And P.C. Board Made At Separate Locations	0	0
High Operating Temp	8	+ 1250C	5	40	+ 1250C	5	40
Low Operating Temp	8	- 650C	5	40	- 650C	5	40
TOTALS				430			260

Weighting Factors: Most Important = 10
 Very Important = 8
 Important = 5
 Somewhat Important = 3
 Least Important = 1

Rating Factor: Most Applicable = 10
 (RF) Acceptable = 5
 Not Recommended = 0

E-6216

TABLE B-5 HIGH PERFORMANCE LAMINATE COMPARISON

[illegible]

Weighting Factors:	Most Important	Rating Factor:	Passes Mil-Spec Qualifications and is much better than Other Alternatives
{dr}	Very Important	{10}	10
	Important	5	5
	Somewhat Important	3	8
	Least Important	1	5
			Exceeds Mil-Spec Qualifications but is Poor Compared to Other Alternatives
			Does Not Pass Mil-Spec Qualifications but is Acceptable
			1

- No plans for M11-Spec Qualification at the present time.

TABLE B-6 THICK FILM SUBSTRATE COMPARISON

CRITERIA	RELIABILITY WEIGHTING FACTOR (WF)	PORCELAIN ENAMEL ON STEEL	RELATIVE RATING FACTOR (RF)	OVERALL RATING (WFXRF)	96% AL2O3 ALUMINA	RELATIVE RATING FACTOR (RF)	OVERALL RATING (WFXRF)	REF
General Experience	10	Very Little Printed Cir- cuit Exper- ience	3	30	Widespread Use In Multilayer Hybrids For Military And Commercial Products	8	80	
Peak Processing Temp. (°C)	5	675	6	30	1000	9	45	63/
Thick Film Conduc- tor Stability	10	Fair	3	30	Good	8	80	22/
Thermal Conductiv- ity (G/CAL/cm²/cm/ sec/°C)	8	.0027	4	32	.084	10	80	17/ 64/
Dimensional Stabili- ty *(Panels Larger Than 4" X 4")	5	Excellent	10	50	Fair	5	25	22/
Dissipation Factor at 1MHz And 250C	1	.008	5	5	.0003	10	10	22/
Dielectric Constant at 1MHz and 250C	1	6.4	4	4	9.3	2	2	22/
Volume Resistivity at 200 VDC and 250C (ohms - cm)	1	>10 ¹⁴	8	8	> 10 ¹⁴	8	8	22/
Wire Bonding of Conductor Metalli- zation	5	Poor	3	15	Good	8	40	22/
TOTALS				204			370	

Weighting Factors: (WF) Most Important = 10
Very Important = 8
Important = 5
Somewhat Important = 3
Least Important = 1

Rating Factor: (RF) Passes Mil-Spec Qualifications and is
Much Better Than Other Alternatives = 10
Passes Mil-Spec Qualification and is
Slightly Better Than Other Alternatives = 8
Passes Mil-Spec Qualifications and is
Equal to Other Alternatives = 5
Passes Mil-Spec Qualifications but is
Poor Compared to Other Alternatives = 3
Does Not Pass Mil-Spec Qualifications
but is Acceptable = 1

* Both have excellent stability for smaller size panels.

E-6217

TABLE 8-7 SOLDER JOINT COMPARISON

FAILURE MODE	SOLDER JOINT CONFIGURATION									
	WF	LEAD IN P.T.H. (DIP)	RF	WF X RF	BEAM LEAD (FLAT PACK)	RF	WF X RF	METALLIZED SUBSTRATE (LCC)	RF	WF X RF
10 Repair: Cycles	9	< 5 Cycles Lifted Pads Cracked Barrels	1	9	≈ 5 Cycles Lifted Pads Cracked Barrels	3	27	T.L. Test ≈ 15 Cycles No Failures	9	81
Thermal Cycling	10	Coeff. Of Expansion Not Closely Matched	5	50	Coeff. Of Expansion Not Closely Matched	5	50	Coeff. Of Expansion Closely Matched	9	90
Vibration	10	Leads Load The P.T.H.	6	60	Lead Stresses Solder Joint	7	70	No Leads To Impose High Stress	8	80
Humidity	6	Leakage Path Thru Glass Sealed Lead	6	36	Leakage Path Thru Lead Seal	8	48	No Leads ∴ Leakage Very Low	10	60
Salt	6	Sharp Point Hard To Coat	5	30	Sharp Edge Hard To Coat	7	42	No Exposed Metal Package Leads	9	54
Ionic Contamin- ation	5	Sufficient Provision For Flux Removal	9	45	Sufficient Provision For Flux Removal	9	45	Adequate Clearance For Flux Removal	8	40
TOTAL				230			282			405

Weighting Factor: Most Important = 10 Rating Factor: Not Likely To Fail = 10
 (WF) Important = 5 (RF) Possibility Of Failure = 5
 Not Important = 0 High Possibility Of Failure = 0

APPENDIX C
TECHNOLOGY TRANSFER VISIT TO ROME AIR DEVELOPMENT CENTER

RELIABILITY ADVANCEMENT
FOR
ELECTRONIC ENGINE CONTROLLERS

Discussion Topics

RADC

December 8, 1977

1. Review of the engine control problems.
2. Discussion of the failure modes, problems, advantages, disadvantages of CMOS, SOS CMOS, N Channel MOS, I²L, and low power Schottky for high reliability applications in the 1977-1987 time frame.
3. Discussion of the process steps associated with each technology and the potential jeopardy of each step.
4. Recommend the semiconductor and microcircuit technology which shows the most promise for reliable performance in a hostile environment. Consider the need for advanced performance in multiple function and circuit types.
5. Suggestions and recommendations relative to optimum derating for various component types and technologies.
6. Discussion of the impact of "VSLI" on reliability, e.g., new design rules, new testing problems, new process steps.
7. Discussion of advantages/disadvantages of using hybrid technology in high reliability applications.

SUBJECT:

Reliability Advancement for EEC
Technology Transfer Trip Report
Rome Air Development Center
December 8, 1977

A five hour discussion was conducted at RADC along the lines outlined in the discussion topics (attached). The following persons participated:

Messrs. Joe Brauer	RADC
Clyde Lane	RADC
Chuck Ryan	AFAPL
Phil Lefkowitz	HS
Vic Mosca	HS
Dick Potetz	HS
Chas. Rabinowitz	HS
Bill Peck	HS
Dr. Al Shuskas	UTRC

Following the introduction of the engine control problem, a discussion of JFC 90 experience followed with an examination of the failure history. The failure history was examined in order to determine whether high temperature over-stress testing (HTOT) of components could have a beneficial impact on JFC90 reliability. Clyde Lane expressed the consensus opinion by saying that HTOT testing will have little benefit unless it is preceded by a successful reduction in vibration and temperature environment.

CMOS

Highlights

- The greatest problem with CMOS is the variability from lot to lot and the lack of understanding of the failure mechanism.
- CMOS from some vendors cannot presently be HTOT tested.
- Despite problems, RADC has compiled a record with 4000 series metal gate CMOS devices in both field and laboratory which shows CMOS and comparable bi-polar circuits to be about equal at 0.4 failures/million hours of operation at 50°C.
- RADC believes the TTL has a slight edge in reliability and that CMOS reliability can be improved with more stringent screening.
- This discussion centered primarily on digital circuitry constructed with CMOS technology. These circuits comprise less than 12% of the parts list of a typical electronic control. The significance of this discussion is overshadowed by the fact that the reliability of linear integrated circuits is markedly lower than that of digital circuits and, coupled with their greater number, will likely play the dominant role in establishing the system reliability.

The discussion then swung to item 2 and a Joe Brauer/Clyde Lane presentation of the CMOS situation. Their presentation is summarized as follows:

The greatest problem with CMOS is the variability of CMOS product from lot to lot. While CMOS is theoretically capable of being manufactured with reliable characteristics, as are TTL, I²L, lower power Schottky, and others, every practitioner of the CMOS art currently introduced his own variation in the manufacturing recipe. This is done for economic reasons but results in distinct built-in failure modes. All manufacturers suffer from this problem at the present time, even though the variability seems to be slowly improving over the last two years.

The major concern that the RADC personnel expressed about CMOS circuits was that although good devices were being turned out by a given line, occasionally bad batches were turned out which showed excessive failure rates during accelerated life testing. What is particularly puzzling, is that conventional

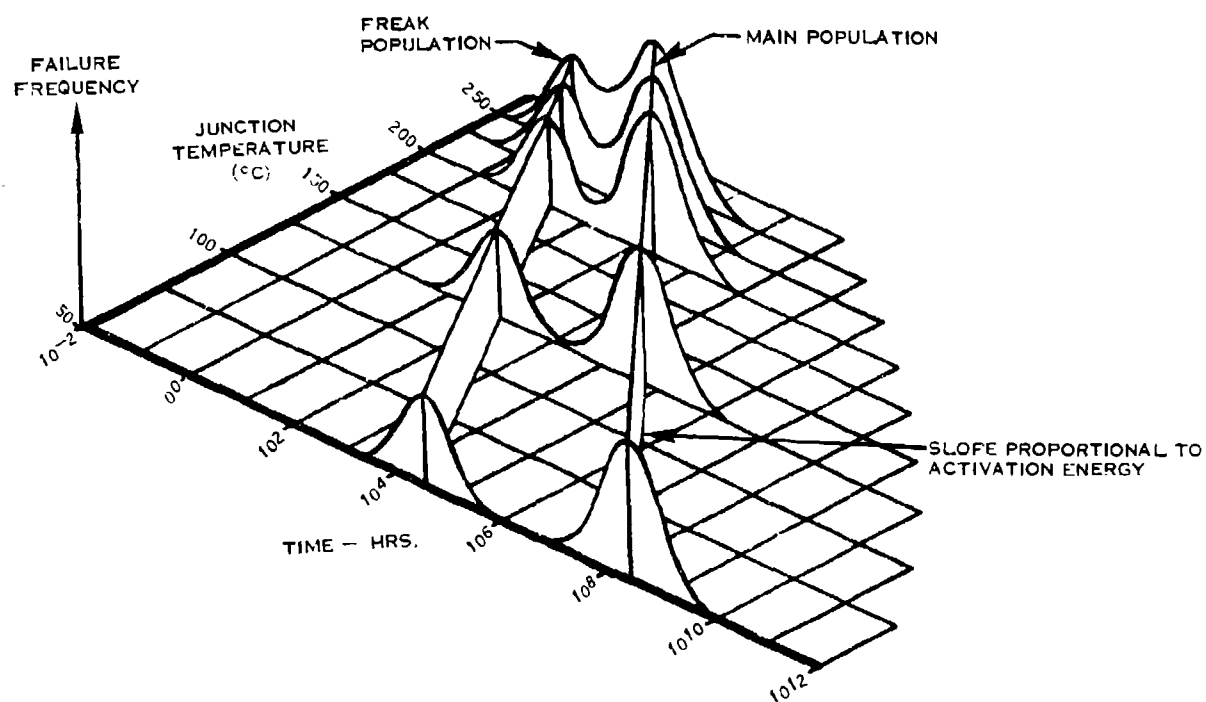
screening techniques such as C-V measurements and bias-temperature stressing cannot distinguish between the batches which show an abnormal failure rate and long lived devices. The lack of understanding of the failure mechanism introduced in the manufacturing process makes for a bad feeling from a reliability standpoint. Any lack of knowledge or control indicates a potential reliability problem.

Long term failure predictions for CMOS for applications with warm to hot environments are a concern. Figure C-1 shows the acceleration of some of the failure modes with temperature. It is significant that the slope of the temperature-time line is a direct function of activation energy. Lot variations from some manufacturers have been documented to vary over a 4 to 1 range with a corresponding variation in slope of 4 to 1.

Although CMOS has fewer construction process steps than T²L, there are more critical steps such as the oxide process which is not well understood. Problems identified under high temperature overstress testing (HTOT) include threshold shift and surface leakage. In particular, some products use epoxy die attach which releases moisture with time and temperature ultimately leading to surface leakage problems. The epoxy utilized for the die bonding was not subjected to a vacuum bake cycle, and hence, released water when the test devices were raised to the elevated temperatures required for accelerated life testing. This resulted in an excessive failure rate due to leakage. In the face of this evidence and repeated suggestions to certain manufacturers by RADC to vacuum bake the epoxy prior to chip bonding, or to revert to eutectic die bonding, they chose to ignore these suggestions until recently. Several lots of devices which were fabricated employing vacuum baked epoxy were reported to exhibit a considerably improved failure rate when subjected to accelerated life testing. One company has persistently declined to use a eutectic die attach which would be the obvious solution to this problem, but instead has elected to try another type epoxy that supposedly would not release moisture in the package. Devices with the new type epoxy material have not yet been made available to RADC for evaluation. RADC suggests that the moisture problem may not affect real applications, however, they must do accelerated testing for SAMSO applications and the moisture problem prohibits meaningful results on these devices. Other devices had a problem with lid seal integrity. Lids popped off at high temperature. Although resolution for these problems is in process, RADC's prime concern is that there still remains excessive lot to lot variation in reliability.

Recent HTOT tests completed by Motorola for Goodyear/MCAIR on CAPTOR program indicated excellent results which were certainly comparable to T²L. In the final analysis, tradeoffs have to be conducted to determine the failure rate effect of lower operating temperatures of CMOS vs T²L.

Preliminary testing of radiation hardened devices has shown good reliability. This has been attributed to the clean oxide low temperature processing needed to meet radiation requirements which also reduced contamination significantly thereby reducing threshold shift and leakage.



E-10

FIGURE C-1 LIFE - TEMPERATURE RELATIONSHIPS MFR NO. 1 LOT A-4007 CMOS

The standard 168 hour 125°C burn-in is not adequate to remove infant mortality; RADC can recommend special testing for hi-rel application.

With regard to the relative merits of CMOS and T²L, RADC implied that TTL is twice as reliable as CMOS. This comment has to be examined in the context that it was made. The reliability comparison was made between CMOS RAM circuits and TTL ROM chips. Clearly the comparison is not being made for circuits of the same level of complexity and the CMOS circuits are at a disadvantage in this comparison. One further caution that must be made when comparing technologies such as CMOS and bi-polar is whether the process technologies used in the fabrication of devices are of a comparable level of sophistication; for example: diffused guard rings vs oxide isolation, epoxy die bonding vs metallic die attachment, diffused junctions vs ion implanted, polysilicon gates vs. metal gates.

Despite the problems detailed above, RADC has compiled a record with 4000 series metal gate CMOS devices in the field and in the laboratory as follows:

Measured at 50°C

LAB	0.37 failures/million hours operation
FIELD	0.39 failures/million hours operation

These CMOS results compare favorably with RADC tests on TTL as follows:

TTL at 70°C

LAB	0.5 failures/million hours operation
-----	--------------------------------------

CMOS device reliability is quite respectable, by today's standards for reliable semiconductor devices, even though some of these parts cannot be tested with HTOT.

SOS/CMOS

SOS has the same problems as CMOS plus an additional one. The oxide SOS interface by process nature has poor strength yielding to failure under thermal cycling. This defect can be screened via thermal cycling. A bad device will last 1-10 cycles, a good one 300 cycles. RADC is concerned in a temperature cyclic environment that 300 cycles will be exceeded.

Device isolation in one process is achieved by means of etching away the silicon between devices. In the subsequent oxidation for device passivation, the oxide film formed near the silicon-sapphire interface tends to grow thinner than the remainder of the film. This is a weak point and tends to fail by rupturing when the devices are thermally cycled. RADC has found that devices which usually can withstand ten temperature cycles will not fail in this mode. There are fixes for this problem and the simplest is to deposit a film over the oxide to shore up the weak point. The best approach is to avoid the problem completely, which has been accomplished by means of oxidizing the silicon between devices down to the sapphire substrate. The local oxidation results in added benefits such as planar surfaces which eliminate metallization step coverage problems encountered in conventional processing.

SAMSO on the Missile X (MX) program spend much money trying to use CMOS SOS and finally gave up and converted to low power Schottky. Reason -- reliability, producibility and limited suppliers on the SOS.

There is a lot of military interest in CMOS SOS, however RADC feels that if the commercial market doesn't expand the technology would not go far.

N-Channel MOS

Although N-Channel would theoretically be less reliable than P-Channel, experience has shown the reverse to be true. RADC stated that BTL is recommending N-Channel for severe environment application because it doesn't have contamination susceptibility, is comparable to SOS speed and MOS power, and is easier to produce.

I²L

Navy appears to be going with I²L and a general DOD attitude favors I²L. No testing has been done by RADC. RADC is being pushed to generate MIL specs but has no basis for assessing inherent reliability. One manufacturer has made a major commitment in this technology, it having high commercial promise.

Hybrid

Messrs. Brauer/Lane commented on hybrids as follows:

Many manufacturers who make hybrid circuits for the open market are small, have inadequate financial resources, and inadequate quality control. Aerospace companies making hybrids for their own internal use have, in general, not been evaluated by RADC but may not suffer from these problems.

Hybrid devices must be recognized as complex assemblies with demanding processes which must be defined and maintained with hard discipline. Most small suppliers lack adequate process control and discipline and are not capable of making reliable hybrids.

The difficult problems of making repeatable reliable hybrids grow enormously as the size of the hybrid increases. It appears that the compounding of severe testing and repair problems on top of original manufacturing problems make the 6" X 7" hybrid device impractical.

At the end of the discussion, it was brought out that the concern over the relative reliability of various technologies employed to fabricate the digital circuits is overridden by the fact that the reliability of linear integrated circuits is markedly lower than that of digital circuits. As long as linear circuits are employed in the electronic engine control, they will play the dominant role in establishing the ultimate system reliability.

CONCLUSIONS

This is only the first of several in-depth technology transfer discussions of semiconductor components and technologies. Therefore, it appears premature to draw final conclusions until more discussions are held and a more complete picture available.

Our next technology transfer visit will be made on December 14, 1977 to Bell Laboratories in Murray Hill, New Jersey. The Bell System, widely recognized as a maker of highly reliable equipment, purchases and uses millions of CMOS devices per year in their telephone switching gear. They have also been one of the pioneers in the use of High Temperature Overstress Testing (HTOT) to eliminate premature failures from semiconductor components. They appear to have solved the HTOT testing problem for their purchased CMOS devices.

APPENDIX D
VIBRATION AND TEMPERATURE TRADEOFF STUDY

D.1 Scope

The purpose of this study is to establish design guidelines so that assessments can be conducted on the Vibration/Failure Rate and Temperature/Failure Rate relationships inherent in electronic equipments. The study also established a method to determine the optimum combination of temperature and vibration level so that the lowest possible failure rate is achieved.

D.2 Temperature/Failure Rate Tradeoff Analysis

The phenomenon of the Temperature/Failure Rate relationship is a well documented process. There are also several ways that the Temperature/Failure Rate relationship can be quantified. In this study the relationship between failure rate and temperature was derived using MIL-HDBK-217B as the basis with all other factors held constant.

The Temperature/Failure Rate relationship was studied using an electronic fuel control parts compliment. A series of failure rate predictions was performed using 217B as the basis and varying the temperature through a range of discrete values. The results are plotted in Figure D-1. Using straight line approximations it can be seen that the slope of the failure rate index increased significantly for temperatures greater than 84°C. For temperatures above this break-point, the failure rate is more sensitive to changes in temperature than for temperatures below the breakpoint. The breakpoint delineates critical regions with respect to operating temperature.

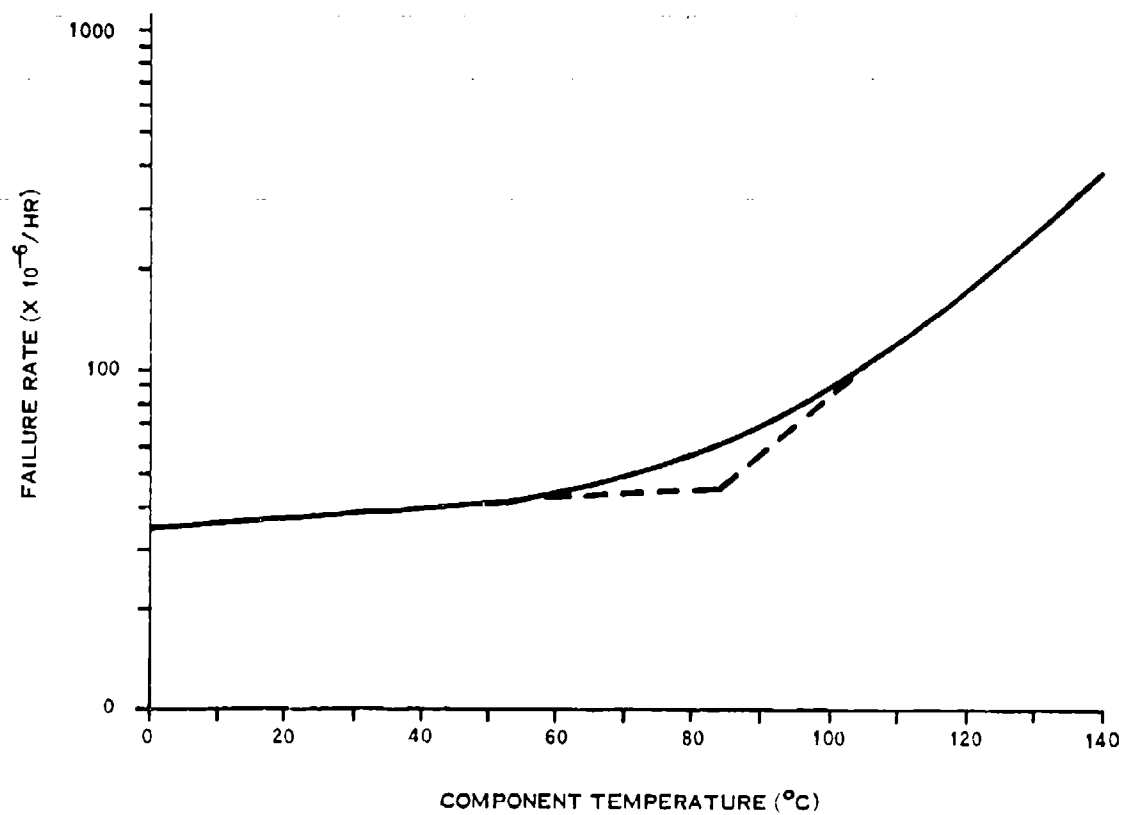
The curve in Figure D-1 can be used to determine the impact of temperature upon failure rates for other systems. For example consider a system with a failure rate of 100×10^{-2} F/Hr and operating at 90°C. If the system was re-designed such that the operating temperature was reduced to 60°C, what would be the corresponding failure rate? From Figure D-1 it can be seen that at 90°C the failure rate is 70×10^{-6} F/Hr and at 60°C the failure rate is 43.5×10^{-6} F/Hr, for a ratio of $0.62 = 43.5 \times 10^{-6} / 70 \times 10^{-6}$. Therefore, the new failure rate, at the reduced temperature, is 62×10^{-3} F/Hr = $(0.62) (100 \times 10^{-3})$.

This type of analysis can be conducted for most equipment/systems. However, it should be kept in mind that the curve in Figure D-1 was developed from a fuel control system, and as such, the closer, in terms of function and environment, the system under analysis is to a fuel control the more accurate the results will be.

D.3 Vibration/Failure Rate Tradeoff Analysis

The purpose of this section of the analysis was to attempt to quantitatively identify the relationship between vibratory stress and the failure rate with all other parameters constant.

A portion of the data for the analysis was drawn from a report prepared for the Eustis Directorate of the U.S. Army Air Mobility Research and Development Laboratory by Sikorsky Aircraft (Reference 65). This study assessed the reliability



E-6161

FIGURE D-1 FAILURE RATE VS. TEMPERATURE

impact of vibration levels upon two groups of helicopters. The groups were identical in construction except that one group had a device which reduced the vibration induced by the rotor. Vibration measurements were made on selected aircraft from both groups to determine the vibration environment. The vibration level, at the mounting location, for each piece of equipment was linearly extrapolated from the measured data points. Failure data was collected through normal Air Force channels using the USAF AFM 66-1 Maintenance Data Reporting System.

The second part of the data was drawn from internal Hamilton Standard sources dealing with the JFC90 Fuel Control. A design improvement to add isolators to the JFC90 has resulted in a reduced vibration level and increased reliability. The data was collected in a manner such that the before and after parameters for vibration level and failure rate were discernable. Therefore, the impact of vibration levels upon reliability can be assessed for the pre-improvement fuel control versus the post-improvement fuel control.

The last part of the data was drawn from information presented in "RADC Reliability Notebook - Volume III" (Reference 66).

The search for further data was conducted in three general areas. These areas were: (1) library literature; (2) people working in the fields of stress, and vibration and reliability; and (3) government, and government-supported, organizations. A representative sample of the contacts made during the search is:

UTC Research Library, East Hartford
Marshall Library, Huntsville
Mr. D.S. Steinberg, Litton Industries
Mr. E. Kimball, Martin Marietta
GIDEP
RADC, Mr. Lester Gubbins
IITRI (RADC), Mr. C. Ehrenfried and Mr. H. Rickers

The search did not uncover any data pertinent to this study.

Due to the large number of subsystems within the aircraft, the Sikorsky report (Reference 55) elected to breakout only the top 13 subsystems as determined by the number of failures (Table D-1). Of the top 13 subsystems only one, Radio Navigation, and portions of three others, Utility, Electrical and Fuel, are of interest in an analysis concerning electronic components. From these four subsystems, seven pieces of equipment were applicable to the analysis (see Table D-2). The complexity of this group ranges from switches and relays to radio transceivers.

In order to obtain a consistent data base, only equipments of roughly the same relative complexity were considered. Therefore the following equipments were deleted from the data base: Fire Sensing Element, Cargo Switches, Pressure Switches and Engine Start Relay.

The equipments remaining in the data base are shown in Table D-3.

TABLE D-1 TOTAL AIRCRAFT SYSTEM COMPARISON

Aircraft Subsystem	W/O Absorber	Failure Rate (10 ⁻³)	
		W/Absorber	Δ Failure Rate
1. Airframe	223.7	107.8	115.9
2. Drive	108.7	47.6	61.1
3. Utility	64.1	13.8	50.3
4. Landing Gear	91.5	44.8	46.7
5. Lights	119.6	29.3	90.3
6. Fuel	56.2	22.8	33.4
7. Flight Controls	58.4	22.8	35.6
8. Cockpit/Fuselage	33.1	9.9	23.2
9. Electrical	35.6	12.4	23.2
10. Hydraulic Power	37.1	17.1	20.0
11. Intercommunications	39.5	21.2	18.3
12. Radio Navigation	65.5	50.2	15.3
13. Airconditioning/Heating	27.1	18.3	8.8

TABLE D-2 COMPONENT FAILURE RATE

Component Name	Failure Rate (10 ⁻³)		Vibration Level (g's)	
	W/O Absorber	W/Absorber	W/O Absorber	W/Absorber
1. Fire Sensing Element	5.5	1.3	1.34	0.47
2. Fire Detector Control	4.1	0.6	1.34	0.47
3. Cargo Switches	3.6	3.2	0.61	0.25
4. Pressure Switches	4.7	1.5	1.48	0.60
5. Voltage Regulator	1.4	0.8	0.52	0.33
6. Engine Start Relay	2.4	1.4	0.36	0.29
7. LF/ADF RCVR (ARN-59)	6.3	4.2	0.75	0.35

Before the analysis could proceed, the failure rates for the control group (without absorber) had to be adjusted for the difference in temperature that the two groups experienced. The two groups were stationed in different climatic zones. The group without the absorber was stationed in a zone where the annual mean temperature was 64.5°F, and the group with the absorber was stationed in a zone where the annual mean temperature was 23.8°F. This difference in annual mean temperature produces a difference in the temperature to which the operating electronics were subjected. The temperature experienced by the electronics was assumed to be the sum of the outside ambient temperature and the temperature rise associated with the electronic's own dissipation. The internal temperature rise of the electronics was estimated to be 75°F.

Therefore, the control group electronics experienced an operating temperature of 139.5°F and the other group of electronics was subjected to an operating temperature of 98.8°F. Due to the higher operating temperature, the control group electronics will exhibit a higher failure rate than the group of electronics associated with the absorber equipped helicopter. To compensate for the temperature induced failure rate differences, the failure rates for the control group (without absorber) were adjusted downward by the use of a multiplicative factor.

The factor was developed from the Failure Rate/Temperature curve of Figure D-1. From the curve it can be seen that at 37.1°C (98.8°F) the corresponding failure rate is 39.0×10^{-6} F/Hr. For 59.7°C (139.5°F) the failure rate is 43.5×10^{-6} F/Hr. Therefore, the failure rates at 139.5°F reduced by the factor $.897 = 39.0 \times 10^{-6} / 43.5 \times 10^{-6}$ are equivalent to the failure rates at 98.8°F. The important assumption is that the Failure Rate/Temperature Curve developed from the EEC 103 Fuel Control can be used as a tradeoff tool for the helicopter equipment with different form, function and environment.

The relevant data is displayed in Table D-3.

In order to make the JFC90 data consistent with the helicopter data the failure rates were adjusted downward to take into account the JFC90's higher operating temperature. A multiplicative factor was used to accomplish the adjustment.

The factor was developed from the Failure Rate/Temperature Curve of Figure D-1. From the curve it can be seen that at 37.1°C (98.8°F) the corresponding failure rate is 39.0×10^{-6} F/Hr. For 125°C (257°F) the failure rate is 210×10^{-6} F/Hr. Therefore, the failure rates at 125°C reduced by the factor $0.186 = 39.0 \times 10^{-6} / 210 \times 10^{-6}$ are equivalent to failure rates at 37.1°C.

The relevant data is displayed in Table D-3.

The data drawn from "RADC Reliability Notebook - Volume II" (66) was derived from Table I-3, Nominal Ranges of Environmental Stress Characteristics, and Table XII-7, Environmental Adjustment Factor for microcircuits. From Table I-3 the following three pairs of environments were chosen for analysis: Ground Fixed (GF) and Ground Portable (GP), Airborne Inhabited and Airborne Uninhabited (AU), Satellite Launch (SL) and Missile (M). The pairs were chosen so

TABLE D-3

	FAILURE RATE ($\times 10^{-3}$)						VIBRATION LEVEL				LOCATION			
	TEMP COMP			TEMP COMP			W/O		W/		RATIO	STA	BL	WL
	W/O	W/	ABSORBER	W/O	ABSORBER	W/	ABSORBER	ABSORBER	ABSORBER	ABSORBER				
HELICOPTER														
FIRE DETECTOR CONTROL	4.1	0.6	3.68	0.6	3.08	6.25	1.34	0.47	0.87	2.86	180	30L	185	
VOLTAGE REGULATOR	1.4	0.8	1.26	0.8	0.46	1.59	0.52	0.83	0.19	1.59	150	40L	145	
LF/ADF PCVR	6.3	4.2	5.65	4.2	1.45	1.35	0.75	0.35	0.40	2.13	130	30L	170	
JFC-90	2.5	1.67	0.47	0.31	0.16	1.52	32.0	22.5	9.5	1.43				

404

HELICOPTER

$$\text{AVG TEMP W/O ABSORBER} = \frac{40 + 89}{2} + 75^{\circ}\text{F}$$

$$= 139.5^{\circ}\text{F}$$

$$= 59.72^{\circ}\text{C}$$

$$\text{AVG TEMP W/ ABSORBER} = \frac{5 + 42.6}{2} + 75^{\circ}\text{F}$$

$$= 98.8^{\circ}\text{F}$$

$$= 37.11^{\circ}\text{C}$$

HELICOPTER

$$\text{@ } 59.7^{\circ}\text{C} = 43.5$$

$$\text{@ } 37.1^{\circ}\text{C} = 39.0$$

$$43.5\text{K} = 39.0$$

$$\text{K} = .897$$

JFC-90

$$\text{@ } 125^{\circ}\text{C} = 210.0$$

$$\text{@ } 37.1^{\circ}\text{C} = 39.0$$

$$210\text{K} = 39.0$$

$$\text{K} = .186$$

that the environmental stress characteristics other than vibration were as similar as possible within pairs. The vibration ratio for each pair was obtained by forming the ratio of the maximum vibration level for each environment within the pair. The failure rate ratio was obtained by forming the ratio of the Environmental Adjustment Factor for each environment within the pair. This information is presented in Table B-4.

In Figure B-2 a "Best Fit" curve was drawn through the points obtained from the helicopter data and the JFC90 data. A separate curve was drawn through the data points derived from the RADC report (Reference 66). Because of the coarseness and scarcity of data points, the two lines do not coincide but serve as upper and lower bounds for a range of possible values. Also, for vibration ratios greater than 2.25, sufficient data does not exist to support a smooth extension of the curves. Therefore, a maximum upper bound of 2.3 for the Failure Rate Ratio was established for vibration ratios greater than 2.25.

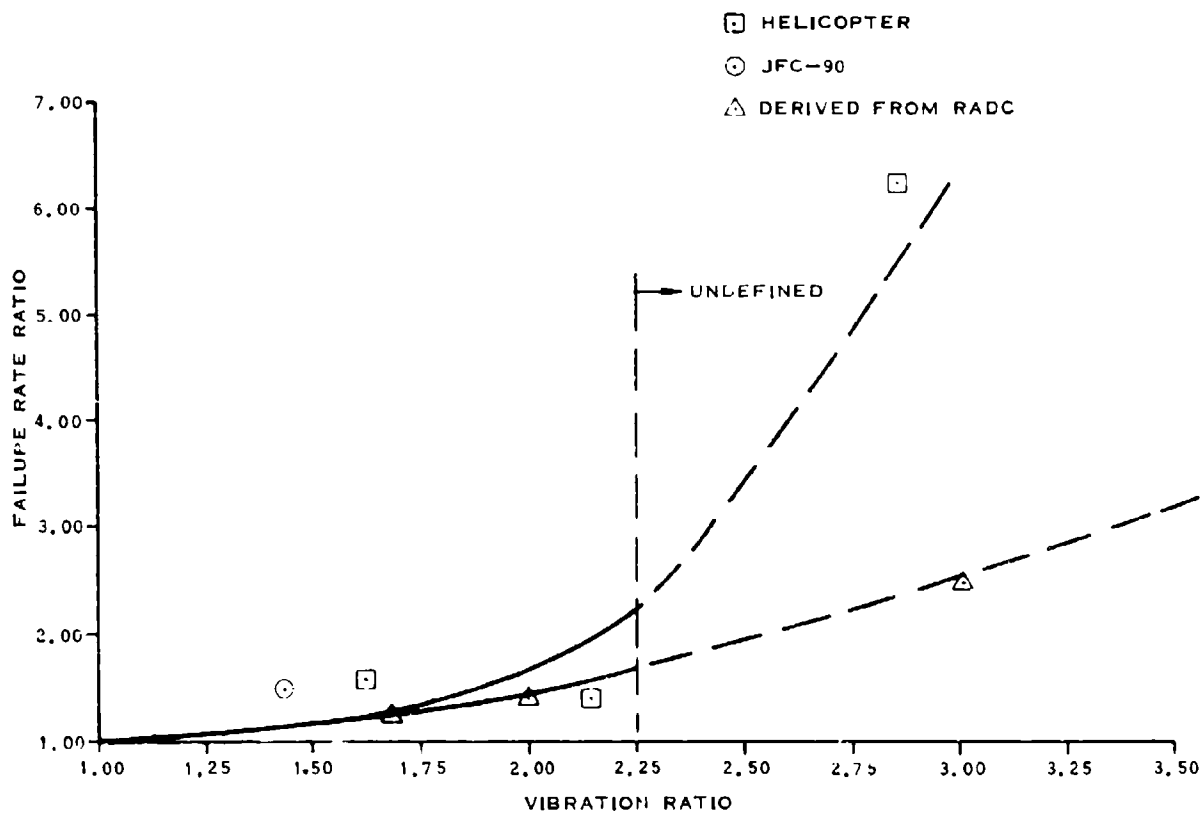
The curve in Figure B-2 provides the means for identifying the Failure Rate/Vibration level tradeoff in terms of relative vibration levels. The curve is dependent upon the assumption that the vibration levels of interest do not exceed equipment design capabilities.

The curve in Figure B-2 can be applied to other systems to determine the impact of vibration upon failure rates. For example consider a system with a failure rate of 100×10^{-3} F/Hr and a vibration level of 10 G's. If the system was redesigned such that the vibration level was reduced to 5 G's, what would be the corresponding failure rate? From Figure B-2 it can be seen that for a vibration ratio of 2, the failure rate ratio is 1.67 using the upper curve. Therefore, the new failure rate, at the reduced vibration level is 59.88×10^{-3} F/Hr = $100 \times 10^{-3}/1.67$.

If both the operating temperature and the vibration level are altered because of a design change, then the net effect of the changes upon the failure rate can be calculated by independently applying the temperature/failure rate and vibration/failure rate techniques. For example consider a system with a failure rate of 100×10^{-6} F/Hr, a vibration level of 10 G's, and an operating temperature of 70°C. If the system was redesigned such that the vibration level was reduced to 4 G's and the temperature increased to 90°C, what would be the corresponding failure? From Figure B-1 it can be seen that at 70°C the failure rate is 48.5×10^{-6} F/Hr and at 90°C the failure rate is 70×10^{-6} F/Hr for a ratio of 1.44. Therefore, the original failure rate is increased by 44×10^{-6} F/Hr due to temperature effects. From Figure B-3 it can be seen that for a vibration ratio of 2.5, the failure rate ratio is 2.3. Therefore, the original failure rate is decreased by 56.52×10^{-6} F/Hr due to vibration effects. For the combined Temperature/Vibration effects, the failure rate is reduced by a net 12.52×10^{-6} F/Hr. Therefore, the new failure rate is 87.48×10^{-6} F/Hr.

TABLE D-4 RADC VIBRATION/FAILURE RATE RELATIONSHIP

Environment	Vibration	Environment Factor	Vibration Ratio	Failure Rate Ratio
Ground Fixed	5	2	3.00	2.5
Ground Portable	15	5		
Airborne Inhabited	30	5	2.00	1.40
Airborne Uninhabited	60	7		
Satellite Launch	60	8	1.67	1.25
Missile	100	10		



E-2694

FIGURE D-2 FAILURE RATE RATIO VS. VIBRATION LEVEL RATIO

APPENDIX 1
PARAMETRIC AND FUNCTIONAL SERVICE TESTING

This appendix is included to define the specific electrical tests, conditions and end point limits used by MDAC-St. Louis in the performance of this program. Table C-1 is a list of the parametric tests, conditions and limits and Table E-2 is the truth table used for functional testing. The tests listed in these tables are identical to the tests used by the manufacturer in order to establish correlation between the MDAC-St. Louis and manufacturer test systems. As a result, the tests differ slightly from those contained in the Hamilton Standard Statement of Work. These differences are:

- a) Low Level Input Voltage (V_{IL}) and High Level Input Voltage (V_{IH}) were not measured directly and do not appear on the Table D-1 parametric electrical test list. V_{IL} and V_{IH} were inherently verified during the noise margin functional tests. Two Noise Margin (N.M.) tests are performed using the functional test pattern. The first N.M. test was performed with $V_{DD} = 15.0$ V, input levels of 11.0 V and 4.0 V for high and low levels, and output compare limits of 13.5 V and 1.5 V for high and low levels. The second N.M. test was performed with $V_{DD} = 5.0$ V, input levels of 3.5 V and 1.5 V and output compare limits of 4.5 V and 0.5 V. The N.M. testing, therefore, inherently verified that V_{IL} and V_{IH} are within the specified limits.
- b) Low Level Output Voltage (V_{OL}) and High Level Output Voltage (V_{OH}) were only measured with $V_{DD} = 15.0$ V, the worst case condition.
- c) The conditions of the High Level Output Current (I_{OH}) test at $V_{DD} = 5.0$ V were modified. The V_{OHT} voltage was changed from 4.6 volts to 2.5 volts and the end point limit from -0.51 mA to -2.4 mA.
- d) Negative and positive Output Saturation currents were included in the electrical parametric test list.
- e) The functional test sequence is not defined in the Statement of Work and the manufacturer's test sequence was followed. This test sequence consists of a clear cycle, load seven, count around to six, disable via PE, disable via TE, load fifteen and clear. The sequence is performed at $V_{DD} = 3.0$ V and $V_{DD} = 18.0$ V with a 0.2 MHz clock frequency.

TABLE E-1 PARAMETRIC TEST CONDITIONS

TEST SYMBOL	TEST NUMBER	CONDITIONS	MEASURE PIN	MIN	MAX	UNITS
I_{SSL}	1	$V_{DD} = 15.0 \text{ V}$ ALL INPUTS = 0 V	V_{DD}	0	20	μA
I_{SSH}	2	$V_{DD} = 15.0 \text{ V}$ ALL INPUTS = 15.0 V	V_{DD}	0	20	μA
I_{IL}	3	$V_{DD} = 15.0 \text{ V}$ ALL INPUTS = 0.0 V	$\overline{\text{CLR}}$	-0.1	0	μA
	4		CLK			
	5		D1			
	6		D2			
	7		D3			
	8		D4			
	9		PE			
	10		$\overline{\text{LD}}$			
	11		TE			
I_{IH}	12	$V_{DD} = 15.0 \text{ V}$ ALL INPUTS = 15.0 V	$\overline{\text{CLR}}$	0	0.1	μA
	13		CLK			
	14		D1			
	15		D2			
	16		D3			
	17		D4			
$V_{OHD} = V_{DD} - V_{OH}$	18	$V_{DD} = 15.0 \text{ V}$	Q4	-50	0.001	mV
	19		Q3			
	20		Q2			
	21		Q1			
	22		C0			
V_{OL}	23	$V_{DD} = 15.0 \text{ V}$	Q4	0	50	mV
	24		Q3			
	25		Q2			
	26		Q1			
	27		C0			

TABLE E-1 PARAMETRIC TEST CONDITIONS (Continued)

TEST SYMBOL	TEST NUMBER	CONDITIONS	MEASURE PIN	MIN	MAX	UNITS
I_{OH}	28	$V_{DD} = 15.0 \text{ V}$ $V_{OUT} = 13.5 \text{ V}$	Q4	-99	-3.4	mA
	29	↓	Q3	↓	↓	↓
	30		Q2	↓	↓	↓
	31		Q1	↓	↓	↓
	32		C0	↓	↓	↓
I_{OL}	33	$V_{DD} = 15.0 \text{ V}$ $V_{OUT} = 1.5 \text{ V}$	Q4	3.4	99	mA
	34	↓	Q3	↓	↓	↓
	35		Q2	↓	↓	↓
	36		Q1	↓	↓	↓
	37		C0	↓	↓	↓
I_{SSL}	38	$V_{DD} = 10 \text{ V}$ ALL INPUTS = 0 V	V_{DD}	0	10	μA
I_{SSH}	39	V_{DD} , ALL INPUTS = 10 V	V_{DD}	0	10	μA
I_{OH}	40	$V_{DD} = 10.0 \text{ V}$ $V_O = 9.5 \text{ V}$	Q4	-99	-1.3	mA
	41	↓	Q3	↓	↓	↓
	42		Q2	↓	↓	↓
	43		Q1	↓	↓	↓
	44		C0	↓	↓	↓
I_{OL}	45	$V_{DD} = 10.0 \text{ V}$ $V_O = 0.5 \text{ V}$	Q4	1.3	99	mA
	46	↓	Q3	↓	↓	↓
	47		Q2	↓	↓	↓
	48		Q1	↓	↓	↓
	49		C0	↓	↓	↓
I_{SSL}	50	$V_{DD} = 5 \text{ V}$ ALL INPUTS = 0 V	V_{DD}	0	5	μA
I_{SSH}	51	V_{DD} , ALL INPUTS = 5 V	V_{DD}	↓	↓	↓

TABLE E-1 PARAMETRIC TEST CONDITIONS (Continued)

TEST SYMBOL	TEST NUMBER	CONDITIONS	MEASURE PIN	MIN	MAX	UNITS
I_{OH}	52	$V_{DD} = 5.0 \text{ V}$ $V_O = 2.5 \text{ V}$	Q4	-99	-2.4	μA
	53		Q3			
	54		Q2			
	55		Q1			
	56		CO			
I_{OL}	57	$V_{DD} = 5.0 \text{ V}$ $V_O = 0.4 \text{ V}$	Q4	0.51	99	mA
	58		Q3			
	59		Q2			
	60		Q1			
	61		CO			
INSAT	62	$V_{DD} = 5.0 \text{ V}$ $V_{OUT} = 5.0 \text{ V}$	Q4	1.7	99	mA
	63		Q3			
	64		Q2			
	65		Q1			
	66		CO			
IPSAT	67	$V_{DD} = 5.0 \text{ V}$ $V_{OUT} = 0.0 \text{ V}$	Q4	-99	-1.7	mA
	68		Q3			
	69		Q2			
	70		Q1			
	71		CO			

TABLE E-2 FUNCTIONAL TEST TRUTH TABLE

PIN STEP	CLEAR 1	CLOCK 2	P1 3	P2 4	P3 5	P4 6	PE 7	VSS 8	LOAD 9	TE 10	Q4 11	Q3 12	Q2 13	Q1 14	CO 15	VDD 16
1	0	1/	1	1	1	0	0	0	1	0	0	0	0	0	0	1
2	1	1	1	0	0	0	0	0	1	0	0	1	0	0	0	1
3	1	1	0	0	0	0	0	0	1	0	0	0	0	0	0	1
4	1	1	0	0	0	0	0	0	1	0	0	0	0	0	0	1
5	1	1	0	0	0	0	0	0	1	0	0	0	0	0	0	1
6	1	1	0	0	0	0	0	0	1	0	0	0	0	0	0	1
7	1	1	0	0	0	0	0	0	1	0	0	0	0	0	0	1
8	1	1	0	0	0	0	0	0	1	0	0	0	0	0	0	1
9	1	1	0	0	0	0	0	0	1	0	0	0	0	0	0	1
10	1	1	0	0	0	0	0	0	1	0	0	0	0	0	0	1
11	1	1	0	0	0	0	0	0	1	0	0	0	0	0	0	1
12	1	1	0	0	0	0	0	0	1	0	0	0	0	0	0	1
13	1	1	0	0	0	0	0	0	1	0	0	0	0	0	0	1
14	1	1	0	0	0	0	0	0	1	0	0	0	0	0	0	1
15	1	1	0	0	0	0	0	0	1	0	0	0	0	0	0	1
16	1	1	0	0	0	0	0	0	1	0	0	0	0	0	0	1
17	1	1	0	0	0	0	0	0	1	0	0	0	0	0	0	1
18	1	1	0	0	0	0	0	0	1	0	0	0	0	0	0	1
19	1	1	0	0	0	0	0	0	1	0	0	0	0	0	0	1
20	1	1	0	0	0	0	0	0	1	0	0	0	0	0	0	1
21	1	1	0	0	0	0	0	0	1	0	0	0	0	0	0	1
22	1	1	0	0	0	0	0	0	1	0	0	0	0	0	0	1
23	1	1	0	0	0	0	0	0	1	0	0	0	0	0	0	1
24	1	1	0	0	0	0	0	0	1	0	0	0	0	0	0	1
25	1	1	0	0	0	0	0	0	1	0	0	0	0	0	0	1
26	1	1	0	0	0	0	0	0	1	0	0	0	0	0	0	1
27	0	1/	1	1	1	1	1	0	0	0	0	0	0	0	0	1

1/ ONE FULL CLOCK CYCLE DURING EACH STEP.

APPENDIX F
CONSTRUCTION EVALUATION FOR ACCELERATED LIFE TESTS

An analysis was made of the physical characteristics of a 16-pin cerdip to determine if there existed any physical construction features that might preclude high temperature accelerated life tests at the temperatures specified (150°C, 175°C, and 200°C). In this analysis one of the devices was delidded and a microscopic inspection was made with attention given primarily to determining the materials used in constructing the device. Table F-1 contains a summary of the results of this analysis. No device features were found that would limit high temperature operation at elevated temperatures below 250°C.

TABLE F-1 PHYSICAL CHARACTERIZATION SUMMARY

PACKAGE TYPE:	16 LEAD DUAL-IN LINE CERDIP
PACKAGE MATERIAL:	TOP: BLACK CERAMIC BOTTOM: BLACK CERAMIC LID SEAL & LEAD INSULATOR: GREY GLASS FRIT
GLASSIVATION:	SiO ₂
DIE SCRIBE METHOD:	MECHANICAL SCRIBE
DIE SIZE:	85 MIL x 57 MIL
DIE ATTACHMENT:	GOLD-SILICON EUECTIC
WIRE MATERIAL:	ALUMINUM; 1 MIL DIAMETER
WIRE BONDING METHOD:	LEAD FRAME: ULTRASONIC BOND DIE BOND PAD: ULTRASONIC BOND
INTRACONNECT MATERIAL:	ALUMINUM
LEAD MATERIALS:	EXTERNAL: KOVAR TYPE WITH TIN PLATING LEAD FRAME: KOVAR TYPE WITH ALUMINUM PLATING

APPENDIX G
COST BENEFITS OF SELF-TRIM CONTROL MODES

6.1 Summary

For the Reliability Advancement Study for Electronic Engine Controllers, a life cycle cost analysis was made of the controllers' self-trim capability (Task II of Hamilton Standard Purchase Order BE 067639). The application used for the study was an advanced variable-cycle engine mounted in a two-engine tactical fighter aircraft combat fleet of 540 operation aircraft using 1,728 engines over a 15-year life. The self-trim feature provides a life cycle cost savings of \$472.7 million.

The primary savings (85%) resulting from the self-trim feature were in the area of reduced spare parts costs due to the elimination of trim "hot" time and an increase in the ratio of engine flight hours to operating hours. Fuel, labor, and support equipment savings related to trims were relatively small.

The total life cycle cost savings attributed to the self-trim control modes were added to the total life cycle cost analysis conducted for this program.

6.2 Introduction

A life cycle cost (LCC) study of the self-trim benefits of an advanced engine electronic controller was performed as part of Task II of the overall program, which is to achieve high reliability for engine-mounted electronic controls. For the purpose of this study, it was assumed that the application is an advanced variable cycle engine equipped with an electronic control having self-trim capability.

The objective of this analysis was to evaluate the operating and support cost savings associated with the self-trim feature. The term "self-trim" means that once an engine is put into service no manual action is required to maintain engine thrust. A closed loop control approach is implemented to eliminate the need to trim the engine to maintain desired thrust and engine airflow. The control mode utilizes engine parameters for automatic regulation of desired thrust setting and engine airflow.

6.3 Results

The following is a summary of the results of the self-trim control modes study:

	<u>ΔLCC (\$ Millions)</u>
RDT&E Cost	No Change
Acquisition Cost	No Change
Operation and Support Cost	
Spare parts and associated labor	-401.8
Support equipment	- 8.9
Trim fuel	- 52.5
Trim labor	- 9.5
TOTAL	-472.7

The cost driver in this analysis, as shown by the breakdown above, was the spare parts and associated labor costs with a predicted savings of \$401.8 million (about 85% of the total savings).

G.4 Study Groundrules

The force structure and utilization groundrules for this study are as follows:

- 729 total aircraft
- 1728 total engines (including 270 spares)
- 540 operational aircraft (6 bases and 1 training base)
- Each operational aircraft flies 25 hr/month for 15 years

Economic assumptions are as follows:

- 1978 dollars
- Base Level Labor Rate: \$16.25 per maintenance man-hour (mmh)
- Depot Level Labor Rate: \$26.00 per mmh
- Fuel Cost: \$0.45 per gallon

G.5 Discussion

G.5.1 Development and Acquisition Costs

This study did not consider any RDT&E or acquisition costs associated with the electronic engine control system. Small differences in development and production costs between an advanced controller with and without self-trim capabilities were considered insignificant to this study.

G.5.2 Self-Trim Savings

Elimination of manual trim provides a hot section life improvement in two ways. A conventional engine mode which controls to engine speed requires occasional trim action to maintain thrust above an acceptable minimum level. This trims the engine to a nominal thrust condition and then allows it to deteriorate back to the minimum level where it is then retrimmed. The self-trim modes continually maintain the desired engine thrust at the desired level and eliminate any uptrimming, thus saving hot section life. The second benefit in hot section life comes from the elimination of engine hot time (intermediate power and above) required for ground trim runs. This increases the life of hot section parts and increases the ratio of engine flight hours to total operating hours.

G.5.3 Spare Parts and Associated Labor

A major portion of the self-trim LCC savings is from reduced spare parts and labor requirements caused by: (1) hot section life improvements and (2) increased ratio of engine flight hours to total operating hours.

The electronic control self-trimming capability would eliminate all trim time, which represents 75% of the total ground hot time, the other 25% being associated with diagnostic runs. This decrease in engine hot time (intermediate power and above) resulted in a 25% increase in the lives of the erosion and creep-limited parts. Hot section life improvement accounted for 73%, or about \$66 per engine flight hour, of spare parts and labor savings. The increase in the lives of the erosion and creep-limited parts reduces the number of spares used over the operating life of the engine, saving \$321.2 million in spare parts.

An increase in the ratio of engine flight hours to total operating hours means that for a fixed number of flight hours, the total number of operating hours for each engine decreases. The savings attributed to the reduction in total operating hours was determined based on overall engine maintenance cost per flight hour. With the decrease in total operating time, the total maintenance cost of the "cold" engine parts is decreased, producing an additional saving of \$80.6 million.

G.5.4 Support Equipment

Support equipment savings were based on the assumption that diagnostic capability at the organizational and intermediate levels would be equivalent to that of the current F100 engine. All trim-related support equipment at the organizational and intermediate maintenance levels was eliminated and considered as savings, including any nonrecurring costs. Since trim runs presently account for a major portion of ground operating time, it was assumed that one portable test stand could be eliminated at each base as a result of the elimination of trim runs.

At the Depot maintenance level, it was assumed that the work load would remain constant, with no net cost difference in required support equipment.

A summary of the support equipment savings is shown below:

<u>Eliminated Support Equipment</u>	<u>Δ LCC (\$ Millions)</u>
Organizational Level	-6.9
● Mach number simulators (two per wing)	
● Remote trimmers (two per wing)	
● SCS test set and engine trim set (four per wing)	
Intermediate Level	-2.0
● Mach number simulator (one per wing)	
● Remote trimmers (two per wing)	
● Test stand (one per wing)	

Eliminated Support EquipmentΔ LCC (\$ Millions)

Depot Level

- No change

0

TOTAL SUPPORT EQUIPMENT SAVINGS

-8.9

G.5.5 Trim Fuel and Labor

The average fuel consumed during a trim run is 2400 gallons, based on F-15 trim data from Langley AFB scaled to reflect the variable cycle engine complexity. At engine maturity, the mean time between trims is projected to be 100 engine flight hours. With fuel costs at \$0.45 per gallon, the elimination of all trim runs would save \$52.5 million over the 4.86 million total engine flight hours of the fleet. A labor saving of \$9.48 million would result from the elimination of trim runs based on the average 12 man-hours required per trim, the labor rate of \$16.25 per mmh, and the projected number of trims that would have been required.

Eliminated Support EquipmentΔ LCC (\$ Millions)

Depot Level

- No change

0

TOTAL SUPPORT EQUIPMENT SAVINGS

-8.9

G.5.5 Trim Fuel and Labor

The average fuel consumed during a trim run is 2400 gallons, based on F-15 trim data from Langley AFB scaled to reflect the variable cycle engine complexity. At engine maturity, the mean time between trims is projected to be 100 engine flight hours. With fuel costs at \$0.45 per gallon, the elimination of all trim runs would save \$52.5 million over the 4.86 million total engine flight hours of the fleet. A labor saving of \$9.48 million would result from the elimination of trim runs based on the average 12 man-hours required per trim, the labor rate of \$16.25 per mmh, and the projected number of trims that would have been required.

REFERENCES

1. W.A. Wulf, "Reliable Hardware/Software Architecture." IEEE Trans. on Software Engineering, June 1975.
2. W.S. Feller, An Introduction to Probability Theory and Its Application. Volume I, Wiley, New York, 1957.
3. W.C. Bouricius, W.C. Carter, and P.R. Schneider, "Reliability Modeling Techniques for Self-Repairing Computer Systems." Proc. of the 24th National Conference of ACM, 1969.
4. T.F. Westermeier, "Redundancy Management of Digital Fly-By-Wire Systems." Proc. Joint Automatic Control Conference (IEEE), Volume I, 1977.
5. C.E. Shannon and E.F. Moore, "Reliable Circuits Using Less Reliable Relays." J. Franklin Inst., Vol. 262, pp 191-203 and 281-297, Sept/Oct 1956.
6. J.G. Tyron, "Quadded Logic." Redundancy Techniques for Computing Systems, Spartan Books, 1962.
7. J. Von Neumann, "Probabilistic Logics and The Synthesis of Reliable Organisms From Unreliable Components." Automata Studies, Annals of Mathematics, No. 34, pp 43-98, Princeton, 1956.
8. I. Bazovsky, Reliability Theory and Practice. Prentice-Hall Inc., NJ, 1961.
9. M.L. Shooman, Probabilistic Reliability: An Engineering Approach. pp 136-140, McGraw-Hill, NJ.
10. Heckelman, Knight, and Straub, "A Self Diagnosing Fault Tolerant Micro-processor." pp 124 and 125, GCMAC Digest of Papers, General Electric, 1978.
11. J. Prokop and D.W. Williams, Chip Carriers As A Means For High-Density Packaging. Texas Instruments, Inc., Dallas, TX, 1977.
12. M.C. Burch, and D.M. Hargis, Ceramic Chip Carrier - The New Standard in Packaging. Electronics Division, 3M Company.
13. R.E. Gordon, RCA Advanced Technology Laboratories, NJ, "Airborne Packaging Using Compound Hybrids with LSI." Electronic Packaging and Production, November 1978.

14. H.W. Markstein, "Chip Carrier Update." Electronic Packaging and Production, April 1979.
15. D. Aney, "Looking Ahead At High Density Packaging." Electro. '78, Electronics Show and Convection, sponsored by IEEE and ERA, May 23-25, 1978.
16. R.J. Clark, General Electric Co., "Microelectronic Packaging Trends: An IEPS Review." Electronic Packaging and Production, January 1979.
17. Captain R.E. Settle, Jr., Air Force Avionics Laboratory, "A New Family Of Microelectronic Packages For Avionics." Solid-State Technology, June 1978.
18. Dr. J.S. Sallo, Fortin Laminating Corp., "Selecting Laminates For Multilayer and Two-Sided Rigid PCB's." Circuits Manufacturing.
19. R. Castonguay, MICA Corp., "Resin Systems For High-Performance Laminates." Electronic Packaging and Production, July 1979.
20. Anon., "Guidelines For Designing Multilayer Ceramic Substrates." Electronic Products Division, 3M Company.
21. R.L. Morey and P.J. Pijoan, "Thick Film Multilayer Boards: Specialized Problem Areas." C.S. Draper Laboratory, Inc., ISHM, 1978.
22. D.P. Wicker and W.B. Hatfield, "Porcelain Steel Technology: A Bona-fide Alternative?" The Singer Company, Corporate R&D Laboratory, ISHM, 1978.
23. F.A. Fisher and J.A. Plumer, General Electric Company, "Lightning Protection of Aircraft." NASA Reference Publication 1008, Prepared for Aerospace Safety Research and Data Institute, NASA Lewis Research Center, October 1977.
24. Anon., "Electromagnetic Compatibility." Air Force Systems Command Design Handbook DH1-4, Third Edition, January 5, 1975.
25. J.D. Robb, "Lightning Protection Approaches For Gas Turbine Controls." AMSE Publication No. 71-GT-29, Applied Research, Lightning and Transients Research Institute, St. Paul, Minn., April 1971.
26. Anon., "Space Shuttle Lightning Protection Criteria Document." NASA Publication JSC-07636, Shuttle Lightning Protection Committee, Lyndon B. Johnson Space Center, Houston, Texas, September 11, 1973.

27. J.A. Plumer, General Electric Company, "Analysis and Calculation of Lightning-Induced Voltages in Aircraft Electrical Circuits." NASA Contractor Report CR-2349, Prepared for NASA Lewis Research Center, January 1974.
28. Anon., "Final Draft, Aerospace Recommended Practice, Lightning Effects Tests on Aerospace Vehicles and Hardware." SAE Publication, SAE Committee AE4 on Electromagnetic Compatibility, Special Task F, May 1, 1974.
29. Anon., "Lightning and Static Electricity Conference, Part II: Conference Paper." Air Force Avionics Lab Technical Report AFAL-TR-68-290, December 3-5, 1968.
30. Anon., "Protection of Aircraft Fuel Systems Against Lightning." FAA Advisory Circular AC 20-53, Washington, D.C., October 1967.
31. Anon., "Lightning and Static Electricity Conference." Air Force Avionics Lab Technical Report AFAL-TR-72-325, December 12-15, 1972.
32. Anon., "Bonding, Electrical, and Lightning Protection For Aerospace Systems." MIL-B-5087B, October 15, 1964.
33. L.L. Oh, "Measured and Calculated Spectral Amplitude of Lightning Sferics." Commercial Airline Group, Boeing, IEEE Trans. on EMC, November 1969.
34. R.A. Weck, "Thin-Film Shielding for Microcircuit Applications and a Useful Laboratory Tool for Plane-Wave Shielding Evaluation." Electronic Components Lab, USAECOM, Fort Monmouth, N.J., IEEE Trans. on EMC, March 1968.
35. P.J. LeBlanc and D.L. Reinhard, "EMI Shielding of Plastic Housings," General Electric Co., Pittsfield, Mass., Electronic Packaging and Production, February 1975.
36. Anon., "Control Mode Studies For Advanced Variable Geometry Turbine Engines." AFAPL-TR-75-7, March 1974.
37. Anon., "Aircraft Fuel Heat Sink Utilizations." AFAPL-TR-73-51.
38. Anon., "FADEC, Full Authority Digital Electronic Control." NAPTIC Contract N00019-76-C-0422.
39. N. Sissenwine, "Extremes of Hydrometers at Altitude For MIL-STD-210B." AFICRL-72-0369, AFSC No. 242, 1972.

40. B. Litovicz and F.E. Ostrem, "A Survey of Environmental Conditions Incident to The Transportation of Materials", Dept. of Transportation Bulletin, PB 204 442, Final Report, Phase I General American Transportation Corp., October 1971.
41. Anon., "Long-Life Assurance Study For Manned Spacecraft Long-Life Hardware." Summary of Long-Life Assurance Guidelines, Vol. I, Martin-Marietta Corporation, September 1972.
42. D. Edgerton, Jr. and I. Quart, "Hughes Aircraft Company Stress Screening Studies." Proceedings-Institute of Environmental Sciences, 1979.
43. J.W. Bathke, General Dynamics/Pomona, "Standardizing Environmental Testing in a Multi-Program Orientation." Proceedings-Institute of Environmental Sciences, 1979.
44. J.D. Branum, "Selection and Evaluation of Environmental Screening Tests For Trident I (C4) Electronics Black Boxes." Lockheed Missiles and Space Company.
45. D.S. Peck and C.H. Zierdt, Jr., "The Reliability of Semiconductor Devices in The Bell System." Proceedings of The IEEE, Vol. 62, No. 2, pp 185-211, February 1974.
46. D.S. Peck, "New Concepts About Integrated Circuit Reliability." Bell Telephone Laboratories, IEEE Transactions Electronic Devices (USA), Vol. ED-26, No. 1, pp. 38-43, January 1979.
47. Anon., "Long-Life Assurance Study for Manned Spacecraft Long-Life Hardware." Special Long-Life Assurance Studies, Vol. 4, Martin-Marietta Corporation, September 1972.
43. J. Cardinal, "Establish Manufacturing Processes for Polyimide/Glass Printed Circuit Boards." Hamilton Standard Division, Windsor Locks, Conn., March 23, 1978.
49. Anon., "Digital Evaluation and Generic Failure Analysis Data." RADC document no. MDR-10, ITI Research Institute, January 1979.
50. J.L. Duane, "Learning Curve Approach to Reliability Monitoring", IELL Aerospace, 2: pp. 563-566, 1964.
51. L.H. Crow, "Reliability Analysis for Complex Repairable Systems", AMSAA, TR138, 1974.

52. O. Kempthorne and L. Folk, "Probability Statistics and Data Analysis", Iowa State University Press, 1971.
53. M. Engle and L.J. Bain, "Prediction Intervals for Weibull Process", Technometrics, 20: pp 167-169, 1978.
54. W.M. Bassin, "Increasing Hazard Functions and Overhaul Policy", Annual Reliability Symposium, pp 173-178, 1969.
55. L.H. Crow, "On Tracking Reliability Growth", Reliability and Maintainability Symposium, pp 438-443, 1975.
56. L.H. Crow, "Confidence Interval Procedures For Reliability Growth Analysis", AMSAA, TR197, AD-A044788, 1977.
57. J.M. Finkelstein, "Confidence Bounds On The Parameters of The Weibull Process", Technometrics, 18: pp 115-117, 1976.
58. I. Lee and S.K. Lee, "Some Results on Inference for the Weibull Process", Technometrics, 20: pp 41-45, 1978.
59. M. Kusner, "Systems Analysis-Nonlinear Estimating Techniques", Reliability and Quality Control Symposium, pp 203-207, 1961.
60. Anon., "Logistics Support Cost Model", U.S. Air Force AFALD, Wright-Patterson Air Force Base, Ohio, August 1976.
61. G.F. Guth, "Development of Nonelectric Part Cyclic Failure Rates", Martin-Marietta Corp., (RADC-TR-77-417), December 1977.
62. Donald F. Cottrell and Thomas E. Kirejczyk, "Crimp Connection Reliability", Martin-Marietta Corp., (RADC-TR-78-15), January 1978.
63. Walter B. Hatfield and Daniel P. Wicker, The Singer Company, Corporate R&D Laboratory, "A Microelectronic Packaging Technology For Consumer Product Applications", presented at the Electronic Component Conference, April, 1978.
64. The Erie Ceramic Arts Company, "Porcelain Enamel Substrates For Thick Film Hybrids and P.C. Boards", Erie, PA.
65. Sikorsky Aircraft Division, "Vibration Effects On Helicopter Reliability and Maintainability." Prepared for Eustis Directorate, U.S. Army Air Mobility Research and Development Laboratory, Fort Eustis, VA, (contract # DAAJ02-71-C-0037), April, 1973.
66. Anon., "RADC Reliability Notebook", Volume II, Technical Report No. RADC-TR-67-108, September, 1967.